

GENERAL DECLASSIFICATION SCHEDULE

**IN ACCORDANCE WITH
DOD 5200.1-R & EXECUTIVE ORDER 11652**

THIS REPORT HAS BEEN DELIMITED
AND CLEARED FOR PUBLIC RELEASE
UNDER DOD DIRECTIVE 5200.20 AND
NO RESTRICTIONS ARE IMPOSED UPON
ITS USE AND DISCLOSURE.

DISTRIBUTION STATEMENT A

APPROVED FOR PUBLIC RELEASE,
DISTRIBUTION UNLIMITED.

UNCLASSIFIED

25837

Armed Services Technical Information Agency

Reproduced by

DOCUMENT SERVICE CENTER

KNOTT BUILDING, DAYTON 2, OHIO

This document is the property of the United States Government. It is furnished for the duration of the contract and shall be returned when no longer required, or upon recall by ASTIA at the following address: Armed Services Technical Information Agency, Document Service Center, Knott Building, Dayton 2, Ohio.

WHEN GOVERNMENT OR OTHER DRAWINGS, SPECIFICATIONS OR OTHER DATA ARE FURNISHED FOR ANY PURPOSE OTHER THAN IN CONNECTION WITH A DEFINITELY RELATED GOVERNMENT PROCUREMENT OPERATION, THE U. S. GOVERNMENT THEREBY INCURS NO LIABILITY, NOR ANY OBLIGATION WHATSOEVER; AND THE FACT THAT THE GOVERNMENT MAY HAVE FORMULATED, FURNISHED, OR IN ANY WAY SUPPLIED THE DRAWINGS, SPECIFICATIONS, OR OTHER DATA IS NOT TO BE REGARDED BY ANY PERSON OR OTHERWISE AS IN ANY MANNER LICENSING THE HOLDER OR ANY OTHER PERSON, CORPORATION, OR CONVEYING ANY RIGHTS OR PERMISSION TO MANUFACTURE, OR TO USE ANY PATENTED INVENTION THAT MAY IN ANY WAY BE RELATED THERETO.

UNCLASSIFIED

126887

WADC TECHNICAL REPORT 55-173

FC

AEROELASTICITY IN STABILITY AND CONTROL

J. B. REA COMPANY, INC.

MARCH 1957

WRIGHT AIR DEVELOPMENT CENTER

NOTICES

When Government drawings, specifications, or other data are used for any purpose other than in connection with a definitely related Government procurement operation, the United States Government thereby incurs no responsibility nor any obligation whatsoever; and the fact that the Government may have formulated, furnished, or in any way supplied the said drawings, specifications, or other data, is not to be regarded by implication or otherwise as in any manner licensing the holder or any other person or corporation, or conveying any rights or permission to manufacture, use, or sell any patented invention that may in any way be related thereto.

Qualified requesters may obtain copies of this report from the ASTIA Document Service Center, Knott Building, Dayton 2, Ohio.

This report has been released to the Office of Technical Services, U. S. Department of Commerce, Washington 25, D. C., for sale to the general public.

Copies of WADC Technical Reports and Technical Notes should not be returned to the Wright Air Development Center unless return is required by security considerations, contractual obligations, or notice on a specific document.

WADC TECHNICAL REPORT 55-173

AEROELASTICITY IN STABILITY AND CONTROL

J. B. REA COMPANY, INC.

MARCH 1957

FLIGHT CONTROL LABORATORY
CONTRACT No. AF 33(616)-2424
PROJECT 1365 TASK No. 13542

WRIGHT AIR DEVELOPMENT CENTER
AIR RESEARCH AND DEVELOPMENT COMMAND
UNITED STATES AIR FORCE
WRIGHT-PATTERSON AIR FORCE BASE, OHIO

FOREWORD

This handbook was prepared under Air Force Contract No. AF 33(616)-2424 by the J. B. Rea Company, Santa Monica, California. The contract was initiated under Research and Development Project 1365 - Task No. 13542, and was administered under the direction of the Flight Control Laboratory, Directorate of Laboratories, Wright Air Development Center, with Mr. R. J. Woodcock and Lt. H. M. Davis acting successively as project engineers.

The project was carried on by the Dynamics Group of the J. B. Rea Company with Mr. L. G. Campbell, Jr. (Chapters I, VIII, and IX) as project engineer. Members of the Dynamics Group who participated were Mr. R. P. Walton (Chapter VII) and Mr. L. D. Stimpson, Jr. (Chapter VIII). The consultants of the J. B. Rea Company who co-operated in the writing of the material were Dr. J. W. Miles (Chapters II, III, and V), Dr. W. T. Thomson (Chapter IV), both of the University of California at Los Angeles, Dr. K. C. Fung (Chapters II and V) of the California Institute of Technology, and Mr. N. L. Wener (Chapter IX) of Convair, San Diego, California.

ABSTRACT

The purpose of this volume is to present sufficient technical material to enable a practicing dynamics engineer to understand various aeroelastic phenomena and to give methods for incorporating aeroelastic effects in equations of motion as well as techniques for obtaining the solutions. Matrix methods are emphasized throughout because of their generality.

The presentation of the material is by "example" rather than by a manual approach, because many of the techniques of analysis are still in a state of development; moreover these techniques are highly dependent upon the aircraft configuration and flight regime involved.

The first five chapters present basic concepts and theories of elasticity and aerodynamics; Chapters VI and VII contain applications to airplanes (which can be extended to missiles) and helicopters, Chapters VIII and IX describe the solution techniques as well as methods for analyzing flight test data relative to aeroelastic analyses.

PUBLICATION REVIEW

This report has been reviewed and is approved.

FOR THE COMMANDER:



JOHN L. MARTIN, JR.
Colonel, USAF
Chief, Flight Control Laboratory
Directorate of Laboratories

TABLE OF CONTENTS

| <u>Chapter</u> | <u>Page</u> |
|--|-------------|
| I Introduction | 1 |
| 1.0 Scope of Book | 1 |
| 1.1 Purpose of the Book | 1 |
| 1.2 Material Included in Book | 1 |
| II Basic Concepts | 2 |
| 2.0 Introduction | 2 |
| 2.1 Descriptions of Parameters | 2 |
| 2.1.1 Aeroelastic Parameters | 2 |
| 2.1.2 Frequency Parameters | 3 |
| 2.1.3 Structural Damping | 4 |
| 2.2 Static Aeroelastic Effects | 4 |
| 2.2.1 Torsional Deflection and Divergence | 4 |
| 2.2.2 Control Surface Effectiveness and Reversal | 7 |
| 2.2.3 Fuselage Bending | 15 |
| 2.2.4 Swept Wing Deflections | 18 |
| 2.2.5 Static Aeroelastic Correction of Stability Derivatives | 22 |
| 2.3 Lift Distribution on an Elastic Wing | 23 |
| 2.3.1 The Lift Curve Slope | 23 |
| 2.3.2 Spanwise Lift Distribution at Subsonic Speeds | 27 |
| 2.3.3 Aerodynamic Influence Coefficients at Subsonic Speeds | 36 |
| 2.3.4 The Effect of Elastic Deformation on the Lift Distribution | 39 |
| References | 47 |
| Nomenclature | 49 |
| III Derivation of Equations of Motion | 53 |
| 3.0 Introduction | 53 |
| 3.1 Modal Approach | 56 |
| 3.2 Collocation Approach Using Matrices | 60 |
| 3.2.1 Dynamic Stability Equations for Rigid Airplane | 60 |
| 3.2.1.1 Equations of Motion in Body Axes | 61 |
| 3.2.1.2 Dimensionless Notation | 65 |
| 3.2.1.3 Dimensionless Longitudinal Stability Equations | 66 |

TABLE OF CONTENTS (continued)

| <u>Chapter</u> | | <u>Page</u> |
|----------------|---|-------------|
| III | 3.2.1.4 Dimensionless Lateral Stability Equations | 70 |
| | 3.2.2 Dynamic Stability Equations for Elastic Airplane | 73 |
| | 3.2.2.1 Longitudinal Stability Equations for Elastic Airframe | 73 |
| | 3.2.2.2 Lateral Stability Equations for Elastic Airframe | 80 |
| | 3.2.2.3 Quasi-Static Solution for Elastic Deflections | 85 |
| | 3.2.2.4 Steady Flight Aeroelastic Problem | 87 |
| | 3.2.2.5 Free Vibration Problem | 88 |
| | 3.2.2.6 Galerkin Formulation of Aeroelastic Equations | 89 |
| | 3.2.2.7 Breakdown of Aeroelastic Problem | 93 |
| | 3.3.1 Autopilot Effects | 94 |
| | References | 96 |
| | Nomenclature | 101 |
| | Appendix | 103 |
| IV | Determination of Elastic Effects | 106 |
| | 4.0 Introduction | 106 |
| | 4.1 Elastic Concepts | 106 |
| | 4.1.1 Dynamic Representation of Elastic Structures | 107 |
| | 4.1.1.1 Elastic Effects | 107 |
| | 4.1.1.2 Inertial Mass and Moment Effects | 110 |
| | 4.1.1.3 Structural Damping Effect | 111 |
| | 4.1.2 Principal and Normal Modes of Oscillation | 112 |
| | 4.1.3 Coupling of Motion | 113 |
| | 4.1.4 Equations for a Beam in Bending and Torsion | 115 |
| | 4.1.4.1 Bending | 115 |
| | 4.1.4.2 Torsion | 116 |
| | 4.1.4.3 Bending-Torsion | 117 |
| | 4.2 Methods for Computing Normal Modes | 117 |
| | 4.2.1 Rayleigh's Energy Method | 120 |
| | 4.2.1.1 Rayleigh-Ritz Extension | 121 |
| | 4.2.2 Stodola Method | 122 |
| | 4.2.3 Tabular Methods | 123 |
| | 4.2.3.1 Holzer Method | 123 |
| | 4.2.3.2 Holzer-Myklestad Method for Bending Vibrations | 124 |
| | 4.2.3.3 Uncoupled Bending Vibrations | 124 |

TABLE OF CONTENTS (continued)

| <u>Chapter</u> | | <u>Page</u> |
|----------------|---|-------------|
| IV | 4.2.3.4 Influence Coefficients | 128 |
| | 4.2.3.5 Coupled Bending-Torsion Vibration | 130 |
| | 4.2.3.6 Swept Wings | 133 |
| | 4.2.4 Method of Matrix Iteration | 136 |
| | 4.2.4.1 Matrix Representation Including Rigid Body Motion | 140 |
| | 4.2.5 Beam Vibrations in a Centrifugal Field | 144 |
| | 4.2.5.1 Holzer-Myklestad Method for the Rotating Beam | 146 |
| | 4.3 Analysis of Coupled Systems | 147 |
| | 4.3.1 Generalized Coordinates and Lagrange's Equation | 147 |
| | 4.3.1.1 Effective Mass and Inertia Parameters | 150 |
| | 4.3.1.2 Transient Response Parameters | 152 |
| | 4.3.2 Coupled Mode Analysis | 153 |
| | 4.3.3 Coupling of Control Surfaces | 160 |
| | References | 166 |
| | Nomenclature | 169 |
| V | Determination of Aerodynamic Effects | 172 |
| | 5.0 Introduction | 172 |
| | 5.1 Summary | 173 |
| | 5.1.1 Significance of the Unsteady Flow Effect | 173 |
| | 5.2 Survey of Basic Concepts and Analytical Results in the First Order Unsteady Flow Theory | 175 |
| | 5.2.1 Aerodynamic Concepts | 175 |
| | 5.2.1.1 Linearized Aerodynamic Theory | 175 |
| | 5.2.1.2 Quasi-Stationary and First Order Theories | 176 |
| | 5.2.1.3 Aerodynamic Effects of Various Motions | 180 |
| | 5.2.1.4 Basic Wing Problem | 182 |
| | 5.2.2 High Aspect Ratio Wings in Subsonic Flow | 183 |
| | 5.2.2.1 Two-Dimensional Incompressible Flow | 184 |
| | 5.2.2.2 Two-Dimensional Compressible Flow | 188 |
| | 5.2.2.3 Lifting-Line Theory for Incompressible Flow | 190 |
| | 5.2.2.4 Lifting Surface Theories for Subsonic Flow | 193 |
| | 5.2.2.5 Subsonic Compressibility Correction | 194 |
| | 5.2.2.6 Swept Wings in Subsonic Flow | 196 |
| | 5.2.3 Supersonic Wings, Piston Theory | 198 |

TABLE OF CONTENTS (continued)

| <u>Chapter</u> | | <u>Page</u> |
|----------------|---|-------------|
| V | 5.2.3.1 Reduction of Unsteady Flow to Steady Flow Problems | 199 |
| | 5.2.3.2 Two-Dimensional Supersonic Flow | 201 |
| | 5.2.3.3 Simple Planforms | 202 |
| | 5.2.3.4 Lifting Surface Integral Equation for Supersonic Flow | 205 |
| | 5.2.3.5 Evvard's Method | 207 |
| | 5.2.3.6 Aerodynamic Influence Coefficients | 219 |
| | 5.2.4 Slender Body Theory | 220 |
| | 5.2.4.1 Slender Body of Revolution | 221 |
| | 5.2.4.2 Low Aspect Ratio Wings | 222 |
| | 5.2.4.3 Slender Wing-Body Combination | 223 |
| | 5.2.4.4 Quasi-Slender Wing Theory | 223 |
| | 5.2.5 Downwash Calculations | 227 |
| 5.3 | Summary of Results in the Theory of Oscillating Airfoil in Two-Dimensional Flow | 228 |
| | 5.3.1 Oscillating Airfoils in Two-Dimensional Incompressible Flow | 228 |
| | 5.3.1.1 Theodorsen's Function | 228 |
| | 5.3.1.2 Rear Aerodynamic Center | 229 |
| | 5.3.1.3 General Solution | 230 |
| | 5.3.1.4 Flutter Aerodynamic Coefficients | 231 |
| | 5.3.1.5 Tabulation of Results - Two-Dimensional Incompressible Flow | 236 |
| | 5.3.2 Oscillating Airfoils in Two-Dimensional Subsonic Flow | 236 |
| | 5.3.3 Oscillating Airfoils in Two-Dimensional Supersonic Flow | 237 |
| | 5.3.4 Oscillating Airfoils in Two-Dimensional Transonic Flow | 244 |
| 5.4 | Oscillating Finite Wings and Bodies | 244 |
| | 5.4.1 Oscillating Finite Wing, Incompressible Flow | 245 |
| | 5.4.2 Oscillating Finite Wing, Subsonic Flow | 247 |
| | 5.4.3 Oscillating Finite Wing, Supersonic Flow | 250 |
| 5.5 | Indicial Response of Airfoil to Step Function Input | 250 |
| | 5.5.1 Aerodynamic Forces Acting on Thin Airfoils in Unsteady Motion - Two-Dimensional Incompressible Flow | 250 |
| | 5.5.2 Wagner's Function, $\phi(\tau)$ | 254 |
| | 5.5.3 Finite Aspect Ratio Effect, Incompressible Flow | 255 |
| | 5.5.4 Kussner's Function, $\psi(\tau)$, Incompressible Flow | 255 |
| | 5.5.5 Indicial Response in Two-Dimensional Subsonic Flow | 256 |
| | 5.5.6 Indicial Response in Two-Dimensional Supersonic Flow | 260 |
| | 5.5.7 Indicial Response at Mach Equal to 1 | 261 |

TABLE OF CONTENTS (continued)

| <u>Chapter</u> | | <u>Page</u> |
|----------------|---|-------------|
| V | 5.5.8 Sinusoidal Gusts | 261 |
| | 5.6 Stability Derivatives | 263 |
| | 5.6.1 Application of Oscillating Wing Theory to Unsteady Motion | 263 |
| | 5.6.2 Transformation of Coordinate Axes | 266 |
| | 5.6.3 Wing Wash Effects in the Vicinity of the Tail | 266 |
| | 5.6.4 Stability Derivatives of the Airplane | 268 |
| | 5.7 The Influence of Elastic Deformation of the Structure | 270 |
| | 5.7.1 Introduction | 270 |
| | 5.7.2 Methods for Investigating the Effects of Structural Distortions | 271 |
| | 5.7.3 Influence of the Flexibility of the Fuselage - An Example of the Modified Derivatives from the Modal Approach | 272 |
| | 5.7.3.1 Quasi-Static Solution, Modified Derivatives | 275 |
| | 5.7.3.2 Static Stability | 279 |
| | 5.7.4 Modified Derivatives from the Collocation Approach | 280 |
| | 5.7.5 Modified Derivatives from the Modal Approach | 281 |
| | 5.7.6 Simplified Estimates of the Static Aeroelastic Effects on the Longitudinal Stability and Control | 282 |
| | 5.7.7 Simplified Estimates of the Static Aeroelastic Effects on the Lateral Stability and Control | 285 |
| | References | 288 |
| | Nomenclature | 298 |
| | Appendix A | 301 |
| | Appendix B | 304 |
| | Appendix C | 307 |
| VI | Aeroelastic Equations of Motion for an Airplane | 309 |
| | 6.0 Introduction | 309 |
| | 6.1 Nomenclature | 309 |
| | 6.1.1 Axis System | 309 |
| | 6.1.2 General Assumptions | 309 |
| | 6.1.3 List of Symbols | 311 |
| | 6.2 General Longitudinal Equations of Motion Including Two Normal Modes | 318 |
| | 6.3 Derivation of the Generalized Forces for the Equations of Motion in ξ_1 and ξ_2 Coordinates | 338 |

TABLE OF CONTENTS (continued)

| <u>Chapter</u> | <u>Page</u> |
|--|-------------|
| VI 6.4 Derivation of Normal Mode Derivatives | 347 |
| 6.5 An Analysis of the Coupling Between an Autopilot System and Airframe Elastic Modes | 353 |
| References | 357 |
| VII Aeroelastic Equations of Motion for a Helicopter | 358 |
| 7.0 Introduction | 358 |
| 7.1 Method of Approach | 358 |
| 7.1.1 Axis System and Coordinate System | 358 |
| 7.1.2 Development of the Linear Equations for the Helicopter | 359 |
| 7.1.3 Modal Analysis | 362 |
| 7.1.3.1 Mode Shapes | 363 |
| 7.2 Equations of Motion - (Rigid Plus Aeroelastic) | 366 |
| 7.2.1 Assumptions | 367 |
| 7.2.2 Coordinates | 368 |
| 7.2.3 Body Forces and Moments | 371 |
| 7.2.4 Total Aeroelastic Equations of Motion | 379 |
| 7.2.5 The Stability Equation | 381 |
| 7.3 Illustrative Example | 384 |
| 7.3.1 Statement of Problem | 384 |
| 7.3.2 Equations of Motion | 387 |
| 7.3.3 Obtaining the Result | 392 |
| 7.4 Illustration of the Use of a Root Locus Plot to Demonstrate the Effect of Torsion and Flexibility of the Blade on Helicopter Stability | 399 |
| 7.4.1 Inclusion of Torsional Effects | 399 |
| 7.4.1.1 Torsional Mode and Stiffness Factor | 400 |
| 7.4.2 Rigid Body | 401 |
| 7.4.3 Aeroelastic Case | 402 |
| 7.5 Summary | 403 |
| Nomenclature | 408 |
| References | 414 |
| Bibliography | 416 |
| VIII Methods for Solving Aeroelastic Equations | 417 |

TABLE OF CONTENTS (continued)

| <u>Chapter</u> | <u>Page</u> |
|---|-------------|
| VIII 8.0 Introduction | 417 |
| 8.1 Development of Solution Forms of Equations of Motion | 419 |
| 8.2 Digital Machines | 422 |
| 8.2.1 Solution of Equations of Motion | 422 |
| 8.2.1.1 Point by Point Solution to Obtain Frequency Responses | 423 |
| 8.2.1.2 Polynomial Solution of Transfer Functions | 426 |
| 8.3 Analog Machines | 432 |
| 8.3.1 Application to Aeroelastic Analysis | 433 |
| References | 440 |
| Bibliography | 441 |
| Appendix | 444 |
| IX Flight Testing | 450 |
| 9.0 Introduction | 450 |
| 9.0.1 Objectives | 450 |
| 9.0.2 Comparison of Experiment and Theory | 450 |
| 9.1 Data Requirements | 451 |
| 9.1.1 General | 451 |
| 9.1.2 Data for Evaluation of Flight Dynamics | 451 |
| 9.1.3 Data for Checking Aeroelastic Theory | 452 |
| 9.2 Ground Tests | 454 |
| 9.2.1 General | 454 |
| 9.2.2 Weight and Balance | 454 |
| 9.2.3 Structural Vibratory Modes | 455 |
| 9.2.4 Structural Influence Coefficients | 455 |
| 9.3 Flight Test Techniques | 457 |
| 9.3.1 Static Stability Tests | 457 |
| 9.3.2 Dynamic Stability Tests | 458 |
| 9.4 Instrumentation | 460 |
| 9.4.1 Sensor Locations | 460 |
| 9.4.2 Sensor Characteristics | 461 |
| 9.4.3 Recording System | 462 |

TABLE OF CONTENTS (continued)

| <u>Chapter</u> | <u>Page</u> |
|--|-------------|
| IX 9.5 Flight Test Procedures | 462 |
| 9.5.1 Flight Conditions | 462 |
| 9.5.2 Test Operations | 464 |
| 9.6 Data Analysis Procedures | 465 |
| 9.6.1 Time-to-Frequency-Plane Transformation | 465 |
| 9.6.2 Techniques for Smoothing Data | 468 |
| 9.6.2.1 Fourier Series | 469 |
| 9.6.2.2 Weighting Functions | 469 |
| 9.6.3 Techniques for Analyzing Dynamic Flight Test Data | 471 |
| 9.6.3.1 Methods for Determining Aerodynamic Co- efficients from Transient Data | 472 |
| 9.6.3.2 Methods for Determining Aerodynamic Co- efficients from Frequency Response Data | 478 |
| 9.6.3.3 Simplified Analysis Procedures | 482 |
| 9.6.4 Techniques for Performing Error Analyses | 484 |
| References | 486 |
| Bibliography | 490 |
| Nomenclature | 493 |

CHAPTER I

INTRODUCTION

1.0 Scope of Book

The phenomenon of coupling between aerodynamics and airframe elasticity is known as aeroelasticity. Aircraft flying at high subsonic and supersonic speeds need both thin wing sections and thin fuselages in order to reduce the drag forces. In general, these thin structures have considerable flexibility which tends to accentuate static and/or dynamic coupling between the aerodynamics and elasticity. For example, the elastic swept wing in bending introduces an effective change in the angle of attack that results in a different aerodynamic force than if the wing were rigid. The structural elasticity also leads to reduced control effectiveness as well as changes in the downwash flow pattern that are important to the tail effectiveness. Transient maneuvers or gusts will cause a flexible aircraft to experience dynamic aeroelastic phenomena which can be very different from static aeroelasticity when the time lag in the build up of the flow pattern is considered.

Of special importance to the dynamic stability and control engineer is the dependence of the latest aircraft upon automatic control equipment. The use of automatic controls in a flexible aircraft can result in undesirable coupling between the elasticity of the structure and the automatic equipment, even to the extent of causing instability in flight. For these and other reasons it is becoming more important to consider the aeroelasticity in the analyses required for the design of new aircraft.

1.1 Purpose of the Book

The purpose of this book is to present the basic concepts needed by engineers in understanding the techniques for incorporating aeroelastic effects in stability and control analyses of aircraft as well as to give practical procedures for performing such analyses. To accomplish this in a single volume only those concepts necessary for understanding the methods are covered and only the most practical and currently used procedures are outlined. References are made to many books and articles which cover the technical details and theories associated with each subject discussed.

1.2 Material Included in Book

The earlier chapters contain the background material needed for understanding the methods employed and the physical principles involved. The later chapters include applications of the methods to the analysis of airplanes (missiles) and helicopters. The final chapters cover the use of automatic computers in solving the equations as well as flight test analysis methods relative to aeroelastic analyses.

CHAPTER II

BASIC CONCEPTS

2.0 Introduction

The proper assessment of aeroelasticity is facilitated by the introduction of dimensionless parameters, which, in the absence of additional dynamic effects, provide some measure of the elastic deflection due to a given aerodynamic load as compared with the displacement of the rigid airframe required to produce this load. However, then dynamic effects are associated with elastic deflections, consideration required the introduction of additional parameters based on the relative time scale of the motions, both with respect to the motion of the airframe itself and also to the disturbances set up in the air. The first class of parameters may be termed "static aeroelastic", while the term "frequency parameters" provides an adequate description of the second class.

2.1 Descriptions of Parameters

2.1.1 Static Aeroelastic Parameters. As a first example of an aeroelastic parameter the ratio of airspeed to torsional divergence speed may be cited. The torsional divergence speed is defined as that speed at which the aerodynamic moment about the elastic axis of a wing, due to an incremental twist about this axis, is just equal to moment due to twisting of the structure. It follows from this definition that any initial twist at this critical speed continues to increase until structural failure occurs (or until some equilibrium is reached by virtue of nonlinear effect). In any practical design, attainable flight speeds must be well below the divergence speed; however, the importance of torsional deflection of the wing may be inferred from the ratio of the actual speed to the divergence speed, and the latter therefore appears as an important design parameter (see section 2.2.1 for further details).

A second aeroelastic parameter of considerable importance is the ratio of flight speed to the aileron reversal speed. The latter is defined as that speed at which the adverse rolling moment due to the structural deformation associated with aileron deflection just cancels the favorable rolling moment produced by the ailerons. Again, a satisfactory design must never achieve this speed, but aileron effectiveness falls off rapidly as it is approached, and therefore the ratio of actual airspeed to reversal speed serves as a significant measure of this important aspect of aeroelasticity.

The existence of a sharply defined parameter in the two examples just cited was associated with the hypothetical occurrence of a catastrophic event, but there are equally important examples in which the measure of significance of an elastic deflection is indicated by some arbitrarily defined ratio of an aeroelastic airframe parameter to a corresponding rigid airframe parameter. For example, fuselage bending always is in a direction to relieve the load on the tail, and to reduce elevator effectiveness; and the bending is proportional

to net tail load. It is therefore appropriate to introduce an airspeed at which fuselage bending reduces elevator effectiveness by some arbitrary amount, say 50 percent.

2.1.2 Frequency Parameters. Aeroelastic parameters such as the foregoing serve to measure the possible magnitude of aeroelastic effects and are adequate for essentially static considerations (e.g., the calculation of static margin or available rate of roll). For dynamic considerations, on the other hand, it is necessary to establish some measure of the time lag between the application of load to the structure and the subsequent structural deflection, this time lag being a consequence of the mechanical inertia of the structure itself. In addition, there generally will exist a first order aerodynamic lag between this deflection and the accession of the aerodynamic load.

In dynamic stability calculations an appropriate measure of mechanical time lag is the ratio of the period of the mode of structural deformation (e.g., wing bending) to that of the rigid body mode under consideration (e.g., phugoid- or short period, longitudinal motions) or, equivalently, the inverse ratio of frequencies (or better, the inverse squares of these frequencies, since dynamic coupling is of this order). If the frequency of an elastic mode of vibration is much in excess of the highest frequency of a rigid body mode with which it might couple, the elastic deflections of the airframe may be assumed to be in phase with the corresponding motion of the airplane as a whole, even though it may be necessary to correct the aerodynamic forces on the airplane for these deflections. If, on the other hand, these two frequencies are proximate,* there will be significant differences in phase between the motions of the various parts of the airframe, and it becomes imperative to introduce an additional degree of freedom for the elastic mode of motion.

The mixing of rigid body and elastic modes tends to blur the conventional line of demarcation between the field of dynamic stability and control and that of flutter; ultimately, it appears that the two may be distinguished, if at all, only by the purpose of the particular investigation rather than the types of motion involved. Thus, the subject of dynamic stability and control is concerned primarily with the motion of the airplane as a whole, particularly in response to a prescribed excitation (e.g., a gust or a control surface deflection). Flutter, on the other hand, is concerned primarily with the possibility of self-excited oscillations of particular parts of the airframe, usually involving coupling between two or more elastic modes, in consequence of a motion that extracts energy from the surrounding airflow. In this respect, it should be remarked that the flutter analyst has found it necessary to incorporate certain rigid body motions in

* A rule-of-thumb generally applied is that if one natural frequency is within a factor of three of the other, then a coupling effect may be evidenced; for under the square-law coupling, one is roughly ten percent affected by the other.

his formulation of the flutter problem, so that it should not be surprising to discover a reciprocal obligation on the part of the dynamic stability analyst.

Turning to the question of aerodynamic lag or unsteady flow effects, the parameter most commonly introduced is the "reduced frequency":

$$K = \frac{\omega L}{U} = \frac{(\text{angular frequency}) (\text{characteristic length})}{(\text{flight velocity})} \quad (2-1)$$

The frequency to be used in calculating K is that of the mode responsible for the aeroelastic forces in question. The characteristic length usually chosen is the wing semi-chord, but in dealing with downwash effects the distance between wing and tail is more significant, with correspondingly larger effective values of K. In most dynamic stability calculations, K is found to be quite small in connection with wing-tail downwash effects. Accordingly, with this single exception, it has been customary to neglect aerodynamic lag in the calculation of the stability derivatives. When dealing with conventional aircraft this proves to be an adequate approximation, but it may not be so for high speed aircraft and for less conventional configurations such as flying wings, helicopters or missiles. Nevertheless, K almost always will be sufficiently small in dynamic stability studies to justify neglecting terms of order K^2 in the aerodynamic calculation. In studying the dynamic transfer function of the control surface, servo-tab, etc., it may become necessary to consider higher order terms in reduced frequency.

2.1.3 Structural Damping. A third type of time lag in aeroelastic calculations is associated with structural hysteresis, also known as "structural damping". While the structural damping forces often are of decisive importance in flutter calculations, they usually are negligible compared with the much larger aerodynamic damping forces that are associated with the rigid body motions of the aircraft. Accordingly, structural damping will be neglected throughout the following discussion.

2.2 Static Aeroelastic Effects

It has been pointed out in Section 2.1.1 that static aeroelastic effects are characterized by certain aeroelastic parameters, such as the torsional divergence speed. The more important of these now will be considered on the basis of simplified models, after which the transition to actual configurations may be made by reference to the literature.

2.2.1 Torsional Deflection and Divergence. Consider the two-dimensional model of a wing shown in Figure 2-1. If the wing is rotated initially to an angle of attack α_0 , a lift force L arises, generally forward (a distance ec, where c is the chord) of the elastic axis.

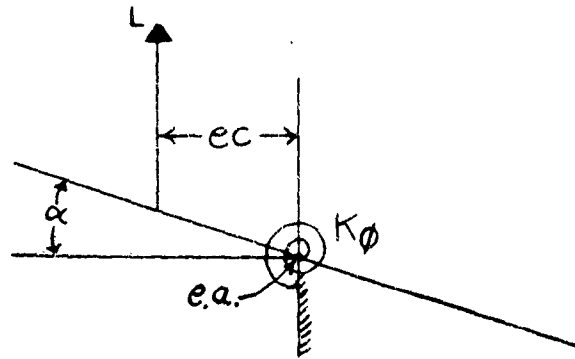


Figure 2-1. A Two Dimensional Wing Having a Torsional Stiffness

The resulting moment produces a twist ϕ and the total angle of attack is given by

$$\alpha = \alpha_0 + \phi \quad (2-2)$$

The system will be in static equilibrium when the total aerodynamic moment (M_α) is just balanced by the torsional moment ($K_\phi \phi$) produced by the twist ϕ ; thus,

$$K_\phi \phi = M_\alpha (\alpha_0 + \phi) \quad (2-3)$$

Where M_α and K_ϕ are, respectively, the pitching moment due to angle of attack and aeroelastic torsional moduli (per radian). Solving (2-2) and (2-3) for ϕ and α yields

$$\phi = \left[\frac{M_\alpha / K_\phi}{1 - (M_\alpha / K_\phi)} \right] \alpha_0 \quad (2-4a)$$

$$\alpha = \left[\frac{1}{1 - (M_\alpha / K_\phi)} \right] \alpha_0 \quad (2-4b)$$

In terms of the dynamic pressure q , the wing area S , the lift curve slope $a = dC_L / d\alpha$ and the moment arm ec , M_α is given by

$$M_\alpha = ec L_\alpha = ecq S a \quad (2-5)$$

As for K_ϕ , if the wing were a uniform, cantilever beam of length $b/2$ * and of uniform torsional modulus GJ , the ratio of applied (tip) moment to tip deflection (in radians) would be given by (section 4.1.4.2):

$$K_\phi = 2GJ/b \quad (2-6)$$

The quotient M_α / K_ϕ then would be

$$(M_\alpha / K_\phi) = becq Sa / 2GJ = eq S^2 a / 2GJ \quad (2-7)$$

where bc has been replaced by S .

It is evident that ϕ becomes infinite (wing divergence) when $M_\alpha = K_\phi$ or, equivalently, when q attains that critical value, say q_d , at which the right hand side of (2-7) becomes equal to one. Moreover, it is evident from dimensional considerations that the departure of a real wing from the above simplified model may be taken into account by the introduction of a suitable constant, which may be determined either by a more refined analysis or by semi-empirical means. Accordingly, the divergence value of the dynamic pressure may be placed in the form

$$q_d = A(GJ/eaS^2) \quad (2-8)$$

where GJ is the section modulus at some reference station (usually the wing root), and e is an appropriately averaged value of the "eccentricity", i.e., the average distance of the line of aerodynamic centers forward of the elastic axis, divided by the average wing chord.

In terms of the parameter q_d the ratio of total angle of attack α to

* $b/2$ is the half-span of the wing

that which would exist for an infinitely stiff wing, viz., α_0 , as given by (2-4b), becomes (noting that q is proportional to the square of the flight speed*)

$$\frac{\alpha}{\alpha_0} = \frac{1}{1 - (q/q_d)} = \frac{1}{1 - (U/U_d)^2} \quad (2-9)$$

The comparison with the amplification factor of a single degree of freedom oscillator is immediately evident, the divergence speed (U_d) being analogous to the resonant frequency. The effective amplification of α predicted by (2-9) is equivalent to an amplification of the lift curve slope with respect to the root section incidence α_0 . This may represent an adverse effect in respect to gust loading and also may promote tip stall.

A fairly extensive analysis¹ of straight, tapered wings, based on a variational method and including aerodynamic induction effects, reveals that an adequate approximation to q_d (within 3 percent of the exact value for ratios of tip chord to root chord less than 0.65) for wings of uniform structure (so that $(G \cdot J)$ varies as the fourth power of the wing chord) is provided by substituting the three-dimensional lift curve slope C_{L_α} for a in (2-8)

$$q_d = 64(GJ)_{\text{root}} / 9eC_{L_\alpha} S^2 \quad (2-10)$$

The result (2-9) is less readily generalized, but, as it stands, gives a rough approximation to the ratio of effective (i.e., averaged over elastic wing) to root section values of the angles of attack. In addition, the right hand side of (2-9) is representative of the increase of the roll damping coefficient (C_{l_p}) for an elastic wing relative to the corresponding rigid wing value. In dealing with antisymmetric loading, however, the lift curve slope (a) should be calculated for half the wing, i.e., half the true aspect ratio should be used in correcting for induction effects.

2.2.2 Control Surface Effectiveness and Reversal. A second basic aero-elastic phenomenon is the reduction of control surface effectiveness due to twist of the wing (or tail). Consider the model of Figure 2-1 modified by the addition of an aileron (or elevator), as shown in Figure 2-2. An initial rotation of the aileron (δ , positive down) will produce two types of

* It should be noted that q_d is not entirely independent of flight speed in consequence of the dependence of the lift curve slope a and eccentricity e on Mach number and, less importantly, the variation of load distribution, and therefore A , with speed.

elastic deflection. First, the lift associated with this initial deflection, acting aft of the elastic axis (Figure 2-2a) for normal configurations, produces a nose down twist ($-\phi$) of the wing, resulting in an adverse increment of lift due to decrease of angle of attack. Secondly, the aileron hinge moment (M_h) will tend to restore the aileron to its neutral position, thereby reducing its effectiveness. However, if the aileron were to be aerodynamically over-balanced (Figure 2-2b), the opposite effect would be experienced, and "aileron divergence" could occur, (the aileron hinge moment still being negative).

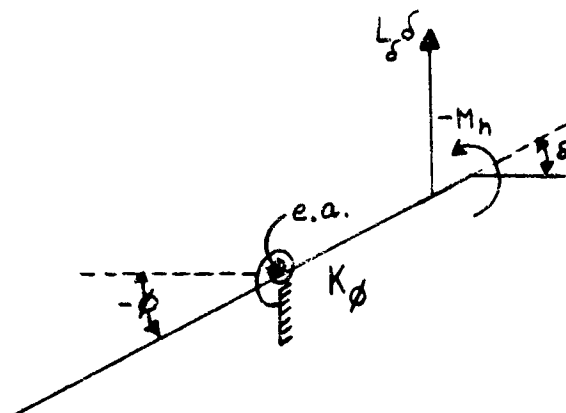


Figure 2-2a. Lift Due to Control Surface Deflection.

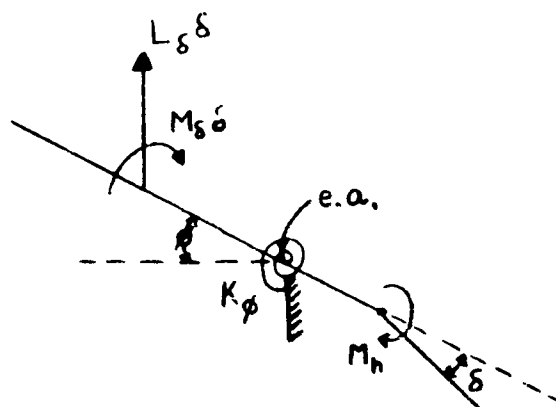


Figure 2-2b. Moment Due to Control Surface Deflection.

In modern aircraft having irreversible, direct actuators the hinge moment effect may be neglected, and only the loss of effectiveness due to wing twist need be considered. In addition, it should be remarked that bending of a swept wing also contributes to reduction of control surface effectiveness in consequence of the reduction of effective angle of attack.

Let ϕ be the increment of wing twist due to the control surface deflection δ . Then the equation of elastic equilibrium, obtained by taking moments about the elastic axis and subtracting $(M_{\alpha})_0$ is

$$K_{\phi} \phi_{\delta} = M_{\alpha} \phi_{\delta} + M_{\delta} \delta + ec L_{\delta} \delta \quad (2-11)$$

where M_{α} and K_{ϕ} are defined in the preceding section 2.2.1 and M_{δ} and L_{δ} ** are the control surface moment and lift moduli, referred to the elastic axis. In terms of the control surface lift and moment coefficients $C_{l_{\delta}}$ * and $C_{m_{\delta}}$, M_{δ} and L_{δ} are given by

$$M_{\delta} = q S c C_{m_{\delta}} \quad (2-12a)$$

$$L_{\delta} = q S C_{l_{\delta}} \quad (2-12b)$$

It again should be emphasized that the total control surface moment about the elastic axis usually is negative for practical ailerons, viz.,

$$M_{\delta} \delta + ec L_{\delta} \delta < 0 \quad (2-13a)$$

$$C_{m_{\delta}} + ec C_{l_{\delta}} < 0 \quad (2-13b)$$

although positive values of this combination may characterize exceptional elevator configurations.

The control surface effectiveness factor, here defined as the ratio of actual section lift to that which would exist in the absence of elastic deflection, is given by

$$\frac{L_{\delta}}{(L_{\delta})_0} = \frac{C_{l_{\delta}} \delta + a \phi_{\delta}}{C_{l_{\delta}} \delta} = 1 + \left(\frac{a \phi_{\delta}}{C_{l_{\delta}} \delta} \right) \quad (2-14)$$

* The small "l" in the sectional lift coefficient, $C_{l_{\delta}}$, is customarily used and still implies a lift effect ($C_{L_{\delta}}$ is the "overall" lift coefficient). This is not to be confused with the rolling coefficient C_{l_p} .

** The elevator contributions are computed for the same eccentricity as the angle of attack contributions.

Solving (2-11) for ϕ yields

$$\phi_s = \left(\frac{M_s + ec L_s}{K_\phi - M_\alpha} \right) \delta \quad (2-15)$$

and (2-14) becomes

$$\frac{L_s}{(L_s)_0} = \frac{1 - M_\alpha / K_\phi + (M_s + ec L_s)(a / K_\phi c l_s)}{1 - M_\alpha / K_\phi} \quad (2-16)$$

It is evident, since M_α , M_s and L_s all are proportional to the dynamic pressure q , that there must exist not only the previously calculated divergence speed at which the denominator of (2-16) vanishes, but also a reversal speed at which the numerator vanishes. Moreover, due to (2-13), this reversal speed usually must be less than the divergence speed. The dynamic pressure for divergence remains as defined by Equation (2-7) and (2-8),

$$\frac{M_\alpha}{K_\phi} = \frac{q}{q_d} \quad (2-17)$$

while that for reversal is defined by

$$\frac{M_\alpha - (M_s + ec L_s)(a / c l_s)}{K_\phi} = \frac{q}{q_r} \quad (2-18)$$

so that (2-16) may be placed in the form

$$\frac{L_s}{(L_s)_0} = \frac{1 - (q / q_r)}{1 - (q / q_d)} \quad (2-19)$$

Substituting M_α , K_ϕ , M_s and L_s in (2-18) from (2-5) and (2-6), and (2-12a,b) above, solving for q_r , and multiplying by a correction factor B to account for three dimensional effects yields

$$q_r = B(GJ/S^2 X c l_s / -a c m_s) \quad (2-20)$$

Since the constant B depends on the ratio of control surface span to wing span, as well as wing taper and aspect ratios, it is not possible to assign it a universal value. An extensive numerical analysis is given in ref. 1, and it is found convenient to re-express q_r as follows:

$$q_r = A_\delta (G J)_{root} / e c_{l_\alpha} S^2 \quad (2-21)$$

where c_{l_α} is the section (two-dimensional) lift curve slope, and the factor A_δ depends on stiffness distribution, taper ratio, aspect ratio, control surface span to wing span ratio, and, most importantly, on the quantity:

$$\Gamma_\delta = 1 + (c_{m_\delta} / e c_{l_\delta}) \quad (2-22)$$

The dependence of A_δ on Γ_δ for a wing of 2:1 taper, aspect ratio 6, and 30 percent span ailerons is plotted in Figure (2-3). This curve also furnishes a reasonable approximation of other, practical values of taper, aspect and span ratios (see ref. 1 for details). Using NACA test data², the parameter Γ_δ is plotted vs. chord ratio and the product of eccentricity and section lift curve slope in Figure (2-4).

Having q_d and q_r , the control surface effectiveness factor for a three-dimensional wing (or tail) may be computed from (2-19). In this connection it should be made clear that the three-dimensional lift curve slope C_{L_α} is to be used in computing q_d , from equation (2-10), whereas the two-dimensional value c_{l_α} is to be used in computing q_r from (2-21) and (2-22).* Moreover, as mentioned previously, in estimating rolling power, the value of C_{L_α} used in q_d should be calculated on the basis of one half of the aspect ratio for the complete wing, whereas in elevator (or elevon) calculations the full aspect ratio of the tail should be used.

Perhaps more important than the actual rolling moment produced by a given aileron deflection is the resulting rate of roll. It is found (cf. section 2.2.1) that the roll damping coefficient** of a straight wing is increased approximately in the ratio

$$\frac{C_{l_p}}{(C_{l_p})_0} = \frac{1}{1 - (q/q_d)} \quad (2-23)$$

* This is an empirical conclusion based on the analysis of Ref. 1.

** C_{l_p} is to be distinguished from c_{l_α} and c_{l_δ} which are sectional lift coefficients.

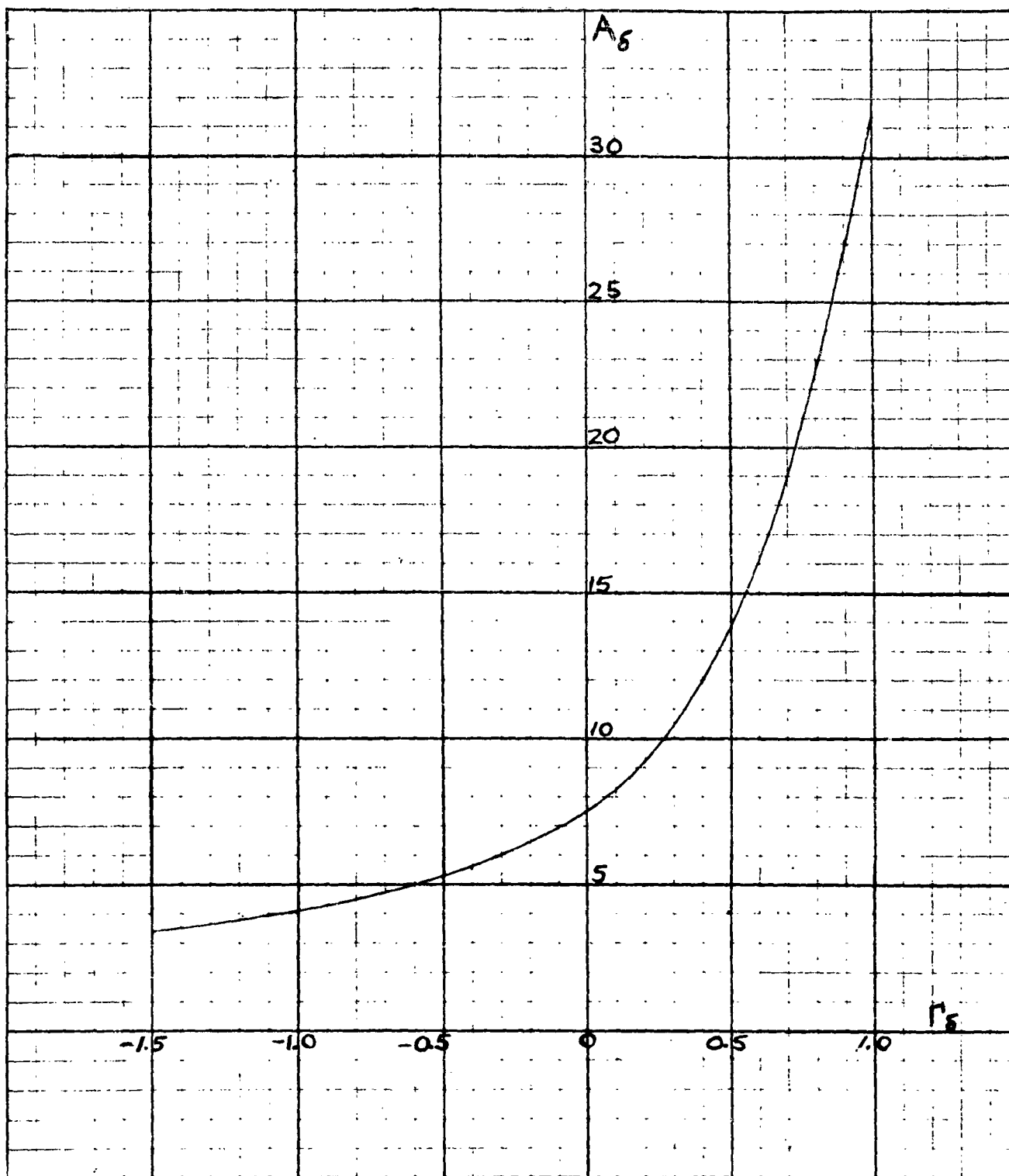


Figure 2-3. Factor A_δ Defined by Equation (2-21)

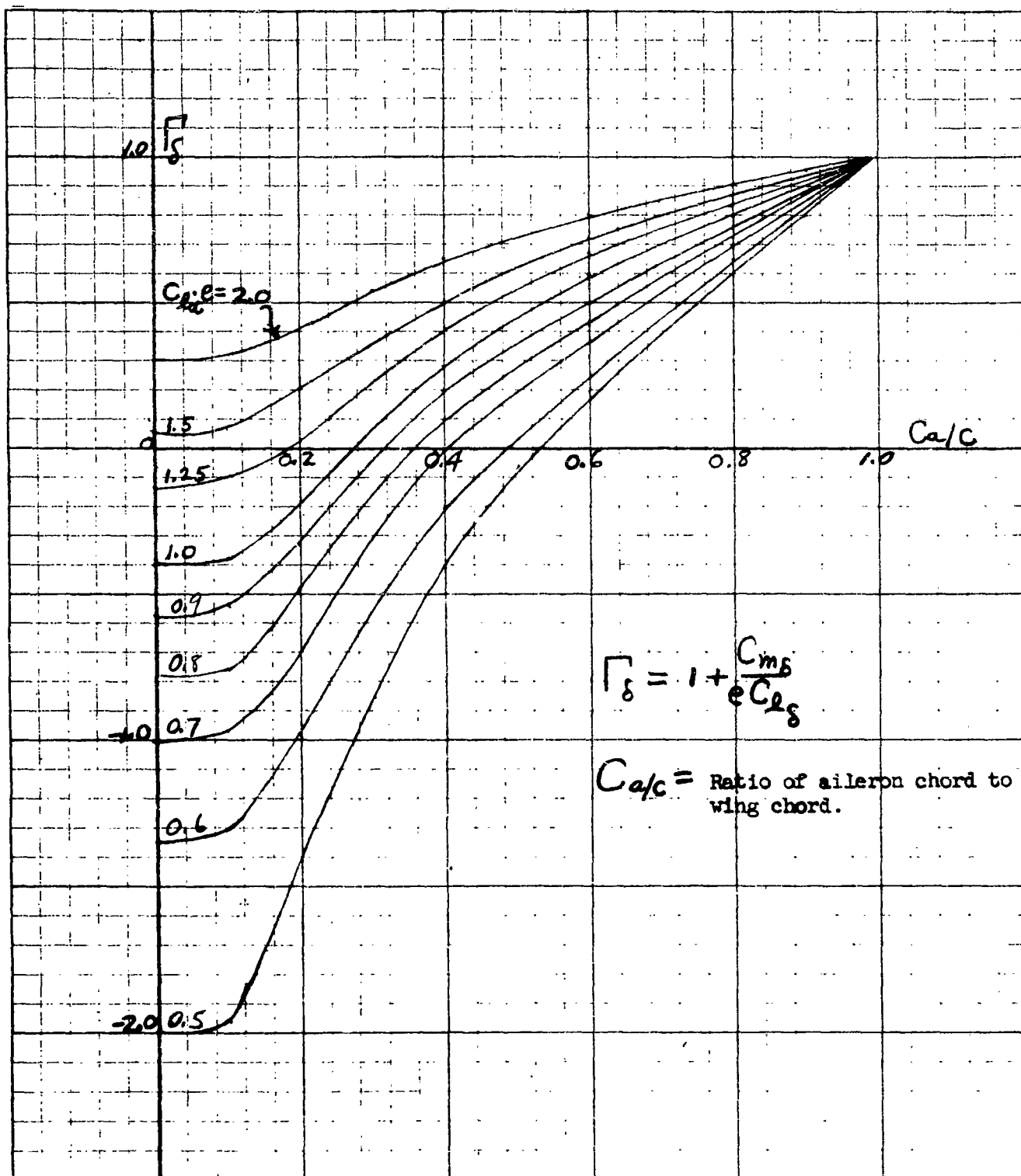


Figure 2-4. Control Surface Parameter Defined by (2-22)

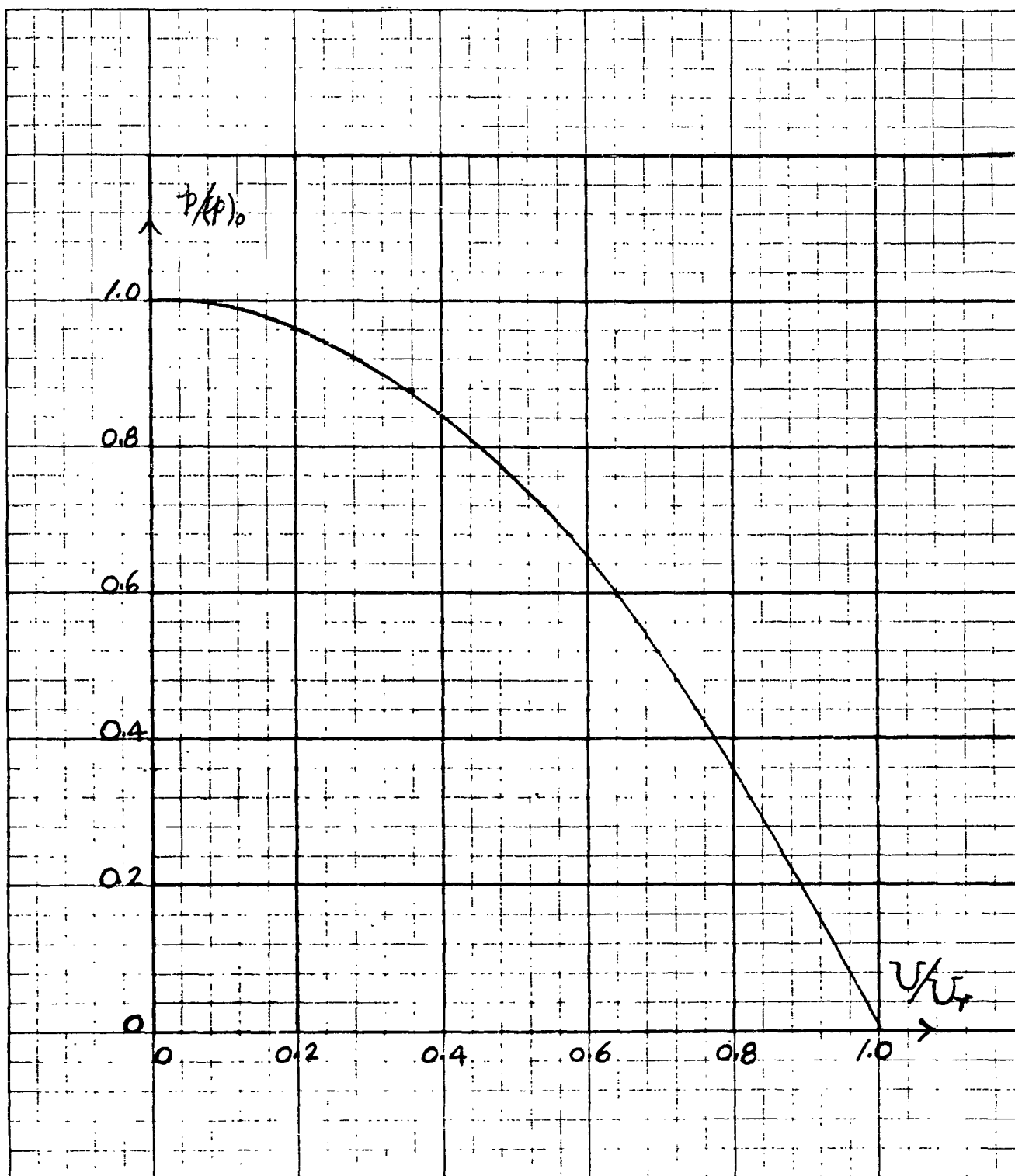


Figure 2-5. Rolling Effectiveness with Speed Given by Equation (2-24)

The corresponding reduction factor for available rate of roll using (2-9), then is given by

$$\frac{p}{(p)_0} = \frac{C_{ls}/(C_{ls})_0}{C_{lp}/(C_{lp})_0} = 1 - (q/q_r) \quad (2-24)$$

Therefore the variation of rolling effectiveness with speed is parabolic, as shown in Figure 2-5. It is evident that the reversal speed cannot be approached too closely without accepting a severe loss in rolling effectiveness (50 percent at $U = 0.7 U_r$).

The decisive factor in setting the allowable reversal speed for the elevator is not the available rate of pitch, but either loss of static margin or the possibility of tailplane failure in consequence of the very large elastic deflections that may arise. Elastic deflections of the tail usually are far more serious (in the structural sense) than those of the wing, due to the larger elevator to horizontal tail (span and chord) ratios of typical elevators and the relatively small torsional structure of the fixed tailplane (as contrasted with the wing).

2.2.3 Fuselage Bending. A third example of a basic aeroelastic effect is fuselage bending. In many designs this may be the dominant factor in determining the effectiveness of both the horizontal and vertical tail surfaces, particularly the latter, since the lateral fuselage stiffness can be quite low.

Let K_f be a stiffness constant defined such that a load L_t applied to the fuselage at the tailplane attachment produces a rotation

$$\theta_f = \frac{L_t}{K_f} \quad (2-25)$$

as shown in Figure 2-6 (note that θ_f constitutes a negative incidence).

Then if L_{α_t} is the tail lift due to tail angle of attack and α_{t_0} the effective angle of attack at the tail in the absence of fuselage deflection, the equation of elastic equilibrium must be

$$L_t = K_f \theta_f = L_{\alpha_t} (\alpha_{t_0} - \theta_f) \quad (2-26)$$

The reduction in tail effectiveness due to fuselage bending is given by

$$\frac{L_t}{(L_t)_0} = \frac{\alpha_{t_0} - \theta_f}{\alpha_{t_0}} \quad (2-27)$$

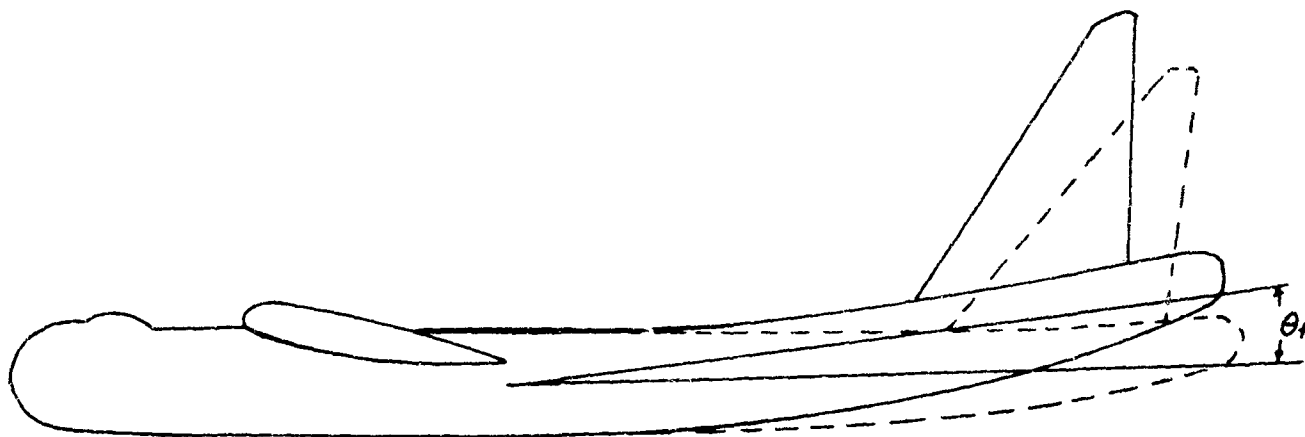


Figure 2-6. Tail Plane Rotation θ_f Produced by Tail Load L_t

Solving (2-26) for θ_f and substituting in (2-27) yields

$$\frac{L_t}{(L_t)_0} = \frac{1}{1 + (L_{\alpha_t}/K_f)} \quad (2-28)$$

or, more conveniently

$$\frac{L_t}{(L_t)_0} = \frac{1}{1 + (q/q_f)} \quad (2-29)$$

where the parameter q_f represents that value of the dynamic pressure at which fuselage bending causes a 50 percent reduction in tail effectiveness. Comparing (2-29) to (2-28) and writing

$$L_{\alpha_t} = q S_t C_{L_{\alpha_t}} \quad (2-30)$$

where S_t and $C_{L_{\alpha_t}}$ represent tail area and lift (coefficient) curve slope, q_f is given by

$$q_f = K_f q / L_{\alpha_t} = K_f / S_t C_{L_{\alpha_t}} \quad (2-31)$$

It is not practical to give a simple formula for K_f due to the wide variations that occur in fuselage design, but it may be noted that

$$K_f \sim EI_f / l_f^2 \quad (2-32)$$

where E is Young's modulus for the fuselage structure, I_f its cross-sectional moments of inertia, and l_f a representative fuselage length; (e.g., distance from c.g. to tail, l_t) therefore

$$q_f \sim EI_f / l_f^2 S_t C_{L_{\alpha_t}} \quad (2-33)$$

It should be remarked that fuselage bending of itself, tending only to relieve the applied load, can have but little effect on either the divergence or the reversal speeds for the tail. Moreover, torsional deflection of the horizontal tail partially compensate for the reduction in horizontal stabilizer effectiveness due to vertical fuselage bending. Likewise, torsional

deflection of the vertical tail partially compensates for the reduction in vertical stabilizer effectiveness due to sidewise fuselage bending. On the other hand, elevator effectiveness is reduced both by horizontal tail plane torsion and fuselage bending, with the latter effect often the more important.

2.2.4 Swept Wing Deflections. Consider the simplified model of a swept wing shown in Figure 2-7, where x and y constitute a coordinate system oriented by the direction of flight, and x' and y' a coordinate system obtained by rotation of the x and y axes through the sweepback angle Λ . If rotations about these axes are treated as infinitesimals, they may be resolved as vectors according to

$$\theta_x = \theta_{x'} \cos \Lambda + \theta_{y'} \sin \Lambda \quad (2-34a)$$

$$\theta_y = -\theta_{x'} \sin \Lambda + \theta_{y'} \cos \Lambda \quad (2-34b)$$

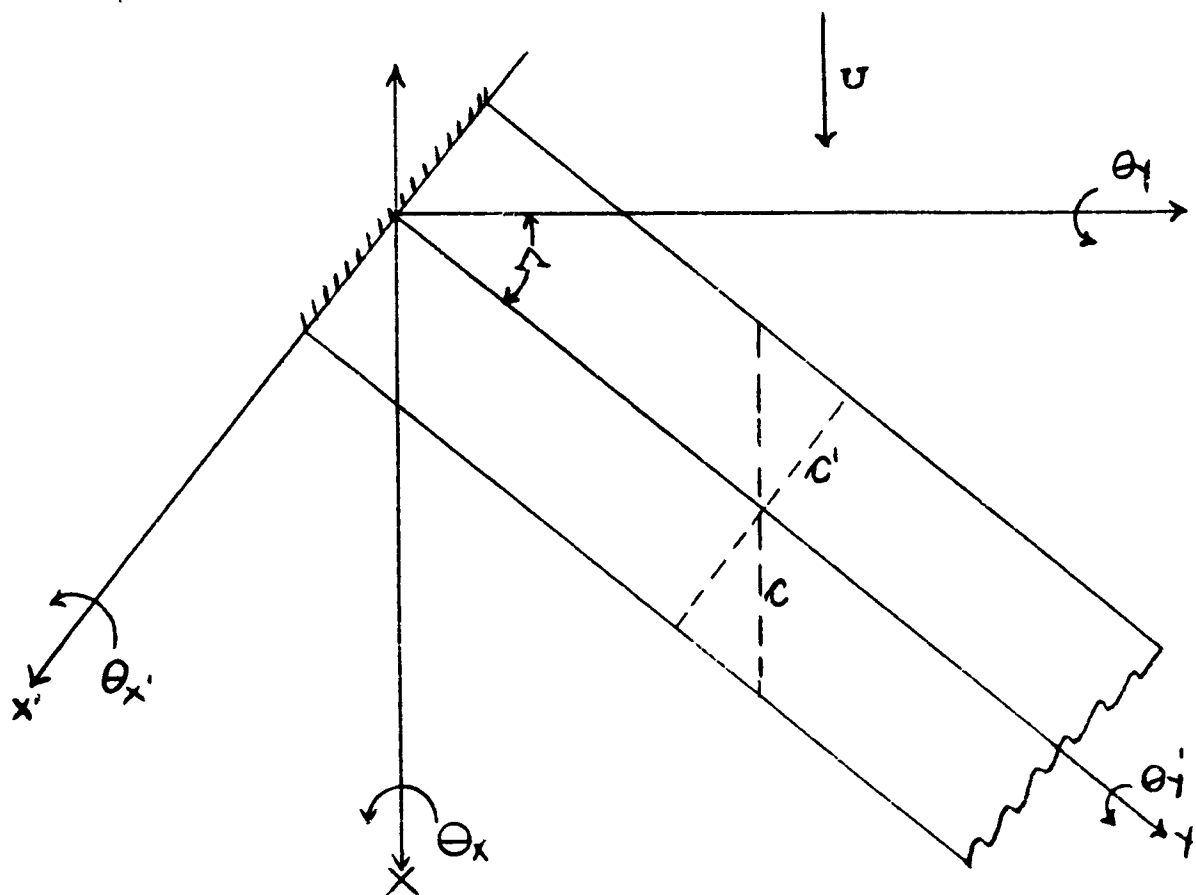


Figure 2-7. A Swept Wing of Constant Chord

The actual bending deflection of the wing of course depends upon the lift distribution, but for the present simplified study it suffices to consider the single chordwise section shown as c' in Figure 2-7. The wing bending slope ψ at this section due to a lift l' per unit span can then be calculated by the introduction of a stiffness coefficient K_b , defined such that

$$K_b \psi = l' = c' q a' \alpha \quad (2-35)$$

where q is the dynamic pressure of the free stream, a' a lift curve (coefficient) slope appropriately corrected for sweepback, and α the effective angle of attack measured as a rotation about the y axis. The elastic contributions to the total angular rotation then are $\theta_{x'} = \psi$ and $\theta_{y'} = 0$ (torsion would give a $\theta_{y'}$ component), and the additional angle of attack due to bending is given by the first term of (2-34b) as $-\psi \sin \Lambda$. Thus, if α_0 is the rigid wing angle of attack, the effective angle of attack of the elastically deflected wing is given by

$$\alpha = \alpha_0 - \psi \sin \Lambda \quad (2-36)$$

Solving (2-35) and (2-36) for α yields

$$\alpha = \left[\frac{1}{1 + (q c' a' \sin \Lambda / K_b)} \right] \alpha_0 \quad (2-37)$$

In applying the result (2-37) to a three-dimensional wing of span b (measured from wing tip to wing tip, i.e., along the y axis), it may be deduced from elementary beam theory that the influence coefficient K_b must be proportional to the section bending modulus EI and inversely proportional to the cube of the beam length $1/2 b \sec \Lambda$. Thus following the analyses of the preceding sections, (2-37) may be recast in the form

$$\alpha = \left[\frac{1}{1 + (q / q_b)} \right] \alpha_0 \quad (2-38)$$

where

$$q_b = K_b / c' a' \sin \Lambda \quad (2-39a)$$

$$\sim E I / c' a' \sin \Lambda (b \sec \Lambda)^3 \quad (2-39b)$$

$$= C E I / a' S^2 A \sec^2 \Lambda \sin \Lambda \quad (2-39c)$$

where C is an as yet undetermined constant that includes the effects of distributed load, taper ratio, varying stiffness, etc.; S is the wing area (proportional to $b c' \sec \Lambda = b c$); and A is the aspect ratio based on the aerodynamic span b (as opposed to the "structural span" $b \sec \Lambda$); viz.,

$$A = b^2 / S \quad (2-40)$$

If the structural or "panel aspect ratio" is introduced according to

$$A' = (b \sec \Lambda)^2 / S = A \sec^2 \Lambda \quad (2-41)$$

(2-39c) becomes

$$q_b = C E I / a' S^2 A' \sin \Lambda \quad (2-42)$$

In calculating the parameter q_b for an actual wing the section lift curve slope a' may be replaced by the mean lift curve slope $C_{L\alpha}^*$ and Λ taken as the average sweepback angle of the elastic axis. The constant C is more difficult to calculate than its counterpart A in the torsional problem of section 2.2.1. However, if a tapered wing is approximated by a cantilever beam having a straight elastic axis and bending about a virtual root chord transverse to this axis (see section 4.2.3.6 for a more detailed discussion of the actual deformation of swept wings), and if the stiffness is assumed to vary as the fourth power of the chord, and EI is taken as the root section (perpendicular to the elastic axis) stiffness; and if aerodynamic strip theory is used in calculating the aerodynamic forces (an approximate value for C is 45); then (2-39c) becomes

* $C_{L\alpha}$ is based on c rather than c' , and is the usual three dimensional lift curve slope.

$$q_b = 45(EI)_{\text{ROOT}} \cos^2 \Lambda / C_{L\alpha} A S^2 \sin \Lambda \quad (2-43)$$

In order to compare the effects of bending with those of torsion, it may be noted that the contribution of a torsional rotation of a swept wing to effective angle of attack is reduced by a factor of $\cos \Lambda$ (see eq. 2-34b). Accordingly, if a swept wing were to deflect in pure torsion, the appropriate modification of (2-10) would yield (although the value of $A = 64/9$ would be less reliable)

$$q_d \approx 64(GJ)_{\text{ROOT}} / 9e C_{L\alpha} S^2 \cos \Lambda \quad (2-44)$$

The relative importance of bending and torsion then may be inferred from the ratio

$$\frac{q_b}{q_d} \approx 7 \left(\frac{EI}{GJ} \right)_{\text{ROOT}} \left(\frac{e \cos^3 \Lambda}{A \sin \Lambda} \right) \quad (2-45)$$

Noting that the stiffness ratio EI/GJ will be of the order of unity for practical structures (somewhat large in the presence of cutouts, which reduce GJ more than EI), it is clear that bending of even a moderately swept wing will be much more important than torsion insofar as static aeroelastic effects are concerned. Thus, for a sweepback angle of 45° , aspect ratio 6, and eccentricity 0.15 (subsonic wing with line of aerodynamic centers at 25 percent chord and elastic axis at 40 percent chord) (2-45) yields $q_b \approx q_d/13$.

The predominance of swept back wing bending over torsion implies that the elastic deflection will tend to reduce rather than increase the effective angle of attack. Accordingly, wing divergence disappears (approximately when $q_b = q_d$) as a practical problem, whereas aileron effectiveness is even further reduced (but since the damping in roll also would be reduced, the reduction in available rate of roll may not be greatly different. Conversely, q_b would be negative for sweepforward, whence bending divergence would occur at $q = -q_b$ (see (2-38) above) for a wing infinitely stiff in torsion and at an even lower q in the presence of torsion. The very low divergence speeds that would result, together with the large magnification of gust loading and tip stall problems, virtually rule out the swept forward wing as a practical possibility.

Finally, it should be remarked that bending of a swept back wing, tending

to relieve the outboard (wingtip) load, not only reduces the effective angle of attack but also shifts the center of pressure forward. The resulting loss of static margin, supplemented by an additional loss of margin due to fuselage bending or, in the case of a flying wing, a loss of elevon effectiveness, is probably the most serious of all aeroelastic effects and often must be a dominant factor in designing the wing. Moreover, unless the wing can be designed for some single cruise condition, the redistribution of wing load due to elastic deflection and the much greater range of control surface deflection required to provide for this redistribution may occasion important increases in drag.

2.2.5 Static Aeroelastic Correction of Stability Derivatives. The results of the preceding sections, particularly the expressions for q_d , q_r , q_α and q_β given by equations (2-10), (2-21), (2-31) or (2-33), and (2-43), respectively, render possible a quick appraisal of the over-all importance of aeroelastic effects for conventional aircraft. If the maximum dynamic pressure at which a particular aircraft is intended to operate is found to be comparable in magnitude (say 25 percent or more) with these parameters it then will be necessary to carry out more detailed calculations of the various aerodynamic coefficients for the elastic wing. Extensive charts for the calculation of the static derivatives for straight wings and, assuming that frequency comparisons so permit (cf., section 2.1.2), also the dynamic stability derivatives have been developed in Ref. 1, using lifting line theory. Corresponding charts for swept wings also have been prepared on the basis of an approximate Galerkin type analysis³ using simple beam theory and aerodynamic strip theory⁴. Diederich and Foss^{5, 6} also have contributed graphical data for conventional aircraft which is based upon the assumption of an elastic axis representation for the elastic wing.

The general principles are also discussed in greater detail in references 7 and 8. In addition, references 7 and 8 give a detailed list of references that are itemized according to the subject matter.

2.3 Lift Distribution on an Elastic Wing

The basic problem in static aeroelasticity is the determination of the lift distribution on a swept or unswept elastic wing. Specified for the problem are the wing geometry, structural properties (most conveniently expressed as influence functions), and the rigid-body geometric angle-of-attack distribution which is determined by the attitude of the airplane, the built-in twist, control surfaces deflection, or steady-state motion of the airplane. The wing of course deflects under the aerodynamic load. The final aerodynamic load distribution is to be calculated. From the solution of this basic problem all static aeroelastic characteristics of the wing can be determined, such as the divergence speed, wing deflection and stresses, control surfaces effectiveness, and static aeroelastic correction of the stability derivatives.

It is necessary to be able to determine the spanwise lift distribution for a wing whose elastic deflection were known. The simplest procedure is to use the "strip" assumption, under which the local lift coefficient is proportional to the local angle of attack. The overall effects of aspect ratio, sweep angle, and Mach number are accounted for by an appropriate correction of the lift curve slope. In Section 2.3.1 the lift curve slope corrections are summarized. When a more accurate analysis is desired, a simple empirical method developed by Diederich may be used; this method is described in Section 2.3.2. In Section 2.3.3 the aerodynamic influence coefficients concept is discussed. Finally, in Section 2.3.4, the formulation of the elastic wing problem is discussed and the method of solution is indicated.

The reader is referred to Chapter 5 of Ref. 8 (Bisplinghoff, Aeroelasticity), for detailed presentation of the theory of lift distribution over finite wings and for references to original papers. For charts and tables of calculated spanwise lift distribution covering a wide range of sweep angle, taper ratio, and aspect ratio, see Diederich and Zlotnik, Refs. 9 and 10 Groth, Ref. 18, gives useful graphical data for swept wings.

2.3.1 The Lift Curve Slope

To avoid complicated aeroelastic analyses, the "strip theory" is usually employed. In this theory each chordwise section is supposed to act as if it were in a two-dimensional flow without aerodynamic induction effect, the finite span effect is then partially accounted for by an overall correction of the lift curve slope. This approximation, without aerodynamic induction effect, is a crude one; but is sufficient for certain purposes.

The lift curve slope per radian for a thin airfoil in a two-dimensional incompressible flow will be denoted by a_0 (theoretical value, 2π ; experimental, $2\pi\gamma$, γ generally of order 0.9). The effect of the compressibility of the fluid is expressed in terms of the free-stream Mach number, M .

If $M < 1$, Glauert gives

$$a'_0 = \frac{1}{\sqrt{1-M^2}} a_0 \quad (2\text{-dimensional}) \quad (2-46)$$

where a'_0 is the value of $\partial C_l / \partial \alpha$ for a compressible fluid, and a_0 is that for $M = 0$. The effect of finite span is approximately given by the following formulas:

$$a' = \frac{a'_0}{1 + \frac{a'_0}{\pi R} \frac{1+\tau}{\pi R}} = \frac{a_0}{\sqrt{1-M^2} + \frac{a_0}{\pi R} \frac{1+\tau}{\pi R}} \quad \begin{matrix} \text{(unswept, subsonic,} \\ \text{symmetric loading,} \\ \text{moderate } R) \end{matrix} \quad (2-47)$$

where a' is the lift-curve slope of a wing of finite aspect ratio in a compressible flow, a_0 is the Glauert's correction factor for non elliptic planform. (Fig. 2-8).

For very small R ,

$$a' = \frac{a'_0}{\sqrt{1 + \left(\frac{a'_0}{\pi R}\right)^2} + \frac{a'_0}{\pi R} \frac{1+\tau}{\pi R}} \quad \begin{matrix} \text{(unswept, subsonic,} \\ \text{symmetric loading,} \\ \text{small } R) \end{matrix} \quad (2-48)$$

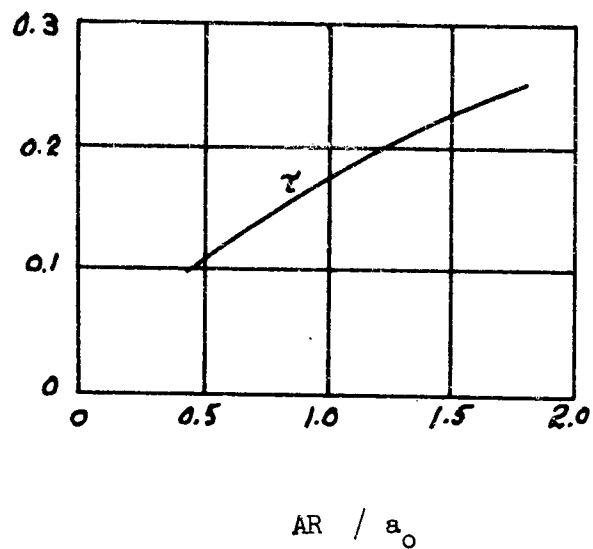
The effect of sweep is incorporated in the following formulas:

$$(a_0)_{\text{swept}} = a_0 \cos \Lambda \quad \begin{matrix} \text{(incompressible,} \\ \text{infinite span,} \\ \text{swept wing)} \end{matrix} \quad (2-49)$$

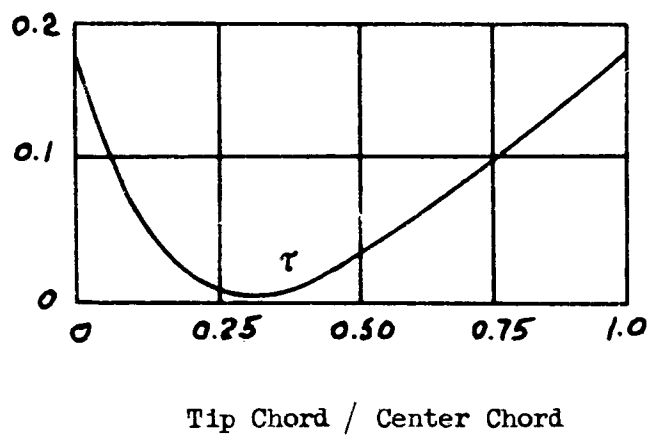
where a_0 is the lift-curve slope of the airfoil section normal to the leading edge.

$$(a'_0)_{\text{swept}} = \frac{a_0 \cos \Lambda}{\sqrt{1 - M^2 \cos^2 \Lambda}} \quad \begin{matrix} \text{(subsonic, infinite} \\ \text{span)} \end{matrix} \quad (2-50)$$

$$a' = \frac{(a'_0)_{\text{swept}}}{\sqrt{1 + \left(\frac{(a'_0)_{\text{swept}}}{\pi R}\right)^2} + \frac{(a'_0)_{\text{swept}}}{\pi R} \frac{1+\tau}{\pi R}} \quad \begin{matrix} \text{(finite } R, \text{ subsonic} \\ \text{symmetric} \\ \text{loading)} \end{matrix} \quad (2-51)$$



(a) Rectangular Planforms



(b) Tapered Planforms with $AR = a_0$

Figure 2-8. Variation of τ with Airfoil Plan-form

where R is the aspect ratio b^2/S , (b = the wing span from tip to tip, S = wing area). If the wing is tapered, the sweep angle Λ should be measured along the 1/4-chord line.

For antisymmetric spanwise lift distribution, the lift curve slope is obtained by replacing R in the above formulas by the effective aspect ratio:

$$R_e = \frac{R}{2} \quad (\text{antisymmetric loading}) \quad (2-52)$$

In the general case the spanwise angle of attack $\alpha(y)$ should be separated into two parts, one symmetric in y and the other antisymmetric in y , ($y = 0$ on the airplane centerline) =

$$\alpha(y) = \alpha_{\text{sym}}(y) + \alpha_{\text{antisym}}(y) \quad (2-53)$$

then one may write

$$C_l(y) = a \alpha_{\text{sym}}(y) + \tilde{a} \alpha_{\text{antisym}}(y) \quad (2-54)$$

where a and \tilde{a} are corrected respectively for R and R_e .

The above formulas are not valid when α is so large as to cause stalling, or when $M > M_{\text{cr}}$, where M_{cr} is the "Mach number of divergence", which is defined as the point of inflection of the curve of C_L vs M . In the transonic range, $M > M_{\text{cr}}$, experimental data should be used as the variation between individual wings becomes difficult to generalize.

In the supersonic flow, $M > 1$, if the free-stream Mach number is sufficiently high, the linearized theory again gives a good approximation. Then the two-dimensional-flow lift curve slope is

$$a'_0 = \frac{4}{\sqrt{M^2 - 1}} \quad \text{2-dim., supersonic} \quad (2-55)$$

and

$$(a'_0)_{\text{swept}} = \frac{4 \cos \Lambda}{\sqrt{M^2 \cos^2 \Lambda - 1}} \quad (\text{supersonic leading edge, } M \cos \Lambda > 1) \quad (2-56)$$

For wings of small aspect ratio, and delta wings, simple strip theory generally does not apply.

2.3.2 Spanwise Lift Distribution at Subsonic Speeds

A simple approximate method for calculating spanwise lift distribution at subsonic speeds, developed by Diederich, (Ref. 11) will be given below. This method is more complicated than the strip theory, but is much simpler than Weissinger's lifting-line theory or Falkner's lifting-surface theory. Its justification is entirely empirical. Numerical examples can be found in the original paper.

Symmetric Lift Distributions

Let the lift distribution be expressed in terms of the loading coefficient γ :

$$\gamma = \frac{c C_l}{c} \quad (2-57)$$

Since, at small angle of attack, γ is a linear function of α , one may write

$$\gamma = \left(\frac{\partial C_l}{\partial \alpha} \right) \bar{\alpha} \gamma_a + \gamma_b \quad (2-58)$$

where $\bar{\alpha}$ = average angle of attack, radians, measured in streamwise direction

γ_a = "additional" lift distribution coefficient

γ_b = "basic" lift distribution coefficient

The integral of γ_a across the span is 1, and that of γ_b is zero.

The lift-curve slope $\partial C_l / \partial \alpha$ is given by formulas of the previous Section. To account for the effect of airfoil thickness empirically, a further refinement is made. This refinement consists of replacing the Glauert correction factor, $\frac{a_o'}{a_o} = \frac{1}{\sqrt{1-M^2}}$, by empirical curves which are functions of airfoil thickness ratios (perpendicular to the 1/4-chord line). The final expression may be written:

$$\frac{\partial C_l}{\partial \alpha} = k_o \left(\frac{a_o'}{a_o} \right) a_o \cos \Lambda \quad (2-59)$$

where

k_o is given in Fig. 2-9, as a function of F -defined below.

(a'_o/a_o) is given in Fig. 2-10.

a_o = lift-curve slope in two-dimensional incompressible flow,
($R = \infty$, $M = 0$) of airfoil section perpendicular to 1/4-chord line.

Λ = angle of sweepback at 1/4-chord line.

The "planform parameter", F , from which k_o is determined, is

$$F = \frac{2 \pi R}{a_o \left(\frac{a'_o}{a_o} \right) \cos \Lambda} \quad (2-60)$$

For very large angles of sweepback ($\Lambda_e > 60^\circ$) another factor k'_o , also shown in Fig. 2-9, should be used instead of k_o .

The additional lift distribution γ_a may be estimated as follows:

$$\gamma_a = C_1 \frac{c}{\bar{c}} + C_2 \frac{1}{\pi} \sqrt{1 - y^{*2}} + C_3 f \quad (2-61)$$

where c = chord, measured parallel to plane of symmetry.

\bar{c} = average chord, S/b

y^* = lateral coordinate/semispan.

f = empirical sweep-correction function, Fig. 2-11.

C_1, C_2, C_3 functions of F , Eq. (2-60) given in Fig. 2-12.

The function f depends on the "effective" angle of sweep Λ_e defined by

$$\Lambda_e = \tan^{-1} \frac{\tan \Lambda}{\sqrt{1 - M^2}} \quad (2-62)$$

The elliptic distribution $\frac{4}{\pi} \sqrt{1 - y^{*2}}$ is also shown in Fig. 2-11 as the value of the function f for $\Lambda_e = 0$.

The basic lift distribution γ_b is given by

$$\gamma_b = k_1 \left(\frac{\partial C_L}{\partial \alpha} \right) (\alpha - \bar{\alpha}) \gamma_a \quad (2-63)$$

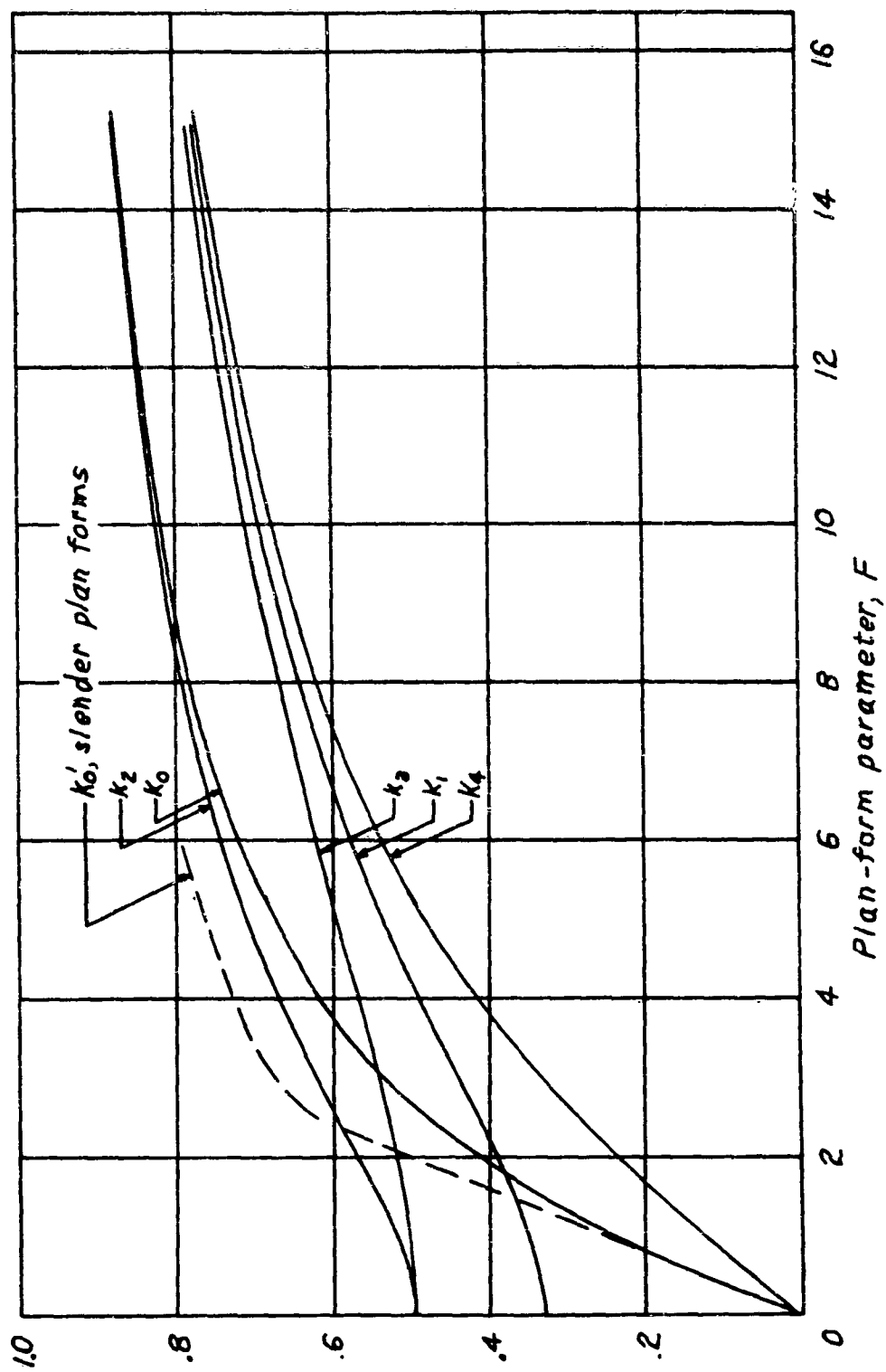


Figure 2-9. Factors k_0 , k_1 , k_2 , k_3 , and k_4 (from NACA TN 2751).

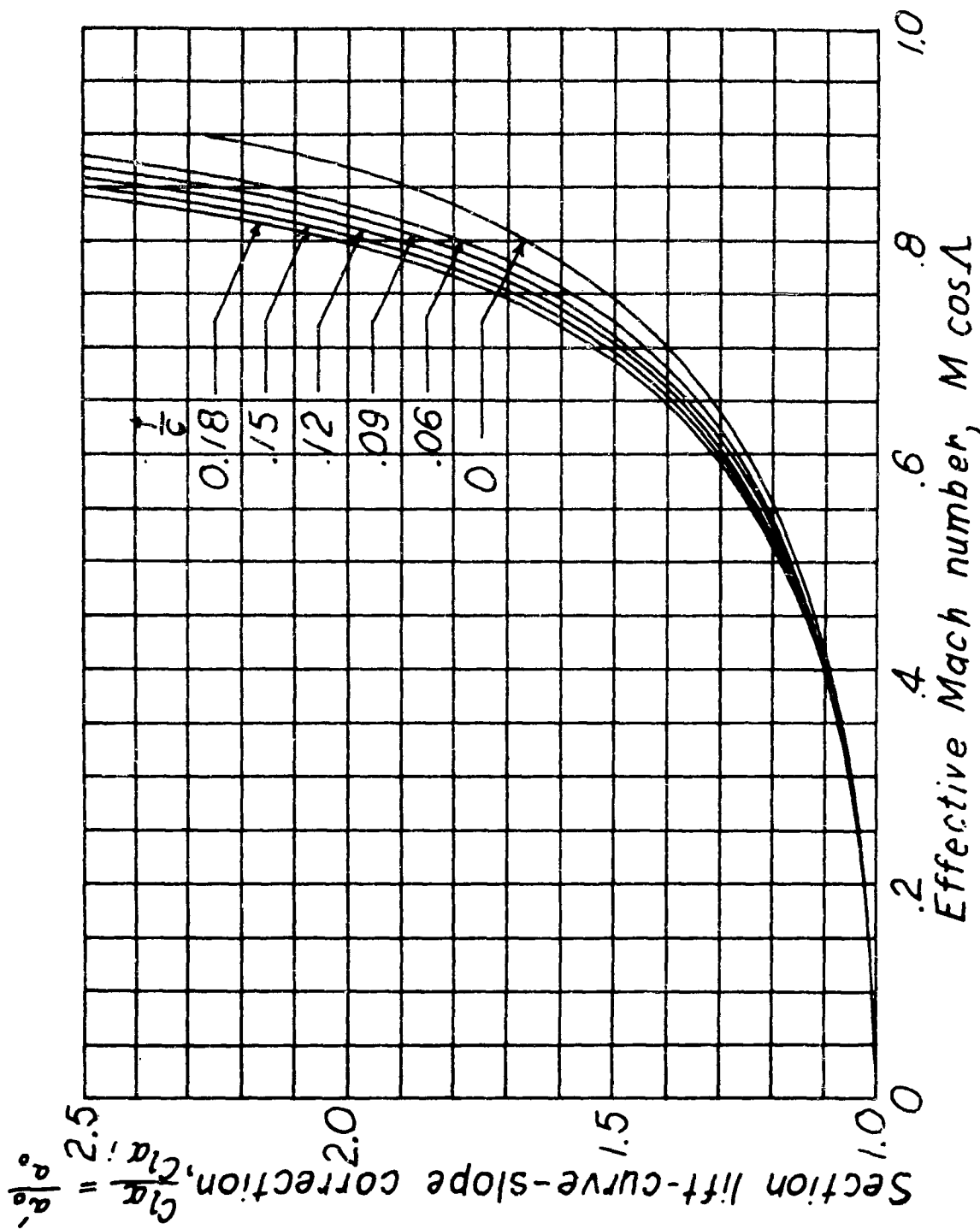


Figure 2-10. Section Lift-Curve-Slope Correction (Plot taken from NACA TN 2751).

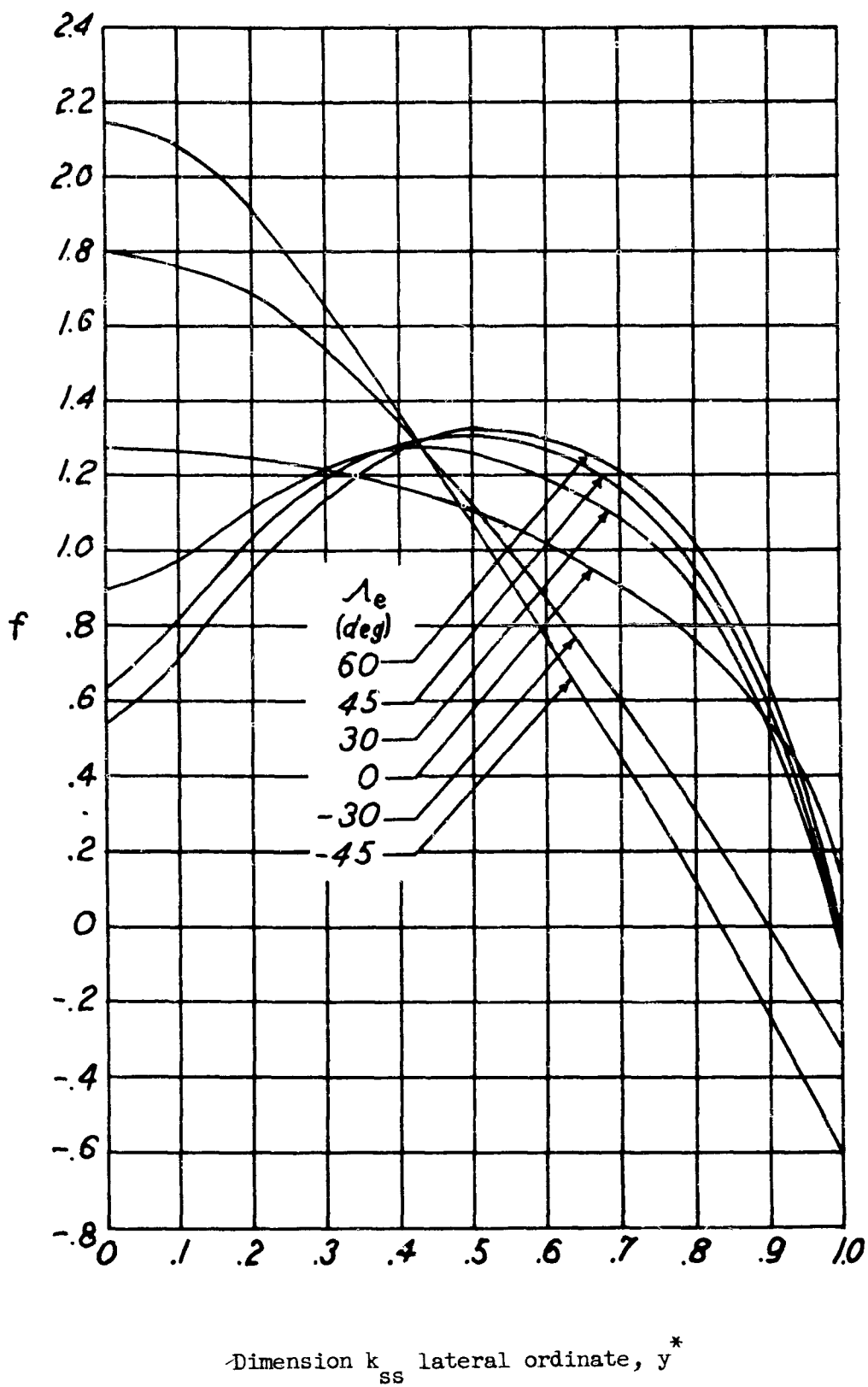


Figure 2-11. The Lift-Distribution Function f (from NACA TN 2751).

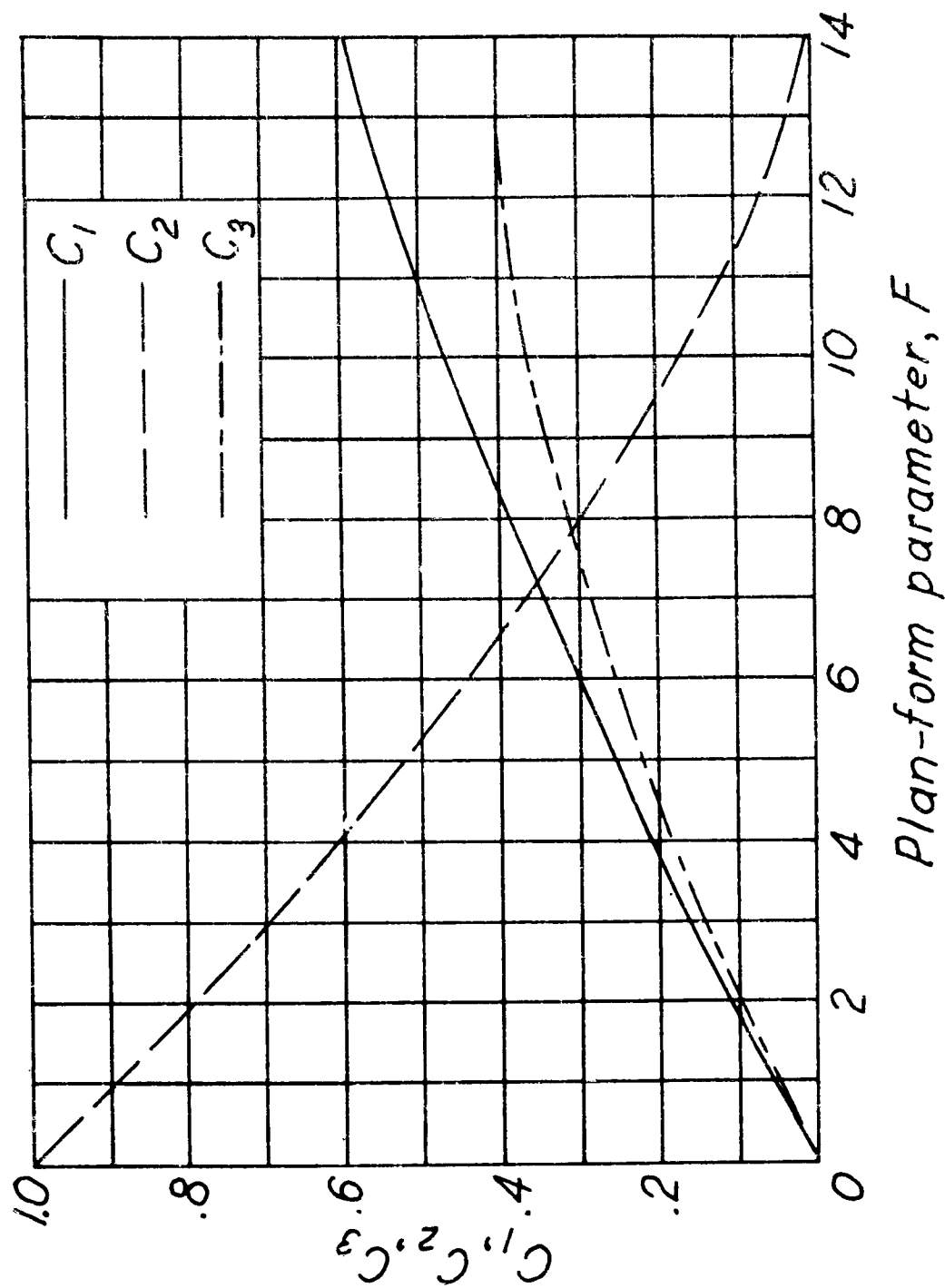


Figure 2-12. The Lift-Distribution Constants C_1 , C_2 , and C_3 (from NACA TN 2751).

where k_L is given in Fig. 2-9 whereas $\partial C_L / \partial \alpha$ and γ_a are given above in Eqs (2-59) and (2-61). The angle-of-attack α is measured in streamwise direction. The average angle of attack is

$$\bar{\alpha} = \int_0^1 \alpha \gamma_a dy^* \quad (2-64)$$

If there are discontinuities in the angle-of-attack distribution, they should be faired before α is used in Eqs. (2-63) and (2-64). Apparently the best results are obtained, on the average, when the fairing extends about 0.3 semispan on either side of the discontinuity and passes through the midpoint of the discontinuity; the faired curve should have the same area as the unfaired one.

Center of Pressure

The lateral coordinate of the center of pressure \bar{y}^* of the additional lift distribution, or of any lift distribution for a constant angle of attack across the span, is numerically equal to the moment about the origin of the function γ_a , since the area under γ_a is 1. Therefore

$$\bar{y}^* = C_1 \int_0^1 \frac{c}{c} \gamma^* dy^* + C_2 \frac{4}{3\pi} + C_3 J \quad (2-65)$$

where J is the abscissa of the centroid of area of the function f , and is given in Fig. 2-13. For linearly tapered wing, with taper ratio λ ,

$$\lambda = \text{tip chord/root chord,}$$

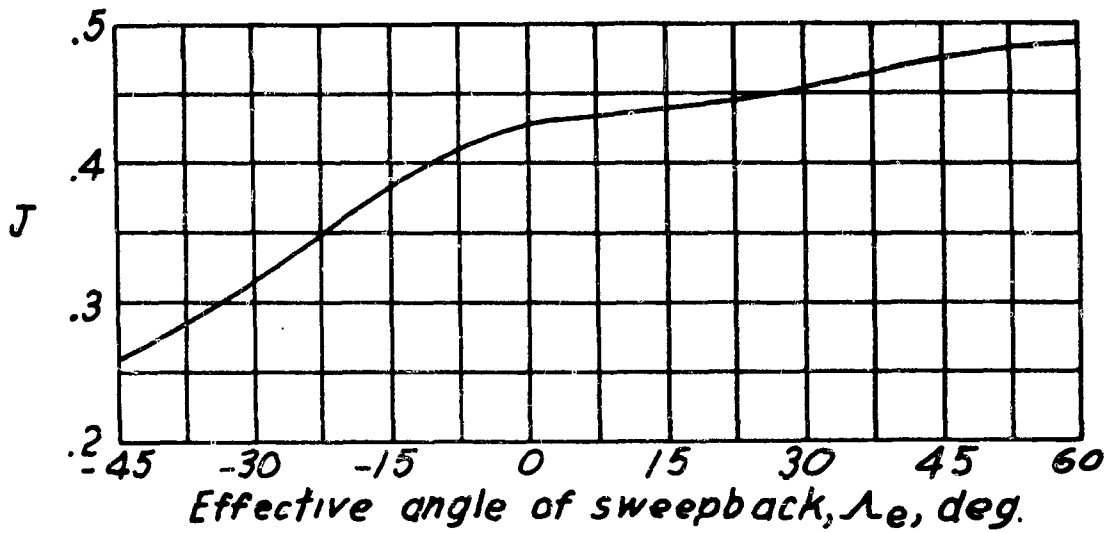
the integral in the first term is reduced to

$$\int_0^1 \frac{c}{c} \gamma^* dy^* = \frac{1+2\lambda}{3(1+\lambda)} \quad (2-66)$$

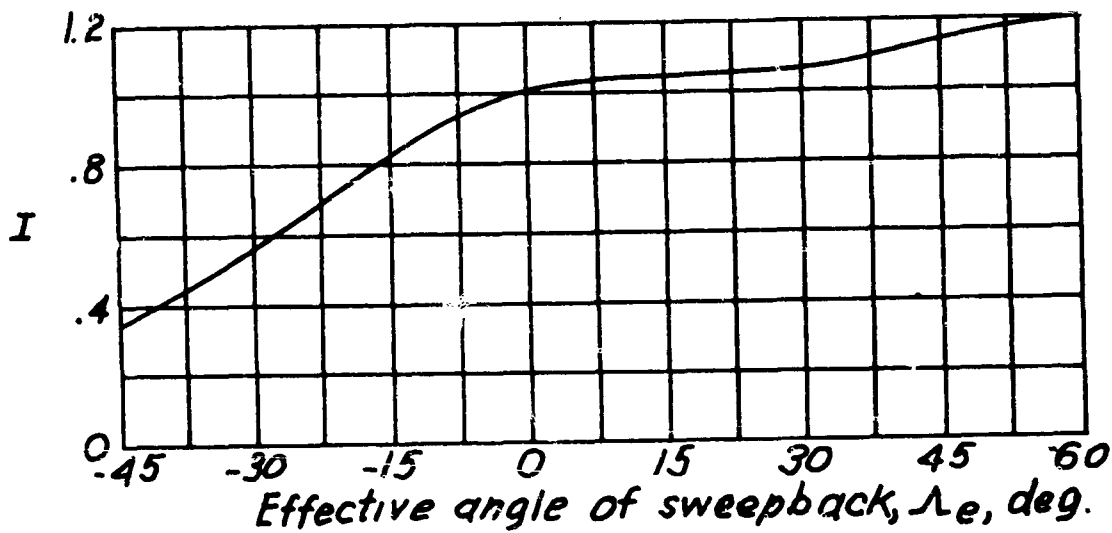
Antisymmetric Lift Distribution

The lift distribution for any antisymmetric twist may be resolved into two parts: a rolling-type distribution, which is the distribution for the given wing with a linear antisymmetric twist of sufficient magnitude to have the same rolling moment as the twist distribution of interest, and a residual distribution, which is the difference between the rolling-type and the true distribution and which, by definition, has no rolling moment. Hence the antisymmetric lift distribution may be written

$$\gamma = \frac{c C_L}{c} = C_{L_a} \alpha_e \gamma_a + \gamma_r \quad (2-67)$$



(a) Spanwise center of pressure J



(b) Moment of Inertia I

Figure 2-13. Centroid of Area and Moment of Inertia of Lift-Distribution Function f (from NACA TN 2751).

where

- C_{l_d} = rolling-moment coefficient for linear antisymmetric twist with unit angle at the tip
 $C_{l_d} = -C_{l_p}$, rolling-moment coeff. due to rolling.
 α_e = tip angle required for a linear antisymmetric distribution with the same rolling moment as the distribution of interest.
 γ_d = unit-rolling type distribution.
 γ_r = residual distribution.

These coefficients are estimated as follows:

$$C_{l_d} = \frac{1}{8} a_o \left(\frac{a_o'}{a_o} \right) \cos \Lambda k_4 \left(\frac{2}{3} \frac{1+3\lambda}{1+\lambda} C_1 + C_2 + I C_3 \right) \quad (2-68)$$

where a_o , a_o'/a_o , C_1 , C_2 , C_3 , λ are given above, k_4 is a function of the plan-form parameter and is given in Fig. 2-9, and

$$I = 4 \int_0^1 f \gamma^{*2} d\gamma^* \quad (2-69)$$

is given in Fig. 2-13. If the wing does not have a linear taper the expression

$4 \int_0^1 \frac{c}{c} \gamma^{*2} d\gamma^*$ must be substituted for the term $\frac{2}{3} \frac{1+3\lambda}{1+\lambda}$.

$$\gamma_d = \frac{1}{C_{l_d}} k_2 \left(\frac{\partial C_L}{\partial \alpha} \right) \gamma^* \gamma_d \quad (2-70)$$

$$\gamma_r = k_3 C_{l_d} \left(\frac{\alpha}{\gamma^*} - \alpha_e \right) \gamma_d \quad (2-71)$$

$$\alpha_e = \frac{1}{2} \int_0^1 \alpha \gamma_d d\gamma^* = \frac{1}{2} \int_0^1 \frac{\alpha}{\gamma^*} \gamma_d \gamma^* d\gamma^* \quad (2-72)$$

The factors k_2 , k_3 are functions of F , given in Fig. 2-9. The corrections k_0 , k_1 , ..., k_4 are all derived for theoretical finite aspect ratio corrections and modified on the basis of lift-curve slope formulas of Section 2.3.1.

Any discontinuity in the angle-of-attack distribution must be faired before the distribution is used in Eqs. (2-71), (2-72). A convenient procedure is

to plot the ratio α/y^* over the span and to fair it as suggested for discontinuous symmetric distributions.

The empirical information embodied in the curves presented above was derived for plan forms with nearly straight quarter-chord lines and for effective angles of sweepback which are not greater than, say, 60° . However, for very small aspect ratio, the agreement between the above empirical method and the slender wing theory seems quite good.

If experimental values of $\partial C_L / \partial \alpha$, C_{L_s} , γ_a , γ_d and C_{L_d} are known,

they may, of course, be used instead of the values given herein. For wings with fuselage, nacelles, etc., an effective value of the planform parameter F can be obtained from Fig. 2-9 if the lift-curve slope is known from experiment. The factors k_1, k_2, k_3, k_4 can be obtained for this effective F .

2.3.3 Aerodynamic Influence Coefficients at Subsonic Speeds

In practical aeroelastic analysis the angle of attack and the lift distributions are specified or computed for a number of stations across the span; and the structural (or elastic) properties of the wing are specified by matrices of influence coefficients. Hence it is natural to employ matrix representation. Let the lift distribution coefficient γ ,

$$\gamma = \frac{c C_L}{c}$$

the additional lift distribution γ_a , and angle-of-attack α be all taken at the same set of stations, say points 1, 2, ... n , and write $\{\gamma\}$ the column matrix which consists of the values of γ at these points, etc.; the equations of the last section, 2.3.2, can be collected together and posed in the matrix form:

$$(a) \text{ Symmetric case } \{\gamma\} = \frac{\partial C_L}{\partial \alpha} [Q_s] \{\alpha\} \quad (2-73)$$

$$(b) \text{ Antisymmetric case } \{\gamma\} = C_{L_a} [Q_a] \{\alpha\} \quad (2-74)$$

where $[Q_s]$, $[Q_a]$ are square matrices of the aerodynamic influence coefficients in the symmetric and antisymmetric cases, respectively.

To derive the aerodynamic influence coefficients, certain integration must be replaced by a matrix operation. In the symmetric case, combination of Eqs. (2-58) and (2-63) of Section 2.3.2 yields

$$\gamma = \frac{\partial C_L}{\partial \alpha} \left((1-k_1) \bar{\alpha} \gamma_a + k_1 \alpha \gamma_a \right) \quad (2-75)$$

where

$$\bar{\alpha} = \int_0^1 \alpha \gamma_a d\gamma^* \quad (2-76)$$

Diederich (Ref. 11) shows that by a proper modification of the Simpson's rule of numerical integration, one may write

$$\begin{aligned} \bar{\alpha} = \alpha_{root} \frac{w}{6b} & \left((\gamma_a)_{\gamma^*=0} + 4(\gamma_a)_{\gamma^*=\frac{w}{2b}} + (\gamma_a)_{\gamma^*=\frac{w}{b}} \right) \\ & + \frac{b-w}{b} [I_1] [\gamma_a] \{\alpha\} \end{aligned} \quad (2-77)$$

where

b = wing span

w = width of fuselage

$\{\alpha\}$ = a column matrix $\{\alpha_1, \alpha_2, \dots, \alpha_n\}$

$[\gamma_a]$ = a diagonal matrix the nonzero elements of which are the values of γ_a at the stations 1, 2, ..., n, as given by Eq. (2-61) of Section 2.3.2.

$[I_1]$ = an integrating matrix.

If the interval from the wing root to the wing tip, $(b-w)/2$, is divided into 6 equal segments, so that the stations are located at

$$\gamma^* = 0, 0.1667, 0.3333, 0.5000, 0.6667, 0.8333, 1 \quad (2-78)$$

where γ^* is the ratio of the lateral distance of the given station from the wing root to the length $(b-w)/2$; then

$$[I_1]_{root} = [0.05556, 0.20833, 0.15278, 0.16667, 0.14913, 0.22500, 0]_{tap} \quad (2-79)$$

When the row matrix $\frac{b-w}{b} [I_1] [\gamma_a]$ is calculated, and the factor

$\frac{w}{6b} \left((\gamma_a)_0 + 4(\gamma_a)_{\frac{w}{2b}} + (\gamma_a)_{\frac{w}{b}} \right)$ is added to its first element, the result

may be written as $\overline{[I_1] [\gamma_a]}$. A square matrix $\overline{[I_1] [\gamma_a]}$ can

then be constructed which consists of rows all equal to $\overline{[I_1] [\gamma_a]}$. With this square matrix, Eqs. (2-77) and (2-75) may be combined into

$$\{ \gamma \} = \frac{\partial C_L}{\partial \alpha} [\gamma_a] \left[(1-k_1) \overline{[I_1] [\gamma_a]} + k_1 [1] \right] \{ \alpha \} \quad (2-80)$$

where $[1]$ is the unit matrix. This is then of the form of Eq. (2-73). Hence the symmetric aerodynamic-influence-coefficient matrix is

$$[Q_s] \equiv [\gamma_a] \left[(1-k_1) \overline{[I_1] [\gamma_a]} + k_1 [1] \right] \quad (2-81)$$

Unless tip tanks or end plates are present, γ_a and γ vanish at the wing tip. Hence the last station in (2-78) and the last element, 0, in (2-79), may be dropped.

A similar reduction of the antisymmetric case leads to (Ref. 11).

$$[Q_a] \equiv [\gamma_a] \left[\frac{1-k_3}{2} \overline{[I_1] [\gamma_a]} + k_3 \left[\frac{1}{y^*} \right] \right] \quad (2-82)$$

The matrix $\overline{[I_1] \gamma_a}$ is a square matrix with rows all equal to $\frac{b-w}{b} [I_1] [\gamma_a]$ and with a constant H' added to the first element:

$$H' = \frac{w}{12b} \left(2 (\gamma_a)_{y^* = \frac{w}{2b}} + (\gamma_a)_{y^* = \frac{w}{b}} \right) \quad (2-83)$$

The matrix $\left[\frac{1}{y^*} \right]$ can be calculated at the given stations from the relation

$$y^* = \frac{b-w}{b} \eta^* + \frac{w}{b} \quad (2-84)$$

An alternative procedure is to use Multhopp's integration formula, which states that for a function $F(\eta)$ which behaves like the spanwise lift distribution at the wing tip,

$$\int_{-1}^1 F(\eta^*) d\eta^* = \frac{\pi}{n+1} \sum_{m=1}^n F_m \sin \theta_m \quad (2-85)$$

where

$$\eta_m^* = \cos \theta_m, \quad \theta_m = \frac{m\pi}{n+1} \quad (2-86)$$

and

$$F_m = F(\eta_m^*), \quad \left(\begin{array}{l} m=1, 2, \dots, n \\ n, \text{ odd} \end{array} \right) \quad (2-87)$$

Hence if, instead of η^* of Eq. (2-78), the stations were chosen according to Eq. (2-86), with $m = 1$ near the wing tip, and $m = (n+1)/2$ at the wing root, then

$$[I_1] = \left[\frac{\pi}{n+1} \sin \theta_m \right] \quad (2-88)$$

2.3.4 The Effect of Elastic Deformation on the Lift Distribution

The methods of the preceding sections yield the lift distribution for swept wings for a given angle-of-attack distribution. If the wing is elastic, it is necessary to resolve the angle-of-attack into two parts, one part due to the rigid-body motion of the airplane, as if it were perfectly rigid, and another part due to the elastic deformation. The elastic deformation is caused in turn by the aerodynamic load. Thus the nature of the lift distribution problem of an elastic wing is that of a feedback system.

For problems concerned with the stability and control of aircraft it generally suffices to use the method of successive approximation. On the premise that the flight speed is substantially lower than the critical speed of wing divergence or that of aileron reversal, the effect of elastic deformation is not too large. In this case one computes first the lift distribution for a rigid airplane. Then the elastic deformation for this lift distribution is computed. Next the change of the lift distribution due to the elastic deformation is computed, and the process is repeated until convergence is reached.

In the general case, it may be necessary to treat the lifting surface as a plate-like structure. For the following illustration, however, it will be assumed that reasonable accuracy can be obtained by considering the deformation pattern at each chordwise section as characterized by a deflection at a reference point and a rotation in the chordwise section about that point. Generalization to the plate-like structure is quite evident, and detailed formulation can be found in Ref. 8.

For a wing other than a normal simple beam, the concept of elastic axis loses its simplicity, and it is more straightforward to define the wing deformation with respect to a suitable reference line. Let the wing under consideration be shown in Fig. 2-14 whose cross sections normal to a reference line may be assumed rigid. Let s be the distance measured from an origin

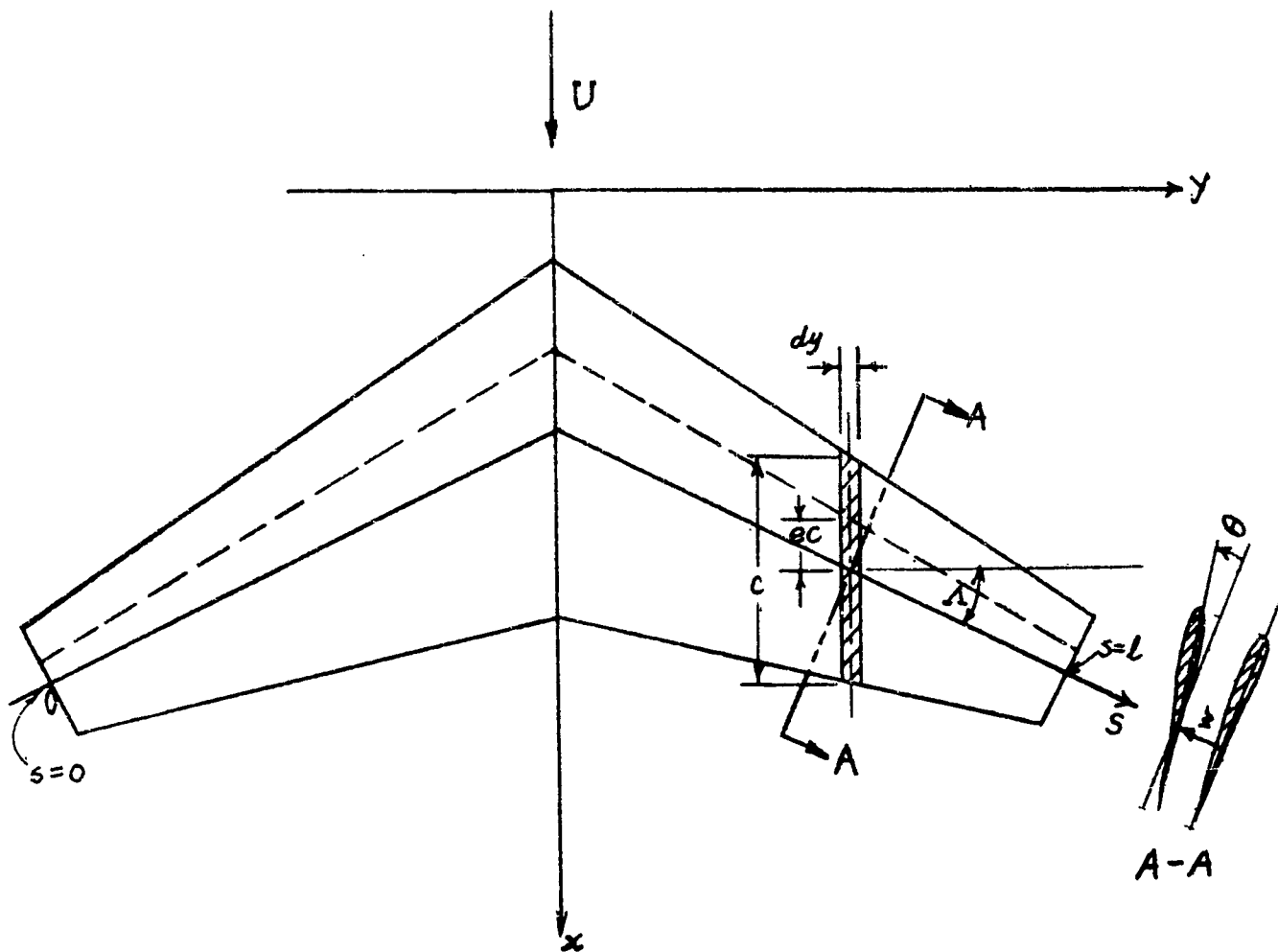


Figure 2-14. Swept Wing

along the reference line. Let $w(s)$ be the deflection at a point s on the reference line, normal to the plane of the wing, and let $\theta(s)$ be the angle of twist of a normal cross section at s about the reference line. In the aerodynamic load problem, the slope $\Gamma(s) = \partial w / \partial s$, rather than w itself, is of importance. The elastic property of the wing can be characterized by the following influence functions:

$F_1(s, \sigma)$ giving Γ at s due to a unit force at σ

$F_2(s, \sigma)$ giving θ at s due to a unit force at σ

$H_1(s, \sigma)$ giving Γ at s due to unit external twisting moment at σ

$H_2(s, \sigma)$ giving θ at s due to unit external twisting moment at σ

By an external twisting moment is meant a couple whose vector is tangent to the reference line. If there acts a unit couple whose vector is perpendicular to the reference line, this couple will be referred to as a unit external bending moment. The influence functions for Γ and θ due to unit external bending moment are $\frac{\partial F_1(s, \sigma)}{\partial \sigma}$ and $\frac{\partial F_2(s, \sigma)}{\partial \sigma}$ respectively.

These influence functions are defined by assuming the structure being rigidly supported in a manner appropriate to the particular problem under consideration. The positive senses of force and deflection, and couples and rotation, must agree respectively.

By the principle of superposition,

$$\Gamma(s) = \int_0^l F_1(s, \sigma) f(\sigma) d\sigma + \int_0^l \frac{\partial F_1(s, \sigma)}{\partial \sigma} m(\sigma) d\sigma + \int_0^l H_1(s, \sigma) t(\sigma) d\sigma \quad (2-89)$$

$$\theta(s) = \int_0^l F_2(s, \sigma) f(\sigma) d\sigma + \int_0^l \frac{\partial F_2(s, \sigma)}{\partial \sigma} m(\sigma) d\sigma + \int_0^l H_2(s, \sigma) t(\sigma) d\sigma \quad (2-90)$$

where $f(s)$ =normal external load per unit length acting on the reference line,

$m(s)$ =distributed external bending moment, per unit length, about the reference line,

$t(s)$ =the distributed external twisting moment per unit length about the reference line.

The integration covers the entire length of the wing.

Now the angle of attack at any section s , measured in the flight direction and denoted by $\alpha(s)$, can be expressed as

$$\alpha(s) = \alpha^{(r)} + \alpha^{(e)} \quad (2-91)$$

where

$\alpha^{(r)}$ = value of α if the airplane were perfectly rigid,

$\alpha^{(e)}$ = that due to elastic deformation.

Expressed in terms of Γ and θ defined with respect to the reference line,

$$\alpha^{(e)} = \theta \cos \Lambda - \Gamma \sin \Lambda \quad (2-92)$$

where Λ is the local sweep-back angle.

From $\alpha(s)$, the aerodynamic forces can be determined. The local lift and moment coefficients are defined by considering the lift and moment acting on an elementary strip of small width dy parallel to the x -axis (see Fig.2-1). The length of the strip is the chord length c measured in the free-stream direction. The lift force on the strip is $q C_l c dy$ and the moment about the aerodynamic center of this strip is $q C_m c^2 dy$. Assume that the drag force is negligible and that the force normal to the wing is equal to the lift. Let the distance from the aerodynamic center and the reference line be ec also measured in the free-stream direction, and taken as positive if the reference line lies behind the aerodynamic center. Then the moment about a point on the reference line due to forces on the elementary strip is $q C_l ec^2 dy + q C_m c^2 dy$, with its vector parallel to the y -axis.

Resolving along and normal to the reference line, and replacing dy by $\cos \Lambda d\sigma$, one obtains

$$t(\sigma) = q \left[C_l(\sigma) e(\sigma) + C_m(\sigma) \right] c^2(\sigma) \cos^2 \Lambda(\sigma) \quad (2-93)$$

$$m(\sigma) = -q \left[C_l(\sigma) e(\sigma) + C_m(\sigma) \right] c^2(\sigma) \sin \Lambda(\sigma) \cos \Lambda(\sigma) \quad (2-94)$$

and

$$f(\sigma) = q C_l(\sigma) c(\sigma) \cos \Lambda(\sigma) \quad (2-95)$$

The integral equations for $\Gamma(s)$ and $\theta(s)$ are then obtained by substituting (2-93), (2-94), (2-95), into (2-89) and (2-90).

In practice, these integral equations are reduced into matrix equations.

Let $\alpha(s)$, $C_L(s)$, $c C_L(s)$ be represented by column matrices $\underline{\alpha}$, $\underline{C_L}$, and $\underline{c C_L}$ with elements $\alpha_1, \alpha_2, \dots, \alpha_n$; $C_{L1}, C_{L2}, \dots, C_{Ln}$; and $c_1 C_{L1}, c_2 C_{L2}, \dots, c_n C_{Ln}$, specified at $s = s_1, s_2, \dots, s_n$, respectively. For

conciseness in notation all matrices will be written underscored, without particular distinction for column, row, or square matrices. The relation between $\underline{\alpha}$ and $\underline{c C_L}$ may be written as

$$\underline{c C_L} = \underline{A} \underline{\alpha} \quad (2-96)$$

where \underline{A} is a matrix of aerodynamic influence coefficients. If strip theory is used, \underline{A} is equal to a diagonal matrix whose nonzero elements are the values of the local chord length c_1, c_2, \dots, c_n times the lift curve slope $\partial C_L / \partial \alpha$ (corrected for aspect ratio). If the flow is subsonic, more refined methods as presented in Section 2.3.3 may be used, and $\underline{A} = (\partial C_L / \partial \alpha) \underline{Q_s}$ or $\underline{A} = \underline{C_{Ld}} \underline{Q_a}$ for the symmetric and antisymmetric cases respectively.

Combining the above equations after they are all converted into matrix approximation form, one obtains

$$\begin{aligned} \underline{c C_L} &= \underline{A} [\alpha^{(r)} + \alpha^{(e)}] \\ &= \underline{A} [\alpha^{(r)} + \underline{\cos \Lambda} \underline{\theta} - \underline{\sin \Lambda} \underline{\Gamma}] \\ &= \underline{A} [\alpha^{(r)} + \underline{q} \underline{E} \underline{c C_L} + \underline{q} \underline{G} \underline{c^2 C_m}] \end{aligned} \quad (2-97)$$

where

$$\begin{aligned} \underline{E} &= (\underline{\cos \Lambda} \underline{F_2} - \underline{\sin \Lambda} \underline{F_1}) \underline{\cos \Lambda} \underline{S} + [(\underline{\cos \Lambda} \underline{H_2} - \underline{\sin \Lambda} \underline{H_1}) \underline{\cos^2 \Lambda} \\ &\quad - (\underline{\cos \Lambda} \frac{\partial F_2}{\partial \sigma} - \underline{\sin \Lambda} \frac{\partial F_1}{\partial \sigma}) \underline{\sin \Lambda} \underline{\cos \Lambda}] \underline{c e} \underline{S}. \end{aligned} \quad (2-98)$$

$$\underline{G} = [(\underline{\cos \Lambda} \underline{H_2} - \underline{\sin \Lambda} \underline{H_1}) \underline{\cos^2 \Lambda} - (\underline{\cos \Lambda} \frac{\partial F_2}{\partial \sigma} - \underline{\sin \Lambda} \frac{\partial F_1}{\partial \sigma}) \underline{\sin \Lambda} \underline{\cos \Lambda}] \underline{S} \quad (2-99)$$

In these equations \underline{e} , $\underline{\sin \Lambda}$, $\underline{\cos \Lambda}$ are diagonal matrices whose nonzero elements are, respectively, values of e , $\sin \Lambda$, and $\cos \Lambda$ evaluated at the stations (s_1, s_2, \dots, s_n) . $\underline{F}_1, \underline{F}_2$, etc. are the elastic influence

coefficients matrices. \underline{S} is a diagonal matrix of "weights" used in converting an integral into a finite sum. For example, if the points (s_1, \dots, s_n) were taken at uniform spacing, then:

Trapezoid rule:

Simpson's rule: (n odd)

$$\underline{S} = h \begin{pmatrix} \frac{1}{2} & & & 0 \\ & 1 & & \\ & & \ddots & \\ 0 & & & 1 \\ & & & & \frac{1}{2} \end{pmatrix},$$

$$\underline{S} = h \begin{pmatrix} \frac{1}{4} & & & 0 \\ & 2 & & \\ & & \ddots & \\ 0 & & & 2 & \\ & & & & \frac{1}{4} \end{pmatrix}$$

where $h = (b-a) / \sum_{m=1}^n$ (diagonal elements in \underline{S})

provided that b and a are the upper and lower limits of integration. Eq. (2-97) can be written as

$$(\underline{I} - q \underline{A} \underline{E}) \cdot \underline{c} \underline{C}_e = \underline{A} [\underline{\alpha}^{(r)} + q \underline{G} \underline{c}^2 \underline{C}_m] \quad (2-100)$$

Hence

$$\underline{c} \underline{C}_e = (\underline{I} - q \underline{A} \underline{E})^{-1} \underline{A} [\underline{\alpha}^{(r)} + q \underline{G} \underline{c}^2 \underline{C}_m] \quad (2-101)$$

The lift per unit span $q c C_l$ can therefore be obtained by matrix operations.

The value of q that satisfies the determinant equation

$$|\underline{I} - q \underline{A} \underline{E}| = 0 \quad (2-102)$$

which is the dynamic pressure at divergence.

Solution by Matrix Iteration

Instead of Eq. (2-101) which involves an inversion of a matrix, approximate solution may be obtained by iterated matrices as follows. Let

$$\underline{u}_0 = \underline{A} [\underline{\alpha}^{(r)} + q \underline{G} \underline{c}^2 \underline{C}_m] \quad (2-103)$$

From \underline{u}_0 , compute successively the iterated matrices

$$\begin{aligned}\underline{u}_1 &= \underline{A} \underline{E} \underline{u}_0 \\ \underline{u}_2 &= \underline{A} \underline{E} \underline{u}_1 \\ &\dots \\ \underline{u}_m &= \underline{A} \underline{E} \underline{u}_{m-1}\end{aligned}\tag{2-104}$$

Then the solution (2-101) may be approximated by

$$\underline{C} \underline{C} = \underline{u}_0 + q \underline{u}_1 + \dots + q^{m-1} \underline{u}_{m-1} + \frac{q^m}{1 - \frac{q}{q_{div}}} \underline{u}_m\tag{2-105}$$

This series holds for the dynamic pressure $q < |q_{div}|$. Theoretically, m should be so large that \underline{u}_m has converged to a unique limiting vector with negligible error. In practice it often suffices to take $m = 2$ or 3 .

If q_{div} is the smallest (in absolute value), simple, real eigenvalue of Eq. (2-102), the divergence dynamic pressure is given by

$$\lim_{m \rightarrow \infty} \frac{u_{m-1}}{u_m} \rightarrow q_{div}\tag{2-106}$$

and, aside from a numerical factor,

$$\lim_{m \rightarrow \infty} \underline{u}_m \rightarrow \underline{u}\tag{2-107}$$

where \underline{u} is an eigenvector of the equation

$$\left(\underline{A} \underline{E} - \frac{1}{q_{div}} \underline{I} \right) \underline{u} = 0\tag{2-108}$$

In Eq. (2-106), the ratio u_{m-1}/u_m means the ratio of the corresponding elements in the column matrices \underline{u}_{m-1} and \underline{u}_m .

Note that q_{div} may be negative for sweptback wings. Then the wing does not diverge, and Eq. (2-105) is valid only for those values of q which is less than the absolute value of q_{div} .

Other methods of solution are available. See Ref. 7, Chapter 8. An alternative formulation and method of solution, based on information of EI and GJ of a slender wing, is given by Diederich, Ref. 12.

CHAPTER II

REFERENCES

1. Miles, J. W., Aeroelastic Properties of Unswept Wings, Lifting Line Theory, Northrop Aircraft Company Report GM-115 (1947).
2. Ames, M. B. and Sears, R. I., Determination of Control Surface Characteristics from NACA Plain Flap and Tab Data, NACA Report 721 (1941).
3. Miles, J. W., A Formulation of the Aeroelastic Problem for a Swept Wing, Northrop Aircraft Report GM-119 (1948), Journal Aeronautical Sciences, Vol. 16 pp. 477-490 (1949).
4. Miles, J. W., Aeroelastic Properties of a Swept Wing, Northrop Aircraft Report GM-103-LV (1948).
5. Diederich, F. W., and Foss, K. A., Charts and Approximate Formulas for the Estimation of Aeroelastic Effects on the Loading of Swept and Unswept Wings, NACA Report 1140 (1953).
6. Foss, K. A., and Diederich, F. W., Charts and Approximate Formulas for the Estimation of Aeroelastic Effects on the Lateral Control of Swept and Unswept Wings, NACA Report 1139 (1953).
7. Fung, Y. C., An Introduction to the Theory of Aeroelasticity, John Wiley, 1955.
8. Bisplinghoff, R. L., Ashley, H., Halfman, R. L., Aeroelasticity, Addison, Wesley, 1955.
9. Diederich, F. W. and Zlotnick, M.: Calculated Spanwise Lift Distribution and Aerodynamic Influence Coefficients for Unswept Wings in Subsonic Flow, NACA Tech. Note 3014 (1953).
10. Diederich, F. W. and Zlotnick, M.: Calculated Spanwise Lift Distributions and Aerodynamic Influence Coefficients for Swept Wings in Subsonic Flow, NACA TN 3476 (1955) 173 pp.
11. Diederich, F. W.: A Simple Approximate Method for Calculating Spanwise Lift Distributions and Aerodynamic Influence Coefficients at Subsonic Speeds, NACA TN 2751 (1952).
12. Diederich, F. W.: Calculation of the Aerodynamic Loading of Swept and Unswept Flexible Wings of Arbitrary Stiffness, NACA Report 1000, (1950), supersedes NACA TN 1876 (1949).
13. Benscoter, S. U.: Matrix Development of Multhopp's Equations for Spanwise Air-Load Distribution, J.A.Sc 15 (Feb. 1948) 113-120.
14. Diederich, F. W., and Foss, K. A.: The Calculation of Certain Static Aeroelastic Phenomena of Wings with Tip Tanks or Boom-Mounted Lifting Surfaces, NACA RM L52A22 (1952).

REFERENCES (contd.)

15. Diederich, F. W.: Charts and Tables for Use in Calculations of Downwash of Wings of Arbitrary Plan Form, NACA TN 2353 (1951).
16. Lyon, H. M.: A Method of Estimating the Effect of Aero-elastic Distortion of a Sweptback Wing on Stability and Control Derivatives, Aero. Res. Coun. R and M 2331 (1946).
17. Pai, S. I. and Sears, W. R.: Some Aeroelastic Properties of Swept Wings, Jour. Aero. Sciences 16, 2, (1949), 105-115.
18. Groth, E.: Aeroelastic Design Data for Swept Wings at Subsonic Speeds. Part 1. Wings with 35° Sweepback. Part 2. Wings with 50° Sweepback and Wings with Small Angle of Sweep. USAF WADC Tech. Rept. 6742, Parts 1 and 2. (1952).

NOMENCLATURE

- a = lift curve slope
- a' = lift curve (coefficient) slope corrected for sweepback
- b = wing span, feet
- c = wing chord, feet
- $c_{l_{\alpha}}$ = sectional lift coefficient due to α
- $c_{l_{\delta}}$ = sectional lift coefficient due to δ
- e = eccentricity, the non-dimensional distance of the aerodynamic center forward of the elastic axis.
- l_f = characteristic fuselage length, feet
- l_t = fuselage length from c.g. to tail, feet
- l' = lift per unit span = $c' a' q \alpha$
- p = rate of roll
- q = dynamic pressure = $1/2 \rho U^2$
- q_t = dynamic pressure at wing bending divergence
- q_d = dynamic pressure at divergence (in twist)
- q_f = dynamic pressure at which fuselage bending causes 50 percent reduction in tail effectiveness
- q_r = dynamic pressure at reversal (in twist)
- w = width of fuselage
- $\left. \begin{matrix} x \\ y \end{matrix} \right\}$ = coordinates oriented by the direction of flight (cf. fig. 2-7)
- $\left. \begin{matrix} x' \\ y' \end{matrix} \right\}$ = coordinates obtained by rotating x and y through sweepback angle (cf. fig. 2-7)
- A = $\frac{64}{9}$ = a correction factor used in determining the divergence speed for a group of wings
- \underline{A} = matrix of aerodynamic influence coefficients
- AR = aspect ratio = $\frac{b^2}{S}$
- B = correction factor for three dimensional effects

- C_L = lift coefficient = $\frac{L}{qS}$
 C_{L_α} = three dimensional lift curve slope = $\frac{dC_L}{d\alpha}$
 C_{l_p} = roll damping coefficient = $\frac{dC}{d\left(\frac{pb}{2v}\right)}$
 C_{L_δ} = control surface lift coefficient
 C_{M_δ} = control surface moment coefficient
 $C_{L_{\alpha_t}}$ = lift coefficient of tail

 E = Young's modulus of fuselage material, pounds per sq. ft.
 F = planform parameter

 $\left. \begin{matrix} F_1' \\ F_2' \\ \text{etc.} \end{matrix} \right\}$ = matrices of elastic influence coefficients

 I_F = cross sectional moment of inertia of fuselage, ft.⁴
 GJ = uniform torsional modulus, ft.² lbs.
 K = "reduced frequency" = $\frac{\omega L}{U}$

 K_b = stiffness coefficient of wing in bending
 K_ϕ = stiffness coefficient of wing in torsion
 K_f = stiffness coefficient of fuselage in bending

 L = lift force
 L_α = lift due to angle of attack
 L_δ = lift due to control surface deflection
 L_{α_t} = tail lift due to tail angle of attack

 L_t = tail load

 M = Mach number

M_α = pitching moment due to angle of attack (M is generally a pitching moment, N a yawing moment, etc.)
 M_h = control surface hinge moment = $(M_h) + (M_h)_\alpha + (M_h)_{\dot{\alpha}} + \dots$
 M_δ = moment due to control surface deflection
 S = wing area
 \underline{S} = diagonal matrix
 S_t = tail area
 U = flight velocity
 U_d = divergence speed
 α = total angle of attack
 α_{t_0} = tail angle of attack in absence of fuselage deflection
 α_0 = angle of attack due to initial rotation of wing
 Γ_δ = control surface parameter = $1 + \frac{C_{M_\delta}}{eC_{l_\delta}}$
 γ = loading coefficient
 λ = taper ratio
 δ = control surface deflection angle
 θ_f = tail plane rotation
 $\left. \begin{matrix} \theta_x \\ \theta_y \end{matrix} \right\}$ = rotations about x and y axes (cf. fig. 2-7)
 $\left. \begin{matrix} \theta_{x'} \\ \theta_{y'} \end{matrix} \right\}$ = rotations about x' and y' axes (cf. fig. 2-7)
 Λ = sweepback angle of elastic axis
 ϕ = wing twist

ψ = wing bending slope along elastic axis

ω = angular frequency

CHAPTER III

DERIVATION OF EQUATIONS OF MOTION

3.0 Introduction

The first step in deriving the dynamic stability equations for an elastic airplane is the establishment of a coordinate description of the distorted airframe (see the appendix at the end of this chapter for a discussion of axes systems). It is convenient to retain the rigid airplane coordinates as part of this description, at least insofar as the primary motivation of the analysis is to describe the motion of the airplane as a whole (in contrast to flutter analysis, where the primary motivation is to describe the elastic distortion). Moreover, it is convenient to separate the distortion relative to the (hypothetical) rigid airframe into equilibrium, or steady flight components and additional components associated with the dynamic perturbations ($u, v, w, p, q, r, \phi, \theta, \psi$) about this equilibrium. The steady flight distortions will enter the dynamic stability equations through the specification of the equilibrium values of not only C_D , C_L , and C_m but also the angle of attack and dihedral distributions of the wing and the downwash at the tail.

The foregoing separation of equilibrium and dynamic distortion is not intended to preclude "quasi-static" aeroelastic corrections* to some or all of the dynamic stability derivatives; indeed, such corrections should be made at all points in the analysis where elastic distortion is not taken into account by specific degrees of freedom, unless, of course, such distortion is known to be negligible. It usually will be entirely adequate to apply quasi-static corrections to all derivatives with respect to u , which changes rather slowly, and to handle wing and tail torsional deflections in this manner in virtue of the relatively high frequencies of the torsional modes. It should be remarked, however, that the coupling between torsion and bending of swept wing may render it difficult to apply quasi-static torsional corrections directly, i.e., without including torsion in the equations of motion; on the other hand, torsional effects on the aerodynamic characteristics of a heavily swept wing usually are negligible compared with the bending effects. Quasi-static corrections are discussed in section 3.2.2.3 and in Chapter V.

*A "quasi-static" aeroelastic correction is one in which the effect of distributed inertia forces on elastic distortion is neglected, so that this distortion depends only on the instantaneous values of the dynamic stability variables ($u, v, w, p, q, r, \phi, \theta, \psi$); thus, elastic distortion does not lead to additional degrees of freedom in this approximation.

The precise description of a complete elastic airframe or even a wing alone would lead to either partial differential and/or integral equations, and even the invocation of such simplifying approximations as aerodynamic strip theory and simple beam theory still would leave an ordinary differential equation. There are very few cases in which an exact solution to these equations could be formulated, but even if an exact solution were possible, it usually would not be warranted by the accuracy of available data. Accordingly, it is common practice to reduce to a finite number the coordinates describing the elastic airplane, either by assuming a finite set of deflection modes or by dealing with the deflections of a finite set of collocation points on the airframe.

The number of degrees of freedom in these approximate treatments is equal to the number of rigid body modes plus the number of elastic modes or collocation points. The accuracy obtainable for a fixed number of degrees of freedom generally is better when the modal description is used, especially if the mode shapes are judiciously chosen. On the other hand, the collocation point method not only eliminates much of the judgment (based on experience) required in the selection of mode shapes but also leads to a simple and direct matrix formulation that is readily mechanized for digital computing machines; in addition, the experimental (and, in the presence of high order redundancies, the analytical) determination of the purely structural properties of the airframe is greatly simplified by this approach. Moreover, having the general matrix formulation of the equations of motion for an arbitrary set of points, Galerkin's method may be used to obtain a modal formulation identical with that which might otherwise have been deduced from Lagrange's equations through the expansions of the energies in modal amplitude coordinates.

The matrix formulation of the equations of motion should not be assumed to preclude the use of analog computers for the solution thereof. Indeed, while it may be expedient to carry out the entire solution on a digital computer, it frequently may be more advantageous to carry out the algebraic manipulation of the matrices on a digital machine but solve the final differential equations on an analog computer, particularly if the various dimensionless parameters are to be varied during the course of the solution. These questions will be discussed further in Chapter VIII.

The choice between the modal and collocation methods must rest, in large measure, on the judgment and experience of the analyst and on the personnel and facilities available to him. In general, the modal method necessarily would be used where computations must be carried out by hand or desk-type machines; the collocation method usually would be the choice for computations to be carried out on high-speed, digital computers of sufficient capacity, but machine capacity often might be sufficiently limited to render the modal approach superior.

COMPARISON OF TWO AEROELASTIC ANALYSIS METHODS

| MODAL APPROACH | | COLLOCATION APPROACH | |
|---|--|--|---|
| ADVANTAGES | DISADVANTAGES | ADVANTAGES | DISADVANTAGES |
| <ol style="list-style-type: none"> 1. Fewer equations 2. Lower cost 3. Easily solved by either digital or analog computing equipment. 4. Elastic and aerodynamic data is usually available or readily computed. | <ol style="list-style-type: none"> 1. Success depends for the most part upon the right choice of modes and mode shapes. 2. More assumptions are made. 3. Answers are approximate. | <ol style="list-style-type: none"> 1. Fewer assumptions are made. 2. Doesn't specify a particular mode. 3. Readily mechanized for digital computing equipment. 4. Answers provide more information about elastic distortion. 5. Approaches the more exact way to analyze an elastic airframe. | <ol style="list-style-type: none"> 1. Higher cost and longer time to perform. 2. Not as easily solved on analog equipment. 3. User must be familiar with matrix operation. |

3.1 Modal Approach*

A simple form for the equations of motion of an elastic structure is the form based on normal** coordinates. A normal coordinate d_r describes the motion of the elastic system vibrating in its r^{th} undamped, orthogonal mode. References 1 and 2 contain detailed derivations of these equations; for brevity, only a short outline of the derivation will be presented here.

Lagrange's equations of motion form the basis of a widely used method of dynamic analysis of structures, and are written as follows:

$$\frac{d}{dt} \left(\frac{\partial T}{\partial \dot{q}_r} \right) - \frac{\partial T}{\partial q_r} + \frac{\partial U}{\partial q_r} = Q_r \text{ for } r=1,2,3,\dots,n \quad (3-1)$$

where q_r is the r^{th} of n "generalized" coordinates (defined later) for the system, T and U are the kinetic and potential energies, respectively, of the system, and Q_r is the "generalized" force input to the system. We might define (somewhat loosely) the generalized coordinates q_r as any n independent coordinates which completely specify the configuration of the system***. (It is always possible to describe the configuration of a system having a finite number of elements by a finite number of coordinates, but in many cases these coordinates are not independent of each other due to the constraints on the system.) The generalized force Q_r is defined mathematically as

$$Q_r = \frac{\delta W}{\delta q_r}$$

where δW is the virtual work done by the external forces acting on the system in a virtual displacement δq_r of the system (provided the displacement conforms to the constraints on the system).

If we approximate a continuous structure by a system of lumped masses (or inertias) connected by appropriate springs and viscous dampers, and if we restrict the motions of the system to small oscillations about the equilibrium (minimum potential energy) position, we then can obtain, by application of the Lagrangian equations, the following form of the dynamical equations for the structure:

$$\sum_{j=1}^n M_{ij} \ddot{q}_j + \sum_{j=1}^n D_{ij} \dot{q}_j + \sum_{j=1}^n K_{ij} q_j = Q_i \text{ for } i=1,2,3,\dots,n \quad (3-2)$$

* From J. B. Rea Co. Report 103, Methods for Solution of Combined Aeroelastic-Missile-Plus-Autopilot Stability Problem for the RTV-A-5 Missile by J. P. Zemlin.

** A normal coordinate expresses the displacement in a natural mode.

*** For a more complete definition, see reference 2, pp. 55-57.

where n is the number of lumped masses, q_i is the generalized coordinate (but not a normal coordinate) of the i^{th} mass, and the M_{ij} , D_{ij} and K_{ij} are the inertia, damping, and spring coefficients needed to approximate the actual structure. (Coefficients having a non-zero value for $i \neq j$, are coupling coefficients). Q_i is the generalized force input to the structure. These equations describe the motions of each lumped mass, and are linear but cumbersome, since n might need to be as high as 30 or more to result in an adequate approximation of the structure. For pure bending or torsion of an aircraft wing or fuselage, the M_{ij} usually vanish for $i \neq j$, and the damping is small enough (compared to the aerodynamic damping terms in the Q_i) so that it is often neglected, thus simplifying these equations considerably. It is still necessary, however, to include all n equations.

The general solution of the above n equations indicates that each of the i elements oscillates in s elastic modes, which are characteristic of the system.* These s harmonic modes are exponentially damped if damping terms are included in the equations. The relative amplitudes of oscillation of the n masses in the k^{th} mode (of circular frequency ω_k) determine the k^{th} mode shape of the structure. For small damping (as in aircraft structures), the damped and undamped mode shapes and frequencies are very similar. If, then, we describe the motion of the undamped structure by coordinates d_k , called normal coordinates, describing the instantaneous deflections in the modes $k = 1, 2, 3, \dots, s$, we obtain the following forms for the kinetic energy T and potential energy U of the system (using the equilibrium position for $U = 0$):

$$T = \frac{1}{2} M_k (\dot{d}_k)^2 \quad (3-3)$$

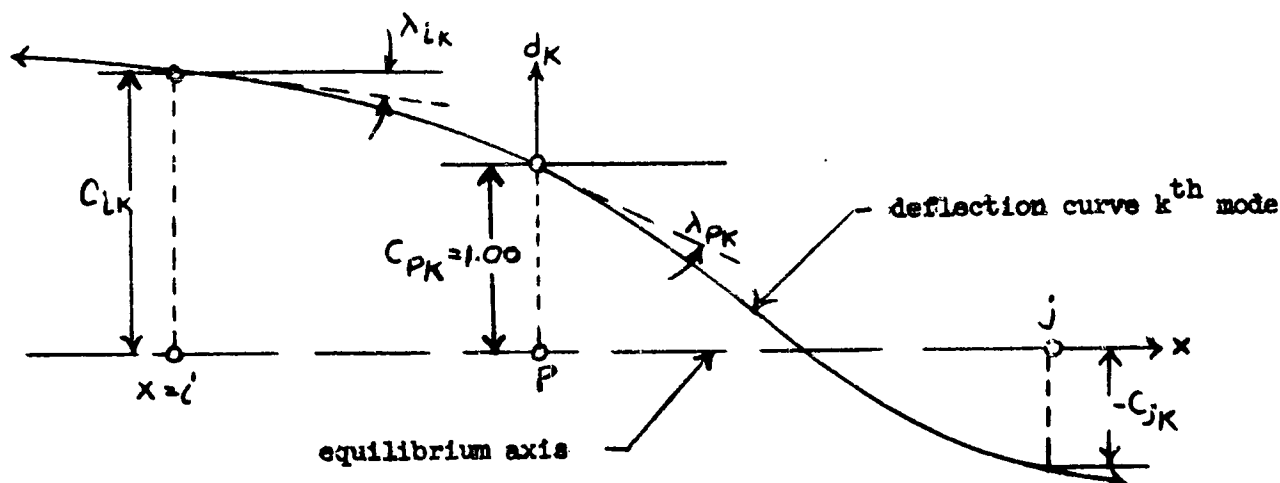
$$U = \frac{1}{2} \omega_k^2 M_k (d_k)^2 \quad (3-4)$$

where M_k is given by

$$M_k = \sum_{i=1}^n \sum_{j=1}^n C_{ik} M_{ij} C_{jk}$$

* The total number of modes will be n , but one or more of these may be modes of motion of the centroid of the system; $s \leq n$ (Reference 3).

and is called the generalized mass for the k^{th} mode, and the constant c_{ik} is the relative amplitude at element i , with respect to unit amplitude at some element p , in the k^{th} mode. The mode shape is said to be "normalized" at p (p may be any point at which it is desired to have unit relative amplitude, or $c_{pk} = 1$). d_k then gives the actual motion in the k^{th} mode, of the structure at point p , and the corresponding motion at any point i in the k^{th} mode is given by $c_{ik} d_k$.



Note: as shown, c_{jk} is negative

Figure 3-1. Fuselage Bending Mode Shape

If the deflection curve in the sketch is a fuselage bending mode, the aerodynamic forces acting on i along the structure in the k^{th} mode will be a function of the slope of the deflection curve at i as well as the deflection (translational in this case) at i . For small deflections, this slope is given by $\lambda_{ik} d_k$. (λ_{ik} is usually taken in radians for convenience.)

If we substitute the expressions for T and U , in normal coordinates, into the Lagrangian equations, we obtain the equations of motion for the normal modes:

$$M_k(\ddot{d}_k + \omega_k^2 d_k) = Q_k \text{ for } k = 1, 2, 3, \dots, s \quad (3-5)$$

where Q_k , the generalized force, is now defined as $\delta W / \delta d_k$. Since the actual system contains damping, the above equations for the undamped case represent an additional approximation over equations (3-2). In particular, equations (3-5) give an infinite response (for the structure alone) at the resonant frequencies, and indicate neutral stability at other frequencies. As a refinement of the approximation, we add to equation (3-5) empirical viscous damping terms to obtain

$$M_k (\ddot{d}_k + 2 \xi \omega_k \dot{d}_k + \omega_k^2 d_k) = Q_k \text{ for } k = 1, 2, 3, \dots, s \quad (3-6)$$

(using a common terminology for second-order systems) where ξ is an empirical damping ratio (ratio of viscous damping to critical damping). The usual range of ξ is from 0.01 to 0.05; in most cases the aerodynamic damping is large compared to the damping in the structure, and the value of ξ selected is not too critical.

Equations (3-6) are the desired equations of motion of the structure and each mode is treated independently*. As previously stated, for pure bending or torsion of aircraft wings and fuselages the inertia coupling terms in equations (3-2) vanish (i.e., $M_{ij} = 0$ for $i \neq j$). The generalized masses for equation (3-6) are then given by:

$$M_k = \sum_{l=1}^n M_{ll} (c_{lk})^2 \text{ for } k = 1, 2, 3, \dots, s \quad (3-7)$$

or for continuously defined mode shapes and inertia distributions,

$$M_k = \int_M y_{ik}^2 dM \quad (3-8)$$

where the integral is taken along the structure with mass or moment of inertia distribution given by dM and deflection curve given as the curve y_{ik} .

An example of the determination of the generalized force Q_k is given in Chapter 6.

* If we transform directly from the damped equation (3-2), the resulting equations are similar to equation (3-6) but contain inertia, damping, and spring coupling terms, and the modes are not structurally independent. Since the damping of the structure is small, these coupling terms are small, and may usually be neglected (for this order of approximation). Hence Equation (3-6) is satisfactory.

3.2 Collocation Approach Using Matrices

Most of the methods of aeroelastic analysis at the present time are based on a modal description, but the increasing capacity and speed of digital computers in manipulating high order matrices, together with the growing complexities (both structural and aerodynamic) of high speed aircraft, indicate a future trend toward the collocation point method. This fact, reinforced by the conceptual simplicity of presentation, supports the choice of a matrix formulation of the aeroelastic problem in the subsequent sections of this chapter.

3.2.1 Dynamic Stability Equations for Rigid Airplane. The equations of motion of a rigid airframe will be formulated as a preliminary to the consideration of a flexible airframe. This formulation, albeit self-contained, will be made relatively brief, and the reader is referred to standard references 4, 5, and 6 for further details. Except as noted, the following assumptions are made (See P-II-35, Reference 4):

1. The airframe is assumed to be rigid;
2. The atmosphere through which the airplane flies is assumed fixed in space (i.e., it constitutes an inertial reference frame in the Newtonian sense);
3. The mass of the airframe is constant;
4. The airframe has a vertical (x,z) plane of symmetry;
5. All disturbances from the initial steady flight condition are assumed small in the sense that only terms of first order in the disturbance amplitudes are considered;
6. The axis system is defined as being an orthogonal system having the origin at the center of gravity, the z axis in the plane of symmetry and perpendicular to the initial relative wind, the x axis in the plane of symmetry perpendicular to the z axis and the y axis perpendicular to the plane of symmetry. (These axes, often referred to as "stability axes", are not, in general, principal axes; however, in virtue of assumption 4, the only non-vanishing product of inertia is I_{xz});
7. The reduced frequency is assumed to be so small that the only unsteady flow derivatives that need be introduced in the equations of motion for the rigid airplane are $(\partial M / \partial \dot{w})$ and $(\partial N / \partial \dot{v})$. On the other hand the flow is not necessarily assumed to be quasi-steady (in contrast to Reference 4), as discussed in more detail in Chapter V.

It should be remarked that, from the analytical viewpoint, body axes are not necessarily more convenient than axes fixed in space ("wind tunnel axes"), especially in connection with flexible airframes. In particular, the assumption of small disturbances (5 above) does away with the objection to variable moments of inertia that often is advanced against fixed axes. Body axes, nevertheless are chosen in the following in recognition of the fact that internal instrumentation (e.g., an autopilot) necessarily is referred to such axes.

3.2.1.1 Equations of Motion in Body Axes.

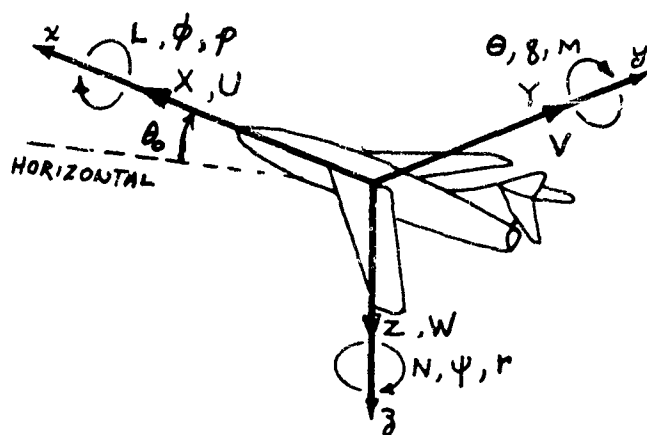


Figure 3-2. Body Axes System and Velocity Components.

Let (x, y, z) be a set of axes fixed in the airframe, as described in assumption 6 above (See Figure 3-2); (U, V, W) the total velocity components of the c.g.; $(\dot{X}, \dot{Y}, \dot{Z})$ the components of angular rotation; (P, Q, R) the angular velocity components; (X, Y, Z) the components of force; (L, M, N) the components of torque; m the total mass; (I_{xx}, I_{yy}, I_{zz}) the moments of inertia; and I_{xz} the product of inertia ($I_{xy} = I_{yz} = 0$ in virtue of assumption 4). The Eulerian equations of motion then read

$$X = m(\dot{U} + QW - RV) \quad (3-9a)$$

$$Y = m(\dot{V} + RU - PW) \quad (3-9b)$$

$$Z = m(\dot{W} + PV - QU) \quad (3-9c)$$

$$L = I_{xx}\dot{P} + (I_{zz} - I_{yy})QR - I_{xz}(PQ + \dot{R}) \quad (3-10a)$$

$$M = I_{yy}\dot{Q} + (I_{xx} - I_{zz})PR + I_{xz}(P^2 - R^2) \quad (3-10b)$$

$$N = I_{zz}\dot{R} + (I_{yy} - I_{xx})PQ + I_{xz}(QR - \dot{P}) \quad (3-10c)$$

The assumption of small disturbances, not yet introduced in (3-9) and (3-10), now is invoked by writing*

$$(U, V, W) = (U_0 + u, v, w), \quad u, v, w \ll U_0 \quad (3-11)$$

$$(P, Q, R) = (p, q, r) \quad p, q, r \ll U_0 / \ell \quad (3-12)$$

where U_0 is the steady flight velocity, and ℓ is an appropriately chosen characteristic length (say mean aerodynamic chord in longitudinal motion or wing span in lateral motion). Substituting (3-11) and (3-12) in (3-9) and (3-10) and neglecting all terms involving products of the small disturbances (u, v, w, p, q, r) then yields the small perturbation equations.

$$X = m \ddot{u} \quad (3-13a)$$

$$Y = m(\ddot{v} + U_0 r) \quad (3-13b)$$

$$Z = m(\ddot{w} - U_0 q) \quad (3-13c)$$

$$L = I_{xx} \dot{p} - I_{xz} \dot{r} \quad (3-14a)$$

$$M = I_{yy} \dot{q} \quad (3-14b)$$

$$N = I_{zz} \dot{r} - I_{xz} \dot{p} \quad (3-14c)$$

It is of interest to note that the steady velocity of the axis system enters the approximate equations (3-13) and (3-14) only through the terms $U_0 r$ and $U_0 q$ of (3-13b) and (3-13c).

The forces and moments acting on the airframe may be considered in five categories: the force of gravity, the steady flight forces (aerodynamic and thrust), the control surface or other input forces and moments initiating disturbances from steady flight, the aerodynamic forces and moments associated with these disturbances, and inertia loads (e.g., $m \ddot{u}$).

* If large excursions from the steady state conditions are to occur, it will, of course, be necessary to retain the gravity and coupling terms that are normally neglected in a small disturbance type of analysis.

If in steady flight the x axis makes an angle θ_0 with the horizontal, the y axis is horizontal, and the airframe then receives small rotations* (ϕ, θ, ψ) about (x, y, z) respectively, the components of gravitational force along the disturbed positions of the axes are (see Section II-5 of Reference 4 for detailed derivation).

$$[X^{(8)}, Y^{(8)}, Z^{(8)}] = mg[-(\sin \theta_0 + \theta \cos \theta_0), (\phi \cos \theta_0 + \psi \sin \theta_0), (\cos \theta_0 - \theta \sin \theta_0)] \quad (3-15)$$

The steady flight force has only components X_0 and Z_0 , while the steady flight moment about the c.g. vanishes identically in consequence of the assumed equilibrium.

Turning to the aerodynamic forces, the velocities (u, w, q) produce only (X, Z, M) forces in virtue of symmetry considerations similarly, the (v, p, r) velocities produce only (Y, L, R) forces (no aerodynamic forces are associated with the angular perturbations (ϕ, θ, ψ) due to the use of body axes). Moreover, in accordance with assumption 7, time lags between velocity perturbations and the forces that are produced thereby may be neglected except as noted, whence the forces are in phase with (or opposite in phase to) the velocity perturbations. The only exception to this last statement that usually is considered is the lag between M and w , which leads to the introduction of a term $(\partial M / \partial \dot{w}) \dot{w}$. That $(\partial M / \partial \dot{w})$ is the only unsteady flow-derivative of importance in the equations of longitudinal stability can be inferred from an order analysis (in Glauert's mass parameter μ of the dimensionless equation 7, Reference 7). It should be emphasized, however, that this conclusion does not necessarily lend support to a quasi-steady flow hypothesis, and there may be important contributions to $(\partial M / \partial \dot{w})$ from unsteady flow effects other than the conventional downwash lag; moreover, the quasi-steady flow hypothesis may not form an adequate basis for the calculation of downwash lag (Reference 8). It follows by analogy that a term $(\partial N / \partial \dot{v}) \dot{v}$, also should enter the lateral stability equation; while it appears that unsteady flow contributions to this term are not too important for fin alone (Reference 9), little data is available on the effects of wing sidewash lag.

On the basis of the foregoing discussion, the total forces can be expanded as follows (the derivatives in these expressions are to be evaluated in the equilibrium configuration in virtue of the assumption of small disturbances):

$$X = [X_0 - mg \sin \theta_0] - mg \theta \cos \theta_0 + \left(\frac{\partial X}{\partial u}\right) u + \left(\frac{\partial X}{\partial w}\right) w + \left(\frac{\partial X}{\partial q}\right) q + X, \quad (3-16a)$$

* The final position of the airframe is independent of the order of these small rotations, in contrast to the result for non-small rotations (i.e., those for which products of angles can not be neglected) which are non-commutative.

$$Y = mg(\phi \cos \theta_0 + \psi \sin \theta_0) + \left(\frac{\partial Y}{\partial v}\right) \dot{v} + \left(\frac{\partial Y}{\partial p}\right) p + \left(\frac{\partial Y}{\partial r}\right) r + Y_1 \quad (3-16b)$$

$$Z = [Z_0 + mg \cos \theta_0] - mg \theta \sin \theta_0 + \left(\frac{\partial Z}{\partial u}\right) u + \left(\frac{\partial Z}{\partial w}\right) w + \left(\frac{\partial Z}{\partial q}\right) q + Z_1 \quad (3-16c)$$

$$L = \left(\frac{\partial L}{\partial v}\right) \dot{v} + \left(\frac{\partial L}{\partial p}\right) p + \left(\frac{\partial L}{\partial r}\right) r + L_1 \quad (3-17a)$$

$$M = \left(\frac{\partial M}{\partial u}\right) u + \left(\frac{\partial M}{\partial w}\right) \dot{w} + \left(\frac{\partial M}{\partial w}\right) w + \left(\frac{\partial M}{\partial q}\right) q + M_1 \quad (3-17b)$$

$$N = \left(\frac{\partial N}{\partial v}\right) \dot{v} + \left(\frac{\partial N}{\partial v}\right) v + \left(\frac{\partial N}{\partial p}\right) p + \left(\frac{\partial N}{\partial r}\right) r + N_1 \quad (3-17c)$$

where $(X_1, Y_1, Z_1, L_1, M_1, N_1)$ represent small disturbances due to control surface deflections or other sources.* Moreover, in consequence of the assumed equilibrium condition of steady flight, the terms in square brackets in (3-16a) and (3-16c) vanish identically.

Finally, substituting the force and moment expansions (3-16) and (3-17) in the equations of motion (3-13) and (3-14), regrouping the latter into longitudinal and lateral equations, and ordering the terms in the conventional manner, the results are:

$$m \dot{u} - \left(\frac{\partial X}{\partial u}\right) u - \left(\frac{\partial X}{\partial w}\right) w - \left(\frac{\partial X}{\partial q}\right) q + (mg \cos \theta_0) \theta = X_1 \quad (3-18a)$$

$$-\left(\frac{\partial Z}{\partial u}\right) u + m \dot{w} - \left(\frac{\partial Z}{\partial w}\right) w - \left(m U_0 + \frac{\partial Z}{\partial q}\right) q + (mg \sin \theta_0) \theta = Z_1 \quad (3-18b)$$

$$-\left(\frac{\partial M}{\partial u}\right) u - \left(\frac{\partial M}{\partial w}\right) \dot{w} - \left(\frac{\partial M}{\partial w}\right) w + I_{yy} \dot{q} - \left(\frac{\partial M}{\partial q}\right) q = M_1 \quad (3-18c)$$

$$m \dot{v} - \left(\frac{\partial Y}{\partial v}\right) v - \left(\frac{\partial Y}{\partial p}\right) p - (mg \cos \theta_0) \phi + \left(m U_0 - \frac{\partial Y}{\partial r}\right) \psi - (mg \sin \theta_0) \psi = Y_1 \quad (3-19a)$$

$$-\left(\frac{\partial L}{\partial v}\right) v + I_{xx} \dot{p} - \left(\frac{\partial L}{\partial p}\right) p - I_{xz} \dot{r} - \left(\frac{\partial L}{\partial r}\right) r = L_1 \quad (3-19b)$$

$$-\left(\frac{\partial N}{\partial v}\right) \dot{v} - \left(\frac{\partial N}{\partial v}\right) v - I_{xz} \dot{p} - \left(\frac{\partial N}{\partial p}\right) p + I_{zz} \dot{r} - \left(\frac{\partial N}{\partial r}\right) r = N_1 \quad (3-19c)$$

* In stick-free stability studies control surface deflections must be considered as separate degrees of freedom rather than input sources; see, e.g., Reference 6.

These are dimensional forms of the equations of motion about the "stability axes" used herein. In the following sections they will be recast in dimensionless form.

3.2.1.2 Dimensionless Notation. It is expedient to place the equations of motion developed in the preceding section in dimensionless form, both in order to exhibit scale effects more clearly and as a preliminary to the examination of the importance of aeroelastic terms. Following the original analysis of Glauert, Reference 10 (but in revised notation), dimensional consideration of the motion of a rigid airplane leads to the introduction of the dynamical parameters

$$\mu = m/\rho S l = \text{relative density} \quad (3-20)$$

$$F = U^2/l g = \text{Froude number} \quad (3-21)$$

where ρ is the air density, S the wing area, l an appropriately defined characteristic length, and U the flight velocity (the subscript zero now being dropped). In addition, there exist the well known, aerodynamic parameters

$$M_a = U/a = \text{Mach number} \quad (3-22)$$

$$R = U l / \nu = \text{Reynolds number} \quad (3-23)$$

where a is the velocity of sound and ν the coefficient of kinematic viscosity of the air. Two geometrically similar aircraft having identical values of these four parameters will respond in essentially identical fashion in proportion to their scale to similar disturbances from similar initial conditions.

The relative density parameter μ , being proportional to the ratio of airplane density to air density, is probably the most important of the dimensionless parameters in the equations of motion of a rigid airplane. In general, a large value of μ may be regarded as typical of dynamic stability studies; conversely, a small value of μ would call for a reconsideration of some of the basic assumptions, particularly 7, set forth in Section 3.2.1.

The parameter F , usually designated as the Froude number, is proportional to the ratio of aerodynamic to gravitational forces. This ratio is determined by the equilibrium flight requirement (neglecting the contribution of thrust to lift) that the lift force must balance the component of weight normal to the flight path, viz.

$$\frac{1}{2} \rho U^2 S C_L = m g \cos \theta_0 \quad (3-24)$$

where C_L is the steady flight lift coefficient. Substituting U^2 in (3-24) from (3-21) and m from (3-20), it is found that

$$F = \frac{2m\cos\theta_0}{\rho S l C_L} = \frac{2\mu\cos\theta_0}{C_L} \quad (3-25)$$

In view of the over-all importance of the lift coefficient C_L , it is customary to use μ and C_L , rather than μ and F , as the principal similarity parameters in dynamic stability studies.

The parameters M_a (Mach number) and R (Reynolds number), representing the ratios of aerodynamic inertial forces to compression and viscous forces, respectively, enter only through the aerodynamic derivatives. These derivatives are relatively insensitive to variations in the Reynolds number (although stalled flight may be an important exception), whence it usually may be relegated to the background. On the other hand, especially in the transonic regime, the aerodynamic derivatives (particularly C_{L_u} , C_{D_u} and C_{m_u}) may exhibit important dependences on the Mach number M_a , as borne out in Chapter V.

In order to place the equations of motion in dimensionless form it is necessary to choose a set of fundamental units. Following Glauert, (Reference 11), the unit of time will be defined by

$$\tau = m/\rho U S = \mu l/U \quad (3-26)$$

and the unit of mass by m . In contract to Glauert's choice of l as the unit of length, however, it is more in keeping with modern practice to choose U as the unit of velocity, whence the derived unit of length is $U\tau = \mu l$. In this connection, it should be remarked that the length l is still undefined, and it will be found expedient to define it differently in dealing with the longitudinal and lateral equations.

3.2.1.3 Dimensionless Longitudinal Stability Equations. The longitudinal equations of (3-18) now will be placed in dimensionless form, following the discussion of the preceding section. Throughout this section the characteristic length l will be chosen as the mean aerodynamic chord c , so that the relative density parameter becomes

$$\mu = m/\rho S c \quad (3-27)$$

In addition, it is convenient to introduce the moment of inertia parameter

$$K_B = I_{yy}/mc^2 = \frac{h_y^2}{c^2} \quad (3-28)$$

Based on the choices of T and U as units of time and velocity, the dimensionless variables are defined as follows:

$$\bar{t} = t/\tau = Ut/\mu l \quad (3-29)$$

$$\bar{u} = u/U \quad (3-30)$$

$$\bar{w} = w/U \quad (3-31)$$

The variable θ , being already dimensionless, requires no modification.

The non-dimensional forms of the stability derivatives in conventional notation are (see Section II-14 of Reference 4 for detailed derivations):

$$\frac{\partial X}{\partial u} = -\rho U S (C_D + C_{Du}), \quad C_{Du} = \frac{U}{2} \left(\frac{\partial C_D}{\partial u} \right) \quad (3-32)$$

$$\frac{\partial Z}{\partial u} = -\rho U S (C_L + C_{Lu}), \quad C_{Lu} = \frac{U}{2} \left(\frac{\partial C_L}{\partial u} \right) \quad (3-33)$$

$$\frac{\partial M}{\partial u} = \rho U S c (C_m + C_{mu}), \quad C_{mu} = \frac{U}{2} \left(\frac{\partial C_m}{\partial u} \right) \quad (3-34)$$

$$\frac{\partial X}{\partial w} = \frac{1}{2} \rho U S (C_L - C_{D\alpha}), \quad C_{D\alpha} = \frac{\partial C_D}{\partial \alpha} \quad (3-35)$$

$$\frac{\partial Z}{\partial w} = -\frac{1}{2} \rho U S (C_{L\alpha} + C_D), \quad C_{L\alpha} = \frac{\partial C_L}{\partial \alpha} \quad (3-36)$$

$$\frac{\partial M}{\partial w} = \frac{1}{2} \rho U S c C_{m\alpha}, \quad C_{m\alpha} = \frac{\partial C_m}{\partial \alpha} \quad (3-37)$$

$$\frac{\partial M}{\partial \dot{w}} = \frac{1}{4} \rho S c^2 C_{m\dot{\alpha}}, \quad C_{m\dot{\alpha}} = \frac{\partial C_m}{\partial \left(\frac{\partial \alpha}{\partial t} \right)} \quad (3-38)$$

$$\frac{\partial Z}{\partial q} = -\frac{1}{4} \rho U s c C_{Lq}, \quad C_{Lq} = \frac{\partial C_L}{\partial \left(\frac{qc}{2U}\right)} \quad (3-39)$$

$$\frac{\partial M}{\partial q} = \frac{1}{4} \rho U s c^2 C_{mq}, \quad C_{mq} = \frac{\partial C_m}{\partial \left(\frac{qc}{2U}\right)} \quad (3-40)$$

$$X_i = -\frac{1}{2} \rho U^2 s C_D, \quad (3-41)$$

$$Z_i = -\frac{1}{2} \rho U^2 s C_L, \quad (3-42)$$

$$M_i = \frac{1}{2} \rho U^2 s c C_m, \quad (3-43)$$

The "input coefficients" (C_D , C_L , C_m) usually will be associated with control surface deflections, but there is no need to restrict them at this point.

Substituting (3-27) - (3-43) above in (3-18), using (3-24) to eliminate g , and replacing θ_0 by γ_0 , the initial angle of climb, there result the dimensionless equations

$$\frac{d\bar{U}}{d\bar{t}} + (C_D + C_{Du})\bar{U} + \frac{1}{2}(C_{Da} - C_L)\bar{W} + \frac{1}{2}C_L\theta = -\frac{1}{2}C_D, \quad (3-44a)$$

$$(C_L + C_{Lu})\bar{U} + \frac{d\bar{W}}{d\bar{t}} + \frac{1}{2}(C_{La} + C_D)\bar{W} - \left(1 - \frac{C_{Lg}}{2\bar{U}}\right)\frac{d\theta}{d\bar{t}} + \frac{1}{2}C_L \tan \gamma_0 \theta = -\frac{1}{2}C_L, \quad (3-44b)$$

$$-\mu(C_m + C_{m\alpha})\bar{U} - \frac{C_{m\dot{\alpha}}}{4} \frac{d\bar{W}}{d\bar{t}} - \frac{\mu}{2} C_{m\alpha} \bar{W} + K_B \frac{d^2\theta}{d\bar{t}^2} - \frac{C_{m\dot{\theta}}}{4} \frac{d\theta}{d\bar{t}} = \frac{\mu}{2} C_m, \quad (3-44c)$$

The fact that the displacement θ introduces no aerodynamic forces makes it convenient to introduce θ and the dimensionless angular velocity

$$\bar{q} = \tau q = \frac{d\theta}{d\bar{t}} = \frac{m}{\rho S U} q \quad (3-45)$$

as separate coordinates. The result is to replace (3-44a, b, c) by four, first order equations, consisting of (3-44a, b, c) with $(d\theta/d\bar{t})$ replaced by \bar{q} , and (3-45). These first order equations have the advantage of being more directly adaptable to a differential analyzer.

In connection with the assumption that μ is large, it may be noted that $(4\mu)^{-1} C_{L_q}$ is negligible compared with one in the coefficient of $(d\theta/d\bar{t})$ in (3-44b). On the other hand, terms not containing the μ factor in (3-44c) may not be omitted (there being no terms dominating them). In addition, for all practical configurations (stalled flight excepted) C_D may be neglected compared with C_{L_α} in (3-44b).

The manipulation of the stability equations and their extension to the elastic airframe is expedited by placing them in the matrix form

$$\underline{C}^{(r)} \underline{y}^{(r)} = \underline{F}^{(r)} \quad (3-46)$$

where $\underline{y}^{(r)}$ denotes the dependent variable, column matrix*

$$\underline{y}^{(r)} = \left\{ \frac{u}{U}, \frac{w}{U}, \tau q, \theta \right\} \quad (3-47)$$

* Column matrices will be designated by braces.

$\underline{F}^{(r)}$ the "forcing" or "input" column matrix

$$\underline{F}^{(r)} = \frac{1}{2} \left\{ -C_{D_i}, -C_{L_i}, \mu C_{m_i}, 0 \right\} \quad (3-48)$$

$\underline{C}^{(r)}$ the square matrix (neglecting $C_{L_q}/4\mu$ compared with one and C_D compared with C_{L_α})

$$\underline{C}^{(r)} = \begin{bmatrix} \lambda + (C_D + C_{D_u}) & \frac{1}{2}(C_{D_\alpha} - C_L) & 0 & \frac{1}{2}C_L \\ C_L + C_{L_u} & \lambda + \frac{1}{2}C_{L_\alpha} & -1 & \frac{1}{2}C_L \tan \gamma \\ -\mu(C_m + C_{m_u}) & -\frac{C_{m_\alpha}}{4}\lambda - \frac{\mu}{2}C_{m_\alpha} & K_B\lambda - \frac{C_{m_q}}{4} & 0 \\ 0 & 0 & -1 & \lambda \end{bmatrix} \quad (3-49)$$

and λ the dimensionless operator defined by

$$\lambda = \frac{d}{dt} = \tau \frac{d}{dt} = \frac{m}{\rho S U} \frac{d}{dt} \quad (3-50)$$

The superscript r on these matrices signifies that they apply only to the rigid airplane (see (3-97) - (3-104)) for the corresponding results for the elastic airplane) and may be dropped if there is no danger of confusion. In addition, a superscript "s" could be added to denote their connection with the symmetric, or longitudinal motion (in contrast to the antisymmetric, or lateral motion), but the type of motion usually will be clear from the context of the discussion.

3.2.1.4 Dimensionless Lateral Stability Equations. In transforming the lateral equations of (3-19) to dimensionless form the characteristic length l will be chosen as the wing span b , so that the relative density parameter becomes

$$\mu = m/\rho S b \quad (3-51)$$

while the required moment of inertia parameters are defined according to

$$K_A = I_{xx}/mb^2 = K_x^2 \quad (3-52)$$

$$K_C = I_{zz}/mb^2 = K_z^2 \quad (3-53)$$

$$K_{AC} = I_{xz}/mb^2 = K_{xz} \quad (3-54)$$

The dimensionless time \bar{t} remains as defined in (3-29), being independent of the choice of characteristic length. The dimensionless sideslip velocity is denoted by

$$\beta = v/u \quad (3-55)$$

while the roll and yaw angles, ϕ and ψ , require no modification.

The non-dimensional forms of the stability derivatives in conventional notation are (cf. Section II-14, of Reference 4):

$$\frac{\partial Y}{\partial v} = \frac{1}{2} \rho U s C_{Y\beta} \quad , \quad C_{Y\beta} = \frac{\partial C_Y}{\partial \beta} \quad (3-56)$$

$$\frac{\partial L}{\partial v} = \frac{1}{2} \rho U s b C_{L\beta} \quad , \quad C_{L\beta} = \frac{\partial C_L}{\partial \beta} \quad (3-57)$$

$$\frac{\partial N}{\partial v} = \frac{1}{2} \rho U s b C_{N\beta} \quad , \quad C_{N\beta} = \frac{\partial C_N}{\partial \beta} \quad (3-58)$$

$$\frac{\partial N}{\partial \dot{v}} = \frac{1}{4} \rho s b^2 C_{N\dot{\beta}} \quad , \quad C_{N\dot{\beta}} = \frac{\partial C_N}{\partial (\frac{\dot{\beta} b}{2U})} \quad (3-59)$$

$$\frac{\partial Y}{\partial p} = \frac{1}{4} \rho U s b C_{Yp} \quad , \quad C_{Yp} = \frac{\partial C_Y}{\partial (\frac{pb}{2U})} \quad (3-60)$$

$$\frac{\partial L}{\partial p} = \frac{1}{4} \rho U s b^2 C_{Lp} \quad , \quad C_{Lp} = \frac{\partial C_L}{\partial (\frac{pb}{2U})} \quad (3-61)$$

$$\frac{\partial N}{\partial p} = \frac{1}{4} \rho U s b^2 C_{Np} \quad , \quad C_{Np} = \frac{\partial C_N}{\partial (\frac{pb}{2U})} \quad (3-62)$$

$$\frac{\partial Y}{\partial r} = \frac{1}{4} \rho U s b C_{Yr} \quad , \quad C_{Yr} = \frac{\partial C_Y}{\partial (\frac{rb}{2U})} \quad (3-63)$$

$$\frac{\partial L}{\partial r} = \frac{1}{4} \rho U s b^2 C_{Lr} \quad , \quad C_{Lr} = \frac{\partial C_L}{\partial (\frac{rb}{2U})} \quad (3-64)$$

$$\frac{\partial N}{\partial r} = \frac{1}{4} \rho U s b^2 C_{Nr} \quad , \quad C_{Nr} = \frac{\partial C_N}{\partial (\frac{rb}{2U})} \quad (3-65)$$

$$Y_i = \frac{1}{2} \rho U^2 s C_{Y_i} \quad (3-66)$$

$$L_i = \frac{1}{2} \rho U^2 s b C_{L_i} \quad (3-67)$$

$$N_i = \frac{1}{2} \rho U^2 s b C_{N_i} \quad (3-68)$$

As in the longitudinal analysis, the input coefficients (C_{y_1} , C_{η_1} , C_{n_1}) are not restricted as to source, albeit usually generated by control surface (aileron or rudder) deflections.

Substituting (3-51) - (3-68) above in (3-19 a,b,c) and proceeding as in the longitudinal analysis, there result the dimensionless equations

$$\frac{d\beta}{d\bar{t}} - \frac{1}{2}C_{y\beta}\beta - \frac{C_{yp}}{4\mu}\frac{d\phi}{d\bar{t}} - \frac{1}{2}C_L\phi + \left(1 - \frac{C_{yr}}{4\mu}\right)\frac{d\psi}{d\bar{t}} - \frac{1}{2}C_L\tan\gamma\psi = \frac{1}{2}C_{y_1} \quad (3-69a)$$

$$-\frac{\mu}{2}C_{\ell\beta}\beta + K_A\frac{d^2\phi}{d\bar{t}^2} - \frac{1}{4}C_{\ell p}\frac{d\phi}{d\bar{t}} - K_{AC}\frac{d^2\psi}{d\bar{t}^2} - \frac{1}{4}C_{\ell r}\frac{d\psi}{d\bar{t}} = \frac{\mu}{2}C_{\ell_1} \quad (3-69b)$$

$$-\frac{1}{4}C_{n\beta}\frac{d\beta}{d\bar{t}} - \frac{\mu}{2}C_{n\beta}\beta - K_{AC}\frac{d^2\phi}{d\bar{t}^2} - \frac{1}{4}C_{np}\frac{d\phi}{d\bar{t}} + K_C\frac{d^2\psi}{d\bar{t}^2} - \frac{1}{4}C_{nr}\frac{d\psi}{d\bar{t}} = \frac{\mu}{2}C_{n_1} \quad (3-69c)$$

Alternatively, following the longitudinal analysis and introducing the angular velocities and angular displacements as separate coordinates, (3-69) may be recast in the matrix form

$$\underline{C}^{(r)}\underline{V}^{(r)} = \underline{F}^{(r)} \quad (3-70)$$

$$\underline{V}^{(r)} = \{\beta, \tau p, \tau r, \phi, \psi\} \quad (3-71)$$

$$\underline{F}^{(r)} = \frac{1}{2}\{C_{y_1}, \mu C_{\ell_1}, \mu C_{n_1}, 0, 0\} \quad (3-72)$$

$$\underline{C}^{(r)} = \begin{bmatrix} \lambda - \frac{1}{2}C_{y\beta} & -\frac{C_{yp}}{4\mu} & \left(1 - \frac{C_{yr}}{4\mu}\right) & -\frac{1}{2}C_L & -\frac{1}{2}C_L\tan\gamma \\ -\frac{\mu}{2}C_{\ell\beta} & K_A\lambda - \frac{1}{4}C_{\ell p} & -K_{AC}\lambda - \frac{1}{4}C_{\ell r} & 0 & 0 \\ -\frac{C_{n\beta}}{4}\lambda - \frac{\mu}{2}C_{n\beta} & K_{AC}\lambda - \frac{1}{4}C_{np} & K_C\lambda - \frac{1}{4}C_{nr} & 0 & 0 \\ 0 & -1 & 0 & \lambda & 0 \\ 0 & 0 & -1 & 0 & \lambda \end{bmatrix} \quad (3-73)$$

If necessary, a superscript "a" could be added to these matrices to denote their connection with the antisymmetric or lateral motion.

3.2.2 Dynamic Stability Equations for Elastic Airplane

3.2.2.1 Longitudinal Stability Equations for Elastic Airframe. In dealing with the longitudinal, or symmetric motion of an elastic airplane, only the transverse (z) deflections are of aerodynamic importance. In the case where the airframe is divided into a number of rigid segments, the torsion is, of course, of aerodynamic importance also, but in the following formulation torsion is assumed to be taken into account by appropriate choice of the h_i with respect to the elastic axis (or other nodal line for twist). Moreover, in virtue of the fact that changes in u, the fore and aft velocity perturbation, can occur only very slowly (compared with the motions of elastic deformation), the aeroelastic modifications of the derivatives entering the u equation may be calculated on a quasi-static basis (see Section 3.2.2.3), and only the w and q equations need be considered in the following discussion. To be investigated are the effects of the motions of the center of gravity on the flexible degrees of freedom, the mutual effects of the elastic degrees of freedom, and finally the effects of the flexibility on the rigid equations. Using the complete equation approach, quasi-static or steady state corrections for transverse deflections are not needed for the rigid derivatives as these effects are accounted for in the above mentioned flexibility calculations. Simplifications to the complete equations are treated at the end of this chapter.

Let the transverse deflections at points $i = 1, 2, \dots, n$ be incorporated in a column matrix* $\underline{z}^{(e)}$ according to

$$\underline{z}^{(e)} = \underline{\ell} \underline{h} = \underline{\ell} \{h_i(x_i, y_i, \bar{t})\} \quad (3-74)$$

where h_i is the deflection of the i'th point, rendered dimensionless with respect to the characteristic length ℓ (eventually ℓ will be chosen as the mean aerodynamic chord in the longitudinal equations, but there is no need to restrict its choice until the equations governing elastic deflections are combined with those governing rigid body motion) and as a function of the coordinates (x_i, y_i) and the dimensionless time \bar{t} . Further, let the transverse deflection at the point i due to a transverse force f_j at the

point j be given by $z_i = (\ell^2/B) a_{ij} f_j$, where B** is a characteristic stiffness (e.g., B is $Ed^3/12(1 - \mu^2)$ for a thin plate of flexural modulus E, thickness d, and Poisson ratio μ), and a_{ij} is a dimensionless influence coefficient (cf. Section 4.1.1.1, where the a_{ij} are not dimensionless);

then the response to the column matrix of forces \underline{f} may be exhibited in the form

$$\underline{z}^{(e)} = [\ell^2/B] \underline{a} \underline{f}, \quad \underline{a} = [a_{ij}] \quad (3-75)$$

* The matrix notation used herein follows that of Reference 12. All symbols representing matrices are underscored.

** The units of B are lb-ft = $L^2 \text{ MT}^{-2}$.

where \underline{a} denotes the square influence matrix comprising the set of influence coefficients.

The forces comprised by \underline{f} may be distinguished as either aerodynamic or inertial, writing

$$\underline{f} = F_{\text{aero}} + F_{\text{c.g. accel.}} + F_{\text{weight}} + F_{\text{elastic}},$$

$$\underline{f} = -\frac{1}{2}\rho U^2 S \underline{A} \underline{c}_l + m \underline{M} [\underline{U}_q - \dot{\underline{w}} + \dot{\underline{q}} \underline{x}_i - g \sin \gamma \underline{e}] - m \underline{M} \ddot{\underline{z}}^{(e)} \quad (3-76)$$

where \underline{A} is a diagonal matrix comprising the dimensionless (with respect to s) areas associated with the individual points*, viz.

$$\underline{A} = \begin{bmatrix} A_1 & 0 & 0 & 0 & \text{---} & \text{---} & \text{---} \\ 0 & A_2 & 0 & 0 & \text{---} & \text{---} & \text{---} \\ 0 & 0 & A_3 & 0 & \text{---} & \text{---} & \text{---} \\ \text{---} & \text{---} & \text{---} & \text{---} & \text{---} & \text{---} & \text{---} \end{bmatrix} \quad (3-77)$$

\underline{c}_l is a column matrix comprising the local lift coefficients at the points, \underline{M} is a diagonal matrix comprising the dimensionless (with respect to m , the total airplane mass) masses associated with the points, the braces denote a column matrix having as its elements the reversed transverse accelerations due to the rigid body motion, and $\ddot{\underline{z}}^{(e)}$ is the acceleration matrix resulting from elastic motion. If the acceleration terms are rendered dimensionless by introducing the notation of the preceding sections (using the length ℓ in defining $\underline{\mu}$) and (1) above and the column matrices**

$$\underline{1} = \{1\} \quad (3-78)$$

$$\underline{\xi} = \ell^{-1} \{x_i\} \quad (3-79)$$

* In dealing with non-planar portions of the airframe, such as the fuselage, the A_i must be defined as equivalent areas to which the C_{l_i} are referred

(but usually aerodynamic forces on such surfaces may be neglected). In general it is not convenient to choose all the area elements equal, but if such a choice is made, the matrix \underline{A} may be replaced by a scalar, viz. the dimensionless element of area.

** n.b., $\underline{1}$ is a unit column matrix, whereas the standard unit (square) matrix is denoted by \underline{I} .

(3) may be rewritten

(3-80)

$$\underline{f} = -\frac{1}{2} \rho U^2 S \left[\underline{A} \underline{c}_\ell + 2 \underline{M} \underline{1} (\lambda \bar{w} - \bar{q} + \frac{1}{2} C_L \tan \delta \theta) - 2 \mu^{-1} \underline{M} \underline{f} \lambda \bar{q} + 2 \mu^{-1} \lambda^2 \underline{M} \underline{h} \right]$$

It may be noted that $\underline{M} \underline{1}$ is a column matrix having the elements M_i of the diagonal matrix \underline{M} , while $\underline{M} \underline{f}$ is a column matrix having the elements $M_i x_i / \ell$.

The lift coefficient matrix \underline{c}_ℓ may be conveniently decomposed according to

$$\underline{c}_\ell = 2 \left(\frac{U}{U} \right) (\underline{c}_{\ell_0} + \underline{c}_{\ell_u}) + 2 \underline{P} \underline{\alpha} + \underline{c}_{\ell_i} \quad (3-81)$$

representing the effects of change in flight velocity, change in incidence (due to both rigid body and elastic motions), and input disturbances, respectively. Autopilot terms must be regarded as included in the input coefficient \underline{c}_{ℓ_i} , but it should be emphasized that the autopilot response may depend on both the rigid body and elastic motions (the latter in consequence of the locations of sensing elements), so that such terms should be separated out in the final equations, (3-97) - (3-104) below. The column matrix \underline{c}_{ℓ_0} comprises

the equilibrium values of local lift coefficient, and \underline{c}_{ℓ_u} is defined by (cf. 3.2.1.3 (3-33))

$$\underline{c}_{\ell_u} = \frac{U}{2} \frac{\partial \underline{c}_{\ell_0}}{\partial u} \quad (3-82)$$

$2 \underline{P}$ is a square matrix (the factor of 2 being simply a convenience) by which the (column) incidence matrix* $\underline{\alpha}$ must be multiplied to obtain the corresponding (column) lift coefficient matrix (cf. Chapter V, Basic Wing Problem). The incidence matrix is given by

$$\underline{\alpha} = \underline{U}^{-1} (\underline{W} \underline{1} - \underline{q} \underline{x} + \underline{\dot{z}}^{(e)} + \frac{\partial \underline{z}}{\partial x}) \quad (3-83a)$$

$$= \bar{W} \underline{1} - \mu^{-1} \bar{q} \underline{1} \underline{f} + (\underline{D} + \mu^{-1} \lambda) \underline{h} \quad (3-83b)$$

where \underline{D} is a streamwise differentiation, square matrix defined in such a way that

$$\underline{D}(\underline{\quad}) = \left\{ \frac{\partial(\underline{\quad})_i}{\partial(x/\ell)} \right\} \quad (3-84)$$

* It should be emphasized that $\underline{\alpha}$ represents a distribution of local incidence and not simply the rigid wing angle of attack.

The determination of the matrix \underline{P} rests on aerodynamic theory and will be discussed further in Chapter V, but it should be specifically remarked that, in consequence of induction effects, \underline{P} is not generally diagonal (but if the only deflecting aerodynamic surface were a wing with chordwise sections selected as the area elements A_i strip theory would render \underline{P} diagonal).

It also may be remarked that \underline{P} may contain the time differentiation operator λ unless the quasi-steady hypothesis is invoked; in particular, \underline{P} is assumed to account for downwash lag when operating on w .

If (3-74) and (3-80) are substituted in (3-75) and if (3-81) and (3-83b) are introduced, the result may be placed in the form:

$$\begin{aligned} h = & - \left[\frac{\rho U^2 \ell}{B} \right] a \left[\underline{A}(\underline{C}_{\ell_0} + \underline{C}_{\ell_u}) \bar{u} + (\underline{M}\lambda + \underline{A}\underline{P}) \underline{1} \bar{w} - (\mu^{-1} \underline{M} \underline{\mathcal{P}} \lambda + \mu^{-1} \underline{A} \underline{P} \underline{\mathcal{P}} + \underline{M} \underline{1}) \bar{q} \right. \\ & \left. + \frac{1}{2} C_L \tan \delta \underline{M} \underline{1} \theta + (\mu^{-1} \underline{M} \lambda^2 + \mu^{-1} \underline{A} \underline{P} \lambda + \underline{A} \underline{P} \underline{D}) h + \frac{1}{2} \underline{A} \underline{C}_{\ell_1} \right] \end{aligned} \quad (3-85)$$

Introducing the aeroelastic parameter

$$\kappa = B / \rho U^2 \ell \quad (3-86)$$

(3-85) may be written in the form

$$\begin{aligned} & a \underline{A}(\underline{C}_{\ell_0} + \underline{C}_{\ell_u}) \bar{u} + a (\underline{M}\lambda + \underline{A}\underline{P}) \underline{1} \bar{w} - a (\mu^{-1} \underline{M} \underline{\mathcal{P}} \lambda + \underline{M} \underline{1} + \mu^{-1} \underline{A} \underline{P} \underline{\mathcal{P}}) \bar{q} \quad (3-87) \\ & + \frac{1}{2} C_L \tan \delta a \underline{M} \underline{1} \theta + (\mu^{-1} a \underline{M} \lambda^2 + \mu^{-1} a \underline{A} \underline{P} \lambda + a \underline{A} \underline{P} \underline{D} + \kappa \underline{I}) h = - \frac{1}{2} a \underline{A} \underline{C}_{\ell_1} \end{aligned}$$

where \underline{I} denotes the unit (diagonal) matrix.

The foregoing development was based on the influence matrix a because of its conceptual simplicity, the greater ease (compared with the stiffness matrix) with which it may be determined experimentally and the fact that it is required if the dominant mode of natural oscillation is to be calculated by matrix iteration. Alternatively, (3-75) may be replaced by the inverse relation

$$\underline{f} = (B / \ell^2) \underline{K} \underline{\hat{z}}^{(e)}, \quad \underline{K} = \underline{a}^{-1} \quad (3-88)$$

where the (dimensionless) stiffness matrix \underline{k} is the inverse of \underline{a} . Premultiplying (3-87) by \underline{k} then yields (since $\underline{a}^{-1}\underline{a} = \underline{I}$, the unit matrix)

$$\underline{A}(\underline{c}_{\ell_0} + \underline{c}_{\ell_u})\underline{q} + (\underline{M}\lambda + \underline{A}\underline{P})\underline{z}\underline{w} - (\mu^{-1}\underline{M}\underline{g}\lambda + \underline{M}\underline{z} + \mu^{-1}\underline{A}\underline{P}\underline{g})\underline{\bar{q}} + \frac{1}{2}\underline{c}_L \tan \gamma \underline{M}\underline{z}\underline{\theta} + (\mu^{-1}\underline{M}\lambda^2 + \mu^{-1}\underline{A}\underline{P}\lambda + \underline{A}\underline{P}\underline{D} + \underline{x}\underline{k})\underline{h} = -\frac{1}{2}\underline{A}\underline{c}_\ell. \quad (3-89)$$

A second modification of (3-87) might be motivated by the fact that it could be more expedient to deal with the inverse aerodynamic matrix \underline{P}^{-1} , rather than \underline{P} . Thus, the usual aerodynamic problem requires the solution of an integral equation to obtain the lift distribution from a prescribed incidence distribution, and the resulting matrix formulation is (including only the effects of incidence)

$$\underline{P}^{-1}\underline{c}_\ell = 2\underline{\alpha} \quad (3-90)$$

Then, rather than invert (3-90) directly, (3-89) may be premultiplied by $\underline{P}^{-1}\underline{A}^{-1}$ to obtain the modified result

$$2(\underline{\alpha}_0 + \underline{\alpha}_u)\underline{q} + (\underline{Q}\lambda + \underline{z})\underline{w} - (\mu^{-1}\underline{Q}\underline{g}\lambda + \underline{Q}\underline{z} + \mu^{-1}\underline{g})\underline{\bar{q}} + \frac{1}{2}\underline{c}_L \tan \gamma \underline{Q}\underline{z}\underline{\theta} + (\mu^{-1}\underline{Q}\lambda^2 + \mu^{-1}\underline{z}\lambda + \underline{D} + \underline{x}\underline{P}^{-1}\underline{A}^{-1}\underline{k})\underline{h} = -\underline{\alpha}_1, \quad (3-91)$$

where \underline{Q} denotes the matrix

$$\underline{Q} = \underline{P}^{-1}\underline{A}^{-1}\underline{M} \quad (3-92)$$

and the $\underline{\alpha}$ matrices are defined according to (3-90), viz.

$$\underline{P}^{-1}\underline{c}_{\ell_0} = 2\underline{\alpha}_0 \quad (3-93a)$$

$$\underline{P}^{-1}\underline{c}_{\ell_u} = 2\underline{\alpha}_u \quad (3-93b)$$

$$\underline{P}^{-1}\underline{c}_{\ell_1} = 2\underline{\alpha}_1 \quad (3-93c)$$

The $\underline{\alpha}_0$ and $\underline{\alpha}_1$ matrices will be specified directly in most problems, so that (3-93a) and (3-93c) need not be solved; however, the matrix $\underline{\alpha}_u$ does not represent a true incidence and must be evaluated via (3-93b).

The matrix equations (3-89) will be designated as the basic description of the elastic degrees of freedom, although it often might prove more convenient to choose one of the alternative forms (3-87) or (3-91). It then remains to calculate the aeroelastic forces introduced in the original, rigid body equations. As remarked earlier, the aeroelastic contribution to the X component of force will be neglected except insofar as the equilibrium values of the stability derivatives in the \bar{u} equation are modified for static deflections.

The summation over the entire airplane of the aeroelastic contribution to the Z force is given by the sum of those elements in \underline{f} that arise from elastic deflection, viz. (cf. (3-80) and (3-83b)),

$$\underline{Z}^{(e)} = -\rho U^2 S \underline{1}' (\mu^{-1} \underline{M} \lambda^2 + \mu^{-1} \underline{A} \underline{P} \lambda + \underline{A} \underline{P} \underline{D}) \underline{h} \quad (3-94)$$

since the effect of multiplying a column matrix by the unit, row matrix $\underline{1}'$ (the transpose of the unit, column matrix $\underline{1}$) is to sum the elements of the former. Similarly, $M^{(e)*}$ is obtained by summing the products of the elastic deflection elements of \underline{f} and the $-x_i$ components; this operation may be effected by premultiplication by $-\underline{\ell} \underline{\xi}$, viz.

$$M^{(e)} = \rho U^2 S \underline{\ell} \underline{\xi}' (\mu^{-1} \underline{M} \lambda^2 + \mu^{-1} \underline{A} \underline{P} \lambda + \underline{A} \underline{P} \underline{D}) \underline{h} \quad (3-95)$$

The modified equations of motion for \bar{w} and \bar{q} then follow after setting $\underline{\ell} = c$ and subtracting $(\rho U^2 S)^{-1} \underline{Z}^{(e)}$ and $\mu (\rho U S^2)^{-1} M^{(e)}$ from the left hand sides of (3-44b) and (3-44c), respectively, with the results

$$\begin{aligned} (C_L + C_{L_u}) \bar{u} + [\lambda + \frac{1}{2}(C_{L_\alpha} + C_D)] \bar{w} - (1 - \frac{C_{L_\beta}}{4\mu}) \bar{q} + \frac{1}{2} C_L \tan \gamma \theta \\ + \underline{1}' (\mu^{-1} \underline{M} \lambda^2 + \mu^{-1} \underline{A} \underline{P} \lambda + \underline{A} \underline{P} \underline{D}) \underline{h} = -\frac{1}{2} C_L \end{aligned} \quad (3-96a)$$

$$\begin{aligned} -\mu (C_m + C_{m_u}) \bar{u} - (\frac{C_{m_\alpha}}{4} \lambda + \frac{\mu}{2} C_{m_\alpha}) \bar{w} + (K_B \lambda - \frac{C_{m_\beta}}{4}) \bar{q} \\ - \underline{\xi}' (\underline{M} \lambda^2 + \underline{A} \underline{P} \lambda + \mu \underline{A} \underline{P} \underline{D}) \underline{h} = \frac{\mu}{2} C_m, \end{aligned} \quad (3-96b)$$

* $M^{(e)}$ = elastic moment.

The original, matrix formulation of the longitudinal stability equations for the rigid airframe, as set forth in (3-46) - (3-49), now may be extended to the elastic airframe by combining (3-89) and (3-96a,b) above with (3-44a) and (3-45). The results are

$$\underline{C}^{(e)} \underline{v}^{(e)} = \underline{F}^{(e)} \quad (3-97)$$

where $\underline{v}^{(e)}$ denotes the partitioned column matrix

$$\underline{v}^{(e)} = \{ \underline{v}^{(r)} \mid \underline{h} \} \quad (3-98)$$

$$= \{ \frac{u}{U}, \frac{w}{U}, \tau q, \theta \mid h_i \} \quad (3-99)$$

$\underline{F}^{(e)}$ the partitioned column matrix

$$\underline{F}^{(e)} = \{ \underline{F}^{(r)} \mid -\frac{1}{2} \underline{A} \underline{C}_q \} \quad (3-100)$$

and $\underline{C}^{(e)}$ the partitioned square matrix

$$\underline{C}^{(e)} = \begin{bmatrix} \underline{C}^{(r)} & \mid & \underline{R}^{(e)} \\ \hline \underline{E}^{(r)} & \mid & \underline{E}^{(e)} \end{bmatrix} \quad (3-101)$$

In this last matrix, $\underline{C}^{(r)}$ is the rigid body matrix given by (3-49), $\underline{R}^{(e)}$ denotes the column of row matrices comprising the aeroelastic forces in the rigid body mode equations, viz.

$$\begin{aligned} \underline{R}^{(e)} = \{ & 0, (\mu^{-1} \underline{1}' \underline{M} \lambda^2 + \mu^{-1} \underline{1}' \underline{A} \underline{P} \lambda + \underline{1}' \underline{A} \underline{P} \underline{D}), \\ & -(\underline{\xi}' \underline{M} \lambda^2 + \underline{\xi}' \underline{A} \underline{P} \lambda + \mu \underline{\xi}' \underline{A} \underline{P} \underline{D}), 0 \} \end{aligned} \quad (3-102)$$

$\underline{E}^{(r)}$ the row of column matrices comprising the rigid body mode forces in the elastic mode equations, viz. (cf. (3-89))

$$\underline{E}^{(r)} = [\underline{A}(\underline{C}_{\ell_0} + \underline{C}_{\ell_q}) ; (\underline{M} \underline{1} \lambda + \underline{A} \underline{P} \underline{1}) ; (\mu^{-1} \underline{M} \underline{\xi} \lambda + \mu^{-1} \underline{A} \underline{P} \underline{\xi} + \underline{M} \underline{1}) ; \frac{1}{2} \underline{C}_{L \tan \gamma} \underline{M} \underline{1}] \quad (3-103)$$

and $\underline{E}^{(e)}$ the square matrix

$$\underline{E}^{(e)} = \mu^{-1} \underline{M} \lambda^2 + \mu^{-1} \underline{A} \underline{P} \lambda + (\underline{A} \underline{P} \underline{D} + \underline{\kappa} \underline{\kappa}) \quad (3-104)$$

It again should be emphasized that the formulation of (3-97) - (3-104) does not include autopilot terms explicitly, but that such terms may be regarded as included implicitly in the input matrix \underline{c}_{ℓ_1} . To recover an ex-

PLICIT formulation it would be necessary to: (a) introduce an appropriate equations (s) for the autopilot degree(s) of freedom, allowing, in particular, for the effect of the elastic deflection \underline{h} on the autopilot sensing elements; and (b) separate out the autopilot terms from \underline{c}_{ℓ_1} , and therefore $\underline{F}^{(e)}$, and incorporate them on the left hand side of (3-97) by introducing the appropriate, additional terms in $\underline{C}^{(e)}$. As mentioned in section 3.3, it may be adequate to take the autopilot degrees of freedom into account by means of appropriate, time lag factor.

3.2.2.2 Lateral Stability Equations for Elastic Airframe. The elastic deflections of interest in connection with the lateral stability equations are of three types: (a) the static, symmetric, transverse deflections, which affect the equilibrium values of the angle of attack and dihedral distributions of the wing; (b) the dynamic, anti-symmetric, vertical z deflections, which are produced by all of the lateral motions but which sensibly affect only the rolling moment; (c) the dynamic, lateral (y) deflections of the fuselage and fin, which affect all of the lateral stability derivatives to some extent. The static deflections* must be included in the calculation of the stability derivatives entering the "rigid airframe" equations (3-69) but will not be considered further in this section. It is convenient to treat the antisymmetric, vertical and the lateral deflections separately; the latter, being more closely analogous in effect to the symmetric deflections of longitudinal motion, will be considered first.

* of type (a)

Let the lateral deflections be incorporated in the column matrix

$$\underline{y}^{(e)} = \underline{\ell} \underline{h}_1 \quad (3-105)$$

where $\underline{\ell}$ now denotes a length characteristic of the lateral motions (later to be chosen as the wing span b). Further, following the discussion of Section 3.2.1.4, let \underline{a}_1 be a dimensionless structural influence matrix such that

$$\underline{y}^{(e)} = (\underline{\ell}^2 / B_1) \underline{a}_1 \underline{f}_1 \quad (3-106)$$

The lateral force matrix \underline{f}_1 may be placed in the form (see equation 3-53)

$$\underline{f}_1 = \frac{1}{2} \rho U^2 S \underline{A}_1 \underline{c}_y - m \underline{M}_1 \{ \ddot{v} + U \dot{r} - \dot{p} z_i + \dot{r} x_i - g(\phi \cos \gamma + \psi \sin \gamma) \} - m \underline{M}_1 \ddot{\underline{y}}^{(e)} \quad (3-107)$$

where \underline{A}_1 is a diagonal matrix, defined as in (3-54), \underline{c}_y a column matrix comprising the local side-force coefficients at the points, \underline{M}_1 a similar, mass matrix, and the matrix element in the braces the lateral acceleration at the point located at x_i and z_i . Introducing the previously defined dimensionless notation and column matrices $\underline{1}$ and \underline{z}_1 as defined by (3-7b) and (3-79) as well as

$$\underline{z}_1 = \underline{\ell}^{-1} \{ \underline{z}_i \} \quad (3-108)$$

(3-107) may be rewritten

$$\underline{f}_1 = \rho U^2 S \left(\frac{1}{2} \underline{A}_1 \underline{c}_y - \underline{M}_1 \underline{1} (\lambda \beta + \bar{r} - \frac{1}{2} C_L \phi - \frac{1}{2} C_L \tan \gamma \psi) + \mu^{-1} \underline{M}_1 \lambda (\underline{z}_1 \bar{p} - \underline{\xi}_1 \bar{r}) - \mu^{-1} \lambda^2 \underline{M}_1 \underline{h}_1 \right) \quad (3-109)$$

The local aerodynamic incidence (a positive incidence being one that would produce a positive side force in steady flow) is given by

$$\underline{\alpha}_1 = U^{-1} \{ -v + p z_i - r x_i \} - \frac{\partial \gamma^{(e)}}{\partial x} - U^{-1} \dot{\underline{y}}^{(e)} \quad (3-110a)$$

$$= -\underline{1} \beta + \mu^{-1} \underline{z}_1 \bar{p} - \mu^{-1} \underline{\xi}_1 \bar{r} - (\underline{D} + \mu^{-1} \lambda) \underline{h}_1 \quad (3-110b)$$

where \underline{D} is the streamwise differentiation matrix defined by (3-61). Adding the side force coefficient associated with $\underline{\alpha}_1$ to the input term \underline{c}_{y_1} then yields

(there being no change of flight speed to consider here)

$$\underline{c}_y = -2 \underline{P}_1 (\underline{1} \beta - \mu^{-1} \underline{z}_1 \bar{p} + \mu^{-1} \underline{\xi}_1 \bar{r} + (\underline{D} + \mu^{-1} \lambda) \underline{h}_1) + \underline{c}_{y_1} \quad (3-111)$$

Combining (3-105) - (3-109) and (3-111) and premultiplying by \underline{a}_1^{-1} then yields

$$(\underline{M}_1 \lambda + \underline{A}_1 \underline{P}) \underline{1} \beta - \mu^{-1} (\underline{M}_1 \lambda + \underline{A}_1 \underline{P}) \underline{\xi} \bar{P} - \frac{1}{2} \underline{C}_L \underline{M}_1 \underline{1} \Phi +$$

$$(\mu^{-1} \underline{M}_1 \underline{\xi} \lambda + \mu^{-1} \underline{A}_1 \underline{P} \underline{\xi} + \underline{M}_1 \underline{1}) \bar{r} - \frac{1}{2} \underline{C}_L \tan \gamma \underline{M}_1 \underline{1} \Psi + \quad (3-112)$$

$$(\mu^{-1} \underline{M}_1 \lambda^2 + \mu^{-1} \underline{A}_1 \underline{P} \lambda + \underline{A}_1 \underline{P} \underline{D} + \underline{x}_1 \underline{k}_1) \underline{h}_1 = \frac{1}{2} \underline{A}_1 \underline{C}_y,$$

where

$$\underline{x}_1 = \underline{B}_1 / \rho U^2 S \ell \quad (3-113)$$

$$\underline{k}_1 = \underline{a}_1^{-1} \quad (3-114)$$

Of course, as in (3-64), it may be preferable to deal with the influence matrix \underline{a}_1 rather than the stiffness matrix \underline{k}_1 , but the required modification may be obtained from (3-112) by premultiplying by \underline{a}_1 . Similarly, it may prove convenient to premultiply (3-112) by $\underline{P}_1^{-1} \underline{A}_1^{-1}$ (cf. (3-68)).

The total side force due to the lateral elastic deflection is given by (cf. (3-71))

$$\underline{Y}_1^{(e)} = -\rho U^2 S \underline{1}' (\mu^{-1} \underline{M}_1 \lambda^2 + \mu^{-1} \underline{A}_1 \underline{P} \lambda + \underline{A}_1 \underline{P} \underline{D}) \underline{h}_1 \quad (3-115)$$

while the corresponding rolling and yawing moments are

$$\underline{L}_1^{(e)} = \rho U^2 S \ell \underline{\xi}' (\mu^{-1} \underline{M}_1 \lambda^2 + \mu^{-1} \underline{A}_1 \underline{P} \lambda + \underline{A}_1 \underline{P} \underline{D}) \underline{h}_1 \quad (3-116)$$

$$\underline{N}_1^{(e)} = -\rho U^2 S \ell \underline{\xi}' (\mu^{-1} \underline{M}_1 \lambda^2 + \mu^{-1} \underline{A}_1 \underline{P} \lambda + \underline{A}_1 \underline{P} \underline{D}) \underline{h}_1 \quad (3-117)$$

Turning now to the antisymmetric transverse deflections, let them be incorporated in the matrix (antisymmetric in y)

$$\underline{\ddot{z}}^{(e)} = \ell \underline{h}_2 \quad (3-118)$$

Noting that, in the antisymmetric case, the only rigid body motion contributing to the relevant inertial forces is roll, the corresponding force matrix may be placed in the form

$$\underline{f}_2 = -\frac{1}{2} \rho U^2 \underline{A}_2 \underline{C}_\ell^{(a)} - m \underline{M}_2 \{ \dot{P} \gamma_i \} - m \underline{M}_2 \underline{\ddot{z}}^{(e)} \quad (3-119a)$$

$$= -\rho U^2 S \left[\frac{1}{2} \underline{A}_2 \underline{C}_\ell^{(a)} + \mu^{-1} \underline{M}_2 (\lambda \underline{n}_2 \bar{P} + \lambda^2 \underline{h}_2) \right] \quad (3-119b)$$

where η_2 denotes the column matrix

$$\eta_2 = \ell \{ \gamma_i \} \quad (3-120)$$

and $\underline{c}_\ell^{(a)}$ the antisymmetric (in y) lift coefficient matrix

$$\underline{c}_\ell^{(a)} = \underline{c}_{\ell\beta} \beta + \underline{c}_{\ell p} \left(\frac{pb}{2U} \right) + \underline{c}_{\ell r} \left(\frac{rb}{2U} \right) + 2 \underline{P}_2 (\underline{D} + \mu^{-1} \lambda) h_2 + \underline{c}_{\ell_1}^{(a)} \quad (3-121)$$

The calculation of the local lift coefficient derivatives, $\underline{c}_{\ell\beta}$, $\underline{c}_{\ell p}$ and $\underline{c}_{\ell r}$

is relatively more complex than in the two preceding cases, and further consideration thereof will be delayed until Chapter V. The matrix $\underline{c}_{\ell_1}^{(a)}$ represents the antisymmetric, input forces, including autopilot effects.

Proceeding as before, (3-118) - (3-121) lead to the equations of motion

$$\begin{aligned} \frac{1}{2} \underline{A}_2 \underline{c}_{\ell\beta} \beta + \mu^{-1} (\underline{M}_2 \eta_2 \lambda + \frac{1}{4} \underline{A}_2 \underline{c}_{\ell p}) p + \frac{1}{4} \mu^{-1} \underline{A}_2 \underline{c}_{\ell r} \bar{r} \\ + (\mu^{-1} \underline{M}_2 \lambda^2 + \mu^{-1} \underline{A}_2 \underline{P}_2 \lambda + \underline{A}_2 \underline{P}_2 \underline{D} + \underline{\chi}_2 \underline{K}_2) h_2 = -\frac{1}{2} \underline{A}_2 \underline{c}_{\ell_1}^{(a)} \end{aligned} \quad (3-122)$$

where \underline{K}_2 is the stiffness matrix associated with the antisymmetric set of points in h_2 , and $\underline{\chi}_2$ is obtained by substituting B_2 for B_1 in (3-113). The total rolling moment resulting from the motion h_2 is given by

$$\underline{L}_2^{(e)} = -\rho U^2 s \ell \eta_2' (\mu^{-1} \underline{M}_2 \lambda^2 + \mu^{-1} \underline{A}_2 \underline{P}_2 \lambda + \underline{A}_2 \underline{P}_2 \underline{D}_2) h_2 \quad (3-123)$$

The modified, rigid body mode equations now may be obtained by setting $\ell = b$ and subtracting

$$(\rho U^2 s)^{-1} \gamma_i^{(e)}, \quad \mu (\rho U^2 s \ell)^{-1} (\underline{L}_1^{(e)} + \underline{L}_2^{(e)}),$$

and

$$\mu (\rho U^2 s \ell)^{-1} \underline{N}_i^{(e)}$$

from the left hand sides of (3-69a,b,c), respectively, the end result being

$$(\lambda - \frac{1}{2} C_{\gamma\beta})\beta - \frac{C_{\gamma\bar{p}}}{4\mu}\bar{p} + (1 - \frac{C_{\gamma r}}{4\mu})\bar{r} - \frac{1}{2} C_L \phi - \frac{1}{2} C_L \tan \gamma \psi \\ + \Sigma' (\mu^{-1} M_1 \lambda^2 + \mu^{-1} A_1 P_1 \lambda + A_1 P_1 D) h_1 = \frac{1}{2} C_{\gamma_1} \quad (3-124a)$$

$$-\frac{\mu}{2} C_{\ell\beta} \beta + (K_A \lambda - \frac{1}{4} C_{\ell p})\bar{p} - (K_{AC} \lambda + \frac{1}{4} C_{\ell r})\bar{r} - \Sigma' (M_1 \lambda^2 + A_1 P_1 \lambda + \mu A_1 P_1 D) h_1 \\ + \Sigma'_2 (M_2 \lambda^2 + A_2 P_2 \lambda + \mu A_2 P_2 D) h_2 = \frac{\mu}{2} C_{\ell_1} \quad (3-124b)$$

$$-(\frac{1}{4} C_{n\beta} \lambda + \frac{\mu}{2} C_{n\bar{p}})\beta - (K_{AC} \lambda + \frac{1}{4} C_{n p})\bar{p} + (K_c \lambda - \frac{1}{4} C_{n r})\bar{r} \\ + \Sigma' (M_1 \lambda^2 + A_1 P_1 \lambda + \mu A_1 P_1 D) h_1 = \frac{\mu}{2} C_{n_1} \quad (3-124c)$$

Finally, combining (3-112), (3-122), and (3-124) together with $\bar{p} = \lambda\phi$ and $\bar{r} = \lambda\psi$ the matrix formulation of (3-70)-(3-73) is extended to read

$$\underline{C}^{(e)} \underline{V}^{(e)} = \underline{F}^{(e)} \quad (3-125)$$

$$\underline{V}^{(e)} = \{ \underline{V}^{(r)} \mid h_1 \mid h_2 \} \quad (3-126a)$$

$$= \{ \beta, \tau p, \tau r, \phi, \psi \mid h_{1c} \mid h_{2c} \} \quad (3-126b)$$

$$\underline{F}^{(e)} = \{ \underline{F}^{(r)} \mid \frac{1}{2} A_1 C_{\gamma_1} \mid -\frac{1}{2} A_2 C_{\ell_1}^{(a)} \} \quad (3-127)$$

$$\underline{C}^{(e)} = \begin{bmatrix} \underline{C}^{(r)} & R_1^{(e)} & R_2^{(e)} \\ \underline{E}_1^{(r)} & \underline{E}_1^{(e)} & 0 \\ \underline{E}_2^{(r)} & 0 & \underline{E}_2^{(e)} \end{bmatrix} \quad (3-128)$$

where $\underline{c}^{(r)}$ is given by (3-73) and the remaining terms in (3-128) by

$$\underline{R}_1^{(e)} = \left\{ \underline{1}' (\underline{\mu}^{-1} \underline{M}_1 \lambda^2 + \underline{\mu}^{-1} \underline{A}_1 \underline{P}_1 \lambda + \underline{A}_1 \underline{P}_1 \underline{D}), -\underline{5}' (\underline{M}_1 \lambda^2 + \underline{A}_1 \underline{P}_1 \lambda + \underline{\mu} \underline{A}_1 \underline{P}_1 \underline{D}), \right. \\ \left. \underline{5}' (\underline{M}_1 \lambda^2 + \underline{A}_1 \underline{P}_1 \lambda + \underline{\mu} \underline{A}_1 \underline{P}_1 \underline{D}), 0, 0 \right\} \quad (3-129)$$

$$\underline{R}_2^{(e)} = \left\{ 0, \underline{7}'_2 (\underline{M}_2 \lambda^2 + \underline{A}_2 \underline{P}_2 \lambda + \underline{\mu} \underline{A}_2 \underline{P}_2 \underline{D}), 0, 0, 0 \right\} \quad (3-130)$$

$$\underline{E}_1^{(r)} = \left[(\underline{M}_1 \lambda + \underline{A}_1 \underline{P}_1) \underline{1} \mid -\underline{\mu}^{-1} (\underline{M}_1 \lambda + \underline{A}_1 \underline{P}_1) \underline{5}' \mid \underline{\mu}^{-1} (\underline{M}_1 \lambda + \underline{A}_1 \underline{P}_1) \underline{5} \mid + \underline{M}_1 \underline{1} \mid \right. \\ \left. - \frac{1}{2} C_L \underline{M}_1 \underline{1} \mid - \frac{1}{2} C_L \tan \gamma \underline{M}_1 \underline{1} \right] \quad (3-131)$$

$$\underline{E}_2^{(r)} = \left[\frac{1}{2} \underline{A}_2 C_{\ell \beta} \mid \underline{\mu}^{-1} (\underline{M}_2 \underline{7}_2 \lambda + \frac{1}{4} \underline{A}_2 C_{\ell \beta}) \mid \frac{1}{4} \underline{\mu} \underline{A}_2 C_{\ell r} \mid 0 \mid 0 \right] \quad (3-132)$$

$$\underline{E}_1^{(e)} = \underline{\mu}^{-1} \underline{M}_1 \lambda^2 + \underline{\mu}^{-1} \underline{A}_1 \underline{P}_1 \lambda + \underline{A}_1 \underline{P}_1 \underline{D} + \underline{\alpha}_1 \underline{K}_1 \quad (3-133)$$

$$\underline{E}_2^{(e)} = \underline{\mu}^{-1} \underline{M}_2 \lambda^2 + \underline{\mu}^{-1} \underline{A}_2 \underline{P}_2 \lambda + \underline{A}_2 \underline{P}_2 \underline{D} + \underline{\alpha}_2 \underline{K}_2 \quad (3-134)$$

It is again emphasized that autopilot effects are not included explicitly in the formulation of (3-125) - (3-134) but may be incorporated through $\underline{c}_{\lambda_1}^{(a)}$ and \underline{c}_{y_1} .

3.2.2.3 Quasi-static Solution For Elastic Deflections. If the mass parameter $\underline{\mu}$ is sufficiently large, and λ is not large, as it will not be in those problems where the motion of the airplane as a whole is of principle interest (in the flutter problem, where the elastic motions are of principle interest, λ would be large) it evidently is permissible to omit those terms of $(\underline{\mu}^{-1} \underline{h})$ in (3-85). The neglect of those terms is tantamount to the assumption that the elastic deflections are in phase with the loads that produce them, and the resulting approximation may be designated as "quasi-static". Only the longitudinal equations will be considered in this section, but an entirely similar treatment may be accorded the lateral equations.*

Neglecting the terms of $(\underline{\mu}^{-1} \underline{h})$ in (3-85) and solving for \underline{h} yields (the rigid body motions being as yet undetermined)

* It should be remarked that the method of this section might be used to calculate quasi-static aeroelastic effects on some derivatives (e.g., all \underline{u} derivatives), even though elastic degrees of freedom were incorporated in the complete analysis; moreover, some portions of the airframe might be treated quasi-statically and others by adding degrees of freedom e.g., wing and tail, respectively.

$$\underline{h} = -(\alpha \underline{I} + \underline{a} \underline{A} \underline{P} \underline{D})^{-1} \underline{a} [\underline{A} (\underline{C}_{L_0} + \underline{C}_{L_u}) \bar{u} + (\underline{M} \lambda + \underline{A} \underline{P}) \underline{1} \bar{w}] \quad (3-135)$$

$$-(\mu^{-1} \underline{M} \underline{\xi} \lambda + \mu^{-1} \underline{A} \underline{P} \underline{\xi} + \underline{M} \underline{1}) \bar{q} + \frac{1}{2} C_L \tan \gamma \underline{M} \underline{1} \theta + \frac{1}{2} \underline{A} \underline{C}_{L_i}]$$

The terms in $\mu^{-1} \bar{q}$ also may be neglected in many applications but could prove important in dealing with swept wing or fuselage deflections. Various modifications of (3-135) are possible; thus, if it is desired to make use of the stiffness matrix \underline{k} rather than the influence matrix \underline{a} , (3-135) goes over to

$$\underline{h} = -(\alpha \underline{k} + \underline{A} \underline{P} \underline{D})^{-1} [\underline{A} (\underline{C}_{L_0} + \underline{C}_{L_u}) \bar{u} + (\underline{M} \lambda + \underline{A} \underline{P}) \underline{1} \bar{w} - (\mu^{-1} \underline{M} \underline{\xi} \lambda + \mu^{-1} \underline{A} \underline{P} \underline{\xi} + \underline{M} \underline{1}) \bar{q} + \frac{1}{2} C_L \tan \gamma \underline{M} \underline{1} \theta + \frac{1}{2} \underline{A} \underline{C}_{L_i}] \quad (3-136)$$

The implicit solution of (3-135) may be used for a direct calculation of the aeroelastic forces in the modified, rigid body mode equations of (3-96). Neglecting the terms of $(\mu^{-1} \underline{h})$ in these equations, it is required to calculate $\underline{A} \underline{P} \underline{D} \underline{h}$, which may be evaluated from (3-135) as

$$\underline{A} \underline{P} \underline{D} \underline{h} = -\underline{Y} [\underline{A} (\underline{C}_{L_0} + \underline{C}_{L_u}) + (\underline{M} \lambda + \underline{A} \underline{P}) \underline{1} \bar{w} + \frac{1}{2} \underline{A} \underline{C}_{L_i} - (\mu^{-1} \underline{M} \underline{\xi} \lambda + \mu^{-1} \underline{A} \underline{P} \underline{\xi} + \underline{M} \underline{1}) \bar{q} + \frac{1}{2} C_L \tan \gamma \underline{M} \underline{1} \theta] \quad (3-137)$$

where \underline{Y} represents the aeroelastic inversion matrix

$$\underline{Y} = \underline{A} \underline{P} \underline{D} (\alpha \underline{1} + \underline{a} \underline{A} \underline{P} \underline{D})^{-1} \underline{a} \quad (3-138a)$$

$$= (\alpha \underline{D}^{-1} \underline{P}^{-1} \underline{A}^{-1} + \underline{a})^{-1} \underline{a} \quad (3-138b)$$

$$= (\alpha \underline{D}^{-1} \underline{P}^{-1} \underline{A}^{-1} \underline{k} + \underline{I})^{-1} \quad (3-138c)$$

Substituting (3-137) in (3-96) then yields

$$[(\underline{C}_L + \underline{C}_{L_u}) - \underline{1}' \underline{Y} \underline{A} (\underline{C}_{L_0} + \underline{C}_{L_u})] \bar{u} + [(1 - \underline{1}' \underline{Y} \underline{M} \underline{1}) \lambda + \frac{1}{2} (\underline{C}_{L_a} + \underline{C}_D) - \underline{1}' \underline{Y} \underline{A} \underline{P} \underline{1}] \bar{w} + [\mu^{-1} \underline{1}' \underline{Y} \underline{M} \underline{\xi} \lambda - 1 + \underline{1}' \underline{Y} \underline{M} \underline{1} + \frac{\underline{C}_{L_i}}{q \mu} + \mu^{-1} \underline{1}' \underline{Y} \underline{A} \underline{P} \underline{\xi}] \bar{q} + \frac{1}{2} C_L \tan \gamma (1 - \underline{1}' \underline{Y} \underline{M} \underline{1}) \theta = -\frac{1}{2} (\underline{C}_L - \underline{1}' \underline{Y} \underline{A} \underline{C}_{L_i}) \quad (3-139a)$$

$$\begin{aligned}
& -\mu[(C_m + C_{m_1}) - \xi' Y A (C_{l_0} + C_{l_1})] \bar{u} - \left[\left(\frac{C_{m_0}}{4} - \mu \xi' Y M_1 \right) \lambda + \mu \left(\frac{C_{m_0}}{2} - \xi' Y A P_1 \right) \right] \bar{w} \\
& + \left[\left(K_0 - \xi' Y M_1 \right) \lambda - \frac{C_{m_0}}{4} - \xi' Y A P_1 - \mu \xi' Y M_1 \right] \bar{q} \\
& = \frac{\mu}{2} (C_{m_1} - \xi' Y A C_{l_1})
\end{aligned} \tag{3-139b}$$

The equations (3-139), together with (3-44a) and (3-45), now may be attacked exactly as would be the original equations of (3-44a,b,c) and (3-45); in particular, the order of the system of differential equations has not been raised by the incorporation of the quasi-static, aeroelastic correction terms.

In concluding this section, it again should be remarked that the quasi-static, aeroelastic correction of the rigid body derivatives usually will be adequate for torsion of a straight wing or tail, even though wing bending may have to be introduced as a separate degree of freedom (cf. the discussion of Section 3.2.2.1).

3.2.2.4 Steady Flight Aeroelastic Problem. The steady flight aeroelastic problem may be solved as a special case of the results of the preceding section.* Starting from (3-135), \underline{c}_{l_1} , may be replaced by $\underline{c}_{l_0}^{(r)}$ representing the lift coefficient distribution calculated on the assumption of a rigid airframe, the terms in \bar{u} , \bar{w} and \bar{q} dropped, and $\frac{1}{2} C_L \tan \gamma \theta$ replaced by $-\frac{1}{2} C_L$ (cf. (3-15) where the transverse gravitational load is proportional to $(\cos \gamma - \theta \sin \gamma)$ to represent the effects of dead weight load; the result is

$$h_0 = -(\alpha \underline{I} + \underline{A A P D})^T \underline{a} \left(\frac{1}{2} \underline{A C_{l_0}}^{(r)} - \frac{1}{2} C_L M_1 \right) \tag{3-140}$$

Having h_0 , the lift distribution over the elastic airframe is given by

$$\underline{A C_{l_0}}^{(e)} = \underline{A C_{l_0}}^{(r)} + 2 \underline{A P D} h_0 \tag{3-141}$$

* It is not implied that the steady flight distortions should be calculated from the identical equations used for the quasi-static correction problem, but only that the formulation is similar. Indeed, the steady flight distortions usually should be calculated more accurately, since they may have important effects on stress distributions and drag.

Substituting (3-140) in (3-141) and incorporating \underline{Y} from (3-138) yields*

$$\underline{A} \underline{C}_{\underline{L}_0}^{(e)} = (\underline{I} - \underline{Y}) \underline{A} \underline{C}_{\underline{L}_0}^{(r)} + \underline{C}_L \underline{Y} \underline{M} \underline{1} \quad (3-142)$$

Similarly, static control surface effectiveness may be calculated simply by replacing $\underline{C}_{\underline{L}_0}$ by $\underline{C}_{\underline{L}_\delta}$ and neglecting the dead weight term in (3-142), whence

$$\underline{A} \underline{C}_{\underline{L}_\delta}^{(e)} = (\underline{I} - \underline{Y}) \underline{A} \underline{C}_{\underline{L}_\delta}^{(r)} \quad (3-143)$$

The result (3-140) also is required for the calculation of effective dihedral, but the details of this calculation depend on the type of wing under consideration.

3.2.2.5 Free Vibration Problem. The free vibration problem will be discussed in detail in Chapter IV, but it is of some interest to consider it as a special case of the results of Section 3.2.2.1 (or, for antisymmetric vibrations, Section 3.2.2.2). If all aerodynamic and rigid body terms are neglected in (3-87) the result is

$$(\mu^{-1} \underline{a} \underline{M} \underline{\lambda}^2 + \underline{x} \underline{I}) \underline{h} = 0 \quad (3-144)$$

Now for simple harmonic motion of angular frequency ω the operator $\underline{\lambda}$ is given by (assuming the harmonic time dependence $\exp(i\omega t)$)

$$\underline{\lambda} = \tau \frac{d}{dt} = i\omega \tau \quad (3-145)$$

Moreover, it may be verified that

$$\frac{\mu \underline{x}}{\tau^2} = \frac{\underline{B}}{m \ell^2} \quad (3-146)$$

Then, substituting (3-145) and (3-146) in (3-144) yields

$$[(m \ell^2 \omega^2 / B) \underline{a} \underline{M} + \underline{I}] \underline{h} = 0 \quad (3-147)$$

* It may be noted that $\sum_i \underline{A}_i \underline{C}_{oi}^{(r)} = \underline{C}_L \sum_i \underline{A}_i$

which constitutes a system of homogeneous, algebraic equation in h_1 , the characteristic values of which are the values of $(m \omega^2 / B)$ for free oscillations.

An expression for ω^2 that is of particular value in approximate calculations is obtained by premultiplying (3-147) by the inverse matrix $\underline{h}^{-1} = \underline{h}'$ and solving to obtain

$$\frac{m \ell^2}{B} \omega^2 = \frac{\underline{h}' \underline{h}}{\underline{h}' \underline{A} \underline{M} \underline{h}} \quad (3-148)$$

Rayleigh's principal then states that if an estimate for h that has an error ϵ is substituted in (3-148) the resulting approximation to the lowest ("dominant") value of ω^2 is in error only by a term of ϵ^2 .

3.2.2.6 Galerkin Formulation of Aeroelastic Equations. In the formulations and discussions of the preceding sections it was implicit that the number of elastic degrees of freedom was equal to the number of elements in \underline{h} (or the sum of the elements in \underline{h}_1 and \underline{h}_2 in Section 3.2.2.2).

The corresponding methods of direct solution will be discussed in Chapter VI. An alternative approach, which yields results equivalent to those based on the assumption of a prescribed set of deflection modes in a Lagrangian formulation (cf. Section 4.3.1) is afforded by the application of Galerkin's method of solution (Reference 12, p. 288; also Reference 13). This will be carried out for the longitudinal equations, after which the results for lateral motion may be established by analogy.

The first step in the conversion to a modal formulation is to expand the deflection matrix $\{h_i(x_i, y_i, \bar{t})\}$ in a set of prescribed space dependent modes $\{e_i^{(j)}(x_i, y_i)\}$ having the time dependent amplitudes $d^{(j)}(\bar{t})$, viz.

$$\underline{h} = \sum_{j=1}^m d^{(j)} \underline{e}^{(j)} \quad (3-149)$$

A similar decomposition of the area, mass and lift coefficient matrices in (3-87) also must be made, the end result being m equations for the $d^{(j)}$. The longitudinal analysis will be restricted to the simplest case $m = 1$, viz. $h = de$, but the results may be extended readily to the more general case. In the latter respect, it should be remarked that coupling between elastic modes generally is negligible in dynamic stability analyses (in contrast to flutter analyses, where mass coupling usually is the decisive factor), although there may be exceptions such as bending-torsion coupling when the corresponding deflection modes are based on an elastic axis approximation for a swept wing. The case of two uncoupled modes will be illustrated by the Galerkin formulation of the lateral aeroelastic equations of motion. It also should be remarked that it often might be expedient to assume a deflection matrix for one elastic motion while retaining a collocation description of a second motion, e.g., a fuselage deflection mode might be assumed but wing bending treated by collocation.

Substituting $\underline{h} = d\underline{e}$ in (3-87) and premultiplying both sides of the equation by $\underline{e}^{-1} = \underline{e}'$, the result is

$$\begin{aligned} & \underline{e}' \underline{a} (\underline{c}_{\underline{e}_0} + \underline{c}_{\underline{e}_q}) \underline{q} + \underline{e}' \underline{a} (\underline{M} \lambda + \underline{A} \underline{P}) \underline{1} \bar{w} + \frac{1}{2} \underline{c}_{\underline{L}} \tan \gamma \underline{e}' \underline{a} \underline{M} \underline{1} \theta \\ & + \underline{e}' (\mu^{-1} \underline{a} \underline{M} \lambda^2 + \mu^{-1} \underline{a} \underline{A} \underline{P} \lambda + \underline{a} \underline{A} \underline{P} \underline{D} + \underline{x}) \underline{e} d \\ & \cdot \underline{e}' \underline{a} (\mu^{-1} \underline{M} \underline{\xi} \lambda + \mu^{-1} \underline{A} \underline{P} \underline{\xi} + \underline{M} \underline{1}) \bar{q} = -\frac{1}{2} \underline{e}' \underline{a} \underline{A} \underline{c}_{\underline{e}}, \end{aligned} \quad (3-150)$$

In this result the coefficients of \bar{u} , $\lambda \bar{w}$, \bar{w} etc. are simple scalars (rather than matrices of order higher than one). Moreover, if \underline{h} is replaced by $d\underline{e}$ in (3-96a,b), the results together with (3-150) above and (3-44a) and (3-45), constitute a set of five simultaneous differential equations in the (time dependent) unknowns \bar{u} , \bar{w} , \bar{q} , θ and d . The corresponding matrix formulation is given by (cf. (3-97) - (3-104))

$$\underline{C}^{(e)} \underline{V}^{(e)} = \underline{F}^{(e)} \quad (3-151)$$

$$\underline{V}^{(e)} = \{ \underline{V}^{(r)} \mid d \} \quad (3-152a)$$

$$= \{ \frac{\underline{u}}{\underline{U}}, \frac{\underline{w}}{\underline{U}}, \tau \underline{q}, \theta, d \} \quad (3-152b)$$

$$\underline{F}^{(e)} = \{ \underline{F}^{(r)} \mid -\frac{1}{2} \underline{e}' \underline{a} \underline{A} \underline{c}_{\underline{e}} \} \quad (3-153)$$

$$\underline{C}^{(e)} = \left[\begin{array}{c|c} \underline{C}^{(r)} & \underline{R}^{(e)} \\ \hline \underline{E}^{(r)} & \underline{E}^{(\bar{e})} \end{array} \right] \quad (3-154)$$

where $\underline{C}^{(r)}$ is given by (3-49), $\underline{R}^{(e)}$ denotes the column matrix (cf. (3-102);

$$\begin{aligned} \underline{R}^{(e)} = & \{ 0, (\mu^{-1} \underline{1}' \underline{M} \underline{e} \lambda^2 + \mu^{-1} \underline{1}' \underline{A} \underline{P} \underline{e} \lambda + \underline{1}' \underline{A} \underline{P} \underline{D} \underline{e}), \\ & -(\underline{\xi}' \underline{M} \underline{e} \lambda^2 + \underline{\xi}' \underline{A} \underline{P} \underline{e} \lambda + \mu \underline{\xi}' \underline{A} \underline{P} \underline{D} \underline{e}), 0 \} \end{aligned} \quad (3-155)$$

$\underline{E}^{(r)}$ the row matrix (cf. (3-103))

$$\underline{E}^{(r)} = [\underline{e}' \underline{a} \underline{\Delta} (\underline{C}_{\underline{e}_0} + \underline{C}_{\underline{e}_2}), (\underline{e}' \underline{a} \underline{M} \underline{\Delta} + \underline{e}' \underline{a} \underline{A} \underline{P})] \quad (3-156)$$

$$-(\mu^{-1} \underline{e}' \underline{a} \underline{M} \underline{\xi} \underline{\lambda} + \mu^{-1} \underline{e}' \underline{a} \underline{A} \underline{P} \underline{\xi} + \underline{e}' \underline{a} \underline{M} \underline{1}), \frac{1}{2} \underline{C}_L \tan \gamma \underline{e}' \underline{a} \underline{M} \underline{1}]$$

and $\underline{E}^{(e)}$ the scalar (cf. (3-104))

$$\underline{E}^{(e)} = \mu^{-1} \underline{e}' \underline{a} \underline{M} \underline{e} \underline{\lambda}^2 + \mu^{-1} \underline{e}' \underline{a} \underline{A} \underline{P} \underline{e} \underline{\lambda} + \underline{e}' \underline{a} \underline{A} \underline{P} \underline{D} \underline{e} + \chi \underline{e}' \underline{e} \quad (3-157)$$

Various modifications of the formulation provided by (3-151) - (3-157) above are possible, in particular those starting from (3-89) or (3-91). If (3-89) is used as the starting point the only modifications required in the end results of (3-151) - (3-157) are: (a) strike out the influence matrix \underline{a} from the last term in $\underline{F}^{(e)}$ and from each of the terms in $\underline{E}^{(r)}$ and $\underline{E}^{(e)}$; and (b) replace $\chi \underline{e}' \underline{e}$ by $\chi \underline{e}' \underline{k} \underline{e}$ in the last term in $\underline{E}^{(e)}$. A Galerkin approximation based on the influence matrix, such as the foregoing, is generally more accurate than one based on the stiffness matrix; however the amount of labor involved in the latter approach usually is less (depending, to some extent, on whether \underline{k} is given or must be determined by inverting \underline{a}).

A possible modification that generally would increase the accuracy of the foregoing approximation would be to estimate the derivative of \underline{e} , say

$$\underline{e}^* = \underline{D} \underline{e} \quad (3-158)$$

rather than \underline{e} , which then would be replaced by $\underline{D}^{-1} \underline{e}^*$. This would eliminate the relatively inaccurate operation of differentiation at the expense of some increase in complexity of the resulting equations.

A Galerkin formulation of the lateral aeroelastic equations may be derived by an analysis paralleling the foregoing. Introducing the elastic modes $d_1 \underline{e}_1$ and $d_2 \underline{e}_2$ the end results are (cf. (3-126) - (3-134))

$$\underline{V}^{(e)} = \{ \underline{V}^{(r)} | d_1 | d_2 \} \quad (3-159a)$$

$$= \{ \beta, \tau, \phi, \psi, d_1, d_2 \} \quad (3-159b)$$

$$\underline{F}^{(e)} = \{ \underline{F}^{(r)} | \frac{1}{2} \underline{e}'_1 \underline{a}_1 \underline{A}_1 \underline{C}_{\gamma_1} | - \frac{1}{2} \underline{e}'_2 \underline{a}_2 \underline{A}_2 \underline{C}_{\gamma_2} \} \quad (3-160)$$

$$\underline{C}^{(e)} = \begin{bmatrix} \underline{C}^{(r)} & \underline{R}_1^{(e)} & \underline{R}_2^{(e)} \\ \underline{E}^{(r)} & \underline{E}_1^{(e)} & \underline{E}_2^{(e)} \\ \underline{E}_2^{(r)} & 0 & \underline{E}_2^{(e)} \end{bmatrix} \quad (3-161)$$

$$R_1^{(e)} = \{(\mu^{-1} \underline{1}' M_1 \underline{e}_1 \lambda^2 + \mu^{-1} \underline{1}' A_1 P_1 \underline{e}_1 + \underline{1}' A_1 P_1 D_1 \underline{e}_1) - (\underline{\xi}' M_1 \underline{e}_1 \lambda^2 + \underline{\xi}' A_1 P_1 \underline{e}_1 \lambda + \mu \underline{\xi}' A_1 P_1 D_1 \underline{e}_1), 0, 0, \}$$

(3-162)

$$R_2^{(e)} = \{0, (\eta_2' M_2 \underline{e}_2 \lambda^2 + \eta_2' A_2 P_2 \underline{e}_2 \lambda + \mu \eta_2' A_2 P_2 D_2 \underline{e}_2), 0, 0, 0\}$$

(3-163)

$$E_1^{(r)} = [(\underline{e}'_1 \underline{a}_1 M_1 \underline{1} \lambda + \underline{e}'_1 \underline{a}_1 A_1 P_1 \underline{1}), -\mu^{-1}(\underline{e}'_1 \underline{a}_1 M_1 \underline{\xi} \lambda + \underline{e}'_1 \underline{a}_1 A_1 P_1 \underline{\xi}),$$

$$(\mu^{-1} \underline{e}'_1 \underline{a}_1 M_1 \underline{\xi} \lambda + \mu^{-1} \underline{e}'_1 \underline{a}_1 A_1 P_1 \underline{\xi} + \underline{e}'_1 \underline{a}_1 M_1 \underline{1})$$

$$- \frac{1}{2} C_L \underline{e}'_1 \underline{a}_1 M_1 \underline{1}, -\frac{1}{2} C_L \tan \gamma \underline{e}'_1 \underline{a}_1 M_1 \underline{1}]$$

(3-164)

$$E_2^{(r)} = [\frac{1}{2} \underline{e}'_2 \underline{a}_2 A_2 C_{\alpha\beta}, \mu^{-1}(\underline{e}'_2 \underline{a}_2 M_2 \eta_2 \lambda + \frac{1}{4} \underline{e}'_2 \underline{a}_2 A_2 C_{\alpha\beta}),$$

$$\frac{1}{4} \mu^{-1} \underline{e}'_2 \underline{a}_2 A_2 C_{\alpha r}, 0, 0]$$

(3-165)

$$E_1^{(e)} = \mu^{-1} \underline{e}'_1 \underline{a}_1 M_1 \underline{e}_1 \lambda^2 + \mu^{-1} \underline{e}'_1 \underline{a}_1 A_1 P_1 \underline{e}_1 \lambda + \underline{e}'_1 \underline{a}_1 A_1 P_1 D_1 \underline{e}_1 + \chi_1 \underline{e}'_1 \underline{e}_1$$

(3-166)

$$E_2^{(e)} = \mu^{-1} \underline{e}'_2 \underline{a}_2 M_2 \underline{e}_2 \lambda^2 + \mu^{-1} \underline{e}'_2 \underline{a}_2 A_2 P_2 \underline{e}_2 \lambda + \underline{e}'_2 \underline{a}_2 A_2 P_2 D_2 \underline{e}_2 + \chi_2 \underline{e}'_2 \underline{e}_2$$

(3-167)

Again, the transition to a stiffness matrix formulation may be achieved by striking out \underline{a}_1 and \underline{a}_2 in $\underline{F}^{(e)}$, $\underline{E}_1^{(r)}$, $\underline{E}_2^{(r)}$, $\underline{E}_1^{(e)}$ and $\underline{E}_2^{(e)}$ and replacing $\chi_1 \underline{e}_1' \underline{e}_1$ and $\chi_2 \underline{e}_2' \underline{e}_2$ by $\chi_1 \underline{e}_1' \underline{k}_1 \underline{e}_1$ and $\chi_2 \underline{e}_1' \underline{k}_2 \underline{e}_2$, respectively.

The foregoing results may be transformed to integral form by taking the limit as the number of elements in the modal matrix tends to infinity. No advantage is to be gained by such a transition; however in those problems where the integrals would have to be evaluated by numerical methods, as would be the case in any practical application.

The selection of a deflection mode (or modes) in the Galerkin formulation is largely a matter of judgment. In the "quasi-static" approximation, the static deflection mode would constitute the most obvious choice, whereas the use of the dominant mode of free vibration would be preferable wherever elastic motion proved to be of primary importance. (In the latter instance, it is of interest to note that the first term in (3-157) would have the equivalent representation (cf. (3-151) and (3-153)).

$$\mu^{-1} \underline{e}' \underline{a} \underline{M} \underline{e} \lambda^2 = \chi \underline{e}' \underline{e} \left(\frac{\lambda}{\omega_T} \right)^2 \quad (3-168)$$

and similarly for the first terms in (3-166) and (3-167). From consideration of the expected accuracy of the end results, it appears that the choice of either deflection function would be satisfactory, but, assuming that the introduction of elastic degrees of freedom is in fact warranted (in comparison with the "quasi-static" approach), the use of the free vibration mode probably should be preferred.

3.2.2.7 Breakdown of Aeroelastic Problem. It is evident from the foregoing discussion that the problem of calculating the response of an elastic airplane to a given input disturbance may be broken down into the following sub-problems:

- (a) the determination of the airframe mass distribution, including in particular, the total mass and the moments of inertia;
- (b) the determination of the stability derivatives for the rigid airplane;
- (c) the determination of the elastic deflection at any point on the airframe due to a load applied at any other point, this information being placed in the form of an influence matrix a or, equivalently, a stiffness matrix k = a⁻¹
- (d) the calculation of the aerodynamic pressure distribution over the airplane (usually only the wing and tail being considered) due to an arbitrary motion, this information being placed in the form of the aerodynamic matrix P and, in the lateral equations, the specification of \underline{C}_{ℓ_B} , \underline{C}_{ℓ_P} and \underline{C}_{ℓ_r} (the

determination of the latter might be better associated with (b) above, since they represent rigid body loads);

- (e) the selection of a collocation point or Galerkin formulation and the specification of an associated set of deflection points or modes, respectively;
- (f) the solution of the resulting equations for a prescribed input.

In addition, it often may be required to replace or supplement (f) with:

- (g) the determination of the solutions to the homogeneous equations of motion and the construction of the corresponding stability boundaries.

The sub-problems (a) and (b), being independent of aeroelastic effects, will not be treated in any detail herein, although (b) will be discussed briefly in Chapter V. The structural, sub-problem (c) and the related problem (e) of determining modes will be discussed in Chapter IV, while the aerodynamic problem (d) will be taken up in Chapter V. Finally, the solution of the over-all problem will be discussed in Chapter VIII.

3.3 Autopilot-Aeroelastic Coupling

The foregoing sections are directed principally toward the dynamic stability problem. In addition, consideration generally must be given to the possibility of coupling between the autopilot and aeroelastic degrees of freedom; the resulting motion, is unstable, and is designated as "autopilot induced flutter" (see e.g., Reference 14).

It should be added that the possibility of autopilot induced flutter depends on the position of the autopilot sensing elements as well as the relevant frequency ratios. Indeed, it appears that autopilot time constants often will be comparable to wing or fuselage bending frequencies for large, flexible aircraft, and the location and type of sensing elements then may be crucial with respect to the possibility of this type of flutter.

3.3.1 Autopilot Effects. The formulations of Section 3.2.1.3 and 3.2.1.4 include all of the stability derivatives arising in consequence of direct aerodynamic effects. The installation of an autopilot may significantly modify these derivatives and also may introduce new derivatives (in particular with respect to ϕ , θ , ψ , and \dot{v}), but the new terms may be incorporated into the equations of motion in an entirely similar manner.

A precise analysis of the disturbed motion of an airplane plus autopilot requires that additional degrees of freedom be provided to describe the dynamic behavior of the latter; however in dynamic stability analyses it often may be adequate to characterize the autopilot by a constant time lag, say t_i . Then, assuming this lag to be small compared with τ (as indeed it must be if the autopilot is to operate properly), it can be taken into account

by multiplying each of the autopilot derivatives by the factor $1 - (t_1/\tau)\lambda$ in the equations of motion (3-15). Strictly speaking, a different t_1 should be assigned to each derivative, but, in view of the approximate nature of the correction, this usually would not be warranted. The autopilot time constants generally may not be neglected when compared with the periods of the natural vibrations of the aircraft as autopilot induced flutter is a serious possibility. Accordingly, the possibility of coupling between the autopilot and the elastic modes (as a result of the response of the autopilot sensing elements to the elastic motion) always must be considered.

REFERENCES

1. von Karman, T., and Biot, M. A., "Mathematical Methods in Engineering", McGraw-Hill Book Company, Inc., New York, 1940.
2. Scanlon, R. H., and Rosenbaum, R., "Introduction to the Study of Aircraft Vibration and Flutter", the Macmillan Company, New York, 1951
3. Blisplinghoff, R. L., Isackson, G., and Pian, T. H. H., "Methods in Transient Stress Analysis", Journal of the Aeronautical Sciences, Volume 17, Number 5, May 1950.
4. McRuer, D. T., et al, Dynamics of the Airframe, Volume II, BuAer Report AE 614, II, Washington, D. C.: BuAer, (1952).
5. Durand, W. F. (Editor), Aerodynamic Theory, Volume V, Pasadena: Durand Reprinting Committee, California Institute of Technology, (1943).
6. Perkins, C. D. and Hage, R. E., Airplane Performance, Stability, and Control, New York, New York, John Wiley and Sons, (1949).
7. Miles, J. W., On the Equations of Longitudinal Stability, Journal of Aeronautical Sciences 17, p. 815, (1950); ibid 18, p. 212 (1951).
8. The Application of Unsteady Flow Theory to the Calculation of Dynamic Stability Derivatives, North American Aviation Report AL-957, (1950)
9. Bird, J. D., Fisher, L. R. and Hubbard, S. M., Some Effects of Frequency on the Contribution of a Vertical Tail to the Free Aerodynamic Damping of a Model Oscillating in Yaw, NACA Report 1130, (1953).
10. Glauert, H., A Non-Dimensional Form of the Stability Equations of an Aeroplane, ARCR and M 1093, (1927); see also Reference 5, pp. 131 ff.
11. Imlay, F. H., A Theoretical Study of Lateral Stability with an Automatic Pilot, NACA TR 693, (1940).
12. Frazer, R. A., Duncan, W. J., and Collar, A. R., Elementary Matrices, Cambridge University Press (1946).
13. Duncan, W. J., Galerkin's Method in Mechanics and Differential Equations, R and M 1799, (1938).
14. Winson, J., The Flutter of Servo-Controller Aircraft, Journal of Aeronautical Sciences 16, pp. 397-404, (1949).

BIBLIOGRAPHY

1. McRuer, D. T., et al, Methods of Analysis and Synthesis of Piloted Aircraft Flight Control Systems, BuAer Rep. AE-61-41 by Northrop Aircraft, Inc. (March, 1952).
2. McRuer, D. T., et al, Dynamics of the Airframe, BuAer Rep. AE-61-411 by Northrop Aircraft, Inc. (Sept. 1952).
3. Perkins, C. D., and Hage, R. E., Airplane Performance, Stability and Control, N. Y.: John Wiley and Sons, Inc., N. Y. (1949).
4. Durand, Wm. F. (Editor), Aerodynamic Theory, Vol. 5, Dynamics of the Airplane, by B. M. Jones, Durand Reprinting Comm., CIT (1943).
5. Bollay, Wm. E., Aerodynamic Stability and Automatic Control, J. Aeron. Sci., pp. 569-624 (Sept. 1951).
6. Milliken, W. F., Jr., Progress in Dynamic Stability and Control Research J. Aeron. Sci., pp. 493-520 (Sept. 1947).
7. Ahrendt, W. R., and Taplin, J. F., Automatic Feedback Control, N. Y.: McGraw-Hill Book Co., Inc., N. Y. (1944).
8. Thaler, G. J., and Brown, R. G., Servomechanism Analysis, N. Y.: McGraw-Hill Book Co., N. Y., (1953).
9. Brown, G. S. and Campbell, D. P., Principles of Servomechanisms, N. Y.: John Wiley and Sons, N. Y., (1948).
10. Gardner, M. F. and Barnes, J. L., Transients in Linear Systems, N. Y.: John Wiley and Sons (1942).
11. Rauscher, M., Introduction to Aeronautical Dynamics, John Wiley and Sons, N. Y.
12. Schetzer, J. D., Notes on Dynamics for Aerodynamicists, Santa Monica: Douglas Aircraft Co. Rep. No. SM-14077 (5 July 1951).
13. Moore, J. R., Application of Servo Systems to Aircraft, Aeron. Engr. Review 8, pp. 32-43 (Jan. 1949).
14. Evans, W. R., Control-System Dynamics, McGraw-Hill Book Co. (1954).
15. Bode, H. W., Network Analysis and Feedback Amplifier Design, N. Y.,: D. Van Nostrand Co. (1945).

16. Chestnut, H., and Mayer, R. W., Servomechanisms and Regulating System Design, John Wiley and Sons, Inc., N. Y., (1951).
17. James, H. M., Nichols, N. B., and Phillips, R. S. Theory of Servomechanisms, MIT Rad. Lab. Series 25, McGraw-Hill Book Co., Inc. (1947).
18. Routh, E. J., Dynamics of a System of Rigid Bodies, 3d. ed., London: Macmillan and Co., Ltd., London (1877).
19. Thomson, Wm. T., Mechanical Vibrations, 2d. ed., Prentice-Hall (1953).
20. Myklestad, N. O., Vibration Analysis, McGraw-Hill (1944).
21. Timoshenko, S., Vibration Problems in Engineering, J.D. Van Nostrand, N. Y., (1948).
22. Karman, T. von and Biot, N. A., Mathematical Methods in Engineering, McGraw-Hill Book Co. (1940).
23. Churchill, R. V., Modern Operational Mathematics in Engineering, McGraw-Hill Book Co., Inc., N. Y., (1944).
24. Michal, A. D., Matrix and Tensor Calculus with Applications to Mechanics, Elasticity and Aeronautics, Galcit Aeron. Ser., John Wiley and Sons, Inc., N. Y., (1948).
25. Thomson, Wm. T., Laplace Transformation, Prentice-Hall (1951).
26. Dickson, L. E., New First Course in the Theory of Equations, John Wiley and Sons, (1946).
27. Frazer, R. A., Duncan, W. J., and Collar, A. R. Elementary Matrices, Cambridge, Univ. Press, London, (1938).
28. Moore, J. R., Unit Sphere Analysis, unpublished paper available from Engineering Dept., U. C. L. A.
29. Rautenberg, H. J., General Relationships Between the Various Systems of Reference Axes Employed in Flight Mechanics, NACATM 958, (Nov. 1940).
30. Seckel, E., Comparison Between Theoretical and Measured Longitudinal Stability Characteristics of a Gyroscopically Stabilized Helicopter in Forward Flight, Cornell Aeron. Lab. Rep. No. TG-641-F-2, (16 March 1951).

31. Seckel, E., Correlation of Some Longitudinal Dynamic Stability Characteristics of a Bell Helicopter from Theory and Flight Tests, I.A.S. Preprint No. 356, (1952).
32. Nikolsky, A. A., Helicopter Analysis, John Wiley and Sons, (1951).
33. Miller, R. H., Helicopter Control and Stability in Hovering Flight, J. Aeron. Sci., pp. 453-472, (Aug. 1948).
34. Arnold, L., and Goland, L., Helicopter Dynamic Stability and Control Studies, Part I: Longitudinal Stability and Control in Hovering and Forward Flight Including the Effects of Blade Flexibility, Cornell Aeron. Lab. Rep. No. BB-437-S-1, (29 Sept. 1950).
35. Warsett, P., Study of Automatic Control Systems for Helicopter, Part IV: Equations of Motion for a Nominally-Hovering Helicopter with Rotor RPM Degree of Freedom, Minneapolis-Honeywell Reg. Co., Rep. No. AD 5143-TR7, (19 June 1953).
36. Donovan, A. F. and Goland, M., The Response of Helicopters with Articulated Rotors to Cyclic Blade Pitch Control, J. Aeron. Sci., 387-398, (Oct. 1944).
37. Holman, J. A., Stabilizing Controller for H-19 Helicopter Theoretical Stability Analysis, Goodyear Aircraft Corp., Rep. GER 2998, R-569, (30 Apr. 1952).
38. Jones, A. L., and Briggs, B. R., A Survey of Stability Analysis Techniques for Automatically Controlled Aircraft, NACA TN 2275, (Jan. 1951).
39. Rea, J. B., Automatic Control of Aircraft, Sc.D. Thesis, M. I. T., (1947).
40. Toll, T. A., Summary of Lateral-Control Research, NACA Rep. 868, (1947).
41. Imlay, F. H., A Theoretical Study of Lateral Stability with an Automatic Pilot, NACA Rep. 693, (1940).
42. Campbell, J. P., and McKinney, M. O., Summary of Methods for Calculating Dynamic Lateral Stability and Response and For Estimating Lateral Stability Derivatives, NACA Rep. 1098, (1952).
43. Bird, J. D., Fisher, L. R., and Hubbard, S. M., Some Effects of Frequency on the Contribution of a Vertical Tail to the Free Aerodynamic Damping of a Model Oscillating in Yaw, NACA Rep. 1130 (1953).

44. Sternfield, L., Some Effects of Nonlinear Variation in the Directional-Stability and Damping-in-Yawing Derivatives on the Lateral Stability of an Airplane, NACA Rep. 1042 (1951).
45. Walkowicz, T. F., Dynamic Longitudinal Response of an Airplane at High Subsonic Mach Numbers, Sc.D., Thesis, M.I.T. (1948).
46. Rea, J. B., Dynamic Analysis of Aeroelastic Aircraft by the Transfer Function-Fourier Method, Douglas Aircraft Co., Rep. No. SM-13868, also presented to the Institute of Aeronautical Sciences in Los Angeles (13 July 1950).
47. Rea, J. B., Analysis of Systems for Automatic Control of Aircraft, Douglas Aircraft Co., Rep. No. SM-14088, also presented to the Institute of Aeronautical Sciences in Los Angeles (27 June 1951).
48. Walters, E. R. and Rea, J. B., Determination of Frequency Characteristics from Response to Arbitrary Input, presented to the Institute of Aeronautical Sciences (June 1950).
49. Johnson, R. L. and Rea, J. B., Importance of Extending Nyquist Servomechanism Analysis to Include Transient Response, Douglas Aircraft Co., Rep. No. SM-14028, (December 1949).
50. Lauber, J. E. and Underhill, D. A., Longitudinal Dynamic Stability Analyses (Including Aeroelasticity) of the Model C-74 and Model C-124A Airplanes, Douglas Aircraft Co. Rep. No. LB-16460 (26 November 1951).
51. Laitone, E. V., Rigid-Body Dynamics of Aircraft Including Non-Stationary Aerodynamics, Douglas Aircraft Co. Rep. No. SM-13820 (5 January 1951).
52. Statler, I. C., Derivation of Dynamic Longitudinal Stability Derivatives for Subsonic Compressible Flow from Non-Stationary Flow Theory and Application to an F-80A Airplane, Cornell Aeronautical Lab. Rep. No. TB-495-F-9 (1 March 1949).
53. Statler, I. C. and Easterbrook, M., Handbook for Computing Non-Stationary Flow Effects on Subsonic Dynamic Longitudinal Response Characteristics of an Airplane, Cornell Aeronautical Lab. Rep. No. TB-495-F-12 (1 March 1950).
54. Ashley, H., Zartarian, G., and Neilson, D.O., Investigation of Certain Unsteady Aerodynamic Effects in Longitudinal Dynamic Stability, Wright Air Development Center, USAF TR No. 5986, (December 1951).
55. Goland, M., and Luke, Y. L., Aerodynamic Lag in Longitudinal Stick-Free Dynamic Stability, Wright Air Development Center, WADC TR 53-28 (Dec. 1952)
56. Goland, M., and Luke, Y. L., Aeroelastic Effects on Dynamic Longitudinal Stability, Wright Air Development Center, WADC TR 53-29 (June 1953).
57. Howard, V. W., The Effects of Structural Elasticity on Aircraft Control Systems, Wright Air Development Center, WADC TR 56-166 (June 1956).

NOMENCLATURE

- \underline{a} = influence matrix
- c_{ik} = relative amplitude of element i with respect to a unit amplitude deflection at some element p , in the k th mode.
- d_k = normal coordinate associated with k th mode
- \underline{f} = force matrix (aerodynamic and/or inertial)
- h_i = deflections of an elastic structure at element i
- i = element number
- \underline{k} = stiffness matrix
- \underline{l} = unit column matrix
- ℓ = characteristic length
- q_r = normalized coordinate in the r th mode
- r, k = mode numbers
- \underline{A} = diagonal area matrix
- B = characteristic stiffness of an elastic structure
- E = flexural modulus
- F = Froude number
- \underline{I} = unit square matrix
- K_A, K_B, K_C, K_{AC} = Moment of inertia parameters
- M_a = Mach number
- \underline{M} = diagonal mass matrix
- M_k = generalized mass of k th mode
- \underline{P} = aerodynamic matrix
- Q_r = generalized force
- R = Reynolds number
- T = kinetic energy
- U = potential energy

γ = angle of flight path with respect to horizon
 δW = virtual work done by external forces
 ξ = empirical damping ratio of the structure
 λ_{ik} = slope at element i in the kth mode
 λ = dimensionless operator
 μ = relative density
 ν = coefficient of viscosity of air
 τ = time parameter
 ω = angular frequency
 ω_k = natural undamped frequency of kth mode
 $\{ \}$ braces signify a column matrix
 - underscoring indicates a matrix

Axis Systems. The choice of an "Eulerian" system can readily facilitate a stability analysis, whereas a fixed (in space) earth system may be mandatory for over-all trajectory work. "Eulerian" coordinates travel along with the aircraft (origin usually at the c.g.) and permits the instantaneous measurement of linear and angular motions with respect to axes which are fixed at a desired instant of time (such as just previous to a maneuver).

Axis Systems for Airplanes and Missiles. Several different axis systems have been used for airplanes and missiles, each suited to a particular type analysis. Some of the more commonly known systems are referred to as:

- (i) Eulerian axes,
- (ii) Inertial axes,
- (iii) Principal axes,
- (iv) Body axes,
- (v) Wind axes,
- (vi) Stability axes,
- (vii) Wind tunnel axes,
- (viii) Wing chordwise axes,
- (ix) Instrument axes,
- (x) Radar axes, and
- (xi) Elastic axes.

In the airplane stability analyses inertial axes (fixed in space) have been set aside in preference of an "Eulerian" system. However, an inertial system translating with the c.g. but with constant orientation is used for the helicopter. Principal axes are fixed in the aircraft having a special symmetry which causes the inertial cross-product terms to vanish (i.e., $I_{xy} = I_{xz} =$

$I_{yz} = 0$). Body axes are simply axes which are fixed in the aircraft, i.e., they move with the aircraft, or equivalently, there is no relative motion between body axes and the aircraft. Hence principal axes are specialized body axes.

A wind axis system is continually oriented with respect to the relative wind, and as the aircraft maneuvers, the x (or V) axis continually adjusts its orientation into the wind. If the y axis is restricted to a principal axis, as is suggested in the Northrop-BuAer volume, (Reference 4), (i. e., perpendicular to the x z plane), then the wind x axis cannot leave the x z plane in the lateral direction to meet the oncoming wind unless a skew system is adopted. Since orthogonality among axes is highly desirable, the alternative then would be to allow y to leave the principal axis direction.

Stability axes are initially oriented with respect to the oncoming wind during steady flight and then fixed to the aircraft (as body axes) during maneuvering or disturbed flight. In the wind tunnel, lift and drag forces are measured with respect to the relative wind and are logically referred to stability axes. In other words, wind tunnel axes are identical to stability axes during steady flight. Stability derivatives obtained from subsonic flow theory are normally calculated with reference to stability axes.

In supersonic flight, it is convenient to use the x axis along the wing chord. Pressure variations between upper and lower wing surfaces are of principal interest wherein the flow streamlines tend to parallel the wing chord. However, in supersonic flight, the stability x axis will nearly parallel the wing chord line which permits simplifications of some of the stability derivatives even when referenced to the stability axis system.

Flight test data are obtained from instruments located in the airplane. If the instrument axes are aligned with the principle axes, then stability derivatives will be referenced with respect to these axes. Care must be taken to include the effects due to the location of instruments away from the c.g. For example, an accelerometer will pick up angular rates and angular accelerations in addition to other linear and angular velocities, linear accelerations and the effects of gravity.

A radar axis system specifies the orientation of a target with respect to the ship through angular displacements of the gimbals upon which the scanner is mounted. For most problems, the target is considered at some distance, so that the resolution of these (gimbal) angles can be accomplished by assuming the radar is mounted at the c.g. and accounting only for angular displacements.

Throughout the remainder of the airplane and missile analyses, the stability axis system will be used. There are intermediate steps when other axes may be used temporarily, but eventually all the stability derivatives will be referenced with respect to stability axes. One will find it convenient, for instance, to use a spanwise wing coordinate for determining elastic modes, the physics of which eventually can be represented as a wing-tip motion superimposed upon the rigid-body stability y -axis (and x -axis component for swept wing) at the wing-tip station.

The notation distinguishing the axis systems is given in subscript form:

| | | | |
|----------|----------|--------------|--------------------------------|
| x_E | y_E | and z_E | earth or inertial axes, |
| x_B | y_B | and z_B | body axes, |
| x_W | y_W | and z_W | wind axes, |
| x | y | and z | stability axes (no subscript), |
| x_{WT} | y_{WT} | and z_{WT} | wind tunnel axes, etc. |

Care must be taken not to confuse the above notation with stability derivatives which are represented by capital X, Y, and Z with the associated

lower case subscripts, e.g.: X_u , Y_v , Z_w , etc. The above could be confused with the nondimensional stability derivatives, however, the two areas are likely to be covered at entirely different times.

At this point, the notation used for elastic deflections should be clarified, particularly for torsion. In partial conformity with flutter work, the following is used:

- h_1 = linear deflection of a specified station (wing tip, nose, etc.) for the first mode of vibration,
- h_2 = same for second mode,
- ϕ_1 = torsional twist at specified station for first torsional mode, etc.

(The first mode is usually considered as that with the lowest natural frequency, and higher modes associated with higher frequencies.) The above are the disturbed deflections from the steady-state flight positions, i.e., under static aeroelastic conditions (see Sections 2.2), the wing tip will be elastically deflected an amount h_0 and twisted ϕ_0 , note that ϕ used for torsion should be distinguished from ϕ used for the perturbation roll angle of the ship.

In analyzing maneuvers in which the small perturbation theory must be modified, there are two important effects that should be considered. First the gravitational or weight vector must be accounted for throughout the maneuver. Second, the aerodynamic effects must be resolved about either a body axis system, a wind axis system (X axis restrained to plane of symmetry) or some combination of the two. There are two advantages associated with the body axis. First, the inertia terms are independent of altitude and second, the autopilot sensing gear is oriented with respect to some fixed body axis system. For these reasons a body axis system is fine for the moment equations. On the other hand a wind axis system is appropriate for simplifying force equations. Transform equations are necessary for relating the two sets of axis systems and tracking the gravitational vector.*

* A. C. Charters, The Linearized Equations of Motion Underlying the Dynamic Stability of Aircraft Spinning Projectiles and Symmetrical Missiles,
NACA T.N. 3350

CHAPTER IV

DETERMINATION OF ELASTIC EFFECTS

4.0 Introduction

The fourth chapter covers the types of elastic vibration that might occur in aircraft, and surveys the more common methods used in calculating the elastic mode shapes. The most useful techniques are covered in detail so as to enable one to apply them to a specific problem. The basic energy concepts are reviewed and relatively simple applications given. From these concepts is evolved the more useful influence coefficient method and its matrix and tabular representations. Finally, the elastic concepts and methods are applied to the transient behavior of an elastic aircraft, excluding unsteady aerodynamic forces.

4.1 Elastic Concepts

The airplane is a complex structure of considerable flexibility. From the standpoint of vibrations, however, its various components such as the wing, fuselage, and tail surfaces, can be considered to be beams of plates capable of bending and twisting. Thus the oscillations of the entire airplane consist of bending and twisting of a number of interconnected beams and plates with possible flapping of attached control surfaces.

In making a vibration analysis of such a complex structure, certain approximations are sometimes justified for the simplified analysis. For instance, in determining the motion of the wing, the fuselage, due to its greater rigidity may be considered to be a rigid cylinder, and the problem becomes one of finding the free-free modes of this wing-cylinder configuration. The natural modes of such a configuration are either symmetric or antisymmetric about the cylinder axis as shown in Figure 4.1. Although

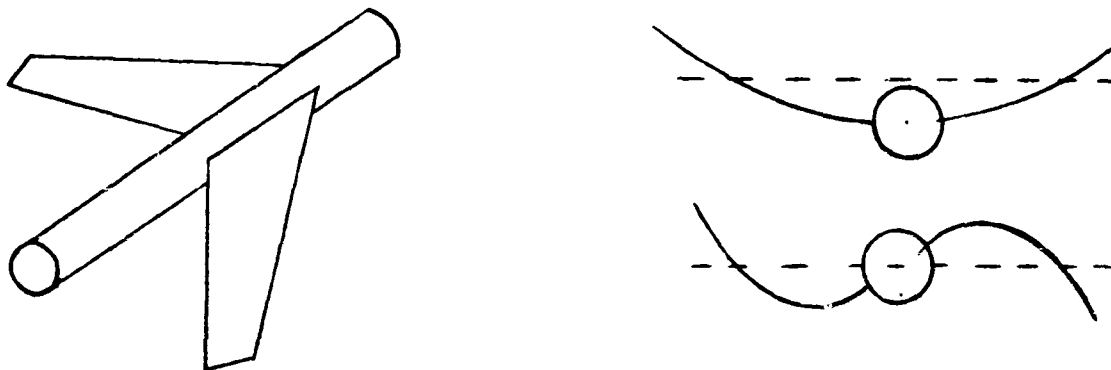


Figure 4-1. Natural Modes

shown by a single line, the wing bending is generally accompanied by torsion, and the symmetric modes result in some pitching motion of the fuselage. Both the symmetric and antisymmetric wing modes may be accompanied by flapping of the ailerons.

Then again the motion of the empennage sometimes can be treated quite independently from that of the wings. In this case, the wings represent a very large mass concentration which enables the fuselage to be treated as a cantilever beam fixed at the wing roots. (As a more accurate case, the fuselage is considered as a free-free beam after having determined the effective mass of the flexible wings plus engines.) Here the vertical bending of the fuselage is accompanied by bending of the stabilizers and flapping of the elevators.

Due to the lack of symmetry about a horizontal plane (e. g., high horizontal tail), the side bending of the fuselage is generally accompanied by fuselage torsion as well as bending of the stabilizer and fin. The fuselage torsion will in this case induce rudder motion and antisymmetric flapping of the elevators. In addition, a rolling motion of the airplane can induce this same type of rudder and elevator response and, in particular, can excite the antisymmetric wing bending modes.

4.1.1 Dynamic Representation of Elastic Structures. The elastic (or spring stiffness) and the inertial (mass and moment of inertia) effects are of primary importance in the aircraft vibration problem and are covered in detail in the following pages. The damping (or structural dissipative) effects are of secondary importance in the presence of induced aerodynamic damping losses. This fact permits one to omit structural damping effects in aircraft stability analyses, but not necessarily in the higher frequency flutter analyses.

4.1.1.1 Elastic Effects. Hooke's law, which states that deformations in the elastic range are proportional to load, together with the principle of superposition, constitute the foundation of all elastic analysis. The relationship between deformation and load can be formulated in two different ways. Thus, the displacement at any point i is the sum of the displacements at that point, independently caused by each of the variously located forces.

$$h_i = \sum_j a_{ij} P_j \quad (4-1a)$$

The quantity a_{ij} which is the deflection at point i , in a given direction, due to a unit force at point j , is referred to as the flexibility influence coefficient.

The second formulation is the reciprocal relation to the above and

expresses the forces in terms of the displacements by the equation,

$$P_i = \sum_j k_{ij} h_j \quad (4-1b)$$

where k_{ij} is the stiffness influence coefficient.

For a system of n forces and displacements, the above equations represent a double set of n equations which can conveniently be expressed in the matrix form

$$\begin{bmatrix} h_1 \\ h_2 \\ \vdots \end{bmatrix} = \begin{bmatrix} a_{11} & a_{12} & \cdots \\ a_{21} & a_{22} & \cdots \\ \vdots & \vdots & \ddots \end{bmatrix} \begin{bmatrix} P_1 \\ P_2 \\ \vdots \end{bmatrix} \quad (4-2a)$$

$$\begin{bmatrix} P_1 \\ P_2 \\ \vdots \end{bmatrix} = \begin{bmatrix} k_{11} & k_{12} & \cdots \\ k_{21} & k_{22} & \cdots \\ \vdots & \vdots & \ddots \end{bmatrix} \begin{bmatrix} h_1 \\ h_2 \\ \vdots \end{bmatrix} \quad (4-2b)$$

Upon examining (4-1a) or (4-1b) the interpretation of these equations becomes self-evident. For instance, in (4-2a), the terms a_{ij} of each row of the square matrix are successively multiplied by the corresponding terms P_j in the adjacent column matrix to form the sum equal to h_i . This operation in matrix algebra is referred to as premultiplying the column matrix by the square matrix to form another column matrix.

On substituting (4-2a) into (4-2b) or vice versa, the reciprocal relationship between the flexibility matrix and the stiffness matrix is evident:

$$[a] = [k]^{-1} \quad (4-3)$$

This operation which is called inversion states that the stiffness matrix can be inverted to form the flexibility matrix. It can also be demonstrated that the individual influence coefficients possess a reciprocal property, $a_{ij} = a_{ji}$ and $k_{ij} = k_{ji}$.

The strain energy of a structure can be expressed in terms of the influence coefficients. For a system of forces P_i acting through displacements h_i , the strain energy is equal to the work done by these forces, which is

$$U = \frac{1}{2} \sum_i h_i P_i \quad (4-4a)$$

This potential energy expression, along with the kinetic and dissipative energy expressions, is substituted into Lagrange's Equations, Section 3.1, to obtain the force equations.

If we substitute for h_i or P_i , two forms for the strain energy become

$$U = \frac{1}{2} \sum_i \sum_j a_{ij} P_i P_j \quad (4-4b)$$

and

$$U = \frac{1}{2} \sum_i \sum_j k_{ij} h_i h_j \quad (4-4c)$$

By differentiation it can be shown that

$$h_r = \frac{\partial U}{\partial P_r} \quad (4-5a)$$

$$P_r = \frac{\partial U}{\partial h_r} \quad (4-5b)$$

which demonstrates Castigliano's first and second theorems (Reference 8 - p. 242).

If the force system applied to the structure is continuous, integral expressions analogous to (4-1a) and (4-1b) exist between deflection and force:

$$h(x) = \int_0^l a(x, \xi) P(\xi) d\xi \quad (4-6a)$$

$$P(x) = \int_0^l k(x, \xi) h(\xi) d\xi \quad (4-6b)$$

Here the quantities $a(x, \xi)$ and $k(x, \xi)$ are the influence functions analogous to the quantities a_{ij} and k_{ij} .

The strain energy for the structure loaded by the continuous force is

$$U = \frac{1}{2} \int_0^l h(x) P(x) dx \quad (4-7a)$$

$$= \frac{1}{2} \int_0^l P(x) \int_0^l a(x, \xi) P(\xi) d\xi dx \quad (4-7b)$$

$$= \frac{1}{2} \int_0^l h(x) \int_0^l k(x, \xi) h(\xi) d\xi dx \quad (4-7c)$$

4.1.1.2 Inertial Mass and Moment Effects. The inertial property of a structure, as established by the mass distribution, is expressed in terms of its kinetic energy. With the motion specified in terms of translation and rotation about the mass center, the kinetic energy may be written as

$$T = \frac{1}{2} \sum_i m_i \dot{h}_i^2 + \frac{1}{2} \sum_i I_i \dot{\psi}_i^2 \quad (4-8a)$$

or

$$T = \frac{1}{2} \int \dot{h}^2 dm + \frac{1}{2} \int \dot{\psi}^2 dI \quad (4-8b)$$

4.1.1.3 Structural Damping Effect. In the vibration of any structure, energy is dissipated in the material itself due to internal friction. For example, in the spring-mass model of Figure 4-2 this form of energy dissipation takes place in the spring and is indicated by the hysteresis loop formed by the plot of the restoring force and the displacement.

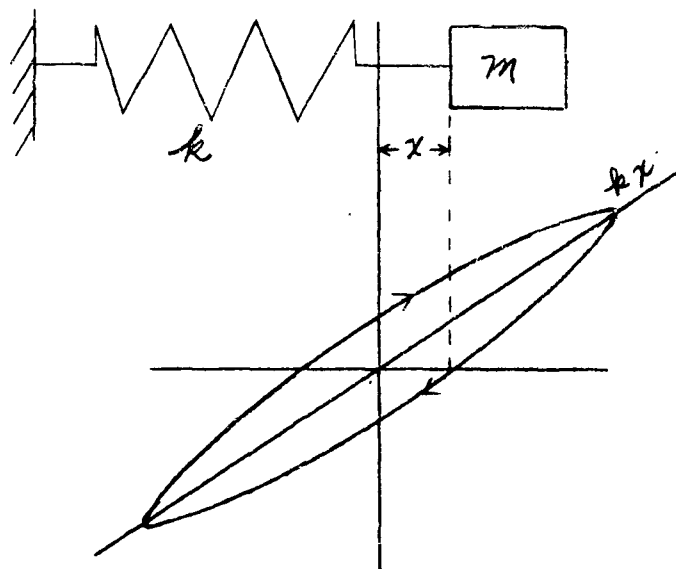


Figure 4-2. Spring-Mass Model

It can be shown that this deviation of the restoring force from the straight line kx can be accounted for by a complex spring force of the form ke^{2bi} where the quantity $2b$ represents a phase angle leading the real spring force (Reference 26). Thus the differential equation including structural damping takes the form

$$m\ddot{x} + ke^{2bi}x = F \quad (4-9)$$

which differs from that of viscous damping which is proportional to the velocity. This indicates that the effective spring force has been reduced from kx to $kx\cos 2b$, and that a damping force $kx\sin 2b$ has been introduced.

When structural damping is small (which is generally the case for aircraft structures), Myklestad (Reference 26) has shown that the solution for free vibration reduces to that of viscous damping. Thus b becomes equal to the damping factor defined as the ratio of the viscous damping coefficient C to the critical damping coefficient $C_{cr} = 2\sqrt{km}$. For forced harmonic vibration with small structural damping, the only difference from the viscous solution lies in the phase angle which is slightly modified

For continuous structures, we can consider a space integrated equation of motion expressed in terms of some specified amplitude. This can be done in terms of normal modes of the system and generalized coordinates (see 3.3.1) which for any mode results in a similar differential equation of second order,

$$M_{ss} \ddot{q}_s + K_{ss} q_s = Q_s \quad (4-10)$$

where M_{ss} and K_{ss} are generalized mass and stiffness. Thus, structural damping can be accounted for in such cases by replacing the stiffness by a complex stiffness $K_{ss} e^{2bi}$.

4.1.2 Principal and Normal Modes of Oscillation. Every dynamic system is associated with the number of principal modes of oscillation equal to the degrees of freedom of the system. A principal mode of oscillation can be defined as a free vibration in which every point in the system undergoes simple harmonic motion of the same frequency so as to pass through their respective equilibrium positions simultaneously. The frequencies of principal mode oscillations are the natural frequencies of the system. *

Principal modes of oscillation are independent of the amplitude; i. e., the mode shape and frequency are not altered with amplitude. Thus, the amplitude of principal oscillations may be chosen arbitrarily to any convenient value. This process of choosing a convenient amplitude scale is referred to as normalizing, and the principal modes after normalization are referred to as normal modes.

Normal modes are established differently according to the problem. For instance the amplitudes A_i may be established by the normalizing condition $\sum_i A_i^2 = 1$. On the other hand, for the method of matrix iteration, it is more convenient to employ the normalizing condition of assigning a unit amplitude at a specified point. Another useful normalizing condition is specified by the equation $\sum_i m_i A_i = 1$.

In general a dynamic system can vibrate in any number of different ways depending on the manner of initiation and excitation. The importance of the normal mode oscillations lies in the fact that any such motion can be represented by the sum of its various normal modes multiplied by time varying coefficients.

Normal modes possess an orthogonal property which can be expressed

* For bending vibrations of beams the natural frequencies are in general not integrally related and hence higher mode frequencies are not referred to as harmonics.

mathematically as

$$\sum_i m_i A_i^{(r)} A_i^{(s)} = 0 \quad r \neq s \quad (4-11)$$

In this equation the superscripts designate the mode number. In the higher mode calculation by any iteration method, the orthogonality relation is used to impose a constraint on the equations to force the computations to converge to the desired mode.

4.1.3 Coupling of Motion. As stated previously, the various components of the airplane can be considered to be beams or plates capable of bending and twisting. In particular the aircraft with long, straight elastic wings (high aspect ratios) can be analyzed as though the wings were flexible beams. On the other hand, the elastic delta wings (low aspect ratios) almost of necessity need to be considered as flexible plates (for which case the influence method still applies). In many cases, though, an elastic axis assumption can be made which simplifies the problem as is indicated in the following discussion.

To establish certain concepts applicable to the elastic-axis bending-torsion vibration, the plan and cross sectional views of a typical swept wing are shown in Figure 4-3.

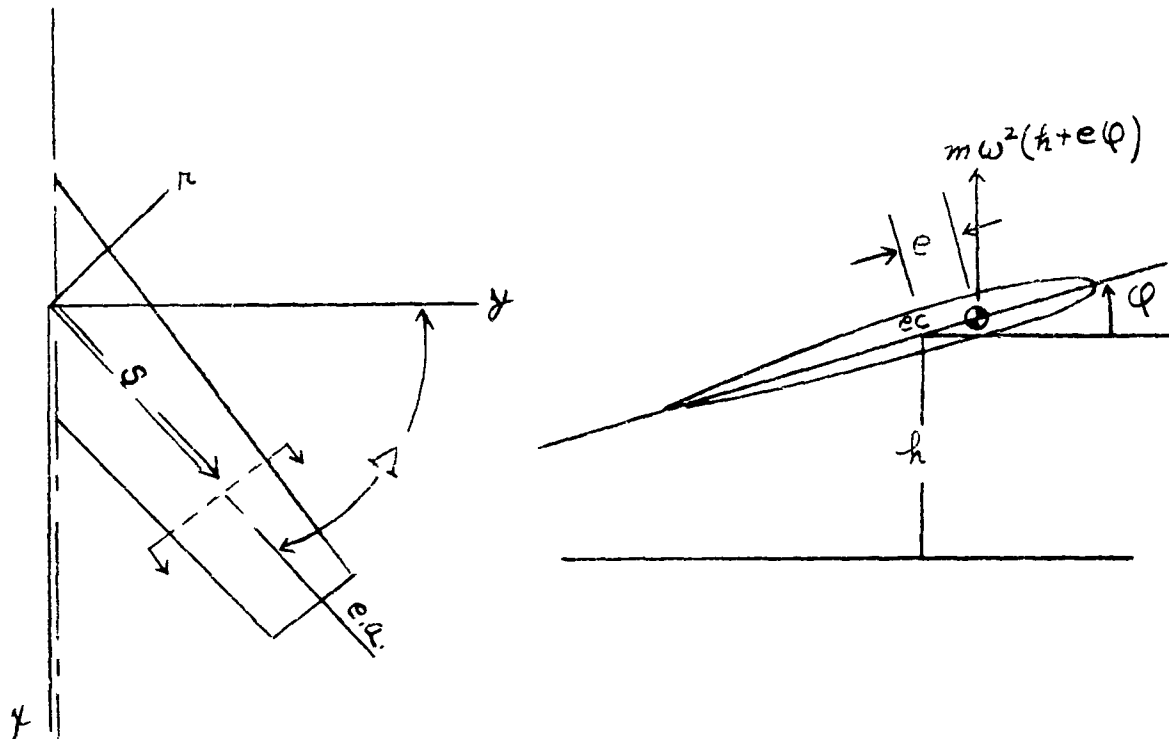


Figure 4-3. Swept Wing Model

The point e.c. on the sectional view is known as the elastic center, which has the following properties: (a) When a pure twisting couple is applied to the section, the cross section rotates about the elastic center. (b) When a force is applied to the elastic center, the cross section translates without rotation. The advantage of choosing the elastic center as a reference is that bending and torsion are not elastically coupled; i.e., bending forces at the elastic center produce only bending displacements h , while pure torsional moments produce rotation without bending.

A line joining all the elastic centers is known as the elastic axis. Such a line is in general not straight and its position is somewhat dependent on the type of loading. In fact, it should be pointed out in satisfying the conditions for the elastic center at the spanwise station of the load, other sections may undergo translation and rotation. However, in many cases no serious error results from assuming the elastic axis to be a straight line approximating the locus of the elastic centers, and the usefulness of the concept of the elastic axis is upheld in spite of its fictitious nature.

If a pure couple is applied to a wing section, its elastic center does not move. However, on releasing the couple both bending and rotation often take place, indicating a coupling due to inertia. This is due to the fact that inertia forces act through the center of gravity of the section, which in general does not coincide with the elastic center. Thus, inertia or dynamic coupling exists between bending and torsion.

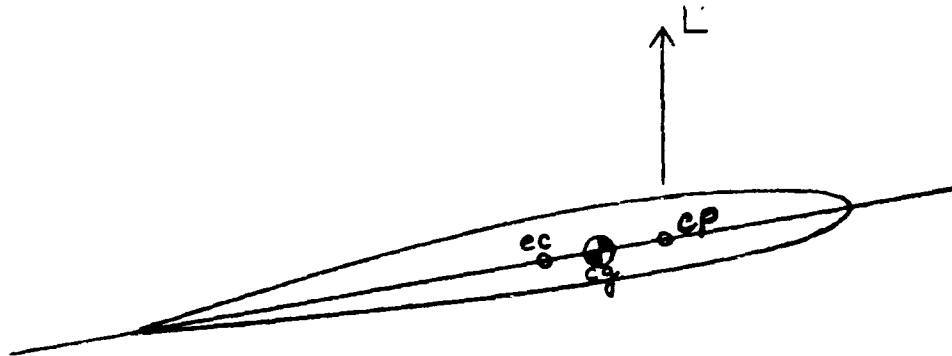


Figure 4-4. Wing Section

Neglecting the effects of camber (which can be treated separately), the center of lift corresponds to the aerodynamic center which is approximately 25 percent of the chord distance from the leading edge at subsonic speeds. The elastic center is usually in the neighborhood of 40 percent of the chord distance from the leading edge. It is evident then that aerodynamic forces produce both bending and twisting and the two types of motion are said to be aerodynamically coupled. (See figure 4-4).

The type of coupling present for the coordinate system chosen can also be established by examining the expressions for the kinetic and potential energies. If cross products of coordinates appear in the expression for the kinetic energy, the system is said to have dynamic coupling. If cross products of coordinates appear in the expression for the potential energy, the system is said to have static coupling.

4.1.4 Equations for a Beam in Bending and Torsion The beam simulating the various components of the airplane is usually nonuniform in mass and stiffness distribution, and special methods must be devised for its vibrational analysis. In the following section the basic equations for the bending and twisting of the nonuniform beam are briefly reviewed.

4.1.4.1 Bending. The basic element of a beam in bending is shown in Figure 4-5. From it the following relationships can be

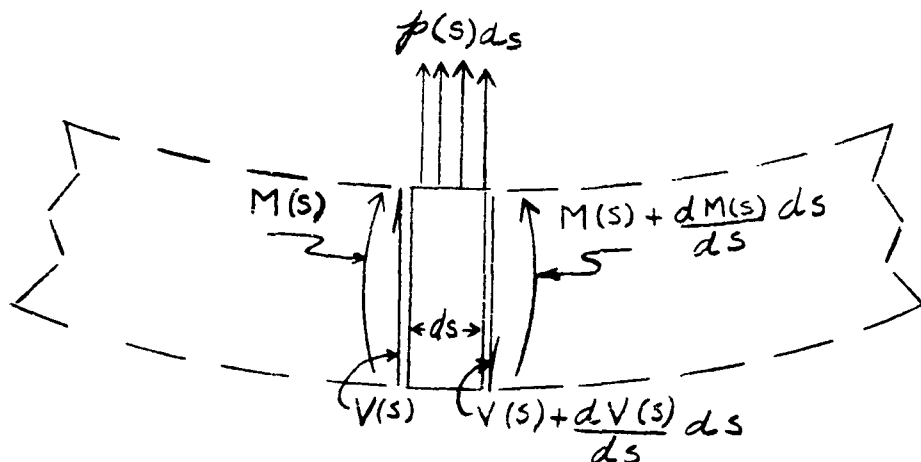


Figure 4-5. Beam Element

obtained from equilibrium considerations

$$p(s) = \frac{dV(s)}{ds} \quad (4-12a)$$

$$V(s) = \frac{dM(s)}{ds} \quad (4-12b)$$

Substituting (4-12b) and (4-12a), a third relationship is obtained

$$\frac{d^2 M(s)}{ds^2} = p(s) \quad (4-12c)$$

Using the conventional assumption of small deflections and Hooke's law, the moment can be expressed in terms of the curvature or deflection, which enables (4-12c) to be written in the form

$$\frac{d^2}{ds^2} \left[E I(s) \frac{d^2 h(s)}{ds^2} \right] = p(s) \quad (4-13)$$

4.1.4.2 Torsion. . For the twisting of the beam, it is generally assumed that the simple equation for the prismatic bar applies. In spite of the limitations imposed on the simple torsion equation, its application to the nonuniform beam results in good agreement with test results.

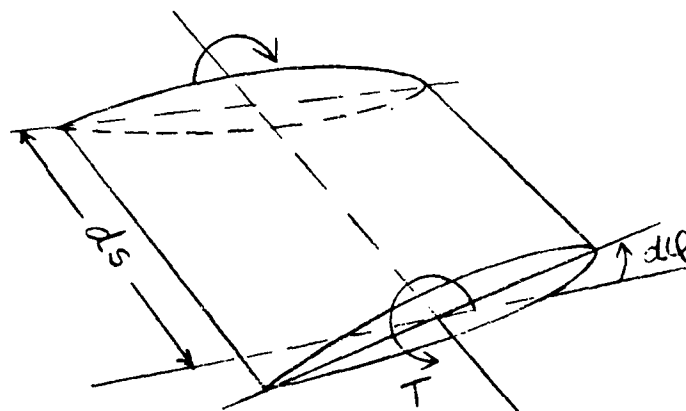


Figure 4-6. Wing-Section in Torsion

Due to torque T , the twist in an elementary length ds is given by the equations

$$d\phi = \frac{T ds}{GJ} \quad (4-14)$$

where GJ is the torsional stiffness per unit length. This equation is often written in the form

$$\frac{d}{ds} \left[GJ(s) \frac{d\phi}{ds} \right] = \frac{dT}{ds} \quad (4-15)$$

which is the counterpart of the bending equation (4-13).

4.1.4.3 Bending-Torsion. Equations (4-13) and (4-15) apply to dynamic problems if inertia terms are included in the loading. Referring to Figure 3-1, the inertia force for harmonic oscillations is

$$p(s) = -m(\ddot{h} + e\ddot{\phi}) = \omega^2(mh + e\phi) \quad (4-16)$$

where m and $s = me$ are the mass and its static moment about the elastic axis per unit length of the beam. Likewise, the torque increment per unit length about the elastic axis is the moment of the inertia forces integrated over the cross section. $I_\phi = \int r^2 dm$ is here the mass moment of inertia about the elastic axis per unit length of the beam.

$$\frac{dT}{ds} = -\int (\ddot{h} + r\ddot{\phi}) r dm = \omega^2(sh + I_\phi\phi) \quad (4-17)$$

Substituting (4-16) and (4-17) into (4-13) and (4-15), respectively, the differential equations for the coupled bending-torsion oscillation of the beam become

$$\frac{d^2}{ds^2} \left[EI(s) \frac{d^2 h(s)}{ds^2} \right] = \omega^2 (mh + e\phi) \quad (4-18a)$$

$$\frac{d}{ds} \left[GJ(s) \frac{d\phi}{ds} \right] = \omega^2 (sh + I_\phi\phi) \quad (4-18b)$$

The above equations reduce to those of the uncoupled bending and torsion when the static moment e is zero:

$$\frac{d^2}{ds^2} \left[EI(s) \frac{d^2 h(s)}{ds^2} \right] = \omega^2 mh \quad (4-19a)$$

$$\frac{d}{ds} \left[GJ(s) \frac{d\phi}{ds} \right] = \omega^2 I_\phi \phi \quad (4-19b)$$

4.2 Methods For Computing Normal Modes

In the case of a nonuniform beam, the analytical solution of the beam equation is not feasible and some approximate method of numerical computation must be used. There are several such methods available, the bases of which will be examined here.

Six basic methods for computing normal modes of vibration are presented in the following section. It is appropriate at this point to summarize the procedures discussed and offer certain comments pertinent to each.

Rayleigh's energy method: The energy method due to its fundamental nature must form the basis for many computing methods. The Rayleigh formulation is one of the simplest and in its original form is applicable to the determination of the fundamental mode. Its accuracy is dependent largely on the adequacy of the assumed deflection in representing the actual vibration mode and the associated boundary conditions. A modification of Rayleigh's method enables one to express the potential energy of the system in terms of the deflection rather than its curvature. This deflection can be computed by any available procedure including the graphical and the influence coefficient method.

Rayleigh-Ritz extension: The Rayleigh-Ritz extension greatly improves the accuracy of the energy method at the expense of added mathematical and numerical work. Here the deflection is assumed as linear combinations of suitable function,

$$h = \alpha_1 h_1(s) + \alpha_2 h_2(s) + \alpha_3 h_3(s) + \dots \quad (4-20)$$

and the frequency equation is minimized with respect to the parameter α_1 .

$$\frac{\partial \omega^2}{\partial \alpha_i} = 0 \quad (4-21)$$

When $h_i(s)$ represent functions such as the uniform beam modes which satisfy the boundary conditions, the accuracy obtained is quite good. It is evident here that the number of assumed functions must be at least one greater than that of the order of the mode to be determined. When using uniform beam modes, the compilation of Young and Felgar, Reference 30, which presents tabulated normal modes and frequencies for various boundary conditions, will be found quite useful.

When the Rayleigh-Ritz procedure is expressed in the form

$$\frac{\partial}{\partial \alpha_i} (T - U) = 0 \quad (4-22)$$

the result is equivalent to the variational method. By representing h as the sum of normal vibrational modes and the rigid body modes, the free-free modes of the airplane can be determined.

The Stodola method: The Stodola method makes use of the inertia loads to reduce the dynamical problem to a static one. In determining the inertia load, a deflection must be assumed and improved upon by successive iteration. When treated from the differential equation approach, the computation from the load to deflection requires four integrations which are generally carried

out in tabular form. For higher mode determination, the lower modes to be used in the orthogonality relation must be computed with considerable accuracy. This statement applies to any iterative procedure which tends to converge to the lowest mode present. The Stodola computations can be carried out much more efficiently by the method of influence coefficients and matrix iteration.

Holzer method: When an elastic system can be represented accurately by lumped torsional parameters, the Holzer method leads to a simple calculation of the normal modes. It appears then that the major problem here is that of being able to accurately represent the continuous system in terms of lumped parameters. Once this representation is adequately made all of the normal modes of the system are easily determined.

Holzer-Myklestad method: The comments made regarding the Holzer method also apply to the Holzer-Myklestad method for bending vibrations. The first step of lumped parameter representation requires experienced judgment. The computation when expressed in matrix form can be systematically performed by automatic machines such as the IBM type. The computation by hand operated computers is tedious and requires constant checking by two individuals carrying out the same computations.

The computation of the higher modes is not dependent on the predetermination of the lower modes. However, due to the fact that the boundary equations are always in the form of small differences between two large numbers, the higher mode computations require the carrying of a large number of significant figures. For the first two modes, six significant figures will in general be sufficient.

When applied to coupled bending-torsion modes the computations become lengthy and an automatic machine procedure is almost essential. One time-saving factor of the Holzer-Myklestad method lies in the fact that both the symmetric and antisymmetric modes can be determined from one computation at the assumed frequency. The inclusion of lumped attachments, such as engines, tip tanks, bombs and rockets offer no added complication to the Holzer-Myklestad method. If the attachments are elastically supported, their effective mass or inertia is used in place of their actual mass or inertia.

Matrix iteration: The method of influence coefficients and matrix iteration offers a systematic computational procedure for vibration analysis. By the use of flexibility influence coefficients, it is possible to express the deflection of the system by an integral equation,

$$h(x,t) = \int a(x,\xi) F(\xi,t) d\xi \quad (4-23)$$

The integral equation can be solved by a numerical procedure; however it is more practical to establish a number of stations over the structure and represent the above equations as a system of linear algebraic equations which is then reduced to matrix form. The coefficients of this set of algebraic equations is then the result of collocation of the integral equations. For

higher mode analysis, the matrix iteration procedure has the disadvantage of requiring accurate lower mode data. Also the symmetric and anti-symmetric modes of the free-free airplane require the solution of different matrix equations. The computations, however, can be easily carried out by a digital computer.

4.2.1 Rayleigh's Energy Method. Rayleigh's method is based on the principle of conservation of energy. Thus, for any conservative system the maximum kinetic energy of the system as it passes through the equilibrium position must equal the maximum potential energy stored in the position of maximum amplitude. The method is limited to the calculation of the fundamental frequency and requires an assumption of the deflection mode of the system.

For the uncoupled beam vibration, the energy expressions are

$$T_{\max} = \frac{1}{2} \omega^2 \int_0^l m(s) h^2(s) ds \quad (4-24a)$$

$$U_{\max} = \frac{1}{2} \int_0^l \frac{M(s)}{EI(s)} ds = \frac{1}{2} \int_0^l EI(s) \left[\frac{\partial^2 h(s)}{\partial s^2} \right]^2 ds \quad (4-24b)$$

Equating the two expressions, the frequency equation becomes

$$\omega^2 = \frac{\int_0^l EI(s) \left[\frac{\partial^2 h(s)}{\partial s^2} \right]^2 ds}{\int_0^l m(s) h^2(s) ds} \quad (4-25)$$

For the torsional vibrations, the counterpart of the above frequency equation is

$$\omega^2 = \frac{\int_0^l GJ \left[\frac{\partial \phi(s)}{\partial s} \right]^2 ds}{\int_0^l I_\phi(s) \phi^2 ds} \quad (4-26)$$

Rayleigh showed that good accuracy can be obtained by this procedure with any reasonable deflection curve. Analytical expressions for the deflection, however, are here impractical since $m(s)$ and $EI(s)$ also vary along the beam. Without an analytical expression, the curvature

$\frac{\partial^2 h(s)}{\partial s^2}$ must be determined by a Stodola iteration technique (Section 4.2.2; Reference 12).

This difficulty is partially avoided by the following procedure. The beam is represented by a series of lumped weights W_1, W_2, W_3, \dots , and the maximum strain energy is determined from the work done by these weights, which is,

$$U_{\max} = \frac{1}{2} [W_1 h_1 + W_2 h_2 + W_3 h_3 + \dots] \quad (4-27)$$

As a first approximation, the static deflection may be used, which can be computed by a graphical procedure or any other known method. The frequency is then expressed entirely in terms of the deflection by the equation,

$$\omega^2 = \frac{8 \sum_i W_i h_i}{\sum_i W_i h_i^2} \quad (4-28)$$

4.2.1.1 Rayleigh-Ritz Extension. Rayleigh's method, which requires one to assume a deflection curve, always leads to a calculated frequency which is somewhat higher than the fundamental frequency. This is due to the fact that a vibrating system tends to take a configuration corresponding to a minimum of potential energy. Since the errors in the assumed curve represent added restraints or stiffness, the computed frequency is higher than the correct value.

Ritz modified Rayleigh's method by expressing the assumed curve in terms of parameters which can be varied to minimize the frequency. With the parameters in the deflection curve designated by a'_s , the Ritz method leads to a set of equations of the form:

$$\frac{\partial}{\partial a_i} \frac{\int_0^L EI(s) \left[\frac{\partial^2 h(s)}{\partial s^2} \right]^2 ds}{\int_0^L m(s) h^2(s) ds} = 0 \quad (4-29)$$

which results in a set of simultaneous algebraic equations in a'_s . The vanishing of the determinant of this set of equations then leads to the natural frequencies of the system.

The Ritz method is essentially a variational method which is well known in mathematics. It has an advantage over the Rayleigh method in that the natural frequencies of higher modes can be found. The accuracy of the higher modes depends, however, on the deflection functions and the number of parameters used. Zahorski (Reference 19) and Anderson (Reference 22) have obtained good results by using the deflection modes of the uniform wing.

4.2.2 Stodola Method. The Stodola method (Reference 4, P. 194) recognizes the fact that the problem of finding the normal modes of vibration of any structure is merely that of determining the static deflection of the structure loaded by inertia forces.

For purposes of discussion consider the uncoupled bending vibration of a beam. Its differential equation from equation (4-19a) can be rewritten in the form

$$\frac{d^2}{ds^2} \left[E I(s) \frac{d^2}{ds^2} \left(\frac{h}{\omega^2} \right) \right] = m h \quad (4-30)$$

which indicates that a loading equal to $m(s)h(s)$ will result in a deflection $\frac{1}{\omega^2} h(s)$.

The Stodola computation is started by assuming a deflection curve $h(s)$ which specifies the loading $m(s)h(s)$. By successive integration which can be performed numerically, the shear, bending moment, slope and deflection multiplied by $\frac{1}{\omega^2}$, can be computed. At first the computed deflection shape will differ from the assumed shape; however, by repeating the computation with the new deflection obtained from the previous step, the procedure will eventually converge to the correct mode shape. At this point the natural frequency can be found from the fact that the ratio of the assumed and computed amplitudes is ω^2 , since the latter is $\frac{h}{\omega^2}$.

Modes above the fundamental may be determined by the present method by introducing the orthogonality property of normal modes, see Section 4.1.2, Equation (4-11). This requires that the first mode be computed with a reasonable degree of accuracy, after which it must be used in the relation,

$$\sum_i m_i h_i^{(1)} h_i = 0 \quad (4-31)$$

where h_i without the superscript is the assumed higher mode. Since the assumed deflection can be considered to be a linear combination of the normal modes, the above equation is equivalent to setting the coefficient of the first mode to zero. Thus, when this condition has been satisfied, the first mode has been eliminated from the assumed curve which then must converge to the second mode.

When carrying out the numerical integration, the boundary conditions corresponding to the type of oscillation must be observed. For the free-free

modes of the airplane, the bending moment and shear at the wing tips must be zero. An exception to this requirement is found for the case where a tip tank is used. The shear and bending moment at the wing tips must then equal that required for the motion of the tip tanks. The boundary conditions at the airplane center line will depend on whether the motion is symmetric or antisymmetric. For the symmetric modes the slope and shear must be zero, whereas for the antisymmetric modes the deflection and bending moments must be zero.

The Stodola method can be extended to coupled bending-torsion modes by solving the two equations (4-18a) and (4-18b) numerically (Reference 23). The boundary conditions at the airplane center line require special considerations for the swept wing, the discussion of which is presented under the section on tabular methods (Section 4.2.3).

4.2.3 Tabular Methods

4.2.3.1 Holzer Method. Holzer (Reference 1) introduced one of the simplest and most widely used methods for the analysis of uncoupled torsional oscillations. The system to be analyzed is first reduced to an idealized torsional system consisting of discrete masses of moments of inertia I_i connected by shafts of torsional stiffness K_i .

Assuming such a system to be oscillating in a free-free mode at frequency ω , the external torque necessary to maintain this oscillation is

$$T = \sum_i I_i \omega^2 \phi_i \quad (4-32)$$

If the amplitude at some specified point is maintained at unity, this torque, which can be applied to any point outside of a nodal point, will depend on the frequency. At the natural frequencies of the system, no external torque is required to maintain this oscillation and thus a plot of the external torque vs. frequency will establish the natural frequencies of the system.

The Holzer computation is conveniently carried out in tabular form. Starting at one end of the system with $\phi_1 = 1$, and with an assumed frequency of ω , the inertia torque of the first mass $I_1 \omega^2$ must be transmitted by the first shaft which twists by an amount $\frac{I_1 \omega^2}{K_1} = 1 - \phi_2$.

The amplitude ϕ_2 of the second mass found from the above equation is then used to determine the inertia torque $I_2 \omega^2 \phi_2$ of the second mass which when added to that of the first mass results in a torque which must be carried by the second shaft. Proceeding in this manner, the external torque requirement for any frequency can be established and plotted.

When the position of a nodal point is known, such as the fuselage station for the antisymmetric modes of the wing, or for the torsion of the fuselage tail assembly, the natural frequencies are those frequencies which result in zero amplitude for this point.

4.2.3.2 Holzer-Myklestad Method for Bending Vibrations. Holzer's method was first extended for beam vibrations by Myklestad (Reference 13) and Prohl (Reference 14). The beam is here divided into n sections with discrete masses and stiffness defined by influence coefficients for each section. The computations are started by choosing a frequency, and the four quantities: shear, bending moment, slope, and deflection are determined progressively from one end of the beam to the other. When the calculated quantities satisfy the actual boundary conditions, the assumed frequency becomes the natural frequency of the beam and the calculated deflection its normal mode.

The Holzer-Myklestad method has certain advantages over the iteration procedure in that higher modes can be determined without a knowledge of the lower modes. Also the symmetric and antisymmetric modes can be determined from one operation, whereas in the iteration procedure a separate treatment is necessary. The computational equations can also be expressed in matrix form for automatic machine computation.

The basis for the Holzer-Myklestad method lies in the fact that in forced harmonic oscillation the deflection, slope, moment and shear are linearly related along the beam. It appears that such problems can be formulated in many different ways. The development here is a modification of the Myklestad method (Reference 9) in which the unnecessary algebraic substitutions have been eliminated in the formulation by redefinition of the initial terms. This results in a clearer insight of the physical concepts which are retained in the computational equations.

4.2.3.3 Uncoupled Bending Vibrations. For the formulation of the equations the beam section is chosen as shown in Figure 7 where the displacement h and the slope $h' = \frac{dh}{ds}$ are shown in their positive sense. This arrangement is identical to that of Reference 9 except that the elementary section is drawn with increasing slope and displacement in the direction of computation to avoid negative signs in the computational equations.

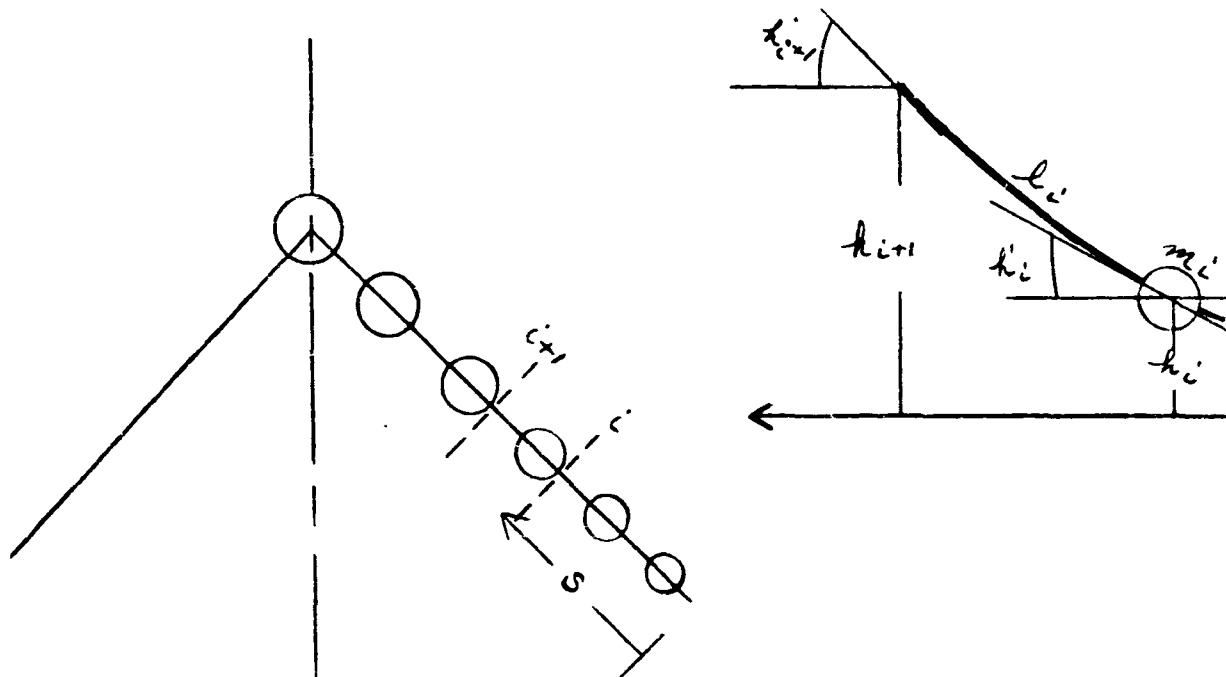


Figure 4-7 Beam Section
124

The computation is also directed from right to left so that the order corresponds to the arrangement of the matrix form of the tabular equations.

In Figure 4-8 a detailed diagram of the elementary section is shown. A cut is taken just to the left of m_i to aid in visualizing the development.

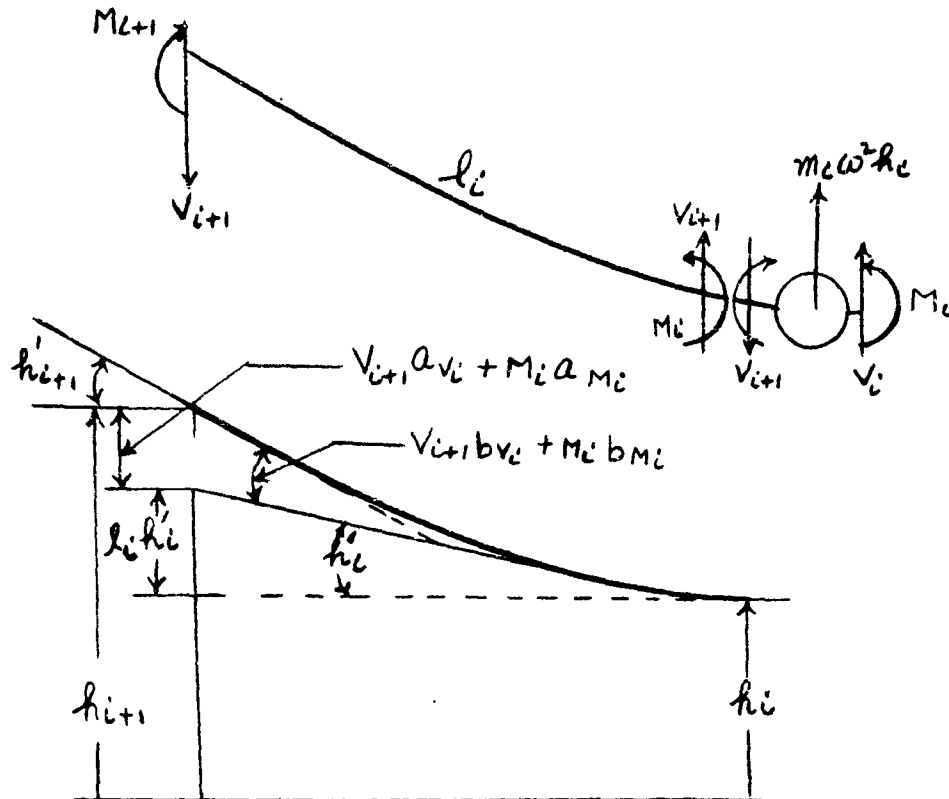


Figure 4-8 Elementary Beam-Section

Summing forces and moments, the first two equations of equilibrium are obtained. The last two equations are obtained from a geometric configuration where the influence coefficients for the section enter into the development. These influence coefficients are the slopes and deflections at station

$$V_{i+1} = V_i + m_i \omega^2 h_i \quad (\text{Shear Forces}) \quad (4-33a)$$

$$M_{i+1} = M_i + V_{i+1} l_i \quad (\text{Moments}) \quad (4-33b)$$

$$h'_{i+1} = h'_i + V_{i+1} b_{V_i} + M_i b_{M_i} \quad (\text{Slopes}) \quad (4-33c)$$

$$h_{i+1} = h_i + l_i h'_i + V_{i+1} a_{V_i} + M_i a_{M_i} \quad (\text{Displacements}) \quad (4-33d)$$

$i + 1$ with respect to a tangent at station i , due to unit shear and moment at station i . It can be shown that this choice of influence coefficients, which differ from those of Myklestad (Reference 13), lead to the simplest form of the matrix equation resulting from a tabular procedure. (Ref. 9)

For an assumed value of ω , these equations enable one to calculate V , M , h' , and h at any point in terms of the corresponding quantities at the starting point. For instance, for a free-ended beam such as an airplane wing or fuselage, the computation is started with the following values at the free end.

$$\begin{aligned} V_1 &= M_1 = 0 \\ h'_1 &= h'_1 \\ h_1 &= 1 \end{aligned} \tag{4-34a}$$

Progressing to the other end, which may be the center line of the airplane or the opposite end of the fuselage, the quantities obtained are in the form

$$V_n = A_1 + B_1 h'_1 \tag{4-34b}$$

$$M_n = A_2 + B_2 h'_1 \tag{4-34c}$$

$$h'_n = A_3 + B_3 h'_1 \tag{4-34d}$$

$$h_n = A_4 + B_4 h'_1 \tag{4-34e}$$

where the A 's and B 's are constants. Specifying the boundary conditions at n , h'_1 is determined, after which all other quantities at n and other stations become known.

As an example, let n correspond to the center line of the airplane for the wing vibrations. For the uncoupled bending vibrations, the boundary conditions are the same for the swept and unswept wings, which are (for the symmetric and antisymmetric modes):

(Symmetric Modes)

$$h'_n = 0, \quad \therefore h'_i = - \frac{A_3}{B_3} \quad (4-35a)$$

$$V_n = A_1 - \frac{A_3 B_1}{B_3} = 0 \quad (4-35b)$$

(Antisymmetric Modes)

$$h_n = 0 \quad \therefore h'_i = - \frac{A_4}{B_4} \quad (4-36a)$$

$$M_n = A_2 - \frac{A_4 B_2}{B_4} = 0 \quad (4-36b)$$

At the natural frequencies, V_n or M_n must become zero. Thus by plotting V_n and M_n vs. ω , the normal modes corresponding to the symmetric and antisymmetric vibrations of the wing are found.

We will next rearrange the computational equations in a more useful matrix form. Replacing all terms on the right side of the equation with $i + 1$ in terms of quantities with subscript i , the rearranged equations take the form:

$$V_{i+1} = V_i + m_i \omega^2 h_i \quad (4-37a)$$

$$M_{i+1} = M_i + V_i l_i + m_i \omega^2 l_i h_i \quad (4-37b)$$

$$h'_{i+1} = h'_i + V_i b_{v_i} + m_i \omega^2 b_{v_i} h_i + M_i b_{m_i} \quad (4-37c)$$

$$h_{i+1} = h_i + h'_i l_i + V_i a_{v_i} + m_i \omega^2 a_{v_i} h_i + M_i a_{m_i} \quad (4-37d)$$

This set of equations in matrix form is:

$$\begin{bmatrix} V_{i+1} \\ M_{i+1} \\ h'_{i+1} \\ h_{i+1} \end{bmatrix} = \begin{bmatrix} 1 & 0 & 0 & m_i \omega^2 \\ l_i & 1 & 0 & m_i l_i \omega^2 \\ b v_i & b m_i & 1 & m_i b v_i \omega^2 \\ a v_i & a m_i & l_i & (1 + m_i a v_i \omega^2) \end{bmatrix} \begin{bmatrix} V_i \\ M_i \\ h'_i \\ h_i \end{bmatrix} \quad (4-38)$$

It should be noted that only the last column of the square matrix need to be changed for different values of ω . For any frequency the computations can be carried out progressively from station to station in a matter of minutes by automatic machines which rapidly perform such matrix multiplications.

4.2.3.4 Influence Coefficients. The influence coefficients may be determined from the actual stiffness curve of the beam by using the area moment procedure. Referring to the stiffness curve of Figure 4-9 and letting the ordinates at station i and $i + 1$ be aEI_0 and $(a + b)EI_0$,

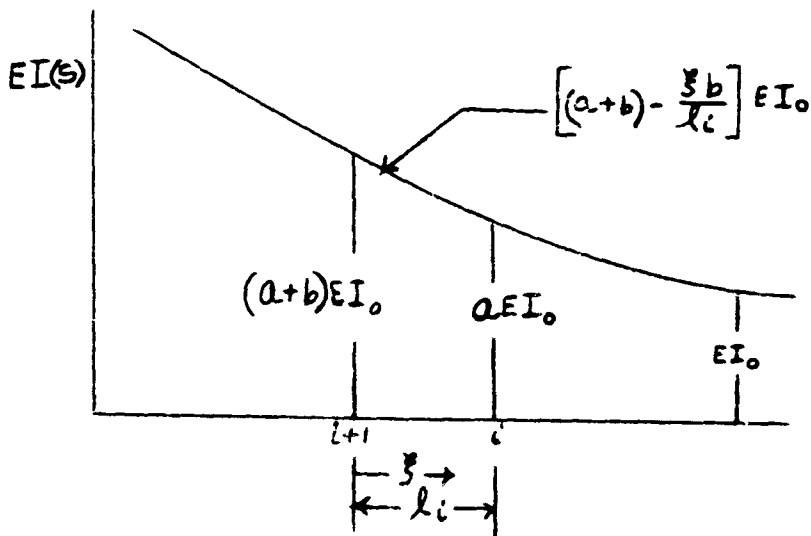


Figure 4-9. Stiffness Curve

where EI_0 is an arbitrary reference value, the equations for the influence coefficients become:

$$b_{Mi} = \int_0^{l_i} \frac{d\xi}{EI} = \frac{l_i}{bEI} \ln\left(\frac{a+b}{a}\right) \quad (4-39a)$$

$$b_{Vi} = \int_0^{l_i} \frac{(l_i - \xi)}{EI} d\xi = \frac{l_i^2}{b^2 EI_0} \left[b - a \ln\left(\frac{a+b}{a}\right) \right] \quad (4-39b)$$

$$a_{Mi} = \int_0^{l_i} \frac{\xi d\xi}{EI} = \frac{l_i^3}{b^2 EI_0} \left[(a+b) \ln\left(\frac{a+b}{a}\right) - b \right] \quad (4-39c)$$

$$a_{Vi} = \int_0^{l_i} \frac{(l_i - \xi)\xi}{EI} d\xi = \frac{l_i^3}{b^3 EI_0} \left[\frac{1}{2} b^2 + ab - a(a+b) \ln\left(\frac{a+b}{a}\right) \right] \quad (4-39d)$$

If a uniform section of some average stiffness EI_i is assumed between stations, the influence coefficients reduce to the simple relations

$$b_{Mi} = \frac{l_i}{EI_i} \quad (4-40a)$$

$$b_{Vi} = a_{Mi} = \frac{l_i^2}{2EI_i} \quad (4-40b)$$

$$a_{Vi} = \frac{l_i^3}{6EI_i} \quad (4-40c)$$

and the matrix equation becomes identical to that suggested by Targoff, (Reference 17).

4.2.3.5 Coupled Bending-Torsion Vibration. Principal modes of vibration of airplane wings are actually coupled bending-torsion modes, for which the uncoupled bending and uncoupled torsion modes represent approximations. If the computed uncoupled bending and torsion modes are widely separated along the frequency spectrum, the principal coupled modes will be predominantly one or the other.

When coupled modes must be computed, the tabular method can be extended in the following manner. We introduce one additional influence coefficient C_i defined as the angle of twist at station $i + 1$ with respect to station i , due to a unit torque at station i . If a torsional stiffness curve $GJ(S)$ is available, C_i can be determined from the equation

$$C_i = \int_0^{l_i} \frac{d\zeta}{GJ} \quad (4-41a)$$

which reduces to the simple expression

$$C_i = \frac{l_i}{GJ_i} \quad (4-41b)$$

when a uniform section of average stiffness GJ_i is assumed between stations.

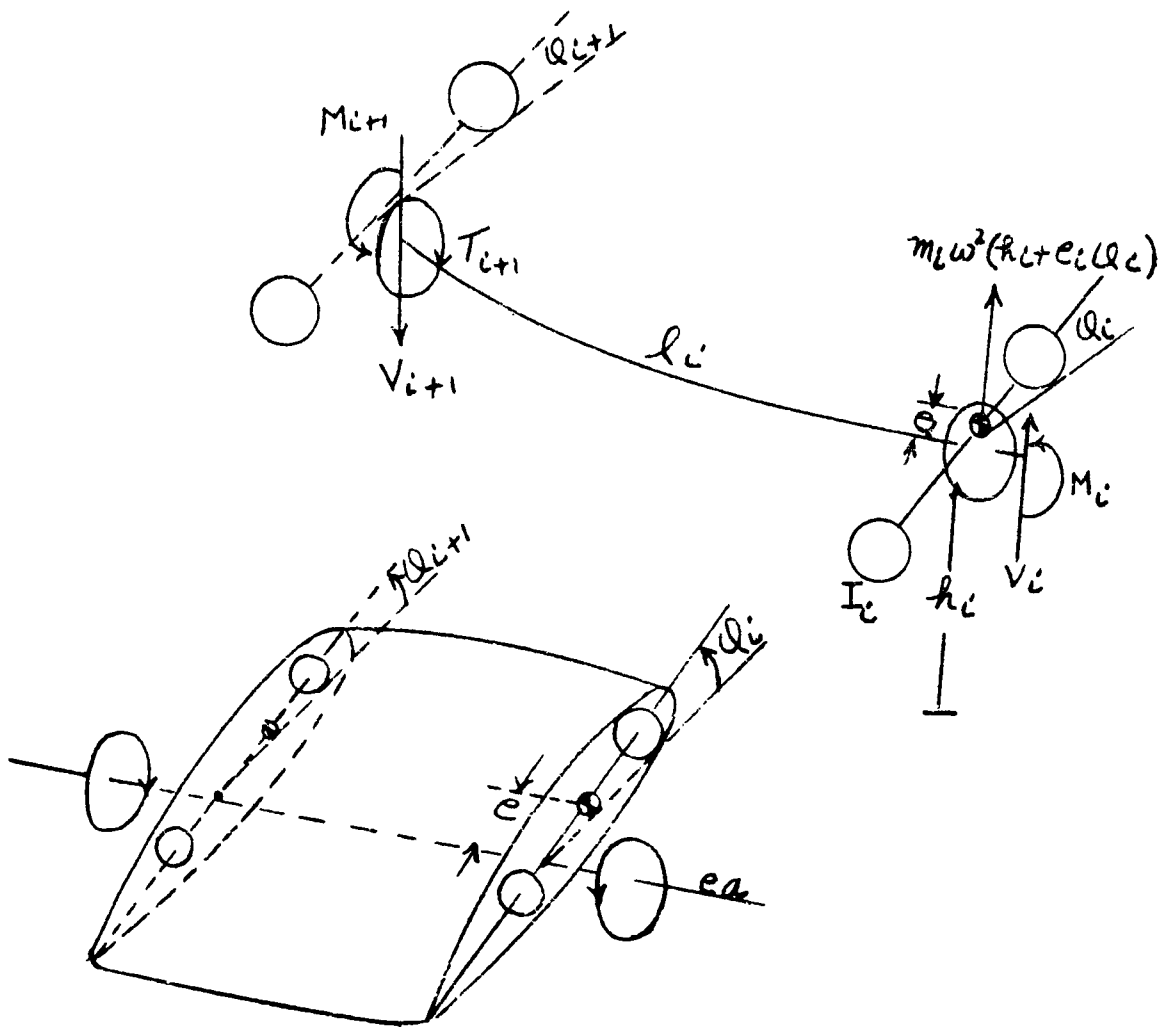


Figure 4-10. Beam Section

Referring to the beam section shown in Figure 4-10, the torsional angle ϕ_i is chosen positive in the direction of increasing angle of attack. The inertia torque of the section is obtained by integrating the moment of the inertia forces over the cross section, which is,

$$\omega^2 \int (h + r\phi) r dm = \omega^2 (\Delta_i h_i + I_i \phi_i) \quad (4-42)$$

I_i is here the mass moment of inertia of the section about the elastic axis, while $\Delta_i = m_i e_i$ is the static moment of the mass about the elastic axis.

With this notation, the computational equations become,

$$V_{i+1} = V_i + \omega^2 (m_i h_i + \Delta_i \phi_i) \quad (\text{Shear Forces}) \quad (4-43a)$$

$$M_{i+1} = M_i + V_{i+1} l_i \quad (\text{Bending Moments}) \quad (4-43b)$$

$$h'_{i+1} = h'_i + V_{i+1} b_{v_i} + M_i b_{m_i} \quad (\text{Slopes}) \quad (4-43c)$$

$$h_{i+1} = h_i + h'_i l_i + V_{i+1} a_{v_i} + M_i a_{m_i} \quad (\text{Displacements}) \quad (4-43d)$$

$$T_{i+1} = T_i + \omega^2 (\Delta_i h_i + I_i \phi_i) \quad (\text{Torque Moments}) \quad (4-43e)$$

$$\phi_{i+1} = \phi_i - T_{i+1} C_i \quad (\text{Torque Angles}) \quad (4-43f)$$

Arranged in matrix form, these equations become:

$$\begin{bmatrix} V_{i+1} \\ M_{i+1} \\ \dot{h}_{i+1} \\ h_{i+1} \\ T_{i+1} \\ \Phi_{i+1} \end{bmatrix} = \begin{bmatrix} 1 & 0 & 0 & m_i \omega^2 & 0 & \Delta_i \omega^2 \\ l_i & 1 & 0 & m_i l_i \omega^2 & 0 & \Delta_i l_i \omega^2 \\ b_{vi} & b_{mi} & 1 & m_i b_{vi} \omega^2 & 0 & \Delta_i b_{vi} \omega^2 \\ a_{vi} & a_{mi} & l_i (1 + m_i a_{vi} \omega^2) & 0 & 0 & \Delta_i a_{vi} \omega^2 \\ 0 & 0 & 0 & \Delta_i \omega^2 & 1 & I_i \omega^2 \\ 0 & 0 & 0 & -\Delta_i C_i \omega^2 & -C_i & (1 - I_i C_i \omega^2) \end{bmatrix} \begin{bmatrix} V_i \\ M_i \\ h'_i \\ h_i \\ T_i \\ \Phi_i \end{bmatrix}$$

(4-44)

When partitioned off as indicated, the square sub-matrices along the diagonal represent the uncoupled bending and torsional equations, whereas the remaining elements represent coupling terms due to Δ_i . Again this equation is identical to that of Targoff (Reference 17) for the coupled bending-torsion vibration.

4.2.3.6 Swept Wings. Of particular interest here are the free-free modes of the airplane with swept wings. The boundary equations derived for this general case will then be applicable to the unswept wing when the sweep angle Λ is made equal to zero.

For the free end corresponding to the wing tip, we have the following boundary conditions to start the computation.

$$h_i = 1.0 \quad h'_i = h'_i \quad \Phi_i = \Phi_i \quad (4-45)$$

Here again, the quantities of interest at any station are linearly related and their numerical value will be of the form,

$$A + Bh' + C\phi, \quad (4-46)$$

The boundary conditions at the center line of the airplane must next be expressed in terms of the beam quantities at the effective root section of the wing. The bending moment and the twisting torque at the root section are in the r and s directions and must first be resolved in the x and y directions corresponding to the airplane axis as shown in Figure 4-11.

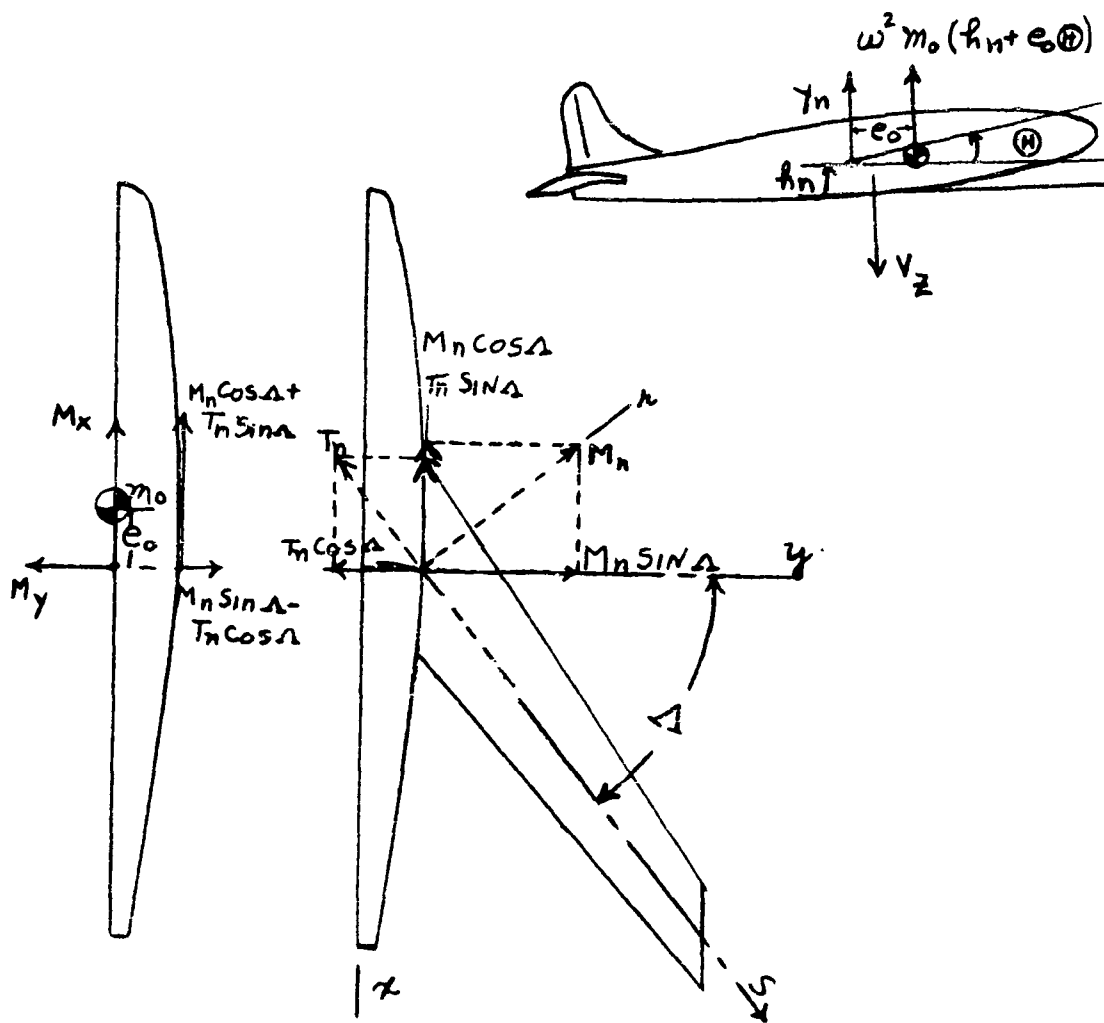


Figure 4-11. Airplane Axis System

It is also necessary to relate the pitching Θ and rolling Φ of the fuselage to the beam bending and twisting angles at the wing root by the following equations:

$$\text{(Pitch)} \quad \Theta = \Phi_n \cos \Lambda - h'_n \sin \Lambda \quad (4-47a)$$

$$\text{(Roll)} \quad \Phi = \Phi_n \sin \Lambda + h'_n \cos \Lambda \quad (4-47b)$$

For the symmetric mode there can be no roll and no component of the vector in the y direction. These conditions are expressed by the equations:

$$\text{(Symmetric Mode)} \quad \Phi_n \sin \Lambda + h'_n \cos \Lambda = 0 \quad (4-48a)$$

$$M_n \sin \Lambda - T_n \cos \Lambda = 0 \quad (4-48b)$$

which enable one to evaluate h'_1 and ϕ_1 . The natural frequencies are then found when the vertical shear V_z at the airplane center line becomes zero.

$$V_z = V_n + m_0 \omega^2 [h_n + e_0 (\phi_n \cos \Lambda - h'_n \sin \Lambda)] = 0 \quad (4-49)$$

In this equation m_0 is half the mass of the fuselage, and e_0 is the distance from the origin of the x,y axis to the fuselage center of gravity.

For the antisymmetric modes, the deflection at the center line of the airplane must be zero. This implies that the pitch angle Θ must also be zero, so that we have the two equations:

$$y_n = 0 \quad (4-50a)$$

(Asymmetric Mode)

$$\Phi_n \cos \Lambda - h'_n \sin \Lambda = 0 \quad (4-50b)$$

for the determination of h'_1 and ϕ_1 . The natural frequencies then correspond to those frequencies for which the rolling moment vanish:

$$M_x = M_n \cos \Delta - T_n \sin \Delta \quad (4-51)$$

4.2.4 Method of Matrix Iteration. The method of matrix iteration is essentially Stodola's method systematized by influence coefficients and matrix algebra. The influence coefficients to be used can be defined in many different ways; however, the latest trend for the modern airplane is to express the transverse deflection a_{ij} of any point i on the wing due to a unit transverse force at any other point j . This viewpoint eliminates the necessity of assuming an elastic axis which for a complex structure like the delta wing would be a highly questionable undertaking. The advantage of the plan form type of influence coefficient is apparent even for the more conventional wing where no chordwise bending is assumed to take place. The stations in this case can be numbered consecutively along the two main spars which then enable one to separate the bending and torsional modes without reference to the elastic axis.

With a_{ij} defined as deflection at i due to a unit force at j , the deflection at any point i due to a force system P_j becomes

$$h_i = \sum_j a_{ij} P_j \quad (4-52)$$

where h_i is the structural deformation in the transverse direction. For a system vibrating in a normal mode with frequency ω , P_j is replaced by the inertia force $m_j \omega^2 Z_j$

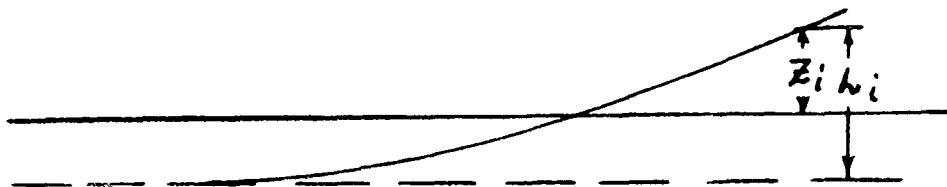


Figure 4-12. Transverse Deflections

where Z_i is the transverse amplitude which in general is different from h_j : as shown in Figure 4-12.

$$h_i = \omega^2 \sum_j a_{ij} m_j Z_j \quad (4-53)$$

The set of equations representing the deflection of n such points is conveniently expressed in the following matrix notation:

$$\frac{1}{\omega^2} \begin{bmatrix} h_1 \\ h_2 \\ h_3 \\ \vdots \\ h_n \end{bmatrix} = \begin{bmatrix} a_{11} m_1 & a_{12} m_2 & \cdots & a_{1n} m_n \\ a_{21} m_1 & a_{22} m_2 & \cdots & a_{2n} m_n \\ a_{31} m_1 & a_{32} m_2 & \cdots & a_{3n} m_n \\ \vdots & \vdots & \ddots & \vdots \\ a_{n1} m_1 & a_{n2} m_2 & \cdots & a_{nn} m_n \end{bmatrix} \begin{bmatrix} z_1 \\ z_2 \\ z_3 \\ \vdots \\ z_n \end{bmatrix} \quad (4-54)$$

where the square matrix $[am]$ is referred to as the dynamic matrix.

In the case of cantilever beams held stationary at the base, $h = Z$ and the two columns of the above equation are equal. In the free-free modes, h can be expressed in terms of Z , and hence in either case matrix equation to be solved takes the form

$$\frac{1}{\omega^2} \begin{bmatrix} z_1 \\ z_2 \\ \vdots \\ z_n \end{bmatrix} = \begin{bmatrix} A_{11} & A_{12} & \cdots & A_{1n} \\ A_{21} & A_{22} & \cdots & A_{2n} \\ \vdots & \vdots & \ddots & \vdots \\ A_{n1} & A_{n2} & \cdots & A_{nn} \end{bmatrix} \begin{bmatrix} z_1 \\ z_2 \\ \vdots \\ z_n \end{bmatrix} \quad (4-55)$$

The solution of this equation is carried out by an iteration procedure as follows. First a set of normalized amplitudes z_1, z_2, z_3, \dots is assumed for the right column, and the indicated matrix multiplication is performed. This results in a new set of $\frac{1}{\omega^2} z$'s as indicated by the left side of the

equation. The resulting mode shape will at first differ from the assumed curve and the procedure must be repeated after normalizing the new curve. When the amplitude stabilizes to a definite mode shape, the matrix equation is satisfied exactly and the natural frequency is established from the ratio of the assumed and computed amplitudes.

The iteration procedure applied to the matrix equation formulated in terms of the flexibility influence coefficients will always converge to the lowest or the fundamental mode of vibration (Reference 10, page 243). If, on the other hand, the fundamental mode is eliminated from the assumed curve, the iteration procedure will converge to the next higher mode, (Reference 10, page 244).

For the elimination of any mode, the principle of orthogonality of normal modes is utilized. Letting the superscripts designate the mode number, the orthogonality principle is expressed by the equation,

$$\sum_i m_i z_i^{(r)} z_i^{(s)} = [m_i z_i]^{(r)} \{z_i\}^{(s)} = \begin{cases} 0 & \text{for } r \neq s \\ 1 & \text{for } r = s \end{cases} \quad (4-56)$$

To eliminate the fundamental mode from an assumed curve which we wish to converge to the second mode, we will express the assumed mode (without superscript) to be represented by the sum of the normal modes as follows:

$$\begin{Bmatrix} z_1 \\ z_2 \\ \vdots \end{Bmatrix} = C_1 \begin{Bmatrix} z_1 \\ z_2 \\ \vdots \end{Bmatrix}^{(1)} + C_2 \begin{Bmatrix} z_1 \\ z_2 \\ \vdots \end{Bmatrix}^{(2)} + C_3 \begin{Bmatrix} z_1 \\ z_2 \\ \vdots \end{Bmatrix}^{(3)} + \dots$$

(4-57)

If both sides of this equation are multiplied by the row matrix $[m_1 z_1, m_2 z_2, \dots]^{(1)}$ corresponding to the first mode, every term on the right side except the first terms will be zero from the orthogonality relationship, and we are left with the equation

$$m_1 \bar{z}_1^{(1)} \bar{z}_1 + m_2 \bar{z}_2^{(1)} \bar{z}_2 + m_3 \bar{z}_3^{(1)} \bar{z}_3 + \dots = C_1 \quad (4-58)$$

The fundamental mode is eliminated from the assumed curve by letting $C_1 = 0$ which leads to the equation

$$\bar{z}_1 = - \frac{m_2}{m_1} \left(\frac{\bar{z}_2}{\bar{z}_1} \right)^{(1)} \bar{z}_2 - \frac{m_3}{m_1} \left(\frac{\bar{z}_3}{\bar{z}_1} \right)^{(1)} \bar{z}_3 + \dots \quad (4-59)$$

Supplying the identities $\bar{z}_2 = z_2$, $\bar{z}_3 = z_3$ etc., this set of equations can be represented in the matrix form

$$\begin{bmatrix} \bar{z}_1 \\ \bar{z}_2 \\ \bar{z}_3 \\ \vdots \end{bmatrix} = \begin{bmatrix} 0 & -\frac{m_2}{m_1} \left(\frac{z_2}{z_1} \right)^{(1)} & -\frac{m_3}{m_1} \left(\frac{z_3}{z_1} \right)^{(1)} & \dots \\ 0 & 1 & 0 & \dots \\ 0 & 0 & 1 & \dots \\ \vdots & \vdots & \vdots & \ddots \end{bmatrix} \begin{bmatrix} z_1 \\ z_2 \\ z_3 \\ \vdots \end{bmatrix} \quad (4-60)$$

Since this equation is the result of $C_1 = 0$, the first mode has been swept out of the assumed curve and the matrix is approximately called the sweeping matrix. The constrained matrix equation to be solved is hence

$$\frac{1}{\omega^2} \begin{bmatrix} \bar{z}_1 \\ \bar{z}_2 \\ \bar{z}_3 \\ \vdots \end{bmatrix} = \begin{bmatrix} a_{11} m_1 & a_{12} m_2 & \dots \\ a_{21} m_1 & a_{22} m_2 & \dots \\ a_{31} m_1 & a_{32} m_2 & \dots \\ \vdots & \vdots & \ddots \end{bmatrix} \begin{bmatrix} 0 & -\frac{m_2}{m_1} \left(\frac{z_2}{z_1} \right)^{(1)} & -\frac{m_3}{m_1} \left(\frac{z_3}{z_1} \right)^{(1)} & \dots \\ 0 & 1 & 0 & \dots \\ 0 & 0 & 1 & \dots \\ \vdots & \vdots & \vdots & \ddots \end{bmatrix} \begin{bmatrix} z_1 \\ z_2 \\ z_3 \\ \vdots \end{bmatrix} \quad (4-61)$$

which will converge to the second mode.

For the remaining higher modes, additional sweeping matrices must be formed from the known modes and introduced into the matrix equation. Due to the first column of zeros in the sweeping matrix, the constrained dynamic matrix will contain a column of zeros for each sweeping matrix, which reduces the number of multiplication necessary for the iteration. The convergence and the accuracy of the higher modes however, will depend greatly on the accuracy of the lower modes used in the orthogonality relationship.

4.2.4.1 Matrix Representation Including Rigid Body Motion. In the free-motion of the airplane, it is necessary to resolve the displacement Z_i of any point into its elastic and rigid body components. Letting the point i be specified by the rectangular coordinates x, y shown in

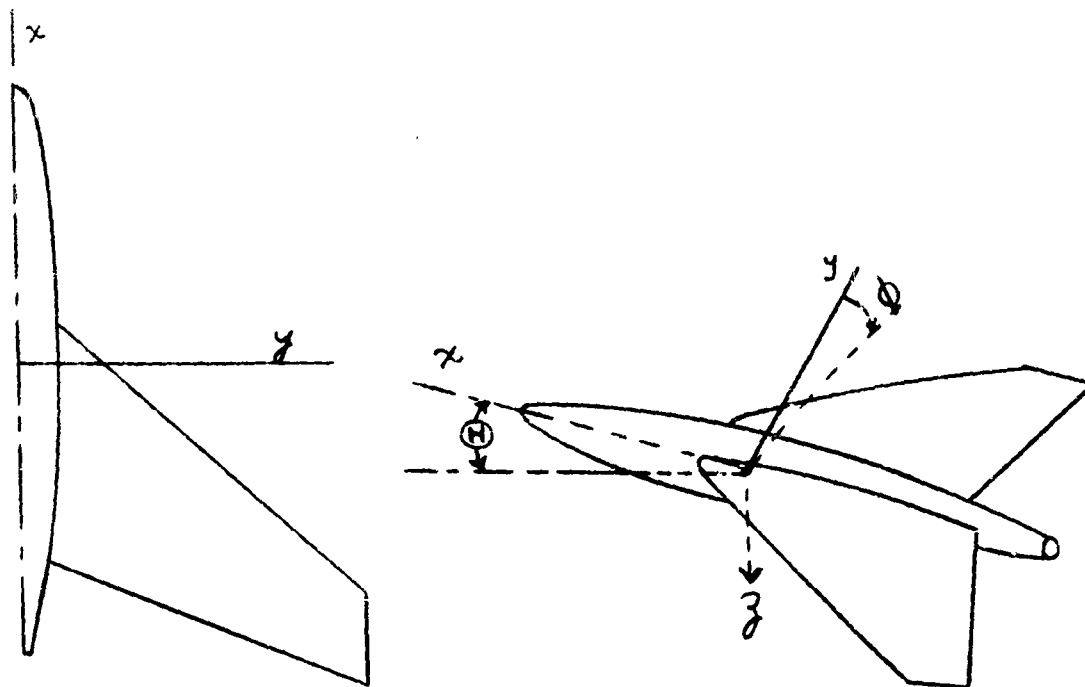


Figure 4-13 Rigid Body Motion

Figure 4-13 the rigid body displacement of the point is

$$Z_o - x \Theta + y \Phi \quad (4-62)$$

where Z_o , Θ and Φ , represent respectively the vertical translation of the origin, pitching about the y axis, and rolling about the x axis. Adding to this the elastic displacement h , considered positive in the downward direction, the total displacement in the z direction becomes

$$Z = Z_o - x \Theta + y \Phi + h \quad (4-63)$$

In the matrix equation (4-54) using influence coefficients, the displacements on the right side of the equation arise from the inertia force which is proportional to the total displacement z , whereas the displacement h on the left side of the equation represent elastic deformation, which can

now be expressed in terms of the total displacement Z , and its rigid body components by 4-63. Thus, the matrix equations including rigid body motion must take the form

$$\frac{1}{\omega^2} \begin{bmatrix} Z_1 - Z_0 + \chi_1 \Theta - \gamma_1 \Phi \\ Z_2 - Z_0 + \chi_2 \Theta - \gamma_2 \Phi \\ \vdots \end{bmatrix} = \begin{bmatrix} a_{11} m_1 & a_{12} m_2 & \dots \\ a_{21} m_1 & a_{22} m_2 & \dots \\ \vdots & \vdots & \ddots \end{bmatrix} \begin{bmatrix} Z_1 \\ Z_2 \\ \vdots \end{bmatrix} \quad (4-64a)$$

The left side of the matrix equation now contains three additional terms Z_0 , Θ and Φ , which can be determined from the fact that for the free-free vibration of the airplane the resultant linear and angular momentums for each wing including half the fuselage must be zero. We therefore have the following three equations in addition to (4-64a) above

$$\text{(Vertical Momentum)} \quad \sum_{i=0}^n m_i Z_i = 0 \quad (4-64b)$$

$$\text{(Angular Momentum about } y \text{)} \quad \sum_{i=0}^n m_i \chi_i Z_i + I_y \Theta = 0 \quad (4-64c)$$

$$\text{(Angular Momentum about } \gamma \text{)} \quad \sum_{i=0}^n m_i \gamma_i Z_i + I_x \Phi = 0 \quad (4-64d)$$

where m_0 , I_x and I_y are the mass and its mass moments of inertia for half the fuselage.

It is evident then that Z_0 , Θ and Φ can now be expressed in terms of Z_i .

Actually all three equations above are not necessary, since, for the symmetric modes, there will be no roll and hence $\Phi = 0$ whereas for the anti-symmetric modes Z_0 and Θ are set equal to zero.

For the symmetric modes then, the vertical momentum and the angular momentum about the y axis must equal zero, which steps lead to the equations,

$$Z_0 = -\frac{m_1}{m_0} Z_1 - \frac{m_2}{m_0} Z_2 - \frac{m_3}{m_0} Z_3 - \dots \quad (4-65a)$$

$$\Theta = -\frac{m_1 x_1}{I_y} Z_1 - \frac{m_2 x_2}{I_y} Z_2 - \frac{m_3 x_3}{I_y} Z_3 - \dots \quad (4-65b)$$

Substituting 4-65a and 4-65b into 4-64a, the left side of the matrix equation becomes

$$\frac{1}{\omega^2} \begin{bmatrix} \left(1 + \frac{m_1}{m_0} - \frac{m_1 x_1^2}{I_y}\right) \left(\frac{m_2}{m_0} - \frac{m_2 x_1 x_2}{I_y}\right) \left(\frac{m_3}{m_0} - \frac{m_3 x_1 x_3}{I_y}\right) - \dots \\ \left(\frac{m_1}{m_0} - \frac{m_1 x_1 x_2}{I_y}\right) \left(1 + \frac{m_2}{m_0} - \frac{m_2 x_2^2}{I_y}\right) \left(\frac{m_3}{m_0} - \frac{m_3 x_2 x_3}{I_y}\right) - \dots \\ \vdots \end{bmatrix} \begin{bmatrix} Z_1 \\ Z_2 \\ \vdots \end{bmatrix} \quad (4-66a)$$

Premultiplying both sides of the equation by the inverse of equation 4-66a, we obtain the final form of the matrix equation,

$$\frac{1}{\omega^2} \begin{bmatrix} Z_1 \\ Z_2 \\ Z_3 \\ \vdots \end{bmatrix} = \begin{bmatrix} A_{11} & A_{12} & A_{13} & \dots \\ A_{21} & A_{22} & A_{23} & \dots \\ A_{31} & A_{32} & & \dots \\ \vdots & \vdots & & \end{bmatrix} \begin{bmatrix} Z_1 \\ Z_2 \\ Z_3 \\ \vdots \end{bmatrix} \quad (4-66b)$$

where

$$\begin{bmatrix} A_{11} & A_{12} & A_{13} & \cdots \\ A_{21} & A_{22} & \cdots \\ A_{31} & \cdots \\ \vdots & \end{bmatrix} = \begin{bmatrix} \left(1 + \frac{m_1}{m_0} - \frac{m_1 x_1^2}{I_y}\right) \left(\frac{m_2}{m_0} - \frac{m_2 x_1 x_2}{I_y}\right) & \cdots \\ \left(\frac{m_1}{m_0} - \frac{m_1 x_1 x_2}{I_y}\right) \left(1 + \frac{m_2}{m_0} - \frac{m_2 x_2^2}{I_y}\right) & \cdots \\ \vdots & \end{bmatrix}^{-1} \begin{bmatrix} a_{11} m_1 & a_{12} m_2 & \cdots \\ a_{21} m_1 & a_{22} m_2 & \cdots \\ \vdots & \end{bmatrix} \quad (4-66c)$$

For the antisymmetric modes, z_0 and ϕ must be zero, and the angular momentum about the x axis must be zero. We then have the equation,

$$\phi = -\frac{m_1 y_1}{I_x} z_1 - \frac{m_2 y_2}{I_x} z_2 - \frac{m_3 y_3}{I_x} z_3 - \cdots \quad (4-67)$$

which on substitution results in the matrix equation for the first antisymmetric mode,

$$\frac{1}{\omega^2} \begin{bmatrix} z_1 \\ z_2 \\ z_3 \\ \vdots \end{bmatrix} = \begin{bmatrix} B_{11} & B_{12} & B_{13} & \cdots \\ B_{21} & B_{22} & B_{23} & \cdots \\ B_{31} & \cdots \\ \vdots & \end{bmatrix} \begin{bmatrix} z_1 \\ z_2 \\ z_3 \\ \vdots \end{bmatrix} \quad (4-68a)$$

where

$$\begin{bmatrix} B_{11} & B_{12} & \cdots \\ B_{21} & B_{22} & \cdots \\ \vdots & \end{bmatrix} = \begin{bmatrix} \left(1 + \frac{m_1 y_1^2}{I_x}\right) \left(\frac{m_2 y_1 y_2}{I_x}\right) & \cdots \\ \left(\frac{m_1 y_1 y_2}{I_x}\right) \left(1 + \frac{m_2 y_2^2}{I_x}\right) & \cdots \\ \vdots & \end{bmatrix}^{-1} \begin{bmatrix} a_{11} m_1 & a_{12} m_2 & \cdots \\ a_{21} m_1 & a_{22} m_2 & \cdots \\ \vdots & \end{bmatrix} \quad (4-68b)$$

The procedure for solving either equation, symmetric or anti-symmetric, is the same, being that of iteration. The equations given for the sweeping matrix to be used for higher modes also applies here.

4.2.5 Beam Vibrations in a Centrifugal Field. For beams vibrating in a centrifugal field, such as helicopter rotor blades, the strain energy is increased by the axial tension developed along its length. This additional strain energy can be determined

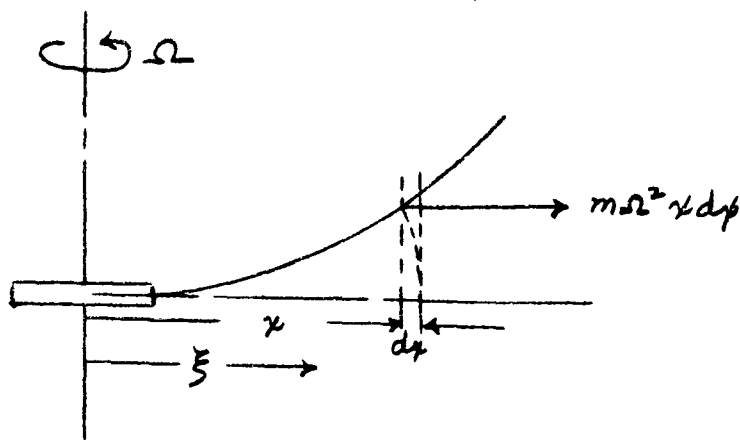


Figure 4-14. Rotating Beam

from the work done by the tensile force in moving inward towards the axis of rotation as the beam deflects.

At any point (see Figure 4-14), the radial motion due to bending is

$$\int_0^x ds - dx = \frac{1}{2} \int_0^x \left(\frac{dh}{d\xi} \right)^2 d\xi \quad (4-69)$$

The work done by the tensile force at this point is

$$\frac{1}{2} m \Omega^2 x dx \int_0^x \left(\frac{dh}{d\xi} \right)^2 d\xi \quad (4-70)$$

which can be integrated along the length of the beam to establish the total strain energy due to the centrifugal field.

$$\frac{1}{2} \Omega^2 \int_0^l m x \int_0^x \left(\frac{dh}{d\xi} \right)^2 d\xi dx \quad (4-71)$$

The total strain energy due to both bending and rotation is then

$$U_{\max} = \frac{1}{2} \int_0^l EI \left(\frac{\partial^2 h}{\partial x^2} \right)^2 dx + \frac{1}{2} \Omega^2 \int_0^l m x \int_0^x \left(\frac{\partial h}{\partial \xi} \right)^2 d\xi \cdot dx \quad (4-72)$$

For the fundamental frequency, Rayleigh's method of equating the maximum kinetic and potential energies results in the frequency equation

$$\omega^2 = \frac{\int_0^l EI \left(\frac{\partial^2 h}{\partial x^2} \right)^2 dx}{\int_0^l m h^2 dx} + \frac{\Omega^2 \int_0^l m x \int_0^x \left(\frac{\partial h}{\partial \xi} \right)^2 d\xi \cdot dx}{\int_0^l m h^2 dx} \quad (4-73a)$$

which can be written in the form (Reference 21):

$$\omega^2 = \omega_b^2 + C \Omega^2 \quad (4-73b)$$

Since the first term on the right side of this equation results from the strain energy of bending, one might be tempted to label ω_b as the natural frequency of bending. It must be remembered however that the bending mode $h(x)$ is dependent on Ω , and hence the effect of rotation is implicitly involved in Ω , making it a variable mildly dependent upon Ω .

The quantity C in the second term is frequently referred to as the rotational constant (known as Horvay's constant), although it too is somewhat dependent on Ω through $h(x)$. Nevertheless, the above frequency equation is a convenient one since the variation of ω_b and C due to Ω is slight.

In fact, Rayleigh's method owes its success to the fact that a first order error in the deflection curve results in a second order error in the frequency.

Equations of this kind are useful in estimating the fundamental frequency of rotor blades of the helicopter. In addition, most helicopter rotor blades are relatively stiff in torsion compared to bending, and its mass center coincides closely with the shear center. Thus, torsional modes are generally insignificant compared to the bending modes.

It should be mentioned here that the Rayleigh-Ritz approach is recommended for the rotating beam problem. Due to the rather gradual variation of the

inertial and elastic properties along the rotor blades, the use of the normal modes of the uniform beam in a non-rotating field results in good accuracy in the Ritz computation.

4.2.5.1 Holzer-Myklestad Method for the Rotating Beam. The Holzer-Myklestad approach discussed previously, can be extended to include rotational effects. It is evident here that only the equilibrium equations are altered

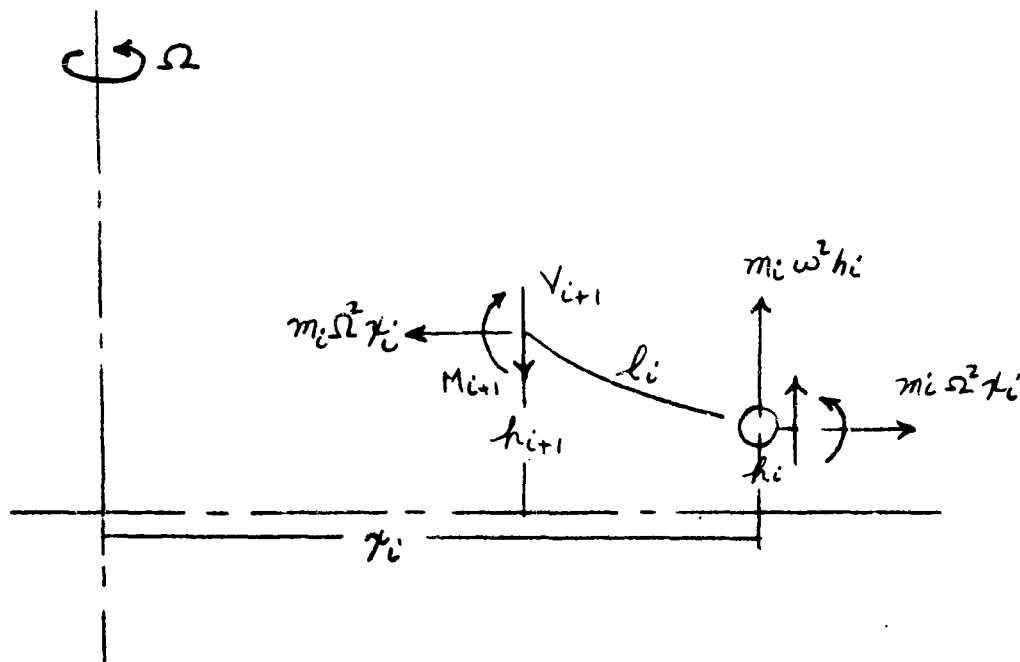


Figure 4-15 Rotating Beam-Element
by the rotation. The four equations from Figure 4-15 are,

$$V_{i+1} = V_i + m_i \omega^2 h_i + m_i \Omega^2 x_i h_i' \quad (4-74a)$$

$$M_{i+1} = M_i + (V_i + m_i \omega^2 h_i) l_i + m_i \Omega^2 x_i (h_{i+1} - h_i) \quad (4-74b)$$

$$= M_i (1 + m_i \Omega^2 x_i a_{m_i}) + V_{i+1} (l_i + m_i \Omega^2 x_i a_{v_i}) \quad (4-74b')$$

$$h_{i+1}' = h_i' + V_{i+1} b_{v_i} + M_i b_{M_i} \quad (4-74c)$$

$$h_{i+1} = h_i + h_i' l_i + V_{i+1} a_{v_i} + M_i a_{M_i} \quad (4-74d)$$

which can be computed in the same manner as in the case of bending vibrations for non-rotating beams.

Equations for the rotating beam can also be expressed in matrix form for machine computation. The elements of the matrix equations however are more involved.

$$\begin{bmatrix} V_{i+1} \\ M_{i+1} \\ h'_{i+1} \\ h_{i+1} \end{bmatrix} = \begin{bmatrix} 1 & 0 & m_i \Omega^2 x_i & m_i \omega^2 \\ (l_i + m_i \Omega^2 x_i a_{v_i}) & (1 + m_i \Omega^2 x_i a_{M_i}) & m_i \Omega^2 x_i (l_i + m_i \Omega^2 x_i a_{v_i}) & m_i \omega^2 (l_i + m_i \Omega^2 x_i a_{v_i}) \\ b_{v_i} & b_{M_i} & (1 + m_i \Omega^2 x_i b_{v_i}) & m_i \omega^2 b_{v_i} \\ a_{v_i} & a_{M_i} & (l_i + m_i \Omega^2 x_i a_{v_i}) & (1 + m_i \omega^2 a_{v_i}) \end{bmatrix} \begin{bmatrix} V_i \\ M_i \\ h'_i \\ h_i \end{bmatrix} \quad (4-75)$$

It is evident that this equation reduces to that of the non-rotating bending mode when $\Omega = 0$.

4.3 Analysis of Coupled Systems

4.3.1 Generalized Coordinates and Lagrange's Equations. In considering the most general type of motion that an airplane can have, it will be recalled that any such motion can be represented in terms of the normal modes of the system. If the amplitudes of the normal modes of the airplane as a whole are designated by $h_r(x, y, z)$ where the subscript r refers to the mode number, the displacement $\xi(x, y, z, t)$ of any point can be expressed in the general form

$$\xi(x, y, z, t) = q_1 h_1(x, y, z) + q_2 h_2(x, y, z) + \dots \quad (4-76)$$

In this equation q_r determines the extent to which the r^{th} mode contributes to the motion, and is referred to as the generalized coordinate corresponding to mode r .

Lagrange introduced a general form of analysis which enables one to determine the equations of motion of the system when the energy expressions of the system are known in terms of the generalized coordinates. The basic form of Lagrange's equation is

$$\frac{d}{dt} \left(\frac{\partial T}{\partial \dot{q}_r} \right) - \frac{\partial T}{\partial q_r} + \frac{\partial U}{\partial q_r} = Q_r \quad (4-77)$$

where T and U are the kinetic and potential energies and $Q_r = \frac{\partial W}{\partial q_r}$ the generalized force determined from that portion of the work not derivable from a potential.

Letting $m(x, y, z)$ be the mass associated with the point (x, y, z) the equation for the kinetic energy takes the form

$$T = \frac{1}{2} \int \dot{\xi}^2(x, y, z) dm(x, y, z) \quad (4-78)$$

where the integral is extended over the entire airplane. Since ξ is of the form

$$\dot{\xi}^2 = \dot{q}_1^2 h_1^2 + \dot{q}_2^2 h_2^2 + \dot{q}_1 \dot{q}_2 h_1 h_2 + \dots + \dot{q}_r \dot{q}_s h_r h_s + \dots \quad (4-79)$$

the kinetic energy expression reduces to the form

$$T = \frac{1}{2} \sum_r \sum_s M_{rs} \dot{q}_r \dot{q}_s \quad (4-80a)$$

where the generalized masses:

$$M_{rs} = M_{sr} = \int h_r(x, y, z) h_s(x, y, z) dm(x, y, z) \quad (4-80b)$$

The potential energy is the strain energy stored in the structure due to deformation, and can be written in the form

$$U = \frac{1}{2} \sum_r \sum_s K_{rs} q_r q_s \quad (4-81)$$

The elastic coefficients $K_{rs} = K_{sr}$ need not be further defined since they can be expressed in terms of mass coefficient and the normal mode frequency as indicated in the following discussion.

For the normal mode vibration of the system we know that each mode satisfies an equation of the form

$$M_{rr} \ddot{q}_r + K_{rr} q_r = 0 \quad (4-82a)$$

$$\ddot{q}_r = -\omega^2 q_r \quad (4-82b)$$

so that the stiffness coefficient is related to the mass coefficient by the equation

$$K_{rr} = \omega^2 M_{rr} \quad (4-83)$$

Since the substitution of T and U into Lagrange's equation for free vibration results in the equation of the form

$$\sum_s M_{rs} \ddot{q}_s + \sum_s K_{rs} q_s = 0 \quad (4-84)$$

it is evident that $M_{rs} = K_{rs} = 0$ for $r \neq s$. We see then that the requirement

$$M_{rs} = \int h_r(x, y, z) h_s(x, y, z) dm(x, y, z) = 0 \quad r \neq s \quad (4-85)$$

defines the orthogonality property for the normal modes.

The above discussion indicates that when normal modes are used, the kinetic and potential energies are given by the equations:

$$T = \frac{1}{2} \sum_s M_{ss} \dot{q}_s^2 \quad (4-86a)$$

$$U = \frac{1}{2} \sum_s K_{ss} q_s^2 \quad (4-86b)$$

and the equations of motion under any form of excitation become

$$(\ddot{q}_s + \omega_s^2 q_s) = \frac{Q_s}{M_{ss}} \quad s = 1, 2, 3, \dots \quad (4-87)$$

where Q may be a function of the generalized coordinates and their derivatives as well as time. Thus, the contribution of each normal mode to the general solution is represented by a second order differential equation.

4.3.1.1 Effective Mass and Inertia Parameters. The fuselage modes tend to couple with the wing modes for large and flexible airplanes. As an example, in the symmetrical wing modes of the free-free airplane, vertical bending of the fuselage and horizontal tail surfaces takes place. This effect can be taken into account by either one of two methods. The first and most obvious method is to include the additional degrees of freedom into the equations of motion by generalized coordinates. The procedure is similar to the technique used in including the control surface rotation into the analysis (see Section 4.3.3). In this case it will be necessary to determine the additional kinetic energy over that of the rigid fuselage motion due to bending of the fuselage-tail assembly. Lagrange's equation then enables one to determine the additional terms in the equations of motion.

In the second method, the flexible modes of the fuselage-tail assembly can be taken into account without increasing the degree of freedom of the equations of motion, by using the effective mass of the fuselage-tail assembly in place of the rigid mass. The effective mass is here defined as an equivalent rigid mass which if acted upon by the acceleration of the reference point, results in the same force as that of the elastic system. Thus, for a distributed elastic system whose reference point is oscillating with an amplitude of z_0 , as shown in Figure 4-16.

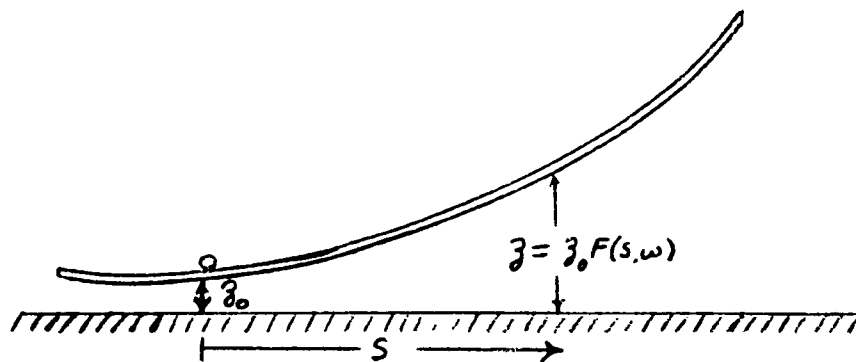


Figure 4-16 Elastic System

the effective mass becomes

$$m_{\text{eff}} = \frac{F_0}{\ddot{z}_0} = \int F(s, \omega) dm \quad (4-88)$$

For a single lumped mass mounted on a spring, the above equation can be reduced to the simple form,

$$m_{\text{eff}} = \frac{m}{1 - \left(\frac{\omega}{\omega_n}\right)^2} \quad (4-89)$$

whereas, for the distributed elastic system, the effective mass can be determined from a Holzer analysis and plotted as a function of the frequency as shown in Figure 4-17.

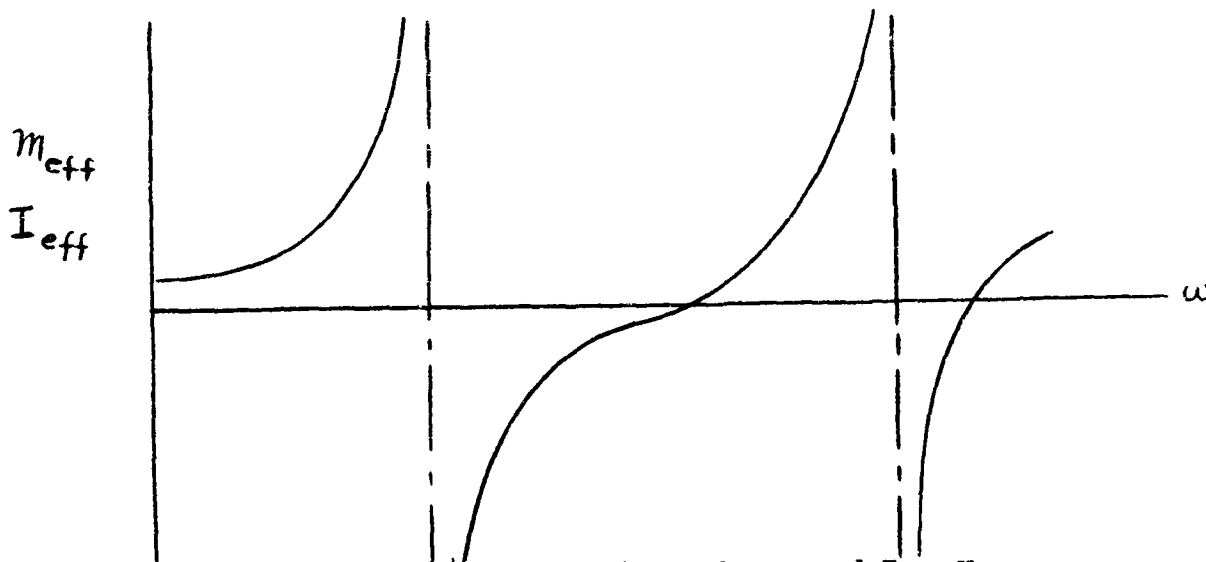


Figure 4-17 Variation of m_{eff} and I_{eff} Versus ω

It is evident then that the effective mass can be negative as well as positive. Assuming that the above curve represents the effective mass of the fuselage for vertical bending, its use in place of the rigid fuselage mass will result in the analysis of the free-free airplane where the fuselage bending modes are coupled to the wing modes.

Similar procedure applies equally well to torsional oscillations. In this case we define the effective inertia as a rigid inertia at a reference point, which acted upon by the torsional acceleration of the reference point will result in the same torque as the elastic system of distributed inertias. The equation for the effective inertia is then,

$$I_{\text{eff}} = \frac{T_0}{\ddot{\phi}_0} = \int F(s, \omega) dI = \frac{\int \phi dI}{\phi_0} \quad (4-90)$$

and its plot as a function of the frequency will be similar to that of effective mass. Here again, for a single flexibly supported mass, the equation reduces to the form,

$$I_{eff} = \frac{I}{1 - \left(\frac{\omega}{\omega_n}\right)^2} \quad (4-91)$$

Equations 4-89 and 4-91 for the single mass can be conveniently used for spring mounted engines and other attachments. It should be noted that in the normal mode analysis of the wing the engine mass to be used should be its effective mass for the frequency under consideration.

4.3.1.2 Transient Response Parameters. In the preceding section it was shown that the transient response of any structure, when represented in terms of its normal modes, leads to a system of second order differential equations (Equation 4-87) which can be determined independently for each mode. Such independent solutions may then be summed as in equation 4-76 for the transient response of the system.

Consider now a force $P(x, y, t)$ applied to the structure. The generalized force Q_s is then determined from the virtual work δW corresponding to a virtual displacement δq_s . The expression for the generalized force becomes,

$$Q_s = \frac{\delta W}{\delta q_s} = \int P(x, y, t) h_s(x, y) dx dy \quad (4-92)$$

and Equation 12 takes the form,

$$\ddot{q}_s + \omega_s^2 q_s = \frac{1}{M_{ss}} \int P(x, y, t) h_s(x, y) dx dy \quad (4-93)$$

where the generalized mass M_{ss} is given by the equation,

$$M_{ss} = \int h_s^2(x, y) dm(x, y) \quad (4-94)$$

In cases where the load $p(x, y, t)$ is expressible in the form,

$$p(x, y) f(t) \quad (4-95)$$

Equation 4-93 may be written as,

$$\ddot{q}_s + \omega_s^2 q_s = \frac{C_s}{M_{ss}} f(t) \quad (4-96)$$

where,

$$C_s = \int p(x, y) h_s(x, y) dx dy \quad (4-97)$$

is the participation factor which determines the extent to which modes contribute to the general motion. The solution of Equation 4-96 can then be written in the following integral form,

$$q_s = \frac{C_s}{\omega_s^2 M_{ss}} \omega_s \int_0^t f(\xi) \sin \omega_s (t - \xi) d\xi \quad (4-98)$$

where the quantity,

$$\omega_s \int_0^t f(\xi) \sin \omega_s (t - \xi) d\xi \quad (4-99)$$

is the dynamic load factor. The significance of this term is evident when one compares the static and dynamic solutions both expressed in terms of normal modes. The dynamic load factor will then be the ratio of the dynamic to the static terms for each mode.

4.3.2 Coupled Mode Analysis. Uncoupled modes are frequently used for the coupled mode analysis of the airplane. As an example, we consider the coupling of the wing bending, wing torsion and the rigid body translation, roll, or pitch of the airplane. We can let the uncoupled modes be expressed as:

$$\text{rigid body motion} \quad \bar{H} H(x, y) \quad (4-100)$$

$$\text{uncoupled wing bending} \quad h = \bar{h}_1 h_1(s) + \bar{h}_2 h_2(s) + \bar{h}_3 h_3(s) + \dots \quad (4-101)$$

$$\text{uncoupled wing torsion} \quad \Phi = \bar{\phi}_1 \phi_1(s) + \bar{\phi}_2 \phi_2(s) + \bar{\phi}_3 \phi_3(s) + \dots \quad (4-102)$$

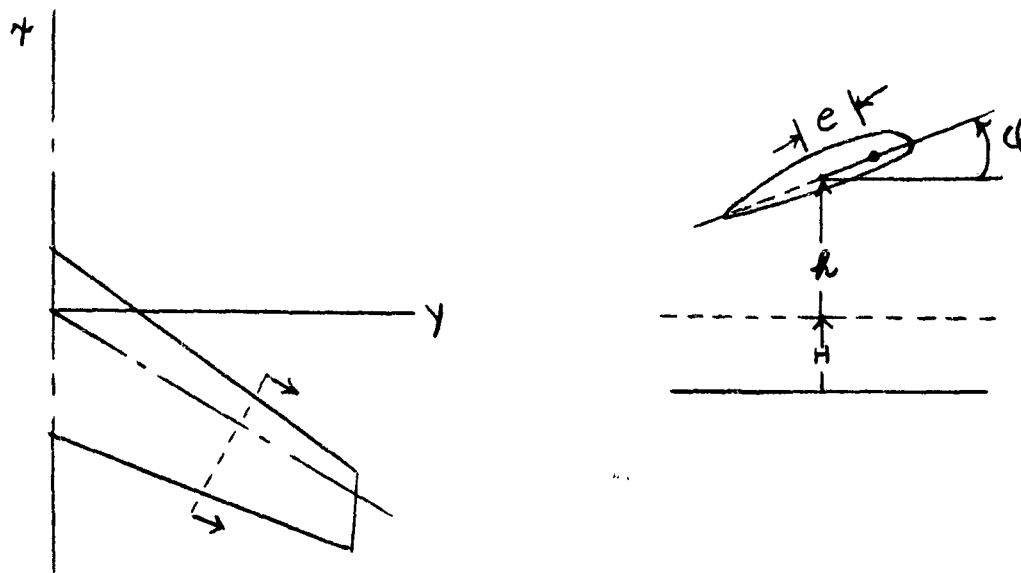


Figure 4-18. Wing Section

For pure translation of the rigid body, $H(x,y) = 1$, whereas for the roll or pitch $H(x,y) = y$ or x respectively. H then is the generalized coordinate for the rigid body translation or rotation. The other terms h and ϕ are the generalized coordinates for the bending and torsion of the wing with normal modes represented by $h(S)$ and $\phi(S)$. Although the modes of the coupled oscillations differ from those of the uncoupled oscillations, they may be accurately represented when sufficient number of modes are included in the analysis.

The displacement of the center of gravity of the wing section at x, y (see Figure 4-18) can now be expressed in terms of the uncoupled components as

$$Z = H + h + e\phi \quad (4-103)$$

Expressions for the kinetic and potential energies then become

$$\begin{aligned} T &= \frac{1}{2} \int (\dot{Z} + e\dot{\phi})^2 dm + \frac{1}{2} \int \dot{\phi}^2 (dI - e^2 dm) \\ &= \frac{1}{2} \dot{H}^2 \int H^2(x,y) dm + \frac{1}{2} \sum_i \dot{h}_i^2 \int h_i^2(s) dm + \sum_i \dot{H} \dot{h}_i \int H(x,y) h_i(s) dm \\ &\quad + \sum_i \dot{H} \dot{\phi}_i \int e H(x,y) \phi_i(s) dm + \sum_i \sum_j \dot{h}_i \dot{\phi}_j \int e h_i(s) \phi_j(s) dm \\ &\quad + \frac{1}{2} \sum_i \dot{\phi}_i^2 \int \phi_i^2(s) dI \end{aligned} \quad (4-104)$$

$$U = \frac{1}{2} \sum_i \bar{h}_i^2 \int EI \left[\frac{\partial^2 \bar{h}_i(s)}{\partial s^2} \right]^2 ds + \frac{1}{2} \sum_i \bar{\Phi}_i^2 \int GJ \left[\frac{\partial \bar{\Phi}_i(s)}{\partial s} \right]^2 ds$$

$$+ \frac{1}{2} \sum_i (K_{hh})_i \bar{h}_i^2 + \frac{1}{2} \sum_i (K_{\phi\phi})_i \bar{\Phi}_i^2 \quad (4-105)$$

where some of the cross products disappear due to orthogonality. Making the following substitutions:

$$M_{hh} = \int H^2(x, y) dm$$

$$M_{hh} = \int H(x, y) h(s) dm$$

$$M_{hh} = \int h^2(s) dm$$

$$M_{h\phi} = \int e H(x, y) \Phi(s) dm$$

$$M_{\phi\phi} = \int \Phi^2(s) dI$$

$$M_{h\phi} = \int e h(s) \Phi(s) dm$$

$$K_{hh} = \omega_{hh}^2 M_{hh}$$

$$K_{\phi\phi} = \omega_{\phi\phi}^2 M_{\phi\phi}$$

the terms in Lagrange's equation become,

$$\frac{d}{dt} \left(\frac{\partial T}{\partial \dot{H}} \right) = M_{hh} \ddot{H} + \sum_i M_{hh_i} \ddot{h}_i + \sum_i M_{h\phi_i} \ddot{\Phi}_i \quad (4-106)$$

$$\frac{d}{dt} \left(\frac{\partial T}{\partial \dot{h}_i} \right) = M_{hh_i} \ddot{h}_i + M_{hh} \ddot{H} + \sum_j M_{h_i\phi_j} \ddot{\Phi}_j \quad (4-107)$$

$$\frac{d}{dt} \left(\frac{\partial T}{\partial \dot{\Phi}_i} \right) = M_{h\phi_i} \ddot{H} + \sum_j M_{h_j\phi_i} \ddot{h}_j + M_{\phi_i\phi_i} \ddot{\Phi}_i \quad (4-108)$$

$$\frac{\partial U}{\partial \bar{h}_i} = (\omega_{hh}^2)_i M_{h_i h_i} \bar{h}_i \quad (4-109)$$

$$\frac{\partial U}{\partial \bar{\phi}_i} = (\omega_{\phi\phi}^2)_i M_{\phi_i \phi_i} \bar{\phi}_i \quad (4-110)$$

At this point it is possible to write down the frequency equation for an analysis including any number of modes. The following equation is for body motion coupled with the first bending and first torsion modes.

$$\begin{vmatrix} \omega^2 M_{HH} & \omega^2 M_{Hh_1} & \omega^2 M_{H\phi_1} \\ \omega^2 M_{Hh_1} & (\omega^2 - \omega_{h,h_1}^2) M_{h_1 h_1} & \omega^2 M_{h_1 \phi_1} \\ \omega^2 M_{H\phi_1} & \omega^2 M_{h_1 \phi_1} & (\omega^2 - \omega_{\phi,\phi_1}^2) M_{\phi_1 \phi_1} \end{vmatrix} = 0 \quad (4-111)$$

It is apparent here that the four lower right terms of this determinant represent the coupled wing bending and torsion modes, whereas the other four terms not including $\omega^2 M_{HH}$, account for the coupling of the wing motions to the rigid body motion.

In considering the modes of vibration of an aircraft, it is usually the case that coupling exists between wing deflection (bending-torsion) and body deflection. Several typical cases are indicated in the following sequence of figures, each of which can be considered as an over-all mode of vibration.

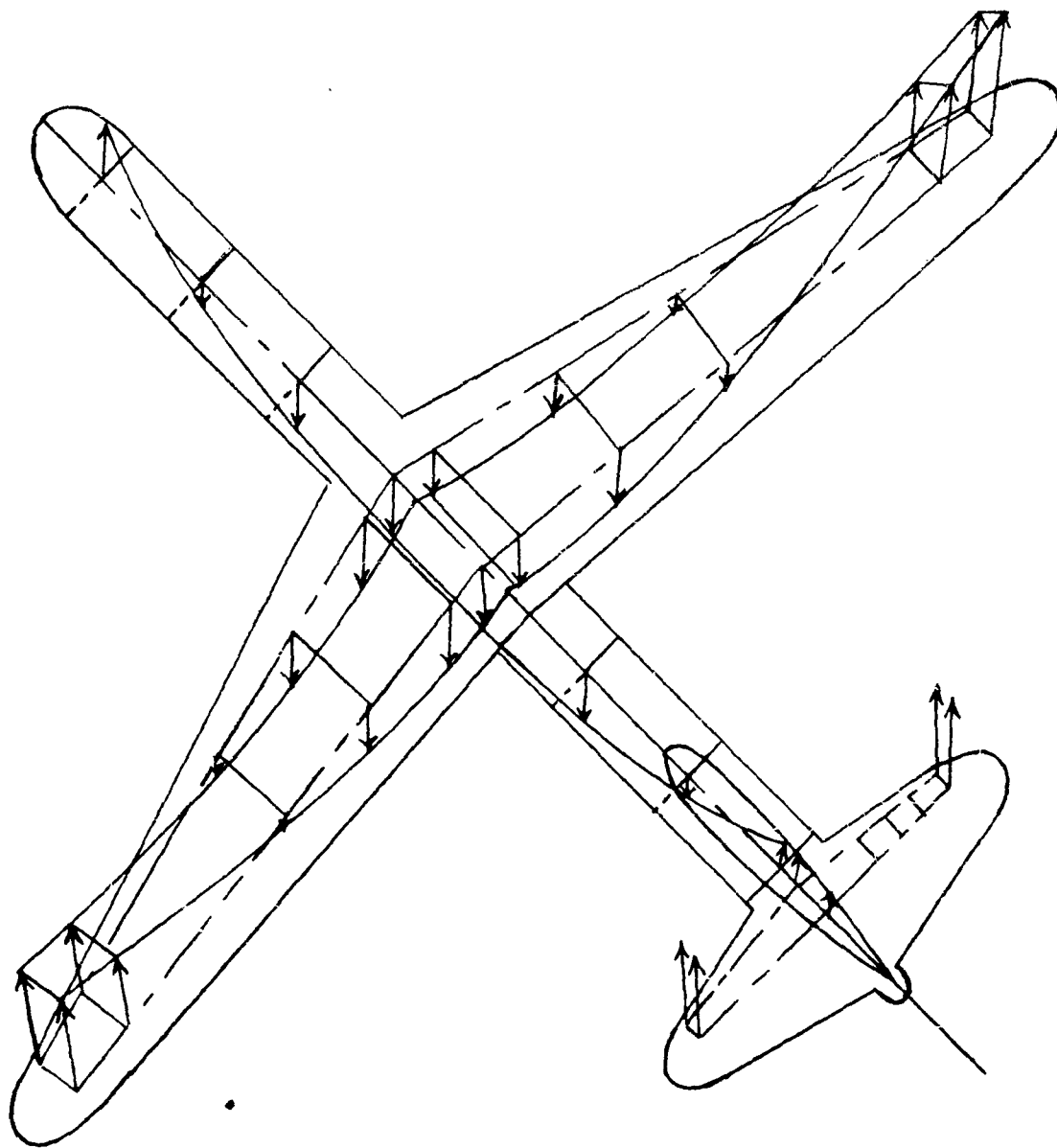


Figure 4-19. Symmetrical Bending Mode

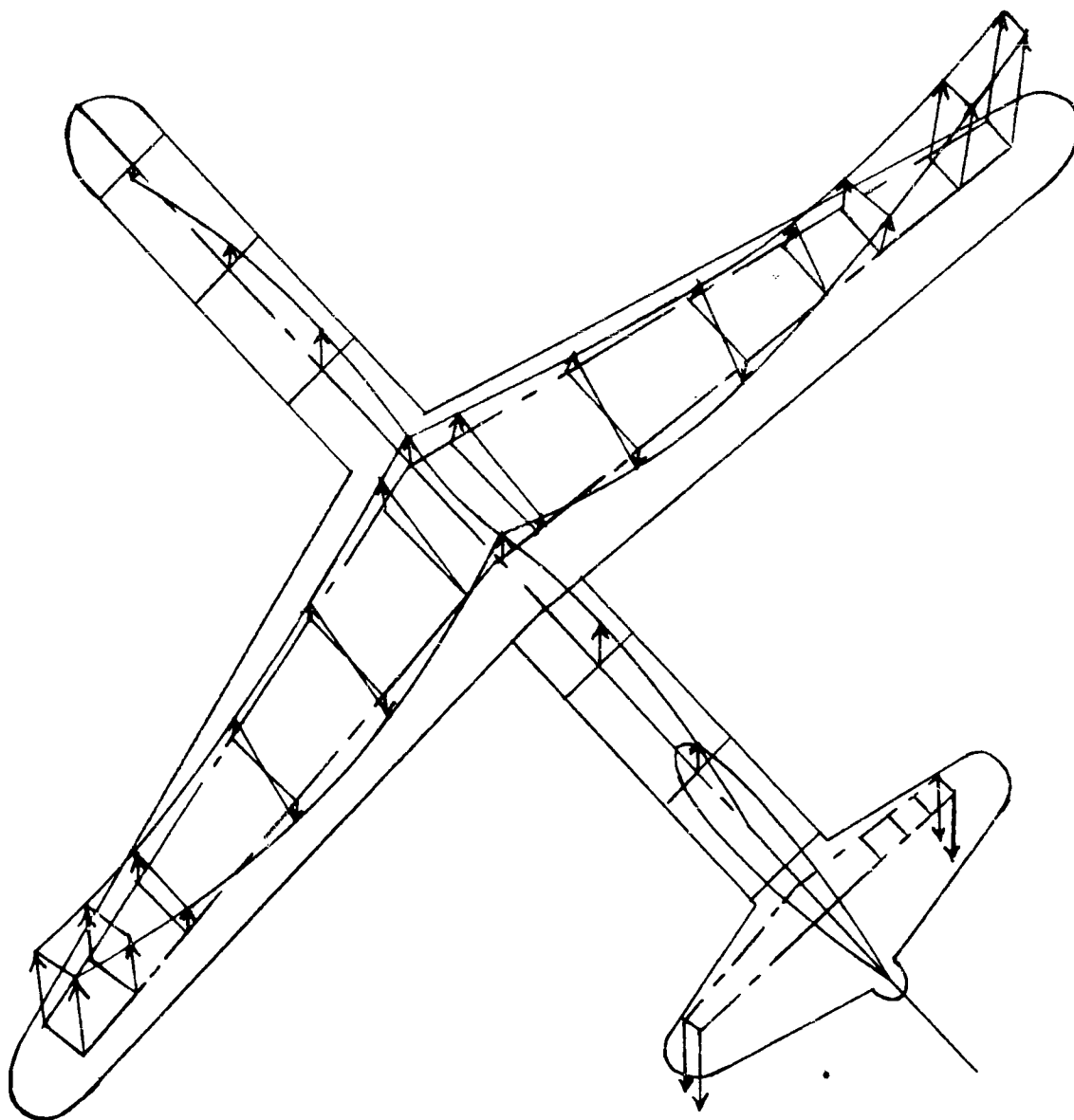


Figure 4-20. Symmetrical Bending Mode

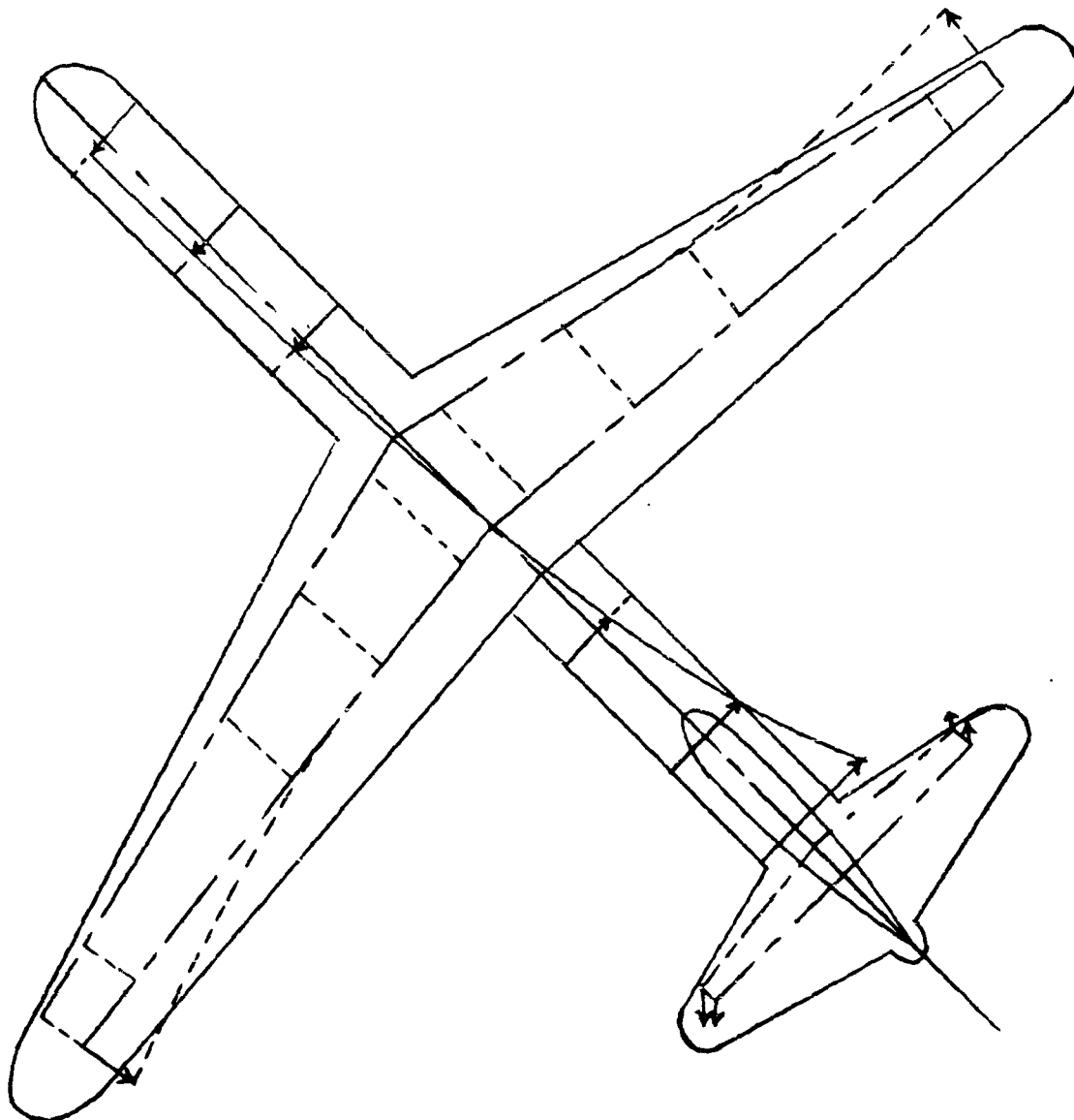


Figure 4-21. Asymmetrical Chordwise Bending Mode

Of course, higher wing and body coupling may occur tending to complicate the analysis a great deal more. In all cases wing torsion associated with wing bending, as previously discussed, introduces more distinct modes. For instance Figure 4-19 may vibrate with either positive or negative wing torsion as the wing bends up (positive torsion means leading edge moves faster than bending elastic axis at the same wing station).

When the over-all mode shapes are known (either from theory or vibration tests), then kinetic and potential energy expressions can be derived knowing the mass, inertial and stiffness distributions. The generalized mass, inertia and spring terms (for each over-all mode) are then determined by the energy averaging methods introduced in Section 3.3 for the simple wing mode case.

4.3.3 Coupling of Control Surfaces. Control surface rotation can be included in the vibration analysis by considering the additional kinetic and potential energies associated with such motion. Since the bending-torsion vibration of the wing structure is generally computed with the control surface locked to it, the additional terms in Lagrange's equations are determined by evaluating the total kinetic energy of the deflected control surface and subtracting from this the kinetic energy of the control surface locked to the wing structure.

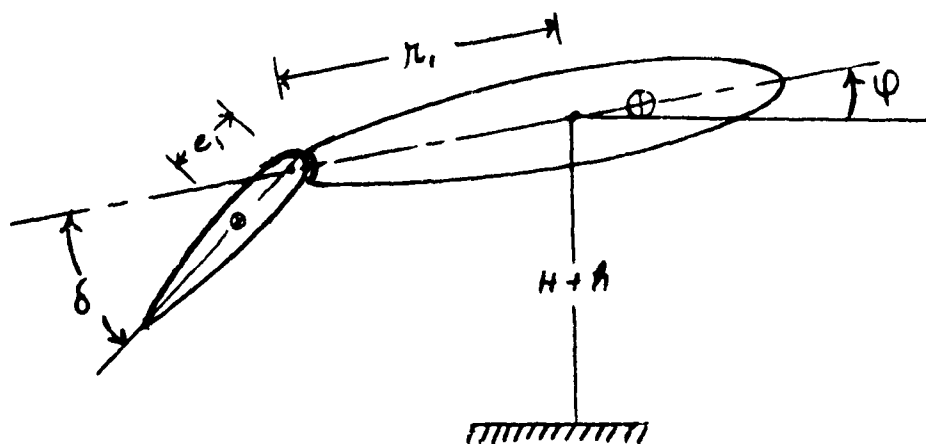


Figure 4-22. Wing and Control Surface Section.

Referring to Figure 4-22, and letting m_δ and I_δ be the control surface mass and its mass moment of inertia about the hinge line, the additional kinetic energy due to δ is

$$T = \frac{1}{2} \int \{ [\dot{H} + \dot{h} - (r_1 + e_1) \dot{\phi} - e_1 \dot{\delta}]^2 - [\dot{H} + \dot{h} - (r_1 + e_1) \dot{\phi}]^2 \} dm_\delta \quad (4-112)$$

$$+ \frac{1}{2} \int \{ [\dot{\phi} + \dot{\delta}]^2 - [\dot{\phi}]^2 \} \{ dI_\delta - e_1^2 dm_\delta \}$$

$$= - \int \dot{H} \dot{\delta} e_1 dm_\delta - \int \dot{h} \dot{\delta} e_1 dm_\delta + \int \dot{\phi} \dot{\delta} (dI_\delta + e_1 r_1 dm_\delta) + \frac{1}{2} \int \dot{\delta}^2 dI_\delta \quad (4-112')$$

Using the notation of Section 4.3.2,

$$H = \bar{H} H(x, y) \quad (4-113)$$

$$h = \sum_i \bar{h}_i h_i(s) \quad (4-114)$$

$$\phi = \sum_i \bar{\phi}_i \phi_i(s) \quad (4-115)$$

we add the control surface coordinate

$$\delta = \bar{\delta}_i \delta(s) \quad (4-116)$$

If the control surface takes no further twisting beyond that due to wing twisting, then $\delta(s) = 1$; however it is convenient to detail the term $\delta(s)$ to identify the various additional integrals in the equations of motion.

Rewriting the kinetic energy equation in terms of these quantities, we have,

$$T = - \dot{\bar{H}} \dot{\bar{\delta}} \int H(x, y) \delta(s) e_1 dm_\delta - \sum_i \dot{\bar{h}}_i \dot{\bar{\delta}} \int h_i(s) \delta(s) e_1 dm_\delta$$

$$+ \sum_i \dot{\bar{\phi}}_i \dot{\bar{\delta}} \int \phi_i(s) \delta(s) [dI_\delta + e_1 r_1 dm_\delta] + \frac{1}{2} \dot{\bar{\delta}}^2 \int \delta^2(s) dI_\delta$$

(4-117)

The stiffness of the control surface to rotation involves the control mechanism as well as the twisting and bending of the control surface induced by $\phi(s)$ and $h(s)$. Lumping these into a single stiffness coefficient, the potential energy associated with δ is

$$U = \frac{1}{2} K_{\delta\delta} \delta^2 = \frac{1}{2} \omega_{\delta\delta}^2 M_{\delta\delta} \delta^2 \quad (4-118)$$

Introducing the notation,

$$M_{H\delta} = - \int H(x, y) \delta(s) e_1 dm_\delta$$

$$M_{h\delta} = - \int h(s) \delta(s) e_1 dm_\delta$$

$$M_{\phi\delta} = \int \phi(s) \delta(s) [dI_\delta + e_1 r_1 dm_\delta]$$

$$M_{\delta\delta} = \int \delta^2(s) dI_\delta$$

the additional terms in Lagrange's equations are:

$$\frac{d}{dt} \left(\frac{\partial T}{\partial \dot{H}} \right) = M_{H\delta} \ddot{\delta} \quad (4-119)$$

$$\frac{d}{dt} \left(\frac{\partial T}{\partial \dot{h}_i} \right) = M_{h_i\delta} \ddot{\delta} \quad (4-120)$$

$$\frac{d}{dt} \left(\frac{\partial T}{\partial \dot{\phi}_i} \right) = M_{\phi_i\delta} \ddot{\delta} \quad (4-121)$$

$$\frac{d}{dt} \left(\frac{\partial T}{\partial \dot{\delta}} \right) = M_{H\delta} \ddot{H} + \sum_i M_{h_i\delta} \ddot{h}_i + \sum_i M_{\phi_i\delta} \ddot{\phi}_i + M_{\delta\delta} \ddot{\delta} \quad (4-122)$$

$$\frac{\partial U}{\partial \delta} = \omega_{\delta\delta}^2 M_{\delta\delta} \delta \quad (4-123)$$

Thus, the frequency equation for the analysis where only the first modes are included takes the form,

$$\begin{vmatrix}
 \omega^2 M_{HH} & \omega^2 M_{Hh_1} & \omega^2 M_{H\phi_1} & \omega^2 M_{H\delta} \\
 \omega^2 M_{Hh_1} & (\omega^2 - \omega_{h_1 h_1}^2) M_{h_1 h_1} & \omega^2 M_{h_1 \phi_1} & \omega^2 M_{h_1 \delta} \\
 \omega^2 M_{H\phi_1} & \omega^2 M_{h_1 \phi_1} & (\omega^2 - \omega_{\phi_1 \phi_1}^2) M_{\phi_1 \phi_1} & \omega^2 M_{\phi_1 \delta} \\
 \omega^2 M_{H\delta} & \omega^2 M_{h_1 \delta} & \omega^2 M_{\phi_1 \delta} & (\omega^2 - \omega_{\delta \delta}^2) M_{\delta \delta}
 \end{vmatrix} = 0$$

(4-124)

This equation is identical to Equation 4-111 of Section 4.3.2 except for the additional terms appearing in the last row and column.

The procedure presented here is quite general and can be applied equally well to the fuselage-tail assembly. The inclusion of the fuselage-tail modes would merely introduce additional terms to the above determinant. With addition of higher modes, the order of the above determinant will be increased.

However, since $h = \sum_i \bar{h}_i h_i(s)$ and $\phi = \sum_i \bar{\phi}_i \phi_i(s)$ are the approximations to the coupled modes, it is possible to replace the summation by the coupled mode itself, i.e., $\bar{h}_c h_c(s)$ and $\bar{\phi}_c \phi_c(s)$, which has the advantage of keeping the order of the determinant to a minimum.

4.3.4 Coupling of Auxiliary Equipment. Airplane structures are frequently burdened by the addition of auxiliary equipment such as tip tanks and rockets. In such cases the question often arises as to the change in natural frequency due to the added mass. Such questions can be answered by carrying out a new set of computations including the additional equipment. It is possible however to avoid a complete recalculation by noting certain pertinent facts regarding the frequency equation of any structure.

Consider for simplicity a rigidly supported structure. We will consider the motion of the system to be harmonic and express the deflections in terms of the influence coefficients.

$$h_i = \omega^2 \sum_j a_{ij} m_j h_j \quad (4-125)$$

The frequency equation resulting from the determinant of these equations takes the form,

$$\left(\frac{1}{\omega^2}\right)^n - \sum_i a_{ii} m_i \left(\frac{1}{\omega^2}\right)^{n-1} + \dots = 0 \quad (4-126)$$

where the coefficient of the second highest term is now of interest. We recall here the fact that when an algebraic equation is arranged in the order of descending powers with the coefficient of the first term equal to unity, the coefficient of the second highest term must be equal to the sum of the roots of the equation. Letting $\omega_1, \omega_2, \omega_3$, etc. be the natural frequencies of the system, corresponding to the roots of the equation, we can write the equation,

$$\frac{1}{\omega_1^2} + \frac{1}{\omega_2^2} + \frac{1}{\omega_3^2} + \dots = a_{11} m_1 + a_{22} m_2 + a_{33} m_3 + \dots \quad (4-127)$$

Since $\omega_1, \omega_2, \omega_3$, etc. are increasing values, the terms on the left side of this equation are diminishing quantities. For instance, for the uniform cantilever beam, these magnitudes are in the proportion

$$\frac{1}{(3.52)^2} + \frac{1}{(22.4)^2} + \frac{1}{(61.7)^2} + \dots \quad (4-128)$$

It is evident here that no serious error will result in assuming the left side of the equation to be $\frac{1}{\omega_1^2}$ in which case we arrive at Dunkerley's equation (Reference 10, page 172).

$$\begin{aligned} \frac{1}{\omega_1^2} &= a_{11} m_1 + a_{22} m_2 + a_{33} m_3 + \dots \\ &= \frac{1}{\omega_{11}^2} + \frac{1}{\omega_{22}^2} + \frac{1}{\omega_{33}^2} + \dots \end{aligned} \quad (4-129)$$

In arriving at the last form of the equation, it is noted that a_{ii} is the deflection at i due to a unit force at i , which implies that a_{ii} is the reciprocal of the stiffness at the point i . Thus, $a_{ii} = \frac{1}{k_i}$ and $a_{ii} m_i = \frac{m_i}{k_i} = \frac{1}{\omega_{ii}^2}$.

To use Dunkerley's equation to answer the question of the effect of the added mass on the natural frequency, we will assume that the fundamental frequency of the original structure is represented by the equation,

$$\frac{1}{\omega_1^2} = a_{11} m_1 + a_{22} m_2 + \dots + a_{jj} m_j + \dots \quad (4-130)$$

We next attach to the structure an additional mass M at some point, say j . Then the new frequency equation becomes

$$\begin{aligned}\frac{1}{\bar{\omega}_1^2} &= a_{11} m_1 + a_{22} m_2 + \dots + a_{jj} (m_j + M) + \dots \\ &= \frac{1}{\omega_1^2} + a_{jj} M \\ &= \frac{1}{\omega_1^2} + \frac{M}{k_j}\end{aligned}\tag{4-131}$$

Thus, the natural frequency ω_1 has been lowered to $\bar{\omega}_1$ by the addition of the mass M . If several masses are added at points i, j, n , etc., the above procedure results in the equation,

$$\frac{1}{\bar{\omega}_1^2} = \frac{1}{\omega_1^2} + \frac{M_i}{k_j} + \frac{M_i}{k_i} + \frac{M_n}{k_n}\tag{4-132}$$

Such equations are applicable to torsional oscillations as well as bending oscillations. For the torsional oscillations the counterpart of the above equation is

$$\frac{1}{\bar{\omega}_1^2} = \frac{1}{\omega_1^2} + \frac{I_i}{K_j} + \frac{I_i}{K_i} + \frac{I_n}{K_n}\tag{4-133}$$

where K_1 is the torsional stiffness at point i , or the reciprocal of the torsional influence coefficient.

REFERENCES

1. Holzer, H., Die Berechnung der Drehschwingungen, J. Springer, Berlin, (1921).
2. Timoshenko, S., Vibration Problems in Engineering, D. Van Nostrand, New York, 2nd Edition, (1937).
3. Karman, T. and Biot, M. A., Mathematical Methods in Engineering, McGraw-Hill, New York, (1940).
4. Den Hartog, J. P., Mechanical Vibrations, McGraw-Hill, New York, 3rd Edition, (1947).
5. Myklestad, N. O., Vibration Analysis, McGraw-Hill, New York, (1944).
6. Frazer, R. A., Duncan, W. J. and Collar, A. R., Elementary Matrices, MacMillan, New York (1947).
7. Pipes, L. A., Applied Mathematics for Engineers and Physicists, McGraw-Hill, (1946).
8. Timoshenko, S. and Young, D. H., Theory of Structures, McGraw-Hill, New York, (1945).
9. Thomson, W. T., A Note on Tabular Methods for Flexural Vibrations, Journal of Aeronautical Sciences, January, 1953.
10. Thomson, W. T., Mechanical Vibrations, Prentice-Hall, 2nd Edition (1953).
11. Karman, T., Use of Orthogonal Functions in Structural Problems, Timoshenko Anniversary Volume, New York, Macmillan, Page 114, (December 1938).
12. Burgess, C. P., The Frequencies of Cantilever Wings in Beam and Torsional Vibrations, National Advisory Committee of Aeronautics, TN 746, (1940).
13. Myklestad, N. O., A New Method of Calculating Natural Modes of Uncoupled Bending Vibration of Airplane Wings and Other Types of Beams, Journal of Aeronautical Sciences, Volume 11, page 153, (April 1944).
14. Prohl, M. A., A General Method of Calculating Critical Speeds of Flexible Rotors, Journal of Applied Mechanics, (September 1945).
15. Beskin, L. and Rosenberg, R. M., Higher Modes of Vibration by a Method of Sweeping, Journal of Aeronautical Science, Page 643, (November 1946).

16. Duncan, W. J., Mechanical Admittances and Their Application to Oscillation Problems, British Aeronautical Research Council, Reports and Memoranda Number 2000, (1947).
17. Targoff, W. P., The Associated Matrices of Bending and Coupled Bending-Torsion Vibrations, Journal of Aeronautical Sciences, Page 576, (October 1947).
18. Lawrence, H. R., Dynamics of a Swept Wing, Journal of Aeronautical Sciences, Page 643, (November 1947).
19. Zahorski, A. T., Free Vibrations of a Sweptback Wing, Journal of Aeronautical Sciences, Page 683, (December 1947).
20. White, W. T., An Integral Equation Approach to the Problem of Vibrating Beams, Journal of the Franklin Institute, Page 25, (January 1948) Page 117, (February 1948).
21. Morduchow, M., A Theoretical Analysis of Elastic Vibrations of Fixed-Ended and Hinged Helicopter Blades in Hovering and Vertical Flight, National Advisory Committee on Aeronautics, TN 1999, (January 1950).
22. Anderson, R. A. and Houbolt, J. C., Determination of Coupled and Uncoupled Modes and Frequencies of Natural Vibration of Swept and Unswept Wings from Uniform Cantilever Modes, National Advisory Committee on Aeronautics, TN 1714, (November 1948).
23. Fettis, H. E., The Calculation of Coupled Modes of Vibration by the Stodola Method, Journal of Aeronautical Sciences, Page 259, (May 1949).
24. Fettis, H. E., A Modification of the Holzer Method for Computing Uncoupled Torsion and Bending Modes, Journal of Aeronautical Sciences, Page 625, (October 1949).
25. Siddall, J. W. and Isakson, G., Approximate Analytical Methods for Determining Natural Modes and Frequencies of Vibration, Massachusetts Institute of Technology, Aero-Elastic and Structures Research, ONR 035-259, (January 1951).
26. Myklestad, N. O., The Concept of Complex Damping, Journal of Applied Mechanics, Page 284, (September 1952).

27. Flomenhoft, H. I., A Method for Determining Mode Shapes and Frequencies Above the Fundamental by Matrix Iteration, Journal of Applied Mechanics, Page 249, (September 1950).
28. Williams, D., Rapid Estimates of the Higher Natural Frequencies and Modes of Beams and Hence of Stress Induced by Transient and Periodic Loads, Reissner Anniversary Volume, Page 152, J. W. Edwards, Ann Arbor, Michigan, (1949).
29. Williams, D., Recent Developments in the Structural Approach of Aeroelastic Problem, Journal of the Royal Aeronautical Society, Page 403, (June 1954).
30. Young, D., and Felgar, R. P., Tables of Characteristic Functions Representing Normal Modes of Vibration of a Beam, University of Texas Engineering Research Publication, Number 4913, (July 1, 1949).

NOMENCLATURE

$a_{ij}, a(x, \xi), a_{v_i}, a_{m_i}, b_{v_i}, b_{m_i}$ = Flexibility influence coefficients

c_i = Torsional flexibility influence coefficient

e = Base (2.718 ---) or eccentricity

$e.a.$ = Elastic axis = locus of elastic centers along wing

e_i = Distance c.g. of section i is from elastic axis

e_o = Distance from origin of xy axis to fuselage c.g.

e_l = Distance from control surface hinge line to control surface center of gravity

h_i = Displacement at point i

$h(x)$ = Bending mode shape

k_{ij} = Stiffness influence coefficient

l_i = Distance between stations i and $i + 1$

m_i = Mass of section i

$p(s)$ = Loading per unit distance

q_r = Generalized coordinates

r = Distance, or mode number

r_l = Distance from elastic center to control surface hinge line

s = Distance along beam (or wing)

\mathcal{A} = Static mass moment about the elastic axis per unit length of beam

x = Axis along fuselage center line

y = Axis perpendicular to center line

A_i = Amplitude associated with i th normal mode
 B = Deflection constant
 C = Rotational Constant (Horvay's Constant)
 C_s = Participation factor
 C_{cr} = Critical Damping
 E = Young's modulus for beam material, lbs/ft^2
 F = Force
 GJ = Torsional stiffness per unit length, lb ft^2
 \bar{H} = Generalized coordinate describing rigid body translation or rotation
 I_Q = Mass Moment of inertia about the elastic axis
 I_δ = Control surface inertia about hinge line
 I_i = Moment of inertia of section i
 K_i = Torsional stiffness at point i
 K_{ss} = Generalized stiffness
 L = Lift
 $M(s)$ = Bending moment at point s along the beam (as wing)
 M_{eff} = Effective Mass
 M_δ = Control surface mass
 M_{ss} = Generalized mass
 P_i = Force
 Q_s = Generalized force
 T = Kinetic Energy or Torque
 U = Potential Energy
 $V(s)$ = Shear
 V_z = Vertical shear at airplane center line
 W = Work
 W_i = Lumped Weights
 Z_i = Normalized amplitudes

- α_1 = Parameter used in equation describing deflection curve
- δ = Control surface deflection angle
- Θ = Pitching angle of fuselage
- Λ = Sweep angle of the elastic axis
- Ω = Angular velocity
- ω = Circular frequency
- Φ = Roll angle of fuselage
- φ = Torsional angle of station
- r = Radial distance to rotational vector, or general spanwise coordinate
- $()^1$ = Slope or first derivative

CHAPTER V

DETERMINATION OF AERODYNAMIC EFFECTS

5.0 Introduction

In the previous chapters the basic concepts of the aeroelastic analysis of aircraft stability and control have been discussed, and the equations of motion of a flexible aircraft have been derived. In these equations it is assumed that the aerodynamic forces acting on a moving and vibrating aircraft may be expressed by the so-called "first-order" theory, which will now be discussed.

In the most general analysis it is necessary to determine the aerodynamic forces corresponding to an arbitrary motion (distortion) of the airplane. This general aerodynamic problem is discussed in Section 5.2. An attempt will be made to put the aerodynamic force evaluations on the foundation of the modern theory of nonstationary airfoils. This theory is ordinarily used in the flutter analysis, and in applying it to the stability and control problems certain simplification is possible in virtue of the smallness of the "reduced frequency" that characterizes dynamic stability problems. In Section 5.2 the basic concepts and general equations are developed. However, solutions are given in the form of integrals which are not necessarily easy to evaluate. Much effort has been spent in the past to accumulate and tabulate special solutions of practical interest to aeroelastic analyses. A summary of known results and a guide to the literature is therefore of interest and value to the analyst. Such a summary is given in Section 5.3 for two-dimensional flow and in Section 5.4 for finite wings. Tables showing a comparison of notations used in the most important references are given.

In Section 5.5, a corresponding summary of the known results on the indicial responses of an airfoil to a step function input is given. These results are of prime importance to problems of gust response, maneuver, or controlled operations. They are also of importance in solving the dynamic problems by the Laplace transformation method.

In Section 5.6, the transformation of stability derivatives in several systems of moving coordinates are examined.

The results of Sections 5.2 - 5.6 are of general applicability, suitable for either the modal approach or the collocation approach as outlined in Chapter III. In Section 5.7, however, the "modified derivatives," to be used in a simplified analysis, are discussed. This is explained as follows:

The analysis of an elastic airplane is usually quite complicated. Simplified approaches are therefore valuable. One of the simplified methods, the so-called "method of modified derivatives," includes the elastic distortion effect in the stability derivatives of a rigid airplane. In this approach the number of dependent variables is the same as that of a rigid airplane. The orders of the differential equations remain unchanged, and the stability determinants are of the same order. Only the stability derivatives are modified. This method is based on the assumption that the elastic distortions occur very slowly in relation to the lowest relevant natural frequency of structural oscillation. It is inapplicable when the forces

and moments proportional to the distortional velocities and accelerations cease to be negligible. It is therefore appropriate to call this method "quasi-static," as was done in Section 3.2.2.3.

Whenever applicable, the method of modified derivatives is to be recommended because it possesses the great merit of simplicity. The validity of this simplified approach can be checked as soon as a solution is obtained. If it is found that the basic assumption of slow oscillation is violated, further corrections can be made subsequently on the basis of more precise equations of greater complexity.

Although the modification of the stability derivatives due to elastic distortion is not merely an aerodynamic problem, but is an aeroelastic problem, it will nevertheless be discussed in this chapter. When one thinks of the stability and control equations in the familiar form applicable to a rigid airplane, it is quite appropriate to include the discussion of the modified derivatives under the present chapter heading.

5.1 Summary

The materials of the present chapter can be used in the following manner: A quick review of the general concepts as well as specific results can be obtained from Sections 5.2 - 5.6. The stability derivatives obtained from the first order unsteady flow theory can be used to replace the conventional quasi-stationary derivatives. The modified derivatives for elastic distortion can be obtained as in Section 5.7. If the solution of the modified-derivatives approach shows violation of conditions presumed for this approach, (Section 5.7.3), a more extensive analysis based either on the modal approach or on the collocation approach must be made.

It suffices in general in the airplane dynamics to use the first order theory; but occasionally it may be necessary to consider higher order terms in reduced frequency. In such an event the information summarized in Sections 5.3, 5.4 may be used.

The general formulas in Section 5.2 may be used as a basis to determine stability derivatives for those modes of elastic distortions or wing plan-forms for which tabulated results are not known.

The evaluation of the rigid body stability derivatives will not be considered in any detail, except insofar as the conventional results may be modified by unsteady flow and elastic effects. Empirical corrections for wing-fuselage interference, power effect, etc., are of great importance, particularly in relation to the lateral derivatives. It is generally advisable to use experimental data wherever possible, relying on purely theoretical calculations only insofar as necessary. Considerable experimental information on unsteady-flow effects exists. See References 22, 95, 146 and 147. A bibliography and review of experimental results can be found in Chapter 15 of Reference 58 and Chapter 13 of Reference 59. Unfortunately, there is still insufficient experience on incorporating these experimental results in the dynamic stability analysis.

5.1.1 Significance of the Unsteady Flow Effect. Incorporation of the unsteady flow theory in the stability and control analysis requires some additional effort in comparison with the labor required in the conventional quasi-stationary analysis. To help judge whether such an elaboration is necessary in each

specific case, the basic reason will be outlined below.

The "quasi-stationary" theory assumes that the aerodynamic loads are linearly dependent on the angular positions and the velocities of the airfoil producing them. The forces and moments are predicted at any instant of the motion as if the airfoil were in steady motion under the conditions pertaining to that instant. Certain aerodynamic lags are neglected in this procedure. Because of the aerodynamic lag, it becomes evident that when rapid maneuvers are considered, the aerodynamic derivatives can no longer be considered constant, but must be variable functions of the acceleration.

In contrast to the "quasi-steady" theory, the unsteady aerodynamic theory accounts for the time lag between the growth of circulation and the motion generating it by considering the influence of the trailing and shed vortices in the wake of the wing. The result, however, is a tremendous complication in the analysis. For stability and control analyses of an aircraft, however, it often happens that the acceleration of the aircraft motion is not large, or, in case of sinusoidal oscillation, the frequency is small. Important simplifications can be obtained in such cases. A proper dimensionless parameter for frequency as a measure of the unsteady aerodynamic effect is the reduced frequency, defined as*

$$k = \frac{\omega l}{U}$$

where ω is the circular frequency in radians per second, l is a characteristic length, often taken as the mean aerodynamic semi-chord length, and U is the true airspeed of the aircraft. If the reduced frequency k is small, say, of order 0.1 or less, the unsteady aerodynamic forces in response to a specific motion may be expanded in series of k . When all terms of higher order of smallness than k are neglected, the result is called the "first-order" theory. In stability and control analysis, the smallness of k often permits one to use the first-order theory instead of the full unsteady flow theory.

Compared with the frequency, damping, and transient-response calculations based on the quasi-steady aerodynamic coefficients, the nonsteady flow considerations seem to show, in some specific instances, considerable influence upon the control surface motion, whereas their effect on the airplane motion as a whole is not large. The unsteady flow effect should be considered, therefore, in studying the control surface motions, and in the design of automatic control of aircraft which operates through the control surfaces, whose dynamic transfer functions must be known in order to avoid instabilities due to coupling between the control system and the aircraft.

To have some idea about the difference in analysis based on quasi-stationary and unsteady flow theory, the stability determinants may be compared. With the usual assumptions of rigid-body airplane dynamics, the stick-free longitudinal stability determinants for horizontal flight are,

(neglecting the u -equation and writing λ for $\frac{\partial}{\partial t}$):

*A sinusoidal oscillation can be represented by a time factor $e^{i\omega t}$, where ω is real and positive. A damped oscillation can be represented by $e^{i\omega t}$ with ω a complex number. The real part of ω is then the frequency, the imaginary part, the damping factor. Similarly k may be complex, with its imaginary part representing reduced damping factor. The first order theory holds when the absolute value of k is small.

(a) First-order-unsteady-flow theory:

$$\left| \begin{array}{ccc} \frac{\partial Z}{\partial w} + \left[\frac{\partial Z}{\partial \dot{w}} - m \right] \lambda & \frac{\partial Z}{\partial \dot{q}} + m U_0 & \frac{\partial Z}{\partial \delta} + \frac{\partial Z}{\partial \dot{\delta}} \lambda \\ \frac{\partial M}{\partial w} + \frac{\partial M}{\partial \dot{w}} \lambda & \frac{\partial M}{\partial \dot{q}} - I_{yy} \lambda & \frac{\partial M}{\partial \delta} + \frac{\partial M}{\partial \dot{\delta}} \lambda \\ \frac{\partial H}{\partial w} + \left[\frac{\partial H}{\partial \dot{w}} - h_e \right] \lambda & \frac{\partial H}{\partial \dot{q}} + h_e - (I_e + h_e l_e) \lambda & \frac{\partial H}{\partial \delta} + \frac{\partial H}{\partial \dot{\delta}} \lambda - I_e \lambda^2 \end{array} \right|$$

(b) Quasi-stationary theory:

$$\left| \begin{array}{ccc} \frac{\partial Z}{\partial w} - m \lambda & \frac{\partial Z}{\partial \dot{q}} + m U_0 & \frac{\partial Z}{\partial \delta} \\ \frac{\partial M}{\partial w} + \frac{\partial M}{\partial \dot{w}} \lambda & \frac{\partial M}{\partial \dot{q}} - I_{yy} \lambda & \frac{\partial M}{\partial \delta} \\ \frac{\partial H}{\partial w} - h_e \lambda & \frac{\partial H}{\partial \dot{q}} + h_e - (I_e + h_e l_e) \lambda & \frac{\partial H}{\partial \delta} - I_e \lambda^2 \end{array} \right|$$

A comparison of the above expressions shows clearly that the additional labor required in adopting the first order theory lies in the evaluation of a number of stability derivatives, and that the labor required in solving the stability determinantal equation or any response problem remains approximately the same for both theories.

It has been shown (Ref. 7 of Chapter III), by an order of magnitude analysis, that for large values of the density ratio, $\mu = m/\rho S c$, many unsteady-flow derivatives have negligible effect on the motion of the aircraft. Thus in the above equations, $\partial Z/\partial \dot{w}$, $\partial Z/\partial \dot{\delta}$, $\partial H/\partial \dot{w}$ may be neglected.

Some conclusions regarding the importance of aerodynamic lag may be drawn on the basis of special numerical examples. Weissinger (Ref. 145), Goland (Ref. 62), Smilg (Ref. 64), Goland, Luke and Sacks (Ref. 69), Statler (Refs. 117, 118) and Walkowicz (Ref. 65) have given various examples to the effects of unsteady flow and elastic distortion to the dynamic characteristics of the airplane. Exhaustive treatment of the problem with many examples is also given by Ashley, Zartarian, and Neilson (Ref. 22), and Goland, Luke, Hager (Ref. 70). A brief survey of their conclusions is presented in Appendix 5C.

5.2 Survey of Basic Concepts and Analytical Results in the First Order Unsteady Flow Theory

5.2.1 Aerodynamic Concepts

5.2.1.1 Linearized Aerodynamic Theory. The linearized aerodynamic theory is based on the hypotheses that all velocity and pressure disturbances

are so small compared with the flight velocity and free stream pressure, respectively, that only linear terms in these disturbances need be retained. In consequence of this approximation, the various aerodynamic forces on a body are linear in the displacements or velocities of this body; e.g., the lift on a wing is linear with respect to angle of attack. The basic equations of fluid flow are nonlinear, so it is necessary to resort to linearized approximations of these equations in order to make any appreciable progress in the calculation of aerodynamic forces. Moreover, the design of the most important lifting surfaces (wing, horizontal tail, fin) for low drag requires that velocity and pressure disturbances be kept small, thereby favoring the linearized theory.*

Linearized aerodynamic theory generally must be distinguished from small perturbation theory; in the latter the aerodynamic forces due to disturbed motion are calculated by considering small perturbations about the undisturbed flow. For example, the values of $C_{L\alpha}$, $C_{m\alpha}$, etc. used in the dynamic

stability equations need not be calculated on the basis on linearized theory but can be taken from nonlinear portions of the approximate curves for steady flight in the equilibrium configuration. Linearized theory however, will be adopted throughout this chapter.

The approximations implicit in linearized theory generally are acceptable in dynamic stability studies. It should be remarked, however, that linearized theory cannot be expected to be satisfactory in analyzing stalled flight or such violent maneuvers as the spin.

5.2.1.2 Quasi-stationary and First Order Theories. The linearized approximations to aerodynamic forces in dynamic stability studies usually are expanded in the disturbance coordinates and their time derivatives with only the first one or two terms retained as in (3-16) and (3-17). Thus, e.g., the lift coefficient due to angle of attack may be expanded according to:

$$C_L = \left(\frac{\partial C_L}{\partial \alpha} \right)_0 \alpha + \left(\frac{\partial C_L}{\partial \dot{\alpha}} \right) \dot{\alpha} + \left(\frac{\partial C_L}{\partial \ddot{\alpha}} \right) \ddot{\alpha} + \dots \quad (5-1)$$

It then is argued that the higher terms in the expansion are negligible for the slow rates of change that occur in the rigid body motions of the airplane. Alternatively, if the motion is regarded as harmonic, it may be established that the n'th term in the expansion (5-1) is of the order of k^n (cf., however, (5-21) and discussions following (5-166)), where k is the reduced frequency

$$k = \omega \ell / U \quad (5-2)$$

comprising the angular frequency ω , a characteristic length ℓ (usually chosen as the wing semi-chord in defining k), and U the flight velocity.

* The pressure disturbances for a body of given dimensions increase with Mach number, however, so that the linearized theory usually breaks down in the hypersonic regime.

The retention of only the first term in expansions of the type (5-1) constitutes the quasi-stationary (or quasi-steady) approximation, in which the air forces are calculated as if the instantaneous flow pattern were steady. In terms of an expansion in the reduced frequency k , the quasi-stationary approximation is not completely consistent, since it neglects terms of first order in frequency in the equations of flow (e.g., the terms $\partial\phi/\partial t$ in Bernoulli's equations, and for compressible flow, the term $\partial\rho/\partial t$ in the equation of continuity).

That approximation retaining all terms that are first order in k will be designated as first order theory, in contrast to quasi-stationary. It should be emphasized that the distinction between the quasi-stationary and first order theories is based on the reduced frequency k , whereas the approximations permitted in the dynamic stability equations for a rigid airplane depend primarily on the relative density factor μ . Thus, it may be established* by an order analysis in μ^{-1} that the only unsteady flow term that need be included in the equations of longitudinal stability for large μ is $C_{m\dot{\alpha}}$.

The foregoing discussion now will be illustrated in more explicit fashion by discussing the calculation of the moment on an airplane due to an angular velocity q , i.e., the pitch damping derivative. There are two distinct situations that are of practical importance viz., flight at constant incidence along a curved flight path (e.g., a dive pullout), as shown in Figure 5-1, and flight at varying incidence along a straight flight path (as in the dynamic stability problem), as shown in Figure 5-2. In the first case the flow is truly steady, and the aerodynamic effect of the flight path curvature is described simply by introducing an additional incidence ($q\ell/U$) at the tail aerodynamic center, where ℓ_t is the distance of this center aft of the c.g., plus an effective camber due to the curved flow, plus similar effects at the wing; however, only the change of tail incidence is of appreciable importance in conventional configurations. It has long been realized that the stability derivative ($C_{m\dot{q}}$) so obtained is not directly applicable to the calculation

of the damping moment on an airplane performing a pitching oscillation as it flies along a straight path, and it is necessary to add the derivative $C_{m\dot{\alpha}}$

to account for changing wing incidence. It usually is assumed that $C_{m\dot{\alpha}}$ is

due entirely to the effect of the wake of the upstream (wing) surface on the downstream (tail) surface** and is given by

$$C_{m\dot{\alpha}} = C_{mq} \cdot \left(\frac{d\epsilon}{d\alpha} \right) \quad (5-3)$$

where ϵ is the induced downwash at the downstream surface due to an angle of attack α of the upstream surface. The total damping derivative for pitching oscillations (with respect to inertial, not body axes) then is given by

* Reference 8, Page 2-59

** In most of the following, the main lifting surface, designated as the wing, is assumed to be forward of the horizontal stabilizer, designated as a tail. However, these positions may be reversed, as in the canard configuration.

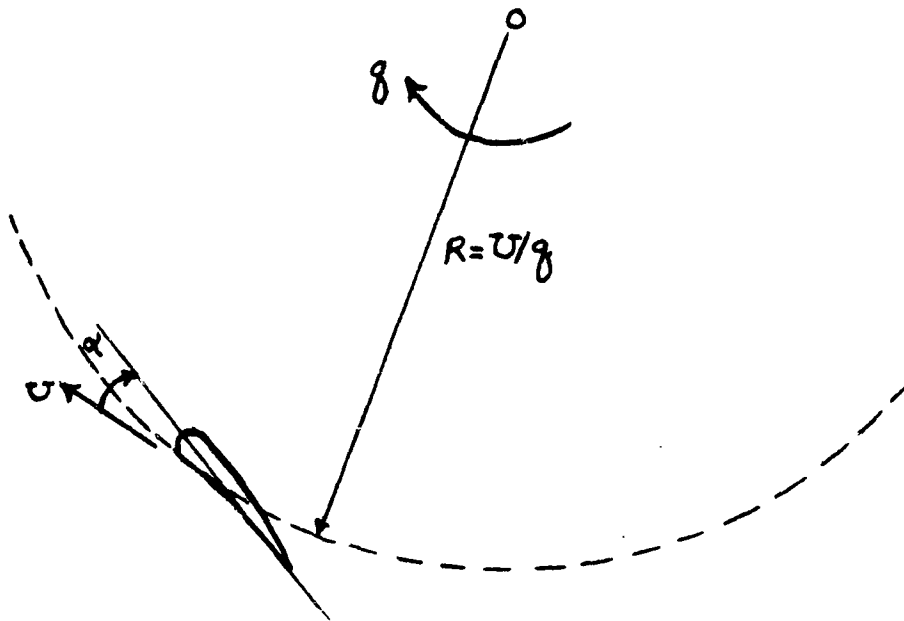


Figure 5-1. An Airfoil Executing a Steady Pullout at an Angular Velocity q about the center O .

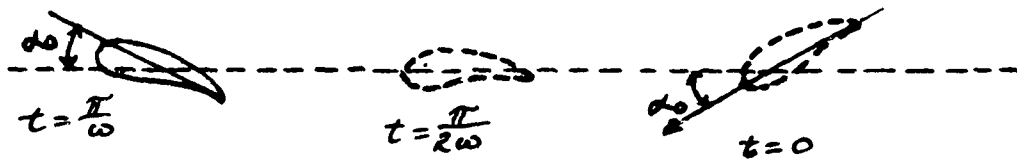


Figure 5-2. An Airfoil Flying Along a Straight Path with Variable Angle of Attack $\alpha = \alpha_0 \cos \omega t$.

$$C_{mq} + C_{m\dot{\alpha}}$$

The derivative $C_{m\dot{\alpha}}$, as given by (5-3), arises essentially in consequence of unsteady flow effects, in contrast to C_{mq} , which is based entirely on steady flow concepts; nevertheless, as given by (5-3), $C_{m\dot{\alpha}}$ fails to account for all terms that contribute to total damping in consequence of being first order in frequency. Thus, while it takes into account the time lag of the wake at the tail due to wing incidence, no allowance is made for the effect of this lag on the wing itself, nor is the downwash at the tail due to effective camber of the wing (associated with the angular velocity q) taken into account. In addition, other terms of first order in frequency may arise, and the consistency of the end result can be best insured by a systematic reduction of the results for unsteady flow, retaining all terms of first order in the reduced frequency k .

It is not to be inferred that all terms of first order in frequency are necessarily of the same importance, but this can be determined only at a later time. Thus, $C_{m\dot{\alpha}}$ for a wing alone is relatively unimportant compared with C_{mq} at low speeds; but in the transonic regime $C_{m\dot{\alpha}}$ may exceed C_{mq} (for wing alone) in magnitude and be of opposite sign. Moreover, in dealing with less conventional configurations, such as tailless aircraft, unsteady flow terms may prove of the greatest importance. In particular, if $C_{m\dot{\alpha}}$ were to cancel C_{mq} in a flying wing design, the results might well be catastrophic.

Before undertaking a detailed study of first order, unsteady-flow results, it is instructive to indicate the structure of the results for the particular case of damping in pitch. The aerodynamic force acting on a wing depends on the normal velocity distribution over the wing, herein designated as the (local) downwash, and the free stream velocity, the former being assumed small compared with the latter. In the case of a pitching oscillation of amplitude α_1 about a transverse axis at $x = a$, as shown in Figure 5-3, the downwash may be placed in the form

$$w(x,t) = R \ell [\bar{w}(x) e^{i\omega t}] \quad (5-4)$$

$$\bar{w}(x) = U \alpha_1 + i \omega \alpha_1 (a-x) \quad (5-5)$$

The first term in (5-5), $U \alpha_1$ represents the effect of incidence and the second, $i \omega \alpha_1 (a-x)$, the effective camber due to the angular velocity (which has the instantaneous value $q = -\omega \alpha_1 \sin \omega t$), the complex exponential time dependence being introduced in the usual manner.

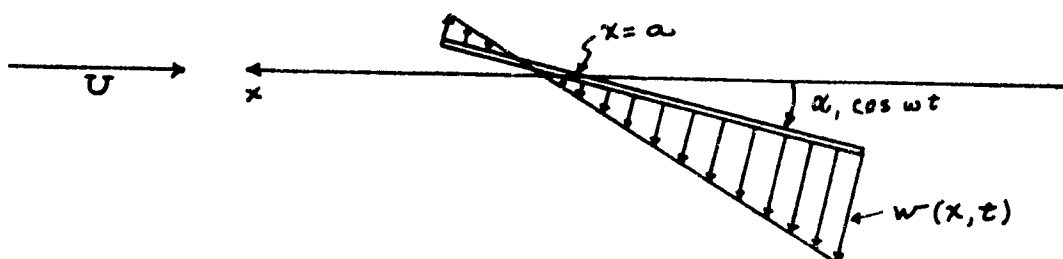


Figure 5-3. A Wing Executing a Pitching Oscillation about $x = a$; the distribution of downwash at a particular instant is depicted by the arrows.

The aerodynamic moment (about $x = a$) due to this downwash may be posed in the form

$$M(t) = Rl [\bar{M}(k) e^{i\omega t}] \quad (5-6)$$

$$\bar{M}(k) = \left[\frac{\partial M}{\partial \alpha} + i k \frac{\partial M}{\partial (q\ell/U)} + i k \frac{\partial M}{\partial (\dot{\alpha}\ell/U)} \right] \alpha \quad (5-7)$$

where $\partial M / \partial \alpha$ is the static moment derivative, $\partial M / \partial (q\ell/U)$ the damping moment derivative calculated from equivalent camber $\omega \alpha(a-x)$, $\partial M / \partial (\dot{\alpha}\ell/U)$ the unsteady flow contribution due to incidence, and k the reduced frequency defined by (5-2). It should be emphasized that $\partial M / \partial (\dot{\alpha}\ell/U)$ arises out of the first order frequency effects in the equations of fluid flow in response to the zero order term $U\alpha$ in the downwash, whereas $\partial M / \partial (q\ell/U)$ arises out of the zero order terms in the equations of flow in response to the first order term $i\omega \alpha(x-a)$ in the downwash. This split-up is, to some extent, artificial, but it has the merit of clearly separating out the quasi-stationary and aero-dynamic lag contributions to the total first order (in frequency) result.

5.2.1.3 Aerodynamic Effects of Various Motions. The basic aerodynamic problem (in the present context) is to establish the pressure distribution, usually over a thin lifting surface, due to a prescribed motion. The direct effects on the flow resulting from this motion may be of the following types:

- a. a change in local incidence;
- b. a change in local flight direction;
- c. a change in local flight speed;
- d. a reorientation of the trailing vortex pattern behind a wing; and
- e. a change in the suction forces at the edges of a lifting surface.

Of the foregoing, effects (a) and (b) are the most important and also the most

amenable to reliable, theoretical calculations. Effect (c)-viz., change in local flight speed, is more difficult to treat theoretically, especially in compressible flow; fortunately, it is of rather less importance, and it generally is adequate to deal with it on the basis of quasi-stationary theory. Reliable theoretical treatments of effects (d) and (e) are not feasible (at the present time), but they are of relatively minor importance for conventional configurations and therefore will be neglected in the following.

The change in incidence associated with a particular motion is calculated simply by dividing the local perturbation velocity normal to the lifting surface, i.e., the prescribed downwash, by the flight velocity. A wing or horizontal tail incidence is reckoned positive when the prescribed downwash is down (so as to produce incidence of the same sign as positive angle of attack). Fin incidence is reckoned positive when the prescribed side-wash is to port (so as to produce incidence of the same sign as a positive angle of yaw). Changes in flight velocity are calculated positive forward.

The change in perturbation pressure (overpressure relative to the free stream value) is given by the linearized Bernoulli equation

$$\Delta p = -\rho_0 \left(\frac{\partial \phi}{\partial t} - U \frac{\partial \phi}{\partial x} \right) \quad (5-8)$$

where $\phi(x,y,z,t)$ is the velocity potential for the perturbed motion, U is the free stream or flight velocity, which is directed along the negative x axis, and ρ_0 is the free stream mass density. The sign of U was chosen as above because the sign conventions in dynamic stability analysis usually specify the x axis to be positive upstream. Thus, if u_0 and v_0 are steady perturbation velocity components along the x and y body axes in the steady flow configuration, and the airplane has a forward velocity component U along the x axis and a sideslip component βU along the y axis, (5-8) can be reduced to

$$\Delta p = -\rho_0 U (u_0 + \beta v_0) \quad (5-9)$$

of which the last term - viz., $-\beta \rho_0 U v_0$, constitutes the change in pressure due to sideslip. The change due to a yawing motion may be deduced in a similar manner, βU being replaced by rx . The result (5-9) is, evidently, a quasi-stationary approximation, but it would be inconsistent to go further without investigating the yawing of the wing wake. The direct aerodynamic effects of the various rigid body motions entering the dynamic stability problem, as inferred from the preceding arguments, are summarized in the following table. The angular rotations are referred to axes through the origin of coordinates. The results for wing incidence also are applicable to the horizontal tail.

A. Longitudinal Motions

| <u>Motion</u> | <u>Wing Incidence</u> | <u>Change in Flight Velocity</u> |
|---------------|-----------------------|----------------------------------|
| u | ----- | u |
| w | w/U | ----- |
| q | $-qx/U$ | ----- |

B. Lateral Motion

| <u>Motion</u> | <u>Wing Incidence</u> | <u>Fin Incidence</u> | <u>Change in Bernoulli's Equation for Pressure on Wing</u> | <u>Change in Local Flight Speed</u> |
|---------------|-----------------------|----------------------|--|---|
| β | $\Gamma\beta$ | $-\beta$ | $-\rho_0 U \beta v_0$ | ----- |
| p | py/U | pZ/U | ----- | ----- |
| r | $\Gamma rx/U$ | $-rx/U$ | $-\rho_0 rx v_0$ | $-ry$ |

Those terms proportional to Γ , the wing dihedral angle, require a change in sign over the port wing ($y < 0$).

The expressions for fin incidence neglect interference effects, which may be appreciable. If experimental measurements of the fin contributions to the derivatives C_{n_β} , C_{n_p} and C_{n_r} were available, it might be possible to establish mean correction factors to be applied to the local side force coefficients C_{y_β} , C_{y_p} and C_{y_r} respectively, but these would be crude at best. Moreover, interference effects in unsteady flow may be quite different than in steady flow, albeit usually less important.

The aerodynamic effects of elastic motions are usually such as to introduce only incidence effects, as treated in Chapter III; see also 5.0 and 5.7.

Given the foregoing results for incidence etc., the problem of obtaining the corresponding pressure distribution may be attacked along the lines set forth in the following sections, depending upon the wing planform and flow regime.

5.2.1.4 Basic Wing Problem. The basic wing problem, as implied by the discussion of the preceding section, is the calculation of the pressure jump across the lifting surface due to a prescribed downwash. It suffices, in the present context, to assume a harmonic time dependence, such that

$$w(x, y, t) = U R_L [\alpha(\xi, \eta) e^{i\omega t}] \quad (5-10)$$

where α is designated as the complex amplitude of the effective incidence or, where no danger of confusion exists, simply the incidence. The coordinates ξ and η , which replace x and y , respectively, are dimensionless quantities obtained through dividing $-x$ and y by a characteristic length, say, the semi-chord length. Moreover, ξ will be measured positive downstream*. See Figure 5-14, the coordinate system used here and throughout Sections 5.2 - 5.5 are so chosen that the x axis is parallel to the mean (steady) motion of the airplane. This system may be referred to as flutter axes, whose relationship with the

* The literature dealing with aerodynamic theory almost universally adopts an x axis that is directed downstream, in opposition to the convention of dynamic stability literature. This difficulty will be at least partially alleviated in the following sections by the introduction of the modified coordinate ξ .

body axes and wind axes are given in Section 5.6.2.

The pressure jump corresponding to the prescribed downwash (5-10) may be expressed in the form

$$\Delta p(x, y, t) = p_{\text{Lower}} - p_{\text{Upper}} = \rho U^2 R \alpha[\gamma(\xi, \eta) e^{i\omega t}] \quad (5-11)$$

where γ is designated as the complex amplitude of the dimensionless (with respect to $\rho_0 U_0^2$) pressure jump, or more simply, the pressure jump. The basic problem then is: given $\alpha(\xi, \eta)$, to find $\gamma(\xi, \eta)$.

The most common formulation of this basic problem results in an integral equation of the type

$$\alpha(\xi, \eta) = \iint_S g(\xi, \eta; \xi', \eta') \alpha(\xi', \eta') d\xi' d\eta' \quad (5-12)$$

where S denotes the projection of the wing planform on $Z = 0$, and g denotes the kernel of the integral equation. Closed form solutions of this integral equation are feasible only in a few special cases in subsonic flow (e.g., the two-dimensional solution of Section 5.2.2.1), and it usually is necessary to resort to approximations of the type introduced in strip theory (Section 5.2.2.1) or lifting line theory (Section 5.2.2.3). In supersonic flow, on the other hand, a great deal more is possible, at least for first order theory (see Sections 5.2.3 and 5.2.3.5).

The direct numerical solution of (5-12) leads naturally to the matrix formulation

$$\underline{\chi} = \underline{P} \underline{\alpha} \quad (5-13)$$

where \underline{P} is the aerodynamic influence matrix already introduced in Chapter III. The construction of the elements of \underline{P} from the kernel function g is, however, complicated by the singularities usually exhibited by the latter. This problem has been accorded only limited study up to the present time, but it doubtless will receive considerable attention as the inversion of large matrices** by high speed digital computers becomes more practical (cf. the discussion on aerodynamic influence coefficients in Section 5.2.3).

5.2.2 High Aspect Ratio Wings in Subsonic Flow. The first aerodynamic problem to be considered will be that presented by a wing of relatively high aspect ratio in subsonic flow. The simplest approach (Section 5.2.2.1) is strip theory, i.e., the approximation of the flow at any wing section as a two-dimensional flow over an infinite wing having that section and having the same motion as the section it represents. This is past, and it probably is adequate if the inequality (see Reference 21),

* g depends parametrically on Mach number and reduced frequency.

** A reliable analysis of a swept wing might call for as many as 100 control points (and certainly at least 20), leading to an influence matrix of 10,000 terms (or at least 4,000 for a matrix of rank 20).

$k AR > 3$

is satisfied,* where k is the reduced frequency based on a representative semi-chord, and AR is the aspect ratio. Unfortunately, it is more than likely that $k AR > 3$ will not be satisfied in the dynamic stability analyses of elastic aircraft, and strip theory then must be regarded as a rather rough approximation.

In the event that strip theory is believed to be inadequate, some form of lifting line theory (Section 5.2.2.3) may be chosen. Except in the quasi-stationary approximation, however, lifting line theories are relatively complicated and may not be warranted in view of other approximations that must be introduced in a particular analysis. It should be remarked, moreover, that the degree of validity to be expected from lifting line theory when applied to a swept wing (even assuming that the difficulties associated with the mid-span kink in the lifting line are removed) is not known with any certainty at the present time, and it is quite possible that lifting surface theory may be required for an adequate treatment when $k AR$ is not large.

Neither strip theory nor lifting line theory should be expected to suffice for wings of relatively low aspect ratio (say $AR < 2$ or 3). An accurate analysis of such wings in unsteady flow almost certainly would call for the application of lifting surface theory, but it appears improbable that aeroelastic problems could be too serious for low aspect ratio wings in subsonic flow, and it may be sufficient to use some form of slender wing theory (Section 5.2.4.2).

5.2.2.1 Two Dimensional Incompressible Flow. The pressure jump across a two dimensional airfoil having the leading and trailing edges $\xi = -1$ and $\xi = +1$ respectively,** due to a prescribed incidence $\alpha(\xi)$ in an incompressible flow of velocity U is given by

$$\gamma = \frac{2}{\pi} \int_{-1}^1 \left\{ \left[\left(\xi' - \xi \right)^{-1} + C(AR) - 1 \right] \left(\frac{1 - \xi}{1 + \xi} \right)^{\frac{1}{2}} \left(\frac{1 + \xi'}{1 - \xi'} \right)^{\frac{1}{2}} + \frac{iAR}{2} \ln \left[\frac{1 - \xi \xi' + (1 - \xi^2)^{\frac{1}{2}} (1 - \xi'^2)^{\frac{1}{2}}}{1 - \xi \xi' - (1 - \xi^2)^{\frac{1}{2}} (1 - \xi'^2)^{\frac{1}{2}}} \right] \right\} \alpha(\xi') d\xi' \quad (5-14)$$

(for equations (5-14) and (5-15) see References 1 or 59).

* Three-dimensional effects may (and usually do) prove more important in the calculation of first order (in k) terms than in steady flow, so that the adequacy of strip theory for steady flow calculations gives no guarantee with respect to unsteady flow. Large values of k , on the other hand, render three-dimensional effects less important, as implied by $k AR > 3$.

** See Section 5.2.1.4 regarding convention of x axis.

where k is the reduced frequency based on the semi-chord, and $C(k)$ is the Theodorsen function

$$C(k) = F(k) + iG(k) = [H_1^{(2)}(k) + iH_0^{(2)}(k)]^{-1} H_1^{(2)}(k) \quad (5-15)$$

expressed in terms of Hankel functions of the second kind. The integral in (5-14) is improper in consequence of the singularity at $\xi' = \xi$, and the principle value is to be taken in the sense of Cauchy, as implied by the C on the integral sign.

The strip theory application of the result (5-14) to a three-dimensional wing having the leading and trailing edges $x_1(y)$ and $x_2(y)$, respectively, requires ξ to be evaluated according to*

$$\xi = 1 - 2 \left[\frac{x - x_2(y)}{x_1(y) - x_2(y)} \right] \quad (5-16a)$$

$$x = [x_1(y) - x_2(y)] \left(\frac{1 - \xi}{2} \right) + x_2(y) \quad (5-16b)$$

as illustrated in Figure 5-4. Moreover, the reduced frequency in (5-14) and (5-15) being based on the local semi-chord, is a function of the spanwise coordinate y according to

$$k = k(y) = \frac{\omega [x_1(y) - x_2(y)]}{2U} \quad (5-17)$$

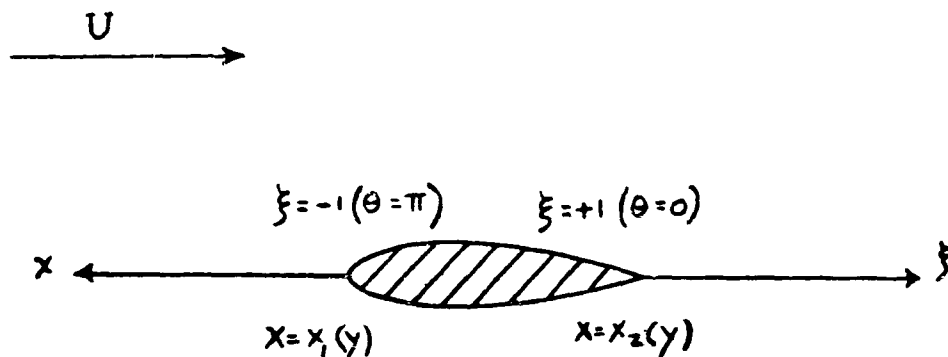


Figure 5-4. A Wing Section Shown in a Freestream of Velocity U , Showing the x and ξ Coordinates Related by (5-16).

* Note that ξ is not, in general, measured orthogonally with respect to y in this application.

In connection with the foregoing change of variable, it should be emphasized that the incidence α , as used in (5-14), is prescribed as a function of the variable ξ , not x .

An alternative form of (5-14), which frequently simplifies the evaluation of the chordwise integrals, is afforded by the trigonometric changes of variable

$$\xi = \cos \theta, \quad \xi' = \cos \phi \quad (5-18)$$

Substituting (5-18) in (5-14) yields

$$\gamma = \frac{2}{\pi} \int_0^\pi \left\{ \left[(\cos \phi - \cos \theta)^{-1} + C(k) - 1 \right] (1 + \cos \phi) \tan\left(\frac{\theta}{2}\right) + i k L(\theta, \phi) \sin \phi \right\} \alpha(\cos \phi) d\phi \quad (5-19)$$

where

$$L(\theta, \phi) = \frac{1}{2} \ln \left[\frac{1 - \cos(\theta + \phi)}{1 - \cos(\theta - \phi)} \right] \quad (5-20)$$

A first order approximation to the foregoing result may be deduced by expanding (5-15) in k - viz.,

$$C(k) = \left(1 - \frac{\pi k}{2}\right) + i k (\ln k - 0.1159 \dots) + O(k^2) \quad (5-21)$$

The term $\pi k/2$ evidently may be neglected compared with unity in the real part of (5-21) in virtue of the hypothesis of small k , but the imaginary term, albeit small, may prove important in the evaluation of damping derivatives. In contrast to the first order result obtained by substituting (5-21) in (5-19) the quasi-stationary approximation neglects all terms of order k in (5-19) except insofar as they appear in α , with the result

$$\gamma^{(0)} = \frac{2}{\pi} \tan\left(\frac{\theta}{2}\right) \int_0^\pi \left(\frac{1 + \cos \phi}{\cos \phi - \cos \theta} \right) \alpha(\cos \phi) d\phi \quad (5-22)$$

All that is required in many applications of strip theory to high aspect ratio wings is the section lift coefficient, as defined by*

$$C_L = \frac{1}{(x_1 - x_2)} \int_{x_1}^{x_2} \frac{(P_{\text{lower}} - P_{\text{upper}}) dx}{(\rho_0 U^2 / 2)} \quad (5-23a)$$

* Of course, the lift coefficient is time dependent. The physical lift coefficient is the real part of $C_L e^{i\omega t}$. The same holds for the other coefficients.

$$c_l = \int_{-1}^1 \gamma d\xi \quad (5-23b)$$

where (5-23b) follows from (5-23a) upon substitution of x from (5-16) above and γ from (5-11). Substituting (5-19) in (5-23) yields

$$c_l = 2 \int_0^\pi [C(k)(1 + \cos \phi) + i k \sin^2 \phi] \alpha(\cos \phi) d\phi \quad (5-24)$$

The corresponding quarter chord moment coefficient is given by

$$C_{m\frac{1}{4}} = \frac{1}{(x_1 - x_2)^2} \int_{x_2}^{x_1} \frac{(x - x_{\frac{1}{4}})(p_{\text{LOWER}} - p_{\text{UPPER}}) dx}{(\rho_0 U^2 / 2)} \quad (5-25a)$$

$$= -\frac{1}{2} \int_{-1}^1 \left(\xi + \frac{1}{2}\right) \gamma d\xi \quad (5-25b)$$

which, upon substitution of (5-19) goes over to

$$C_{m\frac{1}{4}} = -\frac{1}{2} \int_0^\pi [(\cos \phi + \cos 2\phi + i k (1 + \cos \phi) \sin^2 \phi) \alpha(\cos \phi) d\phi \quad (5-26)$$

The prescribed incidence for rigid body motions either is constant along a chordwise section (w, β and p ; cf. Section 5.2.1.3) or varies linearly (q and r). The required results then are

$$\alpha = 1: \begin{cases} c_l = 2\pi [C(k) + \frac{1}{2} i k] \\ c_{m\frac{1}{4}} = -\frac{\pi}{4} i k \end{cases} \quad (5-27a)$$

$$c_{m\frac{1}{4}} = -\frac{\pi}{4} i k \quad (5-27b)$$

$$\alpha = \xi: \begin{cases} c_l = \pi C(k) \\ c_{m\frac{1}{4}} = -\frac{\pi}{4} \left(1 + \frac{i k}{4}\right) \end{cases} \quad (5-28a)$$

$$c_{m\frac{1}{4}} = -\frac{\pi}{4} \left(1 + \frac{i k}{4}\right) \quad (5-28b)$$

In applying these results for c_l and $c_{m\frac{1}{4}}$, it must not be overlooked that they are referred to the local chord - viz., $x_1(y) - x_2(y)$, as also is the reduced frequency k , given by (5-17).

5.2.2.2 Two-Dimensional Compressible Flow. A survey of available results in two-dimensional unsteady flow of a compressible fluid has been prepared by Karp, Shu, Weil, and Biot, (Reference 3); in particular, the wartime work of Dietze (Reference 4) and Schade (Reference 5) is included. Reference also may be made to later (and generally more accurate) work by Timman, van de Vooren and Greidanus (Reference 6); Fettis (Reference 7) and Jones (Reference 8).^{*} The results necessarily appear in numerical form (tables and/or curves), and they will not be presented here. A first order solution, which generally is all that should be required in dynamic stability studies, may be obtained in closed form (Reference 9). The end result for the pressure jump is

$$\gamma^{(1)} = \frac{2}{\pi\beta} \int_0^\pi \left\{ \left[(\cos\phi - \cos\theta)^{-1} - \frac{\pi k}{2\beta^2} + \frac{ik}{\beta^2} (\ln k - 0.1159 - F(M)) \right] \cdot \left((1 + \cos\phi) \tan\left(\frac{\theta}{2}\right) + \frac{ik}{\beta^2} L(\theta, \phi) \sin\phi \right) \right\} \alpha(\cos\phi) d\phi \quad (5-29)$$

where the superscript (1) denotes the first order approximation, θ and ϕ are defined by (5-16) and (5-18), k by (5-17), and

$$\beta = (1 - M^2)^{\frac{1}{2}} \quad (5-30)$$

$$F(M) = M^2 + \ln(2\beta^2/M) - \beta \ln\left(\frac{1+\beta}{M}\right) \quad (5-31)$$

The function $F(M)$ is plotted in Figure 5-5. and is seen to have a maximum value of approximately 0.24 in $0 < M < 0.85$ (F approaches $-\infty$ logarithmically as M approaches unity, but the linearized theory is not valid in this limit due to the neglect of terms of order $\beta^{-4} k^2$). Since $F(M)$ is of relatively small magnitude compared with $\ln k$ for small k , it appears that the principal compressibility corrections appear in the overall factor of β^{-1} , corresponding to the Prandtl-Glauert correction, and, more important, multiplication of ik by β^{-2} (the factor $\pi k/2\beta^2$ being generally negligible compared with the other real terms in (5-29)). The former correction also would appear in the quasi-stationary approximation, but the latter affects only first order terms; accordingly, it may be inferred that the differences between quasi-stationary and first order theories are of greater importance in compressible flow than in incompressible flow.

The lift and quarter-chord moment coefficients corresponding to (5-29) are given by

$$C_z^{(1)} = \frac{2}{\beta} \int_0^\pi \left\{ \left(1 - \frac{\pi k}{2\beta^2} \right) (1 + \cos\phi) + \frac{ik}{\beta^2} \left[\sin^2\phi + (\ln k - 0.1159 - F(M)(1 + \cos\phi)) \right] \right\} \alpha(\cos\phi) d\phi \quad (5-32)$$

^{*} A complete survey is given in References 58, 59.

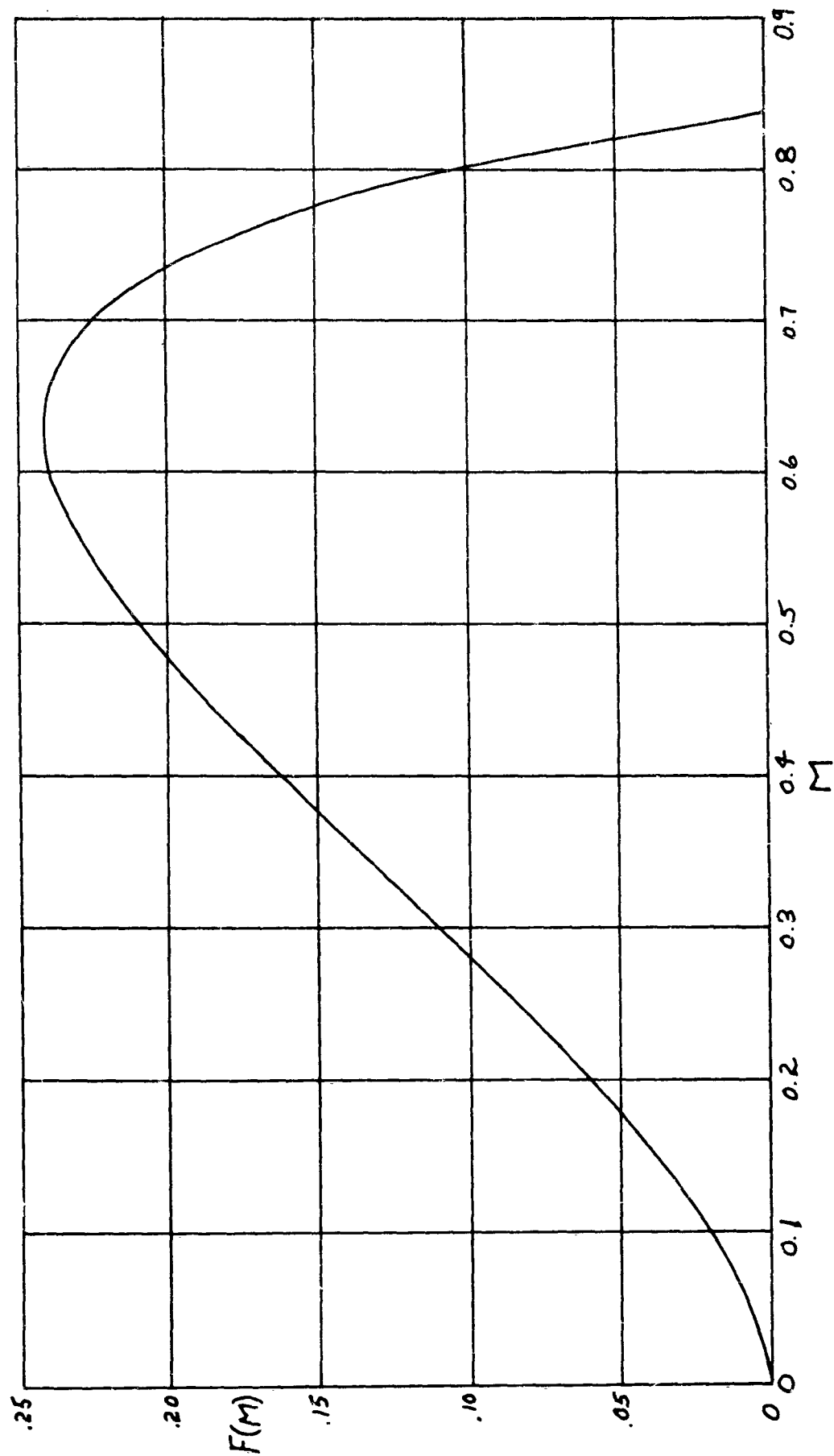


Figure 5-5. $F(M)$ Versus Mach Number

$$C_{m\frac{1}{4}}^{(1)} = -\frac{1}{2\beta} \int_0^\pi \left\{ (\cos\phi + \cos 2\phi) + \frac{ik}{\beta^2} (1 + \cos\phi) \sin^2\phi \right\} \alpha(\cos\phi) d\phi \quad (5-33)$$

$$\alpha = 14 \left\{ \begin{aligned} C_l^{(1)} &= \left(\frac{2\pi}{\beta} \right) \left[\left(1 - \frac{\pi k}{2\beta^2} \right) + \frac{ik}{\beta^2} (\ln k + 0.3841 - F(M)) \right] \\ C_{m\frac{1}{4}}^{(1)} &= -\frac{\pi ik}{4\beta^3} \end{aligned} \right. \quad (5-34a)$$

$$\alpha = 51 \left\{ \begin{aligned} C_l^{(1)} &= \frac{\pi}{\beta} \left[\left(1 - \frac{\pi k}{2\beta^2} \right) + \frac{ik}{\beta^2} (\ln k - 0.1159 - F(M)) \right] \\ C_{m\frac{1}{4}}^{(1)} &= -\frac{\pi}{4\beta} \left(1 + \frac{ik}{4\beta^2} \right) \end{aligned} \right. \quad (5-35a)$$

$$(5-35b)$$

5.2.2.3 Lifting Line Theory for Incompressible Flow. Those theories that effectively separate the problems of determining chordwise and spanwise lift distributions are designated herein as lifting line as opposed to lifting surface theories (see also Section 4.2.4). The various lifting line and lifting surface theories for unsteady flow developed by Cicala (Ref. 10), Lyon (Ref. 11), Jones and Skan (Ref. 12), W. P. Jones (Ref. 13), Sears (Ref. 14), R. T. Jones (Ref. 15), Küssner (Refs. 16 and 17), Biot and Boehnlein (Ref. 18), Wasserman (Ref. 19), Reissner (Refs. 20 and 21), and Zartarian, Hsu and Ashley have been reviewed briefly by Ashley, Zartarian and Neilson (Ref. 22), who conclude that the methods of Biot and Boehnlein (Refs. 18 and 19) and Reissner (Refs. 20 and 21) are usually to be preferred in practical analyses. These Theories require considerable computation at best, but in dynamic stability studies a first order approximation generally will be acceptable and affects a considerable simplification.*

The theory selected for a first order approximation is that of Reissner (Ref. 20). The reduction of this work is presented elsewhere (Ref. 23), and only the results will be presented here. The wing planform to be considered is shown in Figure 5-6.

* As pointed out by Garrick (Ref. 71), the shortcomings of the lifting line methods are their inadequate treatment of the tip and their inability to define the moment characteristics any more reliably than the two-dimensional treatment. Often experimental flutter speeds have fallen about midway between the two-dimensional strip theory results and the three-dimensional lifting line theory results. Thus the latter seems to error often on the unsafe side. However, for the first order theory, a logarithmic singularity $\ln k$ that arises in the two-dimensional theory is removed by the lifting line consideration. See Section 5.4.2.

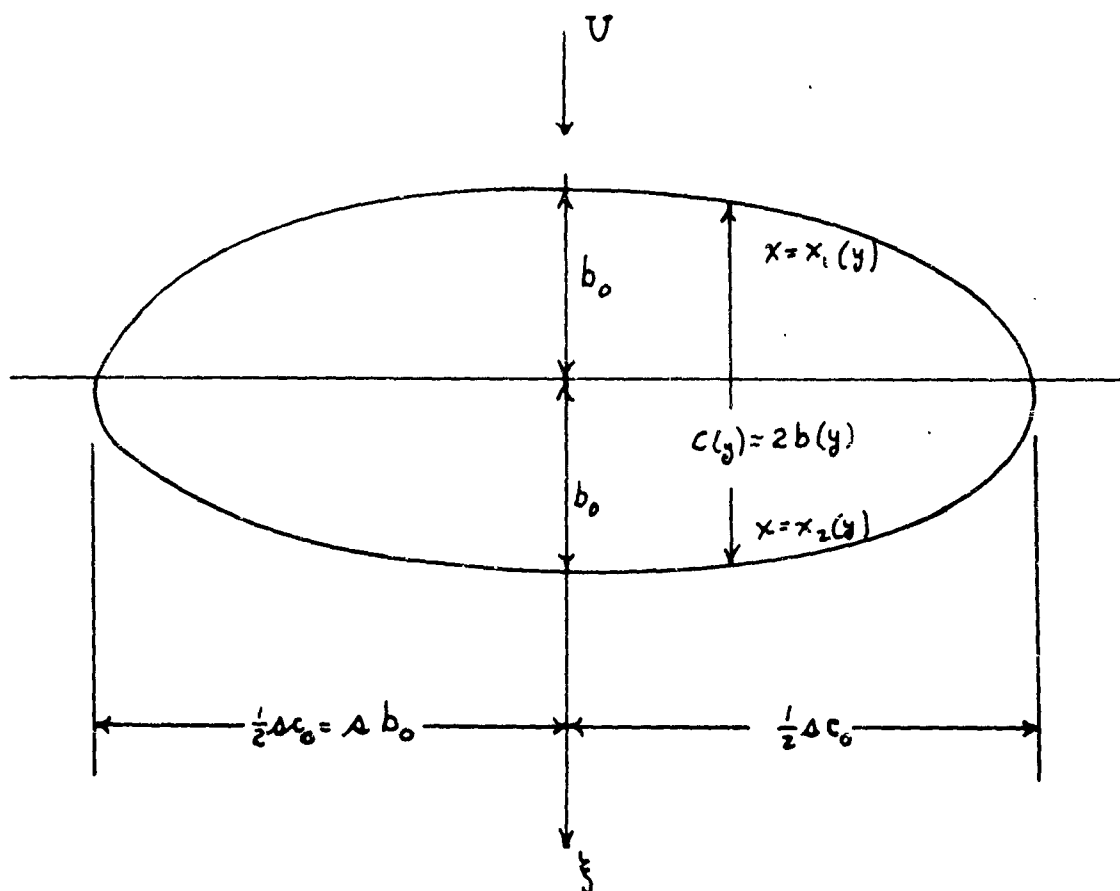


Figure 5-6. Wing Planform of Root Chord $C_0 = 2b_0$ and Span C_0 .

It will be assumed that the incidence may be expressed as the sum of one or more terms like

$$\alpha(\xi, \eta) = f(\eta) \alpha^{(2)}(\xi) \quad (5-36)$$

where ξ is defined by (5-16). Then the corresponding pressure jump across the wing is given by Reference 23 (neglecting real terms of order k and imaginary terms of order k^2)

$$\gamma = \frac{2}{\pi} f(\eta) \oint_0^\pi \left\{ \left[(\cos \phi - \cos \theta)^{-1} - 1 + \chi_0(\eta, s) + i k \left(\frac{1}{2} - \xi_m \right) \chi_0(\eta, s) \right. \right. \\ \left. \left. + i k_0 \chi_1(\eta, s) - \frac{i k^2}{2} \right] (1 + \cos \phi) \tan \left(\frac{\theta}{2} \right) + i k L(\theta, \phi) \sin \phi \right\} \alpha^{(2)}(\cos \phi) d\phi \quad (5-37)$$

where χ_0 and χ_1 satisfy the integral equations

$$f(\eta)\chi_0(\eta, s) + \frac{1}{2} \int_{-s}^s (\eta - \eta')^{-1} \frac{d}{d\eta'} [f(\eta') \bar{c}(\eta') \chi_0(\eta', s)] d\eta' = f(\eta) \quad (5-38)$$

$$\begin{aligned} f(\eta)\chi_1(\eta, s) + \frac{1}{2} \int_{-s}^s (\eta - \eta')^{-1} \frac{d}{d\eta'} [f(\eta') \bar{c}(\eta') \chi_1(\eta', s)] d\eta' \\ = \left[\frac{1}{2} + \xi_m(\eta) \right] \bar{c}(\eta) f(\eta) + \left[\gamma - \frac{1}{2} + \ln\left(\frac{R}{2}\right) \right] \bar{c}(\eta) f(\eta) \chi_0(\eta, s) \\ + \frac{1}{2} \int_{-s}^s |\eta - \eta'|^{-1} (\eta - \eta') F(R_0 |\eta - \eta'|) \frac{d}{d\eta'} [f(\eta') \bar{c}(\eta') \chi_0(\eta', s)] d\eta' \end{aligned} \quad (5-39)$$

and where

$$\xi_m(\eta) = - \left[\frac{\chi_1(\eta) + \chi_2(\eta) - \chi_1(0) - \chi_2(0)}{\chi_1(\eta) - \chi_2(\eta)} \right] \quad (5-40)$$

$$R_0 = \frac{\omega[\chi_1(0) - \chi_2(0)]}{2U} \quad (5-41)$$

$$\bar{c}(\eta) = \frac{c(\eta)}{c(0)} = \frac{R}{R_0} = \frac{\chi_1(\eta) - \chi_2(\eta)}{\chi_1(0) - \chi_2(0)} \quad (5-42)$$

$$F(z) = -\ln z + 0.764 z - 0.27 \quad (5-43)$$

The corresponding results for the section lift and quarter chord moment coefficients are

$$\begin{aligned} C_L = 2f(\eta) \int_0^\pi \left\{ [\chi_0(\eta, s) + iR\left(\frac{1}{2} - \xi_m\right)\chi_0(\eta, s) + iR_0\chi_1(\eta, s) - \frac{iR}{2}] (1 + \cos\phi) \right. \\ \left. + iR \sin^2\phi \right\} \alpha^{(2)}(\cos\phi) d\phi \end{aligned} \quad (5-44)$$

$$C_{m_{\frac{1}{4}}} = -\frac{1}{2} f(\eta) \int_0^{\pi} \left\{ (\cos \phi + \cos 2\phi) + i k \sin^2 \phi (1 + \cos \phi) \right\} \alpha^{(2)} \cos \phi d\phi \quad (5-45)$$

The integral equations (5-38) and (5-39) are similar in form with that which arises in Prandtl, lifting line theory for a straight wing in steady flow. Of the many methods of solution to this integral equation, that which appears best suited to aeroelastic problems is presented in Appendix A.

The results stated in this section have been applied to an elliptic wing executing a pitching oscillation (Reference 23), and it was found that strip theory grossly over-estimates the first order term $C_{m_{\frac{1}{4}}}$ for wings of moderate

aspect ratio and small values of the reduced frequency k ; in particular, the logarithmic term in k that arises through $C(k)$, as in (5-21), is cancelled out in the three-dimensional results, see also, Section 5.4.2.

5.2.2.4 Lifting Surface Theories for Subsonic Flow. Lifting surface theories for unsteady, incompressible flow have been developed and utilized primarily by the British (References 11, 12, and 13), although Reissner (References 20 and 24) has devoted considerable attention to the lifting surface integral equations in developing lifting line approximations. An approximate lifting surface theory for low aspect ratio wings has been developed by Lawrence (References 25 and 26). Each of the various methods requires extensive numerical work, and all that will be given here is the lifting surface integral equation that requires solution.*

The velocity field associated with a lifting surface may be represented as due to a superposition of radiating doublets, the strength of which is proportional to the pressure jump (γ) across the surface. The imposition of the condition of tangential flow at the surface then leads to an integral equation relating the normal velocity of the surface at any point, i.e., the aerodynamic incidence (α), to the pressure distribution, i.e., γ . This calculation for a surface exhibiting an arbitrary motion in a subsonic compressible flow was first carried out by Küssner (Reference 27) and yields

$$\alpha(\xi, \eta, t) = \frac{1}{4\pi} \iint_S d\xi' d\eta' \int_{-\infty}^{\xi-\xi'} \lim_{z \rightarrow 0} \frac{\partial^2}{\partial z^2} \left\{ R^{-1} \gamma \left[\xi', \eta', t - \left(\frac{\xi-\xi'}{U} \right) + \frac{\xi''}{\beta^2 U} - \frac{MR}{\beta^2 U} \right] \right\} d\xi'' \quad (5-46)$$

where

$$R = \left\{ \xi''^2 + \beta^2 [(\eta - \eta')^2 + z^2] \right\}^{1/2} \quad (5-47)$$

* Recently, important advances have been made by Küssner (Refs. 121, 122) Watkins and Runyan, Woolston and Berman (Refs. 28, 123, 124). See review in Ref. 71 by Garrick.

M is the Mach number, $\beta = (1-M^2)^{1/2}$, as in (5-30), and S denotes the wing surface.

If it is further assumed that both α and Δp exhibit the harmonic time dependence $\exp(i\omega t)$, (5-46) may be placed in the reduced form (eliminating the explicit appearance of the time dependence factors)

$$\alpha(\xi, \eta) = \iint_S g(\xi - \xi', \eta - \eta') \alpha(\xi', \eta') d\xi' d\eta', \quad (\xi, \eta) \text{ in } S. \quad (5-48)$$

where the kernel function g is given by

$$g(\xi - \xi', \eta - \eta') = \frac{1}{4\pi} e^{-ik(\xi - \xi')} \lim_{z \rightarrow 0} \int_{-\infty}^{\xi - \xi'} \frac{\partial^2}{\partial z^2} R^{-1} \exp \left[i k (\xi'' - M R) / \beta^2 \right] d\xi'' \quad (5-49)$$

It is necessary in order to avoid improper integrals, to carry out the η integration in (5-48) prior to the z differentiation in (5-49). Alternatively, the z differentiation may be carried out first on the understanding that (5-48) will be integrated formally by parts and the infinite part discarded.

The kernel function g has been expanded in powers of the reduced frequency by Watkins, Fung and Wollston (Reference 28), and also by Lance (Reference 29). The first two terms in this expansion are given by

$$4\pi g(x_0, y_0) = e^{-ikx_0} \lim_{z \rightarrow 0} \frac{\partial^2}{\partial z^2} \left\{ -\ln \left[\sqrt{x_0^2 + \beta^2(y_0^2 + z^2)} - x_0 \right] + \frac{ik}{\beta^2} \sqrt{x_0^2 + \beta^2(y_0^2 + z^2)} + O(k^2) \right\} \quad (5-50)$$

If the z differentiation is carried out directly (vide supra) and if the exponential is expanded, (5-50) reduces to

$$4\pi g(x_0, y_0) = -\left(\frac{x_0 + S}{y_0^2 S} \right) + ik \left[\frac{x_0 + S}{y_0^2} + \frac{M^2}{S} \right] + O(k^2), \quad (5-51)$$

$$S = (x_0^2 + \beta^2 y_0^2)^{1/2}$$

but great care must be exercised in applying this form due to the strong singularity at $y_0 = 0$.

5.2.2.5 Subsonic Compressibility Correction. The pressure distribution over a three-dimensional wing in incompressible flow may be corrected for compressibility effects by a relatively simple extension (Reference 30) of the well known, Prandtl-Glauert rule for steady flow.

Let $p^{(0)} \{ \xi, \eta; \alpha(\xi, \eta); k, AR \}$ denote symbolically the pressure dis-

tribution over a wing of aspect ratio AR due to an arbitrarily prescribed incidence $\alpha(\xi, \eta)$ at reduced frequency k in an incompressible flow. It is assumed that the dimensionless coordinate ξ is measured positive downstream and is referred to the same characteristic length as the reduced frequency k (but ξ is not necessarily defined by (5-16)). The corresponding distribution in a compressible flow of Mach number M then is given by

$$\begin{aligned}
 p\{\xi, \eta; \alpha(\xi, \eta); R, AR, M\} = & \beta^{-1} p^{(0)}\{\xi, \beta\eta; \alpha(\xi, \beta^{-1}\eta); \beta^{-2}R, \beta AR\} \\
 & + i k M^2 \beta^{-3} \left[\xi p^{(0)}\{\xi, \beta\eta; \alpha(\xi, \beta^{-1}\eta); 0, \beta AR\} \right. \\
 & \left. - p^{(0)}\{\xi, \beta\eta; \alpha(\xi, \beta^{-1}\eta); 0, \beta AR\} \right] + O[(k M AR / \beta)^2]
 \end{aligned} \tag{5-52}$$

where β is the Prandtl-Glauert factor, viz.

$$\beta = (1 - M^2)^{1/2}$$

It should be emphasized that this result is not uniformly valid with respect to M near $M = 1$, for the error term involves $(\frac{k}{\beta})^2$. Similarly, it breaks down for large values of AR , where the results of Section 5.2.2.2 must be used.

The compressibility correction (5-52) may be stated in words as follows: the (complex amplitude of the) pressure distribution over a wing of aspect ratio AR that exhibits an incidence of complex amplitude distribution $\alpha(\xi, \eta)$ and reduced frequency k , in a subsonic compressible flow, may be determined for small values of $(k^2 M^2 AR^2 / (1 - M^2))$ by calculating the pressure distribution over an affine* wing of aspect ratio $(1 - M^2)^{1/2} AR$ that exhibits the incidence distribution $\alpha(\xi, \beta^{-1}\eta)$ at a reduced frequency $k(1 - M^2)^{-1}$ in incompressible flow; adding to this $i k M^2 (1 - M^2)^{-1} \xi$ times the pressure distribution calculated over the second wing for the incidence distribution $\alpha(\xi, \beta^{-1}\eta)$ on the assumption of steady flow (quasi-stationary approximation); subtracting $i k M^2 (1 - M^2)^{-1}$ times the pressure distribution calculated over this second wing for the incidence distribution $\xi \alpha(\xi, \beta^{-1}\eta)$ on the assump-

* A similar wing with the same general appearance as the original wing (e.g. having the same angle of sweep) but with different aspect ratio and incidence distribution.

tion of steady flow; and multiplying the sum of these terms by $(1-M^2)^{-1/2}$. It should be specifically remarked that, in carrying out the first of these steps, any dependence of the incidence distribution α on the reduced frequency k is not to be modified; on the other hand, the dependence of α on k may be neglected in the second and third steps in consistency with the approximations already implicit in the transformation.

The transformation (5-52) has been applied to the lifting line results of Section 5.2.2.3 in Reference 23.

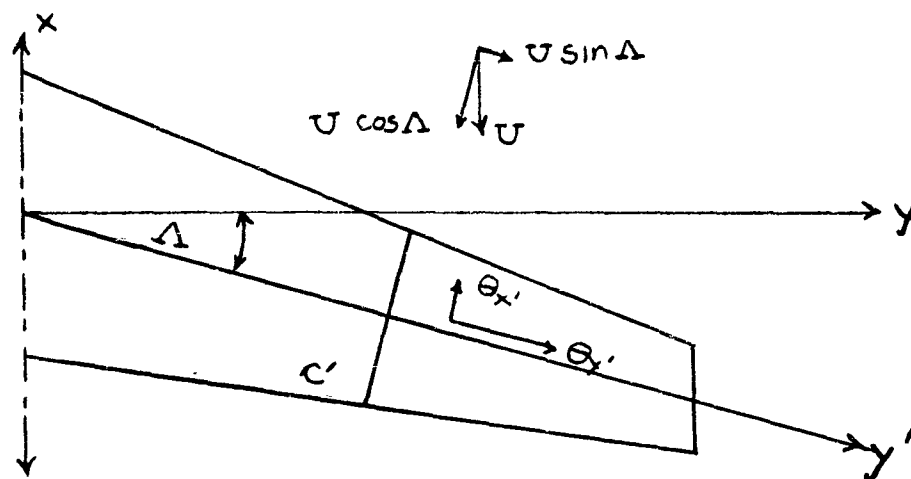
5.2.2.6 Swept Wings in Subsonic Flow. Experience with approximate treatments of swept wings in subsonic unsteady flow is so limited at the present time that it is difficult to assess the reliability of the various methods that have been proposed. Lifting surface theory may be expected to yield results of about the same accuracy for swept wings as would be the case for straight wings using the same number of collocation points. Lifting line theories are, however, rather less reliable due to the mid-span kink; indeed, unless some care is exercised in the formulation, the singularity associated with this kink may render invalid the solution over the entire wing, rather than only in the mid-span neighborhood. This mid-span kink offers no particular difficulty in an appropriately modified strip theory, but such a theory nevertheless must be regarded as crude in consequence of the obviously increased importance (compared with a straight wing) of spanwise effects.

Strip theory approximations for oscillating swept wings have been discussed by Spielberg, Feetis and Toney (Reference 31) and by Miles (Reference 32). Let c' be a strip taken perpendicular to the spanwise reference axis of a swept wing, as shown in Figure 5-7. (It is implicit in the strip theory approximation that differences in sweep angles of the various axes, such as the elastic axis, mid-chord line, quarter-chord line, etc., may be neglected). Viewed as a section of a swept two-dimensional wing, the apparent flight velocity for this section is $U \cos \Lambda$ where Λ is the sweepback angle; in addition, there is a spanwise component of flow $U \sin \Lambda$. The total, effective downwash then consists of three parts: first, there is the local normal velocity \dot{z} (positive down); secondly, there is the product of the rotation $\theta_{y'}$ about the (swept) y' axis and the chordwise velocity component $U \cos \Lambda$ thirdly, there is the product of the rotation $\theta_{x'}$ about the x' axis and spanwise velocity component $U \sin \Lambda$. The total incidence is obtained by dividing this total downwash by the apparent flight velocity $U \cos \Lambda$; this incidence then must be modified by a correction factor of $\cos^2 \Lambda$ to account for the reduction of apparent dynamic pressure (since the end results are referred to the true dynamic pressure $\rho U^2/2$). The end result for the effective incidence on the basis of a strip theory approximation thus is given by

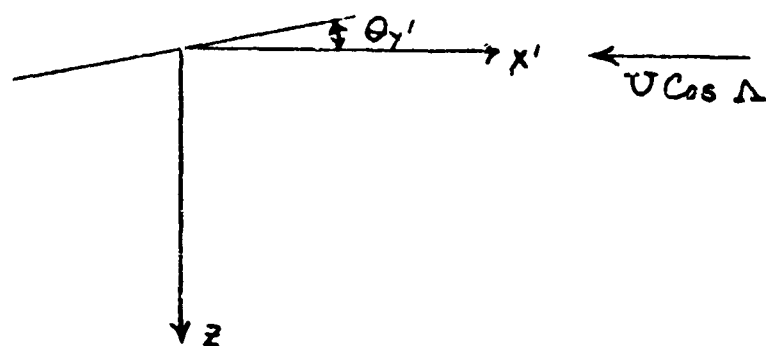
$$\alpha_{\text{eff}} = \cos^2 \Lambda \left[\frac{\dot{z} + U \cos \Lambda \theta_{y'} + U \sin \Lambda \theta_{x'}}{U \cos \Lambda} \right] \quad (5-53a)$$

$$= \cos \Lambda \left[\frac{\dot{z}}{U} + \theta_{y'} \cos \Lambda + \theta_{x'} \sin \Lambda \right] \quad (5-53b)$$

The contribution due to the time rate of change of $\theta_{y'}$, and that due to the spanwise rate of change of $\theta_{y'}$, both depend linearly on the chordwise coordinate, are included in \dot{z}



(a) plan view, showing section c'



(b) the chordwise section c' viewed along the y' axis.

Figure 5-7. A Swept Wing

The result (5-53b) may be used in conjunction with the two-dimensional theories of Sections 5.2.2.1 and 5.2.2.2 (after introducing the dimensionless coordinates ξ and η) for the calculation of the pressure distribution over a swept wing of very high aspect ratio. The effective Mach number to be used in compressible flow is $M \cos \Lambda$. It should be specifically remarked, on the other hand, that the reduced frequency k is independent of Λ , since both flight velocity and chord are modified by a factor of $\cos \Lambda$ in the swept axis system.

Chordwise structural distortion usually may be neglected for those wings of sufficiently high aspect ratio to justify strip theory. Hence $\theta_{y'}$ and $\theta_{x'}$ arise from torsion and bending respectively, while \dot{z} arises from the rigid body motion of the wing plus the contribution due to bending and torsion velocity. The effective camber due to \dot{z} may make important contributions to the loading on a swept wing.

Lifting line theories for oscillating swept wings have been developed by Reissner and his colleagues (References 33, 34 and 35) and by Ashley et al (Reference 22). Both of these methods are, in essence, modifications of Reissner's work for straight wings (References 20 and 21), but that of Reference 22 is considerably simpler (although neglecting effects of taper). Unfortunately, experience with both methods is very slight, and a detailed presentation does not appear to be warranted in the present work.

5.2.3 Supersonic Wings, Piston Theory

The supersonic wing problem differs from its subsonic counterpart primarily in that the wing is influenced only by a finite portion of the total flow field. The resulting pressure distributions over those portions of the wing adjacent to subsonic edges (i.e., edges over which the normal component of flight velocity is subsonic) may be qualitatively similar to that for a subsonic wing, but the pressure distributions over those portions of the wing adjacent to supersonic edges are quite dissimilar.

A particular consequence of supersonic flight speed is that the state of affairs at a given point on a wing is independent of all points that are further downstream.* It is convenient, therefore, to measure the streamwise coordinate ξ downstream from the most upstream point on the wing (rather than from the mid-chord line, as in subsonic flow), and this convention will be adopted in the subsequent sections dealing with supersonic flow. Similarly, it is convenient to choose the characteristic length for aerodynamic calculations either as the local chord or as the streamwise distance between the most upstream and most downstream points on the wing; in particular, the reduced frequency usually will be referred to one of these lengths.

Before the general theory for supersonic wings is presented, a particularly simple result must be mentioned which is generally valid for high Mach numbers or high reduced frequencies of unsteady motion; and sometimes even for subsonic Mach numbers, when the surface involved is nearly a plane and the angle of incidence is small. This is the piston theory, which refers to any method

* A more detailed discussion of the domain of dependence and the various types thereof is given in Section 5.2.3.5.

for calculating aerodynamic loads on aircraft in which the local pressure generated by a body is related to the local normal component of fluid velocity in the same way that these quantities are related at the face of a piston moving in a one-dimensional channel. When a linearized theory is adopted, the piston theory leads to a direct linear proportion between local pressure and downwash. In this case the fundamental equation (5-12) becomes simply

$$\alpha(\xi, \eta) = \text{const.} \cdot \gamma(\xi, \eta) \quad (5-12a)$$

The pressure-downwash relationship and their conditions of validity will now be set forth:

If a piston moves with velocity $w(t)$ in the end of a channel containing perfect gas, whose undisturbed pressure, density and speed of sound are p_0 , ρ_0 , a_0 , the pressure change $p(t)$ on the piston is

$$\frac{p}{p_0} = \left[1 + \frac{\gamma-1}{2} \left(\frac{w}{a_0} \right)^2 \right]^{\gamma/(\gamma-1)}$$

where γ is the ratio of specific heats of the gas, c_p/c_v . Depending on the magnitude of the ratio w/a_0 , the following approximations may be used:

$$p - p_0 = \rho_0 a_0 w$$

$$p - p_0 = \rho_0 a_0^2 \left[\frac{w}{a_0} + \frac{\gamma+1}{4} \left(\frac{w}{a_0} \right)^2 \right]$$

$$p - p_0 = \rho_0 a_0^2 \left[\frac{w}{a_0} + \frac{\gamma+1}{4} \left(\frac{w}{a_0} \right)^2 + \frac{\gamma+1}{12} \left(\frac{w}{a_0} \right)^3 \right]$$

Based on a suggestion of Hayes (Ref. 140), Lighthill (Ref. 141) points out that the above formulas can be used for arbitrary airfoil motion by interpreting w as the local downwash velocity. The conditions under which these relations hold for airfoil motion have been studied by Lighthill (Ref. 141), Landahl (Refs. 142 and 143), and others. For a two-dimensional airfoil the linearized theory is valid whenever (Ref. 142): $M^2 \gg 1$ or $kM^2 \gg 1$, or $k^2 M^2 \gg 1$.

For a three-dimensional wing the linear and second order theory holds if (Ref. 143):

$$(a) \quad \delta/M^3 \ll 1, \text{ and } \delta^2/M^2 \ll 1,$$

$$(b) \quad M\delta \text{ and } kM\delta \text{ not too large}$$

where δ denotes the larger of the wing thickness ratio or the ratio of amplitude of unsteady motion to wing chord. k is the reduced frequency for harmonic motion, on an appropriate measure of the "unsteadiness" of the flow.

The piston theory is not valid in the neighborhood of a cut-off wingtip.

Many interesting applications of the piston theory have been given by Ashley and Zartarian, (Ref. 139).

5.2.3.1 Reduction of Unsteady Flow to Steady Flow Problems. A first order approximation to the pressure distribution over a wing executing a harmonic motion in supersonic flow can be determined from the solution to a modified steady flow problem for the same wing. If the trailing edge of the wing is

nowhere subsonic the result assumes a somewhat simpler form than when this restriction is not satisfied, but, insofar as the steady flow problem for the given wing can be solved, the actual labor involved in constructing the first order approximation is not appreciably greater (see, e.g., Section 5.2.3.5.).

Let $\gamma^{(0)}\{\alpha\}$ denote symbolically the dimensionless pressure jump across a wing in a steady supersonic flow due to a prescribed distribution of incidence α ; further let $\Phi\{\alpha\}$ denote the velocity potential (Ref. 59) over the upper surface of the same wing calculated on the (artificial) hypothesis that subsonic portions of the trailing edge may be treated as subsonic leading edges (i.e., the velocity potential is assumed to be continuous across the wing wake, in particular vanishing along the subsonic portions of the trailing edge). Then the corresponding (complex amplitude of the) pressure distribution over the same wing when the prescribed (complex amplitude of the) incidence α corresponds to a harmonic motion of small reduced frequency k is given by

$$\gamma^{(1)}\{\alpha; k\} = \gamma^{(0)}\{\alpha\} + \frac{ik}{B^2} [M^2 \gamma^{(0)}\{\xi\alpha\} - M^2 \xi \gamma^{(0)}\{\alpha\} - 2\Phi\{\alpha\}] + O(k^2 M^4 / B^4) \quad (5-54)$$

where ξ is measured downstream from the most upstream point on the wing, M is the freestream Mach number, and

$$B^2 = M^2 - 1 \quad (5-55)$$

It should be specifically remarked that $\gamma^{(0)}\{\xi\alpha\}$ represents the steady flow pressure distribution due to the incidence distribution $\xi\alpha$, whereas

$\xi \gamma^{(0)}\{\alpha\}$ represents the product of ξ and the steady flow pressure distribution α . It also may be remarked that, whereas α may depend on the reduced frequency k , it is consistent with the first order approximation to neglect this dependence except in the first term in (5-54).

If the trailing edge of the wing is nowhere supersonic, it follows that

$$2\Phi^{(0)}\{\alpha\} = \int_{\xi_1}^{\xi} \gamma^{(0)}\{\alpha\} d\xi \quad (5-56)$$

where ξ_1 is the ξ coordinate of the leading edge. If, on the other hand, the trailing edge is at least partially subsonic Φ must be determined in accordance with the foregoing instructions (see Section 5.2.3.5 for further details).

It is of interest to note that the foregoing result bears a marked similarity to the subsonic compressibility correction of Section 5.2.2.5. The two results, indeed, are derived by essentially the same transformation (cf. References 30 and 36), but the end results differ in purpose---viz., that of

Section 5.2.2.5 accounts for the effect of the Mach number M , whereas that of the present section accounts for the effect of the reduced frequency k .

5.2.3.2 Two-Dimensional Supersonic Flow. The dimensionless pressure jump across a two-dimensional airfoil having the leading and trailing edges $\xi = 0$ and $\xi = 1$, respectively, in a supersonic flow of Mach number M is given by (Reference 37).

$$\gamma(\xi) = \frac{2}{B} \left\{ \alpha(\xi) + \int_0^\xi \left(\frac{2}{B\xi} + ik \right) \exp \left[-\frac{ikM^2}{B^2} (\xi - \xi') \right] J_0 \left[\frac{RM}{B^2} (\xi - \xi') \right] \alpha(\xi') d\xi' \right\} \quad (5-57)$$

where J_0 denotes a Bessel function of the first kind and zero order. The first term in (5-57), viz., $2\alpha/B$, constitutes the well known result of Ackeret (Reference 38) for steady flow.

If k is assumed small (5-57) may be approximated by

$$\gamma^{(1)} = \frac{2}{B} \left[\alpha(\xi) - \frac{ik}{B^2} \int_0^\xi \alpha(\xi') d\xi' \right] + O(k^2 M^4 / B^4) \quad (5-58)$$

Alternatively, (5-58) could have been derived from the steady flow result with the aid of (5-54). The simplicity of the result (5-58) is to be contrasted with the complexity of its subsonic counterpart, (5-29). This, of course, is a direct consequence of the absence of wake effects.

The strip theory application of the result (5-58) to a three-dimensional wing having the leading and trailing edges $x_1(y)$ and $x_2(y)$ respectively, requires ξ to be transformed according to (5-16).

$$\xi = \frac{x_1(y) - x}{x_1(y) - x_2(y)} \quad (5-59)$$

as shown in Figure 5-8.



Figure 5-8. A Two-Dimensional Airfoil of Chord $x_1(y) - x_2(y)$

The reduced frequency in (5-57), being based on the full local chord, then is given by

$$k = k(\gamma) = \frac{\omega}{U} [x_1(\gamma) - x_2(\gamma)] \quad (5-60)$$

and differs from its subsonic counterpart of (5-17) by a factor of 2.

The section lift coefficient corresponding to the first order approximation (5-58) to the pressure distribution is given by (after integration by parts)

$$C_L^{(1)} = 2 \int_0^1 \gamma^{(1)} d\xi \quad (5-61a)$$

$$= \frac{4}{B} \int_0^1 \left[1 + \frac{i k}{B^2} (\xi - 1) \right] \alpha(\xi) d\xi + O(k^2 M^4 / B^4) \quad (5-61b)$$

The corresponding moment coefficient, referred to the axis $\xi = a$ (a may be a function of y in three-dimensional strip theory applications), is given by

$$C_m^{(1)} = 2 \int_0^1 (a - \xi) \gamma d\xi \quad (5-62a)$$

$$= \frac{4}{B} \int_0^1 \left[(a - \xi) + \frac{i k}{B^2} \left(\frac{1}{2} - a + a \xi - \frac{1}{2} \xi^2 \right) \right] \alpha(\xi) d\xi + O(k^2 M^4 / B^4) \quad (5-62b)$$

The substitution of the more specific incidence distribution $\alpha = \xi^n$ ($n = 0$ or 1 being the more important, particular cases) in (5-61) and (5-62) yields

$$\alpha = \xi^n: \begin{cases} C_L^{(1)} = \frac{4}{(n+1)B} \left[1 - \frac{i k}{(n+2) \cdot B^2} \right] + O(k^2 M^4 / B^4) \end{cases} \quad (5-63a)$$

$$\begin{cases} C_m^{(1)} = a C_L + \frac{4}{B} \left[-\frac{1}{(n+2)} + \frac{i k}{(n+1)(n+3) B^2} \right] + O(k^2 M^4 / B^4) \end{cases} \quad (5-63b)$$

5.2.3.3 Simple Planforms. A simple planform is one having the component of flight velocity normal to its edge everywhere supersonic. If $y_s(x)$ defines the edge of the planform this restriction implies

$$B \left| \frac{dy_s}{dx} \right| > 1 \quad (5-64)$$

An important example of a simple planform is the so-called wide delta wing, as shown in Figure 5-9. The simplest example of such a planform evidently is the two-dimensional wing of the preceding section.

The result of the restriction (5-64) is that the domain of dependence of any point of the wing includes only other points on the wing, and the determination of the pressure distribution due to an arbitrarily prescribed incidence is relatively straightforward. The end result may be placed in the form (Reference 39).

$$\gamma(\xi, \eta) = \frac{2}{\pi} \left(\frac{\partial}{\partial \xi} + i k \right) \iint_S R^{-1} \exp \left[-i k M^2 (\xi - \xi') / B^2 \right] \cos(\lambda M R / B^2) \alpha(\xi', \eta') d\xi' d\eta' \quad (5-65)$$

where ξ and η are dimensionless streamwise and spanwise coordinates, R is the hyperbolic distance defined by

$$R = [(\xi - \xi')^2 - B^2(\eta - \eta')^2]^{1/2} \quad (5-66)$$

and S is that part of the wing planform over which R is real for a given point (ξ, η) , as shown in Figure 5-9.

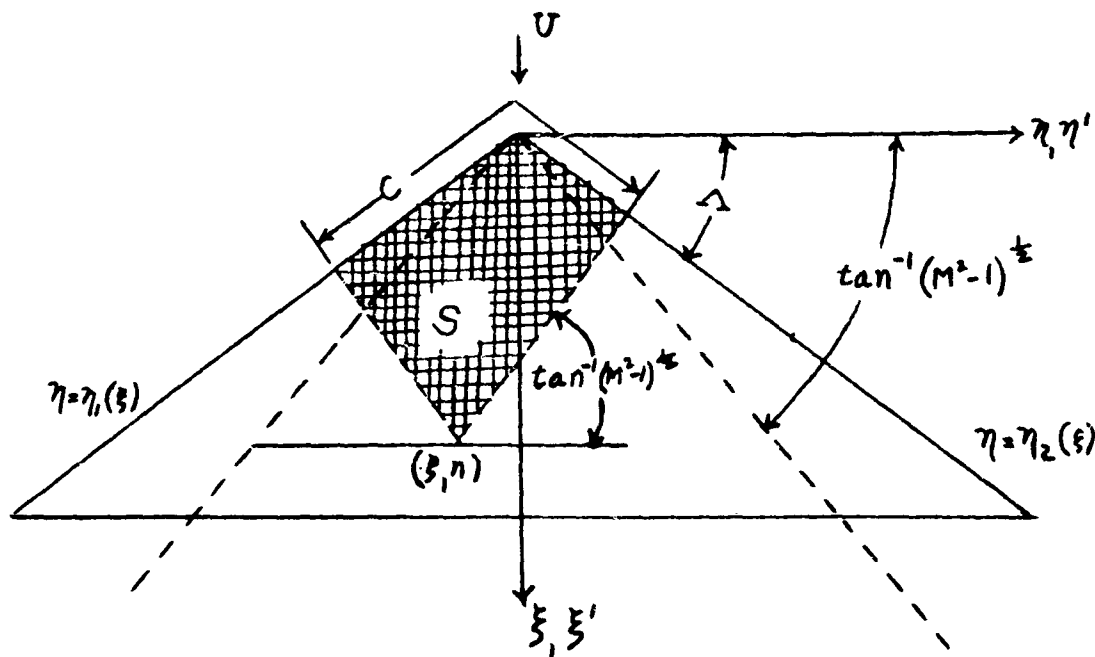


Figure 5-9. Example of a Simple Planform ("Wide Delta" Wing), Showing the Domain of Integration (S) for the Determination of the Pressure.

Setting $k = 0$ in (5-65) yields the quasi-stationary approximation

$$\gamma^{(0)}(\xi, \eta) = \frac{2}{\pi} \frac{\partial}{\partial \xi} \iint_S R^{-1} \alpha(\xi', \eta') d\xi' d\eta' \quad (5-67)$$

in agreement with the steady flow result obtained by Puckett (Reference 40). If terms of order k^2 are neglected in (5-65) there results the first order approximation

$$\gamma^{(1)}(\xi, \eta) = \frac{2}{\pi} \left(\frac{\partial}{\partial \xi} + iA \right) \iint_S \left[1 - \frac{iAM^2}{B^2} (\xi - \xi') \right] R^{-1} \alpha(\xi', \eta') d\xi' d\eta' \quad (5-68)$$

Alternatively, (5-68) could have been derived from (5-67) using (5-54).

The differentiation of the integral in (5-65) as it stands would produce a singular integrand (since $(\partial/\partial \xi) R^{-1} = -(\xi - \xi') R^{-3}$), but if a partial integration with respect to ξ' is effected prior to the ξ differentiation, there results

$$\begin{aligned} \gamma(\xi, \eta) = & \frac{2}{\pi} \iint_S R^{-1} \exp[-iAM^2(\xi - \xi')/B^2] \cos(AMR/B^2) \left(\frac{\partial}{\partial \xi} + iA \right) \alpha(\xi', \eta') d\xi' d\eta' \\ & + \frac{2}{\pi} \int_C R^{-1} \exp[-iAM^2(\xi - \xi')/B^2] \cos(AMR/B^2) \alpha(\xi', \eta') d\eta' \end{aligned} \quad (5-69)$$

where C denotes the curve which the area S intercepts on the leading edge, as shown in Figure 5-9. Similar results, corresponding to the quasi-stationary and first order approximations of (5-67) and (5-68), respectively, may be obtained from (5-69) by setting $k = 0$ or by retaining only first powers of k .

That class of simple planforms for which the trailing edge is restricted to be straight and transverse to the line of flight (i.e., a line of constant ξ) allows further simplification of the above results in the calculation of certain spanwise integrals. Let γ_s denote the strip theory approximation to the pressure distribution, as given by the results of the preceding section; then it may be established (Reference 41) that the spanwise integrals of γ and $\eta\gamma$ are exactly equal to the corresponding integrals of γ_s viz.,

$$\int_{\eta_1(\xi)}^{\eta_2(\xi)} \gamma(\xi, \eta) d\eta = \int_{\eta_1(\xi)}^{\eta_2(\xi)} \gamma_s(\xi, \eta) d\eta \quad (5-70a)$$

$$\int_{\eta_1(\xi)}^{\eta_2(\xi)} \gamma(\xi, \eta) \eta d\eta = \int_{\eta_1(\xi)}^{\eta_2(\xi)} \gamma_s(\xi, \eta) \eta d\eta \quad (5-70b)$$

These results are valid for all values of k , so that if γ is evaluated from (5-65) or (5-68), γ_s is to be evaluated from (5-57) or (5-58), respectively.

The results of (5-70a) and (5-70b) suffice for the calculation of generalized, aerodynamic forces associated with deflection functions that are either independent of ξ or linear in the spanwise coordinate. In dealing with a more general spanwise weighting function $f(\eta)$ it then naturally suggests itself to try the approximation

$$\int_{\eta_1(\xi)}^{\eta_2(\xi)} \gamma(\xi, \eta) f(\eta) d\eta \simeq \int_{\eta_1(\xi)}^{\eta_2(\xi)} \gamma_s(\xi, \eta) f(\eta) d\eta \quad (5-71)$$

The reliability of the approximation (5-71) for a delta wing and polynomial (of degree greater than one) weighting functions has been investigated by Walsh, Zartarian and Voss (Reference 43), who conclude that it should prove satisfactory for most practical flutter analyses. Whether or not the approximation (5-71) is invoked, however, it generally proves expedient to carry out the spanwise weighting integration (with respect to η) prior to the integration (with respect to ξ, η') over the S domain.

It is probable that the simple planform result (5-65) (or (5-68) for small k) would furnish a more reliable approximation to the pressure distribution over non-simple planforms than would strip theory. Such an approximation, indeed, would be exact over those portions of a wing not influenced by subsonic edges; on the other hand, it would be least reliable in the immediate neighborhood of such edges.

5.2.3.4 Lifting Surface Integral Equation for Supersonic Flow. Those wings for which the trailing edge is nowhere subsonic (subsonic leading edges being permitted, however) often are conveniently treated by first solving for the (dimensionless) velocity potential on the upper surface of the wing, which is related to the pressure distribution according to

$$\gamma(\xi, \eta) = 2\left(\frac{\partial \Phi}{\partial \xi} + i k\right) \Phi_+(\xi, \eta) \quad (5-72)$$

It is shown in Appendix B that Φ_+ satisfies the integral equation

$$\alpha(\xi, \eta) = \iint_S g(\xi - \xi', \eta - \eta') \Phi_+(\xi', \eta') d\xi' d\eta', \quad (\xi, \eta) \text{ on wing} \quad (5-73)$$

where g denotes the kernel

$$g(\xi, \eta) = \frac{1}{\pi} \exp(-i k M^2 \xi / B^2) \lim_{z \rightarrow 0} \frac{\partial^2}{\partial z^2} \left\{ \frac{\cos \left[(k M / B^2) \sqrt{\xi^2 - B^2(\eta^2 + z^2)} \right]}{\sqrt{\xi^2 - B^2(\eta^2 + z^2)}} \right\} \quad (5-74)$$

and S denotes that part of the wing planform over which the radical is real, as shown in Figure 5-10 for the particular case of a narrow delta (leading edges behind Mach lines) wing. The treatment of the improper integral that results after carrying out the Z differentiation in (5-74) and substituting in (5-73) is discussed in Appendix B.

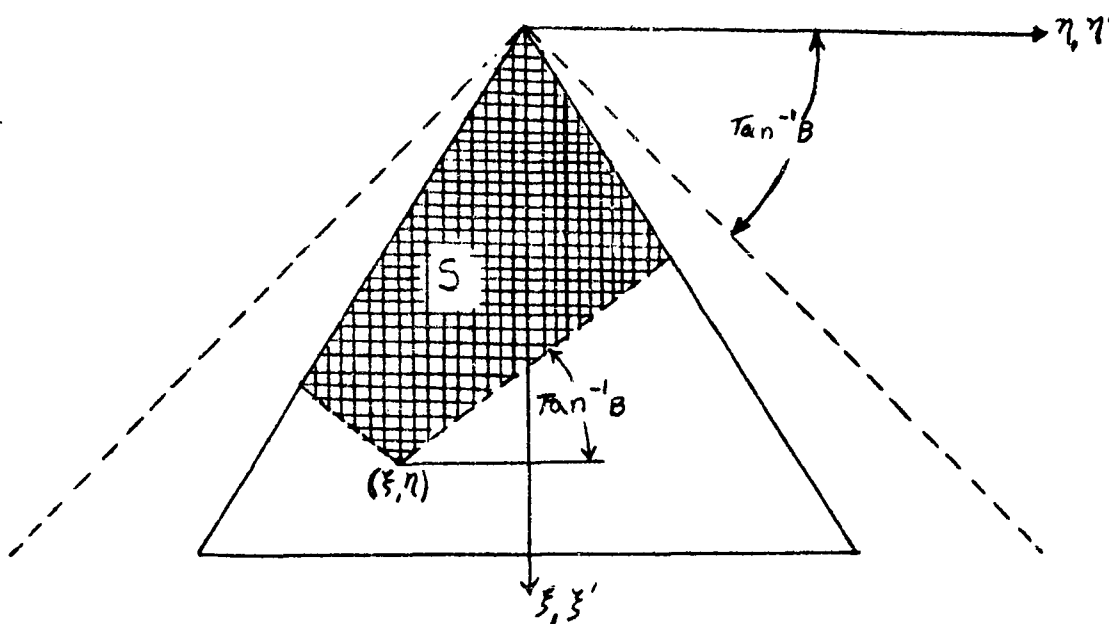


Figure 5-10. The Domain of Integration for the Integral Equation (5-73), Illustrated for a Delta Wing Having Subsonic Leading Edges.

The integral equation (5-73) is not satisfactory for wings having subsonic trailing edges, since points in the wake would enter the calculation. It then is necessary to solve directly for the pressure distribution, which, as shown in Appendix B, satisfies the integral equation

$$\alpha(\xi, \eta) = \iint_S h(\xi - \xi', \eta - \eta') \gamma(\xi', \eta') d\xi' d\eta' \quad (5-75)$$

where the kernel h is related to g according to

$$h(\xi, \eta) = \frac{1}{2} \int_{B|\eta|}^{\xi} e^{-iK(\xi - \xi')} g(\xi', \eta) d\xi' \quad (5-76a)$$

$$= \frac{e^{-iK\xi}}{2\pi} \lim_{z \rightarrow 0} \frac{\partial^2}{\partial z^2} \int_{B(\eta^2 + z^2)^{1/2}}^{\xi} \exp(iK\xi' / B^2) \frac{\cos \left[\frac{(KM/B^2) \sqrt{B^2 - B^2(\eta^2 + z^2)}}{B^2 - B^2(\eta^2 + z^2)} \right]}{B^2 - B^2(\eta^2 + z^2)} d\xi' \quad (5-76b)$$

and where, as before, S denotes that part of the wing planform over which the radical is real. This result again leads to an improper integral, as with (5-73) and (5-74) above. It may be remarked that h resembles, to some extent, the subsonic kernel of (5-49).

The first order approximations to g and h are given by

$$g^{(1)}(\xi, \eta) = \frac{1}{\pi} \left[1 - \frac{i k M^2}{B^2} \xi \right] \lim_{z \rightarrow 0} \frac{\partial^2}{\partial z^2} \left[\xi^2 - B^2(\eta^2 + z^2) \right]^{-\frac{1}{2}} + O(k^2 M^2 / B^4) \quad (5-77)$$

$$h^{(1)}(\xi, \eta) = \frac{1}{2\pi} \lim_{z \rightarrow 0} \frac{\partial^2}{\partial z^2} \int_{B(\eta^2 + z^2)^{1/2}}^{\xi} \left[1 - i k \left(\xi + \frac{z}{B^2} \right) \right] \left[\xi^2 - B^2(\eta^2 + z^2) \right]^{-\frac{1}{2}} dz \quad (5-78a)$$

$$= \frac{1}{2\pi} \lim_{z \rightarrow 0} \frac{\partial^2}{\partial z^2} \left\{ (1 - i k \xi) \cosh^{-1} \left[\xi / B(\eta^2 + z^2)^{1/2} \right] - \frac{i k}{B^2} \left[\xi^2 - B^2(\eta^2 + z^2) \right]^{\frac{1}{2}} \right\} \quad (5-78b)$$

The results of carrying out the limit operations are

$$g^{(1)}(\xi, \eta) = \frac{B^2}{\pi} \left[1 - \frac{i k M^2}{B^2} \xi \right] (\xi^2 - B^2 \eta^2)^{-\frac{3}{2}} + O(k^2 M^2 / B^4) \quad (5-79)$$

$$h^{(1)}(\xi, \eta) = \frac{1}{2\pi} \left[-\frac{\xi}{\eta^2} + i k \left(1 + \frac{\xi^2}{\eta^2} \right) \right] (\xi^2 - B^2 \eta^2)^{-\frac{1}{2}} + O(k^2 M^2 / B^4) \quad (5-80)$$

It should be remarked again that appropriate steps must be taken to circumvent the singularities in these kernels, as noted in Appendix B.

5.2.3.5 Evvard's Method. The steady flow integral equations obtained by setting $k = 0$ in (5-73) and (5-75) may be inverted by a method due to Evvard (Reference 44). The method is, in principle, applicable to planforms of arbitrary shape, but it is of limited value when different subsonic edges are in close proximity; conversely, it assumes a particularly simple form when the subsonic edges of the planform are "non-interfering", whose meaning will become clear in the sequel.

Evvard also has applied his method to a wing exhibiting a slowly varying angle of attack (in particular a linear time variation), and the results so obtained are valid as a first order approximation (the results for a linear

time variation are exact). Only steady flow problems will be considered in the present section, however, in virtue of the transformation of Section 5.2.3.1 which may be used to develop first order approximations to the corresponding unsteady flow problems.

Consider the symmetric* (with respect to the midspan line) wing shown in Figure 5-11. The points a and a' are determined by drawing those tangents to the leading edge that make the Mach angle $\sin^{-1}(\frac{1}{M})$ with the free stream velocity vector. The points c and c' are similarly determined on the trailing edge, while the points b and b' , which separate the leading and trailing edges, are determined by those tangents to the planform boundary that are parallel to the freestream. The component of freestream velocity normal to the wing edge is supersonic along $a'oa$ (supersonic leading edge) and cdc' (supersonic trailing edge), and subsonic along ab and $a'b'$ (subsonic leading edges) as well as bc and $b'c'$ (subsonic trailing edges). These edges serve to define various zones of dependence for the planform, as shown in Figure 5-11, where the dashed lines drawn into the planform from a , a' , b and b' all make the Mach angle with the freestream flow vector. The various zones now will be discussed in the order of the complexity of the corresponding pressure distributions. There is, however, no need to discuss separately the zones II', III' and V', since the required results follow from those of zones II, III and V in virtue of symmetry considerations.

The domain (or zone) of dependence S for a given point P on a wing is determined by constructing the upstream portions of the Mach waves through P and including all points between these lines for which the vertical component of velocity does not vanish. The velocity potential at P (on the upper surface of the wing) is given by (Reference 40)

$$\Phi_+(\xi, \eta) = - \frac{1}{\pi} \iint_S R^{-1} \Phi_z(\xi', \eta', 0) d\xi' d\eta' \quad (5-81)$$

where R is the hyperbolic distance defined by (5-66). The upwash $\Phi_z(\xi', \eta', 0)$ is prescribed (as $-\alpha$) on the wing surface, but in general it does not vanish over the remainder of the plane $z = 0$; however, the upwash does vanish everywhere forward of the supersonic portion ($a'oa$ in Figure 5-11) of the leading edge and the downstream Mach waves terminating this portion, so that the domain of dependence S is always finite in extent.

It follows from the discussion of the preceding paragraph that the potential at any point P in zone I is given by

$$\Phi_I = \frac{1}{\pi} \iint_{S_I} R^{-1} \alpha(\xi', \eta') d\xi' d\eta' \quad (5-82)$$

where S_I is shown in Figure 5-12. The corresponding pressure jump is given by

$$\chi_I = 2 \frac{\partial}{\partial \xi} \Phi_I = \frac{2}{\pi} \iint_{S_I} R^{-1} \frac{\partial}{\partial \xi'} \alpha(\xi', \eta') d\xi' d\eta' + \frac{2}{\pi} \int_{C_I} R^{-1} \alpha(\xi', \eta') d\eta' \quad (5-83)$$

* Evvard's results also are applicable to asymmetric wings, but the latter are of little or no practical interest.

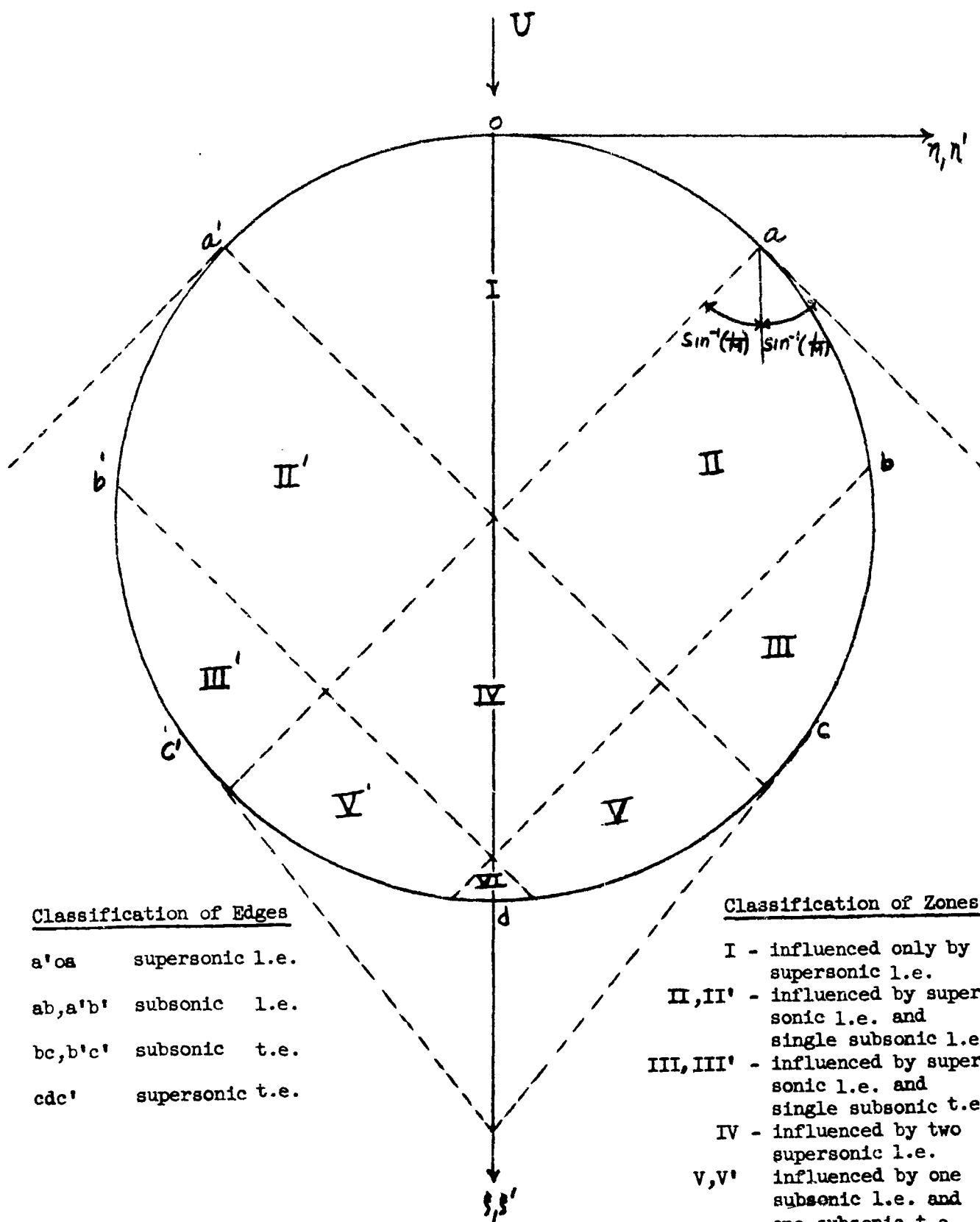


Figure 5-11. Sketch of Supersonic Wing Showing Various Zones of Dependence.

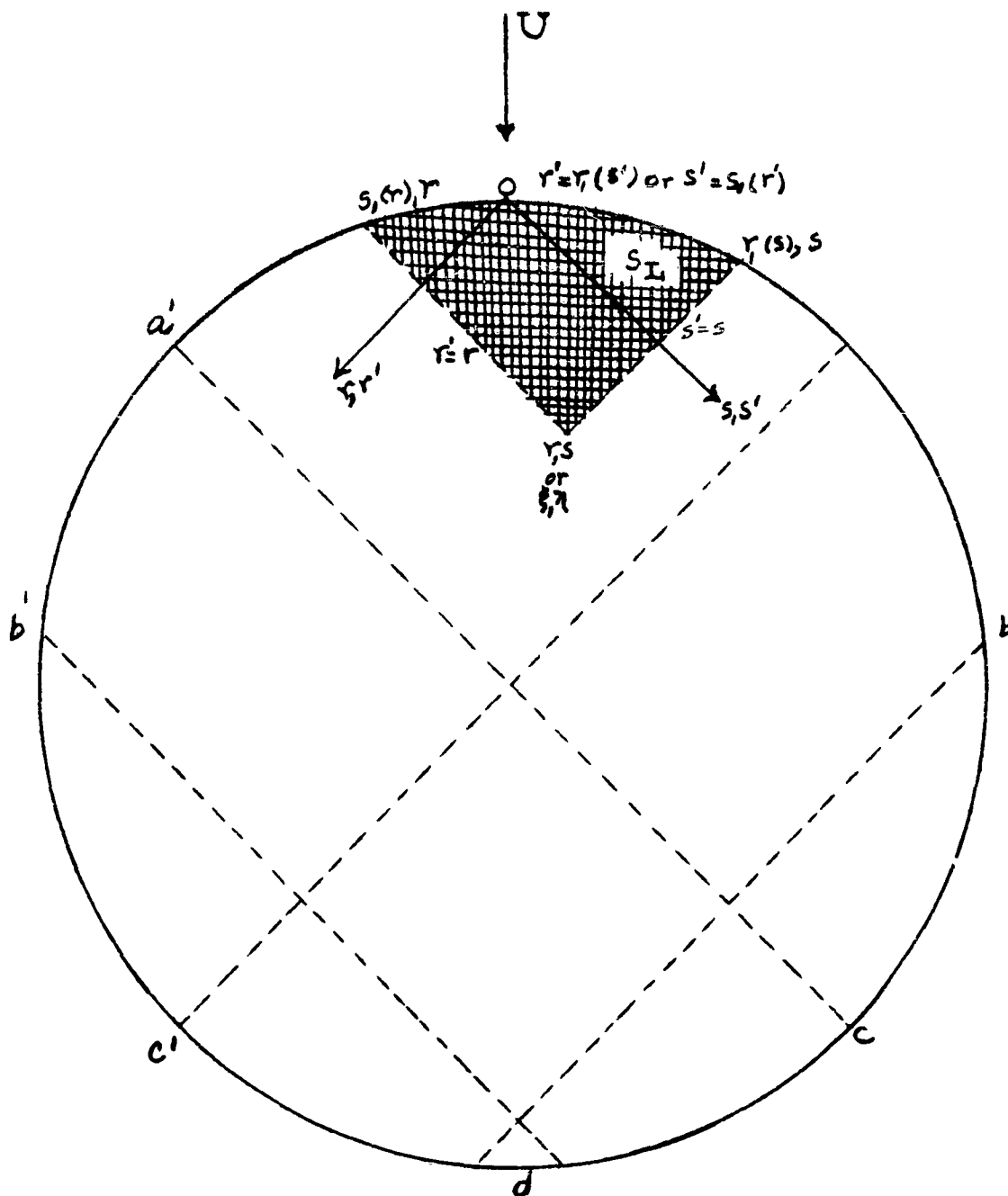


Figure 5-12. The Domain of Integration (S_I) for (5-82), (5-83), (5-85), and (5-86).

where C_I is the curve intercepted on the leading edge by S_I . These results also could have been inferred directly from those of Section 4.2.3.3 since zone I may be regarded as part of a simple planform.

In carrying out the foregoing integrals, it is expedient, following Evvard, to introduce characteristic coordinates r and s , as shown in Figure 5-12. The required transformation is, in matrix form,

$$\begin{Bmatrix} r \\ s \end{Bmatrix} = \frac{M}{2B} \begin{bmatrix} 1 & -B \\ 1 & B \end{bmatrix} \begin{Bmatrix} \xi \\ \eta \end{Bmatrix}. \quad (5-84a)$$

$$\begin{Bmatrix} \xi \\ \eta \end{Bmatrix} = \frac{1}{M} \begin{bmatrix} B & B \\ -1 & 1 \end{bmatrix} \begin{Bmatrix} r \\ s \end{Bmatrix} \quad (5-84b)$$

It also may be noted that

$$\frac{\partial}{\partial \xi} = \frac{M}{2B} \left(\frac{\partial}{\partial r} + \frac{\partial}{\partial s} \right) \quad (5-84c)$$

Under this transformations, (5-82) and (5-83b) go over to

$$\Phi_I = \frac{1}{M\pi} \int_{r_1(s)}^r (r-r')^{-\frac{1}{2}} dr' \int_{s_1(r')}^s (s-s')^{-\frac{1}{2}} \alpha ds' \quad (5-85)$$

where α is assumed to be expressed in terms of r' and s' through (5-84a). Similarly, (5-83b) becomes

$$\begin{aligned} \gamma_I = & \frac{2}{M\pi} \int_{r_1(s)}^r (r-r')^{-\frac{1}{2}} dr' \int_{s_1(r')}^s (s-s')^{-\frac{1}{2}} \frac{\partial \alpha}{\partial \xi'} ds' \\ & + \frac{1}{B\pi} \int_{C_I} (r-r')^{-\frac{1}{2}} (s-s')^{-\frac{1}{2}} \alpha (ds' - dr') \end{aligned} \quad (5-86)$$

In both of these expressions $r_1(s)$ or, equivalently, $s_1(r)$ specifies the leading edge, and this relation may be used to eliminate either r' or s' in the line integral over C_I .

The zone of dependence of a point in zone II evidently includes a region (aef in Figure 5-13) in the upwash field between the subsonic leading edge ab and the downstream Mach wave from a. It was shown by Evvard (Reference 44), that the contribution of this upwash region to the integral (5-82) is just cancelled by that part of the wing downwash in the zone bounded by the leading edge and the reflection in the subsonic leading edge of the upstream Mach wave from the point in question. It follows that the potential in zone II may be calculated by choosing the effective domain of dependence S_{II} , as shown in Figure 5-13. Introducing the characteristic coordinates, and letting $r_1(s)$

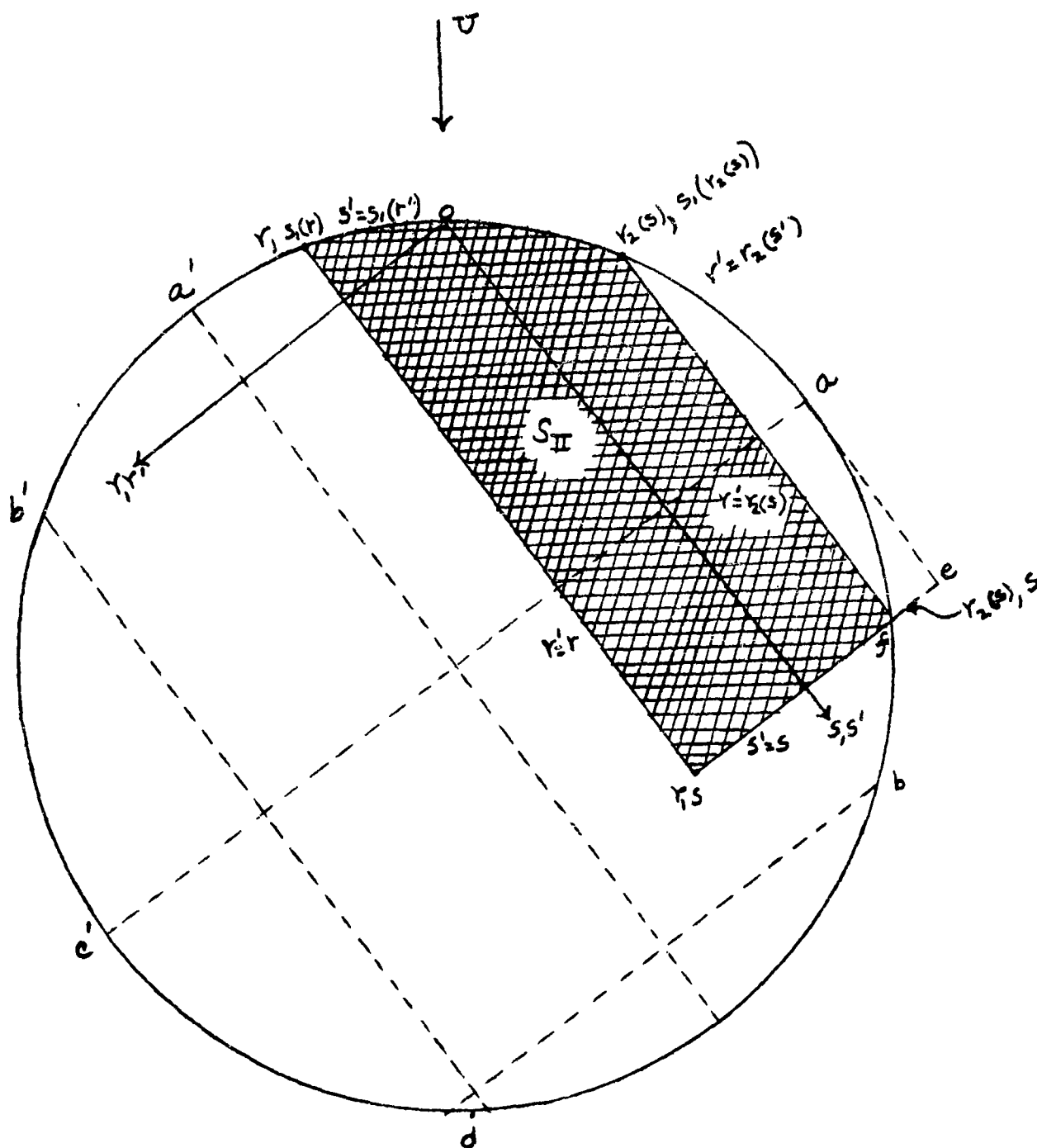


Figure 5-13. The Domain of Integration (S_{II}) for (5-87) and (5-88).

and $r_2(s)$ specify the supersonic (a'oa) and starboard, subsonic leading (ab) edges, respectively, the potential then is given by (cf. (5-85) above)

$$\Phi_{II} = \frac{1}{\pi} \iint_{S_{II}} R^{-1} \alpha d\xi' d\eta' \quad (5-87a)$$

$$= \frac{1}{M\pi} \int_{r_2(s)}^r (r-r')^{-\frac{1}{2}} dr' \int_{s_1(r')}^s (s-s')^{-\frac{1}{2}} \alpha ds' \quad (5-87b)$$

The corresponding pressure jump is obtained by differentiating 2Φ according to (5-84c) with the result

$$\begin{aligned} \gamma_{II} = & \frac{2}{M\pi} \int_{r_2(s)}^r (r-r')^{-\frac{1}{2}} dr' \int_{s_1(r')}^s (s-s')^{-\frac{1}{2}} \frac{\partial \alpha}{\partial \xi'} ds' \\ & + \frac{1}{B\pi} \int_{r_2(s), s_1(r_2(s))}^{r, s_1(r)} (r-r')^{-\frac{1}{2}} (s-s')^{-\frac{1}{2}} \alpha (ds' - dr') \\ & + \left[\frac{1-r_2(s)}{B\pi} \right] \left[r-r_2(s) \right]^{-\frac{1}{2}} \int_{s_1(r_2(s))}^s (s-s')^{-\frac{1}{2}} \alpha ds' \end{aligned} \quad (5-88)$$

It should be remarked that the last term in (5-88) exhibits a square root singularity in the pressure as s approaches $r_2(s)$, i.e., as the subsonic leading edge is approached. This behavior is characteristic of subsonic leading edges and is to be contrasted with the requirement (Kutta condition) that the pressure jump must vanish at a subsonic trailing edge. Evvard has shown that the latter condition, which must be imposed along bc and $b'c'$ in zones III and III', together with the other requirements upon the solution, may be satisfied simply by dropping the last term in (5-88), with the result

$$\begin{aligned} \gamma_{III} = & \frac{2}{M\pi} \int_{r_2(s)}^r (r-r')^{-\frac{1}{2}} dr' \int_{s_1(r')}^s (s-s')^{-\frac{1}{2}} \frac{\partial \alpha}{\partial \xi'} ds' \\ & + \frac{1}{B\pi} \int_{r_2(s), s_1(r_2(s))}^{r, s_1(r)} (r-r')^{-\frac{1}{2}} (s-s')^{-\frac{1}{2}} \alpha (ds' - dr') \end{aligned} \quad (5-89)$$

The domain of integration for the integral in (5-89) is shown as S_{III} in Figure 5-14, but it should be emphasized that S_{III} is not an effective zone of dependence for the potential in zone III. Indeed, this potential is perhaps most simply determined (although seldom required) by integrating (5-89) according to

$$\Phi_{III} = \frac{1}{2} \int_{\xi_1(\eta)}^{\xi} \gamma_{III} d\xi \quad (5-90a)$$

$$= \frac{B}{2M} \int_{\text{leading edge}}^{(r,s)} \gamma_{III} (dr + ds) \quad (5-90b)$$

The construction of a first order approximation in zone III using the result (5-54) requires, in addition to the steady flow pressure distribution α_{III} , the determination of the modified velocity potential ψ , based on the artificial hypothesis that the subsonic trailing edge may be treated as a subsonic leading edge. The required result evidently is given by using the result for Φ_{II} even though (r,s) is in zone III-viz.,

$$\psi_{III} = \frac{1}{\pi} \iint_{S_{III}} R^{-1} \alpha d\xi' d\eta' \quad (5-91a)$$

$$= \frac{1}{M\pi} \int_{r_1(s)}^r (r-r')^{-\frac{1}{2}} dr' \int_{s_1(r')}^s (s-s')^{-\frac{1}{2}} \alpha ds' \quad (5-91b)$$

Zone IV consists of those points influenced by both of the subsonic leading edges ab and $a'b'$. The effective domain of dependence for a point in this zone follows the construction for zone II, except that the upstream Mach waves from the point now must be reflected in both leading edges, as shown in Figure 5-15. The resulting potential is given by

$$\Phi_{IV} = \frac{1}{M\pi} \left[\int_{r_2(s)}^{r_1(s_2^*(r))} \int_{s_1(r')}^s + \int_{r_1(s_2^*(r))}^r \int_{s_2^*(r)}^s \right] (r-r')^{-\frac{1}{2}} (s-s')^{-\frac{1}{2}} \alpha dr' ds' \quad (5-92)$$

where $r_1(s)$, $r_2(s)$ and $s_2^*(r)$ denote the supersonic, starboard subsonic and port subsonic leading edges, respectively. The pressure jump corresponding to (5-92) is given by

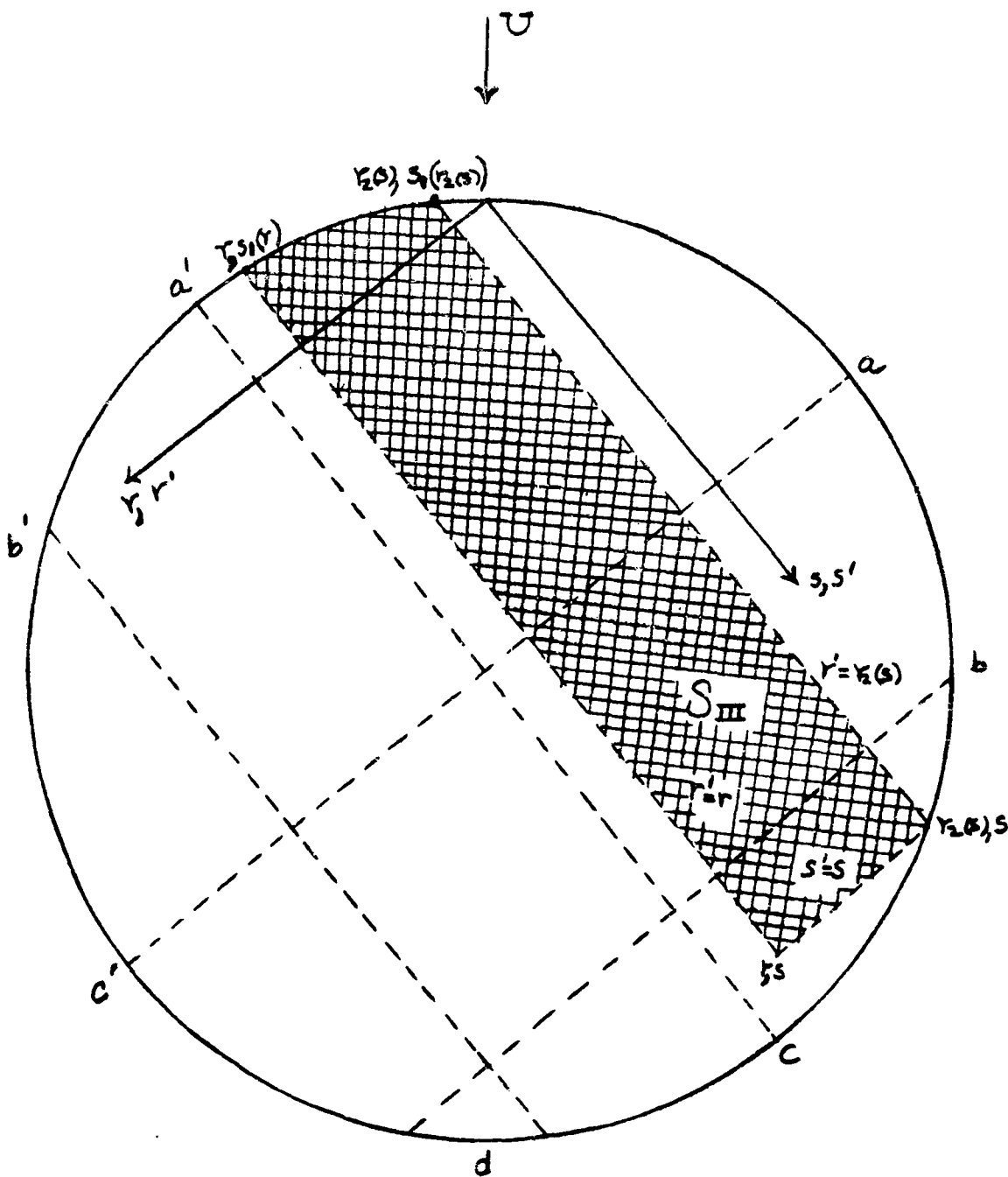


Figure 5-14. The Domain of Integration (S_{III}) for (5-89) and (5-91).

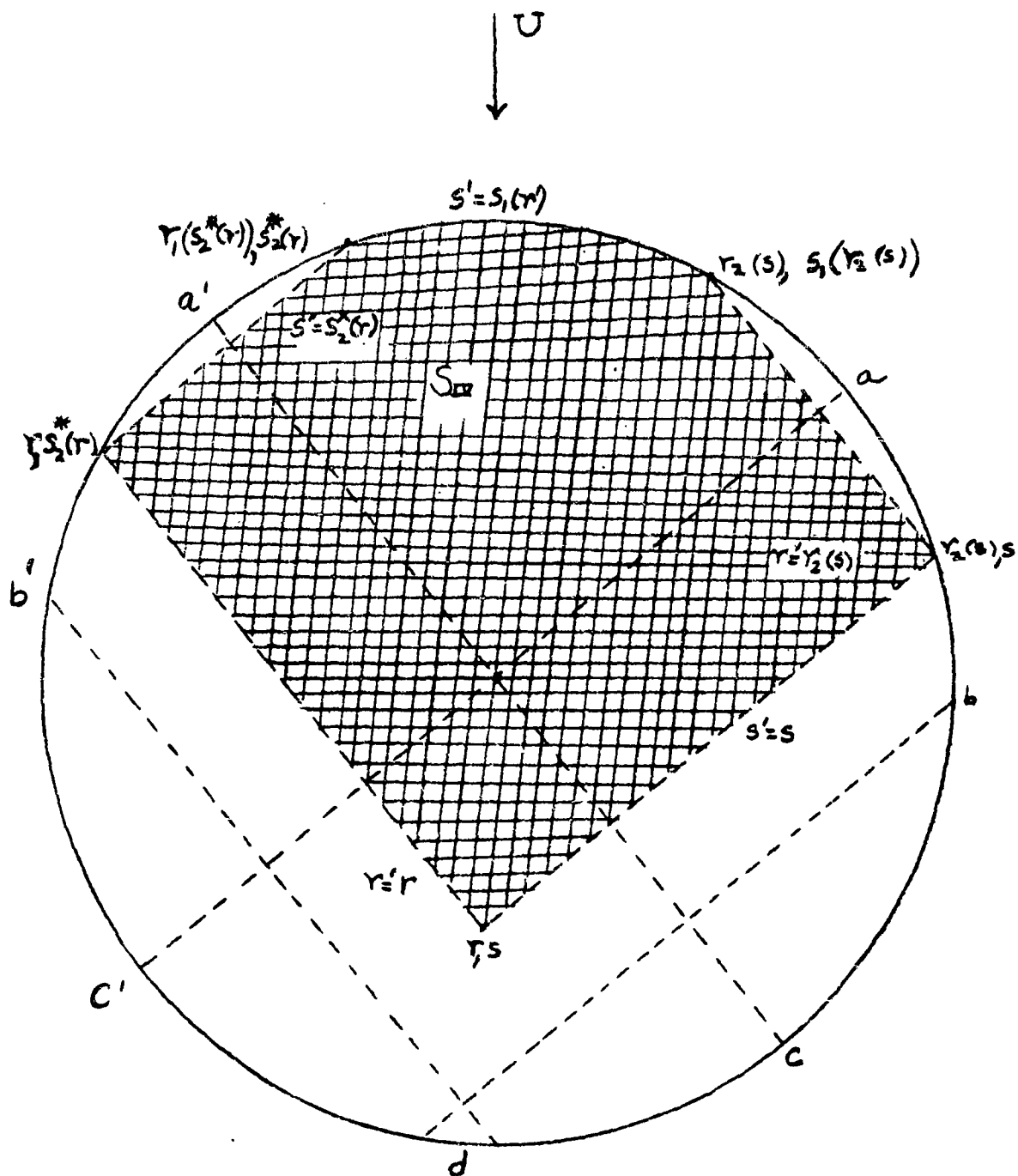


Figure 5-15. The Domain of Integration (S_{IV}) for (5-92) and (5-93).

$$\begin{aligned}
\gamma_{IV} = & \frac{2}{M\pi} \left[\int_{r_2(s)}^{r_1(s_2^*(r))} \int_{s_1(r')}^s + \int_{r_1(s_2^*(r))}^r \int_{s_2^*(r)}^s \right] (r-r')^{-\frac{1}{2}} (s-s')^{-\frac{1}{2}} \frac{\partial \alpha}{\partial \xi'} dr' ds' \\
& + \frac{1}{8\pi} \int_{r_2(s), s_1(r_2(s))}^{r_1(s_2^*(r)), s_2^*(r)} (r-r')^{-\frac{1}{2}} (s-s')^{-\frac{1}{2}} \alpha (ds' - dr') + \left[\frac{1-s_2^*(r)}{8\pi} \right] \left[s-s_2^*(r) \right]^{-\frac{1}{2}} \int_{r_1(s_2^*(r))}^r (r-r')^{-\frac{1}{2}} \alpha dr' \\
& + \left[\frac{1-r_2'(s)}{8\pi} \right] \left[r-r_2(s) \right]^{-\frac{1}{2}} \int_{s_1(r_2(s))}^s (s-s')^{-\frac{1}{2}} \alpha ds'
\end{aligned} \tag{5-93}$$

It is evident that if the supersonic leading edge for the wing of Figure 5-11 were to be extended somewhat further upstream, the reflections of the Mach waves (emanating from a point in zone IV) in the subsonic leading edges would cross on the wing. A planform for which this does occur is illustrated in Figure 5-16. It then is necessary to subtract the downwash integral over the region $S_{IV}^{(-)}$ from the integral over $S_{IV}^{(+)}$ to obtain the effective domain of dependence. The results (5-92) and (5-93) remain formally valid in this case, but it is more convenient in the actual evaluation of the integral to rewrite the potential in the form

$$\Phi_{IV} = \frac{1}{M\pi} \left[\int_{r_2(s)}^r \int_{s_2^*(r)}^s - \int_{r_1(s_2^*(r))}^{r_2(s)} \int_{s_1(r')}^{s_2^*(r)} \right] (r-r')^{-\frac{1}{2}} (s-s')^{-\frac{1}{2}} \alpha dr' ds' \tag{5-94}$$

where the first and second integrals correspond to $S_{IV}^{(+)}$ and $S_{IV}^{(-)}$, respectively. The pressure jump is similarly transformed to

$$\begin{aligned}
\gamma_{IV} = & \frac{2}{M\pi} \left[\int_{r_2(s)}^r \int_{s_2^*(r)}^s + \int_{r_1(s_2^*(r))}^{r_2(s)} \int_{s_1(r')}^{s_2^*(r)} \right] (r-r')^{-\frac{1}{2}} (s-s')^{-\frac{1}{2}} \frac{\partial \alpha}{\partial \xi'} dr' ds' \\
& + \frac{1}{8\pi} \int_{r_2(s), s_1(r_2(s))}^{r_1(s_2^*(r)), s_2^*(r)} (r-r')^{-\frac{1}{2}} (s-s')^{-\frac{1}{2}} \alpha (ds' - dr') + \left[\frac{1-s_2^*(r)}{8\pi} \right] \left[s-s_2^*(r) \right]^{-\frac{1}{2}} \int_{r_1(s_2^*(r))}^r (r-r')^{-\frac{1}{2}} \alpha dr'
\end{aligned}$$

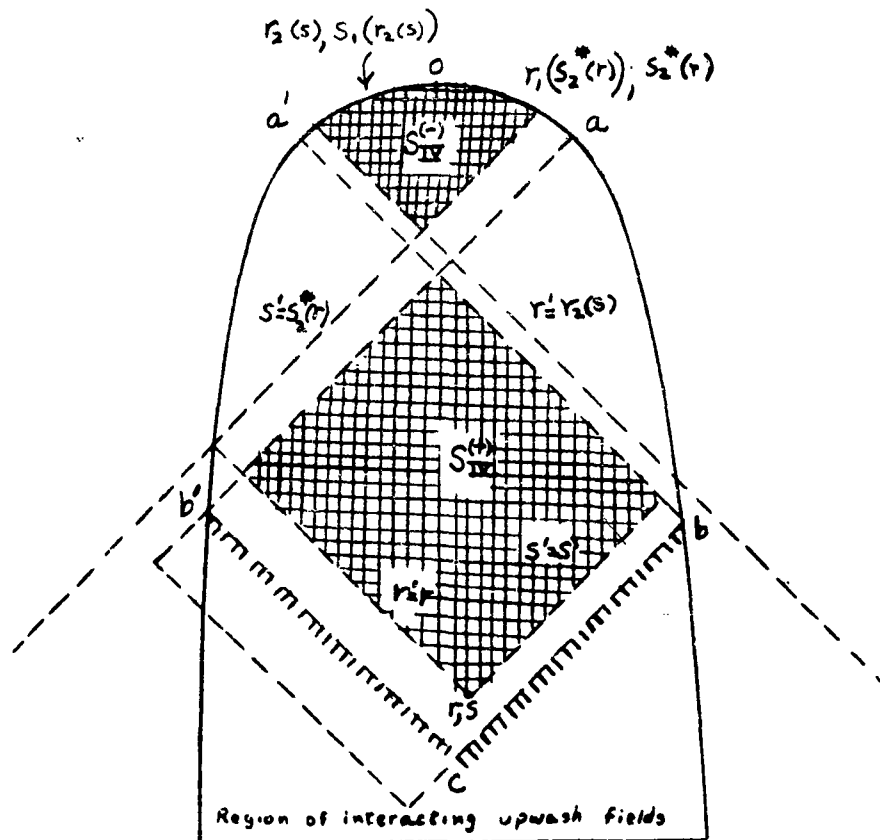


Figure 5-16. A Planform Having a Region of Interacting Upwash Fields and also Illustrating the Domain of Integration for (5-94).

(Equation (5-95) continued)

$$+ \left[\frac{1-r_2'(s)}{8\pi} \right] \left[r-r_2(s) \right]^{-\frac{1}{2}} \int_{s_1(r_2(s))}^s (s-s')^{-\frac{1}{2}} \alpha ds' \quad (5-95)$$

The results (5-94) and (5-95) are not valid for points downstream of b'cb in Figure 5-16 (where b'c and bc are the reflections in the subsonic leading edges of the Mach lines from the points a' and a' that separate the supersonic leading edge from the subsonic leading edges). This is a consequence of the interaction of the upwash fields downstream of the extensions off the wing of the Mach wave ab' and a'b. The derivation of results for points influenced by these interacting upwash fields is discussed by Evvard (Reference 44, page 9), but it does not seem possible to obtain closed form results that are both general and comparable in simplicity with the foregoing formulae. These interactions, moreover, become compounded at each subsequent deflection in the edges of the Mach cone from its apex, having no supersonic leading edge to separate its subsonic leading edges, furnishes an example for which the number of interactions is infinite, so that Evvard's method is incapable of providing a direct solution.

The pressure jump in zone V of Figure 5-11 may be derived from that in zone IV simply by deleting the last integral in (5-93), while that in zone V' follows from (5-93) after the deletion of the third integral (containing the square root singularity at $s = s_2^*(r)$); as already remarked, this last result usually is not required explicitly in virtue of symmetry considerations.. Similarly the pressure jump in zone VI may be obtained by deleting the last two terms in (5-93). Finally, the modified potential for zones V and VI is given by (cf. (5-91))

$$\psi_V = \psi_{IV} = \phi_{IV} \quad (5-96)$$

5.2.3.6 Aerodynamic Influence Coefficients. In Section 5.2.1.4, it is pointed out that a direct numerical solution of the basic wing problem can be posed in the matrix form

$$\underline{\gamma} = \underline{P} \underline{\alpha} \quad (5-13)$$

where \underline{P} is the aerodynamic influence matrix. For supersonic flow this turns to be a powerful method of handling three-dimensional aeroelastic problems. Work in this direction is often referred to as the box method.

Analysis using both structural and aerodynamic influence coefficients is convenient for digital or analog computing machines. Particular promise has been demonstrated for wings with all supersonic edges, because in this case the aerodynamic influence coefficients can be determined with relative ease.

In Section 5.2.3.3, it is shown that according to Garrick and Rubinow (Ref. 39) the local pressure distribution over a wing with supersonic edges is given by integrating, over the portion of the wing that can influence the point, an acoustic-type source that is locally weighted by the prescribed downwash of the wing. See (5-55), et seq. Thus, if any element of area ΔS_1 of a wing

is assumed to have some prescribed motion w_i , (or the dimensionless quantity α_i , according to (5-10)), the lift produced by this motion, (expressed in a dimensionless quantity γ according to (5-11)), on any other element ΔS_j within the region of influence of ΔS_i , is given by an integration of weighted sources over ΔS_i .

Thus the aerodynamic force A_{ji} that acts on the j element due to the i element can be readily calculated. The total aerodynamic forces acting on this j element is given by a matrix equation.

$$\{\gamma_j\} = [A_{ji}] \{\alpha_i\} \quad (5-13a)$$

where all the elements A_{ji} , the aerodynamic influence coefficients, may be considered known. Applications of this method have been demonstrated by Pines and his associates (Ref. 144). An example is also given in Ref. 71.

Extension of this procedure to wings with subsonic edges is discussed in Ref. 144. In Ref. 144, a grid of square boxes is used. Development of other grids which may show greater numerical advantage has been in progress at the Analysis Laboratory of the California Institute of Technology.

It must be added that the use of kernel functions, as developed by Watkins and his associates at NACA, (Refs. 28, 123, 124) leads naturally to the concept of aerodynamic influence coefficients, and may prove to be of great value in future developments.

5.2.4 Slender Body Theory

The approximations that form the basis of lifting line theories in subsonic flow (Section 5.2.2.4) break down for low aspect ratio wings, and it then becomes necessary either to apply the more difficult lifting surface theory or to seek more suitable approximations. Low aspect ratio supersonic wings also are difficult to analyze by those methods suitable for wings of relatively higher aspect ratio; in particular, Evvard's method (Section 5.2.3 5) tends to be impractical in consequence of the inverse relation between the number of Mach wave reflections and the effective aspect ratio. Fuselage interference also becomes more important for low aspect ratio wings, and methods for treating wing-body combinations become correspondingly more important. It should be remarked that, in all of these considerations, the effective aspect ratio, $|1-M^2|^{1/2} AR$ is a more significant measure than the geometric aspect ratio, AR .

A simple solution for steady flow past a slender body of revolution was given by Munk (Ref. 45), who made the approximation that the cross flow could be treated as two-dimensional and introduced the concept of virtual momentum in the calculations of the transverse force. This same approximation

was later applied by Jones (Reference 46), to low aspect ratio wings in steady flow, while the work of both Munk and Jones was extended to unsteady flow by Miles (Reference 47). A formulation of the slender body problem for supersonic flow that was both more rigorous and more general was given by Ward (Reference 48) and extended to unsteady flow by Miles (Reference 49).

The restrictions that must be applied to the slender body results in unsteady flow are as follows: (see References 48 and 49)

$$\delta, k\delta, M\delta, kM\delta \ll 1 \quad (5-97)$$

where k , M and δ denote, respectively, reduced frequency, Mach number and the transverse body dimension (e.g., maximum body diameter or wing span) divided by body length (or, if larger, $\delta = |\alpha_{\max}|$).

5.2.4.1 Slender Body of Revolution. The cross force per unit length, $L'(\xi)$ acting on a slender body of revolution due to a transverse distribution of velocity $U\alpha(\xi)$, positive down, is given by the (linearized theory) approximation (see Reference 47)

$$L'(\xi) = \rho_0 U^2 \left(\frac{\partial}{\partial \xi} + i k \right) [S(\xi) \alpha(\xi)] \quad (5-98)$$

where $S(\xi)$ is the cross sectional area at ξ . The total lift is given by

$$L = \rho_0 U^2 \left[S(1) \alpha(1) + i k \int_0^1 S(\xi) \alpha(\xi) d\xi \right] \quad (5-99)$$

where the characteristic length is chosen as the body length (ℓ). The corresponding moment about $\xi = a$ is

$$M = \rho_0 U^2 \ell \left\{ -(1-a) S(1) \alpha(1) + \int_0^1 [1 + i k(a-\xi)] S(\xi) \alpha(\xi) d\xi \right\} \quad (5-100)$$

The foregoing result may be extended to bodies of non-circular cross section by replacing $\rho_0 S(\xi)$ by the virtual mass (m) of the local cross section, the lift per unit length being given by the (total) time rate of change of the virtual momentum-viz.,

$$L'(\xi) = U^2 \left(\frac{\partial}{\partial \xi} + i k \right) [m(\xi) \alpha(\xi)]^* \quad (5-101)$$

This result assumes the cross sections to remain undistorted, so that the transverse motion of any particular cross section consists of a pure translation of velocity $U\alpha(\xi)$. It also should be emphasized that the result is not valid for steady flow unless the appropriate restrictions are imposed on the cross-sectional distribution (sufficient restrictions being symmetry of the cross section with respect to the y and z axes - Reference 50).

* Equation (5-101) is not valid in unsteady or steady flow when the restrictions mentioned (5-97), are violated.

5.2.4.2 Low Aspect Ratio Wings. The calculation of the lift on any transverse section, due to translation of that section, as the rate of change of virtual momentum may be applied directly to a low aspect ratio wing, following the original work of Jones for steady flow (Reference 46). The virtual mass for a flat plate section of semi-span $b(\xi)$ is given by

$$m(\xi) = \pi \rho_0 b^2(\xi) \quad (5-102)$$

substituting (5-102) in (5-101) then yields (see Reference 47)

$$L'(\xi) = \pi \rho_0 U^2 \left(\frac{\partial}{\partial \xi} + iA \right) [b^2(\xi) \alpha(\xi)] \quad (5-103)$$

The lift coefficient obtained from (5-103)

$$C_L = \left[\frac{1}{2} \rho_0 U^2 S \right]^{-1} \int_0^L L'(\xi) d\xi \quad (5-104a)$$

$$= \frac{\pi AR}{2} \left[\alpha(1) + iA \int_0^1 \frac{b^2(\xi)}{b^2(1)} \alpha(\xi) d\xi \right] \quad (5-104b)$$

where S is wing area and AR is the aspect ratio - viz,

$$AR = 4b^2(1)/S \quad (5-105)$$

Setting $k = 0$ yields the Jones result $(\pi AR/2)$ for the lift (coefficient) curve slope.

The consideration of wing motions that exhibit a spanwise variation is expedited by the introduction of the change of variable (cf. Section 5.2.2.1, where a similar transformation of the chordwise coordinate was introduced)

$$\eta = b(\xi) \cos \theta \quad (5-106)$$

The potential on the upper surface of the wing, $\Phi_+(\xi, \eta)$ due to a prescribed downwash $\alpha(\xi, \eta)$ then is given by (Reference 47)

$$\Phi_+(\xi, b \cos \theta) = \frac{2}{\pi} b(\xi) \sum_{n=1}^{\infty} \frac{\sin(n\theta)}{n} \int_0^{\pi} \alpha(\xi, b \cos \phi) \sin(n\phi) \sin \phi d\phi \quad (5-107a)$$

$$= \frac{1}{\pi} b(\xi) \int_0^{\pi} L(\theta, \phi) \alpha(\xi, b \cos \phi) \sin \phi d\phi \quad (5-107b)$$

where $L(\theta, \varphi)$ is given by (5-20). The pressure jump may be calculated from Φ_+ by (5-72); in the partial differentiation of Φ_+ with respect to ξ , it should be emphasized that θ does not remain constant; rather, it follows from (5-20) and (5-106) that

$$\gamma(\xi, b \cos \theta) = 2 \left(\frac{\partial}{\partial \xi} + i\kappa \right) \eta \Phi_+(\xi, \eta) \quad (5-108a)$$

$$= 2 \left[\left(\frac{\partial}{\partial \xi} \right)_{\theta} + \frac{b'(\xi)}{b(\xi)} \cot \theta \left(\frac{\partial}{\partial \theta} \right)_{\xi} + i\kappa \right] \Phi_+(\xi, b \cos \theta) \quad (5-108b)$$

It is evident from the result (5-107) that the functions $\sin(n\theta)$ would constitute an expedient choice in developing spanwise deflection modes. However, the more common choice of polynomials in n offers very little additional difficulty. Consider, for example, the prescribed downwash

$$\alpha(\xi, \eta) = \eta^2 f(\xi) \quad (5-109)$$

that would arise from a parabolic approximation to spanwise bending. Substituting (5-109) in (5-107a) yields

$$\Phi_+(\xi, b \cos \theta) = \frac{1}{4} b^3(\xi) f(\xi) \left[\sin \theta + \frac{1}{3} \sin(3\theta) \right] \quad (5-110a)$$

$$= \frac{1}{6} f(\xi) \left[b^2(\xi) + 2\eta^2 \right] \left[b^2(\xi) - \eta^2 \right]^{\frac{1}{2}} \quad (5-110b)$$

from which the corresponding pressure jump would follow by substitution in (5-108a) or (5-108b)

5.2.4.3 Slender Wing-body Combination. The wing-body cross section shown in Figure 5-17 may be analyzed in the slender body approximation by conformal transformation to a circular section. A motion of pure translation (at any particular section, so that the incidence α depends only on ξ) is particularly simple, and it is found necessary only to replace $b(\xi)$ in (5-102) through (5-104) by the equivalent semi-span (References 48 and 49)

$$b_{\text{equiv}} = \left[b^2 + \frac{a^4}{b^2} - a^2 \right]^{\frac{1}{2}} \quad (5-111)$$

This reduces to b if either $a = 0$ or $a = b$.

The analysis of more general motions yields a result similar to that of (5-107) (Reference 49). More accurate methods of treating wing-body interference have been discussed by Ashley et. al. (Reference 22).

5.2.4.4 Quasi-slender Wing Theory. The slender wing theory of Section 5.2.4.2 may be regarded as the first step in the development of a solution to

the wing boundary value problem in powers of the aspect ratio. Adams and Sears have obtained the next term in this development for steady supersonic flow, (Reference 51), and their work has been extended to unsteady supersonic flow by Miles (Reference 52). The results are based on an iteration procedure and may be expressed in terms of a modified incidence distribution to be used in the slender wing result of (5-107).

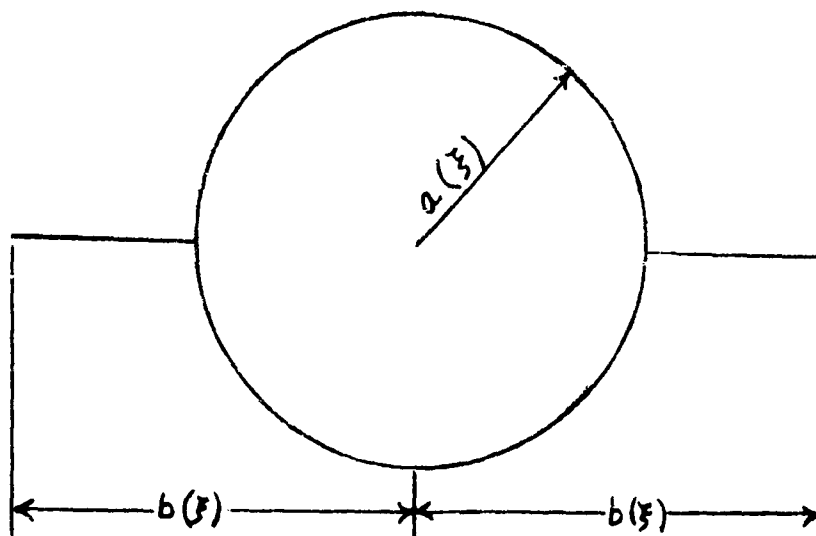


Figure 5-17. The Wing-Body Cross Section of Section 5.2.4.3

The potential on the upper surface of the wing after s iterations may be expressed in the form

$$\Phi_+^{(s)}(\xi, b \cos \theta) = b(\xi) \left\{ \sum_{n=1}^{\infty} a_n^{(s)}(\xi) \sin(n\theta) + O[B^{2s+2} b^{2s+2} \ln(Bb), \right. \\ \left. K^{2s+2} M^{2s+2} \ln(KM \cdot b)] \right\} \quad (5-112)$$

where

$$a_n^{(s)}(\xi) = \frac{2}{\pi n} \int_0^{\pi} \alpha^{(s)}(\xi, b \cos \phi) \sin(n\phi) \sin \phi d\phi \quad (5-113)$$

The simplest approximation, designated by $s = 0$, is obtained by letting $\alpha^0 = \alpha$ so that (5-112) and (5-113) reduce to the slender wing approximation (5-107a). The next approximation is given by (Reference 52)

$$\alpha^{(1)}(\xi, b \cos \theta) = \alpha(\xi, b \cos \theta) + \frac{1}{4} \left(B^2 \frac{\partial^2}{\partial \xi^2} + 2i k M^2 \frac{\partial}{\partial \xi} - k^2 M^2 \right) \left\{ \left[\ln \left(\frac{B b(\xi)}{4} \right) - \frac{1}{2} \right] b^2(\xi) a_1^{(0)}(\xi) \right. \\ \left. - \frac{\partial}{\partial \xi} \int_0^\xi \ln(\xi - \xi') b^2(\xi') a_1^{(0)}(\xi') d\xi' + \int_0^\xi \left[1 - \exp \left\{ -\frac{i k M^2}{B^2} (\xi - \xi') \right\} \cos \left\{ \frac{k M}{B^2} (\xi - \xi') \right\} \right] (\xi - \xi')^{-1} b^2(\xi') a_1^{(0)}(\xi') d\xi' \right. \\ \left. + b^2(\xi) \sum_{m=1}^{\infty} [a_{m-1}^{(0)}(\xi) - a_{m+1}^{(0)}(\xi)] m^{-1} \cos(m\theta) \right\} \quad (5-114)$$

provided that B^2 is not too small. If terms of order $k^2 M^4 / B^4$ may be neglected, (5-114) simplifies further to

$$\alpha^{(1)}(\xi, b \cos \theta) = \alpha(\xi, b \cos \theta) + \frac{1}{4} \left(B^2 \frac{\partial^2}{\partial \xi^2} + 2i k M^2 \frac{\partial}{\partial \xi} \right) \left\{ \left[\ln \left(\frac{B b(\xi)}{4} \right) - \frac{1}{2} \right] b^2(\xi) a_1^{(0)}(\xi) \right. \\ \left. - \frac{\partial}{\partial \xi} \int_0^\xi \ln(\xi - \xi') b^2(\xi') a_1^{(0)}(\xi') d\xi' + b^2(\xi) \sum_{m=1}^{\infty} [a_{m-1}^{(0)}(\xi) - a_{m+1}^{(0)}(\xi)] m^{-1} \cos(m\theta) \right\} \\ + \frac{i k M^2}{4} \frac{\partial}{\partial \xi} \left[b^2(\xi) a_1^{(0)}(\xi) \right] \quad (5-115)$$

It should be emphasized that the partial differentiations with respect to ξ in (5-114) and (5-115) imply η , not θ to be held constant.

If $B^2 \ll 1$ the result (5-114) breaks down and must be replaced by (Reference 52)

$$\alpha^{(1)}(\xi, b \cos \theta) = \alpha(\xi, b \cos \theta) + \frac{1}{4\pi} (2i k \frac{\partial}{\partial \xi} - k^2) \left\{ b(\xi) \right. \\ \left. \cdot \int_0^\pi [2 \ln(\sqrt{\frac{1}{2}} b(\xi) |\cos \theta - \cos \phi|) - 0.423] \Phi^{(0)}(\xi, b \cos \phi) \sin \phi d\phi \right\}$$

(continued (5-116))

(Equation (5-116) continued)

$$+ \frac{\pi}{2} \int_0^{\xi} \left[1 - \exp \left\{ -\frac{iR}{2} (\xi - \xi') \right\} \right] (\xi - \xi')^{-1} b^2(\xi') a_1^{(0)}(\xi') d\xi' \\ - \frac{\pi \partial}{2 \partial \xi} \int_0^{\xi} \ln(\xi - \xi') b^2(\xi') a_1^{(0)}(\xi') d\xi' + O(B^2 b^2) \} \quad (5-116)$$

or, for small kb,

$$\alpha^{(1)}(\xi, b \cos \theta) = \alpha(\xi, b \cos \theta) + \frac{iR}{2\pi} \frac{\partial}{\partial \xi} \left\{ b(\xi) \right. \\ \cdot \int_0^{\pi} \left[2 \ln \left(\sqrt{\frac{iR}{2}} b |\cos \theta - \cos \phi| - 0.423 \right) \right] \Phi^{(0)}(\xi, b \cos \phi) \sin \phi d\phi \\ \left. - \frac{\pi \partial}{2 \partial \xi} \int_0^{\xi} \ln(\xi - \xi') b^2(\xi') a_1^{(0)}(\xi') d\xi' \right\} + O \left[B^2 b^2, R^2 b^2 \ln(Rb) \right] \quad (5-117)$$

As an example, consider the incidence distribution of (5-109) - viz.,

$$\alpha(\xi, b \cos \theta) = \eta^2 f(\xi) = \frac{1}{2} b^2(\xi) f(\xi) (1 + \cos 2\theta) \quad (5-118)$$

Comparing (5-110a) to (5-112) above yields

$$a_1^{(0)} = \frac{1}{4} b^2(\xi) f(\xi), \quad a_3^{(0)} = \frac{1}{12} b^2(\xi) f(\xi) \quad (5-119)$$

while the remaining $a_n^{(0)}$ vanish. Substituting (5-118) and (5-119) in (5-114) yields

$$\alpha^{(1)}(\xi, b \cos \theta) = \frac{1}{2} b^2(\xi) f(\xi) (1 + \cos 2\theta) + \frac{1}{6} \left(B^2 \frac{\partial^2}{\partial \xi^2} + 2iRM^2 \frac{\partial}{\partial \xi} - R^2 M^2 \right)$$

$$\cdot \left\{ \left[\ln \left(\frac{Bb}{4} \right) - \frac{3}{4} \right] b^4(\xi) f(\xi) - \frac{\partial}{\partial \xi} \int_0^{\xi} \ln(\xi - \xi') b^4(\xi') f(\xi') d\xi' \right.$$

$$\left. + \int_0^{\xi} \left[1 - \exp \left\{ -\frac{iRM^2}{B^2} (\xi - \xi') \right\} \right] \cos \left\{ \frac{RM}{B^2} (\xi - \xi') \right\} \right]$$

$$\cdot (\xi - \xi')^{-1} b^4(\xi') f(\xi') d\xi' + \frac{2}{3} f(\xi) \eta^4 \quad (5-120)$$

where η has been introduced in the last term to facilitate the partial differentiation with respect to ξ . Substituting (5-120) in (5-113) then leads to

$$a_1^{(1)} = \frac{1}{4} b^2(\xi) f(\xi) + \frac{1}{16} \left(B^2 \frac{\partial^2}{\partial \xi^2} + 2i k M^2 \frac{\partial}{\partial \xi} - k^2 M^2 \right)$$

$$\cdot \left[\left[\ln \left(\frac{Bb}{4} \right) - \frac{3}{4} \right] b^4(\xi) f(\xi) - \frac{\partial}{\partial \xi} \int_0^\xi \ln(\xi - \xi') b^4(\xi') f(\xi') d\xi' \right.$$

$$\left. + \int_0^\xi \left[1 - \exp \left\{ -\frac{i k M^2}{B^2} (\xi - \xi') \right\} \cos \left\{ \frac{k M}{B^2} (\xi - \xi') \right\} (\xi - \xi')^{-1} b^4(\xi') f(\xi') d\xi' \right. \right.$$

$$\left. + \frac{b^4}{192} \left[B^2 \frac{\partial^2}{\partial \xi^2} + 2i k M^2 \frac{\partial}{\partial \xi} - k^2 M^2 \right] f(\xi) \right] \quad (5-121a)$$

$$a_3^{(1)} = \frac{1}{12} b^2(\xi) f(\xi) + \frac{b^4(\xi)}{384} \left(B^2 \frac{\partial^2}{\partial \xi^2} + 2i k M^2 \frac{\partial}{\partial \xi} - k^2 M^2 \right) f(\xi) \quad (5-121b)$$

$$a_5^{(1)} = \frac{b^4(\xi)}{1920} \left(B^2 \frac{\partial^2}{\partial \xi^2} + 2i k M^2 \frac{\partial}{\partial \xi} - k^2 M^2 \right) f(\xi) \quad (5-121c)$$

while the remaining $a_n^{(1)}$ vanish.

5.2.5 Downwash Calculations

Perhaps the most important unsteady flow problem that arises in studying the dynamic stability of rigid aircraft is the calculation of tail force due to wing wake (and also, in lateral motion, fuselage wake). The usual method of effecting this calculation, already indicated in (5-3), is through a downwash derivative $d\epsilon/d\alpha$ that is evaluated from steady flow theory and/or experiment.

More accurate methods of evaluating the effects of wing downwash on the tail forces have been discussed in References 22 and 23. These methods so far have been applied only to rigid body pitching and plunging, but both are capable of extension at least for straight wings; moreover, the method of Reference 23, which is based on Reissner's work (References 20 and 21), probably could be extended to swept wings, following the procedure applied to the calculation of swept wing forces therein.

No work on downwash due to elastic motion of a wing appears to have been published. Fortunately, it probably is satisfactory to neglect downwash arising from such sources as wing bending and torsion, since these motions

tend to produce appreciable downwash only over the outer portions of the wing span, where it can produce little effect at the tail (assuming a conventional, not a canard, configuration).

5.3 Summary of Results in the Theory of Oscillating Airfoils in Two-Dimensional Flow.

In the present section, existing results of the unsteady airfoil theory will be summarized as a complement to Section 5.2. However, the scope of the present section will not be limited to the first order theory.

The basic problem is an oscillating thin airfoil in a two-dimensional incompressible flow. The mean motion of the airfoil is a rectilinear translation of uniform speed U with respect to the fluid at infinity. To this mean motion a simple-harmonic oscillation of infinitesimal amplitude is superposed. Within the framework of a linearized theory, solutions may be superposed to generate new solutions. It suffices to consider an airfoil of zero thickness and zero camber at zero mean angle of attack.

5.3.1 Oscillating Airfoils in Two-Dimensional Incompressible Flow.

5.3.1.1 Theodorsen's Function. To see the way the important function $C(k)$ enters into the results of the oscillating wing theory, consider the vertical-translation oscillation. Using the complex representation of harmonic oscillations, one may describe the airfoil surface by the real part of the equation

$$\zeta = \zeta_0 b e^{i\omega t} = \zeta_0 b e^{i U k t / b} \quad (5-122)$$

where ζ_0 is a real number representing the ratio of the amplitude of the vertical motion to the semichord length b of the airfoil. (ξ, ζ) are inertial coordinates.* ω is the circular frequency in radians per second. k is the nondimensional reduced frequency defined by the equation

$$k = \frac{\omega b}{U} \quad (5-123)$$

The complex representation of the total lift per unit span is then

$$L = \pi \rho U^2 b k^2 \left[1 - \frac{2i}{k} C(k) \right] \zeta_0 e^{i\omega t} \quad (5-124)$$

The moment per unit span, about the mid-chord point, is (positive in the nose-up sense)

$$M_{\eta_2} = -\pi \rho U^2 b^2 i k C(k) \zeta_0 e^{i\omega t} \quad (5-125)$$

The function $C(k)$ is the so-called Theodorsen's function.

* (ξ, ζ) axes are in the negative directions of x, z axes respectively. See Section 5.2.1.4 and the footnote contained therein.

$$C(k) = F(k) + i G(k) \quad (5-126)$$

$$= \frac{K_1(ik)}{K_1(ik) + K_0(ik)} = \frac{H_1^{(2)}(k)}{H_1^{(2)}(k) + i H_0^{(2)}(k)} \quad (5-127)$$

Eq. (5-126) shows the usual notations $F(k)$ and $G(k)$ for the real and imaginary parts of $C(k)$, respectively, and Eq. (5-127) shows the relationship between $C(k)$ and Bessel functions. K_0 is the modified Bessel function of the second kind or order zero, K_1 is that of order one. $H_0^{(2)}$, $H_1^{(2)}$ are, respectively, Hankel's function of the second kind of order zero and one.

A table of the function $C(k) = F + iG$ is given by Theodorsen and Garrick, (Ref. 127). More extensive numerical tables of $C(k)$ can be found in

- (a) Luke and Dengler, (Ref. 66), J. Aeronaut. Sci., 18, 478-483 (1951).
(This Ref. contains also tables of $C(k)$ for complex valued k .)
- (b) Brower and Lassen, (Ref. 67), J. Aeronaut. Sci., 20, 148-150 (1953).
- (c) Bisplinghoff, et al., (Ref. 116 Appendix V-J).

Approximate expressions for $C(k)$ are:

$$C(k) \doteq 1 - \frac{0.165}{1 - \frac{0.0455}{k}i} - \frac{0.335}{1 - \frac{0.3}{k}i} \quad (5-128)$$

$$C(k) \doteq 1 - \frac{0.165}{1 - \frac{0.041}{k}i} - \frac{0.335}{1 - \frac{0.32}{k}i} \quad (5-129)$$

The expression (5-128) gives somewhat better approximation for $k < 0.5$, whereas (5-129) is better for $k > 0.5$. (See Ref. 58, p. 215 for a detailed comparison.)

5.3.1.2 Rear Aerodynamic Center. If the skeleton airfoil executes a rotational oscillation α with a small amplitude about the mid-chord point, the total lift and moment per unit span about the mid-chord are given by

$$L = \pi \rho U b^2 \dot{\alpha} + 2 \pi \rho U^2 b \left(1 + \frac{ik}{2}\right) C(k) \alpha \quad (5-130)$$

$$M_{\frac{1}{2}} = - \frac{\pi \rho U b^3}{2} \ddot{\alpha} - \frac{\pi \rho b^4}{8} \ddot{\alpha} + \pi \rho U^2 b^2 \left(1 + \frac{ik}{2}\right) C(k) \alpha \quad (5-131)$$

where

$$\alpha = \alpha_0 e^{i\omega t}, \quad \dot{\alpha} = \frac{d\alpha}{dt}, \quad \text{etc.} \quad (5-132)$$

A comparison of the expressions L and $M_{1/2}$ shows that the term $\frac{1}{2}\pi \rho U^2 b^2 \dot{\alpha}$ represents a lift that acts at the $3/4$ -chord point, that the term proportional to $C(k)$ represents a lift that acts at the $1/4$ -chord point, and that the term $\pi \rho b^4 \ddot{\alpha}/8$ is a pure couple.

The lift due to circulation, $2\pi \rho U^2 b (1 + \frac{ik}{2}) C(k) \alpha$, in Eq. (5-130) may be compared with the corresponding term $-2i\pi \rho U^2 b C(k) k \xi_0 e^{i\omega t}$ due to translation (Eq. (5-124) of 5.3.1.1). The "upwash" at the $3/4$ -chord point due to translation is

$$-w_\xi = i U k \xi_0 e^{i\omega t} \quad (5-133)$$

That due to rotation is

$$-w_\alpha = -U \alpha_0 e^{i\omega t} - \frac{1}{2} i U k \alpha_0 e^{i\omega t} \quad (5-134)$$

It is seen that, in both translation and rotation cases, the lift due to circulation can be written as

$$L_c = 2\pi \rho U b C(k) w \quad (5-135)$$

where w stands for either w_ξ or w_α . Thus the upwash at the $3/4$ -chord point has a unique significance. For this reason the $3/4$ -chord point is called the rear aerodynamic center.

5.3.1.3 General Solution. Let the mean position of an airfoil be located from $\xi = -b$ to $\xi = +b$, and let the harmonic oscillation of the points on the airfoil be described by

$$\xi = f(x) e^{i\omega t} \quad (5-136)$$

The "upwash" $-w$ on the airfoil is therefore given by

$$-w = U \frac{\partial \xi}{\partial \xi} + \frac{\partial \xi}{\partial t} = U \left(\frac{\partial \xi}{\partial \xi} + i k \frac{\xi}{b} \right). \quad (5-137)$$

It is convenient to introduce a new variable θ , defined by

$$\xi = b \cos \theta \quad (5-138)$$

so that $\theta = \pi$ at the leading edge, and $\theta = 0$ at the trailing edge. Consider w as a function of θ and t . Let w be expressed by a Fourier series:

$$w(\theta, t) = U e^{i\omega t} \left(P_0 + 2 \sum_{n=1}^{\infty} P_n \cos n\theta \right) \quad (5-139)$$

where

$$U e^{i\omega t} P_0 = \frac{1}{\pi} \int_0^\pi w(\theta, t) d\theta \quad (5-140)$$

$$U e^{i\omega t} P_n = \frac{1}{\pi} \int_0^\pi w(\theta, t) \cos n\theta d\theta \quad (5-141)$$

With the upwash given in this form, the lift distribution can be written as (References 1 and 27).

$$\Delta \dot{p}(\theta, t) = \rho_0 U^2 e^{i\omega t} \left(2 a_0 \tan \frac{\theta}{2} + 4 \sum_{n=1}^{\infty} a_n \frac{\sin n\theta}{n} \right) \quad (5-142)$$

where

$$a_0 = C(k) (P_0 + P_1) - P_1 \quad (5-143)$$

$$a_n = \frac{ik}{2n} P_{n-1} + P_n - \frac{ik}{2n} P_{n+1}, \quad (n \geq 1) \quad (5-144)$$

$C(k)$ being the Theodorsen's function defined in Section 5.3.1.1.

The total lift per unit span is

$$L = 2\pi \rho_0 U^2 b e^{i\omega t} \left[(P_0 + P_1) C(k) + (P_0 - P_2) \frac{ik}{2} \right] \quad (5-145)$$

The nose-up moment about the mid-chord point is

$$M_{\frac{1}{2}} = \pi \rho_0 U^2 b^2 e^{i\omega t} \left\{ P_0 C(k) - P_1 [1 - C(k)] - (P_1 - P_3) \frac{ik}{4} - P_2 \right\} \quad (5-146)$$

These formulas were first given by Küssner and Schwarz. They furnish a convenient method for determining the aerodynamic force acting on an airfoil in harmonic oscillation with arbitrary chordwise deflection (Ref. 27).

5.3.1.4 Flutter Aerodynamic Coefficients. The bulk of oscillating airfoil data exists in the form of aerodynamic coefficients L_α , L_h etc, which are widely used in flutter analysis. They are useful in the dynamics of an airplane when the reduced frequency is not small.

To clarify the definitions, the proper degrees of freedom are first defined. Figure 5-18 shows a two-dimensional airfoil of unit length in the spanwise direction, having four degrees of freedom h , α , β and δ :

h = bending deflection of the elastic axis, positive downward, ft.

α = pitching about the elastic axis, relative to the direction of flow, positive nose up, radians

- β = angular deflection of aileron about aileron hinge line, relative to wing chord, positive for aileron trailing edge down, radians
- δ = angular deflection of tab relative to aileron, positive trailing edge down, radians.

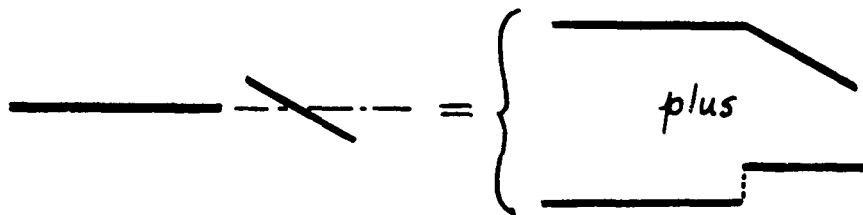


Figure 5-19. Aileron Motions

The standard notations for lengths are shown in the figure. The semichord is denoted by b . Other dimensions are referred nondimensionally to the semichord. Distances are measured with the mid-chord point as origin. Thus,

c_β^b = distance between mid-chord and aileron hinge, positive if aileron hinge is aft of mid-chord,

e_β^b = distance between mid-chord and aileron leading edge, positive if aileron leading edge is aft of mid-chord,

a_h^b = distance between elastic axis and mid-chord, positive if elastic axis is aft of mid-chord.

Similarly, the dimensions d_β^b , f_β^b , x_α^b , etc. can be identified.

For harmonic oscillation, h , α etc. are all represented by complex representation

$$\left. \begin{aligned} \frac{h}{b} &= \frac{h_0}{b} e^{i\omega t} \\ \beta &= \beta_0 e^{i(\omega t + \theta_2)} \\ \alpha &= \alpha_0 e^{i(\omega t + \theta_1)} \\ \delta &= \delta_0 e^{i(\omega t + \theta_3)} \end{aligned} \right\} (5-147)$$

where h_0 , α_0 , β_0 , δ_0 are real numbers (small compared to 1), θ_1 , θ_2 , θ_3 are phase angles by which α , β , δ lead the wing bending displacement, ω is the frequency of oscillation in radians per second.

The standard tables refer the motion and forces to the aerodynamic center. For a subsonic flow the 1/4-chord point aft of the leading edge is used. A notation $(h)_{c/4}$ is introduced to denote the bending displacement at the 1/4-chord point. Furthermore, the aileron motion for an aileron with aerodynamic balance is resolved into two components:

- (a) Rotation of aileron about its leading edge, β .
- (b) Vertical displacement of the aileron with respect to the main airfoil, z , positive downward.

Figure 5-19 shows this resolution. The relations between $(h)_{c/4}$, α , z etc. and h , α , β etc. are:

$$(h)_{c/4} = h - b \left(\frac{1}{2} + a_h \right) \alpha \quad (5-148)$$

$(h)_{c/4}$ = bending displacement of the 1/4-chord point

α = pitching displacement about the 1/4-chord point, also

α = pitching about the elastic axis

β unchanged

$z = -(c_{\beta} - e_{\beta}) b \beta$

δ unchanged if it is hinged at the leading edge, otherwise it should be treated in the same way as the aileron.

These degrees of freedom are denoted by the q notation:

$$\begin{aligned} q_1 &= \frac{(h)_{c/4}}{b} , & q_2 &= \alpha \\ q_3 &= \beta & q_4 &= \frac{z}{b} , & q_5 &= \delta \end{aligned} \quad (5-150)$$

The aerodynamic lift per unit span, $L_{c/4}$, acting at the 1/4-chord point, positive-upward in the usual sense, can be written as

$$L_{c/4} = -\pi \rho b^3 \omega^2 \left[\left(\frac{h}{b} \right)_{c/4} L_h + \alpha L_{\alpha} + \beta L_{\beta} + \frac{z}{b} L_z + \delta L_{\delta} \right] \quad (5-151)$$

or, in shorthand,

$$L_{c/4} = -\pi \rho b^3 \omega^2 \sum_{i=1}^5 q_i L_i \quad (5-152)$$

Similarly, the aerodynamic moment per unit span about the 1/4-chord point, $M_{c/4}$, positive in the nose-up sense, is

$$M_{c/4} = \pi \rho b^4 \omega^2 \sum_{i=1}^5 q_i M_i \quad (5-153)$$

The force per unit span acting on the aileron, $P_{l.e.}$, positive up, is

$$P_{l.e.} = -\pi \rho b^3 \omega^2 \sum_{i=1}^5 q_i P_i \quad (5-154)$$

The moment per unit span about the leading edge of the aileron, $T_{l.e.}$, positive trailing edge down, is:

$$T_{l.e.} = \pi \rho b^4 \omega^2 \sum_{i=1}^5 q_i T_i \quad (5-155)$$

The aerodynamic coefficients L_i, M_i, P_i, T_i are tabulated. A summary of these tables will be given in Section 5.3.1.5.

For the relationship between these aerodynamic coefficients and the conventional stability derivatives, cf. Section 5.6.

5.3.1.5 Tabulation of Results - Two-dimensional Incompressible Flow
Formulas and numerical tables of the aerodynamic coefficients for an airfoil with flap and tab, whose hinge lines do not necessarily coincide with their respective leading edges, have been published by many authors. The most important references are

- (a) Dietze, Luftfahrt-Forsch. Vol 16, 84-96 (1939) (Ref. 75)
Vol 18, 135-141 (1941) (Ref. 76)
- (b) W. P. Jones, Aeronaut. Research Council R and M 1948 (1941) (Ref. 126)
R and M 1958 (1942) (Ref. 72)
- (c) Küssner and Schwarz, Luftfahrt-Forsch. Vol 17, 337-354 (1940).
Translated as NACA TM 991. (Ref. 27)
- (d) Theodorsen and Garrick, NACA TR 496 (1934) (Ref. 2)
NACA TR 736 (1942) (Ref. 127)

The most comprehensive numerical tables are published by Küssner and Schwarz in the references named above. The relations between the special functions tabulated by various authors are listed in a paper by W. P. Jones, (Reference 72).

For flutter calculations, Smilg and Wasserman's tables of L_h , L_α etc. are widely used. These tables are contained in the following references:

- (e) AAF Tech. Rept. 4798, U. S. Air Force (1942) (Ref. 81)
- (f) Introduction to the Study of Aircraft Vibration and Flutter, book by
and Rosenbaum, Macmillan Co., New York (1951) (Ref. 80).
- (g) AF Tech. Rept. 5153, U. S. Air Force (1944) (Ref. 125)

Reference (c) contains tables for both sealed and unsealed gaps between the main wing and the flap and tab. Reference (e) contains only tables for unsealed gaps. Some tables from (e) are omitted in Reference (f). Reference (g) gives more elaborate tab coefficients. Spielberg (Reference 73) gives some values of the coefficients related to a parabolic mode of chordwise deformation.

The notations used by several authors are listed in Table 5-1.

5.3.2 Oscillating Airfoils in Two-Dimensional Subsonic Flow

The basic integral equation relating the lift distribution with the upwash distribution, the so-called Possio's integral equation, is far more complicated than the corresponding equation in the incompressible flow. Practical solutions are obtained by numerical methods. (Possio, Frazer, Frazer and Skan, Schwarz, Schade, Dietz, Fettis.) No simple formulas such as those presented in Sections 5.3.1.1 through 5.3.1.3 have been found except in the first order theory (Cf. Section 5.2.2.2). A different approach, originated by Reissner and Sherman, Biot, Timman, Haskind, Küssner, solves the boundary value problem by orthogonal coordinates and Mathieu functions.

Numerical results have been published by Timman, van de Vooren, and Greidanus.

The principal sources of subsonic data are the papers by Possio, Frazer, Frazer and Skan, Dietze, Schade, Schwarz, Turner and Rabinowitz, Timman, van de Vooren and Greidanus, and Fetti, see Bibliography at the end of this chapter. The numerical results of the first eight authors named above have been compiled and converted into the L_h , M_h , ... coefficients by Luke in the following:

Tables of Coefficients for Compressible Flutter Calculations. (Reference 82) Air Force Tech. Report 6200 (1950) WADC.

A summary of the published tables is given in Table 5-2. In Table 5-3, the notations used in some of the most important references are listed.

In Table 5-2, the symbols L_h , M_h , etc., are defined in Section 5.3.1.4. These coefficients are referred to the 1/4-chord axis for both the rotation α and the moment M_α . In Timman, van de Vooren and Greidanus's paper, the rotation and moment are referred to the mid-chord axis; hence a transformation is needed when comparison of the data is to be made. This is indicated in Table 5-2. Under each column the factors in parentheses are the tabulated quantity expressed in the author's notation. The adjacent coefficients are the factors necessary to convert to the corresponding L_h , L_α , M_h or M_α , which is listed at the left on the same horizontal line. Thus, under Timman and opposite L_h , there is an entry $\frac{1}{2}(k_a)$, which indicates that k_a is given by Timman and that $L_h = (k_a)/k^2$.

5.3.3 Oscillating Airfoils in Two-Dimensional Supersonic Flow.

The linearized supersonic flow theory, applied to the oscillating two-dimensional airfoils, leads to a very simple result (see Section 5.2.3.2). Actual integrations require the evaluation of Schwarz integrals, which are discussed by von Borbely (Reference 89), Schwarz (Reference 128), Garrick and Rubinow (Reference 39), Huckel and Durling (Reference 90). A recent table by Huckel (Reference 91) is very useful.

Comprehensive numerical tables can be found in the following:

(a) Handbook of Supersonic Aerodynamics (Kennedy) (Reference 85)

M : 1.1 (0.1) 2.0 (0.2) 4.0 (0.5) 5.0 (1.0) 12

Ω : 0.01 (0.01) 0.04 (0.02) 0.10 (0.05) 0.40 (0.10)
1.00 (0.20) 3.0 (0.50) 5.0, 7.5, 10, 15, 20 (8 fig.)

The coefficients C_{L_h} , C_{L_α} , C_{M_h} , C_{M_α} listed in this Handbook are, respectively, L_h , L_α , M_h , M_α defined in Section 5.3.1.4. The independent variable in the Handbook is the frequency parameter Ω , which is related to the reduced frequency k and Mach number M by the relation

TABLE 5-1

COMPARISON OF NOTATIONS

| Reference | Duncan Collar Ref. 74 | Theodor- sen Ref. 2 | Küssner Schwarz Ref. 27 | Dietze Ref. 75 76 | Frazer Ref. 77 |
|--|--|---------------------------|-------------------------------|-------------------------|---------------------|
| Chord | c | $2b$ | $2L$ | $L (=t_{FL})$ | c |
| Free stream velocity | W | v | v | v | V |
| Circular frequency | p | $\frac{kv}{b}$ | ν | ω | $\omega (=2\pi f)$ |
| Reduced frequency | $\frac{\lambda}{2}$ | k | $-i\omega$ | ω_r | $\frac{\lambda}{2}$ |
| Translational motion at Ref. point | z | h | $Al e^{i\nu t}$ | δ | z |
| Rotational motion of airfoil | θ | α | $B e^{i\nu t}$ | β | θ |
| Lift vector (Theodorsen function) | $1 - \frac{H}{2} - \frac{i\lambda}{2} G$ | C | $\frac{1+T}{2}$ | $\frac{1+T}{2}$ | $-iC$ |
| Real part of $C(k)$ | $1 - \frac{H}{2}$ | F | $\frac{1+T'}{2}$ | $\frac{1+T'}{2}$ | A |
| Imaginary part of $C(k)$ | $-\frac{\lambda G}{2}$ | G | $\frac{T''}{2}$ | $\frac{T''}{2}$ | $-B$ |
| Lift (+ upward) | $-Z$ | $-P$ | K | $-P$ | $-Z$ |
| Pitching moment (+ nose up) | M | M_α | $-M_o$ | M | M |

TABLE 5-1 (continued)

| | | | | | |
|---------|---------|---------|---------|-----------|--------------|
| Cicala | Lyon | Kassner | Jones | Scanlan | Fung, |
| Ref. 10 | Ref. 78 | Fingado | Ref. 72 | Rosenbaum | Bisplinghoff |
| | | Ref. 79 | | Smilg, | Ref 58, 59 |
| | | | | Wasserman | |
| | | | | Ref 80,81 | |

| $L (=2l)$ or l | $C (=2l)$ | t | c | $2b$ | $c = 2b$ |
|-----------------------|--------------|----------------|-------------------------|----------|----------|
| V | V | v | V | v | U |
| Ω | ν | ν | $\bar{\omega} = 2\pi f$ | ω | ω |
| ω | ω | $\frac{1}{2V}$ | $\frac{\omega}{2}$ | k | k |
| ηL or η | kl | y_h | z | h | h |
| α | θ | ϕ | θ | α | α |
| $1-\lambda$ | $1-\lambda$ | \bar{P} | C | C | C |
| $1-\lambda'$ | $1-\lambda'$ | A | A | F | F |
| $-\lambda''$ | λ'' | $-B$ | $-B$ | G | G |
| P | P | $-$ | $-Z$ | $-L'$ | $+L$ |
| $-M$ | M | $-$ | M | M' | M_y^* |

* y is the point about which the moment is taken.

TABLE 5-2

TABULATED SUBSONIC COEFFICIENTS

| Reference | Luke, Ref. 82 | Timman, et al., Ref. 6, Ref. 86 | Fettis, Ref. 7 |
|-------------------|---|--|--|
| L_h | (L_h) | $\frac{1}{k^2} (k_h)$ | (L_h) |
| L_a | (L_a) | $\frac{1}{k^2} (k_a)$ | (L_a) |
| M_h | (M_h) | $\frac{1}{k^2} (m_h) + \frac{1}{2k^2} (k_h)$ | (M_h) |
| M_a | (M_a) | $\frac{1}{k^2} (m_a) + \frac{1}{2k^2} (k_a)$ | (M_a) |
| Flap coefficients | $(L_\beta), (M_\beta)$ $(T_h), (T_a), (T_\beta)$ $(P_h), (P_a), (P_\beta)$ | $L_\beta = \frac{1}{k^2} (k_c)$ $M_\beta = \frac{1}{k^2} (m_c) + \frac{1}{2k^2} (k_c)$ $T_h = \frac{1}{k^2} (m_h)$ $T_a = \frac{1}{k^2} (m_a)$ $T_\beta = \frac{1}{k^2} (m_c)$ | $(L_\beta), (M_\beta), (L_a), (M_a)$ $(T_h), (T_a), (T_\beta), (T_c)$ $(P_h), (P_a), (P_\beta), (P_c)$ |
| Scope of tables* | For $M = 0.7$, all coefficients, at $e_\beta = 0.16, 0.34, 0.52, 0.70, 1.0$ $k = 0 (0.02) 0.1 (0.1) 0.7$ For $M = 0.5, 0.6$, coeff. $L_h, M_h, L_a, M_a, M_\beta, T_h, T_a, T_\beta$ at $e_\beta = 0.16, 0.70$ Coefficients P_h, P_a, P_β at $e_\beta = 0.70$ | $M = 0.35, 0.5 (0.1) 0.8$ $k = \text{approx. } 0.1 \text{ (irreg.) } 3 \text{ for } L_h, L_a, M_h$ But $k > 1.0$ are omitted for flap coeff. | $M = 0.7$ $k = 0.04 (0.04) 0.52$ $e_\beta = -0.2 (0.1) 0.9$ |
| Remarks | Corrected and extended tables in Ref 86 | | |

* e_β = location of flap leading edge measured from the wing mid-chord point, as a fraction of the wing semichord (+ aft, see Figure 5-18.)

$$\Omega = \frac{2M^2}{M^2 - 1} k$$

(b). Tables of Coefficients for Compressible Flutter Calculations (Luke)*

$$M : \frac{10}{9}, \frac{5}{4}, \frac{10}{7}, \frac{5}{3}, 2, \frac{5}{2}, \frac{10}{3}, 5.$$

$$\frac{1}{k} : \text{approx. } 0.1 \text{ (irreg.) } 100 \text{ (5 dec.)}$$

The scope of these tables is indicated above in the ranges of M and Ω . The notation is as follows: If a table is given for a range of arguments from 0.10 to 0.50 at intervals of 0.05; this is indicated by writing 0.10 (0.05) 0.50. The notation (5 fig.), (6 dec.), etc., implies that most of the figures in the table in question are given to the apparent accuracy of 5 figures or 6 decimals, respectively.

In the supersonic case it suffices to tabulate the four fundamental aerodynamic coefficients named above. The lift and moment coefficients involving the motion of a flap and a tab can be expressed in terms of these four fundamental coefficients. Explicit formulas expressing these relations involving a flap are given in Reference 85. A complete list of formulas including both the flap and the tab is given in Reference 3.

Tables given by Garrick and Rubinow (TR 846, Reference 39) and Huckel and Durling (TN 2055, Reference 90) present aerodynamic loads on an oscillating airfoil-flap combination without aerodynamic balance or gap. Lift and moments are related to the tabulated quantities as follows (in the notation of Ref. 39):

$$L = 4 \rho b^3 \omega^2 \left\{ [L_1 + iL_2] \frac{h}{b} + [L_3 + iL_4] \alpha + [L_5 + iL_6] \beta \right\}$$

$$M_{e.a.} = -4 \rho b^4 \omega^2 \left\{ [M_1 + iM_2] \frac{h}{b} + [M_3 + iM_4] \alpha + [M_5 + iM_6] \beta \right\}$$

$$M_\beta = -4 \rho b^4 \omega^2 \left\{ [N_1 + iN_2] \frac{h}{b} + [N_3 + iN_4] \alpha + [N_5 + iN_6] \beta \right\}$$

$$L_3 = L'_3 - (a_h + 1) L_1$$

$$L_4 = L'_4 - (a_h + 1) L_2$$

$$M_1 = M'_1 - (a_h + 1) L_1$$

$$M_2 = M'_2 - (a_h + 1) L_2$$

* Reference 82.

TABLE 5-3

COMPARISON OF NOTATIONS

| References | Possio Ref 83 | Possio Ref 84 | von Borbély Ref 89 | Küssner Ref. 16 | Schwarz Ref 129 | Dietze Ref 4 |
|---|--------------------------------|------------------|----------------------------|--------------------|--------------------|-----------------|
| Chord | l | l | t | $2l$ | 2 | l |
| Free stream velocity | V_0 | V_i | U_0 | v | v | v |
| Density, undisturbed fluid | ρ | ρ_i | ρ_0 | ρ | ρ | ρ_∞ |
| Circular freq. | Ω | Ω | σ | ν | ν | ω |
| Reduced freq. | ω | ω | $-$ | $\bar{\omega}$ | ω_r | ω_r |
| Frequency parameter ($\frac{2M^2 k}{M^2 - 1}$) | $-$ | $-$ | ω | $-$ | $-$ | $-$ |
| Kernel of Possio's eq. | $\frac{V_f + i V_g}{a \omega}$ | $-$ | $-$ | $-$ | \mathcal{K} | \mathcal{K} |
| Mach no. | λ | λ | Mach angle λ | β | λ | M |
| Downward displacement at Ref. point | $-\eta$ | a | $-\gamma$ | $-$ | $-$ | δ |
| Pitching angle (+ nose up) | α | b | E | $-$ | $-$ | $-$ |
| Lift on wing (+ upward) | P | P | P | $-$ | $-$ | $-$ |
| Pitching moment (+ nose up) | $-M$ | $-M$ | $-M$ | $-$ | $-$ | $-$ |

TABLE 5-3 (continued)

| Temple | Garrick | Karp, et al. | Luke | Turner | Timman | Fettis | Supersonic Handbook | Bispling- hoff | Statler |
|---------------------|----------------|-----------------|----------|--------------|----------|-----------|------------------------|-------------------|----------|
| Ref 88 | Ref 39 | Ref 3 | Ref 82 | Ref 87 | Ref 6 | Ref 7 | Ref 85 | Ref 58 59 | Ref 56 |
| c | $2b$ | $2l$ | $2b$ | l | $2l$ | $2b$ | $2b$ | $2b$ | c |
| V | v | U | v | V | v | v | V | U | U |
| p_o | p | p_o | p | p | p_o | p | p | p | p_o |
| $2\pi f$ | ω | ω | ω | ω | ω | ω | ω | ω | ω |
| $\frac{\lambda}{2}$ | k | ω_r | k | ω_r | ω | ω | k | k | k |
| γ | $\bar{\omega}$ | λ | $-$ | $-$ | $-$ | μ | Ω | Ω | $-$ |
| $-$ | $-$ | K | K | K | $-$ | K | $-$ | K | $-$ |
| M | M | M | M | M | β | λ | M | M | M |
| z_o' | h_o | $-y$ | h | g_s | A | h | h' | h | AL |
| α' | α_o | E | α | g_o | B | α | α | α | B |
| L' | $-P$ | L_o | $-L$ | ΔP_s | $-K$ | $-L$ | $-L$ | L | L |
| M' | M_α | M_o | M | ΔM_o | M | M | M | M_y^* | M |

* y is the point about which the moment is taken. Moment about the mid-chord is written as $M_{1/2}$, etc.

$$M_3 = M_3' - (a_h + 1) [(M_1' + L_3') - (a_h + 1) L_1]$$

$$M_4 = M_4' - (a_h + 1) [(M_2' + L_4') - (a_h + 1) L_2]$$

$$L_5 = \left[\frac{1 - e_\beta}{2} \right]^3 L_3' \left(M, \bar{\omega} \frac{1 - e_\beta}{2} \right), \quad \bar{\omega} = \frac{2 k M^2}{M^2 - 1}$$

$$L_6 = \left[\frac{1 - e_\beta}{2} \right]^3 L_4' \left(M, \bar{\omega} \frac{1 - e_\beta}{2} \right)$$

$L_1, L_2, L_3', L_4',$ etc. are tabulated. $M_{e,a}$ denotes the moment per unit span about the "elastic axis" i.e. the axis of rotation located at $a_h b$ behind the mid-chord point. M_β denotes the moment about the aileron leading edge, which is located at $e_\beta b$ behind the wing mid-chord point (Cf. Figure 5-18).

5.3.4 Oscillating Airfoils in Two-Dimensional Transonic Flow

Whereas the steady-flow airfoil theory is essentially nonlinear in the transonic range, the linearized results for unsteady flow appears to be meaningful if the motion exceeds a certain degree of unsteadiness.

The limiting case of $M \rightarrow 1$ was first studied by Rott, (Reference 92). The various aerodynamic coefficients at $M = 1$ have been computed and tabulated by Nelson and Berman (Reference 93). Their notations are exactly those of Garrick and Rubinow (Reference 39), which are given in Section 5.3.3.

The magnitudes of the (linear) theoretical sonic aerodynamic loads become infinite as the reduced frequency k approaches zero.

The potential flow theory indicates a possible loss of damping in the single-degree-of-freedom modes, particularly in the high subsonic and low supersonic regimes. It must be remembered that the underlying flow usually involves complex shock patterns which are themselves often in motion, and, hence, a great deal of effort is needed to refine and justify the theoretical picture.

5.4 Oscillating Finite Wings

Wings of high aspect ratio are often analyzed by the "strip" theory, i.e., each strip is handled as though part of an infinite wing, having the same normal velocity distribution as that existing at the strip, and all strip effects integrated spanwise in accordance with the mode of vibration chosen. See Sections 5.2.2, 5.2.2.1, 5.2.2.6, and 5.2.3.2 for explicit formulas applicable to the incompressible, subsonic, and supersonic flow according to the strip theory.

Wings of small aspect ratio may be analyzed according to "lifting-line," "lifting-strip", or "lifting-surface" theories, with various degrees of accuracy. There does not exist any comprehensive tabulation of aerodynamic coefficients for finite wings. In the case of the first order (in frequency) theory, analytical solutions are presented in Sections 5.2.2.3; 5.2.2.4; 5.2.2.5; 5.2.2.6; 5.2.3.3; 5.2.3.4; and 5.2.3.5. In the absence of tables, these formulas must be used.

The summary to be presented in the following sections will indicate the numerical information that is available at present.

5.4.1 Oscillating Finite Wing, Incompressible Flow

Among the many theories of oscillating finite wing mentioned in Section 5.2.2.3, Reissner's method is generally preferred because of its simplicity in reasoning and its high degree of systematization. Reissner's method leads to the conclusion that the spanwise induction effect may be expressed in terms of a single function $\sigma(y^*)$ which vanishes when the induction effects are neglected.

The function $\sigma(y^*)$ depends only on the spanwise coordinate and the mode of oscillation of the wing. It has no disturbing influence on the chordwise integration of pressure distribution which yield running lift and moment, being carried through these as an additive correction to $C(k)$. No complete rederivation of two-dimensional formulas like those for $L, M_{e.a.}$ is necessary, all that is necessary is to replace $C(k)$, wherever it appears, by $C(k) + \sigma$ the latter being fixed by the location of station y^* , and by the particular type of motion producing the desired force or moment.

The steps required in Reissner's theory may be summarized as follows:

- (1) The vibration mode is completely specified. The upwash over the wing is written as

$$-\bar{w}_a(\xi, y) e^{i\omega t} = \left[i\omega \bar{\xi}_a(\xi, y) + U \frac{\partial \bar{\xi}_a}{\partial x} \right] e^{i\omega t}$$

where $\bar{\xi}_a(\xi, y, t) = \bar{\xi}_a(\xi, y) e^{i\omega t}$

is the instantaneous vertical coordinate of the vibrating mean surface.

- (2) Determine $\bar{\Omega}^{(2)}(y^*)$:

$$\bar{\Omega}^{(2)}(y^*) = 4 \frac{b}{b_0} e^{ik_m} \frac{\int_{-1}^1 \sqrt{(1+\xi^*)/(1-\xi^*)} \bar{w}_a(\xi^*, y^*) d\xi^*}{\pi i k [H_1^{(2)}(k) + i H_0^{(2)}(k)]}$$

This is the quasi two-dimensional reduced circulation which would be generated by the motion at station y^* in the absence of spanwise induction effects. The notations are: (See Figure 5-6, x, z axes are the negative of ξ, ζ).

$$\xi^* = \frac{2\xi - \xi_2 - \xi_1}{2b}$$

$$y^* = y/b_0$$

$$k_m = \frac{k_0}{2b} (\xi_1 + \xi_2)$$

$$k_0 = \frac{\omega b_0}{U}, \quad b_0 = \text{chord at midspan}$$

$$k = \frac{\omega b}{U}$$

(3) Solve the following equation for $\bar{\Omega}(y^*)$:

$$\bar{\Omega}(y^*) + \mu(k) \frac{b}{b_0} \oint_{-s}^s \frac{d\bar{\Omega}}{d\eta^*} K(k_0(y^* - \eta^*)) d\eta^* = \bar{\Omega}^{(2)}(y^*)$$

where $\mu(k)$ is a function tabulated in Reference 20, TN 1194, and $K(\)$ is related to the Cicala's function tabulated in References 20 and 10 (TN 1194 and TM 887). The details of a method of solving this equation, which is of lifting-line type, are described in Reference 21, (TN 1195).

(4) Compute $\sigma(y^*)$:

$$\sigma(y^*) = \left[\frac{\bar{\Omega}(y^*)}{\bar{\Omega}^{(2)}(y^*)} - 1 \right] \left[C(k) + \frac{i J_1(k)}{J_0(k) - i J_1(k)} \right]$$

(5) The pressure distribution, lift and moments are computed according to the strip theory.

(6) The corrections to the strip theory for the influence of finite span are determined from the $\sigma(y^*)$ and added to the loads determined by the strip theory. Each of these corrections is derived by identifying all terms containing the Theodorsen's function $C(k)$ in the expression for the two-dimensional running load due to the particular type of motion considered, and in these terms replacing $C(k)$ by the value of $\sigma(y^*)$ at the same spanwise station.

The execution of these steps is greatly simplified by using tables prepared by Reissner and Stevens (Reference 21, TN 1195). Reissner's theory agrees well with experiments on rectangular wings for aspect ratios as small as 2.

The corresponding first order in frequency equations are given in Section 5.2.2.3.

For wings of large sweep angle, no three-dimensional theory exists which is not based either on questionable assumptions or on elaborate, poorly systemized computational procedures. Strip theories are often used,

see Section 5.2.2.6; see also Barmby, Cunningham, and Garrick (Reference 94, TR 1014), and Bisplinghoff, Ashley and Halfman (Reference 59, p. 395-400).

Wings of aspect ratio of order 1 are discussed by Lawrence and Gerber (Reference 25), and Laidlaw (Reference 95).

Wings of small aspect ratio (a small fractional value) are discussed by Lomax and Sluder (Reference 96), Voss and Hassig (Reference 97), Merbt and Landahl (Reference 98).

Wing-body combination is discussed by Bryson (Reference 99), and Miles (Reference 52).

A successful empirical correction applicable to low-aspect ratio wing is described by Laidlaw (Reference 100).

5.4.2 Oscillating Finite Wing, Subsonic Flow

The results presented in Sections 5.2.2.5 and 5.2.2.6 give a simple correction of compressibility provided that the parameter $(k M AR)/\sqrt{1-M^2}$ is small compared to 1.

In the general case, a first order solution is given by Statler (Reference 56) under the same assumptions as in Reissner's theory for the incompressible flow. Numerical results are available only in case of an elliptic wing with an elliptic spanwise load distribution.

Statler's first order solution appears in its final form very similar to the corresponding Reissner's solution for $M = 0$. The differential pressure distribution, i.e., the negative lift distribution over the airfoil, is given by the following expression:

$$\frac{2\bar{p}b}{\rho_0 U} = \frac{2e^{iM^2 kX/\beta^2}}{\pi} \left\{ \oint_{-1}^1 \bar{w}(\xi^*, \eta^*) \left[\sqrt{\frac{1-X}{1+X}} \sqrt{\frac{1+\xi^*}{1-\xi^*}} \frac{1}{X-\xi^*} - i \frac{k}{\beta^2} \Lambda_1 \right. \right. \\ \left. \left. + \sqrt{\frac{1-X}{1+X}} \sqrt{\frac{1+\xi^*}{1-\xi^*}} - \sqrt{\frac{1-X}{1+X}} \sqrt{\frac{1+\xi^*}{1-\xi^*}} S\left(\frac{k}{\beta^2}, M, s\right) \right] d\xi^* \right\} \quad (5-156)$$

where

$$S\left(\frac{k}{\beta^2}, M, s\right) = C\left(\frac{k}{\beta^2}, M\right) + \sigma\left(\frac{k}{\beta^2}, M, s\right) \quad (5-157)$$

and

$$\sigma\left(\frac{k}{\beta^2}, M, s\right) = -\frac{2}{\beta R + 2} \left\{ 1 - \frac{\pi \frac{k}{\beta^2} (\beta R + 2)}{4} \right. \\ \left. + \frac{i \frac{k}{\beta^2}}{2(\beta R + 2)} \left[(\beta R + 2)^2 (-M + \ln \frac{\gamma \frac{k}{\beta^2}}{2}) \right. \right. \\ \left. \left. + (\beta R)^2 (-2 - \pi M + \ln 2\pi \beta R) + 2 \right] \right\} \quad (5-158)$$

The definitions of the other terms are:

b = semichord length, ft.

\bar{p} = amplitude of pressure, lbs/ft². $p = \bar{p} e^{i\omega t}$

$\frac{k}{\beta^2}$ = parameter defined by $= \frac{\omega b}{U(1-M^2)}$ (5-159)

$$\beta = \sqrt{1-M^2}$$

X = dimensionless coordinate in free stream direction $= \frac{\xi}{b}$

Y = dimensionless coordinate in spanwise direction $= \beta \frac{y}{b}$

Y^* = parameter defined by $Y = s \beta Y^*$ (5-160)

s = ratio of semispan to semichord at midspan

$$m = \ln \frac{M}{2} - \beta \ln \frac{1-\beta}{M}$$

k = reduced frequency $= \frac{\omega b}{U}$

\bar{W} = downwash function $= \frac{U}{\beta} e^{-iM^2 \frac{k}{\beta^2} X} (ik \bar{H} + \frac{\partial \bar{H}}{\partial X})$ (5-161)

provided that the wing surface is defined by $\bar{S} = \bar{H}(\xi, y) e^{i\omega t}$.

$$\Lambda_1 = \frac{1}{2} \ln \frac{1 - X \xi^* + \sqrt{1 - \xi^{*2}} \sqrt{1 - X^2}}{1 - X \xi^* - \sqrt{1 - \xi^{*2}} \sqrt{1 - X^2}} \quad (5-162)$$

$$C\left(\frac{k}{\beta^2}, M\right) = 1 - \frac{\pi \frac{k}{\beta^2}}{2} + i \frac{k}{\beta^2} \left(\ln \frac{Y \frac{k}{\beta^2}}{2} - m \right), \quad (5-163)$$

(γ = Euler's constant $\doteq 1.781072$)

This equation shows that, as in the incompressible case, the aerodynamic span effect manifests itself as an additive correction, σ , to the basic two-dimensional function C within the limitations of the lifting-strip theory.

To terms of first order in frequency and first order times the logarithm of frequency, the real and imaginary parts of the function S may be written:

$$S = S' + i S'' \quad (5-164)$$

where, with $\beta = \sqrt{1-M^2}$,

$$S' = \frac{\beta R}{\beta R + 2} \quad (5-165)$$

$$\frac{S''}{R/\beta^2} = \frac{2}{(\beta R + 2)^2} \left[(\beta R)^2 \left(1 - \frac{1}{2} \ln 2\pi\beta R + \frac{\pi M}{2} \right) - 1 \right] \quad (5-166)$$

The function S is plotted in Figure 2 of Reference 56.

The function $S(k/\beta^2, M, AR)$ is the three-dimensional analog of the function $C(k/\beta^2, M)$ which is the compressible version of Theodorsen's function $C(k)$. At $M = 0$, $C(k/\beta^2, M)$ represents the first few terms of the series expansion of Theodorsen's function in the neighborhood of the origin.

Although the imaginary part of $C(k/\beta^2, M)$ has a logarithmic singularity in its slope at zero frequency as in the incompressible case, the same is not true for the finite span function S . The singularity cancels out in the finite span case, and S is linear in frequency. Statler relies on this particular property of the S function as a basic justification of the first order theory in application to aircraft dynamics.

Aerodynamic Derivatives

For an airfoil which is undergoing uniform vertical translation and a rotation about its midchord, the instantaneous wing surface may be written, in Statler's notation:

$$\mathcal{S}(x, y, t) = e^{i\omega t} (A b + B x) \quad (5-167)$$

For rotation of a full-span control surface with hinge position φ at its leading edge (see equation 5-167),

$$\begin{aligned} \mathcal{S}(x, y, t) &= 0 \quad \text{for } 0 \leq \theta \leq \varphi \\ \mathcal{S}(x, y, t) &= C b (\cos \varphi - \cos \theta) e^{i\omega t} \quad \text{for } \varphi \leq \theta \leq \pi \end{aligned} \quad (5-168)$$

The total lift force and the total moments about the midchord and the hinge line may be written in the form: (S = wing area)

$$L = -\pi \rho_0 U^2 S e^{i\omega t} \left[i k A (L'_A + i L''_A) + B (L'_B + i L''_B) + C (L'_C + i L''_C) \right] \quad (5-169)$$

$$M = \pi \rho U^2 S b e^{i\omega t} [i k A (M'_A + i M''_A) + B (M'_B + i M''_B) + C (M'_C + i M''_C)] \quad (5-170)$$

$$N = \pi \rho U^2 S b e^{i\omega t} [i k A (N'_A + i N''_A) + B (N'_B + i N''_B) + C (N'_C + i N''_C)] \quad (5-171)$$

Analytical expressions for L'_A , L''_A , M'_C etc. are given in Reference 56. Plots of these derivatives versus aspect ratio are given in Reference 56 for Mach numbers 0, 0.5, 0.7 and 0.8. The hinge moments derivatives are given in Reference 56 for the above Mach numbers and for hinge positions of $\phi = 0.50\pi$, 0.667π , 0.75π , 0.90π , i.e., for hinge positions of 50%, 85.5%, 97.5% chord.

5.4.3 Oscillating Finite Wing, Supersonic Flow.

Sections 5.2.3 - 5.2.3.6 give complete information on the first order supersonic oscillating finite wing theory.

Strip theory is much more accurate and widely applicable in supersonic flow than the subsonic case. Walsh, Voss, Zartarin (Reference 43) studied the generalized forces used in the modal approach of aeroelastic analysis, and showed that for wing with all supersonic leading edges and a straight trailing edge, the strip theory is exact for computing any generalized force acting on a deformation mode which is arbitrary chordwise but contains no higher than the first power of the spanwise variable y . See also, Reference 41 and equations (5-70a) and (5-70b) of Section 5.2.3.3.

Table 5-4 gives a summary of existing literature on finite wing data in supersonic flow.

5.5 Indicial Response of an Airfoil to Step Function Input



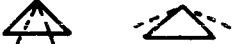
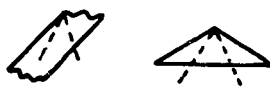
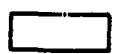

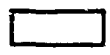


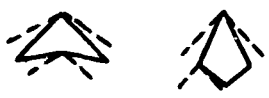
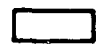
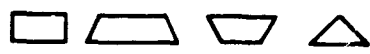


Indicial responses, such as the transient lift due to a sudden sinking motion of the airfoil, or a sudden change of angle of attack, a sharp-edged gust, etc., are important in problems of gust response, maneuver, etc.

Information on the indicial responses of airfoils in a two-dimensional flow is quite complete. Finite aspect ratio corrections in an incompressible flow are known. These are presented below. Finite aspect ratio corrections for indicial responses at finite Mach numbers have not yet been sufficiently studied, and cannot be presented. In Section 5.5.8, the wing responses to a sinusoidal gust are given, which are useful in computing the transfer function for the gust response problem, and also in the generalized harmonic analysis of airplane motion in turbulent air.

5.5.1 Aerodynamic Forces Acting on a Thin Airfoil in Unsteady Motion-- Two-Dimensional Incompressible Flow

The unsteady aerodynamic force acting on a thin airfoil in unsteady motion in a two-dimensional incompressible fluid was obtained by Wagner, Küssner, von Kármán and Sears, and others. In a general motion the pressure distribution over an airfoil is caused partly by the circulation about the

TABLE 5-4
SOURCES OF DATA ON WINGS IN SUPERSONIC FLOW
(Dotted lines - Mach lines)

| Wing Shape | Motion or Derivative | Reference |
|---|---|--|
|  | Plunging, pitching | Nelson, NACA TN 2494 (1951) (Ref. 130) |
|  | | Miles, NAVORD 1234 (1950) (Ref. 131) |
|  | Pitch, roll | Brown, Adams NACA TN 1566 (Ref. 109) |
|  | Longitudinal and lateral | Froehlich, J. Aero. Sc. <u>18</u> , 5(1951) (Ref. 132) |
|  | Plunging, pitching, rolling | Stewart, Li. Quart. Appl. Math, <u>9</u> (1951) (Ref. 133) Li, J. Aero Sc. <u>18</u> , 3(1951) (Ref. 134) |
|  | General, pressure distribution given. | Chang, NACA TN 2467 (1951) (Ref. 135) |
|  | Pitching, plunging | Watkins, NACA Rept. 1028 (Ref. 136) |
|  | Pitching, plunging deforming to quartic law | Watkins, Berman, NACA Rept. 1099 (Ref. 137) Watkins, Berman, NACA TN 3009 (Ref. 138) |
|  | Pitching, plunging | Moskowitz, Moeckel, NACA TN 2034 (Ref. 112) |
|  | Long and lateral | Malvestuto, Margolis, NACA TN 1761 (Ref. 111) |
|  | Long and lateral | Harmon, NACA TN 1706 (Ref. 110) |
|  | Lateral derivatives | Jones, Alksne (Ref. 108) NACA Rept. 1052 |
|  | | |
|  | | |

airfoil, and partly due to non-circulatory origin.

Consider first the growth of circulation about the airfoil which starts impulsively from rest to a uniform velocity U . Let the chord of the airfoil be $2b$, and the angle of attack (assumed small) be α . Let the impulsive motion take place at the origin when $\tau = 0$. (Figure 5-20). The vertical velocity component (downwash) of the fluid is a step-function of time and distributed uniformly across the chord:

$$w = U \sin \alpha \doteq U \alpha \quad (5-172)$$

Then, according to the Kutta condition that the velocity at the trailing edge must be finite, one derives the lift due to circulation on a strip of unit span as a function of time:

$$L_1 = 2\pi b \rho_0 U w \Phi(\tau) \quad (5-173)$$

where

$$\tau = \frac{U t}{b} \quad (5-174)$$

is a non-dimensional quantity proportional to time. The function $\Phi(\tau)$ is called Wagner's function (Section 5.5.2), (Figure 5-21).

Let an airfoil have two degrees of freedom: a vertical translation h , called bending, positive downward, and a rotation α , called pitching, positive nose up, about an axis located at a distance $a_h b$ from the mid-chord point, a_h being positive toward the trailing edge (see Figure 5-18). h and α are assumed to be first order small quantities. As shown in Section 5.3.1.2, in bending and pitching motion the downwash at the rear aerodynamic center (3/4-chord point) is of unique significance. The same holds for arbitrary motion. If one replaces w in equation (5-178) by the increment of downwash at the 3/4-chord point, the circulatory lift can be obtained.

Let a prime denote a differentiation with respect to the nondimensional time τ : $h' = dh/dt$ etc. Then the downwash at the 3/4-chord point due to h and α degrees of freedom is

$$w(\tau) = U \alpha(\tau) + \frac{U}{b} h'(\tau) + \left(\frac{1}{2} - a_h\right) U \alpha'(\tau) \quad (5-175)$$

By the principle of superposition, the circulatory lift is given by the Duhamel's integral (see, for example, Refs. 58 and 59):

$$L_1(\tau) = 2\pi b \rho_0 U \left[w_0 \Phi(\tau) + \int_0^\tau \Phi(\tau - \tau_0) \frac{dw(\tau_0)}{d\tau_0} d\tau_0 \right] \quad (5-176)$$

where

$$w_0 = \lim_{\tau \rightarrow 0^+} w(\tau)$$

In the above equation the motion is assumed to have started at time $\tau = 0$. By substitution of (5-180) into (5-181),

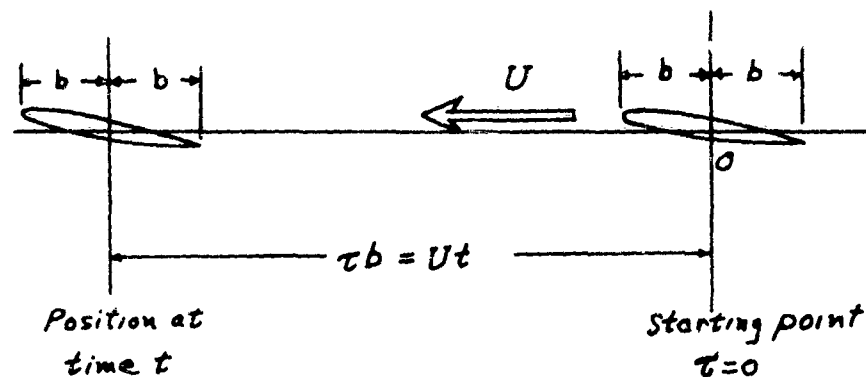


Figure 5-20. Impulsive Motion Of Airfoil

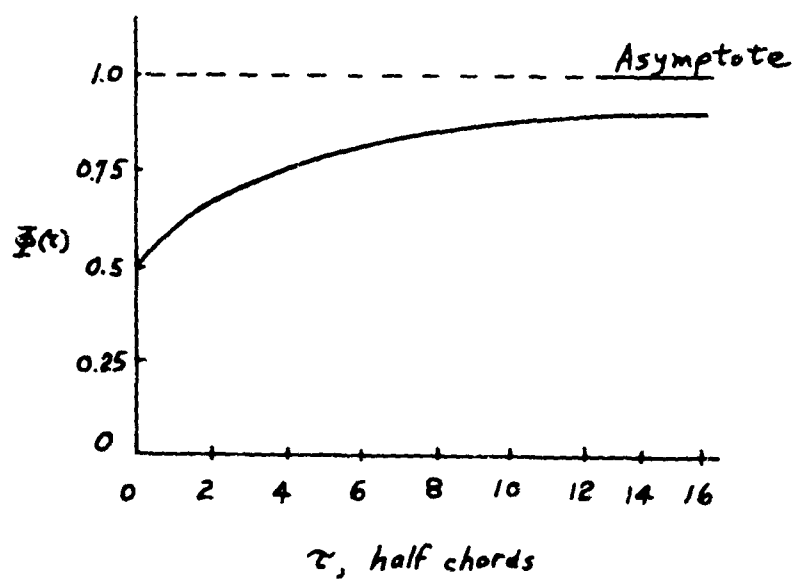


Figure 5-21. Wagner's Function

$$L_1(\tau) = 2\pi b \rho U^2 \left[\frac{w_0}{U} \Phi(\tau) + \int_0^\tau \Phi(\tau - \tau_0) \left[\alpha'(\tau_0) + \frac{1}{b} h''(\tau_0) + \left(\frac{1}{2} - a_h \right) \alpha''(\tau_0) \right] d\tau_0 \right] \quad (5-177)$$

The noncirculatory pressure distribution contributes the following terms:

(a) A lift force with center of pressure at the mid-chord, of amount equal to the apparent mass $\rho \pi b^2$ times the vertical acceleration at the mid-chord point:

$$L_2 = \rho \pi b^2 \left(\frac{d^2 h}{dt^2} - a_h b \frac{d^2 \alpha}{dt^2} \right) = \rho \pi U^2 (h'' - a_h b \alpha'') \quad (5-178)$$

(b) A lift force with center of pressure at the 3/4-chord point, of the nature of a centrifugal force, of amount equal to the apparent mass $\rho \pi b^2$ times $U \frac{d\alpha}{dt}$:

$$L_3 = \rho \pi b^2 U \frac{d\alpha}{dt} = \rho \pi b U^2 \alpha' \quad (5-179)$$

(c) A nose-down couple equal to the apparent moment of inertia $\rho \pi b^2 \left(\frac{b^2}{8} \right)$ times the angular acceleration $d^2 \alpha / dt^2$:

$$M_a = - \frac{\rho \pi b^4}{8} \frac{d^2 \alpha}{dt^2} = - \frac{\rho \pi b^2 U^2}{8} \alpha'' \quad (5-180)$$

The total lift per unit span is then

$$L = L_1 + L_2 + L_3 \quad (5-181)$$

The total moment per unit span about the axis of rotation is, (since L_1 acts at 1/4-chord point):

$$M = \left(\frac{1}{2} + a_h \right) b L_1 + a_h b L_2 - \left(\frac{1}{2} - a_h \right) b L_3 + M_a \quad (5-182)$$

For indicial motion, L_2 and M_a become delta-functions.

5.5.2 Wagner's Function, $\Phi(\tau)$

The exact expression of the Wagner's function $\Phi(\tau)$ (Cf. equation (5-178) Section 5.5.1) is

$$\Phi(\tau) = 1 - \int_0^\infty \left\{ (K_0 - K_1)^2 + \pi^2 (I_0 + I_1)^2 \right\}^{-1/2} e^{-x\tau} x^{-2} dx \quad (5-183)$$

where $K_0, K_1; I_0, I_1$ are modified Bessel functions of the second and first kind, respectively, with argument x implied. An approximate expression which agrees within 2 per cent of the exact value in the entire range $0 < \tau < \infty$ is given by Garrick (Ref. 119):

$$\Phi(\tau) \doteq 1 - \frac{2}{4 + \tau} \quad (\tau > 0) \quad (5-184)$$

Another expression is given by R. T. Jones (Ref. 15):

$$\Phi(\tau) = 1 - 0.165 e^{-0.0455 \tau} - 0.335 e^{-0.300 \tau} \quad (5-185)$$

whereas W. P. Jones gives (Ref. 120):

$$\Phi(\tau) = 1 - 0.165 e^{-0.041 \tau} - 0.335 e^{-0.32 \tau} \quad (5-186)$$

The expression (5-191) gives slightly better approximation than (5-190) for $\tau < 2.2$.

Figure 5-21 shows the Wagner's function. It is seen that half of the final circulatory lift is assumed at once and that the lift approaches asymptotically its steady-state value when $\tau \rightarrow \infty$. The center of pressure of this lift due to circulation is at the $1/4$ -chord point behind the leading edge.

5.5.3 Finite Aspect Ratio Effect, Incompressible Flow

R. T. Jones (Reference 15) gives approximate expressions of $\Phi(\tau)$ at $M = 0$ for finite elliptic wings; τ being based on the half-midspan-chord:

| AR | $\Phi(\tau)$ | $\frac{d C_L}{d \alpha}$ |
|----------|--|--------------------------|
| 3 | $1 - 0.283 e^{-0.540 \tau}$ | 1.2π |
| 6 | $1 - 0.361 e^{-0.381 \tau}$ | 1.5π |
| ∞ | $1 - 0.165 e^{-0.0455 \tau} - 0.335 e^{-0.300 \tau}$ | 2π |

5.5.4 Küssner's Function $\Psi(\tau)$, Incompressible Flow. The lift induced by a gust can be expressed by a fundamental function $\Psi(\tau)$ which represents the ratio of the transient lift to the steady-state lift on an airfoil penetrating a sharp-edged gust normal to the flight path. Let the speed of the sharp-edged gust be w , then by definition the transient lift coefficient is

$$C_L(\tau) = \frac{w}{U} \Psi(\tau) \frac{dC_L}{d\alpha} \quad (5-187)$$

where $dC_L/d\alpha$ is the steady-state lift-curve slope, and τ is the dimensionless time parameter

$$\tau = \frac{2U}{c} t = \frac{U t}{b} \quad (5-188)$$

τ represents the distance traveled by the airfoil, measured in semichords.

The following table gives the Küssner's function for incompressible fluid, as given by von Karman and Sears, and R. T. Jones (Ref. 15):

| AR | $\Psi(\tau)$ | $\frac{dC_L}{d\alpha}$ |
|----------|--|------------------------|
| 3 | $1 - 0.679e^{-0.558\tau} - 0.227e^{-3.20\tau}$ | 1.2π |
| 6 | $1 - 0.448e^{-0.290\tau} - 0.272e^{-0.725\tau} - 0.193e^{-3.00\tau}$ | 1.5π |
| ∞ | $1 - 0.500e^{-0.130\tau} - 0.500e^{-\tau}$ | 2π |

In the above table it is assumed that the leading edge of the airfoil encounters the sharp-edged gust at the instant $\tau = 0$. The finite aspect ratio data refers to elliptical wings. The mid-span semi-chord length being the characteristic length in the definition of τ for finite wings.

Bisplinghoff, Ashley and Halfman (Reference 59) give the following approximate expression for $AR = \infty$:

$$\Psi(\tau) \doteq \frac{\tau^2 + \tau}{\tau^2 + 2.82\tau + 0.80} \quad (5-189)$$

The lift induced by a variable gust can be written as a Duhamel integral. Since $\Psi(0) = 0$, one obtains the following expression if the gust is first encountered at $\tau = 0$:

$$L(\tau) = \frac{1}{2} \rho U^2 S \frac{dC_L}{d\alpha} \int_0^\tau \frac{w(\tau_0)}{U} \frac{d\Psi}{d\tau} (\tau - \tau_0) d\tau_0 \quad (5-190)$$

where S is the wing area, and the strip theory is used. $w(\tau_0)$ is the gust speed at a point at a distance equal to τ_0 semi-chord lengths from initial point of penetration.

The resultant of the gust-induced lift, when $M = 0$, acts at the 1/4-chord point.

5.5.5 Indicical Response in Two-Dimensional Subsonic Flow. Linearized theory for the indicial admittance of a two-dimensional airfoil entering a sharp-edged gust, or making a sudden pitch or a sudden sinking, has been worked out by Lomax, Mazelsky, and others.

Existing tables cover only the case of vertical translation and pitching of a wing whose chordwise sections do not deform.

In a compressible flow the noncirculatory flow patterns do not adjust themselves immediately to changing boundary conditions. The concept of virtual mass becomes meaningless. The 3/4-chord point also loses its significance as the rear aerodynamic center. Hence two indicial-admittance functions, one for vertical translation and another for pitching velocity, replace the single Wagner function. Moreover, the center of pressure does not

remain at a fixed point. Hence both lift and moment expressions must be given.

For an indicial sinking velocity \dot{h} , starting at $t = 0$, let the lift and pitching moment about the axis of rotation at the leading edge be:

$$L'_T(\tau) = 2\pi \frac{\rho_0}{2} U^2 S \frac{\dot{h}}{U} \phi_c(\tau) \quad (5-191)$$

$$M'_T(\tau) = 2\pi \frac{\rho_0}{2} U^2 S (2b) \frac{\dot{h}}{U} \phi_{cM}(\tau) \quad (5-192)$$

where

$$\tau = \frac{U t}{b}$$

For an indicial angular velocity q_0 about the leading-edge axis, let

$$L'_q(\tau) = 4\pi \frac{\rho_0}{2} U^2 S \left(\frac{q_0 b}{U} \right) \phi_{c_f}(\tau) \quad (5-193)$$

$$M'_q(\tau) = 4\pi \frac{\rho_0}{2} U^2 S (2b) \left(\frac{q_0 b}{U} \right) \phi_{cM_f}(\tau) \quad (5-194)$$

The lift and moment for an arbitrary small motion starting at $t = 0$ are:

$$\begin{aligned} L'(\tau) = 2\pi \frac{\rho_0}{2} U^2 S \left\{ \left[\alpha(0) + \frac{\dot{h}(0)}{U} \right] \phi_c(\tau) \right. \\ \left. + \int_0^\tau \frac{d}{d\sigma} \left[\alpha(\sigma) + \frac{\dot{h}(\sigma)}{U} \right] \phi_c(\tau - \sigma) d\sigma \right\} \\ + 4\pi \frac{\rho_0}{2} U^2 S \left\{ \frac{b}{U} \dot{\alpha}(0) \phi_{c_f}(\tau) + \int_0^\tau \frac{b}{U} \frac{d\dot{\alpha}(\sigma)}{d\sigma} \phi_{c_f}(\tau - \sigma) d\sigma \right\} \end{aligned} \quad (5-195)$$

$$\begin{aligned} M'(\tau) = 2\pi \frac{\rho_0}{2} U^2 S (2b) \left\{ \left[\alpha(0) + \frac{\dot{h}(0)}{U} \right] \phi_{cM}(\tau) \right. \\ \left. + \int_0^\tau \frac{d}{d\sigma} \left[\alpha(\sigma) + \frac{\dot{h}(\sigma)}{U} \right] \phi_{cM}(\tau - \sigma) d\sigma \right\} \\ + 4\pi \frac{\rho_0}{2} U^2 S (2b) \left\{ \frac{b}{U} \dot{\alpha}(0) \phi_{cM_f}(\tau) + \int_0^\tau \frac{b}{U} \frac{d\dot{\alpha}(\sigma)}{d\sigma} \phi_{cM_f}(\tau - \sigma) d\sigma \right\} \end{aligned} \quad (5-196)$$

The primes on L' and M' indicate that they were calculated for a pitching axis through the leading edge.

Lomax et al. (Reference 101, TR 1077) suggest a supersonic analogy by which the functions are simply expressed when τ lies between 0 and $2M/(M+1)$.

The limiting values are:

$$\left. \begin{aligned} \phi_c(0) &= \frac{2}{\pi M} & \phi_c(\infty) &= \frac{1}{\sqrt{1-M^2}} \\ \phi_{c_M}(0) &= -\frac{1}{\pi M} & \phi_{c_M}(\infty) &= \frac{-1}{4\sqrt{1-M^2}} \\ \phi_{c_q}(0) &= \frac{1}{\pi M} & \phi_{c_q}(\infty) &= \frac{3}{4\sqrt{1-M^2}} \\ \phi_{c_{Mq}}(0) &= -\frac{2}{3\pi M} & \phi_{c_{Mq}}(\infty) &= \frac{-1}{4\sqrt{1-M^2}} \end{aligned} \right\} (5-197)$$

For smaller values of τ ; $0 \leq \tau \leq \frac{2M}{1+M}$,

$$\left. \begin{aligned} \phi_c(\tau) &= \frac{2}{\pi M} \left[1 - \frac{\tau}{2M} (1-M) \right] \\ \phi_{c_M}(\tau) &= -\frac{1}{\pi M} \left[1 - \frac{\tau}{2M} (1-M) + \frac{\tau^2}{8M} (M-2) \right] \\ \phi_{c_q}(\tau) &= \frac{1}{\pi M} \left[1 - \frac{\tau}{2M} (1-M) + \frac{\tau^2}{4M} \left(1 - \frac{M}{2} \right) \right] \\ \phi_{c_{Mq}}(\tau) &= -\frac{2}{3\pi M} \left\{ 1 - \frac{3\tau}{4M} (1-M) + \frac{3\tau^2}{32M^2} (1-M)^2 \right. \\ &\quad \left. + \frac{\tau^3}{16M^3} \left[M + \frac{1}{4}(1-M)^3 \right] \right\} \end{aligned} \right\} (5-198)$$

For larger values of τ , Mazelsky et al. have obtained the ϕ 's by a Fourier integral transformation from the harmonic oscillation data. References 102 and 103 present data for $M = 0.7$; Reference 104 presents data for $M = 0.5$, 0.6. Mazelsky and Drischler give the following approximate exponential representations which are convenient in solving the gust response or dynamics problem by Laplace transformation method:

$$\phi(\tau) = b_0 + b_1 e^{-\beta_1 \tau} + b_2 e^{-\beta_2 \tau} + b_3 e^{-\beta_3 \tau} \quad (5-199)$$

Table 5-5 lists the various constants associated with the functions for plunging motion. $(\phi_{c_M})_{C/4}$ refers to the moment taken about the quarter-chord axis.

TABLE 5-5
 COEFFICIENTS IN EXPRESSION $b_0 + b_1 e^{-\beta_1 \tau} + b_2 e^{-\beta_2 \tau} + b_3 e^{-\beta_3 \tau}$ FOR APPROXIMATING THE INDICIAL LIFT AND MOMENT FUNCTIONS FOR SUDDEN MOTION AND FOR SHARP-EDGED GUST ENTRY AT $M = 0.5, 0.6, \text{ AND } 0.7$

| Indicial function | Mach number | b_0 | b_1 | b_2 | b_3 | β_1 | β_2 | β_3 |
|-----------------------|-------------|--------|---------|--------|---------|-----------|-----------|-----------|
| $\phi_c(\tau)$ | 0 | 1 | -0.165 | -0.335 | 0 | 0.0455 | 0.300 | |
| | 0.5 | 1.155 | -0.406 | -0.249 | 0.773 | 0.0754 | 0.372 | 1.890 |
| | .6 | 1.250 | -.452 | -.630 | .893 | .0646 | .481 | .958 |
| | .7 | 1.400 | -.5096 | -.567 | -.5866 | .0536 | .357 | .902 |
| $(\phi_{CM})_{c/4}$ | 0 | 0 | 0 | 0 | 0 | - | - | - |
| | .5 | 0 | .0557 | -1.000 | .6263 | 2.555 | 3.308 | 6.09 |
| | .6 | 0 | -.100 | -1.502 | 1.336 | 1.035 | 4.040 | 5.022 |
| | .7 | 0 | -.2425 | .084 | -.069 | .974 | .668 | .438 |
| $(\phi_{Cq})_{3c/4}$ | .5 | 0 | 0 | -2.68 | 2.362 | ----- | 4.08 | 4.90 |
| | .6 | 0 | 0 | 0 | -.2653 | ----- | ----- | 1.345 |
| | .7 | 0 | -.083 | -.293 | .149 | .800 | 1.565 | 2.44 |
| $(\phi_{CMq})_{3c/4}$ | .5 | -.0721 | -.248 | .522 | -.2879 | 1.562 | 2.348 | 6.605 |
| | .6 | -.0781 | -.077 | .380 | -.2469 | .551 | 2.117 | 4.138 |
| | .7 | -.0875 | -.00998 | .1079 | -.02920 | .1865 | 1.141 | 4.04 |
| $\psi_c(\tau)$ | 0 | 1 | -0.500 | -0.500 | 0 | 0.130 | 1.000 | - |
| | .5 | 1.155 | -.450 | -.470 | -.235 | .0716 | .374 | 2.165 |
| | .6 | 1.250 | -.410 | -.538 | -.302 | .0545 | .257 | 1.461 |
| | .7 | 1.400 | -.563 | -.645 | -.192 | .0542 | .3125 | 1.474 |

(From NACA TN 2739)

This is done to demonstrate the rapidity of approach to its final value of zero. Note that

$$(\phi_{CM})_{c/4} = \phi_{CM}(\tau) + \frac{1}{4} \phi_c(\tau) \quad (5-200)$$

Table 5-5 also lists the various constants associated with the pitching motion, for an airfoil rotating about the 3/4-chord point, with the moment taken about the 1/4-chord point.

$$(\phi_{CMq})_{c/4} = \phi_{CMq}(\tau) + \frac{1}{4} \phi_{cq}(\tau) \quad (5-201)$$

The corresponding Küssner's functions for entry into sharp-edged gust are defined by the following equations for two-dimensional lift and moment per unit span:

$$L(\tau) = 2\pi \rho_0 U b w_0 \psi_c(\tau)$$

$$M(\tau) = 2\pi \rho_0 U (2b^2) w_0 \psi_{CM}(\tau) \quad (5-202)$$

where w_0 is the vertical velocity in the uniform gust region, which meets the leading edge at $\tau = 0$.

Only the lift function $\psi_c(\tau)$ has been tabulated in the subsonic case.

For $0 \leq \tau \leq 2M/(1+M)$,

$$\begin{aligned} \psi_c(\tau) &= \frac{\tau}{\pi \sqrt{M}} \\ \psi_{CM}(\tau) &= -\frac{\tau^2}{8\pi \sqrt{M}} \left[\frac{M+1}{M} \right] \end{aligned} \quad (5-203)$$

where the moment acts about an axis through the leading edge.

Table 5-5 lists the various constants in the exponential approximations to $\psi_c(\tau)$ for various Mach numbers. The literal formula to which they refer to is equation (5-199).

5.5.6 Indicial Response in Two-Dimensional Supersonic Flow

The definitions of $\phi_c(\tau)$, $\phi_{CM}(\tau)$, $\phi_{cq}(\tau)$ and $\phi_{CMq}(\tau)$ are retained as in equations (5-191)-(5-194). The limiting values are

$$\begin{aligned} \phi_c(0) &= \frac{2}{\pi M} & \phi_c(\infty) &= \frac{2}{\pi \sqrt{M^2-1}} \\ \phi_{CM}(0) &= -\frac{1}{\pi M} & \phi_{CM}(\infty) &= \frac{-1}{\pi \sqrt{M^2-1}} \end{aligned}$$

$$\phi_{cq}(0) = \frac{1}{\pi M}$$

$$\phi_{cq}(\infty) = \frac{1}{\pi \sqrt{M^2 - 1}}$$

$$\phi_{cMq}(0) = -\frac{2}{3\pi M}$$

$$\phi_{cMq}(\infty) = \frac{-2}{3\pi \sqrt{M^2 - 1}}$$

The functions are given by Lomax et al, (Ref. 101), and are listed in Tables 5-6. The reader is reminded that the pitching moments are assumed to act about the leading edge of the airfoil, and are positive in a sense to depress the trailing edge.

The indicial functions $\psi_c(\tau)$ and $\psi_{cM}(\tau)$ for supersonic entry into a sharp-edged gust are obtained by Biot (Reference 105) and Chang (Reference 106). Formulas and curves of the ψ functions can be found on page 374 of Reference 59.

The indicial functions for a trailing-edge flap are calculated in Reference 106 by Chang.

5.5.7 Indicial Response at Mach Number Equal to 1

Heaslet, Lomax, and Spreiter (Reference 107) give the indicial responses at $M = 1$. The asymptotic (steady-state) values are all infinite. The theoretical indicial responses can be used within the range of the number of chord lengths traveled for which they show reasonable agreement with their subsonic and supersonic counterparts. There exists no experimental confirmation at present.

Tables giving the ϕ and ψ functions at $M = 1$ can be found on pages 378-379 of Reference 59.

5.5.8 Sinusoidal Gust

For a two-dimensional sinusoidal gust acting on a two-dimensional airfoil at uniform forward speed U , let the coordinate axes be fixed on the airfoil and the vertical gust be represented by a velocity distribution

$$w(\xi, t) = W e^{i\omega(t - \frac{\xi}{U})}$$

which expresses the fact that a sinusoidal gust pattern, with amplitude W (a constant), moves past the airfoil with the speed of flight U . If the wave length of the gust is λ , the circular frequency ω with which the waves pass any point of the airfoil is

$$\omega = \frac{2\pi U}{\lambda}$$

If the gust velocity $w(\xi, t)$ is considered positive upward, the relative velocity at any point on the airfoil relative to the fluid (measured positive upward) is

$$v(\xi, t) = -W e^{i\omega t} e^{-i(b\omega/U)\cos\theta}$$

TABLE 5-6. INDICIAL FUNCTIONS IN TWO-DIMENSIONAL FLOW AT SUPERSONIC SPEEDS, FOR SUDDEN SINKING MOTION AND SUDDEN PITCHING ABOUT LEADING EDGE.

| Function | Range of τ | Equation for ϕ |
|--------------------|--|---|
| $\phi_c(\tau)$ | $0 \leq \tau \leq \frac{2M}{M+1}$ | $\frac{2}{\pi M}$ |
| | $\frac{2M}{M+1} \leq \tau \leq \frac{2M}{M-1}$ | $\frac{2}{\pi^2} \left\{ \frac{1}{M} \cos^{-1} \left(M - \frac{2M}{\tau} \right) + \frac{\cos^{-1} \left(\frac{\tau}{2M} + M - \frac{\tau M}{2} \right)}{\sqrt{M^2 - 1}} \right.$ $\left. + \frac{1}{M} \sqrt{\frac{\tau^2}{4M^2} - \left(1 - \frac{\tau}{2} \right)^2} \right\}$ |
| | $\tau \geq \frac{2M}{M-1}$ | $\frac{2}{\pi \sqrt{M^2 - 1}}$ |
| $\phi_{cM}(\tau)$ | $0 \leq \tau \leq \frac{2M}{M+1}$ | $-\frac{1}{2\pi M} \left(2 - \frac{\tau^2}{4M^2} \right)$ |
| | $\frac{2M}{M+1} \leq \tau \leq \frac{2M}{M-1}$ | $-\frac{1}{\pi^2} \left\{ \frac{1}{M} \left(1 - \frac{\tau^2}{8M^2} \right) \cos^{-1} \left(M - \frac{2M}{\tau} \right) + \frac{1}{\sqrt{M^2 - 1}} \cos^{-1} \left(\frac{\tau}{2M} + M - \frac{\tau M}{2} \right) \right.$ $\left. + \frac{1}{4M} (2 + \tau) \sqrt{\frac{\tau^2}{4M^2} - \left(1 - \frac{\tau}{2} \right)^2} \right\}$ |
| | $\tau \geq \frac{2M}{M-1}$ | $-\frac{1}{\pi \sqrt{M^2 - 1}}$ |
| $\phi_{c9}(\tau)$ | $0 \leq \tau \leq \frac{2M}{M+1}$ | $\frac{1}{\pi M} \left(1 + \frac{\tau^2}{8M^2} \right)$ |
| | $\frac{2M}{M+1} \leq \tau \leq \frac{2M}{M-1}$ | $\frac{1}{\pi^2} \left\{ \frac{1}{M} \left(1 + \frac{\tau^2}{8M^2} \right) \cos^{-1} \left(M - \frac{2M}{\tau} \right) \right.$ $\left. + \frac{1}{\sqrt{M^2 - 1}} \cos^{-1} \left(\frac{\tau}{2M} + M - \frac{\tau M}{2} \right) + \frac{6 - \tau}{4M} \sqrt{\frac{\tau^2}{4M^2} - \left(1 - \frac{\tau}{2} \right)^2} \right\}$ |
| | $\tau \geq \frac{2M}{M-1}$ | $\frac{1}{\pi \sqrt{M^2 - 1}}$ |
| $\phi_{cM9}(\tau)$ | $0 \leq \tau \leq \frac{2M}{M+1}$ | $-\frac{2}{3\pi M} \left(1 + \frac{\tau^3}{16M^3} \right)$ |
| | $\frac{2M}{M+1} \leq \tau \leq \frac{2M}{M-1}$ | $-\frac{2}{3\pi^2} \left\{ \frac{1}{M} \left(1 + \frac{\tau^3}{16M^3} \right) \cos^{-1} \left(M - \frac{2M}{\tau} \right) \right.$ $\left. + \frac{1}{\sqrt{M^2 - 1}} \cos^{-1} \left(\frac{\tau}{2M} + M - \frac{\tau M}{2} \right) + \frac{\left(8 - \frac{\tau}{2} - \frac{\tau^2}{2M^2} - \frac{\tau^2}{4} \right) \sqrt{\frac{\tau^2}{4M^2} - \left(1 - \frac{\tau}{2} \right)^2}}{6M} \right\}$ |
| | $\tau \geq \frac{2M}{M-1}$ | $-\frac{2}{3\pi \sqrt{M^2 - 1}}$ |

where the transformation $\xi = b \cos \theta$ has been made for points on the airfoil. Using the general solution given in Section 5.3.1.3, one obtains the lift and moment per unit span; (M about the midchord point) in an incompressible fluid:

$$L = 2 \pi \rho_0 b U W e^{i \omega t} \phi(k)$$

$$M_{\frac{1}{2}} = L \cdot \frac{b}{2}$$

where $k = \omega b / U$ and

$$\phi(k) = [J_0(k) - i J_1(k)] C(k) + i J_1(k)$$

The resultant lift acts through the 1/4-chord point from the leading edge. The factor $2\pi\rho_0 b U \phi(k)$ represents the frequency response (admittance) of the lift to the gust. The function $\phi(k)$ is plotted as a vector diagram in Figure 5-22. An approximate expression for $|\phi(k)|^2$, useful in the gust response analysis using the transfer function method, is

$$|\phi(k)|^2 \approx \frac{1}{1 + 2\pi k}$$

Sinusoidal Gust Acting on a Wing Moving at Supersonic Speed

The lift and the moment per unit span about an axis of rotation located at $a_n b$ behind the mid-chord point (Cf. Figure 5-18) are, for $M > 1$,

$$L = \frac{4 \rho_0 U b W}{\sqrt{M^2 - 1}} e^{i \omega t} e^{i k} f_0(M, \bar{\omega})$$

$$M_{e.a.} = \frac{2 \rho_0 U b^2 W}{\sqrt{M^2 - 1}} e^{i \omega t} e^{i k} \left[(2 a_n + 1) f_0(M, \bar{\omega}) - f_1(M, \bar{\omega}) \right]$$

where

$$\bar{\omega} = \frac{2 M^2 k}{M^2 - 1}, \quad k = \frac{\omega b}{U}$$

The functions f_0, f_1 , are tabulated in References 39 and 91. The first term in the $M_{e.a.}$ -equation can be thought of as the effect of the lift acting at the 1/4-chord point, $a_n = -1/2$. However, the presence of f_1 shows that the gust produces no fixed center of pressure, independent of frequency, such as occurs in the incompressible case.

5.6 Stability Derivatives

5.6.1 Application of Oscillating Wing Theory to Unsteady Motion

The aerodynamic forces acting on an airfoil in general motion may be

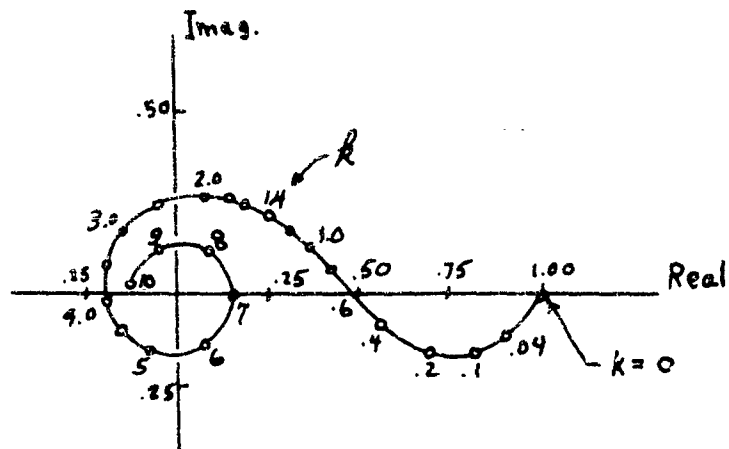


Figure 5-22. Vector diagram showing the real and imaginary parts of Sears' $\phi(k)$ function as function of the reduced frequency k .

written as a Fourier integral if the aerodynamic forces corresponding to simple harmonic oscillations are known. They may also be written as a Duhamel's integral if the forces corresponding to a unit-step motion are known. Simpler results can be obtained, however, if the motion is an exponential function of time: either a nonoscillatory simple exponential divergence or an oscillation with exponentially divergent amplitude.

In the incompressible flow case, Luke and Dengler (Reference 66) proposed that the results obtained by considering simple harmonic motion be applied to damped or divergent oscillations by replacing the reduced frequency in Theodorsen's circulation function $C(k)$ with the appropriate complex argument. The justification of this generalization in the divergent motion case seems evident since a divergent motion implies that the vorticity in the wake decreases exponentially. The generalization in the damped motion case has been discussed by Greidanus and van Heemert (Reference 114), by a physical reasoning based on the damping effect of viscosity on the vorticity in the wake. It was shown that a physical interpretation can be given the generalized $C(k)$ function provided that the damping is small. Dengler, Goland and Luke (Reference 115) also showed that results obtained according to this generalization compare favorably, when the damping is small, with those derived by more rigorous methods. Their result shows that for low damping and small reduced frequencies, the functional dependence of the theodorsen function on the reduced frequency is independent of the amount of damping.

It seems plausible that these arguments should hold also in the compressible flow case. The philosophy of this simplification is generally accepted. Hence in application of the oscillating wing theory, which is derived for a simple harmonic motion with a time factor $e^{i\omega t}$ or $e^{ik\tau}$, one can replace simply in the final result the factor $i\omega$ by λ if the time factor were $e^{\lambda t}$. If the final result can be expanded into a power series in $i\omega$ or λ , then the successive coefficients may be regarded as successive stability derivatives about an equilibrium flight condition. For example, if the lift coefficient due to an oscillating angle of attack is

$$C_L = (a_0 + i\omega a_1 + (i\omega)^2 a_2 + \dots) \alpha \quad (\alpha = \alpha_0 e^{i\omega t}) \quad (5-204)$$

then

$$C_L = (a_0 + \lambda a_1 + \lambda^2 a_2 + \dots) \alpha, \quad (\alpha = \alpha_0 e^{\lambda t}) \quad (5-205)$$

$$C_L = \left(\frac{\partial C_L}{\partial \alpha}\right) \alpha + \left(\frac{\partial C_L}{\partial \dot{\alpha}}\right) \dot{\alpha} + \left(\frac{\partial C_L}{\partial \ddot{\alpha}}\right) \ddot{\alpha} + \dots \quad (5-206)$$

As mentioned before, the Theodorsen's function $C(k)$ cannot be expanded into a power series in k at the origin $k = 0$. Hence the stability derivatives about an equilibrium flight condition cannot be defined from the two-dimensional incompressible flow theory. This difficulty readily disappears when finite aspect ratio is considered. For wings with a finite aspect ratio, power series expansion about the origin ($k = 0$) is legitimate and the stability derivatives are rigorously defined. (See Section 5.4.2)

Data from the two-dimensional incompressible flow theory are useful, of course, when the reduced frequency k , (or the imaginary part of λ) is not zero. Although rigorous derivation of the stability derivative at the steady flight condition is impossible for the two-dimensional case, a plausible procedure has been developed by Goland, Luke, and Sacks (Reference 69, WADC TR 53-425). In this method the real and imaginary parts of $C(k)$ are fitted, in each specific range of frequency, by a linear or quadratic expression. (For example, by the least squares method). The fitted expressions for the aerodynamic coefficients are then truly polynomials from which the stability derivatives are determined. The same procedure has always been used in most British papers on wing flutter, in which the so-called "classical derivative coefficients" are defined for appropriate frequency ranges. (See page 228, Reference 58, and Reference 68).

5.6.2 Transformation of Coordinates

In the literature on the unsteady flow theory, as in practically all of the papers quoted in Sections 5.2 - 5.5, the coordinate system is always chosen parallel and perpendicular to the average motion of the airfoil. Hence, the X-axis is always horizontal and a rigid body wing motion consists of a rotation about a point on this axis through an angle θ and a downward translation of a distance h from this horizontal reference axis. This axis system may be referred to as flutter axes. In dynamic stability analysis, however, it is conventional to use the stability axes or body-fixed axes which are fixed with respect to the airfoil with the origin at the center of gravity and the X' -axis along the initial trimmed flight path. In this system the velocities w and $q = d\theta/dt$, rather than the displacements, are the dependent variables of the motion.

With reference to Figure 5-23, it is seen that the relations among the respective velocities of the two systems are:

$$\dot{h} = w \cos \theta - V \sin \theta$$

$$U = \dot{V} \cos \theta + w \sin \theta$$

V, w are components of velocity along the stability axes; α_0 is the ordinary instantaneous angle of attack equal to w/V .

If θ is small, $w \ll V$, $\dot{h} \ll V$ then

$$\dot{h} \cong w - V \theta$$

$$U \cong V$$

To the same order of approximation, the lift and moments referred to both axes are the same. Hence in order to define the forces and moments in terms of w and θ of the stability axes, it is only necessary to replace h by $w - U\theta$ in the aerodynamic expressions derived in the flutter axes; the pitching angle and flap angle remain unchanged.

5.6.3 Wing Wash Effects in the Vicinity of the Tail

The tail is affected by the oscillating stream due to the wing wake. Cowley and Glauert (1921, R and M 718) first accounted for this unsteady flow condition by approximating the downwash lag by the time required for the flow

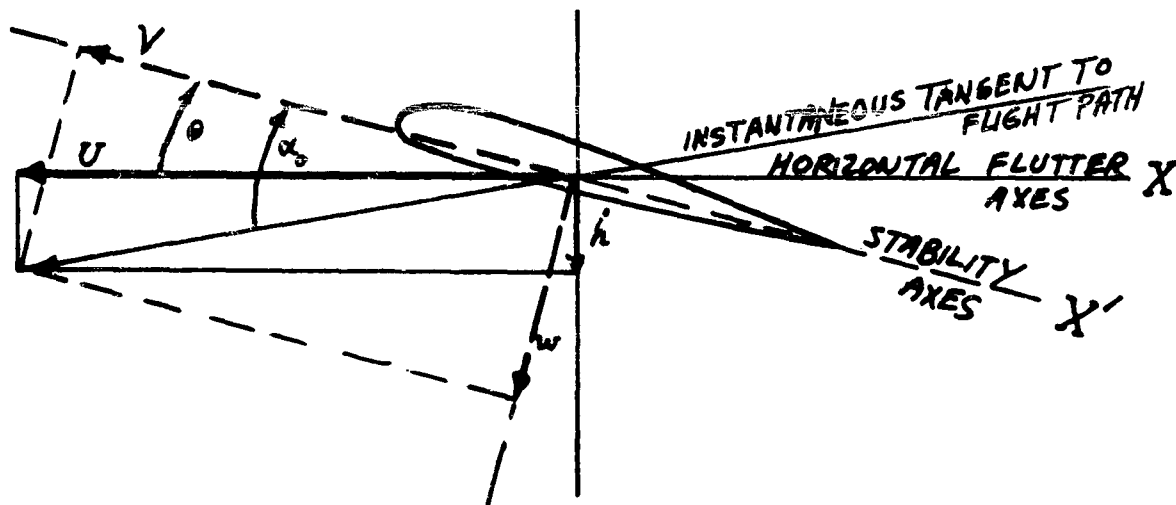


Figure 5-23. Wing Section Showing Velocity Vectors

to travel from the wing to the tail. This leads to the M_w and Z_w derivatives in the quasi-steady theory, \dot{w} being the translational acceleration. These derivatives are modified by the unsteady-flow theory, which accounts for the phase lag of the downwash. The downwash at the vicinity of the horizontal tail due to vertical translation and pitching of the wing in a subsonic compressible flow is tabulated in Reference 56 by Statler. The downwash derivatives w'_A , w''_A etc are defined for the wing motion with a vertical translation of semi-amplitude Ab (b = semichord) and a pitching angle about the mid chord with semi-amplitude B rad. The wing surface is therefore described by the equation

$$z(\xi, y, t) = e^{i\omega t} (Ab + B\xi) \quad (5-207)$$

The downwash velocity at the horizontal tail, $\xi = l_T$, is then given by the following expression:

$$w(l_T, 0, 0) = U e^{i\omega t} \left[ikA(w'_A + iw''_A) + B(w'_B + iw''_B) \right] \quad (5-208)$$

In Reference 56, w'_A , w''_A , w'_B , w''_B are plotted against aspect ratios for Mach numbers of 0, 0.5, 0.7 and 0.8 and for the ratios of (tail length)/(semichord) equal to 4, 6, 8, and 10.

Wing wash effects are strongly influenced by the fuselage interference. The important interference effects probably make the theoretical determination of the wing wash effects on the lateral derivatives rather unreliable.

5.6.4 Stability Derivatives of the Airplane

As an example of putting together the oscillating wing theory and the wing wash effects to form the stability derivatives of an airplane, the subsonic longitudinal derivatives in body coordinates will be quoted.

Let Statler's notation, Section 5.4.2, be used. An unswept airfoil having three degrees of freedom is considered: vertical translation, pitching about the midchord, and flap deflection. The lift, the moment about the midchord, and the hinge moment expressions are given by equations (5-169), (5-170) and (5-171). In transformation to the body axes, it is necessary to replace $i\omega bA$, B , and C in these equations be $w - U\theta$, θ and δ respectively. The wing wash coefficients at the horizontal tail are defined by equations (5-207) and (5-208). If the tail length is sufficiently large, it is reasonable to assume that the rotation of the horizontal tail can be neglected and that rotation of the airplane as a whole about its center of gravity causes a pure translational motion of the tail for small disturbances. Furthermore, the equations quoted above were derived for undamped oscillations so that for damped or divergent oscillations, $\dot{w} = i\omega w$, $\dot{\theta} = i\omega\theta$, $\dot{\delta} = i\omega\delta$, should be substituted. Hence, for an airfoil which is undergoing uniform translation and rotation about the point $\xi = a_h b$, the negative lift force on the wing may be written as

$$\begin{aligned}
\bar{Z}_{wing} &= \pi \rho_0 U^2 S_w [ik(A - \beta a_h) L_A + B L_B]_{wing} \\
&= \pi \rho_0 U^2 S_w [\frac{i \omega b}{U} A L_A + B (L_B - \frac{i \omega b}{U} a_h L_A)]_{wing} \\
&= \pi \rho_0 U^2 S_w [\frac{\bar{w}}{U} L_A + \bar{\theta} (L_B - L_A - \frac{i \omega b a_h}{U} L_A)]_{wing}
\end{aligned}$$

where $L_A = L_A' + i L_A''$ etc. This may be put into the following form for a general motion:

$$Z_{wing} = \frac{1}{2} \rho_0 U^2 S_w \left[\frac{w}{U} Z_{(\frac{w}{U})} + \frac{\dot{w} b}{U^2} Z_{(\frac{\dot{w} b}{U^2})} + \frac{\dot{\theta} b}{U} Z_{(\frac{\dot{\theta} b}{U})} \right]_{wing}$$

Let a subscript $()_w$ refer to wing, then

$$Z_{w(\frac{w}{U})} = 2\pi L_{Aw}'$$

$$Z_{w(\frac{\dot{w} b}{U^2})} = 2\pi \left(\frac{L_A''}{k} \right)_w$$

$$Z_{w(\frac{\dot{\theta} b}{U})} = 2\pi \left[\left(\frac{L_B''}{k} \right)_w - \left(\frac{L_A''}{k} \right)_w - \beta^2 a_h L_{Aw}' \right]$$

Similarly, let $()_T$ denote quantities pertaining to the horizontal tail, the negative lift on the tail is

$$Z_T = \eta_T \pi \rho_0 U^2 S_T \left[\left(\frac{w}{U} + \frac{L_T \dot{\theta}}{U} - \epsilon \right) L_{AT} + \delta L_{CT} \right]$$

where η_T is the horizontal tail efficiency factor, ϵ is the downwash angle:

$$\bar{\epsilon} = \frac{w(L_T, 0, 0)}{U}$$

$$= \frac{i \omega b}{U} A (w_A' + i w_A'') + B (w_B' + i w_B'')$$

$$= \frac{\bar{w}}{U} (w_A' + i w_A'') + \bar{\theta} (w_B' + i w_B'' - w_A' - i w_A'')$$

Substitution of the ϵ expression into Z_T leads to

$$\begin{aligned}
Z_T &= \frac{1}{2} \rho_0 U^2 S_T \left[\frac{w}{U} Z_{T(\frac{w}{U})} + \frac{\dot{w} b}{U^2} Z_{T(\frac{\dot{w} b}{U^2})} + \frac{\dot{\theta} b}{U} Z_{T(\frac{\dot{\theta} b}{U})} \right. \\
&\quad \left. + \delta Z_{T(\delta)} + \frac{\dot{\delta} b}{U} Z_{T(\frac{\dot{\delta} b}{U})} \right]
\end{aligned}$$

where

$$Z_{T(\frac{w}{U})} = 2\pi \frac{S_T}{S_w} L'_{AT} (1 - w'_A) \eta_T$$

$$Z_{T(\frac{\dot{w}b}{U^2})} = 2\pi \frac{S_T}{S_w} \left[\frac{C_T}{C_w} \left(\frac{L''_A}{k} \right)_T (1 - w'_A) - \frac{w''_A}{k} L'_{AT} \right] \eta_T$$

$$Z_{T(\frac{\dot{\theta}b}{U})} = 2\pi \frac{S_T}{S_w} L'_{AT} \left(\beta^2 \frac{L_T}{b} - \frac{w''_B}{k} + \frac{w''_A}{k} \right) \eta_T$$

$$Z_{T(\delta)} = 2\pi \frac{S_T}{S_w} L'_{cT} \eta_T$$

$$Z_{T(\frac{\dot{\delta}b}{U})} = 2\pi \frac{S_T C_T}{S_w C_w} \left(\frac{L'_{cT}}{k} \right)_T \eta_T$$

Similarly the moment derivatives can be derived. Detailed expressions, as well as numerical data for the coefficients L'_A , L''_A , w'_A , w''_B etc. are given in Reference 56.

Lateral derivatives are discussed by Goland, Luke and Hager, Reference 70.

The contributions of fuselage are discussed in Sections 5.2.4 - 5.2.4.3, see also References 56 and 70.

It is advisable in practice to adjust the theoretically determined stability derivatives in such a way that at zero frequency of oscillation they conform with the corresponding experimentally determined static stability derivatives. This adjustment is particularly important when aerodynamic theory is to be used on control surfaces since leading and trailing edge shapes, aerodynamic balance, gaps, and boundary layer characteristics have such predominant effects upon the hinge-moment derivatives that large differences exist between theoretical and experimental results even in the steady case. The calculated derivatives may be replaced by their measured counterparts in a way such that the theoretical variations of the air loads with frequency are unaffected but the correct static air loads are produced at zero frequency.

5.7 Influence of Elastic Deformation of the Structure

5.7.1 Introduction

As mentioned in Chapter II, the influence of the elastic deformation of the structure becomes important when the flight speed is so high that it

becomes comparable with (say, more than 50 percent of) any of the critical aeroelastic speeds, such as the wing divergence speed, the control reversal speed, or the wing and tail flutter speeds.

Structural deformations are of two main types:

(a) Elastic deformation of the main structure, which changes the configuration of the aircraft as a whole.

(b) Local distortions, which may or may not be elastic, and may be of importance in relation to control forces since the "heaviness" of a control flap may be sensitive to small distortions of its surface.

Distortions of type (a) are amenable to mathematical analysis and are of main concern to the stability and control of aircraft. These elastic distortions can be further classified into two kinds, according to their time history:

(a1) Those elastic distortions caused by the aerodynamic, gravity and inertia loads in steady uniform rectilinear flight, or in a steady maneuver, such as rolling at constant angular velocity.

(a2) Those distortions caused by transient loads, such as those due to a gust, a sudden deflection of the control surfaces, or those due to vibrations or flutter of the structure.

In most practical cases, the first kind, the steady state distortions, account for the essential influence of the elastic distortion on the stability and control characteristics of the aircraft. These happen also to be the easier to analyze. The second kind of distortions are of great importance in the gust response, flutter, stall flutter, and buffeting problems, and to airplane stability and control when the flight speed is close to the flutter or buffeting speeds.

5.7.2 Methods for Investigating the Effects of Structural Distortions

The principal methods are:

(a) Solution of the differential equations or integral equations governing the elastic distortions, or the matrix equations approximating these exact equations - the collocation approach.

(b) The method of iteration or successive approximations.

(c) The method of generalized coordinates - the modal approach.

(d) The method of the modification of derivatives.

Method (a) has been discussed in Chapter III (Sections 3.2, 3.3), where the equations of motion of an elastic airplane are derived in the matrix form. This is called the "collocation" approach in Chapter III because of the way by which the approximate matrix equations are derived. Exact equations can be obtained in a similar way, but since exact solutions are difficult to obtain except in the simplest idealized cases, the matrix approximation is usually the most powerful approach.

The method of iteration or successive approximation (b), is conceptually very simple. As an example, consider the effect of elastic deformation on the lift distribution. Let $\alpha^{(r)}(s)$ denote the angle of attack of the airfoil at all sections, if the wing was perfectly rigid. One starts from the angle-of-attack distribution $\alpha^{(r)}(s)$ of a rigid wing, and finds first the lift

and moment distribution corresponding to $\alpha^{(r)}(s)$, and then the elastic deformation $\alpha^{(e)}(s)$ that this lift and moment distribution gives. Next one determines the lift and moment distribution corresponding to $\alpha(s) = \alpha^{(r)} + \alpha^{(e)}$ computed in the first cycle, and then determines the elastic deformation, $\alpha^{(e)}(s)$, again, using the new lift and moment distribution. If, by repeating the process, one arrives at a limiting function $\alpha(s)$, then that limiting function is the equilibrium angle-of-attack distribution of the elastic wing corresponding to $\alpha^{(r)}(s)$.

The actual execution of the method of iteration may take the form of matrix iterations. This method will not be discussed further here. The reader may find detailed expositions in Reference 58.

The method of generalized coordinates (or the so-called modal approach), has been discussed in Chapter III, Sections 3.1 and 3.2.2.6, and will be further illustrated in greater detail in Chapter VI.

The method of modification of derivatives was first used by Gates and Lyon (References 57, 60). In a general form it is presented in Section 3.2.2.3, under the title of quasi-static solutions. The essence of this method is the assumption that the elastic distortions occur very slowly in relation to the lowest relevant natural frequency of structural oscillation. It is inapplicable when the forces and moments proportional to the distortional velocities and accelerations cease to be negligible. Whenever applicable, the great simplicity of this method recommends itself. In this approach the number of dependent variables and the order of the differential equations are identical with those of the rigid aircraft. The stability derivatives are however, modified to account for the elastic deformation.

5.7.3 Influence of the Flexibility of the Fuselage - An Example of Modified Derivatives from the Modal Approach

The formulation of the equations of motion of an elastic airplane according to the modal approach has been given in Section 3.2.2.6 and will be illustrated further in Chapter VI. For the convenience of the reader, however, the equations required for the present example will be derived anew. This example may also be regarded as a simple illustration of the results which were presented in Section 3.2.2.6 in a condensed matrix notation.

Consider the influence of the vertical flexibility of the fuselage in longitudinal-symmetric motion (Reference 57). Assume that the bending of the fuselage gives a displacement in the direction of the body axis oz (see Figure 3.2) equal to

$$z = d(t) e(x) \quad (5-209)$$

where $d(t)$ is the single generalized coordinate, and $e(x)$ is the function that defines the mode of bending. Since z is positive when d is positive, $e(x)$ must be positive when x is negative. The coordinate d is supposed to be a small quantity whose square can be neglected. The components of velocity and acceleration in the direction of the z -axis for any point of the rear fuselage or tail are

$$\text{vel.} = \dot{w} - q x + \dot{d} e(x) \quad (5-210)$$

$$\text{acc.} = \ddot{w} - \dot{q} U_0 - \dot{q} x + \ddot{d} e(x) \quad (5-211)$$

where it is assumed that ox is the wind axis. The inertia force in the z -axis direction is

$$- \sum \left[\ddot{w} - \dot{q} U_0 - \dot{q} x + \ddot{d} e(x) \right] \delta m \quad (5-212)$$

and the inertia pitching moment about the airplane c.g. is (x being positive forward of the c.g.):

$$\sum x \left[\ddot{w} - \dot{q} U_0 - \dot{q} x + \ddot{d} e(x) \right] \delta m \quad (5-213)$$

The summation extends over all mass elements δm of the airplane. From the above expressions the equations of motion can be derived in the manner of Sections 3.2.1 and 3.2.2. (Cf. in particular, equation (3-18)).

The complete equation of the normal forces will be

$$-u \left(\frac{\partial Z}{\partial u} \right) + \dot{w} m - w \left(\frac{\partial Z}{\partial w} \right) + \theta (mg \sin \theta_0) - q \left(m U_0 + \frac{\partial Z}{\partial q} \right) \quad (5-214)$$

$$+ \ddot{d} \sum e(x) \delta m - \dot{d} \left(\frac{\partial Z}{\partial \dot{d}} \right) - d \left(\frac{\partial Z}{\partial d} \right) = Z_1(t)$$

where $\frac{\partial Z}{\partial \dot{d}}$ and $\frac{\partial Z}{\partial d}$ are aerodynamic derivatives for the fuselage bending.

The longitudinal force is unaffected by the fuselage bending except through the aerodynamic derivatives $\frac{\partial X}{\partial \dot{d}}$ and $\frac{\partial X}{\partial d}$. Hence

$$\begin{aligned} \dot{u} m - u \left(\frac{\partial X}{\partial u} \right) - w \left(\frac{\partial X}{\partial w} \right) + \theta mg \cos \theta_0 - q \left(\frac{\partial X}{\partial q} \right) \\ - \dot{d} \left(\frac{\partial X}{\partial \dot{d}} \right) - d \left(\frac{\partial X}{\partial d} \right) = X_1(t) \end{aligned} \quad (5-215)$$

The pitching equation is

$$-u \left(\frac{\partial M}{\partial u} \right) - \dot{w} \left(\frac{\partial M}{\partial \dot{w}} \right) - w \left(\frac{\partial M}{\partial w} \right) + \dot{q} I_{yy} - q \left(\frac{\partial M}{\partial q} \right) \quad (5-216)$$

$$- \ddot{d} \sum x e(x) \delta m - \dot{d} \left(\frac{\partial M}{\partial \dot{d}} \right) - d \left(\frac{\partial M}{\partial d} \right) + d (q \sin \theta_0) \sum e(x) \delta m = \dot{M}_1(t)$$

To formulate the bending equation we must calculate the work done in the virtual normal displacement $\delta z = e(x) \delta d$ and with the associated increment of slope $-\frac{\partial e(x)}{\partial x} \delta d$. Let $F_1(t)$ represent the generalized bending force caused by external forces such as those due to the operation of the controls or the impact of gust, then by definition

$$F_1(t) \delta d = \sum (\text{external force}) \cdot \delta z = \sum (\text{ext. force}) e(x) \delta d.$$

Hence

$$F_1(t) = \sum (\text{external force}) \cdot e(x) \quad (5-217)$$

Similarly, the generalized force caused by the inertia forces is, from equations (5-211) and (5-212).

$$- \sum \left[\dot{w} - q U_0 - \dot{q} x + \ddot{d} e(x) \right] \delta m \cdot e(x) \quad (5-218)$$

The generalized force caused by the aerodynamic and gravitational forces is obtained, as in (5-217), by integrating the product of the aerodynamic force and the function $e(x)$ over the entire airplane. The result may be expressed as generalized aerodynamic derivatives $\frac{\partial F}{\partial u}$, $\frac{\partial F}{\partial w}$, etc. relating to the generalized force of the bending mode. Finally, the generalized elastic restoring force corresponding to the assumed bending mode may be written as $(\frac{\partial f}{\partial d})d$. If the fuselage behaves like a beam, the elastic derivative can be computed simply as follows: Since the generalized bending restoring force corresponding to d is $(\frac{\partial f}{\partial d})d$, it follows that the strain energy is $\frac{1}{2} (\frac{\partial f}{\partial d})d^2$. On the other hand, since the deflection curve is $e(x)d$, the curvature is $e''(x)d$ and the strain energy per unit length is $\frac{1}{2} EI [e''(x)]^2$, where EI is the local bending rigidity. On equating the two expressions for the strain energy one obtains

$$\frac{\partial f}{\partial d} = \int EI [e''(x)]^2 dx \quad (5-219)$$

where the integral covers the fuselage. The generalized rigidity derivative $\frac{\partial f}{\partial d}$ may also be obtained by a static loading test if the airplane is available. Let a load W applied at the tail produce a deflection z relative to the tangent to the fuselage center line at the c.g., and let the corresponding value of the bending coordinate be d , then the strain energy is

$$\frac{1}{2} W z = \frac{1}{2} d^2 \left(\frac{\partial f}{\partial d} \right), \quad d = \left(\frac{z}{e(x)} \right)_{\text{tail}} \quad (5-220)$$

from which $\frac{\partial f}{\partial d}$ can be found. In the analysis it is also convenient to express the generalized rigidity constant $\frac{\partial f}{\partial d}$ in terms of the (hypothetical) frequency ω_f , (rad./sec.) of uncoupled free vibration of the fuselage:

$$\frac{\partial f}{\partial d} = \left(\sum e^2(x) \delta m \right) \omega_f^2 \quad (5-221)$$

where the term in the parenthesis is the generalized mass of the bending mode.

On summing all the generalized forces, the equation for the bending mode is obtained:

$$\begin{aligned}
& - \dot{u} \left(\frac{\partial F}{\partial \dot{u}} \right) - u \left(\frac{\partial F}{\partial u} \right) + \dot{w} \sum e(x) \delta m - \dot{w} \left(\frac{\partial F}{\partial \dot{w}} \right) - w \left(\frac{\partial F}{\partial w} \right) \\
& - \dot{q} \sum x e(x) \delta m - \dot{q} \left(\frac{\partial F}{\partial \dot{q}} \right) - q \left(\frac{\partial F}{\partial q} \right) + \theta g \sin \theta_0 \sum e(x) \delta m \\
& + \ddot{d} \sum e^2(x) \delta m - \dot{d} \left(\frac{\partial F}{\partial \dot{d}} \right) + d \left(- \frac{\partial F}{\partial d} + \frac{\partial f}{\partial d} \right) = F_1(t)
\end{aligned} \tag{5-222}$$

The aerodynamic derivatives $\frac{\partial Z}{\partial d}$, $\frac{\partial M}{\partial \dot{d}}$, etc. are almost wholly attributable to the tail whose effective angle of incidence depends on d and \dot{d} . Let x_t be the coordinate of the tail aerodynamic center, then the angle of incidence of the horizontal tail due to the fuselage bending is

$$-d e'(x_t) + \dot{d} e(x_t) / V_0$$

The increments of X , Z , and M corresponding to this change of incidence can be easily found and the derivatives are determined.

Equations (5-214), (5-215), (5-216), and (5-222) define the longitudinal motion. The corresponding determinantal equation for the free motion is a sextic in λ .

5.7.3.1 Quasi-static Solution, Modified Derivatives. In equation (5-222) the three terms proportional to the generalized coordinate of fuselage bending, d , are

$$\ddot{d} \sum e^2(x) \delta m - \dot{d} \left(\frac{\partial F}{\partial \dot{d}} \right) + d \left(- \frac{\partial F}{\partial d} + \frac{\partial f}{\partial d} \right) \tag{5-223}$$

Now in the stability analysis, d , as well as u , w , q , etc., are assumed to be of the form constant times $e^{\lambda t/\tau}$ where τ is the unit of time employed in the dimensionless system (Section 3.2.1.3). Hence we may write the quantities in (5-223) as

$$\frac{\lambda^2}{\tau^2} d \sum e^2(x) \delta m - \frac{\lambda}{\tau} d \left(\frac{\partial F}{\partial \dot{d}} \right) + d \left(- \frac{\partial F}{\partial d} + \omega_f^2 \sum e^2(x) \delta m \right) \tag{5-224}$$

where the elastic stiffness term $\frac{\partial f}{\partial d}$ has been expressed in terms of the fuselage vibration frequency ω_f as was shown in equation (5-221). Now for the motion of the airplane as a whole the numerical value of λ/τ is usually much smaller than ω_f . If this assumption is made, i.e.

$$\frac{\lambda}{\tau} \ll \omega_f \tag{5-225}$$

then the first two terms in (5-224) are much smaller than the last term and can be neglected. Great simplification results if the assumption (5-225) is valid.

With the assumption (5-225) the equation for fuselage bending, equation (5-222), may be solved for d :

$$\begin{aligned}
d' = & \left(-\frac{\partial F}{\partial d} + \frac{\partial f}{\partial d} \right)^{-1} \left\{ F_1(t) + \left(\frac{\partial F}{\partial \dot{u}} \right) \dot{u} + \left(\frac{\partial F}{\partial u} \right) u - \dot{w} \sum e(x) \delta m \right. \\
& + \dot{w} \left(\frac{\partial F}{\partial \dot{w}} \right) + w \left(\frac{\partial F}{\partial w} \right) + \dot{q} \sum x e(x) \delta m + \dot{q} \left(\frac{\partial F}{\partial \dot{q}} \right) \\
& \left. + q \left(\frac{\partial F}{\partial q} \right) - \theta g \sin \theta_0 \sum e(x) \delta m \right\}
\end{aligned} \tag{5-226}$$

A substitution of (5-226) into the rigid-body motion equations, equations (5-214), (5-215), and (5-216), eliminates the bending coordinate from the equations of motion.

Further simplification is obtained by observing that in general the air-plane relative density parameter μ is large. Now when the last three terms on the left hand side of equation (5-214) are reduced into non-dimensional form, they read:

$$\bar{d} \frac{\lambda^2}{\mu} \frac{\sum e(x) \delta m}{m} + \bar{d} \frac{\lambda}{\mu} C_{z\dot{d}} + \bar{d} C_{z_d} \tag{5-227}$$

where, in addition to the notations introduced in Section 3.2.1.3, we have designated

$$\bar{d} = \frac{d}{c} \quad \begin{array}{l} (d \text{ has dimension of a displacement}) \\ (c = \text{chord}) \end{array} \tag{5-228}$$

$$\frac{\partial Z}{\partial d} = \frac{\rho U^2 S}{c} C_{z_d} \tag{5-229}$$

$$\frac{\partial Z}{\partial \dot{d}} = -\rho U S C_{z\dot{d}} \tag{5-230}$$

The characteristic length ℓ is chosen to be the chord length c in the longitudinal equations, \bar{d} , $e(x)$, C_{z_d} , and $C_{z\dot{d}}$ are dimensionless. C_{z_d} and $C_{z\dot{d}}$

may be assumed to be of the same order of magnitude. $e(x)$ is of order 1, hence if

$$\frac{\lambda}{\mu} \ll 1 \tag{5-231}$$

the first two terms in (5-227) will be negligible in comparison with the last term.

A solution obtained through the incorporating of the assumptions (5-225) and (5-231) is termed a "quasi-static" solution. After a quasi-static solution is obtained, one should check the assumptions (5-225) and (5-231) again to see if they were valid.

The result of eliminating the fuselage bending coordinate from the vertical force equation (5-214) in accordance with the quasi-static assumption is

$$\begin{aligned}
& -u \frac{\partial Z}{\partial u} + \dot{w} m - w \frac{\partial Z}{\partial w} + \theta m g \sin \theta_0 - g \left(m U_0 + \frac{\partial Z}{\partial g} \right) \\
& - \frac{\frac{\partial Z}{\partial d}}{\left(-\frac{\partial F}{\partial d} + \frac{\partial f}{\partial d} \right)} \left\{ F_1(t) + \dot{u} \frac{\partial F}{\partial u} + u \frac{\partial F}{\partial u} - \dot{w} \sum e(x) \delta m + \dot{w} \frac{\partial F}{\partial w} \right. \\
& \quad + w \frac{\partial F}{\partial w} + \dot{g} \sum x e(x) \delta m + \dot{g} \frac{\partial F}{\partial g} + g \frac{\partial F}{\partial g} \\
& \quad \left. - \theta g \sin \theta_0 \sum e(x) \delta m \right\} = Z_1(t) \tag{5-232}
\end{aligned}$$

A comparison of this equation with the corresponding equation for a rigid airplane shows at once that they are of identical form provided that the coefficients are modified as shown in the following table, where

$$K_1 = \frac{\frac{\partial Z}{\partial d}}{-\frac{\partial F}{\partial d} + \frac{\partial f}{\partial d}} \tag{5-233}$$

| <u>Coefficient of</u> | <u>Rigid Airplane</u> | <u>Elastic Airplane</u> |
|-----------------------|--|--|
| \dot{u} | — | $-K_1 \frac{\partial F}{\partial u}$ |
| u | $-\frac{\partial Z}{\partial u}$ | $-\frac{\partial Z}{\partial u} - K_1 \frac{\partial F}{\partial u}$ |
| \dot{w} | m | $m + K_1 \sum e(x) \delta m - K_1 \frac{\partial F}{\partial w}$ |
| w | $-\frac{\partial Z}{\partial w}$ | $-\frac{\partial Z}{\partial w} - K_1 \frac{\partial F}{\partial w}$ |
| \dot{g} | — | $-K_1 \left(\frac{\partial F}{\partial g} + \sum x e(x) \delta m \right)$ |
| g | $-m U_0 - \frac{\partial Z}{\partial g}$ | $-m U_0 + \frac{\partial Z}{\partial g} + K_1 \frac{\partial F}{\partial g}$ |
| θ | $m g \sin \theta_0$ | $(m + K_1 \sum e(x) \delta m) g \sin \theta_0$ |
| Forcing function | $Z_1(t)$ | $Z_1(t) + K_1 F_1(t)$ |

One notices in the above table that the aerodynamic coefficients of \dot{u} , \dot{w} , \dot{q} vanish in the rigid airplane equation, in accordance with a conventional practice in which the only first order unsteady flow term retained is the moment derivative $\partial M / \partial \dot{w}$ in the moment equation. If the full first order unsteady flow aerodynamics were employed the coefficients of these terms would be $\partial Z / \partial \dot{u}$, $\partial Z / \partial \dot{w}$, $\partial Z / \partial \dot{q}$ respectively. Several terms introduced by the flexible fuselage, the F derivatives, could be quite small and negligible. This will become clear in each particular case.

Similarly, the corresponding coefficients for the longitudinal force equation are:

| <u>Coefficient of</u> | <u>Rigid Airplane</u> | <u>Elastic Airplane</u> |
|-----------------------|----------------------------------|--|
| \dot{u} | m | $m - K_2 \frac{\partial F}{\partial \dot{u}}$ |
| u | $-\frac{\partial X}{\partial u}$ | $-\frac{\partial X}{\partial u} - K_2 \frac{\partial F}{\partial u}$ |
| \dot{w} | — | $-K_2 \frac{\partial F}{\partial \dot{w}} + K_2 \sum e(x) \delta m$ |
| w | $-\frac{\partial X}{\partial w}$ | $-\frac{\partial X}{\partial w} - K_2 \frac{\partial F}{\partial w}$ |
| \dot{q} | — | $-K_2 \left(\frac{\partial F}{\partial \dot{q}} + \sum x e(x) \delta m \right)$ |
| q | $-\frac{\partial X}{\partial q}$ | $-\frac{\partial X}{\partial q} - K_2 \frac{\partial F}{\partial q}$ |
| θ | $mg \cos \theta_0$ | $mg \cos \theta_0 + K_2 g \sin \theta_0 \sum e(x) \delta m$ |
| Forcing function | $X_1(t)$ | $X_1(t) + K_2 F_1(t)$ |

where

$$K_2 = \frac{\frac{\partial X}{\partial d}}{-\frac{\partial F}{\partial d} + \frac{\partial f}{\partial d}} \quad (5-234)$$

The corresponding coefficients for the pitching moment equation are

| <u>Coefficient of</u> | <u>Rigid Airplane</u> | <u>Elastic Airplane</u> |
|-----------------------|----------------------------------|--|
| \dot{u} | — | $-K_3 \frac{\partial F}{\partial \dot{u}}$ |
| u | $-\frac{\partial M}{\partial u}$ | $-\frac{\partial M}{\partial u} - K_3 \frac{\partial F}{\partial u}$ |

| <u>Coefficient of</u> | <u>Rigid Airplane</u> | <u>Elastic Airplane</u> |
|-----------------------|--|---|
| \dot{w} | $-\frac{\partial M}{\partial \dot{w}}$ | $-\frac{\partial M}{\partial \dot{w}} - K_3 \frac{\partial F}{\partial \dot{w}} + K_3 \sum e(x) \delta m$ |
| w | $-\frac{\partial M}{\partial w}$ | $-\frac{\partial M}{\partial w} - K_3 \frac{\partial F}{\partial w}$ |
| $\dot{\eta}$ | I_{yy} | $I_{yy} - K_3 \frac{\partial F}{\partial \dot{\eta}} - K_3 \sum x e(x) \delta m$ |
| η | $-\frac{\partial M}{\partial \eta}$ | $-\frac{\partial M}{\partial \eta} - K_3 \frac{\partial F}{\partial \eta}$ |
| θ | — | $K_3 g \sin \theta_0 \sum e(x) \delta m$ |
| Forcing function | $M_1(t)$ | $M_1(t) + K_3 F_1(t)$ |

where

$$K_3 = \frac{\frac{\partial M}{\partial d} - g \sin \theta_0 \sum e(x) \delta m}{-\frac{\partial F}{\partial d} + \frac{\partial f}{\partial d}} \quad (5-235)$$

With the modifications indicated, the resulting equations are of the same form as the rigid airplane equations.

5.7.3.2 Static Stability. On setting $\lambda = 0$ in the equations of motion, the condition for static stability is obtained. In free motion ($X_1 = Z_1 = M_1 = F_1 = 0$) let the value of the determinant of the coefficients be denoted by p_0 . The condition $p_0 > 0$ in isolation gives no information about the stability, except that it is not statically neutral. But if all the other test functions (Hurwitz determinants)* are positive, a change of sign of p_0 from positive to negative indicates the onset of instability and the unstable constituent is a non-oscillatory divergence, corresponding to a real positive root of the determinantal equation. Approach to the neutral condition $p_0 = 0$ is accompanied by increasing sensitiveness to applied forces. (See § 4.10, Duncan, Reference 57)

On noting that $q = \lambda \theta$, the static stability is obtained from the equations of the previous section. Assuming further a horizontal flight with $\theta_0 = 0$, one obtains

$$p_0 = \begin{vmatrix} -\frac{\partial X}{\partial u} - K_2 \frac{\partial F}{\partial u} & -\frac{\partial X}{\partial w} - K_2 \frac{\partial F}{\partial w} & mg \\ -\frac{\partial Z}{\partial u} - K_1 \frac{\partial F}{\partial u} & -\frac{\partial Z}{\partial w} - K_1 \frac{\partial F}{\partial w} & 0 \\ -\frac{\partial M}{\partial u} - K_3 \frac{\partial F}{\partial u} & -\frac{\partial M}{\partial w} - K_3 \frac{\partial F}{\partial w} & 0 \end{vmatrix} \quad (5-236)$$

* See Reference 80, or Reference 58, p. 476.

$$\text{or } \frac{\partial \phi_0}{\partial w} = \frac{\partial z}{\partial u} \frac{\partial M}{\partial w} - \frac{\partial z}{\partial w} \frac{\partial M}{\partial u} + K_1 \left(\frac{\partial F}{\partial u} \frac{\partial M}{\partial w} - \frac{\partial F}{\partial w} \frac{\partial M}{\partial u} \right) + K_3 \left(\frac{\partial F}{\partial w} \frac{\partial z}{\partial u} - \frac{\partial F}{\partial u} \frac{\partial z}{\partial w} \right) \quad (5-237)$$

The last two terms give the influence of the fuselage flexibility. In general, K_1 may be neglected in comparison with K_3 .

5.7.4 Modified Derivatives from the Collocation Approach

The dimensionless longitudinal equations of motion for a rigid-airplane, given in equation (3-39), reads

$$\begin{aligned} \frac{d\bar{u}}{dt} + (C_D + C_{Du})\bar{u} + \frac{1}{2}(C_{D\alpha} - C_L)\bar{w} + \frac{1}{2}C_L\theta &= -\frac{1}{2}C_D \\ (C_L + C_{Lu})\bar{u} + \frac{d\bar{w}}{dt} + \frac{1}{2}(C_{L\alpha} + C_D)\bar{w} - \left(1 - \frac{C_{Lq}}{4\mu}\right)\bar{q} + \frac{1}{2}C_L \tan \gamma \theta &= -\frac{1}{2}C_L \\ -\mu(C_m + C_{m_u})\bar{u} - \frac{C_{m\dot{w}}}{4}\frac{d\bar{w}}{dt} - \frac{\mu}{2}C_{m\alpha}\bar{w} + K_B\frac{d\bar{q}}{dt} - \frac{C_{mq}}{4}\bar{q} &= \frac{\mu}{2}C_m \\ \frac{d\theta}{dt} = \tau\bar{q} = \bar{q} \end{aligned}$$

These equations are written as a single matrix equation in equations (3-41) of Section 3.2.1.3.

For an elastic airplane, the transverse deflections at points $i = 1, 2, \dots, n$ are incorporated in a column matrix $z^{(e)}$ (Section 3.2.2.1) as follows

$$z^{(e)} = \underline{z} \underline{h} = \underline{z} \left\{ h_i(x_i, y_i, \bar{t}) \right\}$$

The quasi-steady solution to the longitudinal motion of an elastic airplane is given in equation (3-139a) of Section 3.2.2.3. A comparison of the quasi-steady equations with the rigid-airplane equations shows that the rigid-airplane equations will be equivalent to the elastic-airplane equations if the following modifications were made, (See 3.2.2.3 for definitions of the underscored matrices).

- (1) The \bar{u} -equation, unchanged, under the assumption that the effect of elastic deformation on this equation is small, (cf. 5.7.3.1, assuming $K_2 \ll 1$).
- (2) The \bar{w} equation:

C_D and its derivatives, unchanged

$$C_L \rightarrow C_L - \underline{1}' \underline{Y} \underline{A} \underline{C}_{\ell}$$

$$C_{Lu} \rightarrow C_{Lu} - \underline{1}' \underline{Y} \underline{A} \underline{C}_{\ell u}$$

$$\lambda \bar{w} \rightarrow (1 - \underline{\underline{1}}' \underline{\underline{Y}} \underline{\underline{M}} \underline{\underline{1}}) \lambda \bar{w}$$

$$C_{L\alpha} \rightarrow C_{L\alpha} - 2 \underline{\underline{1}}' \underline{\underline{Y}} \underline{\underline{A}} \underline{\underline{P}} \underline{\underline{1}}$$

$$\bar{g} \rightarrow (1 - \underline{\underline{1}} \underline{\underline{Y}} \underline{\underline{M}} \underline{\underline{\xi}} \frac{\lambda}{\mu} - \underline{\underline{1}}' \underline{\underline{Y}} \underline{\underline{M}} \underline{\underline{1}} - \frac{1}{\mu} \underline{\underline{1}} \underline{\underline{Y}} \underline{\underline{A}} \underline{\underline{P}} \underline{\underline{\xi}}) \bar{g}$$

$$C_L \tan \gamma \rightarrow C_L \tan \gamma (1 - \underline{\underline{1}}' \underline{\underline{Y}} \underline{\underline{M}} \underline{\underline{1}})$$

$$C_{L_1} \rightarrow C_{L_1} - \underline{\underline{1}} \underline{\underline{Y}} \underline{\underline{A}} C_{\ell_1}$$

(3) The moment equation:

$$C_m \rightarrow C_m - \underline{\underline{\xi}}' \underline{\underline{Y}} \underline{\underline{A}} C_{\ell_0}$$

$$C_{m_u} \rightarrow C_{m_u} - \underline{\underline{\xi}}' \underline{\underline{Y}} \underline{\underline{A}} C_{\ell_{\bar{u}}}$$

$$\frac{C_{m\dot{\alpha}}}{4} \rightarrow \frac{C_{m\dot{\alpha}}}{4} - \mu \underline{\underline{\xi}}' \underline{\underline{Y}} \underline{\underline{M}} \underline{\underline{1}}$$

$$\frac{C_{m\alpha}}{2} \rightarrow \frac{C_{m\alpha}}{2} - \underline{\underline{\xi}}' \underline{\underline{Y}} \underline{\underline{A}} \underline{\underline{P}} \underline{\underline{1}}$$

$$k_B \rightarrow k_B - \underline{\underline{\xi}}' \underline{\underline{Y}} \underline{\underline{M}} \underline{\underline{\xi}}$$

$$\frac{C_{mq}}{4} \rightarrow \frac{C_{mq}}{4} + \underline{\underline{\xi}}' \underline{\underline{Y}} \underline{\underline{A}} \underline{\underline{P}} \underline{\underline{\xi}} - \mu \underline{\underline{\xi}}' \underline{\underline{Y}} \underline{\underline{M}} \underline{\underline{1}}$$

$$C_{m_1} \rightarrow C_{m_1} - \underline{\underline{\xi}}' \underline{\underline{Y}} \underline{\underline{A}} C_{\ell_1}$$

The applicability of the quasi-steady approach is subject to the assumptions of small λ and large μ as examined in Section 5.7.3.1. Not all the modifications listed above are necessarily significant. On close examination of each particular case, a number of modifications may be neglected and the modified scheme may be greatly simplified.

An entirely analogous derivation of the modified scheme for the lateral motion equations can be made under the same assumptions of small λ and large μ .

5.7.5 Modified Derivatives from the Modal Approach

General expressions for the modified derivatives from the modal approach can be derived from the equations of motion given in equations (3-146) to (3-152),

and (3-154) to (3-162), in accordance with the steps illustrated in 5.7.3.

5.7.6 Simplified Estimates of the Static Aeroelastic Effects on the Longitudinal Stability and Control

Under certain assumptions very simple expressions can be obtained which express the elastic efficiency of the horizontal tail and the effect of elastic deformation on the static stability derivative $\partial C_M / \partial C_L$. These formulas are applicable to unswept wings and tails. The shift of the center of pressure on a swept wing due to elastic deformation is so sensitive that a more detailed investigation is needed.

Consider an airplane with unswept wings and tails in horizontal rectilinear symmetric steady flight. When the elevator angle changes, the pitching moment about the airplane c.g. changes. In order to study the efficiency of the tail alone, it is convenient to consider the unbalanced pitching moment itself, instead of the dynamics of the airplane as a whole. For this purpose, the airplane shall be assumed to be held fixed, against any disturbed motion, at the c.g. of the airplane. In this fictitious condition, a measure of the tail efficiency is the rate of change of the pitching moment coefficient with elevator deflection, $\partial C_M / \partial \beta$, β being the elevator deflection angle (positive if deflected downward). Owing to the elastic deformation of the tail and the fuselage, the derivative $\partial C_M / \partial \beta$ for a real airplane is smaller than that of a rigid airplane. The ratio

$$\frac{\partial C_M}{\partial \beta} \bigg/ \left(\frac{\partial C_M}{\partial \beta} \right)_{\text{rigid}} \quad (5-238)$$

is called the elastic efficiency of the elevator.

In order to calculate the elastic efficiency, it is necessary to consider the elastic properties of the airplane. Assume that the elevators are relatively rigid. The angle of attack of the stabilizer will be represented by a characteristic number θ_t measured at a reference section located at a spanwise coordinate η_t . If the tail angle-of-attack distribution is described by $\theta_0 f(y)$, y being the spanwise coordinate, then η_t may be defined according to the following equation:

$$\theta_t = \theta_0 f(\eta_t) = \frac{\theta_0}{S_t} \int_{-s_t}^{s_t} f(\gamma) c_t(\gamma) d\gamma \quad (5-239)$$

where c_t is the tail chord length, s_t is the tail semispan, and S_t is the tail area. Hence θ_t is the weighted average of the tail angle of attack. If a semi-rigid mode $f(y)$ of the tail twisting is assumed, η_t can be evaluated at once. Generally, it may be assumed to lie at 2/3 to 3/4 semi-span outboard from the fuselage.

The elastic property of the tail and fuselage may be described by two stiffness-influence coefficients K_1 and K_2 defined as follows. Let K_1 be the total lift force (with $K_1/2$ acting at each of the reference sections on the two halves of the horizontal tail), that is required to act at the tail aerodynamic

center to produce a rotation of 1 radian at the reference section, (actually only small deflections are of interest and the linearity of the structure may be assumed), with the fuselage assumed clamped at the airplane c.g. Let K_2 be the total pitching moment (with $K_2/2$ acting at each reference section) that is required to act at the tail reference sections to produce the same rotation. Then the total change of the tail angle of attack due to a lift L_t acting at the tail aerodynamic center and a twisting moment M_t about the aerodynamic center, is

$$\theta_t = \frac{L_t}{K_1} + \frac{M_t}{K_2} \quad (5-240)$$

Using the strip assumption, one may write the lift and moment induced by a small deflection angle β of the elevator:

$$L_t = q_t S_t \left[a_t \theta_t + \left(\frac{\partial C_L}{\partial \beta} \right)_t \beta \right] \quad (5-241)$$

$$M_t = -m \beta q_t S_t c_t \quad (5-242)$$

where q_t is the dynamic pressure at the tail, a_t is the lift curve slope of the tail, $\left(\frac{\partial C_L}{\partial \beta} \right)_t$ is the elevator derivative of the tail airfoil section. The derivative m must be considered more carefully. In ordinary situations only the aerodynamic moment acting on the stabilizer contributes to the twisting of the stabilizer, the contribution due to the pressure distribution over the elevator being resisted by the control stick. Hence

$$-m = \frac{\partial C_{M_t}}{\partial \beta} - \frac{\partial C_{H_t}}{\partial \beta} \quad (5-243)$$

where C_{M_t} is the coefficient of the pitching moment about the tail aerodynamic center, C_{H_t} is the hinge moment coefficient, both based on the tail area and tail chord.

On solving equations (5-240), (5-241), and (5-242) for $\partial \theta_t / \partial \beta$, and computing in turn the derivatives $\partial C_{L_t} / \partial \beta$ and $\partial C_{M_t} / \partial \beta$, (the subscript t refers to tail), the pitching moment (about airplane c.g.) derivative $\partial C_M / \partial \beta$ can be computed. The result may be posed in the form (see Reference 58, page 150).

$$\text{Elastic efficiency of elevator} = \frac{1 - q_t / q_{t_{\text{rev}}}}{1 - q_t / q_{t_{\text{div}}}} \quad (5-244)$$

where

$$q_{t_{\text{div}}} = \frac{K_1}{S_t a_t} \quad (5-245)$$

$$q_{t_{rev}} = \frac{K_2}{S_t \bar{c}_t} \frac{1}{\alpha_t m} \left(\frac{\partial C_L}{\partial \beta} \right)_t \quad (5-246)$$

\bar{c}_t is the mean aerodynamic chord of the tail.

The dynamic pressure $q_{t_{div}}$ is the critical divergence pressure of the horizontal tail at which an infinitesimal change in β induces a large tail twist. If K_1 is negative, $q_{t_{div}}$ has no physical meaning, but is merely a parameter showing that the tail is stable. The dynamic pressure $q_{t_{rev}}$ defines the critical horizontal tail-control reversal speed, at which a change of elevator angle produces no change in the pitching moment about the airplane c.g. Note that $q_{t_{rev}}$ is independent of K_1 , because at the reversal speed the tail lift due to elevator deflection vanishes. Since m is in general small, $q_{t_{rev}}$ is in general very high.

The effect of elastic deformation on the longitudinal stability may be estimated under the same approximation. The static longitudinal stability is measured by the derivative $\partial C_M / \partial C_L$ at the symmetric level flight condition, where C_L is the total lift coefficient and C_M is the coefficient of pitching moment about the airplane c.g. An airplane is statically stable when $\partial C_M / \partial C_L$ is negative. In power-off condition and for the rearmost c.g. location, a value of $-\partial C_M / \partial C_L$ from 0.10 to 0.15 usually leads to satisfactory results.

As C_L is contributed mainly by the wing and C_M mainly by the horizontal tail, the above derivative may be computed by evaluating the change of C_M and C_L following a small angle of rotation at the airplane c.g. In the stick-fixed condition (elevator locked), the effect of elastic deformation of the wing, tail, and fuselage may be written in the form (See page 153, Reference 58):

$$\left(\frac{\partial C_M}{\partial C_L} \right)_{elastic} = \left(\frac{\partial C_M}{\partial C_L} \right)_{rigid} + \Delta \left(\frac{\partial C_M}{\partial C_L} \right) \quad (5-247)$$

where, for unswept wing and tail,

$$\Delta \left(\frac{\partial C_M}{\partial C_L} \right) = \frac{l_t}{l} \frac{S_t}{S_w} \frac{q_t}{q_w} \left[\frac{\frac{\partial q_{waiv}}{\partial \beta} - \frac{q_t}{q_{taiv}}}{1 - \frac{\partial q_{taiv}}{\partial \beta}} \right] \quad (5-248)$$

In this equation l is the distance from the airplane c.g. to the tail lift vector through the tail aerodynamic center, and the subscripts w and t refer to wing and tail respectively. Equation (5-248) shows that, for an aeroelastically stable airplane the effect of elastic deformation on $\partial C_M / \partial C_L$ depends on the relative magnitude of the divergence dynamic pressures of the wing and tail. (For wing divergence, see Section 2.2.1.) One might remark again that for most configurations $q_{t_{div}}$ is negative.

The effect of elastic deformation on the longitudinal stability of swept wing aircraft is quite sensitive to the deformation mode due to the shift of center of pressure. For such an aircraft a more detailed study is recommended. (See Sections 2.3, 2.3.1, 2.3.2, and Refs. mentioned therein. See also, Ref. 59, p. 474.)

5.7.7 Simplified Estimates of the Static Aeroelastic Effects on the Lateral Stability and Control.

The static aeroelastic effect on the losses in lateral control and stability may be estimated simply when the one-degree-of-freedom rolling motion is considered. The rigid-body equation of motion, equation (3-69b) reduces to the form

$$K_A \frac{d^2\phi}{dt^2} - \frac{1}{4} C_{\ell p} \frac{d\phi}{dt} = \frac{\mu}{2} C_{\ell} \quad (5-249)$$

The forcing function $C_{\ell 1}$ to be considered here is the rolling moment due to the deflection of aileron and the elastic deformation of the wing. Let

δ_a = total aileron deflection, deg.

ϵ = twist at wing tip, deg.

L_1 = rolling moment, ft. lbs.,

$$\begin{aligned} &= \frac{1}{2} \rho U^2 S b C_{\ell} \\ &= \frac{1}{2} \rho U^2 S b (C_{\ell \delta} \delta_a + C_{\ell \epsilon} \epsilon) \end{aligned} \quad (5-250)$$

$$C_{\ell \delta} = \frac{\partial C_{\ell}}{\partial \delta_a}, \quad C_{\ell \epsilon} = \frac{\partial C_{\ell}}{\partial \epsilon}, \quad C_{\ell} = \frac{L}{\frac{1}{2} \rho U^2 S b}$$

then

$$K_A \frac{d^2\phi}{dt^2} - \frac{1}{4} C_{\ell p} \frac{d\phi}{dt} = \frac{\mu}{2} (C_{\ell \delta} \delta_a + C_{\ell \epsilon} \epsilon) \quad (5-251)$$

It is now desired to eliminate ϵ by proper modification of the coefficients K_A , $C_{\ell p}$, and $C_{\ell \delta}$. The twist at the wing tip, ϵ , can be written as an infinite series (Reference 61) according to the method of successive approximation:

$$\epsilon = \epsilon_1 + \epsilon_2 + \epsilon_3 + \dots \quad (5-252)$$

in which ϵ_1 is the twist resulting from the applied aerodynamic forces and the wing inertia, ϵ_2 is the twist caused by the load due to ϵ_1 , ϵ_3 is caused by the load due to ϵ_2 , etc. ϵ_1 can be expressed as a linear combination of the various angles of attack and accelerations:

$$\epsilon_1 = \epsilon_{\delta} \delta_a + \epsilon_p \left(\frac{pb}{2U} \right) + \epsilon_{\ddot{p}} \ddot{p} \quad (5-253)$$

By assuming that each succeeding twist is proportional to the preceding one in the series

$$\frac{\epsilon_2}{\epsilon_1} = \frac{\epsilon_3}{\epsilon_2} = \frac{\epsilon_4}{\epsilon_3} = \dots = \nu \quad (5-254)$$

then the series for ϵ becomes a geometric series whose sum is

$$\epsilon = \frac{\epsilon_1}{1 - \nu} \quad (5-255)$$

This may be identified with the well-known equation (equation (2-9), Section 2.2.1).

$$\frac{\epsilon}{\epsilon_1} = \frac{1}{1 - \frac{q}{q_{div}}} \quad (5-256)$$

where q_{div} is the divergence dynamic pressure of the wing. For sweptback wings q_{div} may be a negative number.

The deflection pattern across the span due to the three causes: the aileron δ_a , the rolling damping p , the rolling acceleration \dot{p} , may not be the same. Correspondingly, the induced aerodynamic rolling moment due to these twisting modes may be different. Hence it is appropriate to replace the last term in (5-250) and (5-251), by

$$C_{l\epsilon} \epsilon = \frac{1}{1-\nu} \left[(C_{l\epsilon})_{\delta} \epsilon_{\delta} \delta_a + (C_{l\epsilon})_p \epsilon_p \left(\frac{pb}{2U} \right) + (C_{l\epsilon})_{\dot{p}} \epsilon_{\dot{p}} \dot{p} \right] \quad (5-257)$$

The ratio ν is rather insensitive to the twisting mode and can be computed by an average mode. The rolling moment coefficient due to this average mode is denoted by $(C_{l\epsilon})_{\epsilon}$

A combination of equations (5-251) and (5-257) leads to

$$\left(K_A - \frac{\mu}{2\tau^2} \frac{C_{l\epsilon}}{1-\nu} \epsilon_p \right) \frac{d^2 \phi}{dt^2} = \frac{1}{4} \left(C_{lp} + \frac{C_{l\epsilon} \epsilon_p}{1-\nu} \right) \frac{d\phi}{dt} + \frac{\mu}{2} \left(C_{l\delta} + \frac{C_{l\epsilon} \epsilon_{\delta}}{1-\nu} \right) \delta_a \quad (5-258)$$

which, in comparison with (5-249) shows the proper way of modifying the coefficients K_A , C_{lp} , and $C_{l\delta} \delta_a$ for elastic deformation.

The derivatives $(C_{l\epsilon})_{\delta}$, $(C_{l\epsilon})_p$, $(C_{l\epsilon})_{\dot{p}}$ can be computed for a given wing configuration and spanwise twist angle variation by standard methods (see Section 2.3.4). For a crude estimation, one may use the approximation:

$$(C_{l\epsilon})_{\delta} \doteq (C_{l\epsilon})_p \doteq (C_{l\epsilon})_{\dot{p}} \doteq (C_{l\epsilon})_{\epsilon} = C_{lp} \quad (5-259)$$

To compute the coefficients ϵ_p , ϵ_{δ} and $\epsilon_{\dot{p}}$, Rodden (Reference 61) introduces an aeroelastic parameter $\frac{\partial \epsilon}{\partial L}$, which represents the twist at the wing tip corresponding to a unit rolling moment. It is an influence coefficient independent of the magnitude of the applied forces which relates the wing elastic pro-

perties with the spanwise distribution of aerodynamic load. For a given wing rigidity it is only a function of Mach number. Since load distributions are fairly constant in the subsonic and supersonic regimes, the value of $\partial\epsilon/\partial L$ can be found from a subsonic and a supersonic value and faired through the transonic region. From the computed values of $\partial\epsilon/\partial L$ the derivatives are obtained:

$$\epsilon_s = \left(\frac{\partial\epsilon}{\partial L_s} \right) C_{L_s} q S b \quad (5-260)$$

$$\epsilon_p = \left(\frac{\partial\epsilon}{\partial L_p} \right) C_{L_p} q S b \quad (5-261)$$

$$\nu = \left(\frac{\partial\epsilon}{\partial L_e} \right) (C_{L_e})_e q S b \quad (5-262)$$

The inertia coefficient ϵ_p is a constant corresponding to the given rigidity and mass distribution and is the value of tip twist for a unit rolling acceleration.

On setting $\dot{p} = 0$, the ratio of the steady rate of rolling to that of a rigid airplane is obtained

$$\frac{p}{(p)_0} = \frac{1 + \left[\frac{\partial\epsilon}{\partial L_s} (C_{L_e})_s - \frac{\partial\epsilon}{\partial L_e} (C_{L_e})_e \right] q S b}{1 + \left[\frac{\partial\epsilon}{\partial L_p} (C_{L_e})_p - \frac{\partial\epsilon}{\partial L_e} (C_{L_e})_e \right] q S b} \quad (5-263)$$

The reversal condition is obtained by the vanishing of p . From (5-263) one obtains:

$$q_{rev} = \frac{1}{S b \left[\frac{\partial\epsilon}{\partial L_e} (C_{L_e})_e - \frac{\partial\epsilon}{\partial L_s} (C_{L_e})_s \right]} \quad (5-264)$$

If the approximation (5-259) were used (5-263) is simplified into

$$\frac{p}{p_0} = 1 + \left[\frac{\partial\epsilon}{\partial L_s} - \frac{\partial\epsilon}{\partial L_p} \right] C_{L_p} q S b \quad (5-265)$$

i.e., the well known approximate formula

$$\frac{p}{p_0} = 1 - \frac{q}{q_{rev}} \quad (5-266)$$

REFERENCES

1. Schwarz, L., Berechnung der Druckverteilung einer harmonisch sich verformenden Tragfläche in ebener strömung, Luftfahrtforschung 17, pp. 379-386, (1940).
2. Theodorsen, T., General Theory of Aerodynamic Instability and the Mechanism of Flutter, NACA Report 496, (1935).
3. Karp, S. N., Shu, S. S., Weil, H., and Biot, M. A., Aerodynamics of the Oscillating Airfoil in Compressible Flow, A review prepared by Brown University Applied Math Dept. for Air Materiel Command. I. Theory, U.S. Air Force Tech. Rept. F-TR 1167-ND. II. Graphical and Numerical Data, F-TR 1195-ND (GDAM A-9-M III/II).
4. Deitzel, F.: Die Luftkräfte des harmonisch schwingenden Flügels im kompressiblen Medium bei Unterschallgeschwindigkeit (Ebene Probleme). I. Method of Computation ZWB Forsch. Ber. 1733 (1943), Air Force Translation, F-TS 506-Re (1946). II. Tables and Curves ZWB Forsch. Ber. 1733/2 (1944) Air Force Translation F-TS-948-Re.
5. Schade, T.: Numerische Lösung der Possioschen Integralgleichung der schwingenden Tragfläche in ebener Unterschallströmung ZWB, UM 3209, 3210 and 3211 (1944). Curtiss-Wright Corp. Translation N-CGD-621, 622, 623 (1946). British Translation, MAP-VG-197. Also, AVA 46/J/1 (Germany 1946). British, ARC 10,108.
6. Timman, R., van de Vooren, A. I., and Greidanus, J. H.: Aerodynamic Coefficients of an Oscillating Airfoil in Two Dimensional Subsonic Flow, Journal of Aeronautical Sciences 21, pp. 499-500, (1954).
7. Fetti, H. E.: Tables of Lift and Moment Coefficients for an Oscillating Wing-Aileron Combination in Two-Dimensional Subsonic Flow, USAF Technical Report 6085 (1951), First Supplement (1953), Supplement 1 (1954).
8. Jones, W. P., ARC 14,336 (1951) and 15,642 (1953).
9. Miles, J. W.: Quasi-Stationary Airfoil Theory in Subsonic Compressible Flow, Quarterly of Applied Mathematics 8, pp. 351-358, (1951).
10. Cicala, P.: Comparison of Theory with Experiment in the Phenomenon of Wing Flutter, NACA TR 1157 (Translated from L'Aerotechnica, 1939).
11. Lyon, H. M., Jones, W. P., and Skan, S. W.: Aerodynamical Derivatives of Flexural-Torsional Flutter of a Wing of Finite Span, ARC R and M 1900 (1939).
12. Jones, W. P., and Skan, S. W.: Methods of Calculating Derivatives for Rectangular Wings, ARC R and M 2215 (1940).
13. Jones, W. P.: Aerodynamic Forces on Wings in Simple Harmonic Motion, ARC R and M 2026 (1940).

14. Sears, W. R.: A Contribution to the Airfoil Theory for Non-Uniform Motion, Proceedings Fifth International Congress on Applied Mechanics, Cambridge: John Wiley and Sons, pp 483-487, (1938).
15. Jones, R. T.: The Unsteady Lift of a Finite Wing, NACA TN 682 (1939)(see also: Jones, R. T.: The Unsteady Lift of a Wing of Finite Aspect Ratio, Rept. 681, 1940).
16. Küssner, H. G.: General Airfoil Theory, NACA TM 979, (1941), (Translation from Luftfahrtforschung, 17 (1940), 370-378).
17. Dingel, M., and Küssner, H. G.: Contributions to NonStationary Wing Theory, VIII: The Vibrating Wing of Large Aspect Ratio, ZWB Forsch. Ber. 1774 (1943). U.S. Air Force Translation, F-TS-935-RE (1947).
18. Biot, M. A. and Boehnlein, C. T., Aerodynamic Theory of the Oscillating Wings of Finite Span, GALCIT Report Number 5, Pasadena: California Institute of Technology, (1942).
19. Wasserman, L. S., Aspect Ratio Corrections in Flutter Calculations, USAF AMC Report MCREXA 5-4595-8-5 (1948).
20. Reissner, E., Effect of Finite Span on the Airload Distributions for Oscillating Wings: I - Aerodynamic Theory of Oscillating Wings of Finite Span, NACA TN 1194 (1947).
21. Reissner, E. and Stevens, J., Effect of Finite Span on the Airload Distributions for Oscillating Wings: II-Methods of Calculation and Examples of Application, NACA TN 1195 (1947).
22. Ashley, H., Zartarian, G. and Neilson, D. O., Investigation of Certain Unsteady Aerodynamic Effects in Dynamic Longitudinal Stability, USAF Technical Report 5986, WADC, ARDC, USAF, Wright Field, Ohio, (December 1951).
23. Miles, J. W., The Application of Unsteady Flow Theory to the Calculation of Dynamic Stability Derivatives, North American Aviation Report AL-957 (1950).
24. Reissner, E., On the Theory of Oscillating Airfoils of Finite Span in Subsonic Compressible Flow, NACA Report 1002 (1950).
25. Lawrence, H. R., and Gerber, E. H., The Aerodynamic Forces on Low Aspect Ratio Wings Oscillating Wings in Compressible Flow, Journal of Aeronautical Sciences 19, pp. 769-781 (1952); Errata, ibid 20 p. 296 (1953).
26. Lawrence, H. R., The Pressure Distribution on Low Aspect Ratio Wings in Steady or Unsteady Incompressible Flow, Journal of Aeronautical Sciences 20, pp. 218-219 (1953).
27. Küssner, H. G., and Schwarz, L., The Oscillating Wing with Aerodynamically Balanced Elevator, NACA TM 991 (1941). (Translated from Luftfahrt - Forsch, 17, (1940), 337-354).

28. Watkins, C. E., Runyan, H. L., and Woolston, P. S.: On the Kernel Function of the Integral Equation Relating the Lift and Downwash Distributions of Oscillating Finite Wings in Subsonic Flow, NACA TN 3131 (1954).
29. Lance, G. N., The Kernel Function of the Integral Equation Relating the Lift and Downwash Distributions of Oscillating Finite Wings in Subsonic Flow, Journal of Aeronautical Sciences 21, pp. 635-636, (1954).
30. Miles, J. W., On the Compressibility Correction for Subsonic Unsteady Flow, Journal of Aeronautical Science 17, p. 181 (1950).
31. Spielberg, I., Fettis, H. E., and Toney, H. S., Methods for Calculating the Flutter and Vibration Characteristics of Swept Wings, USAF AMC Report MCREXA 5-4595-8-4 (1948).
32. Miles, J. W., Harmonic and Transient Motion of a Swept Wing in Supersonic Flow, Journal of Aeronautical Sciences 15, pp. 343-347 (1948)
33. Hildebrand, F. J., and Reissner, E., Studies for an Aerodynamic Theory of Oscillating Sweptback Wings of Finite Span, Part III, Chance Vought Aircraft Report Number 7039 (1948).
34. Turner, M. J., Aerodynamic Theory of Oscillating Sweptback Wings, Journal of Mathematics and Physics 27, pp. 280-293 (1950).
35. Turner, J. J. and Rabinowitz, Analysis of Sweptback Wing Flutter Models, Part II - Calculation Based on Three-Dimensional Aerodynamic Theory, Chance Vought Aircraft Report Number 7955 (1949).
36. The results of Section 5.3.1, subject to the restriction of no subsonic trailing edges are given by Miles, J. W., On Harmonic Motion at Supersonic Speeds, Journal of Aeronautical Sciences 16, pp. 378-379 (1949); the extension of the result to cover subsonic trailing edges, given by the same writer, is unpublished.
37. Miles, J. W., The Aerodynamic Forces on an Oscillating Airfoil at Supersonic Speeds, Journal of Aeronautical Science 14, p. 351 (1947).
38. Ackeret, J., Luftkräfte auf Flügel, die mit grosserer als Schallgeschwindigkeit bewegt werden, Zeit. für Flugtechnik und Motorluftschiffahrt 16, pp. 72 (1925).
39. Garrick, I. E., and Rubinow, S., Theoretical Study of Air Forces on an Oscillating or Steady Thin Wing in a Supersonic Main Stream, NACA Rpt. 872, (1947).
40. Puckett, A. E., Supersonic Wave Drag of Thin Airfoils, Journal of Aeronautical Sciences 13, pp. 475-484 (1946).
41. Miles, J. W., On Non-Steady Motion of Delta Wings, Journal of Aeronautical Sciences 16, pp. 568-569, (1949).
42. Miles, J. W., On Simple Planforms in Supersonic Flow, Journal of Aeronautical Sciences 17, p. 127 (1950).

43. Walsh, J., Zartarian, G. and Voss, H. M., Generalized Aerodynamic Forces on the Delta Wing with Supersonic Leading Edges, Journal of Aeronautical Sciences 21, pp. 739-748, (1954).
44. Evvard, J. C., Use of Source Distributions for Evaluating Theoretical Aerodynamics of Thin Finite Wings at Supersonic Speeds, NACA Report 951, (1950).
45. Munk, M. M., The Aerodynamic Forces on Airship Hulls, NACA TR 184, (1924).
46. Jones, R. T., Properties of Low Aspect Ratio Pointed Wings at Speeds Below and Above the Speed of Sound, NACA Report 835, (1946).
47. Miles, J. W., On Non-Steady Motion of Slender Bodies, Aeronautical Quarterly 2, p. 183, (1950).
48. Ward, G. N., Supersonic Flow Past Slender Pointed Bodies, Quarterly Journal of Mechanical and Applied Mathematics 2, pp. 75-96, (1949).
49. Miles, J. W., Unsteady Supersonic Flow Past Slender Pointed Bodies, U. S. NOTS, China Lake, California Rept. TM-357, (1950); US NAVORD Rept. 2031 (1953).
50. Sacks, A. H., On Slender-Body Theory and Apparent Mass, Journal of Aeronautical Science 21, pp. 713-714, (1954).
51. Adams, M. C., and Sears, W. R., Slender Body Theory - Review and Extension, Journal of Aeronautical Science 20, pp. 85-98, (1953).
52. Miles, J. W., Unsteady Supersonic Flow, (monograph prepared for ARDC, 1954), Section 9-8.
53. von Karman, T., and Sears, W. R.; A Method for Calculation of Spanwise Lift Distribution, Northrop Aircraft, Rept. A-55, (1945).
54. Sears, W. R., A New Treatment of the Lifting Line Wing Theory, Quarterly Applied Mathematics 6, pp. 239-255, (1948).
55. Hadamard, J., Lectures on Cauchy's Problem, Yale University Press (1923).
56. Statler, I. C., The Effects of Nonstationary Aerodynamics on the Rigid Body Dynamic Stability of an Airplane, Ph.D. Thesis. California Institute of Technology (1956). Reprints available at cost by writing to Aeronautics Library, Calif. Institute of Technology, Pasadena, Calif., See also Reference 117 and 118.
57. Duncan, W. J., The Principles of the Control and Stability of Aircraft, Cambridge University Press (1952).
58. Fung, Y. C., An Introduction to the Theory of Aeroelasticity, Wiley, New York (1955).
59. Bisplinghoff, R. L., Ashley, H., and Halfman, R. L., Aeroelasticity, Addison-Wesley (1955).

60. Gates, S. B. and Lyon, H. M.: A Continuation of Longitudinal Stability and Control Analysis, Part I., General Theory, British ARC R and M 2027 (1944). Part II. Interpretation of Flight Tests, British ARC T and M 2028 (1944).
61. Rodden, W. P.: An Aeroelastic Parameter for Estimation of the Effects of Flexibility on Lateral Stability and Control of Aircraft. Journal Aero. Sci., (July 1956) 660-662.
62. Goland, M.: Stick-Fixed, Short-Period Stability Based on the Wagner Air Forces. Hans Reissner 75th Anniversary Volume. Contributions to Applied Mechanics. Edwards Bros. Ann Arbor (1949), 111-124.
63. Greenberg, H. and Sternfield, L.: A Theoretical Investigation of Longitudinal Stability of Airplane with Free Controls, Including Effect of Friction in Control System. NACA TR 791 (1944).
64. Smilg, B.: The Instability of Pitching Oscillations of an Airfoil in Subsonic Incompressible Potential Flow, J. Aero. Sci., 16, 11 (Nov. 1949), 691-697.
65. Walkowicz, T. F.: Dynamic Longitudinal Response of an Airplane at High Subsonic Mach Numbers, Sc. D. Thesis, MIT (1948).
66. Luke, Y., and Dengler, M. A.: Tables of the Theodorsen Circulation Function for Generalized Motion, J. Aero. Sci. 18 (1951) 478-483.
67. Brower, W. B. and Lassen, R. H.: Additional Values of $C(k)$, J. Aero. Sci., 20 (1953) 148-150.
68. Williams, J.: Methods of Predicting Flexure-Torsion Flutter of Cantilever Wings, British ARC R and M 1990 (1943).
69. Goland, M., Luke, Y. L. and Sacks, I.: Effects of Airplane Elasticity and Unsteady Flow on Longitudinal Stability, WADC TR 53-425 (1953).
70. Goland, M., Luke, Y. L., and Hager, R. G.: Aerodynamic Lag in Lateral Control-Free Dynamic Stability, WADC TR 54-259 (1954).
71. Garrick, I. E.: Aerodynamic Theory and its Application to Flutter. Rept Prepared for Structures and Materials Panel of AGARD, April 1, 1956. Published by NACA (1956).
72. Jones, W. P.: Summary of Formulas and Notations Used in Two-Dimensional Derivative Theory, British ARC R and M 1958 (1942).
73. Spielberg, I. N.: The Two-Dimensional Incompressible Aerodynamic Coefficients for Oscillatory Changes in Airfoil Chamber, USAF, WADC Tech. Note WCNS 52-7 (1952).
74. Duncan, W. J. and Collar, A. R.: Resistance Derivatives of Flutter Theory, Part I, ARC R and M 1500 (1932), Part II, Results for Supersonic Speeds, R and M 2130 (1944).
75. Dietze, F.: Die Luftkräfte der harmonisch schwingenden, in sich verformbaren Platte, Luftfahrt-Forsch, 16, (1939), 84-96.

76. Dietze, F.: Zum Luftkraftgesetz der harmonisch schwingenden, Knickbaren Platte, Luftfahrt-Forsch, 18 (1941), 135-141.
77. Frazer, R. A. and Skan, S. W.: A Comparison of the Observed and Predicted Flexure-Torsion Flutter Characteristics of a Tapered Model Wing, ARC R and M 1943 (1941).
78. Lyon, H. M.: A Review of Theoretical Investigations of the Aerodynamical Forces on a Wing in Non-Uniform Motion, ARC R and M 1786 (1937).
79. Kassner, R. and Fingado, H.: The Two-Dimensional Problem of Wing Vibration, J. Roy. Aeronaut. Soc. 41 (1937), 921-944.
80. Scanlan, R. H. and Rosenbaum, R.: Introduction to the Study of Aircraft Vibration and Flutter, MacMillan Co., N. Y. (1951).
81. Smilg, B., and Wasserman, L. S.: Application of Three-Dimensional Flutter Theory to Aircraft Structures. USAF Tech. Rept. 4798 (1942).
82. Luke, Y. C.: Tables of Coefficients for Compressible Flutter Calculations, USAF WADC Tech. Rept. 6200 (1950).
83. Possio, C.: L'azione aerodinamica sul profilo oscillante in un fluido compressibile a velocita iposonora, Aerotecnica, XVIII, fasc. 4. (1938) 441-458. British Air Ministry Translation 830.
84. Possio, C.: L'azione aerodinamica sul profilo oscillante alle velocita ultrasonora, Acta. Pont. Acad. Sci. 1, 11, (1937, 93-105).
85. U. S. Government Printing Office: Handbook of Supersonic Aerodynamics, Vol. 4. Aeroelastic Phenomena, NAVORD Rept. 1488 (1952).
86. Nationaal Luchtvaartlaboratorium, Amsterdam: Tables of Aerodynamic Coefficients for an Oscillating Wing-Flap System in a Subsonic Compressible Flow, Rept. F. 151 (1954).
87. Turner, M. J. and Rabinowitz, S.: Aerodynamic Coefficients for an Oscillating Airfoil with Hinged Flap, With Tables for Mach Number 0.7, NACA TN 2213 (1950).
88. Temple, G., and Jahn, H. A.: Flutter at Supersonic Speeds, I. Derivative Coefficients, ARC R and M 2140 (1945).
89. von Borbély, S.: Ueber die Luftkraefte, die auf einer harmonisch schwingenden zweidimensionalen Fluegel bei Ueber schallgeschwindigkeit wirken, Z. angew Math. u. Mech. 22 (1942) 190-205.
90. Huckel, V., and Durling, B.: Tables of Wing-Aileron Coefficients of Oscillating Airfoils for Two-dimensional Supersonic Flow, NACA TN 2055 (1950).
91. Huckel, V.: Tabulation of the f^* Functions which Occur in the Aerodynamic Theory of Oscillating Wings in Supersonic Flow, NACA TN 3606 (1956).

92. Rott, N.: Flügelschwingungsformen in ebener kompressibler potentialströmung, Z. angew. Math. Phys. I, fasc 6, (1950) 380-410.
93. Nelson, H. C. and Berman, J. H.: Calculations on the Forces and Moments for an Oscillating Wing-Aileron Combination in Two-Dimensional Potential Flow at Sonic Speed, NACA TN 2590 (1952).
94. Barmby, J. G., Cunningham, H. J. and Garrick, I. E.: Study of Effects of Sweep on the Flutter of Cantilever Wings, NACA Rept. 1014 (1951).
95. Laidlaw, W. R.: Theoretical and Experimental Pressure Distributions on Low Aspect Ratio Wings Oscillating in an Incompressible Flow, MIT Aeroelastic and Structures Lab., Rept. 51-2 (1954).
96. Lomax, H. and Sluder, L.: Chordwise and Compressibility Corrections to Slender-wing Theory, NACA TN 2295 (1951).
97. Voss, H. M. and Hassig, H. J.: Introductory Study of Flutter of Low Aspect Ratio Wings at Subsonic Speeds, MIT Aeroelastic Lab. Rept. on Contract No. (s) 51-109-c (1952).
98. Merbt, H. and Landahl, M.: Aerodynamic Forces on Oscillating Low Aspect-Ratio Wings in Compressible Flow, Swedish K.T.H. Aero TN 30, Royal Institute of Technology, Stockholm (1953).
99. Bryson, A. E.: Stability Derivatives for a Slender Missile, J. Aero. Sci., 20, 5(1953).
100. Laidlaw, W. R. and Hsu, P. T.: A Semi-Empirical Method for Determining Delta Wing Pressure Distribution in an Incompressible Flow, J. Aero. Sci. 21, 12 (1954).
101. Lomax, H., Heaslet, M. A., Fuller, F. B. and Sluder, L.: Two and Three-Dimensional Unsteady Lift Problems in High-Speed Flight, NACA Rept. 1077, (1952).
102. Mazelsky, B.: Numerical Determination of Indicial Lift of a Two-Dimensional Sinking Airfoil at Subsonic Mach Numbers from Oscillatory Lift Coefficients with Calculations for Mach Number 0.7, NACA TN 2562 (1951).
103. Mazelsky, B.: Determination of Indicial Lift and Moment of a Two-Dimensional Pitching Airfoil at Subsonic Mach Numbers from Oscillatory Coefficients with Numerical Calculations for a Mach Number of 0.7, NACA TN 2613, (1952).
104. Mazelsky, B. and Drischler, J. A.: Numerical Determination of Indicial Lift and Moment Functions for a Two-Dimensional Sinking and Pitching Airfoil at Mach Numbers 0.5 and 0.6, NACA TN 2739 (1952).
105. Biot, M. A.: Loads on a Supersonic Wing Striking a Sharp-Edged Gust, Cornell Aero. Lab. Rept. SA-247-S-7 (1948).

106. Chang, C. C.: Transient Aerodynamic Behavior of an Airfoil Due to Different Arbitrary Modes of Nonstationary Motions in a Supersonic Flow, NACA TN 2333 (1951).
107. Heaslet, M. A., Lomax, H. and Spreiter, J. R.: Linearized Compressible-Flow Theory for Sonic Flight Speeds, NACA Report 956 (1950).
108. Jones, A. L. and Alksne, A.: A Summary of Lateral-Stability Derivatives Calculated for Wing Plan Forms in Supersonic Flow, NACA Report 1052, (1951).
109. Brown, C. E. and Mac C. Adams: Damping in Pitch and Roll of Triangular Wings at Supersonic Speeds, NACA TN 1566 (1948).
110. Harmon, S. M.: Stability Derivatives of Thin Rectangular Wings at Supersonic Speeds, Wing Diagonals Ahead of Tip Mach Lines, NACA TN 1706 (1948).
111. Malvestuto, F. S. and Margolis, K.: Theoretical Stability Derivatives of Thin Sweptback Wings Tapered to a Point with Sweptback or Sweptforward Trailing Edges for a Limited Range of Supersonic Speeds, NACA TN 1761 (1949).
112. Moskowitz, B. and Moeckel, W. E.: First-Order Theory for Unsteady Motion of Thin Wings at Supersonic Speeds, NACA TN 2034 (1950).
113. Ribner, H. S.: Time-Dependent Downwash at the Tail and the Pitching Moment Due to Normal Acceleration at Supersonic Speeds, NACA TN 2042 (1950).
114. Greidanus, J. H. and Van Heemert, A.: Theory of the Oscillating Airfoil in Two-Dimensional Incompressible Flow-Part I NLL Rept. F-41 (1948).
115. Dengler, M. A., Goland, M., and Luke, Y. L.: Notes on the Calculation of the Response of Stable Aerodynamic Systems, Reader's Forum, J. Aero. Sci. 19, 3(1952).
116. Bisplinghoff, R. L., et al., An Investigation of Stresses in Aircraft Structures Under Dynamic Loading, Report of the M.I.T. Aeroelastic and Structures Research Laboratory under Contract NOa(s)-8790, 1949.
117. Statler, I. C., Derivation of Longitudinal Stability Derivatives for Subsonic Compressible Flow From Non-Stationary Flow Theory and Application to an F-80A Airplane, Cornell Aeronautical Lab. Rept. No. TB-495-F-9, March 1949.
118. Statler, I. C. and Easterbrook, M., Handbook for Computing Non-Stationary Flow Effects on Subsonic Dynamic Longitudinal Response Characteristics of an Airplane, Cornell Aeronautical Lab., Rept. No. TB-495-F-12, March 1950.
119. Garrick, I. E.: On Moving Sources in Nonsteady Aerodynamics and Kirchhoff's Formula, Proc. 1st U.S. Natl. Cong. Applied Mech., (1951), 733-740.
120. Jones, W. P.: Aerodynamic Forces on Wings in Non-Uniform Motion, ARC R and M 2117 (1945).

121. Küssner, H. G.: A General Method for Solving Problems of the Unsteady Lifting Surface Theory in the Subsonic Range, Journal Aeronautical Sci. 21, 1(1954) 17-27.
122. Küssner, H. G.: Theory of Oscillating Elliptic Wing, Air Force, Office of Scientific Research Rept. (1956).
123. Watkins, C. E., and Berman, J. H.: On the Kernel Functions of the Integral Equation Relating Lift and Downwash Distributions of Oscillating Wings in Supersonic Flow, NACA TN 3438, (1955).
124. Runyan, H. L., and Woolston, D. S.: Method for Calculating the Aerodynamic Loading on an Oscillating Finite Wing in Subsonic and Sonic Flow, NACA TN 3694 (1956).
125. Wasserman, L. S., Mykytow, W. S., and Spielberg, I. N.: Tab Flutter Theory and Applications, Air Force Tech. Rept. 5153 (1944).
126. Jones, W. P.: Aerodynamic Forces on an Oscillating Aerofoil-Aileron-Tab Combination, ARC R and M 1948 (1941).
127. Theodorsen, T. and Garrick, I. E.: Non-stationary Flow about a Wing-Aileron-Tab Combination Including Aerodynamic Balance, NACA Rept. 736 (1942).
128. Schwarz, L.: Ebene Instationaere Theorie des Tragflaechen bei Ueberschallgeschwindigkeit, Göttingen AVA B 43/J/17 (1943). Air Force Translation F-TS-934-RE.
129. Schwarz, L.: Zahlentafeln zur Luftkraftberechnung der schwingenden Tragflaechen im kompressiblen ebenen Unterschallstromung, Forsch. Ber. 1838 (1943).
130. Nelson, H. C.: Lift and Moment on Oscillating Triangular and Related Wings with Supersonic Edges, NACA TN 2494 (1951).
131. Miles, J. W.: On Harmonic Motion of Wide Delta Airfoils at Supersonic Speeds, NAVORD Rept. 1234 (June 1950) U.S. Naval Ord. Test Station.
132. Froehlich, J. E.: Non-Stationary Motion of Purely Supersonic Wings, Journal Aeronautical Sci. 18 (1951) 298-310.
133. Stewart, H. J. and Li, T. Y.: Source-Superposition Method of Solution of a Periodically Oscillating Wing at Supersonic Speed, Quart. Applied Mathematics 9, (1951), 31-45. See, However, Stewartson, Quart. J. Mech. Applied Math, 3 (1950) 182-199.
134. Li, T. Y.: Purely Rolling Oscillations of a Rectangular Wing in Supersonic Flow, Journal Aeronautical Sci. 18 (1951), 191-198.
135. Chang, C. C.: The Aerodynamic Behavior of a Harmonically Oscillating Finite Swept-Back Wing in Supersonic Flow, NACA TN 2467 (1951).
136. Watkins, C. E.: Effect of Aspect Ratio on the Air Forces and Moments of Harmonically Oscillating Thin Rectangular Wings in Supersonic Potential Flow, NACA Rept 1028 (1950).

137. Watkins, C. E., Berman, J. H.: Air Forces and Moments on Triangular and Related Wings with Subsonic Leading Edges Oscillating in Supersonic Potential Flow, NACA Rept. 1099 (1952).
138. Watkins, C. E., and Berman, J. H.: Velocity Potential and Air Forces Associated with a Triangular Wing in Supersonic Flow, with Subsonic Leading Edges, and Deforming Harmonically According to a General Quadratic Equation, NACA TN 3009 (1953).
139. Ashley, H., and Zartarian, G.: Piston Theory - A New Aerodynamic Tool for the Aeroelastician, Journal Aeronautical Sci. 23, 12(1956), 1109-1118.
140. Hayes, W. D.: On Hypersonic Similitude, Quarterly of Applied Mathematics, 5, 1, (1947), 105-106.
141. Lighthill, M. J.: Oscillating Airfoils at High Mach Number, Journal Aeronautical Sci. 20, 6(1953) 402-406.
142. Landahl, M., Mollø - Christensen, E. L. and Ashley, H.: Parametric Studies of Viscous and Nonviscous Unsteady Flows: Air Force OSR Tech. Rept. 55-13 (1955).
143. Landahl, M.: Unsteady Flow Around Thin Wings at High Mach Numbers, Air Force OSR Tech. Note 55-245 (1955).
144. Pines, S., Dugundji, J. and Neuringer, J.: Aerodynamic Flutter Derivatives for a Flexible Wing with the Subsonic Edges, Journal Aeronautical Sci. 22, 10 (1955), 693-700.
145. Weissinger, J.: The Phugoid Oscillation of the Airplane Based on Unsteady Air Forces, Forsch. Ber. 1430 (1941). U.S. Dept. Of Commerce OTS Rept. PB 24024.
146. Mollø - Christensen, E. L.: An Experimental and Theoretical Investigation of Unsteady Transonic Flow, Sc. D. Thesis MIT, May 1954.
147. Tobak, M., Reese, D. E. Jr., and Beam, B. H.: Experimental Damping in Pitch of 45° Triangular Wings, NACA RM A50J26 (1950).

NOMENCLATURE

| | |
|---------------------------------|--|
| a, b, c | = points on an airfoil as determined by the wake locations |
| a_o | = speed of sound in air |
| AR | = aspect ratio |
| b | = semi-span; airfoil semi-chord |
| b_o | = chord at midspan |
| B | = $\sqrt{M^2 - 1}$ |
| c | = chord length |
| c_l | = section lift coefficient |
| c_m | = quarter chord moment coefficient |
| C_L | = lift coefficient |
| $C(k)$ | = Theodorsen function |
| $e(x)d$ | = deflection curve |
| EI | = local bending rigidity |
| $\frac{\partial f}{\partial d}$ | = generalized rigidity constant |
| $F_1(t)$ | = generalized bending force |
| $F(k)$ | = the real part of $C(k)$ |
| g | = kernel function |
| $G(k)$ | = the imaginary part of $C(k)$ |
| h | = kernel function; bending deflection of the elastic axis, positive downward, feet |
| k | = reduced frequency |
| l | = characteristic length |
| L | = total lift per unit span, rolling moment |
| m | = mass of aircraft |
| M | = total moment per unit span; Mach number |
| p | = roll rate |
| \underline{P} | = aerodynamic influence matrix |

q = pitch rate, dynamic pressure
 r = yaw rate
 R = radius of curvature; hyperbolic distance which is a function of ξ and η .
 S = wing area; domain of integration
 u = longitudinal perturbation velocity
 U = true airspeed
 w = upwash velocity
 \bar{w} = downwash function
 x = $\frac{\xi}{b}$
 x, y, z = body axes in steady flow configuration
 y = $\beta \frac{y}{b}$
 z = normal force
 α = pitching about the elastic axis, relative to the direction of flow, positive nose up, radians; angle of attack
 β = angular deflection of aileron about aileron hinge line, relative to wing chord, positive for aileron trailing edge down, radians; sideslip angle; Prandtl-Glauert factor
 γ = complex amplitude of dimensionless pressure jump across a two-dimensional airfoil; ratio of specific heats; Euler's constant
 Γ = wing dihedral angle
 δ = angular deflection of tab relative to aileron, positive trailing edge down, radians; transverse body dimension, (for example, maximum body diameter or wing span)
 ϵ = downwash angle; twist at wing tip
 ζ = complex number representing airfoil motion
 θ = pitch angle; $\cos^{-1} \xi$
 λ = $\frac{d}{dt}$
 Λ = sweepback angle
 μ = relative density factor
 ξ, η = dimensionless coordinates, measured positive downstream

ρ_o = air density

τ = non-dimensional time parameter

$\phi = \cos^{-1} \xi'$

$\left. \begin{array}{l} \varphi_c(\tau) \\ \varphi_{c_M}(\tau) \\ \varphi_{c_q}(\tau) \\ \varphi_{c_{Mq}}(\tau) \end{array} \right\} = \text{indicial functions}$

$\varphi(h)$ = Sear's function

$\bar{\Phi}_+$ = velocity potential on the upper surface of a wing

$\bar{\Phi}(\tau)$ = Wagner's function

$\psi_c(\tau)$ = lift function

$\psi(\tau)$ = Kussner's function

ω = angular frequency

ω_f = fuselage natural frequency

Ω = independent frequency parameter

Solution of lifting line integral equations. The equation to be solved is of the form

$$g(\eta) + \frac{1}{2} \oint_{-s}^s (\eta - \eta')^{-1} \frac{d}{d\eta'} [\bar{c}(\eta') g(\eta')] d\eta' = h(\eta) \quad (1)$$

In 5.2.3 (3), e.g., $g(\eta) = f(\eta) x_0(\eta, s)$ and $h(\eta) = f(\eta)$

While in 5.2.3 (4) $g(\eta) = f(\eta) x_1(\eta, s)$ and $h(\eta)$

is given by the right hand side thereof; in both cases $\bar{c}(\eta)$ denotes the ratio of the chord at station η to the chord at $\eta = 0$.

Introducing the change of variable

$$\eta = s \cos \theta, \quad \eta' = s' \cos \theta' \quad (2)$$

it is expedient to pose the solution to (1) in the form

$$\bar{c}(\eta) g(\eta) = \sum_{n=1}^{\infty} n^{-1} a_n \sin(n\theta) \quad (3)$$

Multiplying (1) by $(2/\pi) \bar{c}(\eta) \sin(m\theta)$ and integrating over $(0, \pi)$ there results the set of simultaneous equations

$$m^{-1} a_m + \sum_{n=1}^{\infty} C_{mn} a_n = b_m \quad (4)$$

where

$$C_{mn} = \frac{1}{s} \int_0^{\pi} \frac{\bar{c}(s \cos \theta)}{\sin \theta} \sin(m\theta) \sin(n\theta) d\theta \quad (5)$$

$$b_m = \frac{2}{\pi} \int_0^{\pi} \bar{c}(s \cos \theta) h(s \cos \theta) \sin(m\theta) d\theta \quad (6)$$

In the particular case of an elliptic planform

$$\bar{c}(\eta) = [1 - (\eta/s)^2]^{-\frac{1}{2}} \quad (7)$$

(5) reduces to

$$C_{mn} = (\pi/2s) \delta_n^m \quad (8)$$

and (3), (4) and (6) yield

$$\bar{C}(s \cos \theta) B(s \cos \theta) = \frac{2}{\pi} \sum_{n=1}^{\infty} [1 + (n\pi/2s)]^{-1} \sin(n\theta) \int_0^{\pi} h(s \cos \theta') \sin(n\theta') \sin \theta' d\theta' \quad (9)$$

The exact solution (9) for an elliptic planform suggests that an approximation for non-elliptic planforms may be obtained by neglecting C_{mn} for $m \neq n$ in (4), with the end result

$$\bar{C}(s \cos \theta) B(s \cos \theta) \approx \frac{2}{\pi} \sum_{n=1}^{\infty} [1 + (n\pi/2s) \chi_n]^{-1} \sin(n\theta) \int_0^{\pi} \bar{C}(s \cos \theta') h(s \cos \theta') \sin(n\theta') d\theta' \quad (10)$$

where

$$\chi_n = \frac{2s}{\pi} C_{nn} = \frac{2}{\pi} \int_0^{\pi} \frac{\bar{C}(s \cos \theta)}{\sin \theta} \sin^2(n\theta) d\theta \quad (11)$$

The further approximation $\chi_n = 1$ may be involved for planforms that are approximately elliptic (e.g., a moderately tapered wing).

The approximation (10) may be regarded as the first step in an iterative solution of (4) following the pattern

$$m^{-1} a_m^{(r)} = [1 + m C_{mm}]^{-1} [b_m - \sum_{n=1}^{\infty} {}' C_{mn} a_n^{(r-1)}] \quad (12)$$

where r denotes the order of the iteration, and the prime on the summation indicates that the term $n = m$ is omitted. Setting $a_n^{(0)} = 0$, the first approximation is given by

$$m^{-1} a_m^{(1)} = (1 + m C_{mm})^{-1} b_m \quad (13)$$

which leads to the result (10). The approximation (13) then may be substituted in (12) to obtain $m^{-1} a_m^{(2)}$ etc.

A method of solving (1) without resorting to iteration has been set forth by von Karman and Sears (References 53 and 54).

The evaluation of the last integral of 5.2.3 (4) leads to (in addition to more elementary integrals) the consideration of the integral

$$I_n^{(a)} = \int_0^{\pi} |\cos \theta - \cos \theta'|^{-1} (\cos \theta' - \cos \theta) \cos(n\theta') d\theta' \quad (14a)$$

$$I_n^{(b)} = \int_0^\pi |\cos \theta' - \cos \theta| (\cos \theta' - \cos \theta) \cos(n\theta') \ln |\cos \theta' - \cos \theta| d\theta' \quad (14b)$$

It has been shown by Reissner and Stevens (Reference 21) that

$$I_n^{(a)} = (2/n) \sin(n\theta) \quad (15)$$

while $I_n^{(b)}$ is given by

$$I_1^{(b)} = 2 [2 \ln |\sin \theta| + \ln 2 - 1] \sin \theta - 2(\theta - \frac{\pi}{2}) \cos \theta \quad (16a)$$

$$I_2^{(b)} = [2 \ln |\sin \theta| + \ln 2 - 1] \sin(2\theta) - \frac{1}{2} \sin(2\theta) - (\theta - \frac{\pi}{2}) \cos(2\theta) \quad (16b)$$

for $n = 1$ and 2 satisfies the recursion formula

$$(1 - \frac{1}{n}) I_{n-1}^{(b)} - 2 \cos \theta I_n^{(b)} + (1 + \frac{1}{n}) I_{n+1}^{(b)} = \frac{2}{n} \left[\frac{\sin(n-1)\theta}{(n-1)} - \frac{\sin(n+1)\theta}{(n+1)} \right] \quad (16c)$$

$n = 2, 3, \dots$

for higher n .

Lifting surface integral equation for supersonic flow. The integral equation relating pressure distribution and prescribed downwash may be derived by inverting the result 5.3.3.(2), in which $-\alpha$ is replaced by the z derivative of a velocity potential, defined such that (regarding z as dimensionless for the moment)

$$-\alpha(\xi, \eta) = \Phi_z(\xi, \eta, 0) = \left. \frac{\partial}{\partial z} \Phi(\xi, \eta, z) \right|_{z=0} \quad (1)$$

$$\gamma(\xi, \eta) = 2 \left(\frac{\partial}{\partial \xi} + i k \right) \Phi(\xi, \eta, 0+) \quad (2)$$

It may be shown (Reference 39) that a valid generalization of 5.3.3 (2) is

$$\Phi(\xi, \eta, z) = -\frac{1}{\pi} \int_{z=0+} R^{-1} \exp \left[-\frac{i k M^2}{B^2} (\xi - \xi') \right] \cos \left(\frac{k M R}{B^2} \right) \Phi_z(\xi', \eta', 0) d\xi' d\eta' \quad (3)$$

where now

$$R = [(\xi - \xi')^2 - \beta^2 (\eta - \eta')^2 - \beta^2 z^2]^{\frac{1}{2}} \quad (4)$$

and the integral is carried out over every part of the plane $z = 0$ for which Φ_z has a non-vanishing value and R is real. As shown in Figure B-1, this includes points off the wing. It then follows, since Φ and Φ_z must satisfy the same, linear differential equation, that

$$\Phi_z(\xi, \eta, z) = -\frac{1}{\pi} \frac{\partial^2}{\partial z^2} \int_{z=0+} R^{-1} \exp \left[-\frac{i k M^2}{B^2} (\xi - \xi') \right] \cos \left(\frac{k M R}{B^2} \right) \Phi(\xi', \eta', 0+) d\xi' d\eta' \quad (5)$$

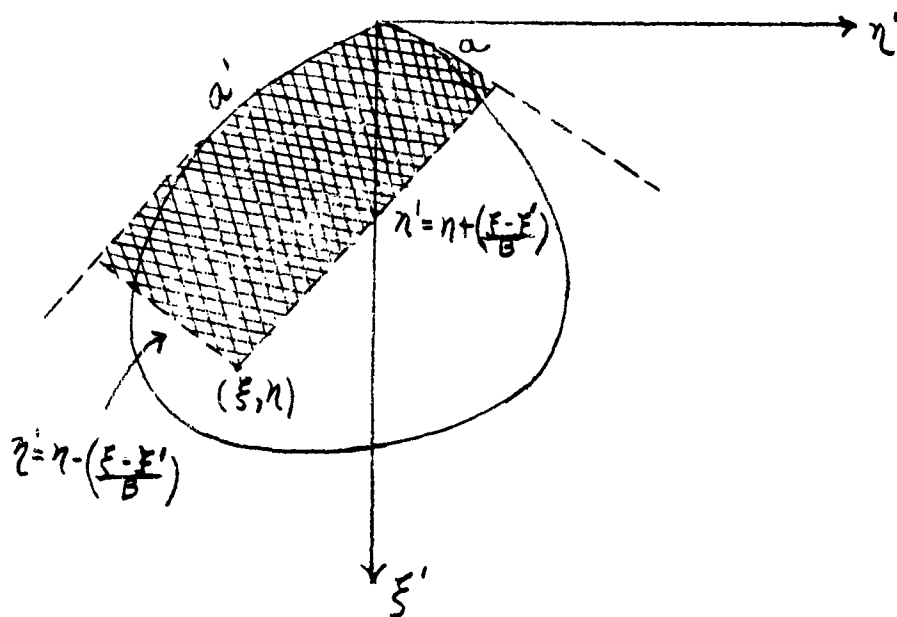


Figure B-1. The Domain of Integration for Equation (5).
The Mach Lines Springing from a and a'
Are Tangent to the Leading Edge at Those Points.

An integral equation relating the velocity potential Φ on the upper surface of the wing to the prescribed downwash then follows from the substitution of (5) in (1). If the order of differentiation and integration is formally reversed, the result may be placed in the form

$$\alpha(\xi, \eta) = \iint g(\xi - \xi', \eta - \eta') \Phi(\xi', \eta', 0+) d\xi' d\eta' \quad (\xi, \eta) \text{ on wing} \quad (6)$$

where g denotes the kernel

$$g(\xi, \eta) = \frac{1}{\pi} \exp \left[-\frac{i\pi M^2}{B^2} \right] \lim_{z \rightarrow 0} \frac{\partial^2}{\partial z^2} \left\{ \frac{\cos \left[\frac{\pi M}{B^2} \sqrt{\xi^2 - B^2(\eta^2 + z^2)} \right]}{\sqrt{\xi^2 - B^2(\eta^2 + z^2)}} \right\} \quad (7)$$

The actual evaluation of the integral (6) is complicated by the strong singularity in g , as given by (7); this difficulty may be circumvented by integration by parts or by adopting Hadamard's (Reference 53) convention of discarding the infinite part of the integral.

The region of integration for (7) comprises those portions of the plane $z = 0$ for which the radical is real and Φ does not vanish. But, in virtue of considerations of symmetry and continuity, the velocity potential $\Phi(\xi, \eta, 0+)$ must vanish over those parts of the plane $z = 0$ not occupied by the wing or its wake; accordingly, if the wing planform in question has no subsonic trailing edges, so that the wake cannot affect the wing, the result (6) is an appropriate integral equation for Φ . If (6) can be solved for Φ , the subsequent calculation of the pressure distribution follows from (2).

Those planforms having subsonic trailing edges require (6) to be modified in consequence of the fact that it becomes necessary to consider points in the wake, where α is not prescribed. It then is expedient to develop an integral equation for γ , which must vanish everywhere on $z = 0$ except across the wing alone. As a first step toward this end, Φ_+ may be expressed in terms of γ -viz.,

$$\Phi_+(\xi, \eta) = \Phi(\xi, \eta, 0_+) = \frac{1}{2} \int_0^\xi e^{iA(\xi-\xi')} \gamma(\xi', \eta) d\xi' \quad (8)$$

and substituted in (6) to obtain

$$\alpha(\xi, \eta) = \frac{1}{2} \iint B(\xi - \xi', \eta - \eta') e^{-iA\xi'} \int_0^{\xi'} e^{iA\xi} \gamma(\xi, \eta) d\xi d\xi' d\eta \quad (9)$$

Integrating (9) by parts yields

$$\alpha(\xi, \eta) = \iint h(\xi - \xi', \eta - \eta') \gamma(\xi', \eta') d\xi' d\eta' \quad (10)$$

where

$$h(\xi, \eta) = \frac{1}{2} \int_{B|\eta|}^\xi e^{-iA(\xi-\xi')} B(\xi, \eta) d\xi \quad (11)$$

The result expressed by (10) and (11) also is improper due to the implied interchange of differentiation (with respect to z) and integration, and the remarks following (7) are again pertinent.

Examples of Effects of Unsteady Flow on Airplane Dynamics

The earliest investigation of the effect of unsteady flow (as against quasi-steady flow) on airplane dynamics seems to be Weissinger's study of phugoid mode (Reference 145, 1941). He concludes that sizable error may result by the quasi-steady approximation. Goland, (Reference 62, 1949), using simplified equations of motion, and restricting attention to the longitudinal, stick-fixed, short-period mode, shows that considerable error in the calculated stability roots may result when approximations of the quasi-steady variety are made.

Other investigations lead to similar conclusions. Smilg (Reference 64) studies the one degree-of-freedom pitching instability of an aircraft and shows that the quasi-steady approach fails to disclose the presence of an instability of this kind. Walkowicz (Reference 65) studies the response of an F-80 airplane, taking into account the effect of compressibility, elastic distortions, and the unsteady flow effects, and demonstrates the importance of all these considerations in determining the stability behavior of the airplane. On the other hand, Statler, (Reference 117) reaches the conclusion that quasi-steady approximation is adequate for studying the longitudinal stability of an F-80A airplane in subsonic flight.

Statler, in a very exhaustive study (Reference 56), maintains it is dangerous to generalize the importance of aerodynamic lags on the basis of a single numerical example. So large a number of airplane parameters become intricately involved that their relative influences are practically inseparable. For F-80A airplane, which is a conventional, high-speed, straight-wing fighter, his conclusion is as follows. The long-period, stick-free modes of F-90A have reduced frequencies of the order of 0.01 - 0.02 which are comparable to the reduced frequencies of the short-period, stick-fixed modes. The dynamic similarity of these two cases is due to the fact that the elevator characteristics have very little influence in the former and do not enter at all in the latter. Although unsteady flow considerations have considerable influence on the damping of the short-period, stick-free modes, (reduced frequencies of order 0.13), apparently they have relatively little effect on the long-period, stick-free modes. The general conclusion is reached, however, that due to the relatively high frequencies involved, a precise estimate of the response of a control surface should include unsteady flow effects. Thus unsteady aerodynamics should be considered in an autopilot design, but may be neglected in the evaluation of handling characteristics and maneuverability of the airplane.

A number of examples worked out in Reference 69 by Goland, Luke, and Sacks show that unsteady flow effects do not play an important role in the stick-fixed, short-period modes. However, all the airplanes examined have well-damped stability modes. For aircraft with marginal stability, it is expected that the effect of unsteady flow will increase. An example of a tailless airplane shows the large influence of unsteady flow effects. All examples show the importance of unsteady flow effects on the longitudinal, stick-free stability modes.

Lateral dynamic stability was studied by Goland, Hager and Luke, (Reference 70). For the cases calculated it is shown that the neglect of unsteady air forces in the stick-free lateral stability analysis leads to a stability prediction that is unconservative, (the predicted stability being greater than that

found from unsteady theory). In the incompressible flight speed range the observed effects are relatively small, but the error increases with increasing rudder aerodynamic balance. It is also found that the wing contribution to the unsteady mechanism is negligible and only the quasi-steady coefficients need be considered. In the majority of the cases studied, the shift in the stability mode afforded by the inclusion of unsteady theory could be predicted from a knowledge of the shift induced in the simplified lateral systems (ψ , δ_r i.e. yaw, rudder) and (β , ψ , δ_r , side slip, yaw, rudder). At flight speeds requiring compressibility considerations similar trends are observed, but calculations indicate a substantial increase in the error resulting from the neglect of the unsteady tail admittance. The sidewash lag contributions appear unimportant in stability calculations.

The work of Ashley, Zartarian and Neilson (Reference 22) was directed at developing and applying a precise method for computing the low speed longitudinal response of an aircraft. The method was applied to twenty rigid and flexible aircraft representing a wide range of parameters. The results show that, in the short-period ranges the predictions compare well with those of simpler theory, especially for short tail lengths and large static stabilities.

CHAPTER VI

AEROELASTIC EQUATIONS OF MOTION FOR AN AIRPLANE*

6.0 Introduction

This chapter presents the derivation of the aeroelastic longitudinal equations of motion for a flexible airplane by the use of the modal approach. The modal approach is considerably shorter than the collocation approach discussed in Chapter III but may be more difficult to grasp initially. The following example demonstrates clearly how the mode shapes are used in the derivation.

6.1 Nomenclature

6.1.1 Axis System. The axis system used throughout this example is illustrated in Figure 6-1 and is called a wind axes system. The longitudinal (X) axis is fixed parallel to the relative wind when the airplane is in steady, level flight, and remains parallel to the instantaneous relative wind as the airplane oscillates. The normal (Z) axis is positive downward. The variables α , θ , γ , δ_e represent small deviations from equilibrium, as shown. For this moving axis system, the following relations exist:

$$\theta = \alpha + \gamma$$
$$\gamma = - \frac{V_z}{u}$$

6.1.2 General Assumptions. The following assumptions are made for all analyses presented herein.

1. Flight motions occur only in the XZ plane.
2. The theory of small deviations from equilibrium applies.
3. There is no variation in forward velocity during the airplane oscillations.
4. The airplane is linear in its response to control inputs.
5. The airplane is initially in trimmed, level flight.

* This example was taken from Convair Report N. FZA-36-271 entitled "An Improved Analytical Method for Predicting the Longitudinal Dynamic Response Characteristics of the B-36D Airplane and Correlations With Flight Tests", by Marx, H. F., Uchimoto, W., Zant, W. L. This report presents in detail a comparison of the results obtained from this method of analysis with the experimental results obtained during a Convair Flight Test Program. Simplifications of this type analysis are also shown (e.g., separation of equations of motion into the high frequency and low frequency portions and then linearly superimposing the results to obtain the overall response; methods for simplifying the kinetic energy expressions.).

DETAIL A

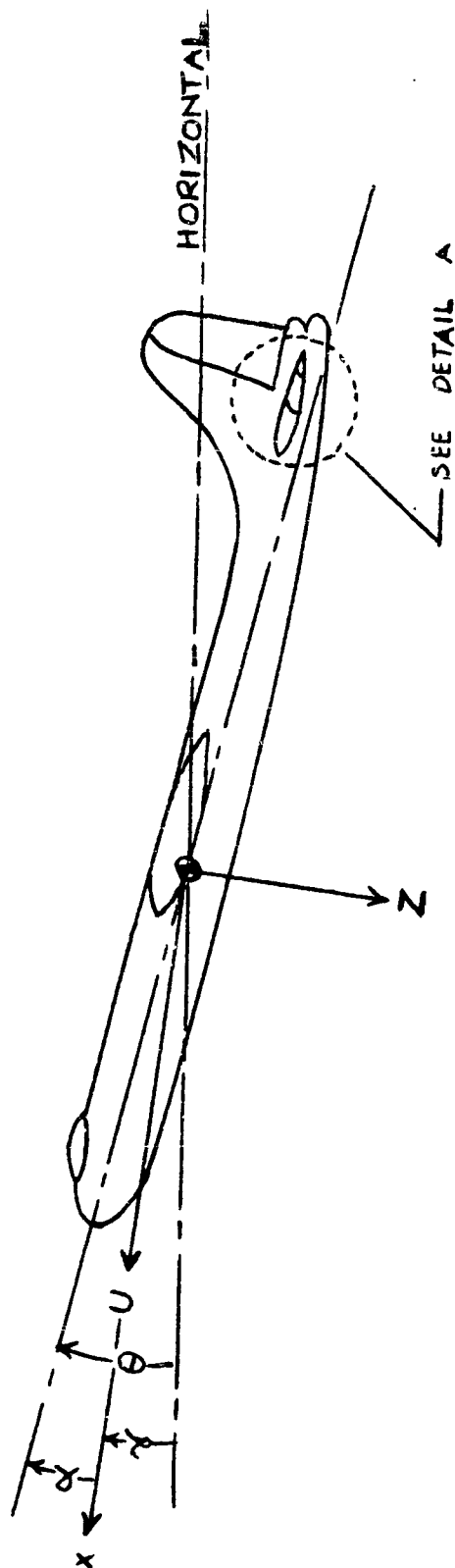
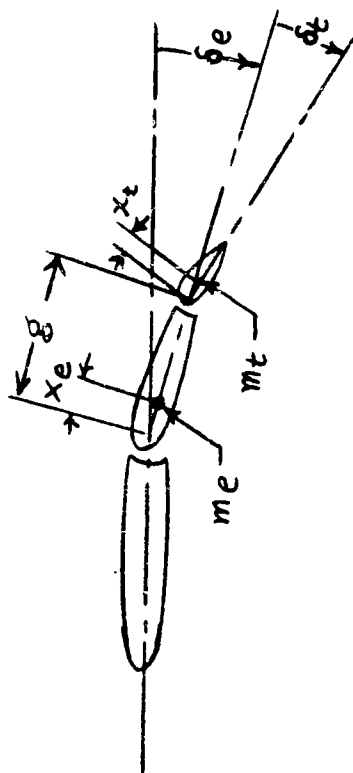


Figure 6-1. Axis System

6.1.3 List of Symbols.

| | | |
|------------|---|---|
| Z | = | vertical displacement |
| α | = | angle of attack |
| θ | = | pitch angle |
| γ | = | flight path angle |
| ξ_1 | = | normal-mode coordinate, normalized on wing tip deflection |
| ξ_2 | = | normal-mode coordinate, normalized on wing tip deflection |
| δ_e | = | elevator deflection |
| δ_t | = | tab deflection |
| Q | = | servo input = amount of input tab deflection which would result if the elevator is held fixed |
| q_i | = | i^{th} generalized coordinate |
| ρ | = | air density |
| U | = | true airspeed; potential energy |
| μ | = | relative density factor = $\frac{2M_A}{\rho S c}$ |
| t | = | time |
| k_y | = | airplane radius of gyration in pitch = $\sqrt{\frac{I_A}{M_A}}$ |
| K_y | = | reduced radius of gyration in pitch = $\frac{2k_y}{c}$ |
| S | = | number of half-chord lengths traveled in t seconds = $\frac{2U}{c} t$ |
| AR | = | amplitude ratio |
| ϕ | = | phase angle |
| D | = | $\frac{d}{dS}$ differentiation operator = $\frac{c}{2U} \frac{d}{dt}$ |

| | | |
|-------------------|---|---|
| q | = | dynamic pressure |
| q_h | = | dynamic pressure at tail |
| ω | = | frequency in rad/sec |
| ω_1 | = | natural frequency of normal mode ζ_1 , rad/sec |
| ω_2 | = | natural frequency of normal mode ζ_2 , rad/sec |
| T | = | kinetic energy |
| W | = | work |
| L | = | lift |
| P_i | = | i^{th} generalized force |
| ϵ | = | downwash angle |
| ϵ_α | = | $\frac{d\epsilon}{d\alpha}$ |
| V | = | linear velocity |
| M | = | Mach number |
| M_a | = | mass of airplane minus mass of elevator and tab |
| M_A | = | mass of airplane |
| M_{ζ_1} | = | generalized mass of airplane for normal mode ζ_1 |
| M_{ζ_2} | = | generalized mass of airplane for normal mode ζ_2 |
| m_e | = | mass of elevator |
| m_t | = | mass of tab |
| m_{f_i} | = | fuselage mass at i^{th} fuselage station |
| m_{w_j} | = | mass of j^{th} wing strip |
| m_{E_k} | = | mass of k^{th} engine |
| I_a | = | moment of inertia in pitch of that part of the airplane represented by M_a about its own c.g. |

$$\begin{aligned}
I_A &= \text{airplane moment of inertia in pitch} \\
I_e &= \text{moment of inertia of elevator about its c.g.} \\
I_t &= \text{moment of inertia of tab about its c.g.} \\
I_{vj} &= \text{moment of inertia of } j^{\text{th}} \text{ wing strip about its c.g.} \\
I_{th} &= \text{moment of inertia of tab about tab hinge line} \\
&= I_t + m_t x_t^2 \\
I_{eh'} &= I_e + m_e x_e^2 + 4I_t + m_t (g + 2x_t)^2 \\
I_e' &= I_e + m_e x_e (l_h + x_e) + 2I_t + m_t (g + 2x_t) (l_h + g + x_t) \\
I_t' &= I_{th} + m_t x_t (g + l_h + x_t) \\
I_{th}'' &= 2I_t + m_t x_t (g + 2x_t) \\
J_{\zeta_n} &= \sum_i m_{f_i} l_{f_i} \phi_{f_{ni}} + \sum_j m_{w_j} (l_{w_j} + d_{w_j}) (\phi_{w_{nj}} + d_{w_j} \psi_{w_{nj}}) \\
&\quad + \sum_j I_{w_j} \psi_{w_{nj}} + \sum_k m_{E_k} (l_{E_k} + d_{E_k}) (\phi_{E_{nk}} + d_{E_k} \psi_{E_{nk}}) \\
&\quad + I_e \psi_{T_n} + m_e \phi_{T_n}'' (l_h + x_e) + I_t \psi_{T_n} + m_t \phi_{T_n}' (l_h + g + x_t) \\
I_{\zeta_n}' &= I_e \psi_{T_n} + m_e x_e \phi_{T_n}'' + 2I_t \psi_{T_n} + m_t \phi_{T_n}' (g + 2x_t) \\
I_{t\zeta_n} &= I_t \psi_{T_n} + m_t x_t \phi_{T_n}' \\
\lambda &= m_e x_e + m_t (g + 2x_t) \\
S &= \text{wing area} \\
\Delta S_j &= \text{area of } j^{\text{th}} \text{ wing strip} \\
s_h &= \text{area of horizontal tail} \\
s_e &= \text{elevator area} \\
c &= \text{mean aerodynamic chord} \\
x_a &= \text{longitudinal distance between airplane c.g. and} \\
&\quad \text{c.g. mass } M_a, \text{ positive aft}
\end{aligned}$$

| | | |
|------------|---|--|
| x_e | = | distance from elevator hinge line to elevator c.g., positive aft |
| x_t | = | distance from tab hinge line to tab c.g., positive aft |
| g | = | distance from elevator hinge line to tab hinge line |
| c_e | = | r.m.s. elevator chord |
| l_h | = | distance between airplane c.g. and elevator hinge line |
| l_{f_i} | = | distance from airplane c.g. to i^{th} fuselage mass station |
| l_{w_j} | = | longitudinal distance from airplane c.g. to elastic axis at j^{th} wing station |
| l_{e_k} | = | longitudinal distance from airplane c.g. to wing elastic axis at k^{th} engine station |
| d_{w_j} | = | longitudinal distance from elastic axis to c.g. of j^{th} wing strip |
| d_{e_k} | = | longitudinal distance from wing elastic axis to c.g. of k^{th} engine |
| ϕ_f | = | modal fuselage linear deflection coefficient |
| ϕ_w | = | modal wing linear deflection coefficient at elastic axis |
| ϕ_E | = | modal engine linear deflection coefficient at wing elastic axis |
| ϕ_T | = | modal tail linear deflection coefficient at elevator hinge line |
| ϕ_T' | = | modal tail linear deflection coefficient at c.g. of tab mass |
| ϕ_T'' | = | modal tail linear deflection coefficient at c.g. of elevator mass |
| ψ_w | = | modal wind torsional deflection coefficient |
| ψ_T | = | modal tail angular deflection coefficient |
| ψ_N | = | modal nose angular deflection coefficient |
| ψ_E | = | modal engine angular deflection coefficient |
| C_L | = | lift coefficient = $\frac{L}{qS}$ |
| C_m | = | pitching moment coefficient = $\frac{M}{qSc}$ |

$$C_h = \text{elevator hinge moment coefficient} = \frac{\text{Elev. H. M.}}{q_h s_e c_e}$$

$$C_{h_t} = \text{tab hinge moment coefficient} = \frac{\text{Tab H.M.}}{q_h s_e c_e}$$

$$\Phi_\alpha = \sum_j \Delta S_j \phi_{w_{1j}}$$

$$\Phi_{\zeta_1} = \sum_j \Delta S_j \psi_{w_{1j}} \phi_{w_{1j}}$$

$$\Phi_{D\zeta_1} = \sum_j \Delta S_j (\phi_{w_{1j}})^2$$

$$\Phi_{\zeta_2} = \sum_j \Delta S_j \psi_{w_{2j}} \phi_{w_{1j}}$$

$$\Phi_{D\zeta_2} = \sum_j \Delta S_j \phi_{w_{2j}} \phi_{w_{1j}}$$

$$\Psi_\alpha = \sum_j \Delta S_j \phi_{w_{2j}}$$

$$\Psi_{\zeta_1} = \sum_j \Delta S_j \psi_{w_{1j}} \phi_{w_{2j}}$$

$$\Psi_{D\zeta_1} = \sum_j \Delta S_j \phi_{w_{1j}} \phi_{w_{2j}}$$

$$\Psi_{\zeta_2} = \sum_j \Delta S_j \psi_{w_{2j}} \phi_{w_{2j}}$$

$$\Psi_{D\zeta_2} = \sum_j \Delta S_j (\phi_{w_{2j}})^2$$

Subscripts

| | |
|----------------------------------|---|
| A | airplane |
| a | airplane less elevator and tab |
| h | horizontal tail |
| T | tail |
| N | nose |
| () _δ | () _{δ_e} + () _{δ_t} |
| c.g. | center of gravity |
| n | n th normal mode |
| f | fuselage |
| w | wing |
| E | engine |
| t | tab |
| i | fuselage mass stations; generalized coordinates |
| j | wing stations |
| k | engine stations |
| y | pitch axis |
| (') = $\frac{d}{dt}$ () | differentiation with respect to time, except when otherwise noted |

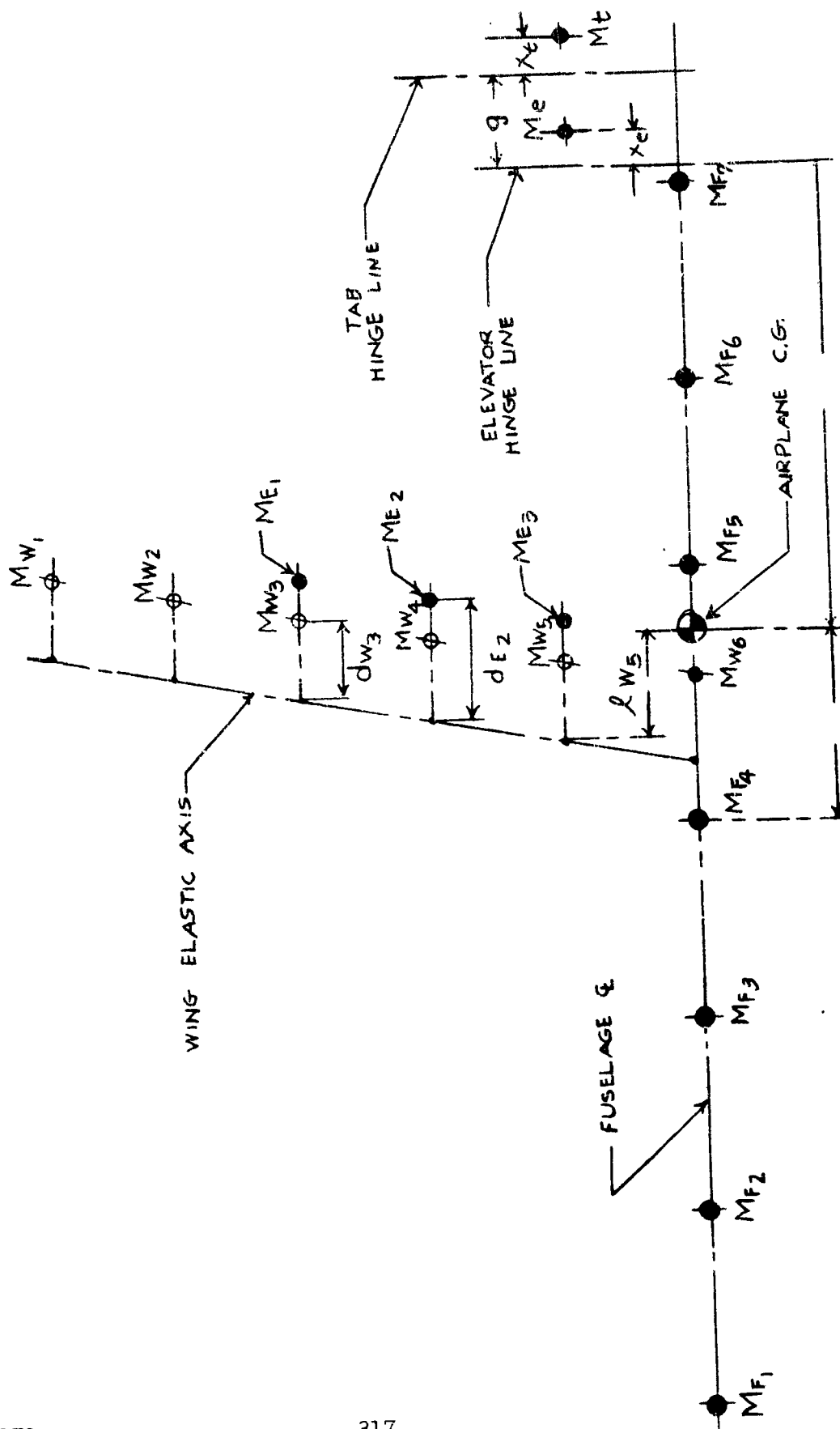


Figure 6-2. Idealized Dynamic Model

6.2 General Longitudinal Equations of Motion Including Two Normal Modes

In this section will be derived the general equations of motion for a flexible airplane, represented as a five-degree-of-freedom system. The degrees of freedom consist of the variables α , $\delta\theta$, δe , ξ_1 , and ξ_2 where ξ_1 and ξ_2 are normal coordinates representing two normal modes of vibration of the airplane. The method of Lagrange will be used to derive these equations of motion.

Symbols for the pertinent mass, inertia, and dimensional quantities are defined in the Table of Symbols.

The kinetic energy of the system may be expressed as

$$T = T_f + T_w + T_E + T_e + T_t \quad (6-1)$$

where the subscripts f, w, E*, e and t refer to fuselage, wing, engines, elevator, and tab, respectively.

By computing the angular and linear velocities of each mass element (Figure 6-1), due to all of the coordinate velocities, it is seen that

$$T_f = \frac{1}{2} \sum_i m_{fi} (v_z + I_{fi} \dot{\theta} + \phi_{fi} \dot{\xi}_1 + \phi_{fz_i} \dot{\xi}_2)^2 \quad (6-2)$$

$$T_w = \frac{1}{2} \sum_j m_{wj} [v_z + (I_{wj} + d_{wj}) \dot{\theta} + (\phi_{wj} + d_{wj} \psi_{wj}) \dot{\xi}_1 + (\phi_{wz_j} + d_{wj} \psi_{wz_j}) \dot{\xi}_2]^2 + \frac{1}{2} \sum_j I_{wj} (\dot{\theta} + \psi_{wj} \dot{\xi}_1 + \psi_{wz_j} \dot{\xi}_2)^2 \quad (6-3)$$

$$T_E = \frac{1}{2} \sum_K m_{EK} [v_z + (I_{EK} + d_{EK}) \dot{\theta} + (\phi_{EK} + d_{EK} \psi_{EK}) \dot{\xi}_1 + (\phi_{Ez_K} + d_{EK} \psi_{Ez_K}) \dot{\xi}_2]^2 \quad (6-4)$$

$$T_e = \frac{1}{2} I_e (\dot{\theta} + \dot{\delta e} + \psi_{T_1} \dot{\xi}_1 + \psi_{T_2} \dot{\xi}_2)^2 + \frac{1}{2} m_e [v_z + (I_h + \lambda_e) \dot{\theta} + \lambda_e \dot{\delta e} + \phi_{T_1} \dot{\xi}_1 + \phi_{T_2} \dot{\xi}_2]^2 \quad (6-5)$$

* Equation 6-4 describes an aircraft with radial engines. However for an airplane using large axial flow jets in or below the wings, the mass point approach might not be a reasonable assumption. In this case it might be necessary to also include the kinetic energy that is a function of the moment of inertia of the jet engine.

If the elevator-servo tab gear ratio is 1:1, the tab deflection may be written as

$$\delta_t = \delta_e + Q \quad (6-6)$$

where Q is the servo input. Therefore, the tab kinetic energy expression becomes

$$T_t = \frac{1}{2} I_t \left[\dot{\theta} + 2 \dot{\delta}_e + \dot{Q} + \psi_{T_1} \dot{s}_1 + \psi_{T_2} \dot{s}_2 \right]^2 \quad (6-7)$$

$$+ \frac{1}{2} m_t \left[v_z + (1_h + \delta + \chi_t) \dot{\theta} + (\delta + 2\chi_t) \dot{\delta}_e + \chi_t \dot{Q} + \phi'_{T_1} \dot{s}_1 + \phi'_{T_2} \dot{s}_2 \right]^2$$

The analysis proceeds by expanding the quadratic factors in Equations (6-2) through (6-7), substituting the results into (6-1) and collecting coefficients of all the resulting terms.

It is noted that all cross-product terms involving products of the normal coordinate derivatives (\dot{s}_1, \dot{s}_2) vanish from the final kinetic energy expression Equation (6-1) because of the orthogonality condition which exists between the two normal coordinates; that is,

$$\sum_i [m_i \phi_{1i} \phi_{2i} + m_i d_i \phi_{1i} \psi_{2i} + m_i d_i \psi_{1i} \phi_{2i} + I_i \psi_{1i} \psi_{2i}] = 0 \quad (6-8)$$

where the summation process is performed over all the mass elements comprising the airplane.

The kinetic energy expression then becomes

$$T = \frac{1}{2} v_z^2 \left[\sum_i m_{f_i} + \sum_j m_{w_j} + \sum_k m_{E_k} + m_e + m_t \right] \quad (6-9)$$

$$+ \frac{1}{2} \dot{\theta}^2 \left[\sum_i m_{f_i} I_{f_i}^2 + \sum_j m_{w_j} (I_{w_j} + d_{w_j})^2 + \sum_j I_{w_j} + I_t \right]$$

Note: Equation (6-9) is continued on the next page.

$$\begin{aligned}
& + I_e + \sum_K m_{EK} (1_{EK} + d_{EK})^2 + m_e (1_h + x_e)^2 + m_t (1_h + g + x_t)^2 \Big] \\
& + \frac{1}{2} \sum_{n=1}^2 \dot{\gamma}_n^2 \left[\sum_i m_{fi} \phi_{fni}^2 + \sum_j m_{wj} (\phi_{wnj} + d_{wj} \psi_{wnj})^2 + \sum_j I_{wj} \psi_{wnj}^2 \right. \\
& + \sum_K m_{EK} (\phi_{EnK} + d_{EK} \psi_{EnK})^2 + I_e \psi_{Tn}^2 + m_e \phi_{Tn}''^2 + I_t \psi_{Tn}^2 + m_t \phi_{Tn}'^2 \Big] \\
& + \frac{1}{2} \dot{\delta}_e^2 [I_e + m_e x_e^2 + 4I_t + m_t (g + 2x_t)^2] + \frac{1}{2} \dot{Q}^2 [I_t + m_t x_t^2] \\
& + V_z \dot{\theta} \left[\sum_i m_{fi} 1_{fi} + \sum_j m_{wj} (1_{wj} + d_{wj}) + \sum_K m_{EK} (1_{EK} + d_{EK}) + m_e (1_h + x_e) \right. \\
& + m_t (1_h + g + x_t) \Big] + V_z \sum_{n=1}^2 \dot{\gamma}_n \left[\sum_i m_{fi} \phi_{fni} + \sum_j m_{wj} (\phi_{wnj} + d_{wj} \psi_{wnj}) \right. \\
& + \sum_K m_{EK} (\phi_{EnK} + d_{EK} \psi_{EnK}) + m_e \phi_{Tn}'' + m_t \phi_{Tn}' \Big] + \dot{\theta} \sum_{n=1}^2 \dot{\gamma}_n \left[\sum_i m_{fi} 1_{fi} \phi_{fni} \right. \\
& + \sum_j m_{wj} (1_{wj} + d_{wj}) (\phi_{wnj} + d_{wj} \psi_{wnj}) + \sum_j I_{wj} \psi_{wnj} + I_e \psi_{Tn} \\
& + \sum_K m_{EK} (1_{EK} + d_{EK}) (\phi_{EnK} + d_{EK} \psi_{EnK}) + m_e \phi_{Tn}'' (1_h + x_e) + I_t \psi_{Tn} \\
& \left. + m_t \phi_{Tn}' (1_h + g + x_t) \right]
\end{aligned}$$

Note: Equation (6-9) is continued on the next page.

$$\begin{aligned}
& + \dot{\theta} \dot{\delta}_e \left[I_e + m_e x_e (1_h + x_e) + 2I_t + m_t (g + 2x_t) (1_h + g + x_t) \right] \\
& + \dot{\delta}_e \sum_{n=1}^2 \ddot{\zeta}_n \left[I_e \psi_{Tn} + m_e x_e \phi_{Tn}'' + 2I_t \psi_{Tn} + m_t \phi_{Tn}' (g + 2x_t) \right] \\
& + V_z \dot{\delta}_e \left[m_e x_e + m_t (g + 2x_t) \right] + \dot{\theta} \dot{Q} \left[I_t + m_t x_t (1_h + g + x_t) \right] \\
& + \dot{\delta}_e \dot{Q} \left[2I_t + m_t x_t (g + 2x_t) \right] + \dot{Q} \sum_{n=1}^2 \dot{\zeta}_n \left[I_t \psi_{Tn} + m_t x_t \phi_{Tn}' \right] + V_z \dot{Q} \left[m_t x_t \right] \quad (6-9)
\end{aligned}$$

Scrutiny of the coefficients in Equation (6-9) reveals the following:

| | |
|--|--|
| Coefficient of $\frac{1}{2} V_z^2$ | = mass of entire airplane = M_A |
| Coefficient of $\frac{1}{2} \dot{\theta}^2$ | = pitching moment of inertia of airplane about its c.g. = I_A |
| Coefficient of $\frac{1}{2} \dot{\zeta}_n^2$ | = generalized mass of n^{th} mode = M_{ζ_n} |
| Coefficient of $V_z \dot{\theta}$ | = \sum static mass moments about airplane c.g. |
| | = 0, by definition of c.g. |
| Coefficient of $V_z \dot{\zeta}_n$ | = summation of mass times linear deflection, in n^{th} mode, performed over entire airplane |
| | = 0 for each of the "n" normal modes |

If the following symbolic notations are assigned to the remaining coefficients,

$$\begin{aligned}
I'_{eh} &= \text{coefficient of } \frac{1}{2} \dot{\delta}_e^2 \\
I_{th} &= \text{coefficient of } \frac{1}{2} \dot{Q}^2
\end{aligned}$$

$$\begin{aligned}
J_{\dot{\varphi}_n} &= \text{coefficient of } \dot{\theta} \dot{\varphi}_n \\
I'_e &= \text{coefficient of } \dot{\theta} \dot{\delta}_e \\
I'_{\dot{\varphi}_n} &= \text{coefficient of } \dot{\delta}_e \dot{\varphi}_n \\
\lambda &= \text{coefficient of } V_z \dot{\delta}_e \\
I'_t &= \text{coefficient of } \dot{\theta} \dot{Q} \\
I''_{th} &= \text{coefficient of } \dot{\delta}_e \dot{Q} \\
I_{t\dot{\varphi}_n} &= \text{coefficient of } \dot{Q} \dot{\varphi}_n
\end{aligned}$$

then the kinetic energy expression becomes

$$\begin{aligned}
T = & \frac{1}{2} M_A V_z^2 + \frac{1}{2} I_A \dot{\theta}^2 + \frac{1}{2} M_{\varphi_1} \dot{\varphi}_1^2 + \frac{1}{2} M_{\varphi_2} \dot{\varphi}_2^2 + \frac{1}{2} I'_{en} \dot{\delta}_e^2 \\
& + \frac{1}{2} I_{tn} \dot{Q}^2 + J_{\varphi_1} \dot{\theta} \dot{\varphi}_1 + J_{\varphi_2} \dot{\theta} \dot{\varphi}_2 + I'_e \dot{\theta} \dot{\delta}_e + I_{\varphi_1} \dot{\delta}_e \dot{\varphi}_1 \\
& + I'_{\varphi_2} \dot{\delta}_e \dot{\varphi}_2 + \lambda V_z \dot{\delta}_e + I'_t \dot{\theta} \dot{Q} + I''_{th} \dot{\delta}_e \dot{Q} + I_{t\varphi_1} \dot{Q} \dot{\varphi}_1 \\
& + I_{t\varphi_2} \dot{Q} \dot{\varphi}_2 + m_t \chi_t V_z \dot{Q}
\end{aligned} \tag{6-10}$$

The potential energy of the system may be expressed as a quadratic function of the two normal mode coordinates and the natural frequencies of these modes.

$$U = \frac{1}{2} M_{\varphi_1} \omega_1^2 \varphi_1^2 + \frac{1}{2} M_{\varphi_2} \omega_2^2 \varphi_2^2 \tag{6-11}$$

Equation of Motion in Variable z:

Lagrange's equation for motion along the Z axis is

$$\frac{d}{dt} \left[\frac{\partial T}{\partial \dot{V}_z} \right] + \frac{\partial U}{\partial z} = P_z \quad (6-12)$$

From Equation (6-10)

$$\frac{d}{dt} \left[\frac{\partial T}{\partial \dot{V}_z} \right] = M_A \dot{V}_z + \lambda \ddot{\delta}_e + m_t x_t \ddot{Q} \quad (6-13)$$

But since

$$V_z = U(\alpha - \theta)$$
$$\frac{d}{dt} \left[\frac{\partial T}{\partial \dot{V}_z} \right] = M_A U(\dot{\alpha} - \dot{\theta}) + \lambda \ddot{\delta}_e + m_t x_t \ddot{Q} \quad (6-14)$$

From Equation (6-11)

$$\frac{\partial U}{\partial z} = 0 \quad (6-15)$$

The generalized force P_z is the work done by the aerodynamic forces in a virtual displacement Δz .

That is, $\Delta W = L \Delta z$ (6-16)

and $P_z = \frac{\Delta W}{\Delta z} = L$

where L represents small changes in lift from that at the equilibrium condition.

$$\Delta W = \left[\frac{\partial L}{\partial \alpha} \alpha + \frac{\partial L}{\partial \dot{\alpha}} \dot{\alpha} + \frac{\partial L}{\partial \theta} \theta + \frac{\partial L}{\partial \beta_1} \beta_1 + \frac{\partial L}{\partial \dot{\beta}_1} \dot{\beta}_1 + \frac{\partial L}{\partial \beta_2} \beta_2 + \right. \\ \left. \frac{\partial L}{\partial \dot{\beta}_2} \dot{\beta}_2 + \frac{\partial L}{\partial \delta_e} \delta_e + \frac{\partial L}{\partial \dot{\delta}_e} \dot{\delta}_e + \frac{\partial L}{\partial \delta_t} \delta_t + \frac{\partial L}{\partial \dot{\delta}_t} \dot{\delta}_t \right] \Delta z \quad (6-17)$$

Therefore

$$P_z = \frac{\partial W}{\partial z} \\ = q_s \left[C_{L_\alpha} \alpha + C_{L_{\dot{\alpha}}} \dot{\alpha} + C_{L_\theta} \theta + C_{L_{\beta_1}} \beta_1 + C_{L_{\dot{\beta}_1}} \dot{\beta}_1 + C_{L_{\beta_2}} \beta_2 + \right. \\ \left. + C_{L_{\dot{\beta}_2}} \dot{\beta}_2 + C_{L_{\delta_e}} \delta_e + C_{L_{\dot{\delta}_e}} \dot{\delta}_e + C_{L_{\delta_t}} \delta_t + C_{L_{\dot{\delta}_t}} \dot{\delta}_t \right]^* \quad (6-18)$$

It is convenient at this stage in the derivation of Equation (6-12) to define a non-dimensional time variable

$$s = \frac{2U}{c} t \quad (6-19)$$

Therefore,

$$\frac{d}{dt} = \frac{2U}{c} \frac{d}{ds} = \frac{2U}{c} D \quad (6-20)$$

* It should be noted that the rate term coefficients are equal to $\frac{2U}{c}$ times the dot derivatives.

By using this non-dimensional time variable and by substituting $\delta_t = \delta_e + Q$ in the expression for P_z the equation of motion (from Equations (6-12), (6-14), (6-15), and (6-18) becomes

$$\begin{aligned}
 & (-C_{LD\beta_1} D - C_{L\beta_1}) \beta_1 + [(2\mu - C_{LD\alpha}) D - C_{L\alpha}] \alpha - (2\mu + C_{LD\theta}) D\theta \\
 & + \left[\frac{\lambda}{9S} \left(\frac{2U}{c} \right)^2 D^2 - C_{LD\delta} D - C_{L\delta} \right] \delta_e + (-C_{LD\beta_2} D - C_{L\beta_2}) \beta_2 = \\
 & \left[\frac{m_t x_t}{9S} \left(\frac{2U}{c} \right)^2 D^2 + C_{LD\delta_t} D + C_{L\delta_t} \right] Q
 \end{aligned} \tag{6-21}$$

where

$$\mu = \frac{2MA}{\rho S c}$$

and

$$\begin{aligned}
 C_{LD\delta} &= C_{LD\delta_e} + C_{LD\delta_t} \\
 C_{L\delta} &= C_{L\delta_e} + C_{L\delta_t}
 \end{aligned}$$

Equation (6-21) may be written in simplified form by assigning symbols to the coefficients of β_1 , α , $D\theta$, δ_e , β_2 and Q as follows:

$$\begin{aligned}
 & (a_2 D + a_3) \beta_1 + (a_4 D + a_5) \alpha + (a_7) D\theta + (a_8 D^2 + a_9 D + a_{10}) \delta_e + (a_{15} D + a_{16}) \beta_2 \\
 & = (a_{11} D^2 + a_{12} D + a_{13}) Q
 \end{aligned} \tag{6-22}$$

where

$$a_2 = -C_{LD\beta_1}$$

$$a_3 = -C_{L\beta_1}$$

$$a_4 = 2\mu - C_{LD\alpha}$$

$$a_5 = -C_{L\alpha}$$

$$a_7 = -2\mu - C_{LD\theta}$$

$$a_8 = \frac{\lambda}{qS} \left(\frac{2U}{c} \right)^2$$

$$a_9 = -C_{LD\delta}$$

$$a_{10} = -C_{L\delta}$$

$$a_{11} = \frac{m_t x_t}{qS} \left(\frac{2U}{c} \right)^2$$

$$a_{12} = C_{LD\delta_t}$$

$$a_{13} = C_{L\delta_t}$$

$$a_{15} = -C_{LD\beta_2}$$

$$a_{16} = -C_{L\beta_2}$$

Equation of Motion in Variable θ ;

Lagrange's equation of motion in variable θ is

$$\frac{d}{dt} \left[\frac{\partial T}{\partial \dot{\theta}} \right] + \frac{\partial U}{\partial \theta} = P_{\theta} \quad (6-23)$$

From Equation (6-10)

$$\frac{d}{dt} \left[\frac{\partial T}{\partial \dot{\theta}} \right] = I_A \ddot{\theta} + J_{\beta_1} \ddot{\beta}_1 + J_{\beta_2} \ddot{\beta}_2 + I_e' \ddot{\delta}_e + I_t' \ddot{Q} \quad (6-24)$$

and

$$\frac{\partial U}{\partial \theta} = 0 \quad (6-25)$$

The force $P_{\theta} = \sum$ aerodynamic pitching moments about the airplane c.g.

$$= \frac{\Delta W}{\Delta \theta}$$

$$P_{\theta} = \left[c_{m_{\alpha}} \alpha + c_{m_{\dot{\alpha}}} \dot{\alpha} + c_{m_{\ddot{\alpha}}} \ddot{\alpha} + c_{m_{\delta_e}} \delta_e + c_{m_{\dot{\delta_e}}} \dot{\delta_e} + c_{m_{\ddot{\delta_e}}} (\ddot{\delta_e} + \ddot{Q}) \right. \\ \left. + c_{m_{\dot{\delta_e}}} (\dot{\delta_e} + \dot{Q}) + c_{m_{\beta_1}} \beta_1 + c_{m_{\dot{\beta}_1}} \dot{\beta}_1 + c_{m_{\beta_2}} \beta_2 + c_{m_{\dot{\beta}_2}} \dot{\beta}_2 \right] q S c \quad (6-26)$$

Upon substituting Equations (6-24), (6-25), (6-26), in (6-23) and changing to the nondimensional time variable s , the equation of motion in variable θ finally becomes

$$\begin{aligned}
& \left[\frac{J_{\beta_1}}{qSc} \left(\frac{2U}{c} \right)^2 D^2 - C_{m_{D\beta_1}} D - C_{m_{\beta_1}} \right] \beta_1 + (-C_{m_{D\alpha}} D - C_{m_{\alpha}}) \alpha \\
& + (\mu \kappa_y^2 D - C_{m_{D\theta}}) D\theta + \left[\frac{I'_e}{qSc} \left(\frac{2U}{c} \right)^2 D^2 - C_{m_{D\delta}} D - C_{m_{\delta}} \right] \delta_e \quad (6-27) \\
& + \left[\frac{J_{\beta_2}}{qSc} \left(\frac{2U}{c} \right)^2 D^2 - C_{m_{D\beta_2}} D - C_{m_{\beta_2}} \right] \beta_2 = \left[-\frac{I'_t}{qSc} \left(\frac{2U}{c} \right)^2 D^2 + C_{m_{D\delta_t}} D + C_{m_{\delta_t}} \right] Q
\end{aligned}$$

where $K_y = \frac{2}{C} \sqrt{\frac{I_A}{M_A}}$ = reduced radius of gyration in pitch.

Equation (6-27) may be written symbolically as follows:

$$\begin{aligned}
& (b_1 D^2 + b_2 D + b_3) \beta_1 + (b_4 D + b_5) \alpha + (b_6 D + b_7) D\theta + (b_8 D^2 + b_9 D + b_{10}) \delta_e \\
& + (b_{14} D^2 + b_{15} D + b_{16}) \beta_2 = (b_{11} D^2 + b_{12} D + b_{13}) Q \quad (6-28)
\end{aligned}$$

where

$$b_1 = \frac{J_{\beta_1}}{qSc} \left(\frac{2U}{c} \right)^2$$

$$b_2 = -C_{m_{D\beta_1}}$$

$$b_3 = -C_{m_{\beta_1}}$$

$$b_4 = -C_{m_{D\alpha}}$$

$$b_5 = -C_{m_{\alpha}}$$

$$b_6 = \mu \kappa_y^2$$

$$b_7 = -C_{mD\theta}$$

$$b_8 = \frac{I_e'}{q_{sc}} \left(\frac{2U}{c} \right)^2$$

$$b_9 = -C_{mD\delta}$$

$$b_{10} = -C_{m\delta}$$

$$b_{11} = -\frac{I_t'}{q_{sc}} \left(\frac{2U}{c} \right)^2$$

$$b_{12} = C_{mD\delta_t}$$

$$b_{13} = C_{m\delta_t}$$

$$b_{14} = \frac{J_{\theta}}{q_{sc}} \left(\frac{2U}{c} \right)^2$$

$$b_{15} = -C_{mD\beta_2}$$

$$b_{16} = -C_{m\beta_2}$$

Equation of Motion in Variable δ_e

Lagrange's equation for the variable δ_e is

$$\frac{d}{dt} \left[\frac{\partial T}{\partial \dot{\delta}_e} \right] + \frac{\partial U}{\partial \delta_e} = P_{\delta_e} \quad (6-29)$$

Again from Equation (6-10),

$$\frac{d}{dt} \left[\frac{\partial T}{\partial \dot{\delta}_e} \right] = I_{th}'' \ddot{\theta} + I_{eh}' \ddot{\delta}_e + I_e' \ddot{\theta} + I_{\beta_1}' \ddot{\beta}_1 + I_{\beta_2}' \ddot{\beta}_2 + \lambda U (\dot{\alpha} - \dot{\theta}) \quad (6-30)$$

and $\frac{\partial U}{\partial \delta_e} = 0 \quad (6-31)$

$$P_{\delta_e} = \frac{\Delta W}{\Delta \delta_e} = \sum \text{aerodynamic moments about the elevator hinge line.}$$

Therefore,

$$\begin{aligned} P_{\delta_e} = q_h S_e C_e \bigg[& C_{h\delta_e} \delta_e + C_{h\dot{\delta}_e} \dot{\delta}_e + C_{h\delta_t} \delta_t + C_{h\dot{\delta}_t} \dot{\delta}_t + C_{h\delta_e\delta_t} \delta_e \delta_t \\ & + C_{h\dot{\delta}_t\delta_t} \dot{\delta}_t \delta_t + C_{h\delta_e\delta_t} \delta_e \delta_t + C_{h\dot{\delta}_e\delta_t} \dot{\delta}_e \delta_t + C_{h\dot{\theta}} \dot{\theta} + C_{h\delta_e\dot{\theta}} \delta_e \dot{\theta} \\ & + C_{h\alpha} \alpha + C_{h\dot{\alpha}} \dot{\alpha} + C_{h\alpha\delta_e} \alpha \delta_e + C_{h\alpha\dot{\delta}_e} \alpha \dot{\delta}_e + C_{h\beta_1} \beta_1 + C_{h\dot{\beta}_1} \dot{\beta}_1 \\ & + C_{h\beta_1\beta_2} \beta_1 \beta_2 + C_{h\dot{\beta}_1\beta_2} \dot{\beta}_1 \beta_2 + C_{h\beta_1\dot{\beta}_2} \beta_1 \dot{\beta}_2 + C_{h\dot{\beta}_1\dot{\beta}_2} \dot{\beta}_1 \dot{\beta}_2 \bigg] \quad (6-32) \end{aligned}$$

By substituting Equations (6-30), (6-31), (6-32), into (6-29), by changing to nondimensional time variables and by collecting terms, the equation of motion in δ_e assumes the following form:

$$\left[\frac{I_{\beta_1}'}{q_h S_e C_e} \left(\frac{2U}{c} \right)^2 D^2 - (C_{hD\beta_1} + C_{h\dot{\theta}D\beta_1}) D - (C_{h\beta_1} + C_{h\dot{\theta}\beta_1}) \right] \beta_1$$

$$\begin{aligned}
& + \left[\frac{\lambda U}{q_h s_e c_e} \left(\frac{2U}{c} \right) - (C_{hD\alpha} + C_{htD\alpha}) \right] D - (C_{h\alpha} + C_{ht\alpha}) \alpha \\
& + \left[\frac{I'_e}{q_h s_e c_e} \left(\frac{2U}{c} \right)^2 D - \left\{ \frac{\lambda U}{q_h s_e c_e} \left(\frac{2U}{c} \right) + C_{hD\theta} + C_{htD\theta} \right\} \right] D\theta \\
& + \left[\frac{I'_{eh}}{q_h s_e c_e} \left(\frac{2U}{c} \right)^2 D^2 - (C_{hD\delta} + C_{htD\delta}) D - (C_{h\delta} + C_{ht\delta}) \right] \delta e \\
& + \left[\frac{I'_{s_2}}{q_h s_e c_e} \left(\frac{2U}{c} \right)^2 D^2 - (C_{hD\beta_2} + C_{htD\beta_2}) D - (C_{h\beta_2} + C_{ht\beta_2}) \right] \beta_2 \\
& = \left[-\frac{I''_{th}}{q_h s_e c_e} \left(\frac{2U}{c} \right)^2 D^2 + (C_{hD\delta_t} + C_{htD\delta_t}) D + (C_{h\delta_t} + C_{ht\delta_t}) \right] \alpha
\end{aligned} \tag{6-33}$$

Equation (6-33) may be written symbolically as follows:

$$\begin{aligned}
& (C_1 D^2 + C_2 D + C_3) \beta_1 + (C_4 D + C_5) \alpha + (C_6 D + C_7) D\theta + (C_8 D^2 + C_9 D + C_{10}) \delta e \\
& + (C_{14} D^2 + C_{15} D + C_{16}) \beta_2 = (C_{11} D^2 + C_{12} D + C_{13}) \alpha
\end{aligned} \tag{6-34}$$

where

$$C_1 = \frac{I'_{s_1}}{q_h s_e c_e} \left(\frac{2U}{c} \right)^2$$

$$C_2 = -C_{hD\beta_1} - C_{htD\beta_1}$$

$$C_3 = -C_{h\beta_1} - C_{ht\beta_1}$$

$$C_4 = \frac{\lambda U}{q_h s_e c_e} \left(\frac{2U}{c} \right) - C_{hD\alpha} - C_{htD\alpha}$$

$$C_5 = -C_{h\alpha} - C_{ht\alpha}$$

$$C_6 = \frac{I_e'}{q_h S_e C_e} \left(\frac{2U}{C} \right)^2$$

$$C_7 = - \frac{\lambda U}{q_h S_e C_e} \left(\frac{2U}{C} \right) - C_{hD\theta} - C_{htD\theta}$$

$$C_8 = \frac{I_{eh}'}{q_h S_e C_e} \left(\frac{2U}{C} \right)^2$$

$$C_9 = -C_{hD\delta} - C_{htD\delta}$$

$$C_{10} = -C_{h\delta} - C_{ht\delta}$$

$$C_{11} = - \frac{I_{th}''}{q_h S_e C_e} \left(\frac{2U}{C} \right)^2$$

$$C_{12} = C_{hD\delta_t} + C_{htD\delta_t}$$

$$C_{13} = C_{h\delta_t} + C_{ht\delta_t}$$

$$C_{14} = \frac{I_{s2}'}{q_h S_e C_e} \left(\frac{2U}{C} \right)^2$$

$$C_{15} = -C_{hD\beta_2} - C_{htD\beta_2}$$

$$C_{16} = -C_{h\beta_2} - C_{ht\beta_2}$$

Equation of Motion in Variable β_1

In the previous manner, Lagrange's equation for the variable β_1 may be written

$$\frac{d}{dt} \left[\frac{\partial T}{\partial \dot{\beta}_1} \right] + \frac{\partial U}{\partial \beta_1} = P_{\beta_1} \quad (6-35)$$

and as before, from Equation (6-10),

$$\frac{d}{dt} \left[\frac{\partial T}{\partial \dot{\beta}_1} \right] = M_{\beta_1} \ddot{\beta}_1 + J_{\beta_1} \ddot{\theta} + I_{\beta_1}' \ddot{\delta}_e + I_{t\beta_1} \ddot{Q} \quad (6-36)$$

Upon changing to non-dimensional variable s , Equation (6-36) becomes

$$\frac{d}{dt} \left[\frac{\partial T}{\partial \dot{s}_i} \right] = M_{s_i} \left(\frac{2U}{c} \right)^2 D^2 s_i + J_{s_i} \left(\frac{2U}{c} \right)^2 D^2 \theta + I'_{s_i} \left(\frac{2U}{c} \right)^2 D^2 \delta e + I_{ts_i} \left(\frac{2U}{c} \right)^2 D^2 Q \quad (6-37)$$

From Equation (6-11)

$$\frac{\partial U}{\partial s_i} = M_{s_i} \omega_i^2 s_i \quad (6-38)$$

$P_{s_i} = \frac{\Delta W}{\Delta s_i} = \sum$ aerodynamic forces associated with deflection in the s_1 coordinate.

$$\begin{aligned} P_{s_i} = q_n S_n \Phi_T, & \left[\left\{ (C_{L s_1})_T + (C_{L s_1})_{w_1} \right\} s_1 + \left\{ (C_{L D s_1})_T + (C_{L D s_1})_{w_1} \right\} D s_1 \right. \\ & + \left\{ (C_{L s_2})_T + (C_{L s_2})_{w_1} \right\} s_2 + \left\{ (C_{L D s_2})_T + (C_{L D s_2})_{w_1} \right\} D s_2 \\ & + \left\{ (1 - \epsilon_\alpha) (C_{L \alpha})_T + (C_{L \alpha})_{w_1} \right\} \alpha + (C_{L \alpha})_T D \alpha + (C_{L D \theta})_T D \theta \\ & \left. + (C_{L \delta})_T \delta e + (C_{L D \delta})_T D \delta e + (C_{L \delta t})_T Q + (C_{L D \delta t}) D Q \right] \end{aligned} \quad (6-39)$$

A detailed explanation of the above expression is given later.

Substitution of Equations (6-37), (6-38), (6-39) into Equation (6-35) yields the equation of motion in \mathcal{S}_1 , which may be symbolically written as follows:

$$(f_1 D^2 + f_2 D + f_3) \mathcal{S}_1 + (f_4 D + f_5) \alpha + (f_6 D + f_7) D\theta + (f_8 D^2 + f_9 D + f_{10}) \delta e + (f_{11} D + f_{12}) \mathcal{S}_2 = (f_{11} D^2 + f_{12} D + f_{13}) Q \quad (6-40)$$

where

$$f_1 = \frac{M \mathcal{S}_1}{q_h S_h \Phi_{T_1}} \left(\frac{2U}{c} \right)^2$$

$$f_2 = -(C_{L D \mathcal{S}_1})_T - (C_{L D \mathcal{S}_1})_{W_1}$$

$$f_3 = \frac{M \mathcal{S}_1 \omega_1^2}{q_h S_h \Phi_{T_1}} - (C_{L \mathcal{S}_1})_T - (C_{L \mathcal{S}_1})_{W_1}$$

$$f_4 = -(C_{L D \alpha})_T$$

$$f_5 = -(1 - \epsilon_\alpha) (C_{L \alpha})_T - (C_{L \alpha})_{W_1}$$

$$f_6 = \frac{J \mathcal{S}_1}{q_h S_h \Phi_{T_1}} \left(\frac{2U}{c} \right)^2$$

$$f_7 = -(C_{L D \theta})_T$$

$$f_8 = \frac{I \mathcal{S}_1'}{q_h S_h \Phi_{T_1}} \left(\frac{2U}{c} \right)^2$$

$$f_9 = -(C_{L D \delta})_T$$

$$f_{10} = -(C_{L \delta})_T$$

$$f_{11} = - \frac{I t \mathcal{S}_1}{q_h S_h \Phi_{T_1}} \left(\frac{2U}{c} \right)^2$$

$$f_{12} = (C_{L\delta_t})_T$$

$$f_{13} = (C_{L\delta_t})_T$$

$$f_{15} = -(C_{LD\beta_2})_T - (C_{LD\beta_2})_{W_1}$$

$$f_{16} = (C_{L\beta_2})_T - (C_{L\beta_2})_{W_1}$$

In a similar manner, Lagrange's equation for the β_2 coordinate is found to be of the form

$$\begin{aligned} & (g_2 D + g_3) \beta_1 + (g_4 D + g_5) \alpha + (g_6 D + g_7) D\theta + (g_8 D^2 + g_9 D + g_{10}) \delta e \\ & + (g_{14} D^2 + g_{15} D + g_{16}) \beta_2 + (g_{11} D^2 + g_{12} D + g_{13}) Q \end{aligned} \quad (6-41)$$

where

$$g_2 = -(C_{LD\beta_1})_T - (C_{LD\beta_1})_{W_2}$$

$$g_3 = -(C_{L\beta_1})_T - (C_{L\beta_1})_{W_2}$$

$$g_4 = f_4 = -(C_{LD\alpha})_T$$

$$g_5 = -(1 - \epsilon_\alpha)(C_{L\alpha})_T - (C_{L\alpha})_{W_2}$$

$$g_6 = \frac{J_{\beta_2}}{2h S_h \phi_{T_2}} \left(\frac{2U}{C} \right)^2$$

$$g_7 = f_7 = -(C_{LD\theta})_T$$

$$g_8 = \frac{I_{32}'}{q_h S_h \Phi_T} \left(\frac{2U}{c}\right)^2$$

$$g_9 = f_9 = -(C_{LD\delta})_T$$

$$g_{10} = f_{10} = -(C_{L\delta})_T$$

$$g_{11} = - \frac{I_{t2}}{q_h S_h \Phi_{T2}} \left(\frac{2U}{c}\right)^2$$

$$g_{12} = f_{12} = (C_{LD\delta_t})_T$$

$$g_{13} = f_{13} = (C_{L\delta_t})_T$$

$$g_{14} = \frac{M g_2}{q_h S_h \Phi_{T2}} \left(\frac{2U}{c}\right)^2$$

$$g_{15} = -(C_{LDg_2})_T - (C_{LDg_2})_{W2}$$

$$g_{16} = \frac{M g_2 \omega_2^2}{q_h S_h \Phi_{T2}} - (C_{Lg_2})_T - (C_{Lg_2})_{W2}$$

The final equations of motion, then, become:

$$(a_2 D + a_3) \ddot{\theta}_1 + (a_4 D + a_5) \dot{\alpha} + (a_7) D \theta + (a_8 D^2 + a_9 D + a_{10}) \delta e \\ + (a_{15} D + a_{16}) \ddot{\theta}_2 = (a_{11} D^2 + a_{12} D + a_{13}) \dot{q}$$

$$(b_1 D^2 + b_2 D + b_3) \ddot{\theta}_1 + (b_4 D + b_5) \dot{\alpha} + (b_6 D + b_7) D \theta + (b_8 D^2 + b_9 D + b_{10}) \delta e \\ + (b_{14} D^2 + b_{15} D + b_{16}) \ddot{\theta}_2 = (b_{11} D^2 + b_{12} D + b_{13}) \dot{q}$$

$$(c_1 D^2 + c_2 D + c_3) \ddot{\theta}_1 + (c_4 D + c_5) \dot{\alpha} + (c_6 D + c_7) D \theta + (c_8 D^2 + c_9 D + c_{10}) \delta e \\ + (c_{14} D^2 + c_{15} D + c_{16}) \ddot{\theta}_2 = (c_{11} D^2 + c_{12} D + c_{13}) \dot{q}$$

$$(f_1 D^2 + f_2 D + f_3) \ddot{\theta}_1 + (f_4 D + f_5) \dot{\alpha} + (f_6 D + f_7) D \theta + (f_8 D^2 + f_9 D + f_{10}) \delta e \\ + (f_{15} D^2 + f_{16}) \ddot{\theta}_2 = (f_{11} D^2 + f_{12} D + f_{13}) \dot{q}$$

$$(g_2 D + g_3) \ddot{\theta}_1 + (g_4 D + g_5) \dot{\alpha} + (g_6 D + g_7) D \theta + (g_8 D^2 + g_9 D + g_{10}) \delta e \\ + (g_{14} D^2 + g_{15} D + g_{16}) \ddot{\theta}_2 = (g_{11} D^2 + g_{12} D + g_{13}) \dot{q}$$

(6-42)

6.3 Derivation of the Generalized Forces for the Equations of Motion in ξ_1 and ξ_2 Coordinates

The generalized force for Lagrange's equations in ξ_1 , is

$$P_{\xi_1} = \frac{\partial W}{\partial \xi_1} \quad (6-43)$$

Let ΔW = incremental work done by the aerodynamic forces in a virtual displacement $\Delta \xi_1$, from the equilibrium condition.

$$\text{Then } \Delta W = L_T \phi_{T_1} \Delta \xi_1 + \left(\sum L_{wj} \phi_{w_{ij}} \right) \Delta \xi_1 \quad (6-44)$$

Then L_T = incremental lift on the horizontal tail

ϕ_{T_1} = vertical deflection of the horizontal tail (at the elevator hinge line) per unit deflection in ξ_1 (See Figure 6-3).

L_{wj} = incremental lift on the j^{th} strip of the wing.

$\phi_{w_{ij}}$ = vertical deflection of the wing elastic axis at the j^{th} strip per unit deflection in ξ_1 (See Figure 6-4).

Therefore,

$$P_{\xi_1} = L_T \phi_{T_1} + \sum_j L_{wj} \phi_{w_{ij}} \quad (6-45)$$

The lift on the horizontal tail may be expressed as follows:

$$\begin{aligned} L_T = q_h S_h & \left[(C_{L_{\xi_1}})_T \xi_1 + (C_{L_{\dot{\xi}_1}})_T \dot{\xi}_1 + (C_{L_{\xi_2}})_T \xi_2 + (C_{L_{\dot{\xi}_2}})_T \dot{\xi}_2 \right. \\ & + (C_{L_\alpha})_T (1 - \epsilon_\alpha) \alpha + (C_{L_{\dot{\alpha}}})_T \dot{\alpha} + (C_{L_\theta})_T \theta + (C_{L_{\delta_e}})_T \delta_e \\ & \left. + (C_{L_{\dot{\delta}_e}})_T \dot{\delta}_e + (C_{L_{\delta_t}})_T \delta_t + (C_{L_{\dot{\delta}_t}})_T \dot{\delta}_t \right] \end{aligned} \quad (6-46)$$

Upon changing to dimensionless time variable s and substituting $\delta_t = \delta_e + Q$ the contribution of the horizontal tail to P_{ξ_1} becomes

$$L_T \Phi_T = q_h S_h \Phi_T \left[(C_{L_{\xi_1}})_T \xi_1 + (C_{L_{D\xi_1}})_T D\xi_1 + (C_{L_{\xi_2}})_T \xi_2 + (C_{L_{D\xi_2}})_T D\xi_2 \right. \\ \left. + (C_{L_\alpha})_T (1 - \epsilon_\alpha)_\alpha + (C_{L_{D\alpha}})_T D\alpha + (C_{L_{D\theta}})_T D\theta + (C_{L_\delta})_T \delta_e \right. \\ \left. + (C_{L_{D\delta}})_T D\delta_e + (C_{L_{\delta_t}})_T Q + (C_{L_{D\delta_t}})_T DQ \right] \quad (6-47)$$

The wing contribution to the generalized force P_{ξ_1} , will be considered next.

The lift on the j^{th} strip* (Figure 6-5) of the wing may be expressed in the following manner

$$L_{Wj} = \frac{\partial L_{Wj}}{\partial \alpha} \alpha + \frac{\partial L_{Wj}}{\partial \xi_1} \xi_1 + \frac{\partial L_{Wj}}{\partial \dot{\xi}_1} \dot{\xi}_1 + \frac{\partial L_{Wj}}{\partial \xi_2} \xi_2 + \frac{\partial L_{Wj}}{\partial \dot{\xi}_2} \dot{\xi}_2 \quad (6-48)$$

Now

$$\frac{\partial L_{Wj}}{\partial \alpha} = (C_{L_\alpha})_W q \Delta S_j \quad (6-49)$$

where $(C_{L_\alpha})_W$ lift curve slope of wing

and ΔS_j area of j^{th} strip wing.

Also,

$$\frac{\partial L_{Wj}}{\partial \xi_1} = \frac{\partial L_{Wj}}{\partial \alpha_{W,j}} \cdot \frac{\partial \alpha_{W,j}}{\partial \xi_1} \quad (6-50)$$

* This is an application of strip theory and constant spanwise load distribution. However, methods for varying the spanwise loading distributions may be applied to equation (6-48).

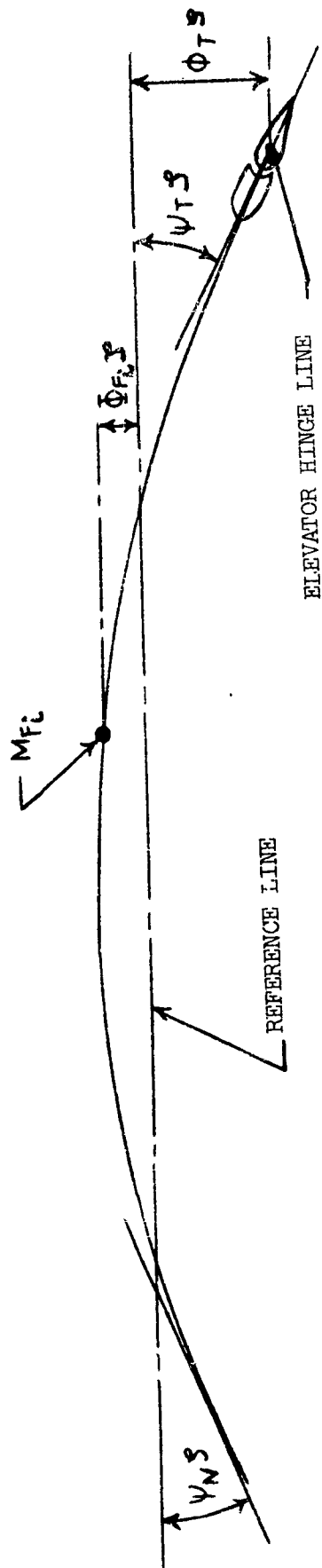
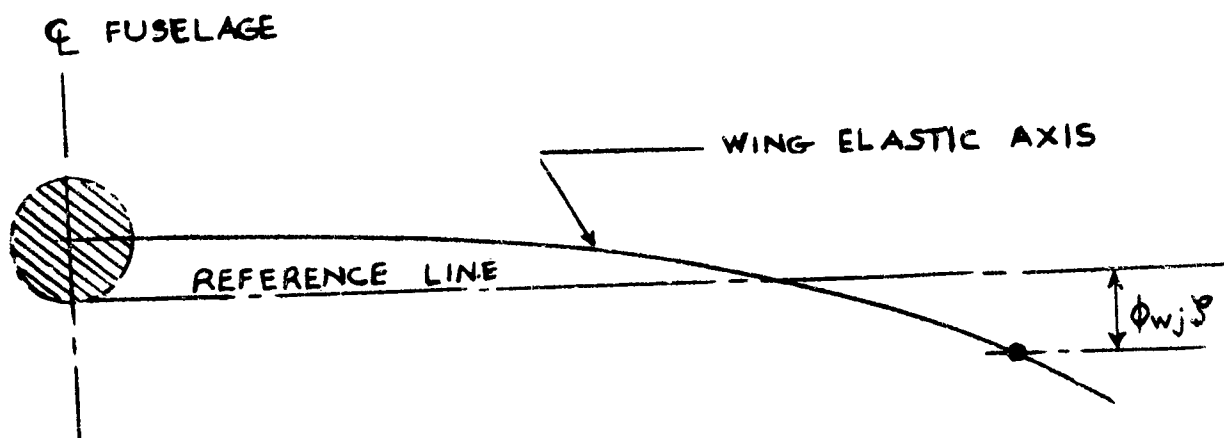
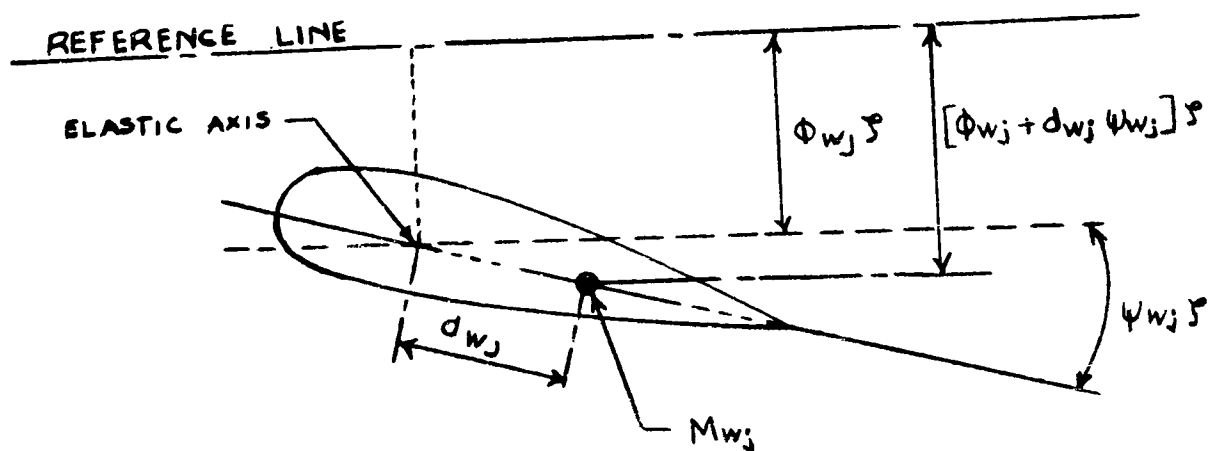


Figure 6-3. Typical Fuselage Bending Mode



TYPICAL WING BENDING MODE



WING TORSION AT TYPICAL CROSS SECTION

Figure 6-4. Wing Bending and Torsion

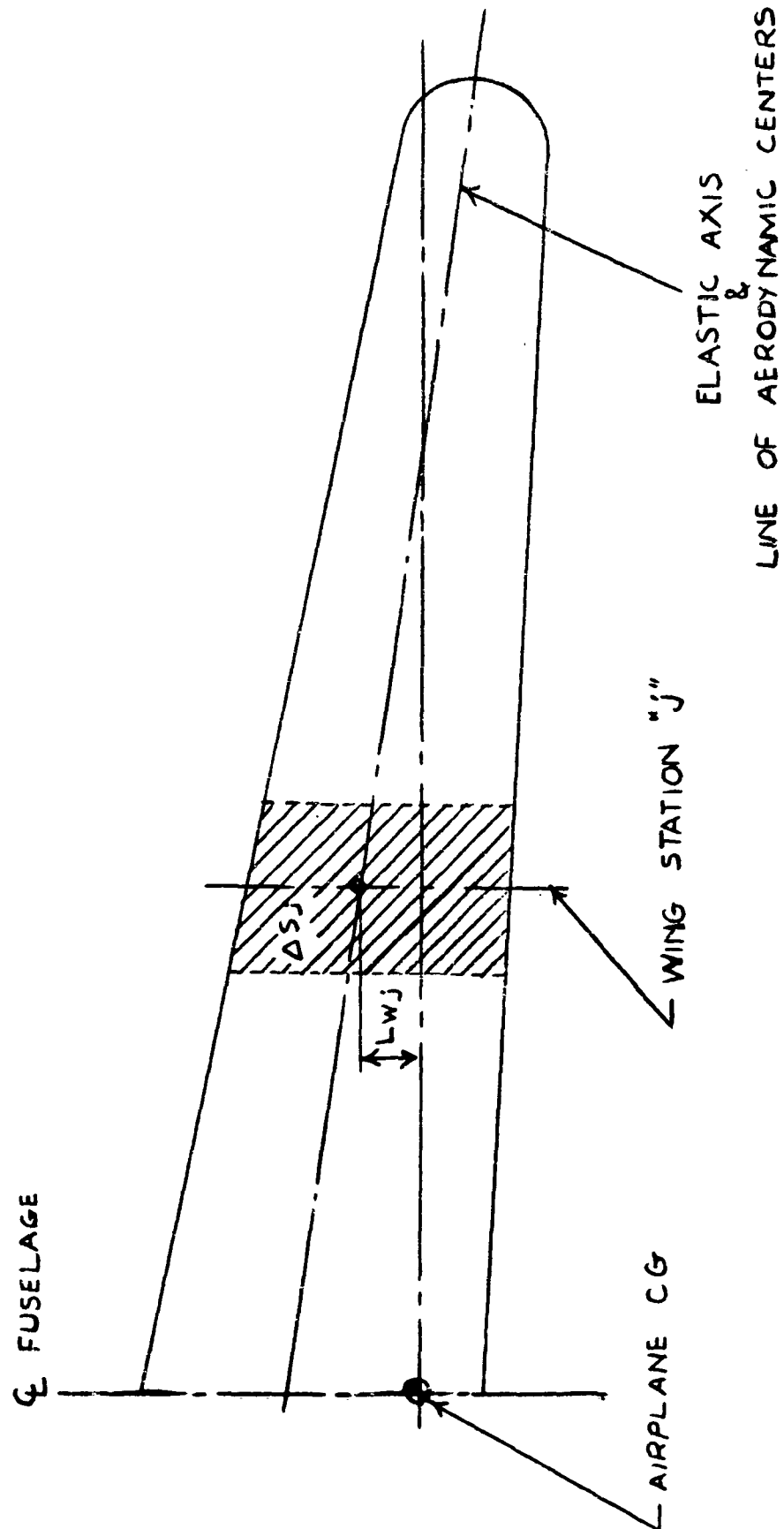


Figure 6-5. Wing Strip Theory Notation

Since

$$\alpha_{w1j} = \psi_{w1j} \dot{\xi}_1 \quad (6-51)$$

Equation (6-50) becomes

$$\frac{\partial L_{wj}}{\partial \dot{\xi}_1} = (C_{L\alpha})_w q \Delta S_j \psi_{w1j} \quad (6-52)$$

where ψ_{w1j} = change in angle of attack of the j^{th} strip of the wing (due to wing torsion) per unit deflection in ξ_1 (See Figure 6-4).

Similarly,

$$\frac{\partial L_{wj}}{\partial \dot{\xi}_2} = (C_{L\alpha})_w q \Delta S_j \psi_{w2j} \quad (6-53)$$

Next consider the damping term

$$\frac{\partial L_{wi}}{\partial \dot{\xi}_1} = \frac{\partial L_{wj}}{\partial \alpha_{w1j}} \frac{\partial \alpha'_{w1j}}{\partial \dot{\xi}_1} \quad (6-54)$$

where α'_{w1j} may be expressed as

$$\alpha'_{w1j} = \frac{\phi_{w1j} \dot{\xi}_1}{U} \quad (6-55)$$

U being the airplane forward velocity. Therefore,

$$\frac{\partial L_{wi}}{\partial \dot{\xi}_1} = (C_{L\alpha})_w q \Delta S_j \frac{\phi_{w1j}}{U} \quad (6-56)$$

By changing to non-dimensional variable s,

$$\frac{\partial L_{wi}}{\partial D \dot{\xi}_1} = \frac{2}{c} (C_{L\alpha})_w q \Delta S_j \phi_{w1j} \quad (6-57)$$

By a similar procedure, it follows that

$$\frac{\partial L_{wi}}{\partial D \dot{\xi}_2} = \frac{2}{c} (C_{L\alpha})_w q \Delta S_j \phi_{w2j} \quad (6-58)$$

From Equations (6-7), (6-10), (6-11), (6-15), and (6-16) the total incremental lift on wing section "j" becomes

$$L_{w,j} = (C_{L\alpha})_w q \left[\Delta S_j \alpha + \Delta S_j \psi_{w1,j} \beta_1 + \frac{2}{c} \Delta S_j \phi_{w1,j} D\beta_1 + \Delta S_j \psi_{w2,j} \beta_2 + \frac{2}{c} \Delta S_j \phi_{w2,j} D\beta_2 \right] \quad (6-59)$$

Hence, the wing contribution to the generalized force P_{β_1} becomes

$$\begin{aligned} \sum_j L_{w,j} \phi_{w1,j} = & (C_{L\alpha})_w q \left[\alpha \sum_j \Delta S_j \phi_{w1,j} + \beta_1 \sum_j \Delta S_j \psi_{w1,j} \phi_{w1,j} \right. \\ & + \frac{2}{c} D\beta_1 \sum_j \Delta S_j (\phi_{w1,j})^2 + \beta_2 \sum_j \Delta S_j \psi_{w2,j} \phi_{w1,j} \\ & \left. + \frac{2}{c} D\beta_2 \sum_j \Delta S_j \phi_{w2,j} \phi_{w1,j} \right] \quad (6-60) \end{aligned}$$

Or, by using symbolic notation,

$$\sum_j L_{w,j} \phi_{w1,j} = (C_{L\alpha})_w q \left[\alpha \Phi_\alpha + \beta_1 \Phi_{\beta_1} + \frac{2}{c} D\beta_1 \Phi_{D\beta_1} + \beta_2 \Phi_{\beta_2} + \frac{2}{c} D\beta_2 \Phi_{D\beta_2} \right] \quad (6-61)$$

where

$$\Phi_\alpha = \sum_j \Delta S_j \phi_{w1,j}$$

$$\Phi_{\beta_1} = \sum_j \Delta S_j \psi_{w1,j} \phi_{w1,j}$$

$$\Phi_{D\beta_1} = \sum_j \Delta S_j (\phi_{w1,j})^2$$

$$\Phi_{\beta_2} = \sum_j \Delta S_j \psi_{w2,j} \phi_{w1,j}$$

$$\Phi_{D\beta_2} = \sum_j \Delta s_j \Phi_{W_{2j}} \Phi_{W_{1j}}$$

By substituting Equation (6-5) and (6-19) into Equation (6-3) and by defining the following new dimensionless parameters,

$$(C_{L\beta_1})_{W_1} = \frac{(C_{L\alpha})_W q \Phi \beta_1}{q_h S_h \Phi_{T_1}}$$

$$(C_{LD\beta_1})_{W_1} = \frac{2(C_{L\alpha})_W q \Phi D\beta_1}{C q_h S_h \Phi_{T_1}}$$

$$(C_{L\beta_2})_{W_1} = \frac{(C_{L\alpha})_W q \Phi \beta_2}{q_h S_h \Phi_{T_1}}$$

$$(C_{LD\beta_2})_{W_1} = \frac{2(C_{L\alpha})_W q \Phi D\beta_2}{C q_h S_h \Phi_{T_1}}$$

$$(C_{L\alpha})_{W_1} = \frac{(C_{L\alpha})_W q \Phi \alpha}{q_h S_h \Phi_{T_1}}$$

The expression for P_{β_1} may finally be written as follows:

$$\begin{aligned} P_{\beta_1} = q_h S_h \Phi_{T_1} \left\{ \left[(C_{L\beta_1})_T + (C_{L\beta_1})_{W_1} \right] \beta_1 + \left[(C_{LD\beta_1})_T + (C_{LD\beta_1})_{W_1} \right] D\beta_1 \right. \\ + \left[(C_{L\beta_2})_T + (C_{L\beta_2})_{W_1} \right] \beta_2 + \left[(C_{LD\beta_2})_T + (C_{LD\beta_2})_{W_1} \right] D\beta_2 \\ + \left[(1-\epsilon_\alpha)(C_{L\alpha})_T + (C_{L\alpha})_{W_1} \right] \alpha + (C_{LD\alpha})_T D\alpha + (C_{LD\theta})_T D\theta \\ \left. + (C_{L\delta})_T \delta e + (C_{LD\delta})_T D\delta e + (C_{L\delta e})_T Q + (C_{LD\delta e})_T DQ \right\} \end{aligned}$$

(6-62)

In a similar manner, the generalized force $P_{\mathcal{Y}_2}$ for the equation of motion in \mathcal{Y}_2 coordinate is found to be

$$\begin{aligned}
 P_{\mathcal{Y}_2} = & q_h S_h \Phi_{T2} \left\{ \left[(C_{L\mathcal{Y}_1})_T + (C_{L\mathcal{Y}_1})_{W2} \right] + \left[(C_{LD\mathcal{Y}_1})_T + (C_{LD\mathcal{Y}_1})_{W2} \right] D\mathcal{Y}_1 \right. \\
 & + \left[(C_{L\mathcal{Y}_2})_T + (C_{L\mathcal{Y}_2})_{W2} \right] \mathcal{Y}_2 + \left[(C_{LD\mathcal{Y}_2})_T + (C_{LD\mathcal{Y}_2})_{W2} \right] D\mathcal{Y}_2 + (C_{LD\theta})_T D\theta \\
 & + \left[(1-\epsilon_\alpha)(C_{L\alpha})_T + (C_{L\alpha})_{W2} \right] \alpha + (C_{LD\alpha})_T D\alpha \\
 & \left. + (C_{L\delta})_T \delta e + (C_{LD\delta})_T D\delta e + (C_{L\delta t})_T Q + (C_{LD\delta t})_T DQ \right\} \quad (6-63)
 \end{aligned}$$

where

$$(C_{L\mathcal{Y}_1})_{W2} = \frac{(C_{L\alpha})_W q \Psi_{\mathcal{Y}_1}}{q_h S_h \Phi_{T2}} \quad \Psi_\alpha = \sum_j \Delta S_j \Phi_{W2j}$$

$$(C_{LD\mathcal{Y}_1})_{W2} = \frac{2(C_{L\alpha})_W q \Psi_{D\mathcal{Y}_1}}{C q_h S_h \Phi_{T2}} \quad \Psi_{\mathcal{Y}_1} = \sum_j \Delta S_j \Psi_{W1j} \Phi_{W2j}$$

$$(C_{L\mathcal{Y}_2})_{W2} = \frac{(C_{L\alpha})_W q \Psi_{\mathcal{Y}_2}}{q_h S_h \Phi_{T2}} \quad \Psi_{D\mathcal{Y}_1} = \sum_j \Delta S_j \Psi_{W1j} \Phi_{W2j}$$

$$(C_{LD\mathcal{Y}_2})_{W2} = \frac{2(C_{L\alpha})_W q \Psi_{D\mathcal{Y}_2}}{C q_h S_h \Phi_{T2}} \quad \Psi_{\mathcal{Y}_2} = \sum_j \Delta S_j \Psi_{W2j} \Phi_{W2j}$$

$$(C_{L\alpha})_{W2} = \frac{(C_{L\alpha})_W q \Psi_\alpha}{q_h S_h \Phi_{T2}} \quad \Psi_{D\mathcal{Y}_2} = \sum_j \Delta S_j (\Phi_{W2j})^2$$

6.4 Derivation of Normal Mode Derivatives

For the following derivations of the normal mode derivatives, refer to Figures 6-2, 6-3, 6-4 and 6-5.

Derivation of $C_{L\beta_1}$ and $C_{L\beta_2}$

Since

$$\alpha_{T_1} = \psi_{T_1} \beta_1 \quad (6-64)$$

$$(C_{L\beta_1})_T = (C_{L\alpha})_T \psi_{T_1} \quad (6-65)$$

and

$$C_{L\beta_1} \dot{\beta}_1 q S = (C_{L\beta_1})_T q_h S_h + \sum_j (C_{L\alpha})_w \Delta S_j q \psi_{w1j} \beta_1 \quad (6-66)$$

Therefore,

$$C_{L\beta_1} = (C_{L\beta_1})_T \frac{q_h S_h}{q S} + \frac{(C_{L\alpha})_w}{S} \sum_j \Delta S_j \psi_{w1j} \quad (6-67)$$

Similarly,

$$C_{L\beta_2} = (C_{L\beta_2})_T \frac{q_h S_h}{q S} + \frac{(C_{L\alpha})_w}{S} \sum_j \Delta S_j \psi_{w2j} \quad (6-68)$$

Derivation of $C_{L_D\dot{\beta}_1}$ and $C_{L_D\dot{\beta}_2}$:

The lift on the horizontal tail due to $\dot{\beta}_1$ is

$$(C_{L\dot{\beta}_1})_T \dot{\beta}_1 q_h S_h = (C_{L\alpha})_T \frac{(\dot{\phi}_{T_1} \dot{\beta}_1)}{U} q_h S_h \quad (6-69)$$

Therefore,

$$(C_{L\dot{y}})_T = (C_{L\alpha})_T \frac{\phi_T}{U} \quad (6-70)$$

Upon changing to dimensionless variable s , Equation (6-7) becomes

$$(C_{LD\dot{y}})_T = \frac{2}{C} (C_{L\alpha})_T \phi_T \quad (6-71)$$

The lift on the wing due to \dot{y} may be expressed as

$$(C_{L\dot{y}})_w q S \dot{y} = \sum_j (C_{L\alpha})_w q \Delta S_j \frac{\phi_{w1j} \dot{y}}{(1)} \quad (6-72)$$

Therefore,

$$(C_{L\dot{y}})_w = \frac{(C_{L\alpha})_w}{S U} \sum_j \Delta S_j \phi_{w1j} \quad (6-73)$$

By substituting dimensionless time variable s in Equation (6-10) and by combining Equations (6-8) and (6-10), the following expression for $C_{LD\dot{y}_1}$ is obtained:

$$C_{LD\dot{y}_1} = (C_{LD\dot{y}_1})_T \frac{q_b S_b}{q S} + \frac{2(C_{L\alpha})_w}{S C} \sum_j \Delta S_j \phi_{w1j} \quad (6-74)$$

Similarly,

$$C_{LD\dot{y}_2} = (C_{LD\dot{y}_2})_T \frac{q_b S_b}{q S} + \frac{2(C_{L\alpha})_w}{S C} \sum_j \Delta S_j \phi_{w2j} \quad (6-75)$$

Derivation of $C_{m\beta_1}$ and $C_{m\beta_2}$:

Pitching moment about the airplane c.g. due to tail deflection in β_1 may be expressed as

$$(C_{m\beta_1})_T q S C_{\beta_1} = (C_{L\beta_1})_T q h S_h l_h \beta_1 \quad (6-76)$$

where the lift force on the horizontal tail is considered to act at the elevator hinge line.

If the line of aerodynamic centers is practically coincident with the wing elastic axis, the wing contribution to pitching moment becomes

$$(C_{m\beta_1})_w q S C_{\beta_1} = \sum_j (C_{L\alpha})_w q \Delta S_j \psi_{w1j} l_{wj} \beta_1 \quad (6-77)$$

where l_{wj} = longitudinal distance from airplane c.g. to wing elastic axis at wing station "j" measured positive aft of c.g. (see Figure 6-5). Therefore, from Equations (6-13) and (6-14)

$$C_{m\beta_1} = (C_{L\beta_1})_T \frac{q h S_h l_h}{q S C_{\beta_1}} + \frac{(C_{L\alpha})_w}{S C_{\beta_1}} \sum_j \Delta S_j \psi_{w1j} l_{wj} \quad (6-78)$$

Likewise,

$$C_{m\beta_2} = (C_{L\beta_2})_T \frac{q h S_h l_h}{q S C_{\beta_2}} + \frac{(C_{L\alpha})_w}{S C_{\beta_2}} \sum_j \Delta S_j \psi_{w2j} l_{wj} \quad (6-79)$$

Derivation of $C_{mD} \dot{y}_1$ and $C_{mD} \dot{y}_2$:

The horizontal tail contribution to pitching moment due to \dot{y}_1 may be obtained from Equation (6-7)

$$(C_{m\dot{y}_1})_T \dot{y}_1 q S C = (C_{L\dot{y}_1})_T \dot{y}_1 q_h S_h l_h \quad (6-80)$$

and from Equation (6-9), the wing contribution becomes

$$(C_{m\dot{y}_1})_w \dot{y}_1 q S C = \sum_j (C_{L\alpha})_w q \Delta s_j \frac{(\phi_{w1j} \dot{y}_1)}{U} l_{wj} \quad (6-81)$$

By combining Equations (6-17) and (6-18) and changing to dimensionless time variable s , there results

$$C_{mD\dot{y}_1} = (C_{LD\dot{y}_1})_T \frac{q_h S_h l_h}{q S C} + \frac{2(C_{L\alpha})_w}{S C^2} \sum_j \Delta s_j l_{wj} \phi_{w1j} \quad (6-82)$$

In a similar manner,

$$C_{mD\dot{y}_2} = (C_{LD\dot{y}_2})_T \frac{q_h S_h l_h}{q S C} + \frac{2(C_{L\alpha})_w}{S C^2} \sum_j \Delta s_j l_{wj} \phi_{w2j} \quad (6-83)$$

Derivation of $C_{h\dot{y}_1}$ and $C_{h\dot{y}_2}$:

By equating hinge moment expression,

$$C_{h\dot{y}_1} \dot{y}_1 = (C_{h\alpha})_T \alpha_{T1}$$

where α_{T1} = change in angle of attack of horizontal tail due to \dot{y}_1 deflection

$$= \psi_{T1} \dot{y}_1$$

Therefore,

$$C_{h\dot{y}_1} = (C_{h\alpha})_T \psi_{T1} \quad (6-84)$$

Similarly,

$$C_{h\dot{y}_2} = (C_{h\alpha})_T \psi_{T2} \quad (6-85)$$

Derivation of $C_{hD\dot{y}_1}$ and $C_{hD\dot{y}_2}$:

Elevator hinge moment due to damping $D\dot{y}_1$ is

$$C_{hD\dot{y}_1} D\dot{y}_1 q_h S_e C_e = (C_{h\alpha})_T \alpha'_T q_h S_c C_e \quad (6-86)$$

where

$$\alpha'_T = \frac{\phi_T \dot{y}_1}{U} = \frac{2\phi_T}{C} D\dot{y}_1 \quad (6-87)$$

Thus,

$$C_{hD\dot{y}_1} = \frac{2(C_{h\alpha})_T}{C} \phi_{T1} \quad (6-88)$$

Derived in like manner,

$$C_{hD\dot{y}_2} = \frac{2(C_{h\alpha})_T}{C} \phi_{T2} \quad (6-89)$$

Summary of Normal Mode Derivatives

Let subscript $n = 1, 2$. Then,

$$(C_{L\beta_n})_T = (C_{L\alpha})_T \psi_{Tn}$$

$$C_{L\beta_n} = (C_{L\beta_n})_T \frac{q_h S_h}{q_s} + \frac{(C_{L\alpha})_w}{S} \sum_j \Delta S_j \psi_{wnj}$$

$$(C_{LD\beta_n})_T = \frac{2(C_{L\alpha})_T}{C} \phi_{Tn}$$

$$C_{LD\beta_n} = (C_{LD\beta_n})_T \frac{q_h S_h}{q_s} + \frac{2(C_{L\alpha})_w}{SC} \sum_j \Delta S_j \phi_{wnj}$$

$$C_{m\beta_n} = (C_{L\beta_n})_T \frac{q_h S_h l_h}{q_s c} + \frac{(C_{L\alpha})_w}{SC} \sum_j \Delta S_j \psi_{wnj} l_{wj}$$

$$C_{mD\beta_n} = (C_{LD\beta_n})_T \frac{q_h S_h l_h}{q_s c} + \frac{2(C_{L\alpha})_w}{SC^2} \sum_j \Delta S_j l_{wj} \phi_{wnj}$$

$$C_{h\beta_n} = (C_{h\alpha})_T \psi_{Tn}$$

$$C_{hD\beta_n} = \frac{2(C_{h\alpha})_T}{C} \phi_{Tn}$$

6.5 An Analysis of the Coupling Between An Autopilot System and Airframe Elastic Modes.*

Past experience in the field of dynamic stability of aircraft has indicated the possibility of coupling between the elastic modes (of the airframe) and the autopilot. This problem has occurred where the natural frequency of the autopilot was near the natural frequency of the first body-bending mode of the airframe. The primary medium of the coupling is through the autopilot sensing elements (accelerometers, rate gyros, and position gyros), which due to their locations pick up the body bending. The effect, on the control surfaces, of the aerodynamic forces due to elastic airframe deflections, also couples the autopilot to the bending mode, but this is usually a relatively unimportant effect.

For the longitudinal case, the aircraft rigid-body and autopilot equations are three in number (the longitudinal velocity equation is omitted, since it contributes primarily to the phugoid motion, which is too low in frequency to enter appreciably into the autopilot dynamics). The rigid-body equations may be written in body-axis form as

$$M(\dot{W} - U_0 \dot{\theta}) = Z_W W + Z_{\dot{\theta}} \dot{\theta} + Z_{\delta_e} \delta_e \quad (6-90)$$

$$I_y \ddot{\theta} = M_W W + M_{\dot{W}} \dot{W} + M_{\dot{\theta}} \dot{\theta} + M_{\delta_e} \delta_e \quad (6-91)$$

where M and I_y are the aircraft's mass and pitching moment of inertia and δ_e is the elevator input. The remaining terminology is conventional. A representative autopilot equation can be written as follows:

$$\ddot{\delta_e} + 25 \dot{\delta_e} + 1000 \delta_e = 500 \dot{\theta}_G + 3000 \theta_G \quad (6-92)$$

where θ_G and $\dot{\theta}_G$ are the pitch angle and rate registered by the autopilot sensing elements. From the autopilot equation, it can be seen that the autopilot servo natural frequency is $\omega_a^2 = 1000$ or $\omega_a = 31.63$ radians per second.

Consider, for example, bending mode data, with natural frequencies for the first two body-bending modes of 30.90 and 53.91 radians per second, respectively. The first mode frequency is too close to the autopilot frequency to be safely ignored. The elastic equations to be included in the analysis are then

$$M_1(\ddot{d}_1 + 2\zeta\omega_1\dot{d}_1 + \omega_1^2 d_1) = Q_1 \quad (6-93)$$

$$M_2(\ddot{d}_2 + 2\zeta\omega_2\dot{d}_2 + \omega_2^2 d_2) = Q_2 \quad (6-94)$$

* This example was taken from J. B. Rea Company Report No. 103 entitled "Methods for Solution of Combined Aeroelastic - Missile - Plus Autopilot Stability Problem for the RIV-A-5 Missile), by J. P. Zemlin.

where the subscripts 1 and 2 refer to the first and second body-bending modes. The generalized masses M_1 and M_2 depend on the mass distribution along the aircraft fuselage and the mode deflection curve. For the bending modes, the M_{ii} in Equation (3-7) are the lumped masses (including wings, fins, etc.) distributed along the fuselage at the stations $i = 1, 2, \dots, n$, and the c_{ik} are the relative deflections in the k^{th} mode at the stations $i = 1, 2, \dots, n$ on the normalized deflection curves. If the deflection curves are normalized at the tail so that $c_{nk} = 1.00$, for n at the tail and $k = 1$ or 2 , d_k gives the deflection at the tail in the k^{th} mode.

The generalized forces Q_k remain to be calculated. The forces acting on the aircraft (in the longitudinal case) must be properly distributed along the fuselage for this purpose. If the forces are distributed at five stations along the aircraft, these stations will be indicated by the symbols x_1, x_2, x_3, x_4 and x_5 , representing distances in feet from the aircraft's nose. These forces are functions of the local α (angle of attack), the elevator deflection δ_e , or the local angle of attack at the flap:

$$F_{x_1} = A \alpha_1$$

$$F_{x_2} = B \alpha_2$$

$$F_{x_3} = C_L \alpha_2^*$$

(6-95)

$$F_{x_4} = D \alpha_4 + E \delta_e + C_L \alpha_2^*$$

$$F_{x_5} = H \delta_e$$

The generalized force Q_k was defined as $\delta W / \delta d_k$; in words, Q_k is the work done by the forces F in a unit displacement ($d_k = 1.00$) of the k^{th} mode. Since d_k is unity, the deflection at any other station i in the k^{th} mode is merely c_{ik} , the displacement at i read off of the k^{th} mode normalized deflection curve, and the work done in this displacement by the force F_{x_1} is $F_{x_1}(c_{1k})$. The generalized force for the k^{th} mode is then

$$Q_k = F_{x_1}(c_{x_1, k}) + F_{x_2}(c_{x_2, k}) + F_{x_3}(c_{x_3, k}) + F_{x_4}(c_{x_4, k}) + F_{x_5}(c_{x_5, k}) \quad (6-96)$$

* Downwash from the flap; lag may be included by adding a term of the form $N \dot{\alpha}_2$, indicating the assumption that $\dot{\alpha}_2$ is constant over the lag interval.

Since the F_{x_i} are linear functions of α_i , δ_e , and α_2 ,

$$Q_k = f(\alpha_i, \delta_e, \alpha_2) \quad (6-97)$$

where f is a linear function. The local angle of attack α_i is in turn given in radians by

$$\alpha_i = \frac{w}{v_0} - \frac{(x_{c.g.} - x_i) \dot{\theta}}{v_0} - \sum_{k=1}^2 \frac{(c_{ik} \dot{d}_k + \lambda_{ik} d_k)}{v_0} \quad (6-98)$$

where c_{ik} is positive upward and λ_{ik} is positive in the nose up sense. (λ_{ik} is here in radians). The coefficients for the α_i are computed from Equation (6-98) and substituted in Equations (6-95), which are in turn substituted in Equation (6-96) to obtain Q_k . Q_k is then a linear function of w , $\dot{\theta}$, δ_e , d_1 , \dot{d}_1 , d_2 , \dot{d}_2 , for either k .

The rigid-body equations will also contain coupling terms from the elastic modes involving the \dot{d}_k and d_k . These terms will arise from the forces F_{x_i} including only the α_i terms of Equation (6-98)

involving the \dot{d}_k and d_k (since the forces due to w , $\dot{\theta}$, and δ_e are already included in the stability derivatives for the rigid-body equations). The normal force equation (6-90) will contain these forces, times their respective lever arms $(x_{c.g.} - x_i)$ about the aircraft c.g.

Since these coupling forces and moments are linear functions of the \dot{d}_k and d_k , equations (6-90) and (6-91) can be rewritten to include elastic mode coupling terms as follows:

$$M(\ddot{w} - v_0 \ddot{\theta}) = Z_w w + Z_{\dot{\theta}} \dot{\theta} + Z_{\delta_e} \delta_e + Z_{d_1} d_1 + Z_{\dot{d}_1} \dot{d}_1 + Z_{d_2} d_2 + Z_{\dot{d}_2} \dot{d}_2 \quad (6-99)$$

$$I_y \ddot{\theta} = M_w w + M_{\dot{w}} \dot{w} + M_{\dot{\theta}} \dot{\theta} + M_{\delta_e} \delta_e + M_{d_1} d_1 + M_{\dot{d}_1} \dot{d}_1 + M_{d_2} d_2 + M_{\dot{d}_2} \dot{d}_2 \quad (6-100)$$

where the coefficients for the last four terms in each equation are found from Equation (6-95) and (6-98) as discussed above.

The autopilot equation (6-92) will be altered by the fact that θ_G is a function of the d_k as well as of the rigid-body θ . The sensing elements are located at some station x_G on the fuselage; the pitch attitude θ_G at this station is given by

$$\theta_G = \theta + \sum_{k=1}^2 \lambda_{x_G k} d_k \quad (6-101)$$

The autopilot equation then becomes

$$\ddot{\delta}_e + 25 \dot{\delta}_e + 1000 \delta_e = 500 \left(\dot{\theta} + \sum_{k=1}^2 \lambda_{x_{\theta k}} \dot{d}_k \right) + 3000 \left(\theta + \sum_{k=1}^2 \lambda_{x_{\theta k}} d_k \right) \quad (6-102)$$

No mention has yet been made of the effects of unsteady aerodynamic flow. The rigid-body equations and generalized forces as presented are based on steady-flow aerodynamics; the possibility of unsteady flow effects affecting the stability of the system should be investigated, since relatively high frequencies are involved. The parameter of primary importance in determining the magnitude of unsteady flow effects is the "reduced frequency" $\omega c/2V$, where c is a length constant (wing chord or span), ω is the circular frequency under consideration and V is the free-stream velocity. If this parameter is sufficiently small (usually taken to mean less than 0.1) at the frequency ω , unsteady flow effects are negligible at this frequency.

CONCLUSIONS

It is probable, in view of the closeness of the body-bending and autopilot natural frequencies, that the longitudinal system would be found to be unstable, or at best marginally stable. It is of interest to consider briefly some possible system alterations. Several alternatives exist for improving the stability of the system; these possibilities include (1) relocating the gyros, (2) reducing the autopilot natural frequency, (3) filtering the gyro signals, (4) stiffening the structure, and (5) using a computing network to eliminate body flexure signals. The first possibility would involve shifting the autopilot sensing elements to a location as close as possible to a constant-slope point of the first or second body-bending modes (whichever is found to be most critical), or to a location representing some compromise between these points. This would serve to minimize the coupling, through these sensing elements, between the autopilot and the body-bending modes. Another possibility would be to reduce the autopilot natural frequency to separate more widely the resonant frequencies of the autopilot and bending modes. Alternatively, direct filtering might be used on the gyro outputs to eliminate the elastic mode frequencies from these signals. Stiffening the fuselage structure would increase the natural frequencies of the elastic modes and thereby tend to separate these frequencies from that of the autopilot. A computing network utilizing signals from strain gauges might be designed to eliminate body flexure components from the gyro signals. The use of strain gauges might seriously reduce the reliability of the system, however, and any considerable stiffening of the structure is usually extremely undesirable, since in most cases it necessitates extensive redesign of the structure itself. The use of direct filtering on the gyro outputs is somewhat impractical, since the first elastic mode natural frequency is very close to the autopilot natural frequency. The possibility of reducing the autopilot natural frequency is limited by the requirements for speed of response of the autopilot, and the possibility of moving the gyros is, of course, limited by

consideration of the available locations for these gyros. All of these possible changes could have a direct adverse effect on the overall system stability, even though the elastic coupling would be reduced.

In general it appears that the most practical possibilities are the relocation of the gyros and the reduction of the autopilot natural frequency. A combination of these two changes might turn out to be the most satisfactory solution of the problem. A final selection of changes (if any) to be made in the system would, of course, depend on the results of the analysis.

REFERENCES

1. Miles, J. W., Aeroelastic Properties of Unswept Wings, Lifting Line Theory, Northrop Aircraft Company Report GM-115(1947).
2. Ames, M. B. and Sears, R. I., Determination of Control Surface Characteristics from NACA Plain Flap and Tab Data, NACA Report 721(1941).
3. Miles, J. W., A Formulation of the Aeroelastic Problem for a Swept Wing, Northrop Aircraft Report GM-119 (1948), Journal Aeronautical Sciences, Vol. 16 pp. 477-490 (1949).
4. Aeroelastic Properties of a Swept Wing, Northrop Aircraft Report GM-103-LV(1948).
5. Diederich, F. W., and Foss, K. A., Charts and Approximate Formulas for the Estimation of Aeroelastic Effects on the Loading of Swept and Unswept Wings, NACA Report 1140(1953).
6. Foss, K. A., and Diederich, F. W., Charts and Approximate Formulas for the Estimation of Aeroelastic Effects on the Lateral Control of Swept and Unswept Wings, NACA Report 1139(1953).
7. Fung, Y. C., An Introduction to the Theory of Aeroelasticity, John Wiley, 1955.
8. Bisplinghoff, R. L., Ashley, H., Halfman, R. L., Aeroelasticity, Addison-Wesley, 1955.

CHAPTER VII

AEROELASTIC EQUATIONS OF MOTION FOR A HELICOPTER

7.0 Introduction

This chapter outlines the procedure for including elastic blade modes into the dynamical equations of the helicopter. The aeroelastic modes of the rotor blades are of special interest from a stability viewpoint, since the large distributive mass of the blade denotes an elastic system with a low natural frequency. It is possible that a coupling between the rigid body modes and the elastic blade modes could exist, but more important is the possible coupling between the elastic blade mode and any automatic control equipment. An introduction to the rigid body dynamics of the helicopter is discussed briefly in order to provide a comparison between the aeroelastic modes and the rigid body modes.

7.1 Method of Approach

The helicopter system is essentially a two-body problem; namely, the rotor and fuselage. The degrees of freedom of such a system are many. For instance, consider a single rotor helicopter to be made up of rigid members. The body has six body motions, three translational and three rotational. The rotor could have seven degrees of freedom whereby the blades are fully articulated and the rotor speed is considered to vary. This does not account for the possibilities of having more than the first harmonic present in the blade flapping and lagging motions. Furthermore, it does not consider the possible tail rotor degrees of freedom.

The technique for performing an aeroelastic study involves the superposition of elastic degrees of freedom on the rigid body motions. The helicopter equations of motion will include the first vertical bending mode of the blade. This will serve to demonstrate how other elastic modes can be included into the helicopter's dynamics. The derived mathematical model will consider a single rotor helicopter in hovering and forward flight.

7.1.1 Axis System and Coordinate System. Almost every conceivable type of axis system used in aircraft stability studies have been used in helicopter stability studies. The most widely used has been the inertial axis system; its popularity probably stems from the fact that the first stability analyses of the helicopter were made for hovering flight. The ground reference makes a very convenient setup in this particular instance. However, in forward flight the description of the helicopter's motion in a steady turn using the ground reference would be extremely difficult. The inertial axis system will be used since it will illustrate this type of axis system plus being consistent with the majority of previous work.

All forces and displacements are referred to an orthogonal coordinate system (x, y, z) which is non-rotating but translates with the undisturbed steady flight velocity of the helicopter. The hub axis system with the origin at the hub (x_0, y_0, z_0) is coincident with the inertial axes (x, y, z) when the helicopter is in the undisturbed state. The origin and the fixed coordinates are the rotor axes at time zero. The motions about the constant velocity axis system are limited to small perturbations and are represented in Figure 7-1.

7.1.2 Development of the Linear Equations for the Helicopter. Throughout this analysis the study of the helicopter dynamics will be determined by linear differential equations. The actual helicopter is a nonlinear system; however a good approximation can be obtained by linearizing the equations for small oscillations about an equilibrium position. The aerodynamic and inertial expressions for the forces and moments can be reduced to a form in which the equilibrium relationships are separated from the perturbation parts. The dependent variable is separated into two parts, a steady state component and a perturbation component. For example,

$$\mu_x = \mu_{x_0} + \bar{\mu}_x$$

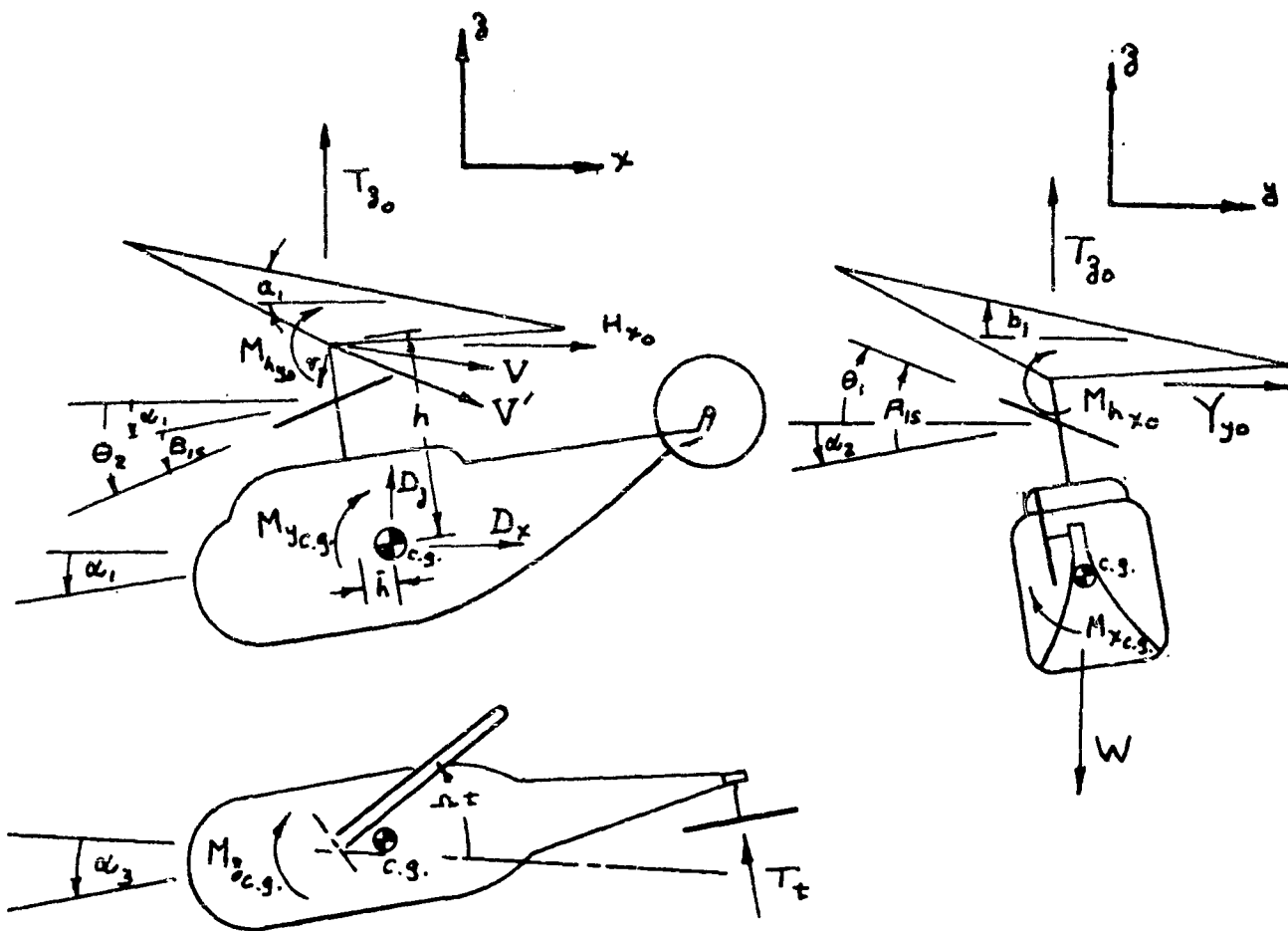
where μ_x is the dimensionless velocity component in the forward direction ($\mu_x = -\frac{\dot{x}_0}{AR}$). Having made the above type of substitutions for all the dependent variables, the "x" forces are written thusly:

$$X = X_0 + \Delta X$$

where X_0 is the equilibrium part and ΔX is the perturbation quantity.

The perturbation part will contain only first order expressions and will become the linear expression used in the stability analysis. The equilibrium expression will contain only the steady state part of the variable and the terms therein will usually be non-linear in nature. The equilibrium expression for X_0 is a performance equation from which the steady state part of the variable is specified or determined.

The rigid body motions include the degrees of freedom associated with the pitch and roll control, the rigid body modes, and the blade motion. The pitch and roll equations of the analysis are represented by eight perturbations from the steady state. These equations include the advance ratios μ_x, μ_y, μ_z the pitch and roll angles α_1 and α_2 (the yaw motion α_3 is decoupled here); the blade coning angle β_0 ; and the longitudinal and lateral inclination of the tip path plane a_1 and b_1 .



Note: Displacements, forces, and moments are all shown in positive direction.

Figure 7-1 Axis System Used for Helicopter Dynamic Analysis

Some important elastic degrees of freedoms will be considered which will include the first mode of the blade vertical bending.

Eleven equations of motion are written by applying Newton's laws of motion first to the helicopter body and then to the elastic rotor blades. Three force and two moment equations are obtained for the body motion and one force and one moment equation describe the elastic blade motions. Since all moments and forces acting on the blade are considered as harmonic functions of blade azimuth angle, every blade equation can be separated into three moment or force equations by equating like terms in the harmonic series. The basic equations of motion for a helicopter using Newton's laws are:

Body Translation

$$\sum X = \bar{m} \ddot{x}_{c.g.} \quad (7-1)$$

$$\sum Y = \bar{m} \ddot{y}_{c.g.} \quad (7-2)$$

$$\sum Z = \bar{m} \ddot{z}_{c.g.} \quad (7-3)$$

Body Rotation

$$\sum M_{y_{c.g.}} + I_y \ddot{\alpha}_1 = 0 \quad (7-4)$$

$$\sum M_{x_{c.g.}} + I_x \ddot{\alpha}_2 = 0 \quad (7-5)$$

Blade Flapping

$$(\bar{M}_y)_a + (\bar{M}_y)_m = 0 \quad (7-6)$$

Blade Vertical Bending

$$(\bar{F}_z)_a + (\bar{F}_z)_m + (\bar{F}_z)_h = 0 \quad (7-7)$$

7.1.3 Modal Analysis. The inclusion of the elastic degrees of freedom into the dynamical analysis of the helicopter can be made through the modal approach. The modes are calculated by using the methods described in Chapter IV. Each vibration mode* is treated as an individual degree of freedom. A sufficient number of modes for approximating the motion are included. The modes can represent any harmonic of a particular elastic deformation. It must be noted that the inclusion of the elastic mode into the dynamical equation cannot be treated in the same manner as the rigid body degree of freedom without making special considerations. Associated with the elastic modes are generalized displacements and forces developed through the energy approach in accordance with Lagrange's equations. The generalized force, corresponding to the generalized coordinate, h , multiplied by the increment δh of the coordinate will give the work produced by the acting forces during the displacement represented by δh . The work done by an elemental force P_i acting at a station i of a beam would be

$$\delta W = P_i c_{ih} \delta h \quad (7-8)$$

where c_{ih} is the deflection at the " i " station for a unit incremental displacement in δh . The total work produced by a unit displacement is

$$W = \sum_{i=0}^{i=N} P_i c_{ih} h(N) = P \quad (7-9)$$

where P (by definition) is the generalized force. If P_i is an elemental lift force then dF_{za} acting at station r along a helicopter blade is given

$$dF_{za} = \frac{1}{2} \rho a c \alpha v^2 dr \quad (7-10)$$

and c_{ih} is given by the blade bending mode shape $\xi(r)$ for a unit deflection at the tip $[h(R)=1]$. Then the generalized force F_z corresponding to the unit tip deflection is

$$(F_z) = \int_0^R \xi(r) dF_z \quad (7-11)$$

* The vibration mode refers to the elastic mode of oscillation. For a hinged blade the non-cyclic, rigid body motion of the blade is referred to as the steady flapping, β_0 . The first mode for such a blade is then that which corresponds to a vibration of one mode and so on.

If the blade bending forces are defined as generalized forces and are developed in the above manner, then the force expression of (7-7) can be handled in a similar way to the rigid body force and moment equations written from Newton's laws of Motion. The above approach is applied to the helicopter blade dynamics in Reference 1 and is developed for the aeroelastic airplane in Chapter VI.

7.1.3.1 Mode Shapes.

Bending

The development of the bending mode shape of a uniform beam is given in Reference 2. The work of this reference is extended to include a beam hinged at one end and free at the other such as an articulated helicopter blade. The differential equation is given by equating the elastic restoring forces of the beam and the inertia forces acting on the beam. Thus, for a uniform beam with EI a constant

$$EI \frac{\partial^4 h}{\partial r^4} = -m \frac{\partial^2 h}{\partial t^2} \quad (7-12)$$

where

E = modulus of elasticity - psi
 I = structural moment of inertia - in²
 m = mass per unit length - lb sec²/in²
 h = deflection at station r - in

If the frequency of vibration is ω , then at any point along the beam the deflection may be assumed to vary harmonically with time such that

$$h(r,t) = h(r) \sin \omega t \quad (7-13)$$

Substituting (7-13) in equation (7-12) the following expression is obtained.

$$\frac{d^4 h}{dr^4} = \frac{m\omega^2}{EI} h = k^4 h \quad (7-14)$$

where

$$k^2 = \frac{\omega}{\sqrt{EI/m}}$$

The general solution of equation (7-14) can be written:

$$h = A \sin kr + B \cos kr + C \sinh kr + D \cosh kr \quad (7-15)$$

in which A, B, C, and D are constants determined by the boundary conditions.

At $r = 0$ (hinged end; bending moment and displacement are zero)

$$\frac{d^2 h}{dr^2} = 0 ; h = 0$$

At $r = R$ (free end; bending moment and shear zero)

$$\frac{d^2 h}{dr^2} = 0 ; \frac{d^3 h}{dr^3} = 0.$$

applying the boundary conditions to equation (7-15), we obtain

from $r = 0$; $B = D = 0$

from $r = R$;

$$-A \sin kR + C \sinh kR = 0 \quad (7-16)$$

or

$$-A \cos kR + C \cosh kR = 0 \quad (7-17)$$

$$-\sin kR \cosh kR + \cos kR \sinh kR = 0 \quad (7-17a)$$

The three smallest roots of this equation are given below:

$$(kR)_0 = 0 \quad (kR)_1 = 3.925 \quad (kR)_2 = 7.06$$

If the natural elastic frequency ω_1 of the blade in mode 1 (for a non-rotating blade; i.e., $\Omega = 0$) is given by

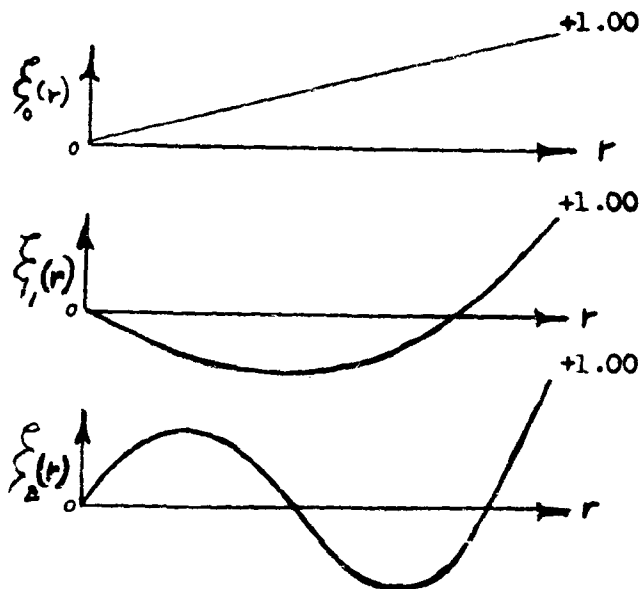
$$\omega_i = \frac{a_i}{k^2} \sqrt{EI/m} \quad \text{then} \quad a_i = (kR)_i^2 \quad (7-18)$$

where

$$a_0 = 0$$

$$a_1 = 15.4$$

$$a_2 = 50.0$$



For the mode shape normalized at the blade tip $h(R) = 1$, the expression for the mode shape $\frac{h(r)}{h(R)} = \xi(r)$ becomes

$$\xi_n(r) = \frac{\sin kr + \frac{\sinh kR}{\sin kR} \sinh kr}{2 \sin kR} \quad (7-19)$$

Torsion. The differential equation for the torsional deflection of a uniform beam can be written as

$$GJ \frac{\partial^2 \phi}{\partial r^2} = I \frac{\partial^2 \phi}{\partial t^2} \quad (7-20)$$

For the blades, having a uniform cross section with fixed pitch at the root, the following solution is obtained for the principle modes of vibration:

$$\eta_n(r) = \sin \frac{n\pi}{2} \frac{r}{R} \quad n \text{ odd} \quad (7-21)$$

The undamped natural frequencies become

$$\omega_n = \frac{n\pi}{2R} \sqrt{GJ/I_P} \quad (7-22)$$

where GJ = torsional rigidity

I_P = mass polar moment of inertia per unit of blade length about the elastic axis.

Effect of Centrifugal Force and Damping on Mode Shapes and Natural Vibration Frequencies.

Many studies have been performed on the influence of the centrifugal force on the mode shapes and vibration frequencies of the rotating blade. References 3 thru 8 are all concerned with some aspect of this problem. The derivation of the mode shapes of this section did not include the effect of centrifugal forces, internal or aerodynamic damping, nor coupling between the torsional and bending vibrations. In Reference 4, it is shown by calculating the mode shapes, that the rotational frequency of the rotor has little influence on the bending deflection curve. The error introduced by using this simplification was found to be less than 3 percent for the example cited (hinge at center of rotation) in this reference. It was concluded by NACA (see Reference 6) that the general shape of the bending deflection curve (rotating cantilever beam fixed at center of rotation) in particular the location of node positions, is unaffected by rotation although relative amplitudes vary. The amplitude of antinode loops relative to tip amplitude decreases with increasing rotational speed. They further stated that the effect of rotational aerodynamic damping or the physical constants have negligible effect upon the mode shape of the beam.

The bending frequency expression of equation (7-18) is for a non-rotating beam; the natural frequency ω_R for a rotating beam is given by the following expression

$$\omega_R^2 = \omega_{NR}^2 + K \Omega^2 \quad (7-23)$$

The constant K is approximately 6.2 for a uniform blade (fixed or hinged) vibrating in the first mode. Reference 8 provides rapid estimation of the constant value K for various types of beams (uniform and tapered) with varying end fixities.

The natural frequencies and mode shapes of the rotating beam in torsion vibration are little effected by the centrifugal forces. It is concluded in Reference 5 that the effect of the free torsional vibrations on the flapping of mass-balanced blades is in practice negligible because of the relatively high natural frequencies in torsion. It was further found that the aerodynamic damping in torsion would decrease with the mode number while the internal damping remained the same for all modes. In the fifth and higher modes, the internal damping exceeds the aerodynamic damping.

7.2 Equations of Motion - (Rigid Plus Aeroelastic)

The linear equations of motion for a single rotor helicopter are developed herein and include the first blade bending mode together with the pitch and roll equations of the rigid body. The basic equations are given by equations (7-1 to -7).

7.2.1 Assumptions. The primary assumptions inherent in the derivation of the total equations of motion are as follows:

1. The angular displacements about the body axis and rotor hinge are considered small. ($\sin \theta = \theta$, $\cos \theta = 1$).
2. The induced velocity can be derived from elementary momentum theory.
3. The profile drag coefficient along the blade is constant and the blade is without twist.
4. The rotor rpm is constant and the oscillation about the drag hinge is highly damped.
5. The yaw motion can be decoupled from pitch and roll.
6. The body forces and moments derived from the rotor can be averaged over a complete cycle of the azimuth.
7. The mode shape can be determined independently of rigid body motions and aerodynamic loading. (uncoupled modes)
8. The inertial axes are assumed to be near the principle body axes and the moments of inertia do not change appreciably with time. Also the products of inertia disappear from the perturbed equations since no steady state angular rates exist.
9. The motions of the rotary wing in the rigid body analysis are usually approximated by the first harmonics of a Fourier Series.

$$\beta = \beta_0 - a, \cos \Omega t - b, \sin \Omega t \quad (7-24)$$

This approximation to the blade motion describes the path of a blade particle by a sinusoidal flapping motion. Using this assumption, the tip path of the rotor forms a plane and its longitudinal and lateral inclinations are the coefficients of the first harmonic cosine and sine terms respectively. Addition of the higher order harmonics would superimpose ripples on the plane produced by the larger first harmonic terms. For the ordinary helicopter and for a travel speed of $1/3$ the tip speed, the amplitude of any harmonic is about $1/10$ of the preceding harmonic. The relative amplitude becomes less at the lower speeds.

The path of the assumed rigid blade elements must be further modified by the elastic deflection of the blade. The deflection of a blade element for a particular mode is represented by a function dependent on time and on the radial position of the blade element. Thus:

$$h = g(t) \xi(r) \quad (7-25)$$

where $q(t)$ can be likened to $\beta(t)$ in that it is a function of time and is usually given by the first harmonics of the blade azimuth position

$$q(t) = q_0 + q_1 \cos \Omega t + q_2 \sin \Omega t + \dots \quad (7-26)$$

and $\xi(r)$ is the mode shape for the elastic mode of the beam under consideration.

7.2.2 Coordinates. Rotor. If x_b , y_b , and z_b are the instantaneous coordinates of a blade element (Figure 7-2) in the inertial reference frame,

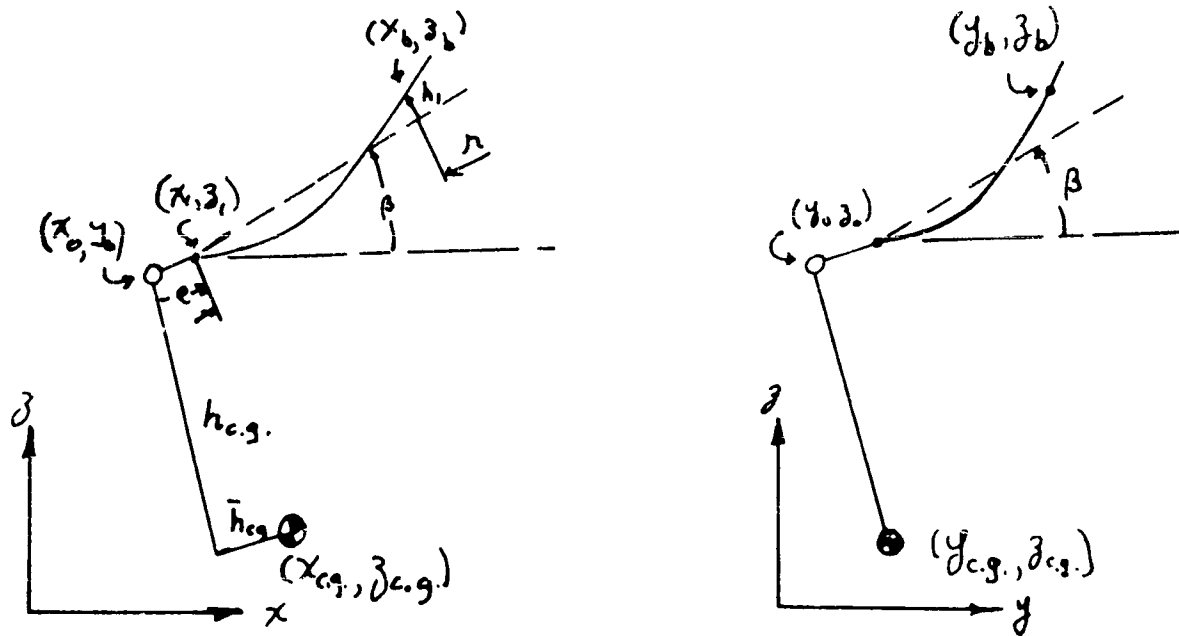


Figure 7-2.

Coordinates

the displacements of the blade element (neglecting the hinge offset) are:

$$x_b = x_0 + r \cos \psi - h_1 \beta \cos \psi \quad (7-27)$$

$$y_b = y_0 + r \sin \psi - h_1 \beta \sin \psi \quad (7-28)$$

$$z_b = z_0 + r \beta + h_1 \quad (7-29)$$

The blade velocities are:

$$\dot{X}_b = -\dot{\mu}_x \Omega R - \Omega r \sin \psi - (\dot{h}_1 \beta + \dot{\beta} h_1) \cos \psi + h_1 \beta \Omega \sin \psi \quad (7-30)$$

$$\dot{Y}_b = -\dot{\mu}_y \Omega R + \Omega r \cos \psi - (\dot{h}_1 \beta + \dot{\beta} h_1) \sin \psi - h_1 \beta \Omega \cos \psi \quad (7-31)$$

$$\dot{Z}_b = -\dot{\mu}_z \Omega R + r \dot{\beta} + \dot{h}_1 \quad (7-32)$$

The blade accelerations are:

$$\begin{aligned} \ddot{X}_b = & -\ddot{\mu}_x \Omega R - \Omega^2 r \cos \psi - (\ddot{h}_1 \beta + 2\dot{h}_1 \dot{\beta} + h_1 \ddot{\beta} - h_1 \beta \Omega^2) \cos \psi \\ & + 2\Omega (\dot{h}_1 \beta + h_1 \dot{\beta}) \sin \psi \end{aligned} \quad (7-33)$$

$$\begin{aligned} \ddot{Y}_b = & -\ddot{\mu}_y \Omega R - \Omega^2 r \sin \psi - (\ddot{h}_1 \beta + 2\dot{h}_1 \dot{\beta} + h_1 \ddot{\beta} - h_1 \beta \Omega^2) \sin \psi \\ & - 2\Omega (\dot{h}_1 \beta + h_1 \dot{\beta}) \cos \psi \end{aligned} \quad (7-34)$$

$$\ddot{Z}_b = -\ddot{\mu}_z \Omega R + r \ddot{\beta} + \ddot{h}_1 \quad (7-35)$$

The products of $h\beta$ and its derivatives can be neglected for all practical purposes because of their relatively small contributions.

Helicopter Body - The instantaneous inertial coordinates of the helicopter fuselage c.g. are $x_{c.g.}$, $y_{c.g.}$, and $z_{c.g.}$ as shown in Figure 7-2. The component displacements of the helicopter c.g. are :

$$x_{c.g.} = x_0 + h_{c.g.} \alpha_1 \quad (7-36)$$

$$y_{c.g.} = y_0 + h_{c.g.} \alpha_2 \quad (7-37)$$

$$z_{c.g.} = z_0 - h_{c.g.} \quad (7-38)$$

The helicopter c.g. velocities are:

$$\dot{x}_{c.g.} = -\mu_x \Omega R + h_{c.g.} \dot{\alpha}_1 \quad (7-39)$$

$$\dot{y}_{c.g.} = -\mu_y \Omega R + h_{c.g.} \dot{\alpha}_2 \quad (7-40)$$

$$\dot{z}_{c.g.} = -\mu_z \Omega R \quad (7-41)$$

The helicopter c.g. accelerations are:

$$\ddot{x}_{c.g.} = -\dot{\mu}_x \Omega R + h_{c.g.} \ddot{\alpha}_1 \quad (7-42)$$

$$\ddot{y}_{c.g.} = -\dot{\mu}_y \Omega R + h_{c.g.} \ddot{\alpha}_2 \quad (7-43)$$

$$\ddot{z}_{c.g.} = -\dot{\mu}_z \Omega R \quad (7-44)$$

7.2.3 Body Forces and Moments. Forces (Rigid Body). The forces considered as acting on the composite system in level flight are given as:

$$\sum X = H_{x_0} + D_x \quad (7-45)$$

$$\sum Y = Y_{y_0} \quad (7-46)$$

$$\sum Z = T_{z_0} + D_z - W \quad (7-47)$$

In developing the forces derived from the rotor, simple aerodynamic relationships are used and are illustrated in Figure 7-3.

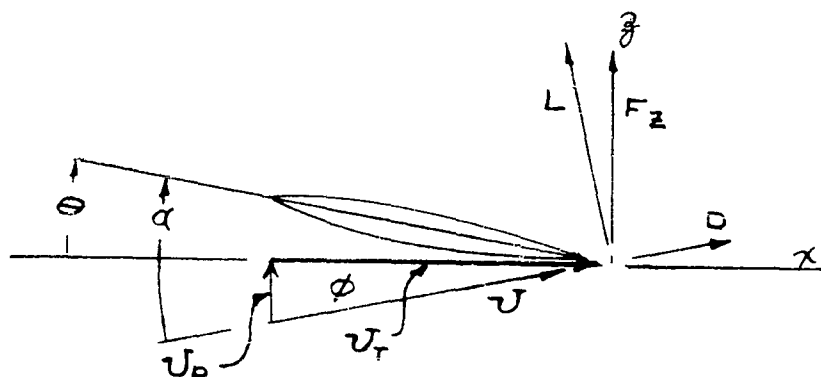


Figure 7-3. Blade Section

Very little work to date has been done to include unsteady flow into the aerodynamics of the rotor. The approach in the past has been to calculate the aerodynamic forces using quasi-static theory (i.e., simple 2-dimensional strip theory). To illustrate, the reduced frequency, $\omega c/2V$ of a typical blade ($\Omega R = 550$ ft./sec., $c = 1.3$ ft.) at its centroid of lift ($3/4$ radius) in the first bending mode, is about 0.08. According to unsteady flow theory, if the reduced frequency is greater than .1 unsteady flow effects should be included in the evaluation of the aerodynamic loading. However, another point must be considered. At high advance ratios ($\mu > .1$) the flow through the rotor appears very much like the flow over a fixed wing. At speeds approaching hovering flight the downwash air velocity through the rotor is of the same order of magnitude as the forward flight velocity. The wake moves downward and backward away from the rotor at velocities that are small compared to the blade velocity, so that the geometrical configuration of the wake is radically different from that considered in fixed wing theory.

The airloads are resolved in the z and x directions by making the usual small angle assumption

$$\frac{dF_{za}}{dr} = \frac{dL}{dr} \quad (7-48)$$

$$\frac{dF_{xa}}{dr} = \frac{dD}{dr} - \phi \frac{dL}{dr} \quad (7-49)$$

From fundamental aerodynamic relationships we have:

$$dL = \frac{1}{2} \rho a c \alpha U_T^2 dr \quad U_T^2 \approx U^2 \quad (7-50)$$

$$dD = \frac{1}{2} \rho c \delta U_T^2 dr \quad (7-51)$$

$$\text{and } \alpha = \theta + \phi \quad (7-52)$$

$$\phi = \frac{U_p}{U_T} \quad \text{where } \tan \phi = \phi$$

Using the above expression the following force equation results:

$$dF_{za} = \frac{1}{2} \rho a c \left(\theta + \frac{U_p}{U_T} \right) U_T^2 dr \quad (7-53)$$

$$dF_{xa} = \frac{1}{2} \rho c \left[\delta U_T^2 - a \left(\theta U_T^2 + U_p U_T \right) \frac{U_p}{U_T} \right] dr \quad (7-54)$$

The blade velocities U_p and U_T may be expressed from the geometric relationship of Section 7.2.2.

$$\dot{V}_p = -\dot{z}_b + (\dot{x}_b \cos \psi + \dot{y}_b \sin \psi)(\beta + \tau) + \lambda_a \Omega R \quad (7-55)$$

$$\dot{V}_T = -\dot{x}_b \sin \psi + \dot{y}_b \cos \psi \quad (7-56)$$

It is assumed that the induced velocity down through the rotor is uniformly distributed over the rotor disc and expressed by the equations.

$$v = -\lambda_a \Omega R = \frac{T}{2\pi R^2 V' \rho} \quad (7-57)$$

where V' is the resultant air velocity at the rotor (Figure 7-1) and is given by

$$V'^2 = V^2 + v^2 + 2Vv \cos(90^\circ + \alpha_1) \quad (7-58)$$

The input blade pitch relative to the horizontal plane can be written as

$$\theta = \theta_0 - \theta_1 \cos \psi - \theta_2 \sin \psi \quad (7-59)$$

where

$$\theta_1 = A_1 - \alpha_2$$

$$\theta_2 = B_1 + \alpha_1$$

The A_1 and B_1 are components of blade pitch due to the cyclic pitch control applied by the pilot and measured at the blade with respect to the rotor shaft.

The resultant rotor blade forces transmitted to the hub can be broken down into its three components, horizontal drag (H_{x_0}), side force (Y_{y_0}) and vertical thrust (T_{z_0}). The expressions for these components may be written

by considering the forces of equations (7-53) and (7-54) derived for a rotating blade which is free to flap.

$$dH_{x_0} = -dF_{z_a} \beta \cos \psi + dF_{x_a} \sin \psi \quad (7-60)$$

$$dY_{y_0} = -dF_{z_a} \beta \sin \psi - dF_{x_a} \cos \psi \quad (7-61)$$

$$dT_{z_0} = dF_{z_a} \quad (7-62)$$

The average rotor forces will be obtained by integrating dH_{x_0} , dY_{y_0} and dT_{z_0} along the blade from $\psi = 0$ to $\psi = 2\pi$.

$$H_{x_0} = \frac{1}{2\pi} \int_0^{2\pi} d\psi \int_0^{BR} \frac{1}{2} \rho b c \left[-a(U_T^2 + U_P U_T) \left(\beta \cos \psi + \frac{U_P}{U_T} \sin \psi \right) + U_T^2 \delta \sin \psi \right] dr \quad (7-63)$$

$$Y_{y_0} = \frac{1}{2\pi} \int_0^{2\pi} d\psi \int_0^{BR} \frac{1}{2} \rho b c \left[-a(U_T^2 + U_P U_T) \left(\beta \sin \psi - \frac{U_P}{U_T} \cos \psi \right) - U_T^2 \delta \cos \psi \right] dr$$

$$T_{z_0} = \frac{1}{2\pi} \int_0^{2\pi} d\psi \int_0^{BR} \frac{1}{2} \rho a b c (\theta U_T^2 + U_P U_T) dr \quad (7-65)$$

Moments. The moments which act on the body and induced by the rotor, or other aerodynamic influences, are defined as follows:

$$\sum M_{y_{c.g.}} = H_{x_0} h_{c.g.} + T_{z_0} (h_{c.g.} \alpha_1 + \bar{h}_{c.g.}) + M_{h_{y_0}} + M_{f_y} = 0 \quad (7-66)$$

$$\sum M_{x_{c.g.}} = Y_{y_0} h_{c.g.} + T_{z_0} h_{c.g.} \alpha_2 + M_{h_{x_0}} = 0 \quad (7-67)$$

If the blade hinges are offset from the hub, a moment will be transmitted through the offset to the body. The moment about the hub, M_h , due to the offset of the flapping hinge can be expressed as

$$M_h \cong -F_1 e \quad (7-68)$$

where F_1 is the total blade force acting normal to the hub at the blade flapping hinge and "e" is the offset of the flapping hinge from the hub center. The blade loading can be represented by its components:

$$F_{z_a} + F_{z_m} = 0 \quad (7-69)$$

The expression for the normal hub force due to aerodynamic loading is given by equation (7-65) before integration with respect to ψ . The loading due to the inertia force can be expressed as follows:

$$F_{z_m} = \int_0^R \left[-\ddot{z}_b + (\ddot{x}_b \cos \psi + \ddot{y}_b \sin \psi)(\alpha_1 \cos \psi + \alpha_2 \sin \psi) \right] m dr \quad (7-70)$$

The moment introduced by the offset blade hinges can be resolved into its pitch and roll components.

$$M_{h y_0} = M_h \cos \psi \quad (7-71)$$

$$M_{h x_0} = M_h \sin \psi \quad (7-72)$$

$$M_{h y_0} = -\frac{eb}{2\pi} \int_0^{2\pi} (F_{z_a} + F_{z_m}) \cos \psi d\psi \quad (7-73)$$

$$M_{h x_0} = -\frac{eb}{2\pi} \int_0^{2\pi} (F_{z_a} + F_{z_m}) \sin \psi d\psi \quad (7-74)$$

These moments have been expanded for the rigid body case in references 11 and 13. In the work of reference 11 the above moments include the elastic blade torsion degree of freedom. The effect of vertical blade bending has been assumed negligible on these moments, Equations (7-73 and 7-74).

The aerodynamic drag forces and body moments acting directly on the fuselage are best obtained from wind tunnel data and corrected for rotor downwash. These forces and moments acting on the body are usually given in coefficient form such as C_{D_f} , $C_{M_{\alpha_f}}$ and expressed as a function

of the fuselage angle of attack and dynamic pressure. If it is assumed that the airstream velocity at the fuselage acts along the resultant velocity vector at the rotor, the fuselage angle of attack α_f for small angles becomes

$$\alpha_f \approx -\alpha_i + \frac{\mu_z + \lambda_a}{\sqrt{\mu_x^2 + (\mu_z + \lambda_a)^2}} \quad (7-75)$$

and the dynamic pressure q is equal to

$$q = \frac{1}{2} \rho (\Omega R)^2 [\mu_x^2 + (\mu_z + \lambda_a)^2] \quad (7-76)$$

Rotor Moments - The rotor equations of motion are obtained by equating the aerodynamic moment about the flapping hinge to the inertia moment about the same hinge.

$$(\bar{M}_y)_a + (\bar{M}_y)_m = 0 \quad (7-77)$$

Since $(\bar{M}_y)_a$ and $(\bar{M}_y)_m$ are harmonic functions of azimuth angle, they can be written:

$$(\bar{M}_y)_a = (M_y)_a + (M'_y)_a \cos \psi + (M''_y)_a \sin \psi \quad (7-78)$$

$$(\bar{M}_y)_m = (M_y)_m + (M'_y)_m \cos \psi + (M''_y)_m \sin \psi \quad (7-79)$$

where the coefficients involve the different degrees of freedom. In this analysis, only first harmonic terms are considered. If these expressions are substituted into equation (7-77) and the coefficients of like trigonometric terms are equated, then the following three equations are obtained:

$$(M_y)_a + (M_y)_m = 0 \quad (7-80)$$

$$(M'_y)_a + (M'_y)_m = 0 \quad (7-81)$$

$$(M''_y)_a + (M''_y)_m = 0 \quad (7-82)$$

The aerodynamic moment about the flapping hinge for an elastic blade in bending is

$$(\bar{M}_y)_a = \frac{1}{2} \rho a c \int_0^{BR} (\theta U_T^2 + U_T U_P) r dr \quad (7-83)$$

where the value of U_p , U_t and θ are given by equations (7-55, -56, and -59).

The inertia moment about the flapping hinge for an elastic blade in bending is

$$(\bar{M}_y)_m = - \int_0^R \left[\ddot{z}_b r - \ddot{x}_b (r\beta + h_1) \cos \psi - \ddot{y}_b (r\beta + h_1) \sin \psi \right] m dr \quad (7-84)$$

where the blade accelerations are given by equations (7-33, -34, and -35).

Blade Bending Equations - The blade bending equation is developed in a manner similar to that of the flapping equation. The bending motion of the blade in the flapping plane may be developed by summing up the generalized aerodynamic, inertia, and elastic forces.

$$(\bar{F}_z)_a + (\bar{F}_z)_{h_1} + (\bar{F}_z)_m = 0 \quad (7-85)$$

Since $(\bar{F}_z)_a$ and $(\bar{F}_z)_{h_1}$ and $(\bar{F}_z)_m$ are harmonic functions of azimuth angle, they can be written:

$$(\bar{F}_z)_a = (F_z)_a + (F'_z)_a \cos \psi + (F''_z)_a \sin \psi \quad (7-86)$$

$$(\bar{F}_z)_{h_1} = (F_z)_{h_1} + (F'_z)_{h_1} \cos \psi + (F''_z)_{h_1} \sin \psi \quad (7-87)$$

$$(\bar{F}_z)_m = (F_z)_m + (F'_z)_m \cos \psi + (F''_z)_m \sin \psi \quad (7-88)$$

If these expressions are substituted into equation (7-85) and the coefficients of like trigonometric terms are equated, the resulting blade bending equations are obtained:

$$(F_z)_a + (F_z)_{h_1} + (F_z)_m = 0 \quad (7-89)$$

$$(F'_z)_a + (F'_z)_{h_1} + (F'_z)_m = 0 \quad (7-90)$$

$$(F''_z)_a + (F''_z)_{h_1} + (F''_z)_m = 0 \quad (7-91)$$

The expressions for the normal blade loading are derived from the following considerations:

The generalized force of the elastic blade element due to the aerodynamic loading is

$$(F_z)_a = \frac{1}{2} \rho a c \int_0^{BR} (\theta U_T^2 + U_T U_P) \xi_1(r) dr \quad (7-92)$$

where $\xi_1(r)$ is the normalized mode shape of the first bending mode.

The elastic restraining force acting on the blade is as follows:

$$(\bar{F}_z)_h = -K_B g(t) \xi_1(r) = -K_B (g_0 + g_1 \cos \psi + g_2 \sin \psi) \quad (7-93)$$

where the blade stiffness constant K_B is obtained by determining a generalized deflection at the tip due to a generalized bending force. The development of this constant will be illustrated in Section 7.3.

The normal loading of the undeflected blade element due to the generalized inertia force can be expressed as follows:

$$(\bar{F}_z)_m = - \int_0^R (\ddot{z}_b - \ddot{x}_b \beta \cos \psi + \ddot{x}_b \theta \sin \psi - \ddot{y}_b \beta \sin \psi - \ddot{y}_b \theta \cos \psi) \xi_1(r) m dr \quad (7-94)$$

7.2.4 Total Aeroelastic Equations of Motion. The inclusion of the three bending equations (7-89, -90 and -91) with the rigid body equations demonstrates the inclusion of elastic modes into the dynamics of the helicopter for level flight.

$$\sum X = H_{x_0} + D_x = - \bar{m}(\dot{\mu}_x \Omega R - h_{c.g.} \ddot{\alpha}_1) \quad (7-95)$$

$$\sum Y = Y_{y_0} = - \bar{m}(\dot{\mu}_y \Omega R - h_{c.g.} \ddot{\alpha}_2) \quad (7-96)$$

$$\sum Z = T_{z_0} - W = - \bar{m} \dot{\mu}_z \Omega R \quad (7-97)$$

$$\sum M_{y_{c.g.}} = H_{x_0} h_{c.g.} + T_{z_0} h_{c.g.} \alpha_1 + T_{z_0} \bar{h}_{c.g.} + M_{h_{x_0}} + M_{f_y} = - I_y \ddot{\alpha}_1 \quad (7-98)$$

$$\sum M_{x_{c.g.}} = Y_{y_0} h_{c.g.} + T_{z_0} h_{c.g.} \alpha_2 + M_{h_{y_0}} = - I_x \ddot{\alpha}_2 \quad (7-99)$$

$$\sum M_y = (M_y)_a + (M_y)_m = 0 \quad (7-100)$$

$$\sum M'_y = (M'_y)_a + (M'_y)_m = 0 \quad (7-101)$$

$$\sum M''_y = (M''_y)_a + (M''_y)_m = 0 \quad (7-102)$$

$$\sum F_z = (F_z)_a + (F_z)_{h_1} + (F_z)_m = 0 \quad (7-103)$$

$$\sum F'_z = (F'_z)_a + (F'_z)_{h_1} + (F'_z)_m = 0 \quad (7-104)$$

$$\sum F''_z = (F''_z)_a + (F''_z)_{h_1} + (F''_z)_m = 0 \quad (7-105)$$

7.2.5 The Stability Equations. To illustrate the derivation of the stability equation from the total equations of the system, the following example is given. Consider the differential equation describing the x degree of freedom of the helicopter as given by the total equation, (7-95)

$$\bar{m} (\dot{\mu}_x \Omega R - h_{c.g.} \ddot{\alpha}_1) + X = 0 \quad (7-106)$$

where X is the summation of external x-forces acting on the system. Then for small deviations from the steady state flight, the equation can be linearized by writing

$$\mu_x = \mu_{x0} + \bar{\mu}_x$$

$$\mu_y = \mu_{y0} + \bar{\mu}_y$$

$$\begin{array}{c} \vdots \\ \vdots \\ \vdots \end{array} \quad \begin{array}{c} \vdots \\ \vdots \\ \vdots \end{array} \quad \begin{array}{c} \vdots \\ \vdots \\ \vdots \end{array}$$

$$g_z = g_{z0} + \bar{g}_z$$

where the variables in the eleven equations of motion can be considered as the sum of a steady state component plus a perturbed value from the initial condition.

The aerodynamic force X can be expressed as a function of the dependent variables by expanding the force in a Taylor series about the steady-state equilibrium condition, X_0 ,

$$X = X_0 + \Delta X \quad (7-107)$$

Since only small perturbations about a steady state flight condition are considered, the summation of all external force at the steady-state flight conditions is zero ($X_0 = 0$). The total change in the force in the above equation is made up from the partial derivatives of these forces taken with respect to each of the dependent variables. These terms are known as the stability derivatives and are written as follows:

$$\Delta X = X_{\mu_x} \bar{\mu}_x + X_{\mu_y} \bar{\mu}_y + \dots \quad (7-108)$$

where

$$\frac{\partial X}{\partial \mu_x} = X_{\mu_x}, \quad \frac{\partial X}{\partial \mu_y} = X_{\mu_y}, \dots$$

Because λ_a is a function of μ_x, μ_y, a_1 , etc. (See equation (7-57) and (7-58)), the effect of a variable λ_a may be included in the stability derivative by the following expression:

$$\frac{\partial X}{\partial ()} = \left. \frac{\partial X}{\partial ()} \right|_{\lambda_a} + \left(\frac{\partial X}{\partial \lambda_a} \right) \frac{\partial \lambda_a}{\partial ()}$$

where () represents the dependent variables μ_x, μ_y , etc. Similar expressions apply to the Y and Z forces. (See Reference 9).

The differential equation describing the dynamic motion of the helicopter from an equilibrium condition can be written as follows:

$$(X_{\mu_x} + D \bar{m} \Omega R) \bar{\mu}_x + X_{\mu_y} \bar{\mu}_y + \dots + (\rho^2 X \ddot{g}_2 + \rho X \dot{g}_2 + X g_2) \bar{g}_2 = -X_{B_1} \bar{B}_1 \quad (7-109)$$

By using operational calculus, the differential equations reduce to a set of algebraic equations with complex coefficients where the complex variable "s" of the form $(\sigma + i\omega)$ replaces the differential operator, D.

$$F_{1,1} \bar{\mu}_x + F_{1,2} \bar{\mu}_y + \dots + F_{1,12} \bar{g}_2 = -F_{1,B_1} \bar{B}_1 \quad (7-110)$$

where

$$F_{1,1} = X_{\mu_x} + \rho \bar{m} \Omega R$$

$$F_{1,2} = X_{\mu_y} + \rho X \dot{\mu}_y$$

$$F_{1,12} = \rho^2 X \ddot{g}_2 + \rho X \dot{g}_2 + X g_2$$

$$F_{1,B_1} = X_{B_1}$$

If the process is applied to the remaining equations of the complete set (Equations (7-96) thru (7-105)), the perturbation equations are obtained. These equations are presented in Figure (7-4).

If a stability analysis is performed on a typical single rotor helicopter with fully articulated blades, the characteristic equation will yield the following rigid-body modes for hovering flight:

Two Unstable Modes with low dampings and long period.

| | <u>Time to Double</u> | <u>Frequency of Mode</u> |
|--------------|-----------------------|--------------------------|
| Longitudinal | ~ 5 sec. | $\sim 1/50 \Omega$ |
| Lateral | ~ 50 sec. | $\sim 1/50 \Omega$ |

Three Rotor Flapping Modes with high damping and short periods.

| <u>Time to Half</u> | <u>Frequency of Mode</u> |
|---------------------|--------------------------|
| $\sim .05$ sec. | $\sim 1/5 \Omega$ |
| $\sim .05$ sec. | $\sim 2 \Omega$ |
| $\sim .05$ sec. | $\sim 1 \Omega$ |

The aeroelastic modes will of course have higher frequencies and lower damping. The frequency of the vertical blade bending mode for a uniform blade is about two and a half times the rotor frequency and the first blade torsion will be greater than three times the rotor frequency.

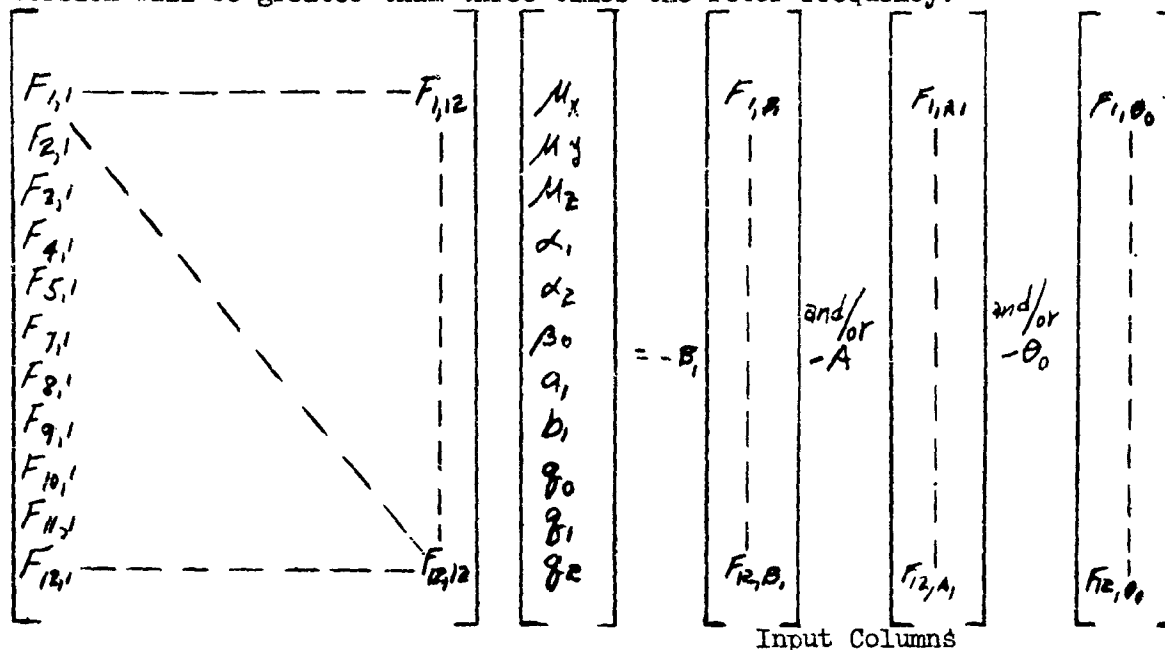


Figure 7-4. Matrix Form of Equations of Motion

Note: (Sixth row and column have been omitted which would have represented yaw)

7.3 Illustrative Example

An illustrative example is given here to demonstrate some of the processes and methods presented in this handbook as applied to the dynamics of an aeroelastic helicopter.

7.3.1 Statement of Problem. In hovering flight the vertical degrees of freedom (μ_z, β_0, q_0) in the stability equations of Figure (7-4) can be decoupled from the remaining equations of the set because the cross coupling terms are zero. Since the system can be decoupled into the vertical three equations and the pitch and roll consisting of 8 equations, the vertical stability of the system will be investigated. The three equations in vertical body motion (μ_z), steady flapping motion (β_0), and the steady blade bending motion (q_0) are given by equations (7-97), (7-100), and (7-103).

$$\sum Z = T_{z_0} - W = -\bar{m} \ddot{\mu}_z \Omega R \quad (7-111)$$

$$\sum M_y = (M_y)_a + (M_y)_m = 0 \quad (7-112)$$

$$\sum F_z = (F_z)_a + (F_z)_h + (F_z)_m = 0 \quad (7-113)$$

A typical helicopter shall be assumed having the following numerical parameters.

- | | | |
|-----------------------------|-------------------------------------|-------------------------|
| 1. Weight | $W = 7000 \text{ Lbs.}$ | $\bar{m} = \frac{W}{g}$ |
| 2. Tip Radius | $R = 26.5 \text{ ft.}$ | $B = 1$ |
| 3. Air Density | $\rho = .002378 \text{ slugs/ft}^3$ | |
| 4. Number of blades | $b = 3$ | |
| 5. Rotor speed | $\Omega = 20.8 \text{ rad/sec.}$ | |
| 6. Lift curve slope | $a = 5.75$ | |
| 7. Steady flight velocities | $\mu_{x0} = 0, \mu_{z0} = 0$ | |
| 8. Induced flow | | |

$$\lambda_a = -\frac{1}{\Omega R} \sqrt{\frac{W}{2\pi R^2 \rho}} = -.0469$$

Bending Mode Shape and Stiffness Factor - An assumed mode shape is used which approximates the exact mode as calculated in section 7.1.3. The assumed first bending mode (see Reference 3) is given by the normalized function (see Figure 7-5).

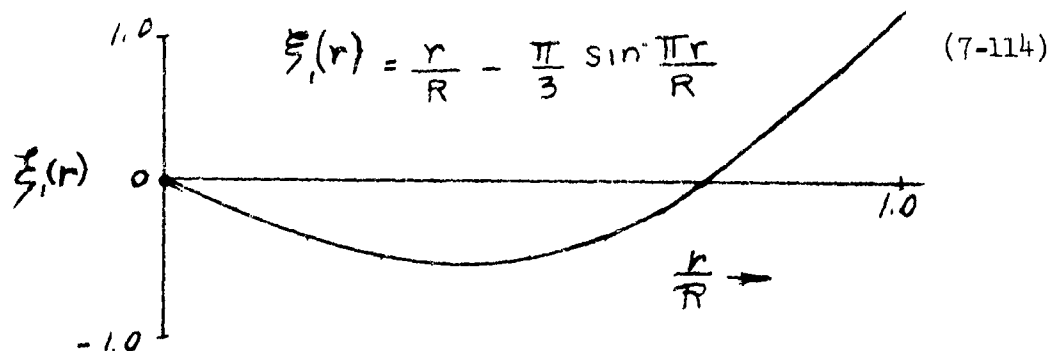


Figure 7-5 Mode Shape

This simplified expression approximates the latter portion of the true curve (Equation (7-19) for $n=1$) to a very high degree; however the antinode loop is decreased in amplitude giving a more realistic mode shape. The reduction in amplitude is in the right direction for the influence of the centrifugal force on the non-rotating mode shape.

The elastic blade deformation for first bending, $h_1(r,t)$ is represented by the expression

$$h_1(r,t) = q_0(t) \xi_1(r) \quad (7-115)$$

where q_0^* is the generalized deflection of the blade tip and is the steady part of the infinite Fourier series for $q(t)$, that is q_0 is independent of the blade azimuth position since the cyclic effect is decoupled in this case.

* The symbol q_0 will replace $q_0(t)$ from here on.

Stiffness Factor - K_B of the blade (see equation (7-93)) is determined from strain energy considerations. The potential energy, U_{BR} for uniform rotating blade in bending is given by the equation,

$$U_{BR} = \frac{1}{2} \int_0^R EI \left(\frac{\partial^2 h}{\partial r^2} \right)^2 dr + \frac{1}{2} \Omega^2 \int_0^R mr \int_0^r \tau(\eta)^2 d\eta dr \quad (7-116)$$

where EI is the bending rigidity of the blade, and $\tau(\eta)$ is slope of the blade at any radial station

$$\tau(\eta) = \frac{1}{R} - \frac{\pi^2}{3R} \cos \frac{\pi \eta}{R} \quad (7-117)$$

The first term of the potential energy equation expresses the energy absorbed by the internal restraint of a non-rotating blade and the second term expresses the additional potential energy absorbed by the rotating blade when the elastic blade particles move against the centrifugal force. The generalized spring force is obtained by differentiating the potential energy expression with respect to the generalized blade tip deflection.

$$\frac{\partial U_{BR}}{\partial q_0} = -K_B q_0 = - \left[\frac{EI \pi^6}{18 R^3} + \Omega^2 m R \left(\frac{\pi^4}{54} - \frac{\pi^2}{72} - \frac{1}{3} \right) \right] q_0 \quad (7-118)$$

The stiffness constant for the first bending is then

$$K_B = \frac{EI \pi^6}{18 R^3} + \Omega^2 m R \left(\frac{\pi^4}{54} - \frac{\pi^2}{72} - \frac{1}{3} \right) \quad (7-119)$$

The numerical value for this example becomes

$$K_B = 279 + 2380 = 2659$$

and it is noted that the stiffness attributed by the centrifugal force is almost ten times that due to the internal restraint of the blade.

7.3.2 Equations of Motion. The summation of the force equations (7-111) in the vertical direction becomes

$$\sum Z = \frac{1}{2} \rho a b c \int_0^{2\pi} d\psi \int_0^R (\theta U_T^2 + U_P U_T) dr - W = -\bar{m} \dot{\mu}_z \Omega R \quad (7-120)$$

The blade velocities and pitch are:

$$U_T = \Omega (r - \beta_0 g_0 \xi_1(r)) \quad (7-121)$$

$$U_P = \dot{\mu}_z \Omega R - r \dot{\beta}_0 - \dot{g}_0 \xi_1(r) + \lambda_a \Omega R \quad (7-122)$$

$$\theta = \theta_0 \quad (7-123)$$

The collective pitch input θ_0 is the only input considered.

Expanding the force equation (7-120) we obtain

$$\begin{aligned} \sum Z = & \frac{\rho a b c \Omega^2 R^3}{36} \left\{ 6 \left(\theta_0 - \frac{\dot{\beta}_0}{\Omega} \right) + 3 \dot{\mu}_z \left(3 + \frac{\beta_0 g_0}{R} \right) + \frac{1}{R^2} g_0 \beta_0 (\pi^2 - 6) \left(g_0 \beta_0 - \frac{\dot{g}_0}{\Omega} \right) \right. \\ & \left. + 9 \lambda_a \left(1 + \frac{\beta_0 g_0}{3R} \right) \right\} - W + \bar{m} \dot{\mu}_z \Omega R = 0 \end{aligned} \quad (7-124)$$

The steady flapping equation (7-112) becomes

$$\begin{aligned} \sum M_y = & \frac{1}{2} \rho a c \int_0^R (\theta U_T^2 + U_T U_P) r dr - m \int_0^R \left[\ddot{z}_b r - \ddot{x}_b (r \beta + h_1) \cos \psi \right. \\ & \left. - \ddot{y}_b (r \beta + h_1) \sin \psi \right] dr = 0 \end{aligned} \quad (7-125)$$

The blade accelerations are given as (see equations (7-33) to (7-35))

$$\dot{\ddot{z}}_b = -\dot{\mu}_z \Omega R + r \ddot{\beta}_0 + \ddot{g}_0 \xi_1(r) \quad (7-126)$$

$$\ddot{x}_b = -r \Omega^2 \cos \psi + g_0 \xi_1(r) \beta_0 \Omega^2 \cos \psi \quad (7-127)$$

$$\ddot{y}_b = -r \Omega^2 \sin \psi + g_0 \xi_1(r) \beta_0 \Omega^2 \sin \psi \quad (7-128)$$

Upon making the substitutions for the blade velocities and accelerations we obtain

$$\begin{aligned} \Sigma M_y = & \frac{\rho a c \Omega^2 R^4}{24} \left[3\theta_0 + 4(\mu_z + \lambda_a) - \frac{3\dot{\beta}_0}{\Omega} + \right. \\ & + \frac{(16-\pi^2)}{R\pi^2} \left(\frac{\beta_0 \dot{g}_0}{\Omega} - \frac{\dot{g}_0}{\Omega} - 2\beta_0 \theta_0 g_0 \right) + \frac{\beta_0 g_0}{3\pi^2 R^2} (\pi^4 - 15\pi^2 + 96) \left(\beta_0 g_0 \theta_0 + \frac{g_0}{\Omega} \right) \Big] \\ & - \frac{m}{3} R^3 \ddot{\beta}_0 + \frac{m}{2} \Omega R^3 \dot{\mu}_z - \frac{m}{3} \Omega^2 R^3 \beta_0 + \frac{m}{18} \Omega^2 R (\pi^2 - 6) \beta_0 g_0^2 = 0 \end{aligned} \quad (7-129)$$

The blade bending equation (7-113) becomes

$$\begin{aligned} \Sigma(F_z) = & \frac{1}{2} \rho a c \int_0^R (\theta v_T^2 + v_T v_P) \xi_1(r) dr - m \int_0^R \left\{ \ddot{z}_b - (\ddot{x}_b \cos \psi + \ddot{y}_b \sin \psi) \beta_0 \right. \\ & \left. + (\ddot{x}_b \sin \psi - \ddot{y}_b \cos \psi) \theta_0 \right\} \xi_1(r) dr - K_B g_0 = 0 \end{aligned} \quad (7-130)$$

Expanding the above equation we obtain

$$\begin{aligned} \Sigma(F_z) = & \frac{\rho a c \Omega R^3}{24 \pi^2} \left[(16 \pi^2)(\Omega \theta_0 - \dot{\beta}_0) + \frac{1}{3R} (\pi^4 - 15 \pi^2 + 96) (-2 \theta_0 \Omega \beta_0 \dot{g}_0 - \dot{g}_0 + \dot{\beta}_0 \beta_0 \dot{g}_0) \right. \\ & \left. - \frac{2 \pi^2 \Omega}{3R} \beta_0 \dot{g}_0 (\pi^2 - 6) (\mu_z + \lambda_a) + \frac{1}{27 R^2} (11 \pi^4 - 24 \pi^2 + 1296) (\theta_0 \Omega \beta_0^2 \dot{g}_0 + \dot{g}_0 \dot{\beta}_0 \beta_0) \right] \\ & - \left[\frac{m \ddot{g}_0 R (\pi^2 - 6)}{18} - \frac{m}{18} \Omega^2 \dot{g}_0 \beta_0^2 R (\pi^2 - 6) + \frac{m \dot{\mu}_z}{6} \Omega R^2 \right] - K_B \dot{g}_0 = 0 \end{aligned} \quad (7-131)$$

Linear Equations. The linear equations of motion are those given by rows three, seven and ten of Figure 7-4. Linearization of equations (7-124) and (7-131) is accomplished by making the substitution for the dependent variables,

$$\mu_z = \mu_{z_0} + \bar{\mu}_z \quad (7-132)$$

$$\beta_0 = \beta_{00} + \bar{\beta}_0 \quad (7-133)$$

$$\dot{g}_0 = \dot{g}_{00} + \bar{\dot{g}}_0 \quad (7-134)$$

$$\theta_0 = \theta_{00} + \bar{\theta}_0 \quad (7-135)$$

and then taking the partial derivatives (stability derivatives) with respect to the bar or perturbed quantities. In writing the linear expressions the following boundary conditions are made:

$$\dot{\mu}_{z_0} = \mu_{z_0} = \dot{\beta}_{00} = \beta_{00} = \dot{g}_{00} = \dot{g}_{00} = 0$$

The linear equations are:

$$F_{3,3} \mu_z + F_{3,7} \beta_0 + F_{3,10} \dot{g}_0 = -F_{3,\theta} \theta_0 \quad (7-136)$$

$$F_{7,3} \mu_z + F_{7,7} \beta_0 + F_{7,10} \dot{g}_0 = -F_{7,\theta} \theta_0 \quad (7-137)$$

$$F_{10,3} \mu_z + F_{10,7} \beta_0 + F_{10,10} \dot{g}_0 = -F_{10,\theta} \theta_0 \quad (7-138)$$

The bar over the variable has been dropped for convenience. The above equation can be decoupled from the larger set in hovering flight, and the helicopter is considered to be stabilized in its pitch and roll motions. The contribution of the blade bending to the stability equations can be had by eliminating the third row and column of the above equation, leaving only the rigid body equations.

Stability Derivatives

$$\frac{\partial Z}{\partial \mu_z} = \frac{\rho abc}{36} \Omega^2 R^2 (9R + 3\beta_{00} g_{00})$$

$$\frac{\partial Z}{\partial \dot{\mu}_z} = + \bar{m} \Omega R$$

$$\frac{\partial Z}{\partial \beta_0} = \frac{\rho abc}{12} \Omega^2 R^2 \lambda_a g_{00}$$

$$\frac{\partial Z}{\partial \beta_0} = \frac{\rho abc}{6} \Omega R^3$$

$$\frac{\partial Z}{\partial \dot{g}_0} = \frac{\rho abc}{12} \Omega^2 R^2 \lambda_a \beta_0$$

$$\frac{\partial Z}{\partial \beta_0} = \frac{mR^2}{2} + \frac{mR}{6} g_{00}$$

$$\frac{\partial Z}{\partial \dot{g}_0} = - \frac{\rho abc \Omega R}{36} (\pi^2 - 6) g_0 \beta_0$$

$$\frac{\partial Z}{\partial \theta_0} = \frac{\rho abc}{6} \Omega^2 R^3$$

$$\frac{\partial Z}{\partial \ddot{g}_0} = - \frac{mR}{6}$$

$$\frac{\partial M_y}{\partial \mu_z} = \frac{\rho ac}{6} \Omega^2 R^4$$

$$\frac{\partial M_y}{\partial \dot{\mu}_z} = \frac{m \Omega R^3}{2}$$

$$\frac{\partial M_y}{\partial \beta_0} = - \frac{\rho ac}{12 \pi^2} \Omega^2 R^3 \theta_{00} g_{00} (16 - \pi^2) - \frac{m}{2} \left\{ \frac{2}{3} \Omega^2 R^3 - \frac{\Omega^2 R}{9} g_{00}^2 (\pi^2 - 6) \right\}$$

$$\frac{\partial M_y}{\partial \beta_0} = \frac{\rho ac}{24 \pi^2} \Omega R^3 \left\{ -3\pi^2 R + g_{00} \beta_{00} (16 - \pi^2) \right\}$$

$$\frac{\partial M_y}{\partial \beta_0} = -\frac{mR^3}{3}$$

$$\frac{\partial M_y}{\partial g_0} = -\frac{\rho a c}{12\pi^2} \Omega^2 R^3 \beta_{00} \theta_{00} (16 - \pi^2) + \frac{m \Omega^2 R}{9} g_{00} \beta_{00} (\pi^2 - 6)$$

$$\frac{\partial M_y}{\partial \dot{g}_0} = \frac{\rho a c}{24\pi^2} \Omega R^2 \left\{ -R(16 - \pi^2) + \frac{\beta_{00} g_{00}}{3} (\pi^4 - 15\pi^2 + 96) \right\}$$

$$\frac{\partial M_y}{\partial \theta_0} = \frac{\rho a c}{24} \Omega^2 R^3 \left\{ 3R - \frac{2\beta_{00} g_{00}}{\pi^2} (16 - \pi^2) \right\}$$

$$\frac{\partial F_z}{\partial \mu_z} = -\frac{\rho a c}{36} \Omega^2 R^2 \beta_{00} g_{00} (\pi^2 - 6)$$

$$\frac{\partial F_z}{\partial \mu_z} = -\frac{m \Omega R^2}{6}$$

$$\frac{\partial F_z}{\partial \beta_0} = -\frac{\rho a c \Omega^2 R^2}{36} \left[\lambda_a g_{00} (\pi^2 - 6) + \frac{(\pi^4 - 15\pi^2 + 96)}{\pi^2} g_{00} \theta_{00} \right] + \frac{m \Omega^2 R^2}{9} g_{00} \beta_{00} (\pi^2 - 6)$$

$$\frac{\partial F_z}{\partial \dot{\beta}_0} = \frac{\rho a c}{24\pi^2} \Omega R^3 \left\{ (\pi^2 - 16) + \frac{\beta_{00} g_{00}}{3R} (\pi^4 - 15\pi^2 + 96) \right\}$$

$$\frac{\partial F_z}{\partial \ddot{\beta}_0} = 0$$

$$\frac{\partial F_z}{\partial g_0} = -\frac{\rho a c}{36\pi^2} \Omega^2 R^2 \left\{ \theta_{00} \beta_{00} (\pi^4 - 15\pi^2 + 96) + \pi^2 \lambda_a \beta_{00} (\pi^2 - 6) \right\} + \frac{m \Omega^2 R}{18} (\pi^2 - 6) \beta_{00}^2 - K_B$$

$$\frac{\partial F_z}{\partial \dot{g}_0} = \frac{\rho a c \Omega R^2}{24\pi^2} \left\{ -\frac{(\pi^4 - 15\pi^2 + 96)}{3} + \frac{g_{00} \beta_{00}}{24R} (11\pi^4 - 243\pi^2 + 1296) \right\}$$

$$\frac{\partial F_z}{\partial \ddot{g}_0} = -\frac{mR}{18} (\pi^2 - 6)$$

$$\frac{\partial F_z}{\partial \theta_0} = \frac{\rho a c \Omega^2 R^3}{24\pi^2} (16 - \pi^2)$$

Determining the Boundary Conditions. The flight trim conditions are obtained by considering only the steady state terms of the total equations (all derivatives terms made zero). The following relationships are used for calculating the equilibrium conditions in hovering flight ($\mu_{x0} = 0$).

$$Z_0 = \frac{\rho a b c \Omega^2 R^3}{2} \left\{ \left(\frac{1}{3} \theta_{00} + \frac{1}{2} \lambda_a \right) + \frac{\lambda_a g_{00} \beta_{00}}{6 R} \right\} = W \quad (7-139)$$

$$M_{y_0} = \rho a c R^4 \left\{ \frac{\theta_{00}}{8} - \frac{(16 - \pi^2)}{12 \pi^2 R} \beta_{00} \theta_{00} g_{00} + \frac{\lambda_a}{6} \right\} = \frac{m R^3}{3} \beta_{00} \quad (7-140)$$

$$(F_{z_0}) = \frac{\rho a c \Omega^2 R^3}{24 \pi^2} \left\{ \theta_{00} (16 - \pi^2) - \frac{2}{3 R} \pi^2 (\pi^2 - 6) \lambda_a \beta_{00} g_{00} \right. \\ \left. - \frac{2}{3 R} (\pi^4 - 15 \pi^2 + 96) \theta_{00} \beta_{00} g_{00} \right\} + \frac{m \Omega^2 R}{18} g_{00} \beta_{00}^2 (\pi^2 - 6) = K_\beta g_{00} \quad (7-141)$$

Solving for the above conditions for β_{00} , q_{00} , and θ_{00} we obtain

$$\beta_{00} = .1274 \text{ radians}$$

$$q_{00} = .2358 \text{ feet}$$

$$\theta_{00} = .1660 \text{ radians}$$

7.3.3 Obtaining the Result. The linear differential equations have been obtained from the total equations of motion for stability studies. The component transfer function (F_{ij} 's) are made up from the individual helicopter stability derivatives. The performance study has been made to provide the boundary or initial conditions for the numerical computation of the F_{ij} 's.

Stability characteristics are determined from both the qualitative and quantitative information derived from the over-all transfer functions, the characteristic equations, and the transient behavior of the system.

Transfer functions will be obtained by using the Laplace transform of the differential equation. The frequency response of the system is given for both the rigid body and the aeroelastic cases.

The characteristic equation gives the characteristic modes of the dynamic system whereby the roots of this equation yield both the damping and frequency associated with each mode.

The stability equation becomes:

$$\begin{bmatrix} 109690 + 122207s & -15.25 - 3514.4s + 57.40s^2 & -8.24 - .0970s - .72s^2 \\ 645708 + 31558.9s & -437723 - 23260s - 1011.2s^2 & -135.5 - 181s \\ -5.866 - 396.82s & +3.123 - 181.401s & -2641 - 16.9s - .928s^2 \end{bmatrix} \begin{bmatrix} \mu_z \\ \beta_o \\ q_o \end{bmatrix} = - \begin{bmatrix} 73099 \\ 484509 \\ 3783 \end{bmatrix} \theta_o \quad (7-142)$$

The transfer functions are easily obtained by applying Kramer's rule to the stability equation.

Aeroelastic (μ_z, β_o, q_o)

$$\frac{\mu_z}{\theta_o} = -.3362 \frac{(s^4 + 42.05s^3 + 7582s^2 + 13611s + 2154000)}{(s^5 + 41.22s^4 + 3648s^3 + 73307s^2 + 1224000s + 1086500)}$$

$$\frac{\beta_o}{\theta_o} = 454.9 \frac{(s^3 + 16.15s^2 + 2831s + 296.1)}{(s^5 + 41.22s^4 + 3648s^3 + 73307s^2 + 1224000s + 1086500)}$$

$$\frac{q_o}{\theta_o} = 5615 \frac{(s^3 + 5.802s^2 + 414.59s + 359)}{(s^5 + 41.22s^4 + 3648s^3 + 73307s^2 + 1224000s + 1086500)}$$

The frequency responses are given by the phase and amplitude plots of

Figures 7-6, -7, and -8. The plots show the separate regions of response and also give the comparison between rigid body and aeroelastic analysis.

The characteristic equations are given for the two cases and the roots are presented where the real part of the root is the damping factor (not to be confused with damping ratio) and the imaginary part is the angular frequency of oscillation (rad./sec.).

Aeroelastic Case

$$\Delta = s^5 + 41.22s^4 + 3648s^3 + 73307s^2 + 122400s + 1086500 = 0$$

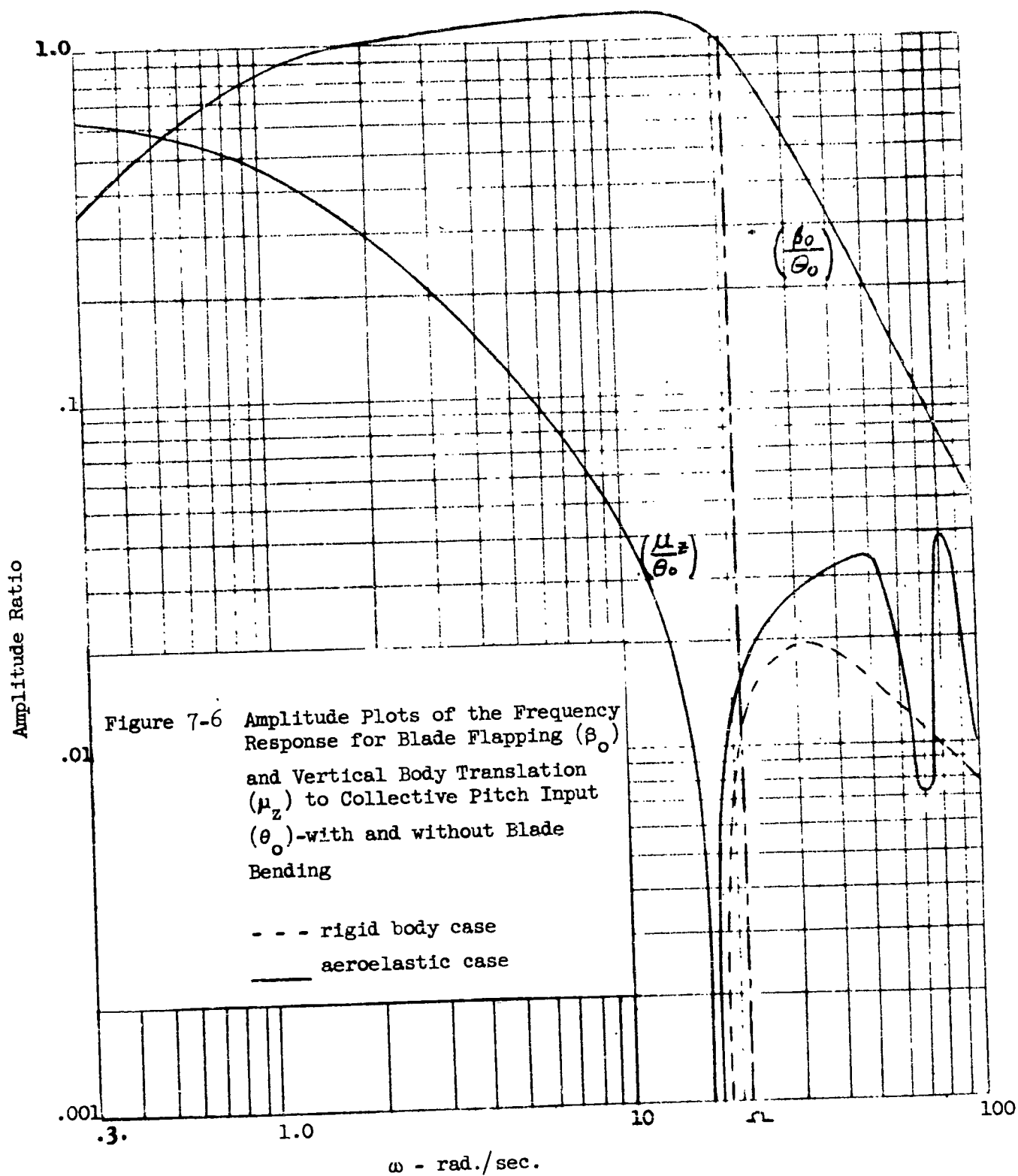
$$\begin{aligned} s_1 &= -.9381 \\ s_{2,3} &= -11.18 \pm 17.01i \\ s_{4,5} &= -8.966 \pm 52.10i \end{aligned}$$

Rigid Body Case

$$\Delta = s^3 + 22.97s^2 + 428.7s + 382.6 = 0$$

$$\begin{aligned} s_1 &= -.9377 \\ s_{2,3} &= -11.02 \pm 16.93i \end{aligned}$$

The transient responses for the aeroelastic case (Equation 7-142) are given in Figure 7-9. In this figure transients in μ_z , β_o , and q_o are obtained from electronic analog computer for a one degree step input in θ_o .



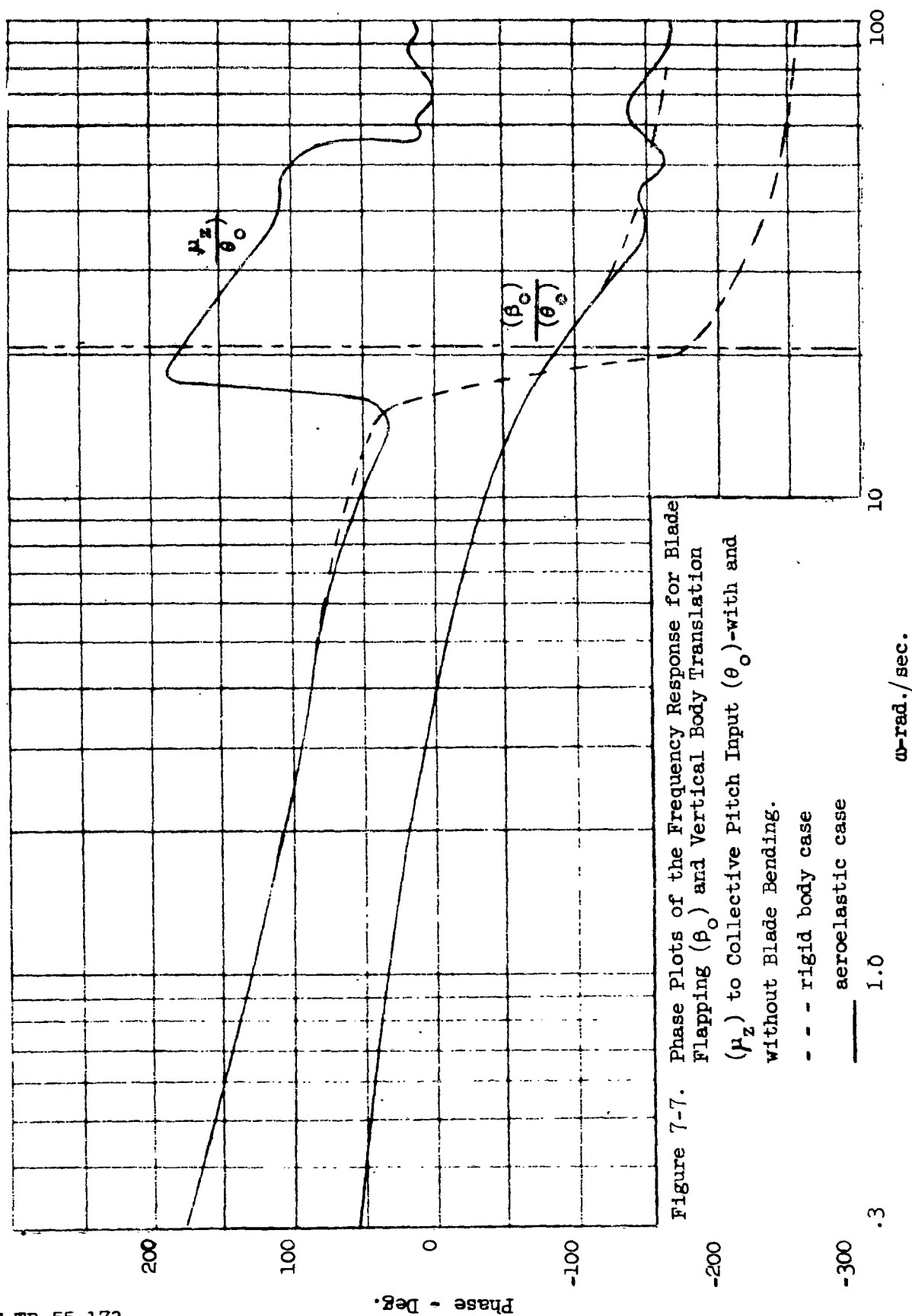


Figure 7-7. Phase Plots of the Frequency Response for Blade Flapping (β_0) and Vertical Body Translation (μ_z) to Collective Pitch Input (θ_0)-with and without Blade Bending.

Amplitude Ratio $\left(\frac{\theta}{\theta_0}\right)$ rad.

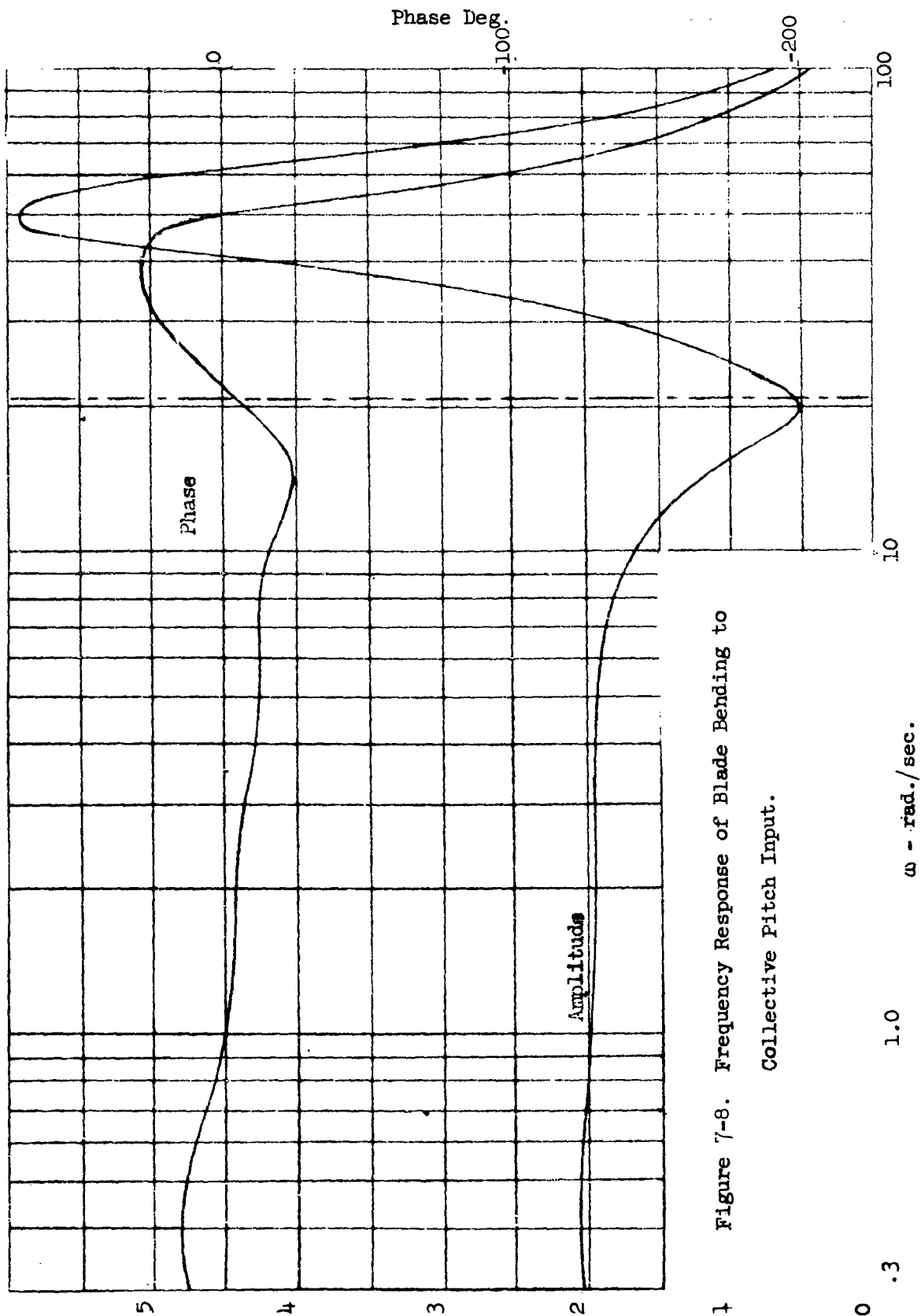
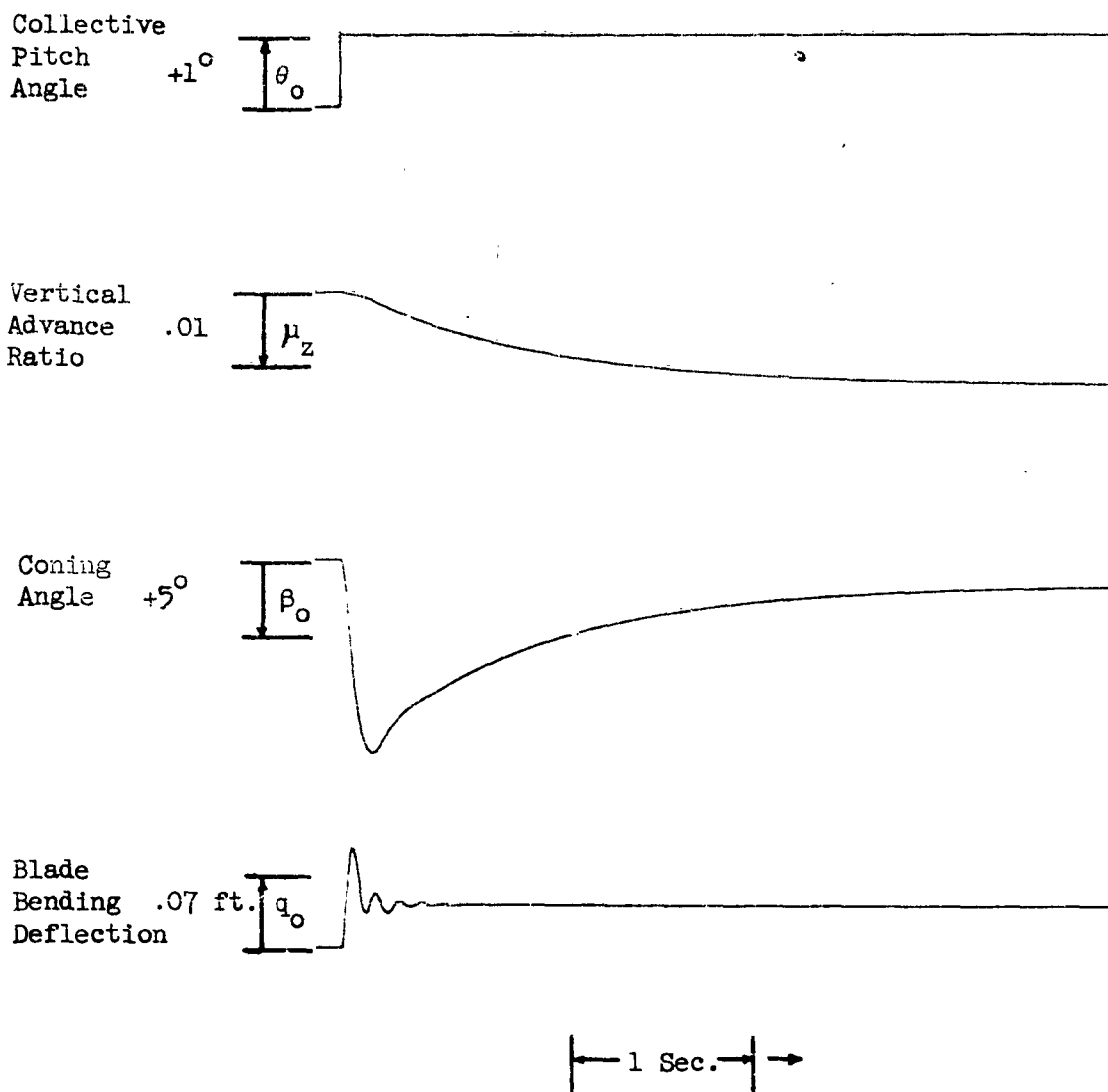


Figure 7-8. Frequency Response of Blade Bending to Collective Pitch Input.



Weight = 7,000 lbs.
 Altitude = Sea Level
 $\mu_{x_0} = \mu_{y_0} = \mu_{z_0} = 0$

Figure 7-9. Vertical Transients of a Helicopter in Hovering Flight ($\mu_{x_0} = 0$)
 Determined By An Aeroelastic Analysis Which Included
 The First Blade Bending Mode.

7.4 Illustration of the Use of a Root Locus Plot to Demonstrate the Effect of Torsion and Flexibility of the Blade on Helicopter Stability.

The root locus method has gained much popularity as a tool for synthesizing automatic controls and for describing the stability of systems with feedback networks. The method has further merit in its ease of yielding the stability characteristics of a system as a function of a change in parameters or the introduction of new degrees of freedom into the characteristic equation of the system. The latter use which is of interest here, is also described in Reference 10.

7.4.1 Inclusion of Torsional Effects

The particular application to be illustrated here is the resulting change in the rigid-body stability analysis of the helicopter by including blade torsion into the longitudinal characteristic equation for hovering flight. The basic data of the helicopter in Section 7.3 will be used and supplemented by the required additions for the insertion of the torsion mode.

In the case of torsion flexibility, it is assumed the blade incidence about the feathering axis is completely restrained by the pilots control (irreversible servo). However, the blades are permitted to twist about the elastic axis in the first torsion mode of the blade. The geometry of the blade is as shown in Figure 7-10.

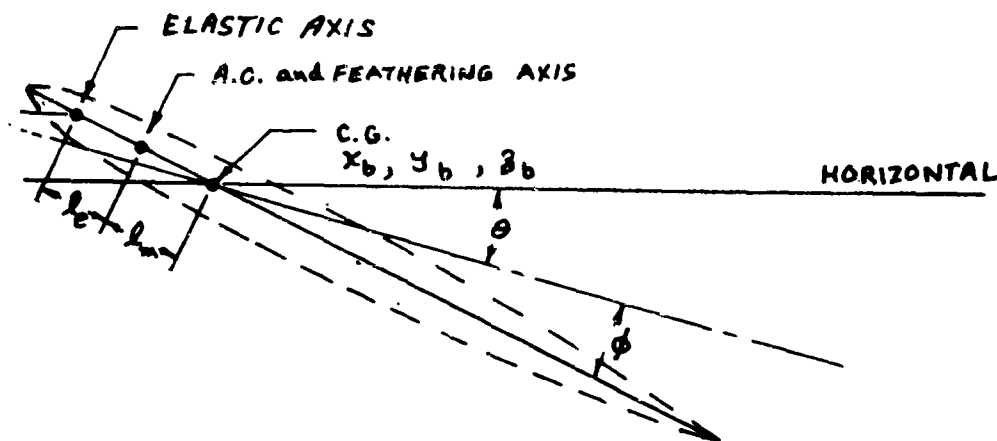


Figure 7-10. Blade Balance

The location of the aerodynamic center and the centers of mass with respect to the blade feathering axis is referred to as the aerodynamic and mass balance respectively. In this example, the blade has a symmetrical airfoil with aerodynamic center and feathering axis coincident. The general case will have the elastic and c.g. axes displaced a distance l_e and l_m from the feathering axis. In adding the elastic degree of freedom to the system, the equation of motion expressing the blade torsion moments about the elastic axis must be considered.

$$(\bar{M}_x) = (\bar{M}_x)_a + (\bar{M}_x)_m + (\bar{M}_x)_\phi \quad (7-143)$$

where

$$(\bar{M}_x)_a = -\frac{1}{2} \rho a c l_e \int_0^{BR} [(\theta + \phi) v_T^2 + v_T v_P] \eta(r) dr$$

$$(\bar{M}_x)_m = - \int_0^R \left[-\ddot{z}_b + \ddot{x}_b (\beta + \tau) \cos \psi - \ddot{x}_b (\theta + \phi) \sin \psi + \ddot{x}_b (\beta + \tau) \sin \psi + \ddot{y}_b (\theta + \phi) \cos \psi \right] (l_e + l_m) \eta(r) m dr$$

$$(\bar{M}_x)_\phi = -K_T \sigma(t) \quad (K_T = \text{generalized torsional stiffness})$$

This moment expression has been expanded and resolved into its Fourier components as shown in Reference 11. In this example, the high frequency effects associated with $\dot{\phi}$ and $\ddot{\phi}$ have been neglected. The purpose is to show the effect of torsion on the low frequency modes of the helicopter.

7.4.1.1 Torsional Mode and Stiffness Factor

The first torsional mode of the blade is represented by the expression

$$\phi = \eta_1(r) \sigma(t)$$

where the function $\sigma(t)$ is the generalized torsional deflection of the blade tip. Here again, the function $\sigma(t)$ will be represented as a harmonic function, i.e., $\sigma(t) = \sigma_0 + \sigma_1 \cos \psi + \sigma_2 \sin \psi$

The first torsional mode shape $\eta_1(r)$ is represented by the following function, normalized at the blade tip (see Equation 7-21).

$$\eta_1(r) = \sin \frac{\pi r}{2R} \quad (7-144)$$

The generalized restoring force is obtained by differentiating the potential energy with respect to the generalized deflection. The potential energy for a blade in torsion is expressed as

$$U_t = \frac{1}{2} \int_0^R GJ \left(\frac{\partial^2 \phi}{\partial r^2} \right)^2 dr \quad (7-145)$$

where GJ is the torsional rigidity of the blade. Solving for the stiffness factor, K_T , of the first mode

$$\frac{\partial U_t}{\partial \sigma} = -K_T \sigma = - \frac{GJ \pi^2}{8R} \sigma$$

and

$$K_T = \frac{GJ \pi^2}{8R}$$

The design value of the blade stiffness for the typical helicopter is

$$K_T = 4914 \quad \frac{\text{ft} - \text{lbs}}{\text{rad.}}$$

7.4.2 Rigid Body

To illustrate the procedure, the longitudinal rigid body equations of motion in hovering flight are used for describing the helicopters motion in forward translation, fuselage pitch, and rotor tip path plane pitch. The characteristic equation for our typical helicopter becomes (see Reference 11 for evaluation of stability derivatives):

$$\begin{aligned} \sum X \quad & (1750 + 122200s) \mu_x + (-2570 - 1359s^2) \alpha_1 + (4285 - 203s) a_1 = 0 \\ \sum M_{y_{cg}} \quad & 15690 \mu_x + (54,640 + 9640s^2) \alpha_1 + (54640 - 2590s) a_1 = 0 \\ \sum M_y'' \quad & 167 \mu_x + -481 \alpha_1 + (-479 - 41.6s) a_1 = 0 \end{aligned} \quad (7-146)$$

Some of the high frequency effects have been suppressed such as the neglect of the $s^2 a_1$ term in order to simplify the example.

The factored form of the characteristic equation is

$$\Delta_R = -.0481(s + 1.117)(s - .1071 \pm .4333i)(s + 10.63) = 0 \quad (7-147)$$

The roots of the above equation are plotted in root locus form in Figure 7-11a. The rigid-body roots are labeled p_{1R} , p_{2R} , p_{3R} , and p_{4R} where the unstable long period mode is represented by the two roots in the right hand plane.

7.4.3 Aeroelastic Case

If an elastic degree of freedom is introduced to the rigid body case, the effect is to give a displacement to all the existing rigid-body roots the magnitude of the displacement will depend upon the stiffness of the blade. Permitting the blade to twist in torsion, an additional degree of freedom is given to the helicopter and the characteristic equation becomes:

$$\begin{aligned} X \quad & (1750 + 109555s)\mu_x + (-2570 - 1359s^2)\alpha_1 + (4285 - 203s)a_1 + 0 = 0 \\ M_{y_{cg}} \quad & 15690\mu_x + (54640 + 9640s^2)\alpha_1 + (54640 - 2590s)a_1 + 0 = 0 \\ M_y'' \quad & 167\mu_x + -481\alpha_1 + (-479 - 41.6s)a_1 + 44.3\sigma_2 = 0 \\ M_x'' \quad & \frac{-l_e}{(l_e + l_m)^2 + .1368} (3545)\mu_x + \frac{9970l_e + 75}{(l_e + l_m)^2 + .1368} \alpha_1 + \frac{9970l_e + 894(l_e + l_m)s}{(l_e + l_m)^2 + .1368} a_1 \\ & + 432 - \frac{9070l_e + .464K_T}{(l_e + l_m)^2 + .1368} \sigma_2 = 0 \end{aligned} \quad (7-148)$$

The characteristic determinant should be expanded about the fourth column so that the rigid body determinant appears as one of the minors. The first locus is to illustrate the effect of the variations in torsional stiffness with l_e and l_m set at their design values.

$$\begin{aligned} l_e &= .1 \text{ ft.} \\ l_m &= 0 \end{aligned}$$

The new characteristic equation in factor form becomes:

$$\begin{aligned} \Delta_A &= (-5545 - 3.17 K_T)\Delta_R \\ -443(.678)(s + .661)(s + .0921 \pm .5781i)(s + 10.33) &= 0 \end{aligned} \quad (7-149)$$

The factors of the second minor become the zeros (z_{1A} , z_{2A} , etc.) of the

root locus plot and the factors of the rigid body determinant become the poles, (p_{1A} , p_{2A} , ---- etc.). In root locus fashion, the above equation (7-149) is expressed as follows:

$$\frac{6240}{(5545 + 3.17 K_T)(s + 1.117)(s - .1071 \pm .433i)(s + 10.63)} = |1| \angle 0 \quad (7-150)$$

The locus of roots for the characteristic equation of (7-149) are displayed in Figure 7-11b where the value of K_T is permitted to vary over a wide range. As K_T becomes infinitely large, the rigid body case is approached.

The variation of blade c.g. position is another important parameter which can be studied to advantage by showing the root locus with change in blade c.g. position, l_m . The characteristic determinant, Eq. (7-148), is again expanded about the fourth column, only this time the term $l_e + l_m$ is left indeterminate with K_T fixed at its design value. If l_e is held at the design value of .1 ft, and l_m is permitted to take on the following values:

$$l_m = 0, l_m = l_e, l_m = -l_e \text{ and } l_m = -2l_e;$$

then the locus of roots for this variation is as described in Figure 7-11c.

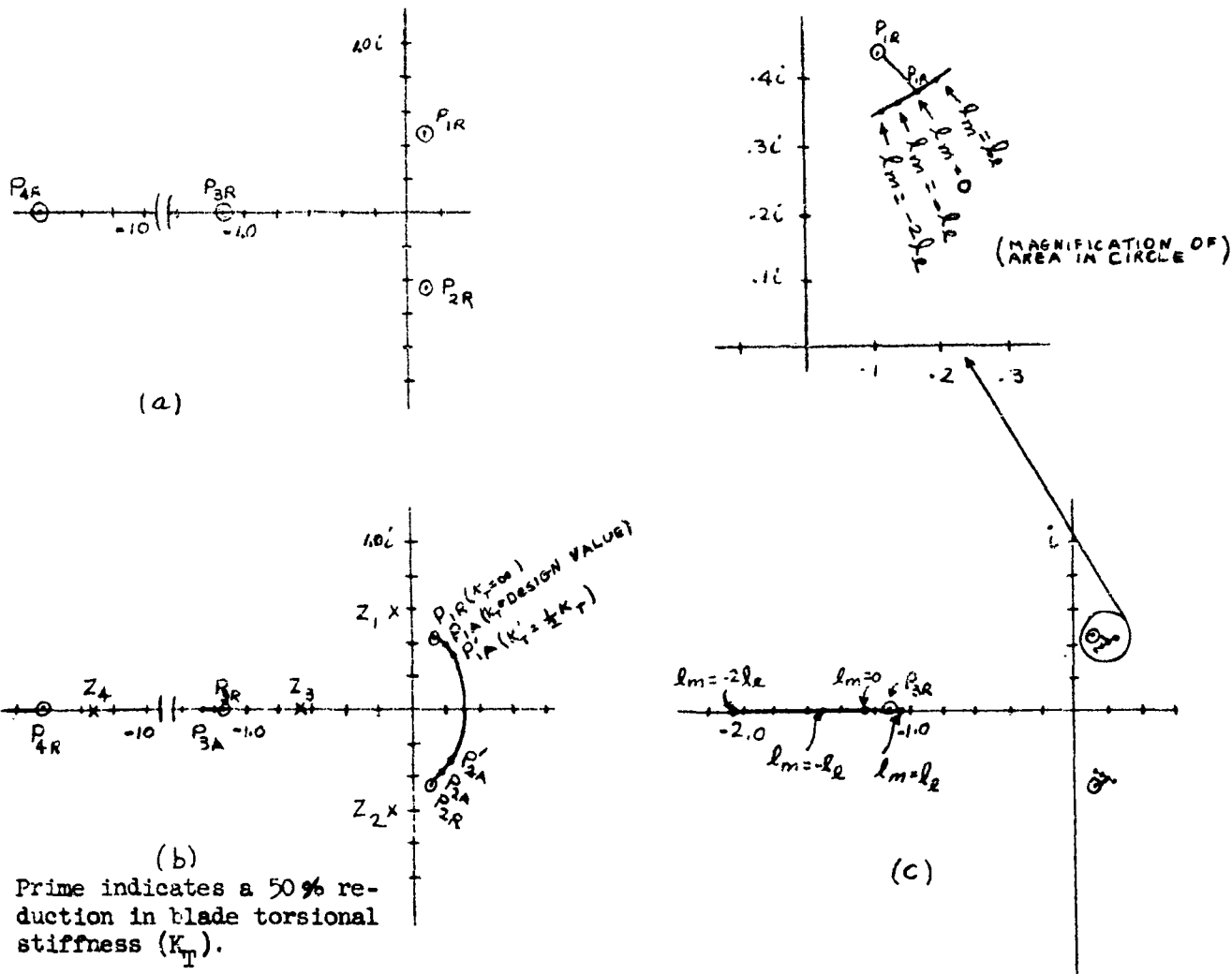
In all of the above cases, the different boundary conditions resulting from changes in blade balance and blade stiffness did not significantly change the stability derivatives of equation (7-148) except the last two elements in the last row as noted.

In Figure 7-12 transients are shown for the above case (where K_T and ($l_e + l_m$) are set at the design values) and are compared with the transients for a rigid body case.

7.5 Summary

The primary purpose of the manual, of course, is the presentation of methods of analysis and in particular the material of Chapter VII has applied these methods to the helicopter. Where possible, numerical examples have been employed to illustrate the procedures. Although some results have been presented, any discussion concerning them has not been made since the method and application were of primary concern. At this point, it might be well to discuss the present state of the art and give a few concluding remarks on some of the results attained thus far.

Comparatively little work has been done concerning the effect of aeroelasticity on the stability and control of the helicopter. However, a large amount of effort has been spent and is being spent on problems dealing with helicopter vibrations, flutter and blade stresses. These analyses are closely akin to the analyses of the manual and overlap in many areas, but actually lie outside of the scope presented here. Many studies deal with isolated cases such as blade or rotor stability, but few are concerned with the aero-



Hovering Helicopter
 $W = 7,000$ lbs.
 Sea Level
 Elastic axis ahead of feathering axis

Figure 7-11. Root Locus Plots Showing: (a) the rigid body poles, (b) the effect of stiffness, and (c) the effect of blade c.g. location.

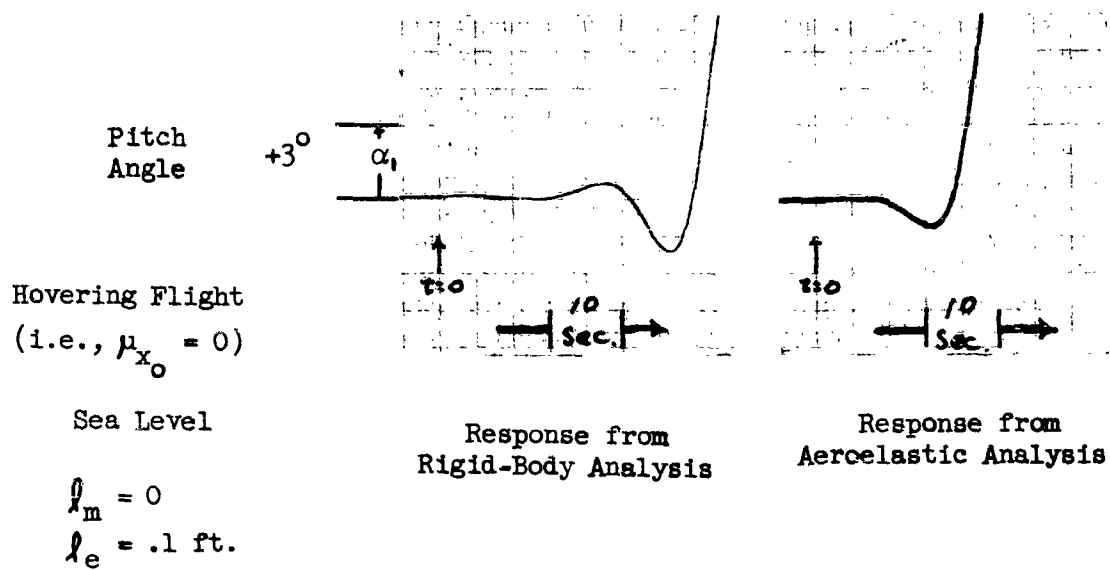


Figure 7-12.

Effect of Blade Torsion on the Pitch Response of the Long Period Mode.

elastic effect on the overall stability and control of the helicopter plus any feedback control equipment.

An early attempt to show the effects of blade restraint about the feathering axis on the long period modes of the helicopter is given in Reference 12. In this work the author, without permitting the blade to twist elastically, shows that the possibility does exist of improving the inherent stability of the helicopter by restraining the blades about the feathering axis, together with proper blade mass and or aerodynamic balance. The performance and results are indicated by transient analysis. In Reference 13, the same problem is pursued further by using elastic and viscous restraints between the non-rotating part of the swash plate and the frame of the aircraft. As in the first article, the analysis permits variations in the blade c.g. and a.c. positions. The equations of motion are developed and applied to an example case for hovering flight. The improvement in helicopter stability achieved by this means is demonstrated by determining the roots of the characteristic equation and transient responses. Reference 14 actually includes rotor blade flexibility into the analyses by the method presented herein. In this work, the first torsion mode of the blade is incorporated into a helicopter stability analysis which permits a variation in the mass and aerodynamic center with respect to the elastic axis of the blade. It is shown by this work that blade flexibility and unbalance can have a noticeable influence on the damping in pitch of the helicopter. The work of Reference 14 further demonstrates that blade twist flexibility and unbalance can materially reduce the effectiveness of an automatic control system design if these items are neglected in the control synthesis.

The examples used in this chapter are primarily to show application but they do contain some significant results. The example of Section 7.3 shows very little effect of blade bending on the vertical response of the helicopter body and rotor near hovering flight. The frequency responses and characteristic roots show little change in the rigid body modes (frequencies below rotor RPM) for having included the bending degree of freedom. The same results have been obtained for the cyclic or pitch and roll cases at low advance ratios ($\mu < .5$).^{*} However, the analysis of Reference 15 demonstrates that the inclusion of blade bending is important at advance ratios near 1.0 and above. This is an important consideration for the case of an unloaded rotor traveling in the airplane speed regime.

The results of Section 7.4 shows a significant change in the low frequency modes of the helicopter due to the inclusion of the blade elastic twist and mass unbalance. In this example, the elastic axis is not coincident with the feathering axis as is the case with most other simplified analyses. For the blade configuration of this example, it shows that the inclusion of blade twist increases the period and divergent rate for decreasing blade stiffness. As in all previous studies moving the c.g. in the aft direction causes a destabilizing influence. As can be seen from the blade geometry, there are many configurations to be investigated where

* These results have been obtained by the J. B. Rea Company and are to be published in WADC TR 55-407.

the analysis permits variation of parameters such as blade mass and aerodynamic unbalance, elastic-axis location and feathering axis location. Of course, many of these variations would be limited by practical blade design and unwanted vibrations.

In conclusion, the following general remarks can be made.

1. The methods presented herein are extremely useful for including structural elasticity into the stability and control analysis of the helicopter.
2. Blade bending can be neglected in most stability analyses except for the high advance ratios $\mu \approx 1$.
3. It is important to include blade twist into analyses for autopilot design equipment, especially when the blades have low stiffness and/or have mass or aerodynamic unbalance.

NOMENCLATURE

- A_1 = Lateral cyclic control input. Tilt angle measured at the blade with respect to shaft line. Right tilt positive.
- a = Lift curve slope of main rotor blade, per radian.
- a_1 = Longitudinal tilt of tip-path plane (or vertical axis) with respect to horizontal (to vertical) backward tilt positive.
- B = Blade tip loss
- B_1 = Longitudinal cyclic control input. Tilt angle measured at blade with respect to the shaft line. Forward tilt positive.
- b = Number of main rotor blades.
- b_1 = Lateral tilt of tip path plane (or vertical axis) with respect to horizontal (to vertical) - right tilt positive.
- c = Chord of main motor blade.
- D_x = Horizontal component of helicopter drag acting at c.g. of helicopter.
- e = Flapping hinge offset.
- $F_{i,j}$ = Component transfer functions = $As^2 + Bs + C$ where A, B, and C are the stability derivatives.
- F_1 = Normal blade force \perp to hub.
- F_{z_a} = Aerodynamic contribution to F_1
- F_{z_m} = Inertial contribution to F_1
- $(F_z), (F'_z), (F''_z)$ = The components of the vertical blade generalized force when described by the first harmonics of a Fourier Series.

$$\bar{F}_1 = (F_z) + (F'_z) \cos \psi + (F''_z) \sin \psi$$

- $(\bar{F}_z)_a$ = Generalized aerodynamic force acting on blade and \perp to undeflected elastic axis.

$$(\bar{F}_z)_a = (F_z)_a + (F_z')_a \cos \psi + (F_z'')_a \sin \psi$$
- $(\bar{F}_z)_h$ = Generalized elastic restraining force of blade in bending.

$$(\bar{F}_z)_h = (F_z)_h + (F_z')_h \cos \psi + (F_z'')_h \sin \psi$$
- $(\bar{F}_z)_m$ = Generalized inertia force normal to undeflected blade in vertical bending.

$$(\bar{F}_z)_m = (F_z)_m + (F_z')_m \cos \psi + (F_z'')_m \sin \psi$$
- g = Acceleration of gravity.
- H_{x_0} = Horizontal hub force of helicopter rotor positive to the rear.
- h = Rotor blade elastic deflection.
- h_1 = Rotor blade generalized deflection in first bending mode.

$$h_1 = g(t) \xi(r)$$
- h_{cg} = Vertical displacement of helicopter c.g. from hub center positive c.g. below hub.
- \bar{h}_{cg} = Fore and aft displacement of helicopter c.g. from shaft line.
- I_x = Moment of inertia of helicopter about longitudinal axis (in horizontal plane) and passing through c.g. (without blades), slug-ft².
- I_y = Moment of inertia of helicopter about lateral axis (in horizontal plane) and passing through c.g. (without blades), slug-ft².
- I_z = Moment of inertia of helicopter about vertical axis passing through c.g. (without blades), slug-ft².
- i = $\sqrt{-1}$
- K_B = Blade bending stiffness, lb per ft.

$M_{h_{x_0}}, M_{h_{y_0}}$ = Components of the hub moments due to the offset of the flapping hinge.

\bar{M}_y = Total blade moments about flapping hinge.

M_y, M'_y, M''_y The Fourier components of the blade moments about the flapping hinge.

$$\bar{M}_y = M_y + M'_y \cos \psi + M''_y \sin \psi$$

$(\bar{M}_y)_a$ = Total aerodynamic moment of blade about flapping hinge.

$$(\bar{M}_y)_a = (M_y)_a + (M'_y)_a \cos \psi + (M''_y)_a \sin \psi$$

$(\bar{M}_y)_m$ = Total inertia moments of blade about flapping hinge.

$$(\bar{M}_y)_m = (M_y)_m + (M'_y)_m \cos \psi + (M''_y)_m \sin \psi$$

$M_{x_{c.g.}}$ = Rolling moment about longitudinal axis which passes through c.g. and parallel to the "X" inertial axis. Positive left roll.

$M_{y_{c.g.}}$ = Pitching moment about lateral axis which passes through c.g. and parallel to the "Y" inertial axis. Positive nose down.

$M_{z_{c.g.}}$ = Yawing moment about vertical axis which passes through c.g. and parallel to the "Z" inertial axis. Positive nose left.

m = Mass per unit length of blade, slugs per ft.

\bar{m} = Total mass of helicopter, slugs.

$q(t)$ = Generalized, blade bending deflection, positive tip up.

q_0, q_1, q_2 = Fourier coefficients of generalized blade bending deflection.

$$q(t) = q_0 + q_1 \cos \psi + q_2 \sin \psi$$

R = Blade radius of main rotor.

r = Elemental blade radius of main rotor.

s = Laplace operator ($= \sigma + i\omega$)
 T = Helicopter thrust
 T_{z_o} = Vertical helicopter thrust component
 t = Time, sec.
 V = Velocity along flight path
 V' = Resultant velocity at rotor, vector sum of $V + v$.
 v = Induced velocity of main rotor.
 W = Weight of helicopter.
 X = Horizontal "X" force acting on helicopter. Positive to the rear.
 $x_o, \dot{x}_o, \ddot{x}_o$ = Horizontal displacement, velocity and acceleration of helicopter hub in direction of "x" axis.
 Y = Horizontal "Y" force acting on helicopter. Positive to the right.
 Y_{y_o} = Y component of horizontal rotor force. Positive to the right.
 $y_o, \dot{y}_o, \ddot{y}_o$ = Horizontal displacement, velocity, and acceleration of helicopter hub in direction of the "y" axis.
 Z = Vertical force acting on helicopter (not including weight). Positive upwards.
 $z_o, \dot{z}_o, \ddot{z}_o$ = Vertical displacement, velocity, and acceleration of helicopter hub.
 α = Blade angle of attack.
 α_f = Fuselage angle of attack.
 $\alpha_1, \dot{\alpha}_1, \ddot{\alpha}_1$ = Angular pitch displacement, rate and acceleration of helicopter shaft line with respect to the vertical and positive nose downward.
 $\alpha_2, \dot{\alpha}_2, \ddot{\alpha}_2$ = Angular roll displacement, rate and acceleration of helicopter body. Positive left roll.

$\alpha_3, \dot{\alpha}_3, \ddot{\alpha}_3$ = Angular yaw displacement, rate and acceleration of helicopter body. Positive nose left.

$\beta(t)$ = Blade flapping angle measured between blade feathering axis and horizontal. Positive blade up.

$$\beta(t) = \beta_0 - a_1 \cos \psi - b_1 \sin \psi$$

β_0 = Coning angle of helicopter blade.

δ = Mean drag coefficient of blades.

θ = Total pitch angle of helicopter blade measured between chord line and horizontal.

$$\theta = \theta_0 - \theta_1 \cos \psi - \theta_2 \sin \psi$$

θ_0 = Collective pitch of helicopter blade.

θ_1 = Swashplate tilt with respect to horizontal for lateral control.

$$\theta_1 = A_1 - \alpha_2$$

θ_2 = Swashplate tilt with respect to horizontal for longitudinal control.

$$\theta_2 = B_1 + \alpha_1$$

$$\lambda_a = -\frac{v}{\Omega R}$$

μ = $\frac{V}{\Omega R}$ forward advance ratio

$\mu_x, \dot{\mu}_x$ = $\frac{-\dot{x}_0}{\Omega R}$ and $\frac{\dot{x}_0}{\Omega R}$ respectively (positive for forward flight).

$\mu_y, \dot{\mu}_y$ = $\frac{\dot{y}_0}{R}$ and $\frac{-\dot{y}_0}{\Omega R}$ respectively (positive for right translation of hub).

$\mu_z, \dot{\mu}_z$ = $\frac{\dot{z}_0}{\Omega R}$ and $\frac{-\dot{z}_0}{\Omega R}$ respectively (positive for downward translation of hub).

- $\xi_1(r)$ = First bending mode shape of blade.
- ρ = Standard air density.
- σ = Real part of operator "s".
- τ = Slope of bending mode shape
- ψ = Blade azimuth angle, positive in direction of rotation, zero aft.
- Ω = Angular frequency of main rotor.
- ω = Angular frequency (imaginary part of operator "s").

REFERENCES

1. Arnold, S. and Goland, L., Helicopter Dynamic Stability and Control Studies, Cornell Aeronautical Laboratory Reports No. BB-437-S-1, Part I, 1950, and No. BB-437-S-2, Part II, 1951.
2. Scanlan, R. H. and Rosenbaum, R., Introduction to the Study of Aircraft Vibration and Flutter, The Macmillan Company, 1951.
3. Prewitt, R. H. and Wagner, R. A., Frequency and Vibration Problems of Rotors, J. A. S., Volume 7, Number 10, August 1940.
4. de Guillenchmidt, P., Calculation of the Bending Stresses in Helicopter Rotor Blades, NACA TM 1312, 1951.
5. Morduchow, Morris, A Theoretical Analysis of Elastic Vibration of Fixed-Ended and Hinged Helicopter Blades in Hovering and Vertical Flight, NACA TN, 1999.
6. Simpkinson, Scott H., Ealberton, L. J., and Millenson, M. B., Effect of Centrifugal Force on the Elastic Curve of a Vibrating Cantilever Beams, NACA TN 1204, 1947.
7. Horvay, G., Chordwise and Beamwise Bending Frequencies of Hinged Rotor Blades, J. A. S., Volume 15, Number 8, 1948.
8. Yntema, Robert Q., Rapid Estimation of Bending Frequencies of Rotating Beams, Langley Aeronautical Laboratory RM L54G02, August 1954.
9. Steffens, J., A Theoretical Analysis of the Lateral Dynamic Stability of Tandem Helicopters, Part I, Princeton University Aeronautical Engineering Report No. 286, Jan. 1955.
10. Bollay, William, Aerodynamic Stability and Automatic Control, Journal of Aeronautical Sciences, Volume 18, September 1951.
11. Walton, R. P., Investigation of Helicopter Stability and Control in Hovering and Forward Flight, J. B. Rea Co. Report, Air Force Contract No. AF 33(616)-108.
12. Miller, R. H., A Method for Improving the Inherent Stability and Control Characteristics of Helicopters, Volume 17, June 1950.
13. Nikolsky, A. A., Helicopter Analysis, John Wiley and Sons, Inc., 1951.
14. Goland, Leonard, The Effects of Rotor Blade Flexibility and Unbalance on Helicopter Hovering Stability and Control, Princeton University, Aeronautical Engineering Laboratory Report No. 218, February 1953.
15. Shulman, Yechiel, Stability of a Flexible Helicopter Rotor Blade in Forward Flight, Journal of Aeronautical Sciences, Volume 23, July 1956.

BIBLIOGRAPHY

Gessow, A., Bibliography of NACA Papers of Rotating-Wing Aircraft, January 1952. Research Memo RM L52B18a (Formerly RM L7J30) NACA.

Wheatley, J. B., An Analytical and Experimental Study of the Effect of Periodic Blade Twist on the Thrust, Torque, and Flapping Motion of an Autogiro Rotor, TR Number 591, NACA, 1937.

Wheatley, J. B., An Analysis of the Factors that Determine the Periodic Twist of an Autogiro Rotor Blade with a Comparison of Predicted and Measured Results, TR Number 600, NACA 1937.

Feingold, Arnold M., Theory of Mechanical Oscillation of Rotors with Two Hinged Blades, NACA ARR 3113, 1943.

Coleman, Robert P., Theory of Self-Excited Mechanical Oscillations of Hinged Rotor Blades, NACA ARR 3G29, 1943.

Rosenburg, Reinhardt, Aero-Elastic Instability in Unbalanced Lifting Rotor Blades, Journal of Aeronautical Sciences, Volume 11, October, 1944.

Coleman, Robert P., A Preliminary Theoretical Study of Helicopter-Blade Flutter Involving Dependence Upon Coning Angle and Pitch Setting, NACA RM L6G12, 1946.

Deutch, M. L., Ground Vibrations of Helicopters, Journal of Aeronautical Sciences Volume 13, Number 5, May 1946.

Flax, Alexander, The Bending of Rotor Blades, Journal of Aeronautical Sciences, Volume 14, Number 1, January 1947.

Horvay, G., Stress Analysis of Rotor Blades, Journal of Aeronautical Sciences,

Reissner, H. and Morduchow, M., A Theoretical Study of the Dynamic Properties of Helicopter-Blade Systems, NACA TN Number 143", 1948.

Horvay, G. and Yuan, S. W., Stability of Rotor Blade Flapping Motion When the Hinges are Tilted, Generalization of the "Rectangular Ripple" Method of Solution. Journal of Aeronautical Sciences Volume 14, Number 10, October 1947.

Moduchow, M., On Internal Damping of Rotating Beams, NACA TN 1996, 1949.

Carpenter, Paul J. and Peitzer, H. E., Response of a Helicopter Rotor to Oscillatory Pitch and Throttle Movements, NACA TN 1888, 1949.

Hirsch, H., Kline, J., and Daughaday, H., H-5 Variable Stiffness Blade Program AFTR-6329, Parts 1-6.

BIBLIOGRAPHY (continued)

Flax, A. H., Determination of Rotor Blade Natural Lagging Frequency Including Effects of Hinge Offset, Blade Flexibility and Root Spring Restraint. Cornell Aeronautical Laboratory, BB Reports, Number BB-538-S-1.

Flax, A. H. and Goland, L., Dynamic Effects in Rotor Blade Bending, Journal of Aeronautical Sciences, Volume 18, Number 12, December 1951.

Hirsch, Harold, the Contribution of Higher Mode Resonance to Helicopter Rotor Blade Bending, Cornell Aeronautical Laboratory, Presented at IAS meeting of January, 1952.

Purcell, T. H., Application of Stress Models to Rotor Blade Design Analysis Ninth Annual Forum, American Helicopter Society, May, 1953.

Brooks, G. W., The Application of Models to Helicopter Vibration and Flutter Research Ninth Annual Forum, American Helicopter Society, May, 1953.

Daughaday, H. and Kline, G., An Approach to the Determination of Higher Harmonic Rotor Blade Stresses, Ninth Annual Forum, American Helicopter Society, May, 1954.

Hirsch, Harold and Rasumoff, Abner, Influence of Rotor Blade Twist and Mass Distribution on Blade Loadings, Western Forum of the American Helicopter Society, Inc., November, 1954.

Myers, Garry C., Flight Measurements of Helicopter Blade Motion with a Comparison Between Theoretical and Experimental Results, NACA TN 1266, 1947.

Berman, Alex, Response Matrix Method of Rotor Blade Analysis, IAS Preprint Number 506, 1955.

CHAPTER VIII

METHODS FOR SOLVING AEROELASTIC EQUATIONS

8.0 Introduction

This chapter presents a few of the more widely used methods for solving aeroelastic equations of motion and discusses the uses of both digital and analog computing equipment in such computations. For the purpose of demonstrating the methods the following set of typical, yet simplified aeroelastic equations of motion for an elastic airframe is chosen:

Summation of Vertical Forces*

$$m(\ddot{z} - U_0 \dot{\theta}) = \frac{\partial Z}{\partial \eta} \dot{\theta} + \frac{\partial Z}{\partial \omega} \omega + \frac{\partial Z}{\partial h_1} h_1 + \frac{\partial Z}{\partial \dot{h}_1} \dot{h}_1 + \frac{\partial Z}{\partial \delta_e} \delta_e \quad (8-1)$$

Summation of Pitching Moments

$$I_y \ddot{\theta} = \frac{\partial M}{\partial \eta} \dot{\theta} + \frac{\partial M}{\partial \omega} \omega + \frac{\partial M}{\partial \dot{\omega}} \dot{\omega} + \frac{\partial M}{\partial h_1} h_1 + \frac{\partial M}{\partial \dot{h}_1} \dot{h}_1 + \frac{\partial M}{\partial \delta_e} \delta_e \quad (8-2)$$

Summation of Generalized Forces for Elastic Degree of Freedom

$$m_1 \ddot{h}_1 + c_1 \dot{h}_1 + k_1 h_1 = \frac{\partial P_1}{\partial \eta} \dot{\theta} + \frac{\partial P_1}{\partial \dot{\eta}} \dot{\eta} + \frac{\partial P_1}{\partial \omega} \omega + \frac{\partial P_1}{\partial \dot{\omega}} \dot{\omega} + \frac{\partial P_1}{\partial h_1} h_1 + \frac{\partial P_1}{\partial \dot{h}_1} \dot{h}_1 + \frac{\partial P_1}{\partial \delta_e} \delta_e \quad (8-3)$$

The above equations are usually written in what is known as the "stability derivative" form.

* If the frequency range of the motion is high (above 1 cps) it is well to add the term $\frac{\partial Z}{\partial \dot{\omega}} \dot{\omega}$.

The stability derivative form is obtained by dividing equations (8-1), (8-2), and (8-3) by m , I_y , and m_1 , respectively, which gives:

$$D^2 \bar{z} = \frac{\sum \bar{z}}{m} = (\bar{U}_0 + \bar{z}_g) D \theta + (\bar{z}_{\dot{w}} D^2 + \bar{z}_w D) \bar{z} + (\bar{z}_{h_1} D + \bar{z}_{h_1}) h_1 + \bar{z}_{\delta_e} \delta_e \quad (8-4)$$

$$D^2 \theta = \frac{\sum M}{I_y} = M_g D \theta + (M_{\dot{w}} D^2 + M_w D) \bar{z} + (M_{h_1} D + M_{h_1}) h_1 + M_{\delta_e} \delta_e \quad (8-5)$$

$$(D^2 + 2\zeta \omega_{n_1} D + \omega_{n_1}^2) h_1 = \frac{\sum P_i}{m_1} = (P_{\dot{\theta}} D^2 + P_{\theta} D) \theta + (P_{\dot{w}} D^2 + P_w D) \bar{z} + (P_{h_1} D + P_{h_1}) h_1 + P_{\delta_e} \delta_e \quad (8-6)$$

where $D = \frac{d}{dt}$ operator. Regrouping terms:

$$[(1 - \bar{z}_w) D^2 - \bar{z}_{\dot{w}} D] \bar{z} = (\bar{U}_0 + \bar{z}_g) D \theta + (\bar{z}_{h_1} D + \bar{z}_{h_1}) h_1 + \bar{z}_{\delta_e} \delta_e \quad (8-7)$$

$$(D^2 - M_g D) \theta = (M_{\dot{w}} D^2 + M_w D) \bar{z} + (M_{h_1} D + M_{h_1}) h_1 + M_{\delta_e} \delta_e \quad (8-8)$$

$$[D^2 + (2\zeta \omega_{n_1} - P_{h_1}) D + (\omega_{n_1}^2 - P_{h_1})] h_1 = (P_{\dot{\theta}} D^2 + P_{\theta} D) \theta + (P_{\dot{w}} D^2 + P_w D) \bar{z} + P_{\delta_e} \delta_e \quad (8-9)$$

or (dividing through by operator expressions on left) we obtain:

$$\bar{z} = \frac{1}{[(1 - \bar{z}_w) D^2 - \bar{z}_{\dot{w}} D]} \left[(\bar{U}_0 + \bar{z}_g) D \theta + (\bar{z}_{h_1} D + \bar{z}_{h_1}) h_1 + \bar{z}_{\delta_e} \delta_e \right] \quad (8-10)$$

$$\theta = \frac{1}{D^2 - M_g D} \left[(M_{\dot{w}} D^2 + M_w D) \bar{z} + (M_{h_1} D + M_{h_1}) h_1 + M_{\delta_e} \delta_e \right] \quad (8-11)$$

$$h_1 = \frac{1}{[D^2 + (2\zeta \omega_{n_1} - P_{h_1}) D + (\omega_{n_1}^2 - P_{h_1})]} \left[(P_{\dot{\theta}} D^2 + P_{\theta} D) \theta + (P_{\dot{w}} D^2 + P_w D) \bar{z} + P_{\delta_e} \delta_e \right] \quad (8-12)$$

8.1 Development of Solution Forms of Equations of Motion

The equations of section 8.0 are not in a form that is readily suitable for solution by computing procedures. Hence, it is desirable to further manipulate the equations to obtain the several forms that can be solved by either digital or analog equipment. The following algebraic manipulations result in several useful forms.

First, stability derivatives in equations 8-7, 8-8, and 8-9 can be replaced by F_{ij} expressions.

An example of this is as follows:

$$(F_{11}\theta + F_{12}z + F_{13}h_1 + F_{14}\delta_e)F_1 = \theta \quad (8-13)$$

$$(F_{21}\theta + F_{22}z + F_{23}h_1 + F_{24}\delta_e)F_2 = z \quad (8-14)$$

$$(F_{31}\theta + F_{32}z + F_{33}h_1 + F_{34}\delta_e)F_3 = h_1 \quad (8-15)$$

where $F_1 = \frac{1}{D^2}$, $F_{11} = M_g D$, $F_{12} = M_{\dot{w}} D^2 + M_{\omega} D$, etc.

An alternate corresponding to equations (8-10), (8-11) and (8-12) is:

$$(F_{12}z + F_{13}h_1 + F_{14}\delta_e)\mu_1 = \theta \quad (8-16)$$

$$(F_{21}\theta + F_{23}h_1 + F_{24}\delta_e)\mu_2 = z \quad (8-17)$$

$$(F_{31}\theta + F_{32}z + F_{34}\delta_e)\mu_3 = h_1 \quad (8-18)$$

where $\mu_1 = \frac{F_1}{1 - F_1 F_{11}}$, $\mu_2 = \frac{F_2}{1 - F_2 F_{22}}$, $\mu_3 = \frac{F_3}{1 - F_3 F_{33}}$

Secondly, the transfer functions relating total aircraft responses to inputs can then be found by algebraic means from equations (8-16) to (8-18) (Cramer's determinate rule); e. g.,

$$\frac{\text{Pitching Motion}}{\text{Elevator Motion}} = \frac{\theta}{\delta_E} = \frac{\Delta_\theta}{\Delta} \quad (8-19)$$

where the determinants:

$$\Delta = \begin{vmatrix} \mu_1^{-1} & -F_{12} & -F_{13} \\ -F_{21} & \mu_2^{-1} & -F_{23} \\ -F_{31} & -F_{32} & \mu_3^{-1} \end{vmatrix} \quad (8-20)$$

and

$$\Delta_\theta = \begin{vmatrix} F_{14} & -F_{12} & -F_{13} \\ F_{24} & \mu_2^{-1} & -F_{23} \\ F_{34} & -F_{32} & \mu_3^{-1} \end{vmatrix} \quad (8-21)$$

Another and perhaps a more familiar approach to obtaining the transfer functions involves either the Laplace or Fourier transformations. The results obtained are equivalent, for if we consider the Laplace transforms of equations (8.0), (8-1) to (8-3), we have:

$$(I_y s^2 + C s + K) \theta(s) = \sum M(s), \quad (8-22)$$

$$(m s^2 + C s + R) z(s) = \sum Z(s), \quad (8-23)$$

$$(m_i s^2 + C_i s + R_i) h_i(s) = \sum P_i(s), \quad (8-24)$$

where the initial condition data is omitted since it is assumed to have no effect on steady-state oscillatory motions.

The expressions on the right of Equations (8-22) through (8-24) are found by transforming the terms on the right side of Equation (8-7) through (8-9). After rearranging all the terms of (8-22) through (8-24) and obtaining the transfer function as before by a similar algebraic process, one sees the analogy of the two approaches in which D has been replaced by s. In either case the transfer function, Equation (8-19), will appear in the form:

$$\frac{\theta}{\delta_e} = \frac{a_m s^m + a_{m-1} s^{m-1} + \dots + a_0}{b_n s^n + b_{n-1} s^{n-1} + \dots + b_0} \quad (8-25)$$

where the coefficients a and b are constants.

The above transfer function (Equation 8-25) can be placed in its actual solution form if the following (Heaviside) substitution is made:

$$S = j\omega \quad (8-26)$$

where ω is the radian measure of frequency, $\omega = 2\pi f$. Equation (8-25) then becomes the analytic representation of a frequency response*:

$$\frac{\theta}{\delta_e} = \frac{a_m (j\omega)^m + \dots + a_0}{b_n (j\omega)^n + \dots + b_0} \quad (8-27)$$

Equation (8-27) could have been obtained more directly through the use of the Fourier transform. In this case the angular frequency, ω , is used immediately rather than passing through the entire s (or z) complex plane first and then restricting interest to the imaginary axis by Equation (8-26).

* A frequency response is a special case of a transfer function, where s has been replaced by $j\omega$. Frequency responses are normally presented in graphical form.

To recapitulate, the transition from time domain to frequency just discussed is performed by either the Laplace transform or the Fourier (series) analysis techniques (Figure 8-1). The Laplace is directly suited for the equations of motion whereas the Fourier harmonic analysis can be used on actual transient traces (such as flight test records). The transition from the frequency to time domain is demonstrated by the two techniques given in references 1 and 2. The first is called "Fourier Synthesis" and the second uses the Duhamel Integral.

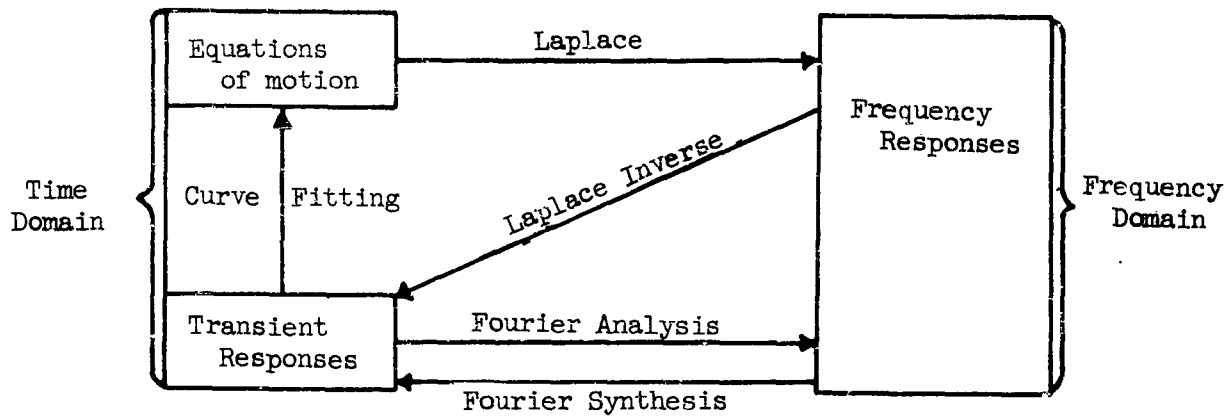


Figure 8-1. Domain Conversion

8.2 Digital Machines

Digital computers perform essentially two basic types of operations: matrix manipulation and step-by-step solution of equations. Matrix operations are primarily restricted to linear equation type results (determinant evaluations, etc.), whereas the step-by-step approach (with iteration schemes) can be used to solve nonlinear as well as linear differential equations through sequencing the integrations, differentiations, summations, etc.

Some of the more common types of high-speed digital computers suitable for solving aeroelastic equations of motion are: IBM 701, IBM 704, IBM 650, IBM CPC, ERA 1103, NCR 102, DATATRON, READIX, SWAC, SEAC, DYSEAC, DINAC, UNIVAC, JOHNIAC, MARK SERIES.

8.2.1 Solution of Equations of Motion. The equations of motion developed in Chapter III and in the examples of Chapters VI and VII are linear in form. The solutions will be in the forms of frequency responses or transient responses (to arbitrary inputs).

8.2.1.1 Point by Point Solution to Obtain Frequency Responses.
Consider Equations (8-16) to (8-18) whose coefficients are in the F_{ij} operator form; e. g.

$$F_{12} = M_{\dot{\omega}} D^2 + M_{\omega} D \quad (8-28)$$

If Equations (8-16) to (8-18) are Laplace transformed and s replaced by $j\omega$, then both the coefficients and variables will become complex functions of ω as follows:

$$\begin{aligned} \mu_1^{-1}(\omega) \theta(\omega) - F_{12}(\omega) z(\omega) - F_{13}(\omega) h_1(\omega) &= F_{14}(\omega) \delta_e(\omega) \\ -F_{21}(\omega) \theta(\omega) + \mu_2^{-1}(\omega) z(\omega) - F_{23}(\omega) h_1(\omega) &= F_{24}(\omega) \delta_e(\omega) \\ -F_{31}(\omega) \theta(\omega) - F_{32}(\omega) z(\omega) + \mu_3^{-1}(\omega) h_1(\omega) &= F_{34}(\omega) \delta_e(\omega) \end{aligned} \quad (8-29)$$

Then, if the following substitutions are made:

$$\begin{aligned} \mu_i^{-1} &= \mu_R^{-1} + j \mu_I^{-1} \\ -F_{12} &= F_{12R} + j F_{12I} \\ -F_{13} &= F_{13R} + j F_{13I} \\ F_{14} &= F_{14R} + j F_{14I} \\ \theta &= \theta_R + j \theta_I \\ z &= z_R + j z_I \\ h_1 &= h_{1R} + j h_{1I} \end{aligned} \quad (8-30)$$

, and

$$\delta_e = \delta_{eR} \quad (\delta_{eI} = 0 \text{ being arbitrarily chosen});$$

Equation (8-30) becomes (upon separating reals and imaginaries):

$$\mu_{1R}^{-1} \theta_R - \mu_{1I}^{-1} \theta_I + F_{12R} Z_R - F_{12I} Z_I + F_{13R} h_{1R} - F_{13I} h_{1I} = F_{14R} \delta_{eR}$$

$$\mu_{1I}^{-1} \theta_R + \mu_{1R}^{-1} \theta_I + F_{12I} Z_R + F_{12R} Z_I + F_{13I} h_{1R} + F_{13R} h_{1I} = 0$$

(8-31)

$$F_{21R} \theta_R - F_{21I} \theta_I + \mu_{2R}^{-1} Z_R - \mu_{2I}^{-1} Z_I + F_{23R} h_{1R} - F_{23I} h_{1I} = F_{24R} \delta_{eR}$$

$$F_{21I} \theta_R + F_{21R} \theta_I + \mu_{2I}^{-1} Z_R + \mu_{2R}^{-1} Z_I + F_{23I} h_{1R} + F_{23R} h_{1I} = 0$$

$$F_{31R} \theta_R - F_{31I} \theta_I + F_{32R} Z_R - F_{32I} Z_I + \mu_{3R}^{-1} h_{1R} - \mu_{3I}^{-1} h_{1I} = F_{34R} \delta_{eR}$$

$$F_{31I} \theta_R + F_{31R} \theta_I + F_{32I} Z_R + F_{32R} Z_I + \mu_{3I}^{-1} h_{1R} + \mu_{3R}^{-1} h_{1I} = 0$$

Equation (8-31) contains real coefficients and real variable components, all of which are functions of frequency, ω . Note that the size of the "matrix" has doubled.

By substituting a specific value of frequency, ω , into equation (8-31) we obtain a set of linear algebraic equations with real numerical coefficients.

The solution for each variable (θ_R , θ_I , Z_R , Z_I , h_{1R} , and h_{1I}) in terms of δ_{eR} is in the form of a ratio of two determinants as in Equation (8-19). Substituting, in turn, other values of frequency, ω_1 , ω_2 , etc., and repeating the determinant solution process, we obtain the real and imaginary terms for θ , Z , and h_1 as expressions of δ_e for a sequence of frequency values. Since δ_e appears as a factorable item, we can find $\frac{\theta}{\delta_e}$, $\frac{Z}{\delta_e}$, and $\frac{h_1}{\delta_e}$ as dependent upon frequency by first converting

real and imaginary components into polar form. These can be represented graphically as follows:

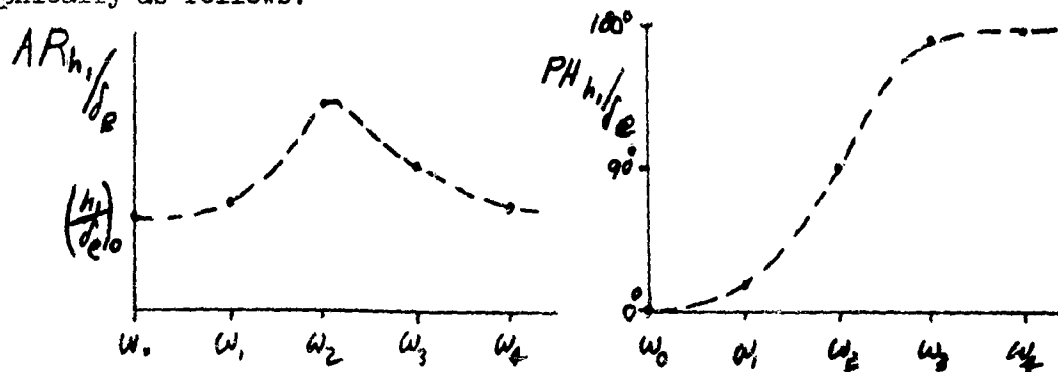


Figure 8-2. Frequency Response in Graphical Form

$$\text{where } AR_{h_1/\delta_e} = \frac{\text{Amplitude of } h_1}{\text{Amplitude of } \delta_e} = \frac{|h_1|}{|\delta_e|} \quad (8-32)$$

$$= \sqrt{\left(\frac{h_{1R}}{\delta_{eR}}\right)^2 + \left(\frac{h_{1I}}{\delta_{eI}}\right)^2},$$

$$\begin{aligned} PH_{h_1/\delta_e} &= \text{Phase angle, the lag of } h, \text{ behind } \delta_e = \arg \delta_e - \arg h_1 \\ &= -\tan^{-1} \frac{h_{1I}}{h_{1R}}, \text{ since } \arg \delta_e = 0. \end{aligned}$$

Once the frequency response of a system is available the transient response of the system to any input can be computed by means of a Fourier Synthesis, providing the Fourier representation of the input is known or can be obtained. The transient response is obtained by evaluating the Fourier Series of the output over the desired time interval. The Fourier Series of the output is obtained by transforming each coefficient of the Fourier Series representing the input by the amplitude ratio and phase indicated by this frequency response.

As an example, consider the response of a system to a step input. The output response can be written in Fourier Series form as

$$f(t) = \sum_{n=1}^N b_n \sin(n\omega_0 t + PA_n),$$

$$n = 1, 3, 5, 7, \text{ etc.}$$

where

$$b_n = B_n \times AR_n.$$

AR_n = Amplitude ratio of the frequency response data at frequency $n\omega_0$.

PA_n = Phase angle of the frequency response data at frequency $n\omega_0$.

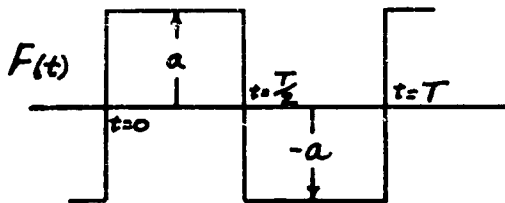
ω_0 = Fundamental frequency whose period should be greater than the time required for the transient output response to come to a steady state value.

$$B_n = \text{Sine coefficient of input at frequency } n\omega_0 = \frac{2}{T} \int_0^T F(t) \sin(n\omega_0 t) dt.$$

For the case of a unit step input:

$$F(t) = a \text{ for } 0 < t < \frac{T}{2}$$

$$\text{and } -a \text{ for } \frac{T}{2} < t < T$$



$$B_n = \frac{4a}{n\pi} \text{ and } n = 1, 3, 5, 7, \text{ etc.}$$

8.2.1.2 Polynomial Solution of Transfer Functions. This step results in the polynomial representations of transfer functions as shown by Equation (8-25). The polynomials can be obtained from a determinant by expanding by minors. However, expanding determinants which have elements of the form:

$$f_n s^2 + g_n s + h_n, \text{ etc} \quad (8-33)$$

by minors is a tedious task, considering that one not only is required to multiply, add and subtract a larger quantity of terms, but that one must also regroup the terms into respective powers of s so that the determinant will now be of the form

$$a(s) = a_n s^n + a_{n-1} s^{n-1} + \dots + a_0 \quad (8-34)$$

An alternate method for finding Equation (8-34) involves first the digital computer evaluation of a set of determinants (each having numerical elements rather than elements similar to Equation (8-33)). The numerical element form of the determinants is obtained by setting $s = s_0, s_1, s_2, \dots, s_n$, in turn, just as was done in the point-by-point frequency response determinant evaluation in the previous section. Hence $n + 1$ numerical-element determinants are obtained for the digital computer to solve.

The second step in the process is to curve-fit the $n + 1$ determinant values found from the digital computer evaluation above. It is convenient to use equally-spaced values in s above, for then curve fitting can be more conveniently accomplished by use of Lagrange's Interpolation Formula* which yields the desired polynomial form for Equation (8-34):

$$a(s) = D_0 L_0^{(n)}(s) + D_1 L_1^{(n)}(s) + \dots + D_n L_n^{(n)}(s) \quad (8-35)$$

$$\text{where } L_j^{(n)}(s) = \frac{(s-s_0)(s-s_1)\dots(s-s_{j-1})(s-s_{j+1})\dots(s-s_n)}{(s_j-s_0)(s_j-s_1)\dots(s_j-s_{j-1})(s_j-s_{j+1})\dots(s_j-s_n)} \quad (8-36)$$

The first formula is known as Lagrange's Interpolation Formula and the coefficients $L_j^{(n)}(s)$ as the Lagrangian Coefficients. The values of D_0, D_1, \dots, D_n are the values of the determinant for the corresponding values of s , i.e., s_0, s_1, \dots, s_n . It is important to note that Lagrange's Formula now becomes an exact (rather than interpolated) fit, since exactly $n + 1$ distinct values of s were used to fit an n th order curve, Equation (8-34).

* Milne, W. E. Numerical Calculus, Princeton University Press, Princeton, N. J. (1949), Page 67.

Each $L_j^{(n)}(s)$ is a polynomial of degree n which vanishes at $s = s_0, s = s_1, \dots, s = s_{j-1}, s = s_{j+1}, \dots, s = s_n$, but at $s = s_j$ it assumes the value of unity. From $L_j^{(n)}(s)$ we get $n + 1$ polynomial coefficients:

$$\begin{aligned} L_0^{(n)}(s) &= A_0 s^n + B_0 s^{n-1} + C_0 s^{n-2} + \dots + K_0 \\ L_1^{(n)}(s) &= A_1 s^n + B_1 s^{n-1} + C_1 s^{n-2} + \dots + K_1 \\ &\dots\dots\dots \\ L_n^{(n)}(s) &= A_n s^n + B_n s^{n-1} + C_n s^{n-2} + \dots + K_n \end{aligned} \quad (8-37)$$

where the coefficients of the final polynomial are given by Equation (8-35)

$$\begin{aligned} a_n &= D_0 A_0 + D_1 A_1 + D_2 A_2 + \dots + D_n A_n && = \text{coefficient of } s^n \\ &&& (8-38) \\ a_{n-1} &= D_0 B_0 + D_1 B_1 + D_2 B_2 + \dots + D_n B_n && = \text{coefficient of } s^{n-1} \\ &\dots\dots\dots \\ a_0 &= D_0 K_0 + D_1 K_1 + D_2 K_2 + \dots + D_n K_n && = \text{constant term} \end{aligned}$$

The over-all polynomial $a(s)$ is of order n and hence is determinable, in a unique manner, from any set of $n + 1$ distinct points, $a(s_i) = D_i$, $i = 0, \dots, n$. Substitution of the $n + 1$ distinct values of s_i into the polynomial while in the determinant form, and solving the resulting $n + 1$ determinants yields the $n + 1$ values of D_i . Using these $n + 1$ values of D_i to calculate Lagrange's D_i are exactly equal to the $a(s_i)$. Hence, the resulting polynomial form will be unique and exact, except for round-off errors.

As an example of the Lagrange method, consider the characteristic determinant of a typical helicopter:

$$\begin{vmatrix} 1837.91 + 109555s & -2458.19 - 1236.27s^2 & 3928.66 - 220.184s & -4579.8 - 35.349s \\ 16579.8 & 48756.7 + 9640s^2 & 48674 - 2687.43s - 56.025s^2 & -55897.94 - 2550.51s \\ -95.484 - 4.03489s & 0 & 27.5s + s^2 & 572 + 41.6s \\ 184.4128 & -572 & -572 - 41.6s & 27.5s + s^2 \end{vmatrix}$$

(8-39)

In making use of the Lagrangian interpolation formula, we take the following values of s ; namely, $s = 0, 1, 2, 3, 4, 5, 6$, and 7 . The Lagrangian coefficients are (by Equation 8-39):

$$\begin{aligned} L_0(s) &= \frac{(s-1)(s-2)(s-3)(s-4)(s-5)(s-6)(s-7)}{(-1)(-2)(-3)(-4)(-5)(-6)(-7)} \\ &= \frac{s^7 - 28s^6 + 322s^5 - 1960s^4 + 6769s^3 - 13132s^2 + 13069s - 5040}{-5040} \end{aligned}$$

$$\begin{aligned} L_1(s) &= \frac{s(s-2)(s-3)(s-4)(s-5)(s-6)(s-7)}{1(-1)(-2)(-3)(-4)(-5)(-6)} \\ &= \frac{s^7 - 27s^6 + 295s^5 - 1665s^4 + 5104s^3 - 8028s^2 + 5040s}{720} \end{aligned}$$

(8-40)

$$\begin{aligned} L_2(s) &= \frac{s(s-1)(s-3)(s-4)(s-5)(s-6)(s-7)}{2(1)(-1)(-2)(-3)(-4)(-5)} \\ &= \frac{s^7 - 26s^6 + 270s^5 - 1420s^4 + 3929s^3 - 5274s^2 + 2520s}{-240} \end{aligned}$$

$$\dots \dots \dots L_7(s) = \frac{s(s-1)(s-2)(s-3)(s-4)(s-5)(s-6)}{7(6)(5)(4)(3)(2)(1)} = \frac{s^7 - 21s^6 + 175s^5 - 735s^4 + 1624s^3 - 1764s^2 + 720s}{5040}$$

The D 's obtained by a digital calculation of the determinants (Equations (8-39) for $s = 0, 1, \dots, 7$), were as follows:

$$\begin{aligned} D_0 &= 48.00306 \times 10^{12} \\ D_1 &= 615.9440 \times 10^{12} \\ D_2 &= 4434.382 \times 10^{12} \\ D_3 &= 15923.93 \times 10^{12} \\ D_4 &= 41450.65 \times 10^{12} \\ D_5 &= 897641.8 \times 10^{12} \\ D_6 &= 724938. \times 10^{12} \\ D_7 &= 3047074. \times 10^{12} \end{aligned}$$

The coefficient of s^7 is (by Equation (8-38):

$$\left(-\frac{48.003055}{5040} + \frac{615.944033}{720} - \frac{4434.38196}{240} + \dots + \frac{3047073.867}{5040} \right) \times 10^{12} = 0.001046 \times 10^{12} \quad (8-41)$$

The coefficient of s^6 is

$$\left(48.003055 \left(\frac{-28}{5040} \right) + 615.944033 \left(\frac{-27}{720} \right) + 4434.38196 \left(\frac{-26}{240} \right) + \dots \right) \times 10^{12} = 0.05897 \times 10^{12}$$

If the constant term $D_0 = 48.003 \times 10^{12}$, then the polynomial of Equation (8-35) becomes:

$$10^{12} (.001046s^7 + .05897s^6 + 2.632s^5 + 50.58s^4 + 361.87s^3 + 144.13s^2 + 8.646s + 48.003) \quad (8-42)$$

In using this method, the amount of work is reduced considerably, since use can be made of digital computing equipment to obtain the values of the determinants. The $L_n(s)$ can be calculated readily with very little work. The order of the polynomial (n) can be obtained by inspection of the determinant and is usually equal to the sum of the highest powers of s along the diagonal (since this is the usual way of arranging terms).

Once the equations have been reduced to polynomials of s or D , there are a number of routine procedures available that are applicable to digital equipment for extracting the roots of the equations, natural frequencies, damping ratios, times to damp to half amplitude, etc. These dynamic parameters provide an insight to the stability of the system. Considerable literature is available describing these various techniques and some of the best known are given in References 3 through 6.

As an example, Equation (8-42) can be factored easily by a method of successive approximations (see Ref. 5). A trial divisor of

$$d^2 + a_1/a_2 d + a_0/a_2$$

works very well if the roots are well separated and if they are complex conjugates. This method is easily mechanized for either desk or larger machine calculators.

The quadratic factors obtained therefrom can be factored further to obtain the final roots. The roots are in the form

$$d = -\omega_n \xi \pm i \omega_n \sqrt{1 - \xi^2}$$

where

$$\xi = \text{damping ratio} = \frac{\text{actual damping coefficient}}{\text{critical damping coefficient}}$$

$$\omega_n = \text{undamped natural frequency}$$

$$\omega = \text{damped natural frequency} = \omega_n \sqrt{1 - \xi^2}$$

and

$$t_{1/2} = \text{time to damp to half amplitude} \\ \text{(or double amplitude if real part of the root} \\ \text{is positive)} = \frac{.693}{\xi \omega_n}$$

Equation (8-42) yields the following roots:

$$s_1 = -.701,$$

$$s_{2,3} = .140 \pm i 1.426,$$

$$s_{4,5} = 13.78 \pm i 5.364 \text{ and}$$

$$s_{6,7} = 14.20 \pm i 35.91.$$

Root one indicates an aperiodic yet convergent mode with a $t_{1/2} = \frac{.693}{.701} = .99$ second. Roots two and three indicate a divergent and oscillatory mode with

$$\xi = .312,$$

$$\omega_n = .45 \text{ rad/sec.},$$

$$\omega = .426 \text{ rad/sec.}, \text{ and}$$

$$t_{1/2} = \frac{.693}{.140} = 4.95 \text{ sec.} \\ \text{(time to double amplitude)}$$

Roots four and five indicate a convergent and oscillatory mode with

$$\xi = .934$$

$$\omega_n = 14.75 \text{ rad/sec.},$$

$$\omega = 5.32, \text{ and}$$

$$t_{1/2} = \frac{.693}{13.78} = .05 \text{ sec.}$$

Roots six and seven also indicate a convergent and oscillatory mode with

$$\begin{aligned}\xi &= .368 \\ \omega_n &= 38.6 \text{ rad/sec.}, \\ \omega &= 36.0 \text{ rad/sec.}, \text{ and} \\ t \frac{1}{2} &= \frac{.693}{14.20} = .049 \text{ sec.}\end{aligned}$$

8.3 Analog Machines

Analog machines are classified into two general groups; namely, direct analog and functional analog. The direct analog group includes such examples as the network analyzer, the electrical potential field (or electrolytic tank) representation for air flow, the thermal analog, etc. In general there is a direct correspondence between the physical quantities and the analog simulator quantities. Table I at the end of this chapter lists some of the more commonly used direct analog correspondences.

The direct analog representation of primary use in analyzing the aeroelastic aircraft is the network analyzer. This can be used as an electrical analog for structural stressing analyses which will yield not only elastic influence coefficient data for the job immediately at hand but also required strength design data. One of the better known facilities is located at California Institute of Technology in Pasadena, California.

The functional analog machine is set up to perform certain operations as prescribed by the mathematical differential equations rather than to obey similar laws of nature like direct analog. These operations include addition, subtraction, (or differencing), multiplication, division, integration, differentiation, and function generation (such as square roots, etc.). Since the functional analog computer is set up from the equations of motion, the remainder of this section will be devoted to its use. Another reason for this emphasis is that functional analog simulators are more easily adapted to dynamic aeroelastic analyses, whereas the network analyzer is reserved more for static aeroelasticity and steady-state structural loading studies. Functional analogs are being used to solve the problems that were originally unique to the network analyzer.

Functional analog computers may be of several types, the more popular being the electronic (operational amplifier) and the mechanical (differential analyzer) computers. The electronic analyzer uses voltages (or current) for variables and feedback amplifiers and other electronic devices, whereas the mechanical analyzer uses shaft rotations for variables and ball-disc integrators as principle units. The electronic has the advantage of being relatively fast and easy to set up, whereas it is more susceptible to break down than is the mechanical. Aside from this difficulty, the electronic operational amplifier computer is more satisfactory for aeroelastic stability and control studies, being more accurate than the mechanical computer. Incidentally, even the electronic computer uses some mechanical components (such as servo-type multipliers and mechanical recorders).

Accuracy of an analog computer is usually a nebulous thing, since the accuracy of end results depends not only upon the component accuracies but also upon the manner in which they are intercoupled. Good component design can yield accuracy of the order of 0.01 percent, while the overall accuracy is likely to be of the order of 0.1 to 1 percent. (Digital computing may be used to check overall accuracy and aid in uncovering errors in programming). In the future analog computing elements may be replaced by digital elements using converters to go from one field to the other. This will also enable printing out analog results in digital form.

8.3.1 Application to Aeroelastic Analysis. The method used to set up an analog computer for simulating the dynamic behavior of an aeroelastic aircraft is demonstrated in the following pages. The simplified mathematical model presented in section 8.0 will be used to demonstrate the technique.

Equations (8-4) to (8-6) are Laplace transformed into:

$$(1 - Z_w) s^2 Z = (U_0 + Z_g) s \theta + Z_w s Z + Z_{h_1} s h_1 + Z_{h_1} h_1 + Z_{\delta_e} \delta_e \quad (8-43)$$

$$s^2 \theta = M_g s \theta + M_{\dot{w}} s^2 Z + M_w s Z + M_{h_1} s h_1 + M_{h_1} h_1 + M_{\delta_e} \delta_e \quad (8-44)$$

$$s^2 h_1 = P_g s^2 \theta + P_g s \theta + P_{\dot{w}} s^2 Z + P_w s Z + (-2f_{h_1} + P_{h_1}) s h_1 - (w_{h_1}^2 - P_{h_1}) h_1 + P_{\delta_e} \delta_e \quad (8-45)$$

Assuming for the moment, the second derivatives $s^2 \theta$, $s^2 Z$, and $s^2 h_1$ are available, they can be integrated to obtain the lower and zero derivatives:

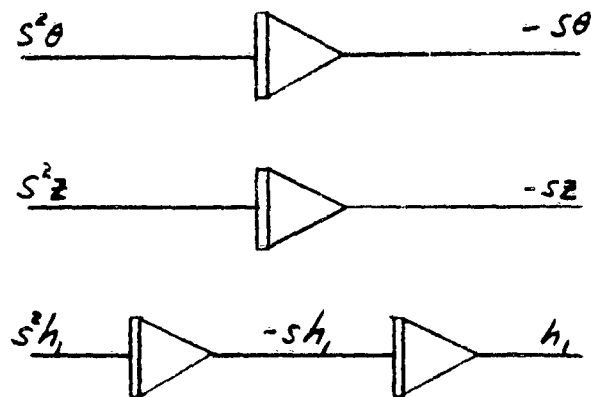


Figure 8-3 Analog Integration

Equation 8-43 is represented on the analog computer by a summing amplifier:

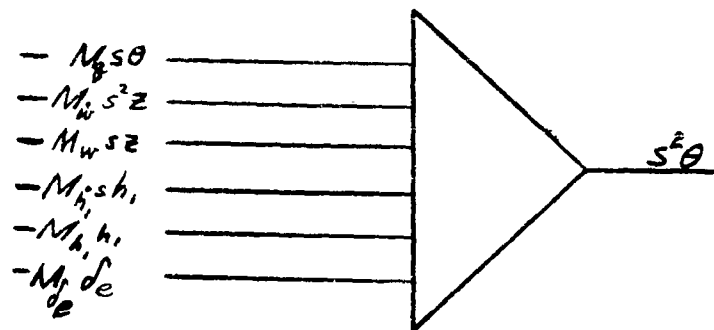


Figure 8-4 Analog Equation Addition

Equations (8-44) and (8-45) are represented in a similar way by two other summing amplifiers. Now that the highest derivatives have been made available, they can be put in as inputs to Figure 8-3.

Several problems arise to complicate the situation, which are:

1. Obtaining the right signs of variables,
2. Determining the appropriate gains (constants),
3. Scaling the variables to suitable amplitudes, and
4. Scaling in time (when necessary).

In order to change the sign of any quantity, one can simply pass it through another amplifier, however, this procedure is apt to lead to an excessive usage of amplifiers. Some investigation of the possible choices of certain variables with different signs may be justifiable in reducing the amplifier requirements.

The coefficients in Equations (8-43) to (8-45) govern the choice of amplifier gains and associated potentiometer settings to be used. In order to multiply a quantity by a constant greater than unity, an amplifier with a suitable gain must first be used with a pot following it in order to get a more accurate result.* This will be seen in the example soon to follow.

Analog computers are limited in the amount of power which can be transferred. In particular, amplifiers tend to limit above a certain voltage depending upon the output loading. Most operational amplifiers are designed to be linear up to 100 volts, hence one must "scale" the problem so that no amplifier output (or variable) exceeds this voltage. On the other hand, output voltages should not be so low as to be cluttered up by extraneous noise. The lower limit can be determined by checking the full scale percentage accuracy specifications for the amplifiers under consideration.

Time scaling may be found convenient (and sometime necessary) in analog analyses. Difficulty is encountered if as an example, an elastic degree of freedom having a natural frequency much greater than five cycles is to be investigated in conjunction with an aircraft having a natural (short-termed) frequency much less than one cycle. The dynamics of the higher elastic degree of freedom hardly couple at all with the aircraft dynamics and can be neglected if the latter is to be investigated**. On the other hand, if one is interested in the higher frequency regime, the slower rigid body aircraft dynamics may tend to become negligible. In this case a time scaling of the problem (slowing down the actual physical motion on the computer) becomes appropriate yielding an analysis that appears to be more like a flutter case.

A simple example will bring out some of the scaling features (for a more detailed example, see Appendix A of this chapter). Consider the elastic degree of freedom as expressed by Equation (8-45) with a natural frequency of one cycle per second:

$$\omega_{n_1}^2 = [2\pi(1)]^2 = 39.48 \frac{\text{rad}^2}{\text{sec}^2} \quad (8-46)$$

Suppose, for simplicity, that the mass normalized "spring" constant of the elastic mode, $P_{h_1} = -9.52$, and that the mass normalized damping constant,

$P_{\dot{h}_1} = -9.8$; then:

* Operational amplifier gains range from one tenth to 10 and possibly larger, while pots usually are accurate to about three decimal places.

** The static "spring" effect due to a higher frequency mode may be significant upon aircraft dynamics, however. This is included if one only sets the inertia term equal to zero (damping already being considered zero).

$$\begin{aligned}
 S^2 h_1 + (P_w - P_h) S h_1 + (\omega_{n_1}^2 - P_{h_1}) h_1 &= S^2 h_1 + 9.8 S h_1 + 49.0 h_1 \\
 &= P_g S^2 \theta + P_g S \theta + P_w S^2 z + P_w S z + P_e \delta_e \quad (8-47)
 \end{aligned}$$

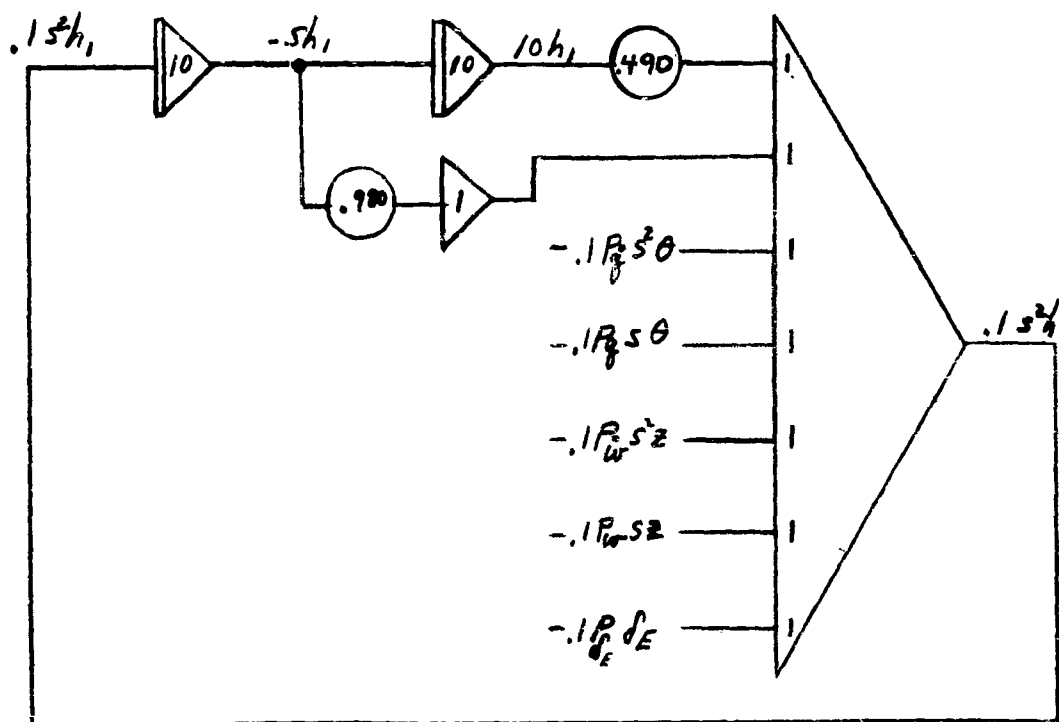
Scaling the variables to suitable amplitudes can now be demonstrated. Suppose the following maxima are known (or have been estimated) from the physical situation:

$$\begin{aligned}
 h_1 \text{ max.} &= \pm 10 \text{ ft.,} & \text{scale factor} &= 10 \text{ volts/ft.} \\
 \dot{h}_1 \text{ max.} &= \pm 75 \text{ ft./sec.,} & \text{scale factor} &= 1 \text{ volt/ft./sec.} \\
 \ddot{h}_1 \text{ max.} &= \pm 500 \text{ ft./sec.}^2, & \text{scale factor} &= 0.1 \text{ volt/ft./sec.}^2
 \end{aligned} \quad (8-48)$$

One can conveniently assign the indicated scale factors to each which would keep the voltage amplitudes on the computer within ± 100 volts. An equivalent method is to multiply each variable by a suitable factor and measure this quantity throughout the analog schematic:

$$\begin{aligned}
 \text{measure: } 10 h_1 &\text{ having a maximum of } \pm 100 \text{ volts,} \\
 \text{measure: } \dot{h}_1 &\text{ having a maximum of } \pm 75 \text{ volts, and} \\
 \text{measure: } .1 \ddot{h}_1 &\text{ having a maximum of } \pm 50 \text{ volts.}
 \end{aligned} \quad (8-49)$$

The analog representation for (the left hand side of) Equation (8-47) becomes:



Gains, pot settings and signs now become evident if Equation (8-47) is rewritten (recalling that amplifiers alternate signs):

$$.1S^2h_1 = -(.490)10h_1 - (.980)Sh_1 + .1(P_\theta S^2\theta + P_\theta S\theta + P_\omega S^2Z + P_\omega SZ + P_{\delta_e}\delta_e) \quad (8-50)$$

A time scaling can be indicated by substituting

$$\lambda = 10s \quad (8-51)$$

into Equation (8-47) (this results in the problem running ten times slower on the analog computer):

$$100\lambda^2h_1 + 98\lambda h_1 + 49h_1 = 100P_\theta\lambda^2\theta + 10P_\theta\lambda\theta + 100P_\omega\lambda^2Z + 10P_\omega\lambda Z + P_{\delta_e}\delta_e \quad (8-52)$$

The analog representation, in part, becomes:

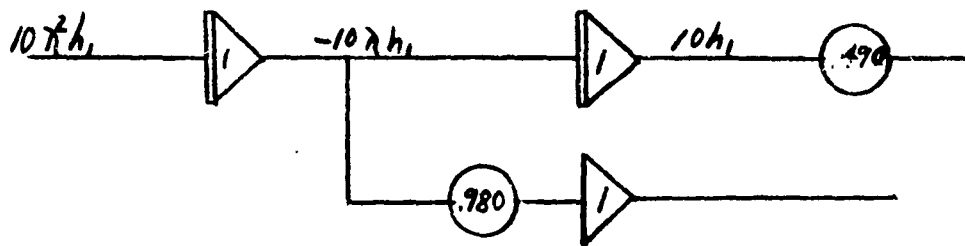


Figure 8-6. Time Scale Change in Analog Representation

since

$$\lambda^2 h_1 = \pm 5 \text{ ft./sec.}^2, \quad \lambda h_1 = \pm 7.5 \text{ ft./sec.}, \quad \text{and } h_1 = \pm 10 \text{ ft.}$$

One is referred to Appendix A for a more detailed example of analog setup procedures and to the bibliography at the end of this chapter for further information.

TABLE I

CORRESPONDENCE BETWEEN ELECTRICAL AND PHYSICAL QUANTITIES

| System | ELECTRICAL | | | FLUID (Gas or Liquid) | | |
|--|----------------------|------------------------------------|----------------|-----------------------------------|---|--------------------------------------|
| <u>Basic Dimension</u> | <u>Quantity</u> | <u>Unit</u> | <u>Sym bol</u> | <u>Quantity</u> | <u>Unit</u> | <u>Sym bol</u> |
| Potential | Electro-motive Force | Volt | e | Pressure | psia | P |
| <u>Quantity</u> | Charge | Coulomb | q | Volume or Weight displacement | in ³ lb | \bar{X} \bar{W} |
| <u>Quantity</u> Time | Current | Ampere | \dot{q} | Volume or Weight Flow | $\frac{\text{in}^3}{\text{sec}}$ $\frac{\text{lb}}{\text{sec}}$ | $\dot{\bar{X}}$ $\dot{\bar{W}}$ |
| <u>Quantity</u> Time ² | Current Change Rate | $\frac{\text{Ampere}}{\text{sec}}$ | \ddot{q} | Volume or Weight Flow Change Rate | $\frac{\text{in}^3}{\text{sec}^2}$ $\frac{\text{lb}}{\text{sec}^2}$ | $\ddot{\bar{X}}$ $\ddot{\bar{W}}$ |
| <u>Quantity</u> Potential | Capacitance | Farads | C _E | Compliance | $\frac{\text{in}^5}{\text{lb}}$ in ² | C _L C _G |
| <u>Pot-Time</u> Quantity | Resistance | Ohm | r _E | Resistance | $\frac{\text{lb-sec}}{\text{in}^5}$ $\frac{\text{sec}}{\text{in}^2}$ | r _L r _G |
| <u>Pot-Time</u> ² Quantity | Inductance | Heneries | L | Inertance | $\frac{\text{lb-sec}^2}{\text{in}^5}$ $\frac{\text{sec}^2}{\text{in}^2}$ | M _L M _G |
| <u>Pot-Time</u> Quantity | Impedance | Ohm | z _E | Impedance | $\frac{\text{lb-sec}}{\text{in}^5}$ $\frac{\text{sec}}{\text{in}^2}$ | z _L z _G |

TABLE I (Continued)

| System | MECHANICAL (Linear or Rotary) | | | THERMAL | | |
|-----------------------------------|---|---|-------------------------------|-----------------------------------|--|------------------|
| | Quantity | Unit | Sym bol | Quantity | Unit | Sym bol |
| Potential | Force or Torque | lb lb-in | f_M f_R | Temper- ature | Degree Rankine | T |
| Quantity | Displace- ment | in radian | x θ | Entropy | $\frac{\text{Btu}}{^\circ\text{R}}$ | \bar{S} |
| Quantity Time | Linear or Angular Velocity | $\frac{\text{in}}{\text{sec}}$ $\frac{1}{\text{sec}}$ | \dot{x} $\dot{\theta}$ | Entropy Flow | $\frac{\text{Btu}}{^\circ\text{R-sec}}$ | $\dot{\bar{S}}$ |
| Quantity Time ² | Linear or Angular Acceler- ation | $\frac{\text{in}}{\text{sec}^2}$ $\frac{1}{\text{sec}^2}$ | \ddot{x} $\ddot{\theta}$ | Entropy Flow Change Rate | $\frac{\text{Btu}}{^\circ\text{R-sec}^2}$ | $\ddot{\bar{S}}$ |
| Quantity Potential | Linear or Angular Inverse Spring const | $\frac{\text{in}}{\text{lb}}$ $\frac{\text{lb}}{\text{lb-in}}$ | C_M C_P | Heat Capaci- tance | $\frac{\text{Btu}}{^\circ\text{R}^2}$ | C_T |
| Pot-Time Quantity | Linear or Rotation- al Damping | $\frac{\text{lb-sec}}{\text{in}}$ $\frac{\text{in}}{\text{lb-in-sec}}$ | r_M r_R | Thermal Resist- ance | $\frac{^\circ\text{R}^2\text{-sec}}{\text{Btu}}$ | r_T |
| Pot-Time ² Quantity | Mass or Moment of Inertia | $\frac{\text{lb-sec}^2}{\text{in}}$ $\frac{\text{in}}{\text{lb-in-sec}^2}$ | m I | Thermal Inertia Concept | $\frac{^\circ\text{R}^2\text{-sec}}{\text{Btu}}$ | M_T |
| Pot-Time Quantity | Mech or Rotation- al impedance | $\frac{\text{lb-sec}}{\text{in}}$ $\frac{\text{in}}{\text{lb-in-sec}}$ | z_M z_R | Thermal Impedance | $\frac{^\circ\text{R}^2\text{-sec}}{\text{Btu}}$ | z_T |

REFERENCES

1. Walters, E. R. and Rea, J. B., Determination of Frequency Characteristics from Response to an Arbitrary Input, Journal of the Aeronautical Sciences, Vol. 17, No. 7, July, 1950.
2. Laitone, E. V.; Rigid Body Dynamics Including Non-Stationary Aerodynamics, Douglas Aircraft Co. Report No. SM-13820, January, 1951.
3. Milne, W. E., Numerical Calculus, Princeton University Press, Princeton, N. J. (1949).
4. Brown, G. S. and Campbell, D. P., Principles of Servomechanisms, John Wiley and Sons, N. Y. (1948).
5. Lin, Shih-Nge, : Method of Successive Approximations of Evaluation the Real and Complex Roots of Cubic and Higher Order Equations, Journal of Mathematics and Physics, Vol. 20, No. 3, August, 1941.
6. Sharp, H. S., Comparison of Methods for Evaluation the Complex Roots of Quartic Equations, Journal of Mathematics and Physics, Vol. 20, No. 3, August, 1941.

BIBLIOGRAPHY

1. McRuer, D. T., et al, Dynamics of the Airframe, BuAer Report AE-61-4II by Northrop Aircraft (Sept. 1952).
2. McRuer, D. T., et al, Methods of Analysis and Synthesis of Piloted Aircraft Flight Control Systems, BuAer Report AE-61-41 by Northrop Aircraft (March 1952).
3. Thaler, G. J. and Brown, R. G., Servomechanism Analysis, McGraw-Hill Book Co. (1953).
4. Brown, G. S. and Campbell, D. P., Principles of Servomechanisms, John Wiley and Sons (1948).
5. Evans, W. R., Control System Dynamics, McGraw-Hill Book Company (1954).
6. Chestnut, H. and Mayer, R. W., Servomechanisms and Regulating System Design, John Wiley and Sons (1951).
7. IBM Electric Punched Card Accounting Machines Principles of Operation: Electronic Calculating Punch-Type 604; Collator-Type 077, and Automatic Reproducing Punch-Type 513; International Business Machines Corp., New York, N. Y. (1945-1948).
8. Rodden, W. P., Static Longitudinal Stability and Dynamic Lateral Stability as Affected by Aircraft Flexibility, Douglas Aircraft Company Report EL-17299 (31 March 1953).
9. Hall, B. M., Energy Method Applied to Aircraft Vibration Problems, Douglas Aircraft Company Report SM-14349.
10. Hall, B. M., Survey of Approaches of Modal Analysis, Douglas Aircraft Company Report SM-14171 (October 1951).
11. Underwood, R., Solution of Matrix and Polynomial Equations, Douglas Aircraft Company Report SM-13568 (July 1949).

12. Barndollar, E. J., Application of Matrix Operations to Flutter Analysis Model General, Douglas Aircraft Company Report SM-13693 (February 1950).
13. Barndollar, E. J., Notes on Computing Methods, Douglas Aircraft Company Report SM-14013 (April 1951).
14. Williams, D., A General Method (Depending on the Aid of a Digital Computer) Deriving the Structural Influence Coefficients of Aeroplane Wings, British Report (RAE Structures 168), available from NACA on loan, N-34956 (November 1954).
15. Williams D., Solution of Aero-Elastic Problems by Means of Influence Coefficients, British Report (RAE Structures 169), available from NACA on loan, N-34929 (November 1954).
16. Milne, W. E., Numerical Calculus, Princeton University Press, Princeton, N. J. (1949).
17. Scarborough, J. B., Numerical Mathematical Analysis, Baltimore, John Hopkins Press (1930).
18. Milne Thompson, L. M., Calculus of Finite Differences, Macmillian and Co., Ltd., London (1933).
19. Dickson, L. E., New First Course in the Theory of Equations, John Wiley and Sons (1946).
20. Frazer, R. A., Duncan, W. J., and Collar, A. R., "Elementary Matrices," Cambridge University Press, London (1938).
21. Andrews, G. M., End Corrections for Frequency Responses by Laplace Transformation, Air Force Technical Report No. AFFTC 52-15.
22. Hall, B. M., Report on the Cal Tech. Analog Computer, Douglas Aircraft Company, Report No. SM-14193.
23. MacNeal, R. H.; McCann, G. D., and Wilts, C. H., The Solution of Aeroelastic Problems by Means of Electrical Analogies, Journal of the Aeronautical Sciences (December 1951), pp. 777-789.
24. Benscoter, S. U. and MacNeal, R. H., Introduction to Electrical Circuit Analogies for Beam Analysis, NACA TN 2785 (September 1952). pp. 273-275.

25. Swenson, G. W., Analysis of Nonuniform Columns and Beams by a Simple DC Network Analyzer, Journal of the Aeronautical Sciences (April 1952), pp. 273-275.
26. Scalan, R. H., A Steady-Flow Aeroelastic Study by Electrical Analogy, Journal of the Aeronautical Sciences, Vol. 20, No. 10 (October 1953).
27. Korn, G. A. and Korn, T. M., Electronic Analog Computers, McGraw-Hill, N. Y. (1952).
28. Mengel, A. S. and Melahn, W. S., RAND REAC Manual, RAND Corporation Report, RM-525, Revised (1 December 1950).
29. Instruction Book for Multiplier Groups 16 31L, 16 31M, 16 31N, Electronic Associates, Inc., Long Branch, N. J. (1953).
30. Greenwood, I. A., Holdam, J. V., and MacRae, D., Electronic Instruments, MIT Radiation Laboratory Series, Vol. 21, McGraw-Hill, N. Y. (1948).
31. Draper, C. S., McKay, W., Lees, S., Methods for Associating Mathematical Solutions with Common Forms, Instrument Engineering, Volume II, McGraw Hill, N. Y. (1953).

APPENDIX A

Mechanization Procedure for Analog Computers-Helicopter Example

Included in this appendix is a numerical example* which demonstrates the analog setup procedure. The helicopter in hovering flight and having three degrees of freedom is used.

The equations of motion of a hovering helicopter may be written as follows:**

$$M'_{y\mu_x}\mu_x - \alpha_1 + (M'_{y\dot{a}_1}S - 1)a_1 = B_1 \quad (1)$$

$$\begin{aligned} &[(H_{\ddot{\mu}_x} - M_{y\mu_x}H_{b_1})S + (H_{\mu_x} - M_{y\mu_x}H_{b_1} + M'_{y\mu_x}H_{a_1} - TM_{y\mu_x})]\mu_x \\ &+ H_{\ddot{\alpha}_1}S^2\alpha_1 + [-M_{y\ddot{a}_1}H_{b_1}S^2 + (M'_{y\dot{a}_1}H_{a_1} - TM'_{y\dot{a}_1})S + T]a_1 = 0 \end{aligned} \quad (2)$$

$$\begin{aligned} &[M_{y\mu_x}M_{y_{\dot{b}_1}}S + M_{y_{\dot{b}_1}\mu_x} - M_{y_{\dot{b}_1}} + M_{y\mu_x}M_{y_{\dot{a}_1}} \\ &- M'_{y\mu_x}(M_{y_{\dot{b}_1}} + M_{y_{\dot{a}_1}})]\mu_x + [M_{y_{\dot{a}_1}}S^2 + (M_{y_{\dot{b}_1}} + M_{y_{\dot{a}_1}})]\alpha_1 \\ &+ \{[M'_{y\dot{a}_1}M_{y_{\dot{a}_1}} - M_{y_{\dot{a}_1}}(M_{y_{\dot{b}_1}} + M_{y_{\dot{a}_1}})]S + (M_{y_{\dot{b}_1}} + M_{y_{\dot{a}_1}})\}a_1 = 0 \end{aligned} \quad (3)$$

* J. B. Rea Company, Determination of the Optimum Autopilot Design for Stabilizing the Longitudinal Mode of a Helicopter in Hovering Flight, published by Beckman Instruments, Inc., Richmond, California, Application Bulletin 5.

** Nikolsky, A. A , Helicopter Analysis, John Wiley and Sons, New York, 1951, Page 219, Equations 6.31b, 6.32b, and 6.33b.

where

$\dot{x}_o = \frac{\dot{x}_o}{\dot{\alpha}_1}$ = the longitudinal linear velocity of the helicopter c.g.,

α_1 = the longitudinal angular displacement

α_r = rotor tip path plane angle

B_1 = swash plate or control element angular displacement

s = d/dt operator

The following transfer functions for pitch angle to swash plate input and forward displacement to pitch angle respectively were derived from these equations.

$$\frac{\alpha_1}{B_1} = .139 \frac{(s + .00161)(s + 6.89 + j24.6)(s + 6.89 - j24.6)}{(s + .712)(s + 13.3)(s - .14 + j.425)(s - .14 - j.425)} \frac{\text{deg.}}{\text{deg.}} \quad (4)$$

$$\frac{\dot{x}_o}{\alpha_1} = 2.29 \frac{(s + .00550 + j1.70)(s + .00550 - j1.70)(s + 8.60 + j25.2)}{s(s + .00161)(s + 6.89 + j24.6)} \quad (5)$$

$$\frac{(s + 8.60 - j25.2)}{s + 6.89 - j24.6} \frac{\text{ft.}}{\text{deg.}}$$

As may be seen from equations (4) and (5), the various roots of each of the two denominators are widely separated. From preliminary investigations it was found that the larger roots contribute practically nothing to the dynamics of the helicopter except gain. It was further determined that neglecting the larger roots does not result in important changes in helicopter plus autopilot over-all response over the range of networks and gains which were used for autopilot stabilization. Thus equations (4) and (5) were reduced to:

$$\frac{\alpha_1}{B_1} = 6.82 \frac{s + .00161}{(s + .712)(s - .14 + j.425)(s - .14 - j.425)} \frac{\text{deg.}}{\text{deg.}} \quad (6)$$

and

$$\frac{\dot{x}_o}{\alpha_1} = 16.4 \frac{s + .00550 + j1.70)(s + .00550 - j1.70)}{s(s + .00161)} \frac{\text{ft.}}{\text{deg.}} \quad (7)$$

Autopilot data were used to obtain the following equation representing the autopilot servo motor dynamics.

$$\frac{B_1}{e} = \frac{K_M}{s+2.3} \quad \frac{\text{deg.}}{\text{volt}} \quad (8)$$

where

B_1 = swash plate control angle due to autopilot correction signal. (degrees)

e = autopilot correction signal to the servo motor (volts)

K_M = servo motor gain constant (deg/volt.)

A double lead-lag network of the form

$$K_B \frac{(s + \frac{1}{T_1})(s + \frac{1}{T_2})}{(s + 10)^2} \quad (9)$$

was chosen in order to provide sufficient lead with α_1 and x_0 feedbacks to obtain acceptable system natural frequency and damping.

Equations (6) and (7) were re-written in the following form in order that they could be mechanized in a straightforward manner on the computer.

$$-s^2 \alpha_1 = (.432s + .0011 + \frac{.143}{s}) \alpha_1 - (6.82 + \frac{.011}{s}) B_1 \quad (10)$$

$$-s^2 x_0 = .00161 s x_0 - (17.8s^2 + .194s + 51.4) x_1 \quad (11)$$

Equation (8) may be mechanized using one integrator amplifier as follows:

$$\frac{B_1}{e} = \frac{K_M}{s + 2.3}$$

$$-B_1 = (-K_M e + 2.3 B_1) \frac{1}{s}$$

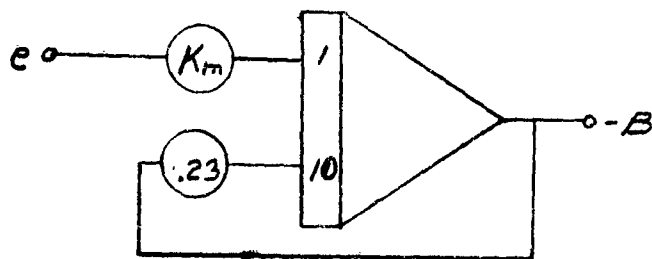


Figure A-1

Equation (8) is most conveniently mechanized using complex impedances on input and feedback paths of a D-C analog amplifier since such an arrangement enables one to vary the several cascaded time constants of the autopilot separately and independently without changing the feedback gain K_β , in the process. For each term of the form $(s + 1/T) / (s + 10)$ one amplifier may be used.

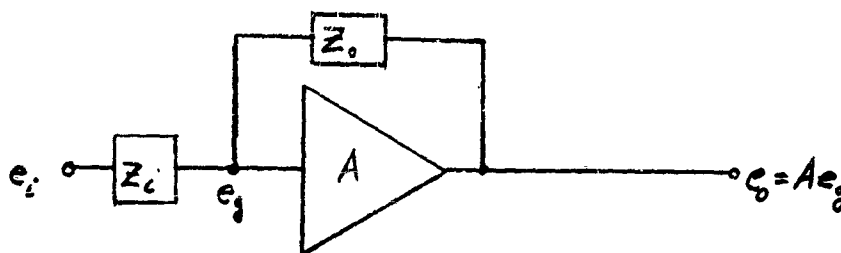


Figure A-2

In Figure A-2, if $A \rightarrow \infty$ then

$$\frac{e_o}{e_i} = \frac{Z_o}{Z_i}$$

$$Z_o = \frac{1}{s + \frac{1}{R_o C_o}}$$

$$Z_i = \frac{1}{s + \frac{1}{R_i C_i}}$$

If $C_1 = C_o$,

$$\text{then } \frac{e_o}{e_i} = \frac{s + \frac{1}{R_1 C_1}}{s + \frac{1}{R_o C_o}}$$

and if $\frac{1}{R_1 C_1} = \frac{1}{T}$

$$\frac{1}{R_o C_o} = 10,$$

$$\text{then } \frac{e_o}{e_i} = \frac{s + \frac{1}{T}}{s + 10}$$

The final mechanization is shown in Figure A-3. The input-output calibrations are as follows:

$$B_1 = 1 \frac{v}{\text{deg.}}, \alpha_1 = 1 \frac{v}{\text{deg.}}, x_o = 1 \frac{v}{10 \text{ ft.}}$$

Since x_o could have easily have a displacement excursion of several hundred feet during transients, the x_o output gain was reduced by a factor of 10. This change eliminated the possibility of amplifier limiting in the x_o section of the computer.

CHAPTER IX.

FLIGHT TESTING

9.0 Introduction

9.0.1 Objectives: The theoretical determination of the dynamics of aeroelastic aircraft, as described in the preceding chapters, is a complex process. Any numerical solution is necessarily an approximate one, subject to various errors due to: representation of the aircraft motion by simplified (e.g., linearized) equations of motion, approximation of continuous functions with values at discrete points, estimation of the coefficients of the assumed equations, etc. Indeed, it is difficult to predict with accuracy the motions of a rigid aircraft in high-speed flight. Addition of degrees of elastic freedom so increases the uncertainty of the results that full-scale verification by flight testing is a practical necessity.

Of course, it might be said that measurement in flight of the dynamic response of an aircraft, rigid or elastic, obviates the need for the laborious prediction by theoretical methods. When the mission is solely that of determining the dynamic characteristics of a particular aircraft at specified conditions, this is true. Such an approach has been followed to obtain airframe data on which to base automatic control design. This merely attests to the need for prediction methods available to the development engineer. In any event, full-scale testing comes far too late in the development cycle to provide timely information for the designer. Its goals should be to verify the predictions and, perhaps most important, to lead to improved prediction techniques.

9.0.2 Comparison of Experiment and Theory. Four forms of verification of the predicted dynamic response require the comparison of theoretical and experimental values of (a) transient response to known disturbances, (b) frequency response, (c) transfer function coefficients, and (d) aerodynamic, structural and inertial coefficients (i.e., coefficients of the equations of motion). The methods are listed in order of increasing value to the aircraft designer. As the value of the result increases, so does the difficulty of obtaining it.

Comparison of transient responses (time histories) measured in flight with those obtained by analytical means is a straightforward approach to the verification of predicted responses. It makes the best use of analogue simulator techniques, with a few reservations. The usual analogue computer approach is to determine the response of the aircraft to step or symmetrical pulse deflections of control surfaces. In practice, these inputs cannot easily be produced. Moreover, they are often not the most desirable inputs. They may fail to excite one or more of the fundamental modes of the aircraft or, as with the step input, will create a steady-state error from the trim condition. It is nevertheless possible to verify the predicted equations of motion "ex post facto" by generating inputs to the analogue computer which match those applied in flight. The subject of desirable inputs is discussed in more detail in Section 9.3.

The comparison of experimental and theoretical data in frequency res-

ponse form is generally more convenient than a transient response comparison because it displays explicitly the agreement, or disagreement for each clearly separate mode.* It thus helps the engineer to decide which modes of motion of the aircraft need more attention in terms of refinement of prediction techniques. Computation of frequency response by analogue computer methods is considerably less convenient than is the computation of transient response. Preparation of arbitrary inputs (for read-in to the computer), low accuracy, and inability to store interim results are major drawbacks to the use of analogue computers for frequency response analysis. Perhaps the greatest disadvantage is its inability to handle transients which do not vanish rapidly. The digital computer can be used here to good advantage.

Comparison of transfer coefficients obtained from theory and test carries the above procedure an additional step, with further benefits to the researcher and designer. Ideally, it permits separate comparison of each coefficient of each mode of the system transfer function. In practice, if more than a few coefficients must be determined from the flight test data the solution becomes difficult. For an aeolastic aircraft with any elastic modes included, this difficulty will certainly be present. Improved techniques for the evaluation of transfer function coefficients from flight measurements may give this approach more practical utility in the future.

Comparison of the stability derivatives (coefficients of the equations of motion) as obtained from theory and from flight test can be considered as the final refinement in the correlation process. The determination of these coefficients from flight data is, of course, beset with the difficulties mentioned above, and more. Separation of some of the stability derivatives is virtually impossible. In many cases the magnitude of the instrumentation installation and the extreme accuracies required will impose practical limits on the determination of the coefficients. Reference 1 gives a method for finding the maximum number of coefficients which may be determined and the conditions under which this maximum number is obtained. Much research remains to be done on the semi-inverse solution of stability equations to yield the coefficients (stability derivatives), as pointed out in Reference 2.

9.1 Data Requirements

9.1.1 General. In Section 9.0.1 it was pointed out that the objectives of flight testing were two-fold: (a) determination of the dynamic characteristics of a particular aircraft and/or (b) verification of prediction theory for aircraft dynamics. In some instances both objectives may not be realized because of limitations of time and money. In general, data requirements of objective (a) are of lesser magnitude than those of (b), and the two will be discussed separately. It should be realized, however, that the two objectives might well be combined in one program. To date only a limited amount of flight research on aeroelastic aircraft dynamics has been conducted (References 3-5) and the need for more such work is great.

9.1.2 Data for Evaluation of Flight Dynamics. As with the rigid aircraft, evaluation of the dynamics of aeroelastic aircraft requires measurement of the response of its center of gravity. The primary items are vertical

* Where two modes are closely coupled, it may not be possible to separate them effectively.

(normal) and lateral acceleration and angular velocity about all three body axes. Angles of attack, α , and sideslip, β , are desirable, but present measurement problems (see Section 9.4). It must be recognized that the free-stream air direction obtained from any measurement applies principally to the point of measurement. For aeroelastic aircraft the variations of relative wind are of considerably greater magnitude than for rigid aircraft; however, this should not lead one to the conclusion that such values of α and β are valueless. Some reference value of α , for example, is necessary from which to determine the α distribution along a flexible, swept wing. An indirect procedure is to compute angle of attack from measured values of normal acceleration and pitching velocity (or sideslip from lateral acceleration and yawing velocity). Because of the limited accuracy presently obtainable from direct measurement of air direction -- within $1/4$ degree at best, more often no better than $\pm 1/2$ degree accuracy -- the indirect approach is preferred by many.

Control surface position measurement poses a problem not shared by the rigid airframe. Because it is subject to spanwise twist, a single point of measurement will not generally suffice. Too, the twisting is a function of indicated airspeed (or dynamic pressure, q) and no single point on the control surface or its torque tube represents a mean value of the control surface deflection at all flight conditions.

Of importance to the design of automatic flight controls is the response of the aircraft to a command input to the control surfaces. Such input command is generally in the nature of a displacement of a servo valve. Thus it becomes important to measure such displacement at the valve or at some point rigidly connected to it. Under manual control by the pilot, inputs should be measured such that they are representative of the stick, wheel or pedal displacements. If there is any suspicion of significant lag between the cockpit controls and the surface actuators, it is wise to measure at both points.

Of major importance in the elastic airframe is the necessity for measuring accelerations and/or angular velocities at points on the structure where it is intended that sensors for any automatic control subsystem may be located. It is quite possible that the sensor will feed back a signal which is markedly different in amplitude and/or phase than was anticipated. In one situation, an otherwise stable airplane was made dangerously unstable because of the effects of fuselage side bending on the yaw rate feedback of the autopilot. The flight test program which followed (Reference 6) resulted in a retrofit affecting numerous airplanes. In the case in question, the yaw rate gyro was relocated and roll rate feedback to rudder was added; also, other improvements to the autopilot were made. Had the dynamic response of this aeroelastic airplane been determined at an earlier date, much of the time and expense of a retrofit program could have been avoided.

Measurement of the quantity of fuel in each tank is necessary to determine changes in weight, center of gravity, and moments of inertia. Determination of the initial (take-off) values of the parameters is discussed in Section 9.2.

9.1.3 Data for Checking Aeroelastic Theory. The requirements for flight data to check theoretical predictions and wind tunnel tests include practically all of the foregoing plus much more. Deformation of elastic

portions of the structure, pressure distribution over these portions of the aircraft, and accelerations at numerous points, are items of which measurements may be needed. The extent to which these are accounted for is dependent upon the extent to which theoretical calculations are to be checked. An example of such a test program is given in References 3, 4 and 5.

Determining deformation of the structure by optical means is the most straightforward approach. The camera(s) must be located at a rigid reference point on the aircraft, such as on the upper or lower fuselage near the main wing spar juncture. Targets must be provided at the points whose deformations are to be measured in order that the perception of such deformation is sufficiently sensitive. For the wing with negligible chordwise bending, a chordwise pair of targets for each of a number of spanwise stations is sufficient. This condition is met for high aspect ratio wings with ribs aligned in the streamwise direction, such as the B-47 airplane. The number of spanwise stations required is determined by the number of mode shapes to be accounted for: the more complex the mode shape, the greater the number of spanwise measurements. In view of the problem of obtaining optical measurement of many deflections, it is not considered practical to attempt more than the number of measurements necessary to define a few important modes. In terms of airframe dynamics, these are the low frequency modes. The existence of an elastic axis simplifies the problem in that it permits describing the aeroelastic deformations in terms of deflections of the axis. The low-aspect-ratio wing (e.g., $AR < 4$) of stressed-skin construction is not amenable to elastic-axis representation. Its chordwise elastic deformations cannot be neglected and, therefore, the problem of deformation measurement necessarily becomes more extensive. It is doubtful that satisfactory optical measurements can be obtained in flight for this type of structure.

Determination of structural deformation by means of a pattern of strain gages is most practical for the beam-type of structure with unstressed skin, but becomes difficult and less accurate for more complex types of structure. Because this type of construction is no longer in use for high-speed fighters and bomber aircraft, the use of strain gages for deformation measurements is of lesser value than are other methods. In the tests of Reference 5, the strain gages were used primarily to determine structural resonance frequencies rather than for deformation measurement.

Another approach to the problem of measuring elastic deformations involves measurement of accelerations at various points in the structure and at a reference point such as the wing-fuselage juncture. Double integration of the accelerations will yield the time history of displacements at each point. the displacement of a point $\delta_p(x, y, t)$ less that of the reference point $\delta_o(0, 0, t)$ gives the relative deformation $\delta_{p-o}(x, y, t)$. Clearly, the presence of a steady-state error in the measurement of acceleration will create an increasing error in computed displacement; however, this should not be too troublesome where the deformations of interest are of a known periodic nature. It is essential that the accelerometers have a high order of accuracy and important that the frequency response characteristics be suitably chosen.

Determination of load distribution by means of strain gages is subject to the limitations already discussed. In addition it requires a laborious

calibration procedure to correlate loading at each station with deformations at numerous stations on the structure. The loads thus determined represent the sum of aerodynamic and inertial loads. A more direct approach is the measurement, by means of an array of pressure taps, of the pressure distribution over a wing (Reference 7). Determination of the airload distribution, the shear forces, and the bending and torsional moments can then be made. This procedure isolates the aerodynamic loading from the inertial effects.

9.2 Ground Tests

9.2.1 General. In order to achieve the goals of flight testing, certain supporting tests must be carried out on the airplane on the ground. Included among these are the determinations of weight (or mass), static moments (center of gravity), moments of inertia, and principal axes. Other tests, which may not be necessary to the flight testing directly, may be desired for correlation with various theoretical predictions. Examples are the determinations of vibratory elastic mode shapes and frequencies and measurement of structural influence coefficients. The calibration of test equipment and instrumentation is, of course, a form of ground testing; however, it is not discussed here, being dealt with (albeit briefly) in Section 9.4.

9.2.2 Weight and Balance. The measurement of aircraft weight and determination of the horizontal location of the center of gravity certainly needs no description here. All that needs be said is that considerable care should be taken to insure accuracy, particularly if the determination of stability derivatives from flight data is to be undertaken. The static longitudinal stability derivative, $C_{m\alpha}$ is directly dependent upon the static

margin, (c.g. - n.p.). An additional measurement required for dynamic flight testing is the vertical location of the center of gravity. This can be found experimentally by the method of Reference 8; however, it can generally be determined by computation (or the manufacturer's detailed weight report, if available) with sufficient accuracy.

Experimental measurement of the moments of inertia in pitch, roll and yaw is described in several NACA reports and others. The techniques vary: swinging the airplane as a pendulum or oscillating it about a fulcrum with restoring force provided by springs are the two major methods. Refer to References 8 - 12 for detailed information on these methods. Reference 13 includes the determination of the products of inertia and inclination of the principal axes from the reference (geometric) axes. Computation of the moments of inertia of an airplane piece by piece is a tedious task which is possible only if the weight and location of each element of the structure is accurately known. Such information is obtained by the manufacturer during the construction of the aircraft. Of most importance, the computed moments of inertia are unconfirmed values which are subject to cumulative errors in mass and moment arm. Despite such limitations, computed values of the moments of inertia must be used in many instances, particularly for very large aircraft which cannot be swung or oscillated.

At least one attempt has been made to determine the pitching moment of inertia from flight test data. The frequency response of a B-25J airplane was measured by the direct oscillation method on two flights. The

flight conditions were identical insofar as possible, except for solid ballast providing a known difference in mass and pitching moment of inertia. Center of gravity and moment of inertia were maintained constant during each flight by means of careful scheduling of fuel consumption and in-flight transfer of liquid ballast. By simultaneous solution of the equations of longitudinal motion, the moment of inertia was determined. In spite of considerable care in carrying out the experiment, the values obtained for I_y lacked consistency and failed to agree even reasonably well with I_y as determined from ground tests. Because of the far greater difficulties in fuel scheduling of jet aircraft and because they do not generally permit the inclusion of large ballasting installations, the flight test method of determining moments of inertia is considered to be unsatisfactory.

Fuel sloshing in partially-full tanks is doubtless the greatest source of error in the computation of moments of inertia in flight. Assuming that the fuel acts as a solid mass leads to considerably erroneous results for pylon mounted tanks, as demonstrated by some much-needed research by Reese and Sewall (Reference 14). For internal tanks* the ratio of the effective moment of inertia to that of an equivalent solid mass varied considerably with the tank fineness ratio (length/height); however, Reference 14 indicates that analytical solutions using the "solid" fuel assumption (no sloshing) offers a good engineering approximation for any degree of tank fullness.

9.2.3 Structural Vibratory Modes. Experimental determination of the modal shapes and natural frequencies of the aircraft structure can be better carried out by ground tests than in flight. Except for very low frequency modes, the absence of aerodynamic damping will have little effect on the measured results. The general procedure is to vibrate the aircraft over a range of frequencies by means of electro-magnetic or hydraulic shakers and to measure the motion of the structure at various points. A wide variety of means are available for measuring the structural motion, including almost all of the many position-measuring instruments. Thorough discussion of ground vibration testing may be found in References 15 and 16.

9.2.4 Structural Influence Coefficients. When the structure under consideration does not possess an elastic axis (e.g., a low aspect wing such as a delta wing) it may be treated as a modified flexible plate. Such an approach makes use of the reciprocal equations (4-1a) and (4-1b). Applying a force at a point $j = 1$ (Figure 9-1), it is possible to measure the resulting deflections at points $i = 1, 2, \dots$. From these can be determined the deflections per unit force P_1 , giving the flexibility coefficients A_{i1} . Repeating the loading at each point j will provide additional series of deflections from which one can obtain the matrix of coefficients A_{ij} . The deformations h_i can be determined from a given load distribution P_j by means of (4-1a). Clearly, the stiffness influence coefficients k_{ij} , cannot be obtained in such a straightforward manner. As indicated in Section 4.1.1.1, the load

* Centrally mounted with respect to the axis of rotation in the experiments of Reference 14.

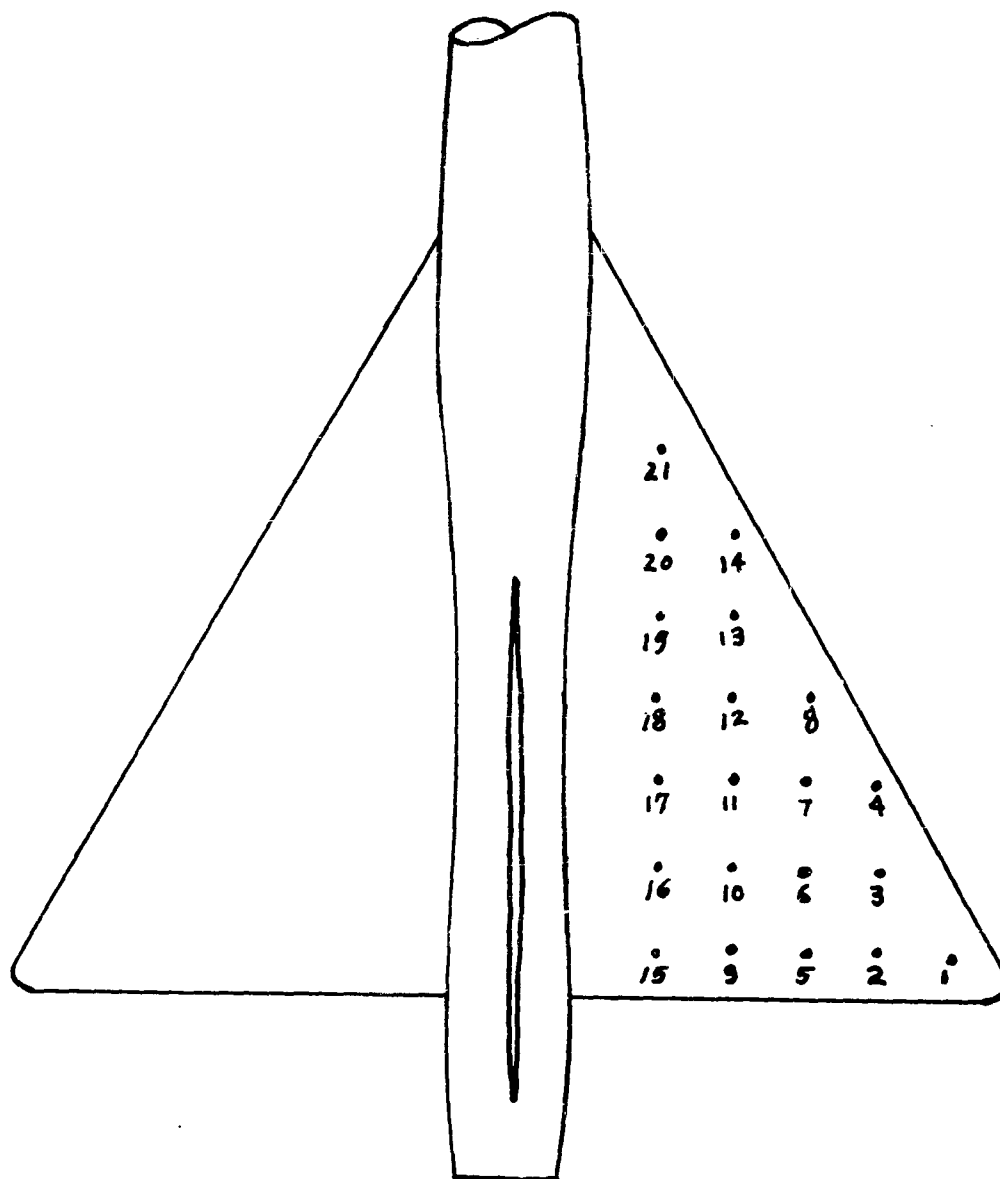


Figure 9-1. Influence Coefficient Stations on a Delta Wing

distribution P_i resulting from a deformation pattern h_j , as expressed by (4-1b), can be determined by inversion of the matrix of flexibility influence coefficients into the matrix of stiffness coefficients. This is expressed by (4-3) and assumes that there is no residual boundary conditions, structural slippage, local plastic deformation and other nonconservative effects.

The experimental equipment needed by measurement of the flexibility influence coefficients is similar, in part, to that required for defining the mode shapes. The main difference is in the application of loads. Exciting modal vibration is a dynamic process, requiring a knowledge of the excitation frequency but not of the force applied. Determining flexibility coefficients, on the other hand, requires static loading of a known magnitude. This is best carried out with hydraulic rams which apply loads to the structure through compression or tension pads. The details of experimental procedures is given in References 15 and 17.

9.3 Flight Test Techniques

9.3.1 Static Stability Tests. The various flight test techniques for determination of static stability derivatives of rigid airplanes should be well-known to the reader and will not be discussed here. References 18 and 19 cover the subject well. Certain modifications are necessary when dealing with an aeroelastic aircraft. Contrary to the common assumption for rigid aircraft, some of the stability derivatives will vary with dynamic pressure, q . The derivatives are functions of Mach number in either case. As an example, $C_{l_{\delta_A}}$, rolling moment coefficient due to aileron deflection, de-

creases with increasing q because of the twisting of the wing is such as to reduce the angle-of-attack change produced by the aileron. As a result, $C_{l_{\delta_A}}$

is not a constant coefficient but is a function of indicated airspeed. In short, the results of static stability flight testing include the effects of static aeroelasticity and cannot be directly compared with the theoretical "rigid-body" condition.*

The fact that the derivatives are not independent of q or Mach number, except at low speeds, invalidates many of the common steady-state tests. For example, the static longitudinal stability has generally been determined by measuring the elevator force required to change airspeed from the trim condition. This procedure is predicted on the assumption that $C_{m_{\alpha}}$ is independent

of α over an appreciable range of α . This not a valid assumption in the transonic region. The major advantages of static stability tests, when valid, are that (1) they tend toward more accuracy by virtue of excluding other variables and (2) they reduce the number of unknowns when the dynamical equations are solved for the remaining stability derivatives.

* Even for rigid airplanes the stability derivatives are not constant coefficients in the high subsonic and transonic regions, but are nonlinear functions of Mach number.

9.3.2 Dynamic Stability Tests. There are presently two basic techniques in use for the flight determination of aircraft dynamic response to control motions: sinusoidal oscillation and transient response. In the former, the frequency response is measured directly by oscillating one of the control surfaces at a number of frequencies sufficient to cover the required spectrum. To create sinusoidal motions of the control surfaces requires some mechanical driving force such as an autopilot. Also, the control system must have a linear characteristic in order that the sinusoidal input be transmitted to the control surface undistorted. If the aircraft has an unstable, oscillatory mode, the control surface must not be oscillated near the resonant frequency as the response will result in a dangerous situation. The major advantage of this method is its accuracy. Each frequency is individually excited, leading to a high signal-to-noise ratio for the measured response. As a drawback, the procedure is time-consuming, resulting in significant variations in aircraft mass and center of gravity during the time required to explore a set of frequencies. References 8 and 20 give a thorough description of the sinusoidal oscillation method.

Because of their high fuel consumption rate and inflexible fuel management, modern fighter aircraft cannot practicably exploit the sinusoidal oscillation method; therefore, the transient response to an "arbitrary" control deflection is measured. The input is generally in the form of a pulse or a step. It is "arbitrary" only in the sense that it need not have a precisely defined form, as in the case of sinusoidal oscillation. The general form of this input pulse should be such as to excite sufficiently the aircraft response throughout its active harmonic spectrum. The need for this will be clarified by the discussion in Section 9.5 of the transformation from transient response to frequency response. When the aircraft being tested exhibits an instability such that the flight attitude becomes rapidly untenable, it becomes impossible to obtain records of sufficient duration to permit analysis. It is possible to ameliorate this situation by stabilizing the aircraft through an autopilot or damper system. The degree of stabilization should not be such as to nullify the motion or we should be faced with the situation of having a continuous input with zero, or near-zero, response. It would be best to provide only a slight margin of stability so that the input and responses tend to vanish in approximately the same finite time. Otherwise, the problem of transforming the data into frequency response form becomes difficult, sometimes impossible, as will be shown in Section 9.6. Without going through a rigorous proof, it should be apparent that the foregoing restrictions on the test method apply equally whether the results are analyzed in the time plane or the frequency plane. The transformation from time to frequency is merely a mathematical operation which does not add to or subtract from the information contained in the measurements.*

The proper shaping of input functions is a matter worthy of discussion. As previously stated, it is important that all of the aircraft modes of interest be sufficiently excited to produce measurable response. The unit impulse has the convenient property of having a flat spectrum (i.e., all fre-

* It is possible to lose information in a transformation if it is not carried out with sufficient accuracy.

quencies are present in identical magnitudes) as shown in Figure 9-2. Such a function is not physically realizable; however, approximations to it by

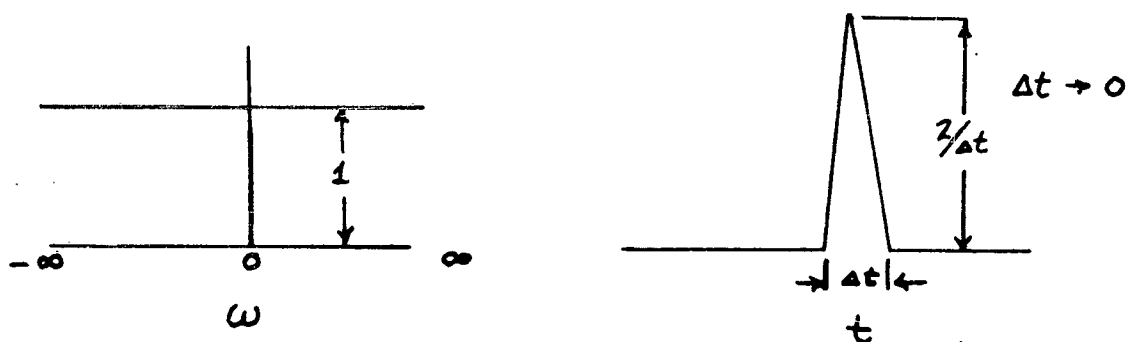


Figure 9-2. Frequency Spectrum of Unit Impulse

triangular impulses can be useful. Figure 9-3 illustrates the effects of pulse duration on the frequency spectrum.* The triangles are of equal area,

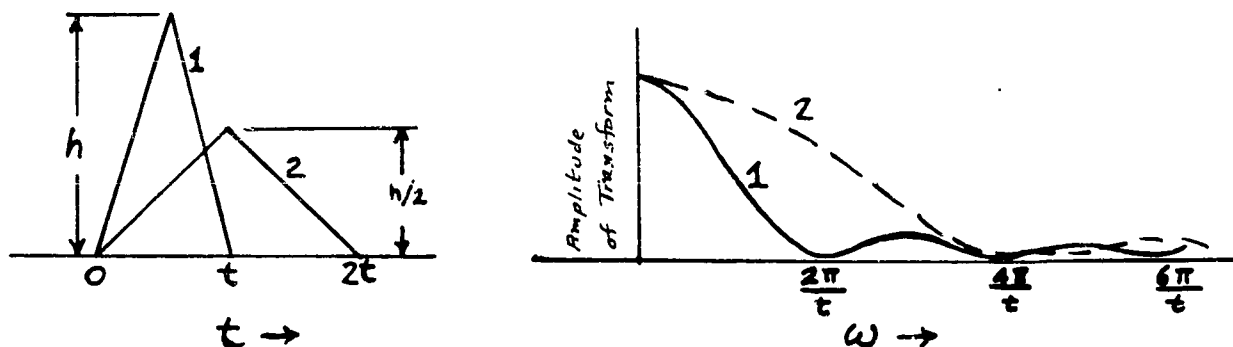


Figure 9-3. Frequency Spectra of Triangular Pulses

giving an equal zero-frequency component in the ω -plane. It can be seen from Figure 9-3 that the harmonic content of the pulses vanishes at regular intervals of frequency, thus no excitation of the aircraft is produced at these frequencies. Of more real interest, there is insufficient disturbance created in the vicinity of the zeroes to insure measurable input and response. A means of overcoming the zeroing or "bottoming" of the frequency spectrum is by the use of unsymmetrical pulses, as illustrated by Figure 9-4. This technique extends the usable bandwidth of the input as compared with a symmetrical pulse of equal duration. Reference 21 contains a good discussion of the shaping of input functions. Additional transients and the associated transforms may be found in References 21-23. In summation, the selection of suitable input functions should be based on the transfer function characteristics of the aircraft to be tested. Where the bandwidth of interest is wide, as for an aero-

* The curves have been omitted for negative values of ω being of no physical significance. They would appear as reflections about the ordinate of the positive ω values.

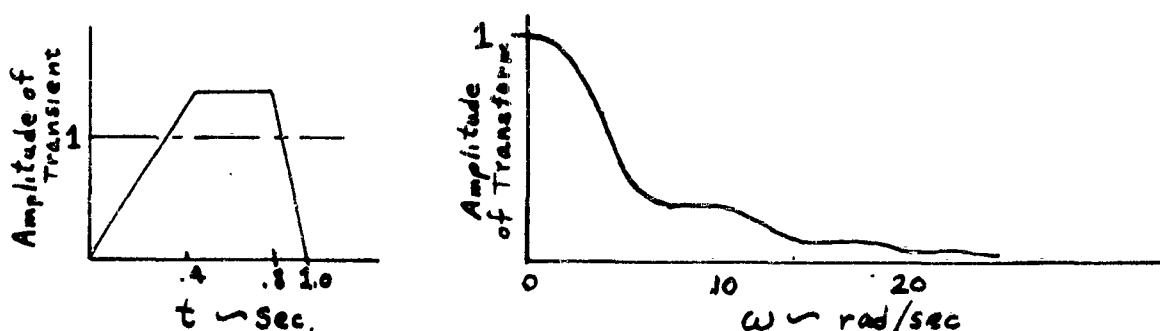


Figure 9-4. Frequency Spectrum of Trapezoidal Pulse

elastic aircraft, it may not be possible to excite all modes sufficiently with a single input pulse. The spectrum can then be covered by two or more inputs, each covering a different portion of the desired spectrum.

9.4 Instrumentation*

9.4.1 Sensor Locations. The location of each sensing element generally becomes a compromise between the position at which the measurement is desired and one which physically permits installation. Mounting of accelerometers in the wing structure, for example, must be made on a spar or rib near an inspection door in order that the instrument be accessible for calibration or replacement. The same holds true for other sensors. Because the center of gravity changes in flight as fuel is consumed, measurement of c.g. accelerations at all times cannot be practicably obtained. Placement of accelerometers at the mean location of the c.g. during the test period is usually satisfactory. It is important that possible spurious inputs to the instrument be kept in mind and such effects be avoided or corrected in the data. As an example, a lateral accelerometer above or below the c.g. will sense rolling accelerations about the c.g. in addition to the lateral acceleration of the c.g. If the accelerometer is placed outside the plane of symmetry ($y \neq 0$), rolling velocity will impose centrifugal forces on the sensing element, but at twice the cyclic frequency of the rolling motion.** When physical restrictions make it impossible to place accelerometers at the c.g., a study of the probable errors due to spurious inputs will greatly aid in selecting the best compromise location. If a location can be found for which sensing errors are negligible, a considerable saving in data correction will result.

* References 24 and 25 contain more detailed discussion of the subjects covered in this section.

** The centrifugal force is outward from the center of rotation, regardless of the direction of rotation, thus it goes through two cycles for each cycle of rolling oscillation.

The measurement of angular velocities at the c.g. is in some respects simpler than that of determining linear accelerations. All points reasonably near the c.g. are coupled to it with sufficient rigidity to permit locating rate gyros. High quality floated gyros are available which respond negligibly to other than angular velocities about their input axes. They must, of course, be mounted in the aircraft with great care to assure that the outboard locations, such as the wing tips or tail, do not present alignment difficulties. As the structure flexes, the input axis of a gyro will be continuously tilted to an orientation which is unknown. Whether this effect is sufficiently serious to limit the use of rate gyros in favor of accelerometers at outboard locations must be decided for the individual case, taking into consideration the maneuvers to be performed, the sensitive axis and the probable errors which will result.

Probably the most difficult measurements to obtain with accuracy are those dealing with relative wind direction (angle of attack and sideslip). Aeroelasticity further complicates the problem. Much experimentation has been done on this subject with the result that relative wind sensors are mounted on nose booms in very many instances. Most other fuselage locations suffer from flow disturbances which render them unsuitable for accurate determination of free-stream relative wind conditions. Wing or tail-mounted sensors are subjected to errors induced by aeroelastic distortion of the aircraft structure. When the nose-boom location is subject to motion relative to the aircraft reference point (c.g. or wing-fuselage junction) it becomes necessary to correct the data for such effects. The boom must be designed for considerable stiffness* to minimize errors due to its flexure. This requirement leads to a short boom which compromises the need to put the sensors ahead of the pressure field of the fuselage.

Accurate measurements of airspeed and Mach number are dependent upon a good static pressure source. The statements regarding suitable relative wind sensor locations generally apply. Unless there is time available to investigate alternate sources -- and this can be a lengthy, or possibly futile, search -- the best solution is a nose boom location for the pitot-static pressure sources.

9.4.2 Sensor Characteristics. The requisite characteristics of sensitivity, linearity, environmental stability and ruggedness of flight test instruments apply equally to testing aeroelastic or rigid aircraft. The extended frequency range of interest for aeroelastic testing may require instruments with higher natural frequencies; where only the lower elastic modes are to be investigated, the frequency characteristics suitable for rigid body dynamics measurement will generally suffice. If the natural frequency of a sensor is too high, the signal-to-noise ratio will be reduced; readability and therefore accuracy, will suffer. On the other hand, too low a cut-off frequency is accompanied by excessive phase lag in the signal. A desirable situation would be identical phase characteristics of all sensors, eliminating the need for relative phase correction of the data. To achieve this,

* Natural vibration frequencies of the boom and sensor must be well above the range of aircraft frequencies being investigated.

such zero-lag* instruments as position transducers should have a phase lag created by low-pass filtering of the output signal.

9.4.3 Recording System. While the details of data recording are outside the scope of this work, certain comments are felt to be appropriate. Too much emphasis cannot be placed on the need for compatibility of the data recording with the analysis to be performed. Dynamic flight testing involves the reduction and analysis of large quantities of data, even in the simplest of cases. When the aeroelastic properties of an aircraft are included, the problem grows rapidly. Wholly manual methods of data processing are ruled out as being overly time-consuming and expensive. Access to automatic or semi-automatic data transcription equipment and an automatic computer is a minimum requirement. The optimum system, in terms of rapid data processing, is digital recording on magnetic type. Although no equipment of this type is presently on the market, development of at least two systems is currently underway and the finished products should be available in the very near future. Analogue magnetic recording is available and can be made compatible with digital computation by analogue-to-digital conversion. Oscillographic recording of data is the most-used technique. Adaptation of the data for digital computation can be carried out by semi-automatic transcribers which convert the data into punched-card form.

In summary, the recording system should be matched to the analysis procedures and computing equipment available, or vice versa. Failure to do so can result in failure of the flight test program to provide useful information in a reasonable time.

9.5 Flight Test Procedures

9.5.1 Flight Conditions. Because of the great expense of flight testing, it is important that a maximum of data be obtained with a minimum of flying. This rules out the measurement of dynamic, aeroelastic responses at all combinations of altitude, airspeed, Mach number, etc. By proper design of the flight program, the effects of each of the important parameters on aircraft response can be evaluated. Figure 9-5 gives a sample of a rather extensive pattern of tests to investigate the effects of Mach number and dynamic pressure on dynamic response of an elastic supersonic airplane. The series of test points at $q = 350 \text{ lb/ft}^2$ is designed to show the effects of Mach number with aeroelastic effects minimized. At $q = 1000$, high Mach number effects can be measured. The sets of data points at constant Mach number should distinguish the effects of dynamic pressure on the aircraft response and the structural distortion.

Fuel scheduling must be planned to give a maximum of test time with variations in c.g. and moments of inertia kept as small as possible. Many current aircraft have automatic fuel management, not controllable by the pilot. Under such circumstances the test period may be severely limited by the normal variations of c.g. and inertia, resulting in numerous test flights.

* In the frequency spectrum of aircraft dynamics, the lag of potentiometer and inductive-type transducers used to measure control surface and attitude gyro positions are negligible.

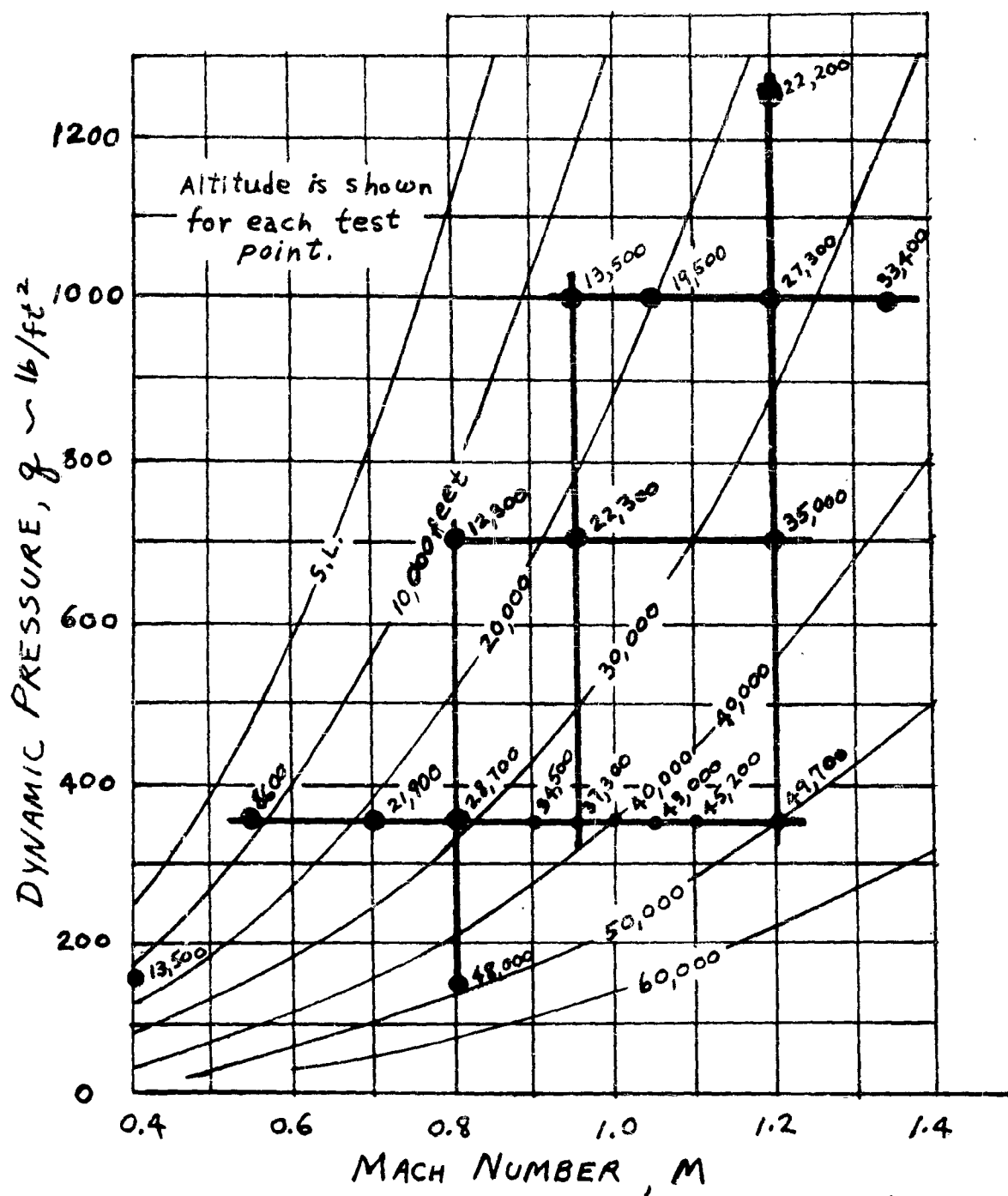


Figure 9-5. Sample Pattern of Flight Tests

Flight tests must be performed in smooth air to prevent the addition of gust inputs. The presence of undesired inputs is detectable on the response to sinusoidal control inputs. The data, while not correctable, may be usable if the distortion is obviously small. For transient response tests, even this visual assessment of the data is not possible. Fortunately, smooth air is generally attainable at the high altitudes, jet stream penetration being an exception. Further research into the power spectra of turbulent air may nullify the requirement for smooth-air testing, at least for certain frequency regions. Meanwhile, the requirement should be retained.

9.5.2 Test Operations. For sinusoidal oscillation testing, a pattern for scheduling the oscillations should be established prior to flight. A procedure which has been found to be satisfactory is to start with a frequency at or near the lower (or upper) end of the region to be investigated. Then move up (or down) the frequency scale, oscillating at alternate frequencies in the pattern. At the end of the spectrum move down (or up) the scale, filling in the frequencies skipped on the first traverse. Figure 9-6 shows this procedure graphically. One advantage to be gained is that the first and last test points are at neighboring frequencies.

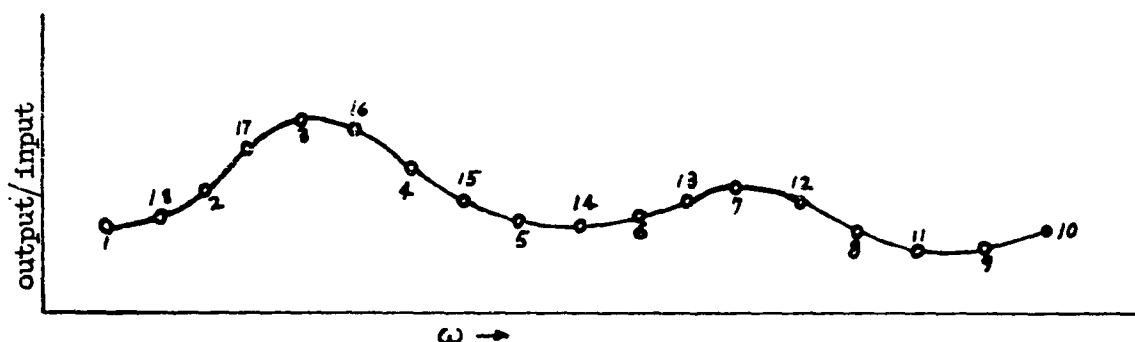


Figure 9-6. Typical Results of Sinusoidal Oscillation Testing With No Changes In Response During The Test Period.

If flight conditions (air density, aircraft inertia, etc.) have changed significantly during the test, it should be apparent from the data. An example is shown in Figure 9-7. A second advantage is evident should the test flight

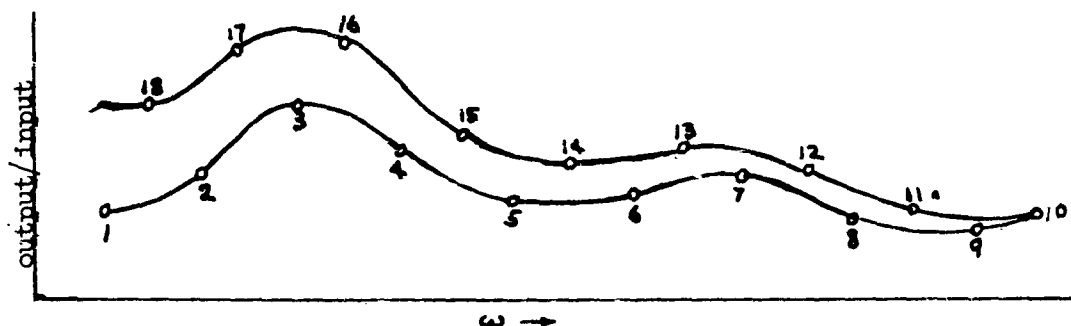


Figure 9-7. Typical Results of Sinusoidal Oscillation Testing With Large Changes in Response During the Test Period.

be aborted prior to completion: half the test points will roughly define the entire spectrum. This is generally preferable to more precise definition of only a portion of the spectrum.

In performing transient response tests, the inputs may be performed manually or, if automatic controls are available in the aircraft, the inputs may be injected by a signal generator. Both methods have been employed successfully. The former is simpler and can be easily modified in flight should the need arise. The latter method makes possible the injection of precisely repeatable inputs. The magnitude of the input should be large enough to provide accurate measurement of itself and the response, without exceeding either the "small disturbance" conditions or safe loads on the aircraft. The requirement for accurate measurement of both input and response will be compromised somewhat at the resonant peaks and the valleys because of small inputs and responses, respectively, in these regions.

9.6 Data Analysis Procedures

9.6.1 Time-to-Frequency-Plane Transformation. There are available to the engineer at least two well-known methods for transforming functions of time into functions of frequency: the Fourier integral and the Duhamel integral. Only the Fourier transformation will be discussed here. Application of the Duhamel integral is treated in Reference 26.

The direct Fourier integral transformation is stated by

$$G(\omega) = \int_{-\infty}^{\infty} F(t) e^{-j\omega t} dt \quad (9-1)$$

and its inverse by

$$F(t) = \frac{1}{2\pi} \int_{-\infty}^{\infty} G(\omega) e^{j\omega t} d\omega \quad (9-2)$$

For systems describable by linear differential equations with constant coefficients, the principle of superposition applies. Stated mathematically for the case at hand,

$$\frac{G_{out}(\omega)}{G_{in}(\omega)} = \frac{\mathcal{F}[F_{out}(t)]}{\mathcal{F}[F_{in}(t)]} \quad (9-3)$$

where $\mathcal{F} F(t) = G(\omega)$ as given by (9-1).

More simply, for each frequency component, $G_{in}(\omega)$, of the input to the system described above, there is a component, $G_{out}(\omega)$, of the output having the same frequency and which is due solely to $G_{in}(\omega)$. Thus, given almost

any* time functions F_{in} and F_{out} of a linear system, we can determine the frequency response by means of (9-3).

Clearly, we cannot hope to evaluate the integrals in (9-1) or (9-2) over the stated intervals. If $F(t)$ has a constant value prior to the desired disturbance, the coordinate axes may be selected such that $F(t) = 0$ for $t \leq 0$. Now the lower limit of integration may be changed to zero. We can then express (9-1) by

$$G(\omega) = \int_0^T F(t) e^{-j\omega t} dt + \int_T^\infty F(t) e^{-j\omega t} dt \quad (9-4)$$

If some finite T can be found such that $F(t) = F_T = \text{constant}$, for $t \geq T$, then the second integral of (9-4) is the Fourier transform of a step function occurring at time T and may be directly evaluated.

$$\mathcal{F}[u(t-T)] = \frac{F_T}{j\omega} e^{-j\omega T} \quad (9-5)$$

The major effort lies in evaluating the finite integral

$$g(\omega) = \int_0^T F(t) e^{-j\omega t} dt \quad (9-6)$$

where $g(\omega)$ means the \mathcal{F} -transform of the "initial transient", $F(t)$ for $0 \leq t \leq T$. The "residual transient" transforms into $g_r(\omega)$.

Applying the Euler relationship, $e^{-j\omega t} = \cos \omega t - j \sin \omega t$, puts (9-1) into the more useful form

$$g(\omega) = \int_0^T F(t) \cos \omega t dt - j \int_0^T F(t) \sin \omega t dt \quad (9-7)$$

$$g(\omega) = a(\omega) - j b(\omega) \quad (9-8)$$

The problem now is to evaluate the integrals in (9-7) when $F(t)$ is an arbitrary function. This can be performed by several analogues: mechanical harmonic analyzer (Reference 27), electromechanical Fourier synthesizer (Reference 27), or electronic analogue computer (Reference 28 and 29). As discussed in Reference 29, the analogue computer performs the Fourier integration rapidly and in a very straightforward fashion. Its major drawbacks are the time-consuming preparation of $F(t)$ for input to the computer and handling the output, and its inability to transform any transient which does not

* The function, $F(t)$ must be such that the integral in (9-1) exists; e.g., the integrand must converge for the range of solution required. See Reference 21, pp. 72-80.

vanish in a reasonably short time. The digital computer, on the other hand, can store interim results for further computation, such that a number of solutions for $G(\omega)$ can be performed sequentially, or simultaneously, without reloading the input, $F(t)$. Furthermore, it is flexible enough to handle the entire data analysis problem with no need for any manual operations during the entire process. The transformation can be wholly automatic from loading the input to tabulating or plotting frequency response, including the effect of $g_r(\omega)$.* The computation can, of course, be continued to include solution of stability derivatives.

Digital evaluation of (9-7) requires that we approximate in some manner the integrand. There is the choice of approximating $F(t) \cos \omega t$ and $F(t) \sin \omega t$, or of approximating only $F(t)$. In view of the fact that the trigonometric functions can be determined as precisely as desired and because their products with $F(t)$ will likely oscillate more rapidly than $F(t)$ alone, it would seem that the latter course might be more desirable. This is, in fact, the case, as demonstrated by References 21 and 31. Approximation of $F(t)$ can be done with functions of any degree. Clearly we would not be justified in using any higher degree of approximating function than is necessary to obtain the result with sufficient accuracy. Figures 9-8a and 9-8b demonstrate the fitting of a portion of $F(t)$ with linear and quadratic functions, respectively.

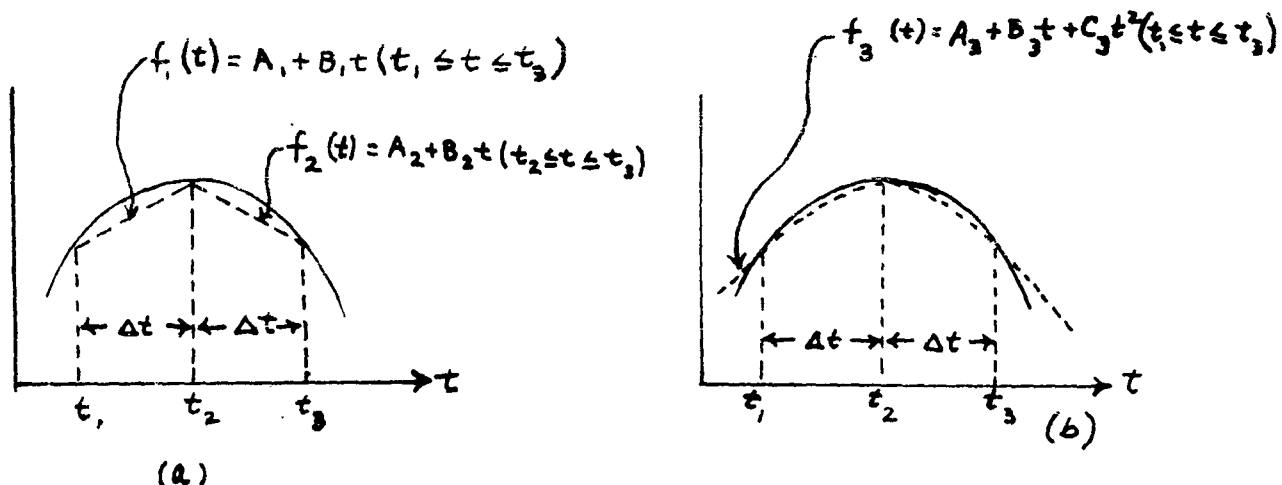


Figure 9-8. Curve Fitting Examples

while equal time intervals, $\Delta t = t_2 - t_1 = t_3 - t_2 = \dots = t_n - t_{n-1}$, are not a mathematical necessity, practical considerations dictate that we use a constant Δt for any given transformation in order to keep the computation relatively simple and to retain generality of application to arbitrary functions, $F(t)$. As indicated by Figure 9-8, for the same value of Δt , the single quadratic function better approximates $F(t)$ than do the pair of linear functions, but at the expense of greater complexity in fitting the curve.** Even this single

* $F(t)$, $T \leq t$, need not be a step function, but may be any \mathcal{F} -transformable function. In fact, some of the usual restrictions on the transform can be voided as discussed in References 21 and 30.

** Fitting the approximating function to a curve consists of determining the coefficients of the function such that it will pass through known points on the curve: $f(t_1)$, $f(t_2)$, etc.

objection becomes of little significance if we precompute a set of coefficients which can be reused for many problems. Such a method is developed by Schumacher in Reference 31, using quadratic approximation of $F(t)$. This method was utilized to compute two sets of coefficients which were applied to a number of sample functions in Reference 29. Filon's method (Reference 32 or 33) is essentially the same.

Where the values of $F(t)$ must be transcribed from oscillograms by manual or semi-automatic methods, the use of higher-order approximation is attractive because of the lesser number of samples, $f(t)$, required for a given accuracy. Use of precomputed coefficients will, for some computers, shorten the problem time by eliminating the need to recalculate the numerous, repeated, trigonometric functions involved. Automatic readout from magnetic tape recordings of $F(t)$ and high-speed digital computers make it practical to read $F(t)$ at frequent intervals and to use linear approximation of $F(t)$, computing the coefficients as they are required. The transformation can be stated as

$$a(\omega) = \int_0^T F(t) \cos \omega t \, dt = \Delta t \sum_{i=1}^m f(t_i) \cos \omega t_i \quad (9-9)$$

where

$$m \Delta t = T$$

Similarly,

$$b(\omega) = - \int_0^T F(t) \sin \omega t \, dt = -\Delta t \sum_{i=1}^m f(t_i) \sin \omega t_i \quad (9-10)$$

The advantage here is that the transformation can be made for any values of ω , whereas the use of precomputed coefficients yields solutions for a pre-determined set of values of ω .

Having determined $a(\omega)$ and $b(\omega)$ from (9-9) and (9-10) or by means of References 29, 31, or 32, the end corrections $a_r(\omega)$ and $b_r(\omega)$ must be applied.

$$A(\omega) = a(\omega) + a_r(\omega) \quad (9-11)$$

$$B(\omega) = b(\omega) + b_r(\omega) \quad (9-12)$$

It is generally desired to express the vector $G(\omega)$ in polar form

$$G(\omega) = |G(\omega)| e^{j\phi(\omega)} \quad (9-13)$$

where

$$|G(\omega)| = \sqrt{[A(\omega)]^2 + [B(\omega)]^2}$$

and

$$\phi(\omega) = \tan^{-1} \frac{B(\omega)}{A(\omega)} = \sin^{-1} \frac{B(\omega)}{|G(\omega)|}$$

9.6.2 Techniques for Smoothing Data. The techniques for data smoothing range from a simple weighting function to complex mathematical methods which utilize the available information to various degrees. The more complex methods seem attractive in that the smoothing of the data is theoretically

better as a greater portion of the given information (i.e., data and noise) is utilized in any one analysis. However, it should be pointed out that in many cases, to make use of the larger amount of information, the complex smoothing methods involve mathematical operations that make use of the small difference of large numbers. (This is common to the solution of a large number of simultaneous equations). This type of mathematical manipulation can result in such large errors that the calculating weighting function is of little value for data smoothing.

9.6.2.1 Fourier Series. A method of data smoothing is suggested by Rice in Reference 34. He points out that random noise can be represented by Fourier series with coefficients a_n and b_n each of which can be regarded as an independent random variable distributed about its mean value according to a normal law. It then follows that if random noise were superimposed on a function $F(t)$ the new Fourier coefficients would be normally distributed about the respective non-noise Fourier coefficients of $F(t)$.

Lanczos, in Reference 35, suggests a second Fourier method which separates the coefficients of the true data from those of the noise by means of a single Fourier analysis of the signal. This method works well if the following two conditions are true:

1. The "noisy" data can be considered to be made up of true data on which random noise is linearly superimposed, and
2. The frequency spectra of both the true data and random noise overlap very little.

These two methods, involving Fourier series, work very well under the proper conditions and, in addition, lead directly into a method of analysis that makes use of flight test data in frequency response form.

9.6.2.2 Weighting Functions. A simple weighting function technique of data smoothing is also described in Reference 35. This technique is a standard interpolation procedure using a simple function, $(\sin x/x)$, commonly called the "si-function".

The choice of a weighting function is dependent upon both the type of noise as well as the nature of the true data. If extrapolated data (i.e., data beyond existing data, in time) were desired, the most recent data would be the most valuable, and hence the weighting function would appear similar to:

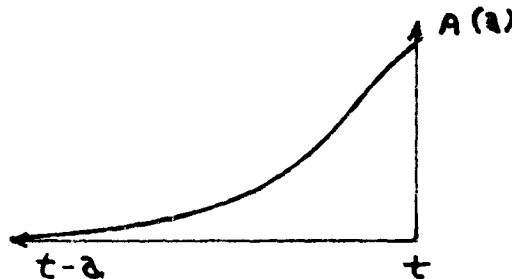


Figure 9-9. Typical "Si-function" Weighting Curve

where $A(t)$ is the weighting function and

$$\int_{-\infty}^{\infty} A(a) da = 1 \quad (9-14)$$

If smoothed data are to be obtained through interpolation (i.e., data among existing data), two different weighting functions are often used. They are:

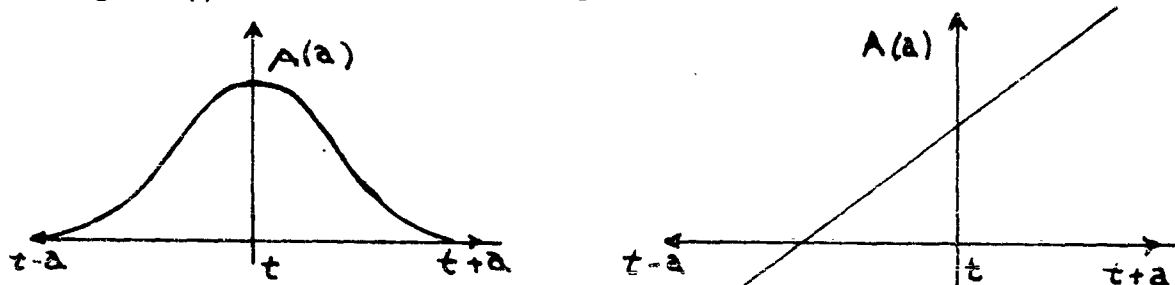


Figure 9-10. Weighting Functions

Lanczos, in Reference 35, gives the si-function ($\frac{\sin x}{x}$) as a standard weighting function. In particular:

$$A(a_k) = \frac{1}{P} \text{si} \left(\frac{\pi}{P} k \right) \quad (9-15)$$

where

$$\text{si}(x) = \frac{\sin x}{x}$$

P = smoothing parameter = $\frac{N}{M}$ = $\frac{\text{total number of observations}}{\text{number of degrees of freedom (harmonic)}}$

K = number of terms being evaluated

Ideally, a properly chosen weighting function for smoothing a signal must account for the statistical nature of the noise, the true data, and any coupling of the noise with the true data. The methods for obtaining theoretical weighting functions, which account for the above correlations, require lengthy computations.

Wiener, in Reference 36 presents a generalized approach for smoothing data using extensive statistical measures. The theory involves many integrals which are rather difficult to solve with sufficient accuracy. Levinson, in an appendix to Reference 36, presents a simplification of Wiener's work. In this method the coefficients of the weighting function are calculated by solving a system of linear equations which incorporate the auto- and cross-correlation functions of the signal and of the true data.

Two variations of wiener's theory use spectral density functions in addition to auto- and cross-correlation functions that are slightly different from those of Levinson's method. The first variation by Bubb is described in Reference 37 and the second variation by Zadeh and Ragazzini is presented in Reference 38.

It has been found through actual application experience that the following conclusions regarding data smoothing processes may be drawn:

1. The most practical method of obtaining true data from a signal appears to be one that makes use of Fourier Analysis. The Fourier Analysis method is particularly suitable for incorporating the distribution of the noise.
2. The simple weighting function approach (such as the "sifunction") will offer considerable smoothing in the time domain when most of the noise spectrum consists of higher frequencies than the true data.
3. The methods involving the more complicated weighting functions (such as Levinson's and Bubb's) are subject to greater inaccuracies due to the inherent mathematical difficulties. (These difficulties include such items as the inaccuracies that arise from solving a high order number of simultaneous equations containing small differences of large numbers, approximations of spectral densities by specific analytic forms, and convergence of power series expansions upon the true data. These methods require high capacity computing facilities.)

9.6.3 Techniques for Analyzing Dynamic Flight Test Data. It has been found convenient to devise the following block diagram as a means of identifying and segregating the various techniques for analyzing dynamic flight test data.

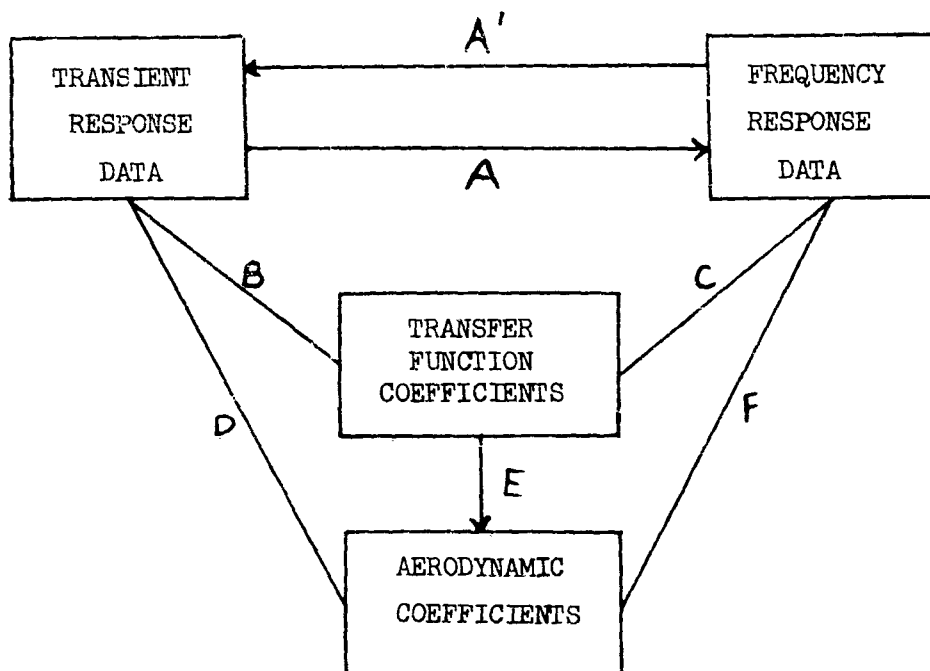


Figure 9-11. Block Diagram for Identifying and Segregating Techniques for Determining Aerodynamic Coefficients from Dynamic Flight Test Data.

In Figure 9-11 the lines labelled A and A' indicate the methods for time-to-frequency domain conversion, and vice versa. Two methods of performing the domain conversion of "A" are presented in References 31 and 39. The domain conversion of line A' can be done by methods explained in References 40 and 41. The techniques for determining transfer function coefficients from transient response data are indicated by line B. In addition, the techniques for deriving aerodynamic coefficients from transient response data, via the transfer function coefficients, also include the methods indicated by line E. The complete technique in this case is designated as B-E. On the other hand, path D represents the techniques for determining the aerodynamic coefficients directly from the transient response data without having to first determine the transfer function coefficients. Alternates C (with E) and F are representative of those methods which incorporate frequency response data.

The techniques represented (in Fig. 9-11) are applicable to two basic types of dynamic flight test data. These types are shown by the blocks designated as follows:

1. Transient response data, which is dynamic flight test data obtained by recording the transient responses to various types of inputs such as:
 - a. Control surface pulses that are asymmetrical and/or arbitrary in shape,
 - b. Control surface step inputs, and
 - c. Other inputs with the control surfaces either fixed or free, as for example in the case of missiles firing cartridges at right angles to the flight path.
2. Frequency response data, which is dynamic flight test data obtained by recording forced steady-state responses of the aircraft or missile to sinusoidal inputs.

It should be pointed out that the analysis methods presented in the following sections (i.e., 9.6.3.1 and 9.6.3.2) are based upon rigid body equations of motion and only two degrees of freedom. The reason for this is that the number of unknowns to be solved for is small enough that the solution yields reasonably accurate values for the unknowns. If these methods are used to analyze the responses of elastic aircraft the values obtained for the unknowns (transfer function coefficients or stability derivatives) will contain the effects of elasticity. These unknowns are usually terms as "modified transfer function coefficients" (or modified stability derivatives). If the analysis methods were extended to account for the elasticity, the number of unknowns that would then have to be solved for would be so large it would be almost impossible to obtain accurate answers.

9.6.3.1 Methods for Determining Aerodynamic Coefficients from Transient Data.

- a. Derivative Method as applied to the Transfer Functions (See Reference 42).

If the assumed form of the transfer function is

$$\frac{q}{\delta_e} = \frac{p\theta}{\delta_e} = \frac{C_{1q}p + C_{0q}}{p^2 + bp + R} \quad (9-16)$$

it is possible to determine the parameters b , k , C_{0q} and C_{1q} from four sets of simultaneous measurements. The above equation can be written as

$$p^3\theta + p^2b\theta + pR\theta - C_{1q}p\delta_e - C_{0q}\delta_e = 0 \quad (9-17)$$

This can be integrated once by dividing through by p which gives

$$p^2\theta + pb\theta + R\theta - C_{1q}\delta_e - C_{0q}\int_0^t \delta_e d\tau = 0 \quad (9-18)$$

If the subscript 1 denotes the value of a quantity at $t = t_1$ etc., then four simultaneous equations for the parameters b , k , C_{1q} and C_{0q} can be obtained from four sets of simultaneous measurements of θ , $p\theta$, $p^2\theta$, δ_e and $\int_0^t \delta_e d\tau$ by making the proper substitutions in Equation (9-16). The equations are as follows:

$$\begin{aligned} (p^2\theta)_1 + b(p\theta)_1 + R\theta_1 - C_{1q}\delta_{e1} - C_{0q}\int_0^{t_1} \delta_e d\tau &= 0 \\ (p^2\theta)_2 + b(p\theta)_2 + R\theta_2 - C_{1q}\delta_{e2} - C_{0q}\int_0^{t_2} \delta_e d\tau &= 0 \end{aligned} \quad (9-19)$$

If it is desirable to use more data (taken at more than four time instants) then a method of least squares may be used to compute values of b , k , C_{1q} and C_{0q} such that $\sum E_i^2$ is a minimum,

where

$$E_i = (p^2\theta)_i + b(p\theta)_i + R(\theta)_i - C_{1q}\delta_{ei} - C_{0q}\int_0^{t_i} \delta_e d\tau \quad (9-20)$$

The normal equations are:

$$\begin{aligned}
 \sum_i (p\theta)_i^2 b + \sum_i (p\theta)_i (\theta)_i k - \sum_i (p\theta)_i (\delta_e)_i C_{1g} - \sum_i (p\theta)_i \int_0^{t_i} \delta_e d\tau C_{0g} &= - \sum_i (p\theta)_i (p^2\theta)_i \\
 \sum_i (p\theta)_i (\theta)_i b + \sum_i (\theta)_i^2 k - \sum_i (\theta)_i (\delta_e)_i C_{1g} - \sum_i (\theta)_i \int_0^{t_i} \delta_e d\tau C_{0g} &= - \sum_i (\theta)_i (p^2\theta)_i \\
 \sum_i (p\theta)_i (\delta_e)_i b + \sum_i (\theta)_i (\delta_e)_i k - \sum_i (\delta_e)_i^2 C_{1g} - \sum_i (\delta_e)_i \int_0^{t_i} \delta_e d\tau C_{0g} &= - \sum_i (\delta_e)_i (p^2\theta)_i \\
 \sum_i (p\theta)_i \int_0^{t_i} \delta_e d\tau b + \sum_i (\theta)_i \int_0^{t_i} \delta_e d\tau k - \sum_i (\delta_e)_i \int_0^{t_i} \delta_e d\tau C_{1g} - \sum_i \left(\int_0^{t_i} \delta_e d\tau \right)^2 C_{0g} &= - \sum_i \int_0^{t_i} \delta_e d\tau (p^2\theta)_i
 \end{aligned}
 \tag{9-21}$$

The derivative method can also be applied to the response to a unit step input in δ_e . For a step response the differential equation relating θ and δ_e is

$$p^2\theta + bp\theta + k\theta - C_{1g} - C_{0g}t = 0 \text{ or } E \tag{9-22}$$

The normal equations resulting from the minimizing of $\sum E^2$ are

$$\begin{aligned}
 \sum_i (p\theta)_i^2 b + \sum_i (p\theta)_i (\theta)_i k - \sum_i (p\theta)_i C_{1g} - \sum_i (p\theta)_i t_i C_{0g} &= - \sum_i (p\theta)_i (p^2\theta)_i \\
 \sum_i (p\theta)_i (\theta)_i b + \sum_i (\theta)_i^2 k - \sum_i (\theta)_i C_{1g} - \sum_i \theta_i t_i C_{0g} &= - \sum_i (p^2\theta)_i \theta_i \\
 \sum_i (p\theta)_i b + \sum_i (\theta)_i k - N C_{1g} - \sum_i t_i C_{0g} &= - \sum_i (p^2\theta)_i \\
 \sum_i (p\theta)_i t_i b + \sum_i (\theta)_i t_i k - \sum_i t_i C_{1g} - \sum_i t_i^2 C_{0g} &= - \sum_i (p^2\theta)_i t_i
 \end{aligned}
 \tag{9-23}$$

where N is the number of time instants at which the variables are known.

If the same procedure is applied to the transfer function

$$\frac{n}{\delta_e} = \frac{C_{2n}p^2 + C_{1n}p + C_{0n}}{p^2 + bp + k} \tag{9-24}$$

the coefficients C_{2n} , C_{1n} and C_{0n} can also be determined.

The relationships between the transfer function coefficients and the stability derivatives are presented in the nomenclature. The stability derivatives may be determined from the transfer function coefficients by the process of simultaneous solution indicated by Path E in Figure 9-11. In making this simultaneous solution it is important that the number of unknown stability derivatives to be solved for be no more than the number of transfer function coefficients available. If the number of stability derivatives is greater, the number can usually be reduced by assuming reasonable values for some of the better known stability derivatives such as static derivatives (i.e., Z_{α} and/or M_{α}).

- b. Matrix Method of Determining Aerodynamic Coefficients from Transient Flight Data. (See Reference 43).

Consider the equation

$$\frac{\dot{\theta}}{\delta_e} = \frac{c_1 p + c_0}{p^2 + b p + R} \quad (9-25)$$

This can be rewritten as follows:

$$p^3 \theta + b p^2 \theta + R p \theta = (c_1 p + c_0) \delta_e \quad (9-26)$$

$$\text{where } \dot{\theta} = p \theta \quad \text{and} \quad p = \frac{d}{dt}$$

If the above equation is multiplied by $\frac{1}{p}$ the integral form of the rearranged equation can be written as,

$$b \theta + R \int_0^t \theta dt - c_1 \int_0^t \delta_e dt - c_0 \int_0^t \int_0^t \delta_e d\tau dt = -\dot{\theta} \quad (9-27)$$

In principle, to solve this equation for the coefficients, it is only necessary to tabulate the recorded values of θ , $\dot{\theta}$ and δ_e at a number of points t_1, t_2, \dots, t_i along a given time history and perform the indicated integrations from $t = 0$ to $t = t_i$.

A number of simultaneous equations containing the unknown constants are then solved. The number of equations can vary from a minimum, in which the number of ordinates is equal to the number of constants, to the case where there are many more equations than unknowns. When the number of ordinates equals the number of unknown coefficients, the usual methods of solving simultaneous equations may be used to obtain the coefficients. However, when there are more equations than unknowns, a least-squares method is often used to reduce the equations. Since the best average value of the coefficients is obtained when many points along the time history are used, a least-squares procedure is generally preferable.

The indicated integration can either be done graphically or by a numerical process. If the latter is chosen, a matrix method of solution proves quite convenient.

The matrix form of the above equation may be written:

$$\left\| \begin{array}{l} \theta_1 \\ \theta_2 \\ \theta_3 \\ \theta_4 \end{array} \right\| \left\{ \begin{array}{l} \int_0^{t_1} \theta dt - \int_0^{t_1} \delta_e dt - \int_0^{t_1} \int_0^{\tau} \delta_e d\tau dt \\ \int_0^{t_2} \theta dt - \int_0^{t_2} \delta_e dt - \int_0^{t_2} \int_0^{\tau} \delta_e d\tau dt \\ \int_0^{t_3} \theta dt - \int_0^{t_3} \delta_e dt - \int_0^{t_3} \int_0^{\tau} \delta_e d\tau dt \\ \int_0^{t_4} \theta dt - \int_0^{t_4} \delta_e dt - \int_0^{t_4} \int_0^{\tau} \delta_e d\tau dt \end{array} \right\} = \left\{ \begin{array}{l} b \\ R \\ C_{1g} \\ C_{0g} \end{array} \right\} \left\{ \begin{array}{l} -\dot{\theta}_1 \\ -\dot{\theta}_2 \\ -\dot{\theta}_3 \\ -\dot{\theta}_4 \end{array} \right\} \quad (9-28)$$

In shorter form this expression can be rewritten as:

$$\|A\| \left\{ \begin{array}{l} b \\ R \\ C_{1g} \\ C_{0g} \end{array} \right\} = \left\{ -\dot{\theta}_i \right\} \quad (9-29)$$

where the matrix $\|A\|$ is in general a rectangular matrix; that is, for every t_i , one equation or one row of the matrix $\|A\|$ is obtained.

The individual elements of matrix $\|A\|$ are evaluated from known values of θ and δ . As mentioned previously, the integration may be performed graphically, but it is more convenient to use integrating matrices. These integrating matrices are derived in Reference 44. Any element in the rectangular

matrix such as $\int_0^t \theta dt$ or $\int_0^t \int_0^{\tau} \delta_e d\tau dt$ may be expressed in matrix

$$\begin{aligned} \text{form as follows:} \quad \left\{ \int_0^{t_i} \theta dt \right\} &= \|C_1\| \left\{ \dot{\theta}_i \right\} \\ \left\{ \int_0^{t_i} \int_0^{\tau} \delta_{e_i} d\tau dt \right\} &= \|C_1\| \left\{ \int_0^{t_i} \delta_{e_i} dt \right\} \end{aligned} \quad (9-30)$$

After the elements of matrix $\|A\|$ have been determined either by applying the integrating matrix or by graphical integration, a method of least-squares can be applied to the solution of the system of simultaneous equations.

In matrix notation the least-squares solution involves multiplication of matrix $\|A\|$ by its transpose $\|A'\|$ so that

$$\|A\| \{b, k, C_{1g}, C_{0g}\} = \{-\dot{\theta}_i\} \quad (9-31)$$

becomes

$$[A'A] \{b, k, C_{1g}, C_{0g}\} = \{-A'\dot{\theta}_i\} \quad (9-32)$$

This equation can now be arranged to be solved directly for the coefficients by multiplying by the inverse matrix $A'A^{-1}$. This gives

$$\{b, k, C_{1g}, C_{0g}\} = [A'A]^{-1} \{-A'\dot{\theta}_i\} \quad (9-33)$$

The application of this matrix method may be applied to the transfer functions n/δ_e in a similar manner. The resulting equation would be:

$$b \int_0^t n dt + k \int_0^t \int_0^t n dr dt - C_{2n} \delta_e - C_{1n} \int_0^t \delta_e dt - C_{0n} \int_0^t \int_0^t \delta_e dr dt = -n \quad (9-34)$$

The aerodynamic coefficients are then evaluated by a simultaneous solution of the transfer function coefficients, providing that the mass and inertia are known.

c. Derivative Method as Applied to the Equations of Motion.

If the assumed form of the lift equation is:

$$(Ump - Z_a)\alpha - (Um + Z_q)\dot{\alpha} = Z_{\delta_e} \delta_e \quad (9-35)$$

it is possible to determine the aerodynamic coefficients Z_α , Z_q and Z_{δ_e} from three sets of simultaneous measurements. The equation above can be written as:

$$Ump\alpha - Z_a\alpha - (Um + Z_q)\dot{\alpha} - Z_{\delta_e}\delta_e = 0 \quad (9-36)$$

If the subscript 1 denotes the value of a quantity at $t = t_1$, etc., then three simultaneous equations are obtained by the proper substitution of three sets of simultaneous values for $p\alpha$, α , q and δ_e (α and $\dot{\alpha}$ are difficult to measure directly but can be computed by making use of the relation, $\dot{\alpha} = q - \frac{gn}{U}$.)

The equations are as follows:

$$\begin{aligned}Um(\rho\alpha)_1 - Z_\alpha \alpha_1 - (Um + Z_q)q_1 - Z_{\delta_e} \delta_{e1} &= 0 \\Um(\rho\alpha)_2 - Z_\alpha \alpha_2 - (Um + Z_q)q_2 - Z_{\delta_e} \delta_{e2} &= 0 \\Um(\rho\alpha)_3 - Z_\alpha \alpha_3 - (Um + Z_q)q_3 - Z_{\delta_e} \delta_{e3} &= 0\end{aligned}\quad (9-37)$$

If it is desirable to use more data (taken at more than three time instants) then, as previously indicated, a method of least-squares may be used to compute values of Z_α , Z_q and Z_{δ_e} . The equations are:

$$\begin{aligned}\sum_i Um(\rho\alpha)_i \alpha_i - \sum_i Z_\alpha \alpha_i^2 - \sum_i (Um + Z_q) q_i \alpha_i - \sum_i Z_{\delta_e} \delta_{ei} \alpha_i &= 0 \\ \sum_i Um(\rho\alpha)_i q_i - \sum_i Z_\alpha \alpha_i q_i - \sum_i (Um + Z_q) q_i^2 - \sum_i Z_{\delta_e} \delta_{ei} q_i &= 0 \\ \sum_i Um(\rho\alpha)_i \delta_{ei} - \sum_i Z_\alpha \alpha_i \delta_{ei} - \sum_i (Um + Z_q) q_i \delta_{ei} - \sum_i Z_{\delta_e} \delta_{ei}^2 &= 0\end{aligned}\quad (9-38)$$

This same procedure can be applied to the moment equation to solve for M_α , M_q and M_{δ_e} .

9.6.3.2 Methods for Determining Aerodynamic Coefficients from Frequency Response Data.

a. Sinusoidal (Frequency) Response (See Reference 42).

This technique is applicable to data that consists of amplitude ratios and phase shifts (between the input and output response) over a given frequency range. For example, in the case of longitudinal motion with two degrees of freedom, the transfer function between pitching velocity q and elevator angle δ_e has been shown to be:

$$\frac{q}{\delta_e} = \frac{C_1 p + C_0 q}{p^2 + pb + k} \quad (9-39)$$

If $\delta_e = \delta_{e0} \sin \omega t$ and $\frac{q}{\delta_{e0}} = R \sin \omega t + \phi = A \sin \omega t + B \cos \omega t$,

then it can be shown that $A + iB$ is the value of the transfer function when $p = i\omega$. If the proper substitutions are made in the above transfer function the following equation is obtained:

$$A(R - \omega^2) - Bb\omega + i[B(R - \omega^2) + Ab\omega] = C_{0g} + C_{1g}i\omega \quad (9-40)$$

Equating the real and imaginary parts results in the two equations:

$$\begin{aligned} AR - B\omega b - C_{0g} &= A\omega^2 && \text{Real equation} \\ BR + A\omega b - C_{1g}\omega &= B\omega^2 && \text{Imaginary equation} \end{aligned} \quad (9-41)$$

If the values of A and B are known at two frequencies, then it is possible to set up four simultaneous equations in four unknowns b , k , C_{0q} and C_{1q} as follows:

$$\begin{aligned} A_1 R - B_1 \omega_1 b - C_{0g} &= A_1 \omega_1^2 \\ A_2 R - B_2 \omega_2 b - C_{0g} &= A_2 \omega_2^2 \\ B_1 R + A_1 \omega_1 b - \omega_1 C_{1g} &= B_1 \omega_1^2 \\ B_2 R + A_2 \omega_2 b - \omega_2 C_{1g} &= B_2 \omega_2^2 \end{aligned} \quad (9-42)$$

where A_1 , A_2 , B_1 , B_2 are the values of A and B at ω_1 and ω_2 . The solution of these equations for the values of b , k , C_{1q} and C_{0q} should yield a frequency response curve that agrees with the measured curve at the two frequencies selected. This has been called the "method of selected points."

Better values for b , k , C_{1q} and C_{0q} can be obtained by using data measured at more than two frequencies. A method of least-squares is used to calculate values of the parameters that make $\sum E_R^2 + \sum E_I^2$ a minimum where E_R and E_I are defined by:

$$\begin{aligned} AR - B\omega b - C_{0g} - A\omega^2 &= E_R \\ BR + A\omega b - C_{1g}\omega - B\omega^2 &= E_I \end{aligned} \quad (9-43)$$

This leads to the following set of normal equations:

$$\begin{aligned}
 \sum (B^2 \omega^2 + A^2 \omega^2) b &+ \sum B \omega c_{0g} - \sum A \omega^2 c_{1g} = 0 \\
 \sum (B^2 + A^2) R &- \sum A c_{0g} - \sum B \omega c_{1g} = \sum (B^2 \omega^2 + A^2 \omega^2) \\
 \sum B \omega b &- \sum A R + N c_{0g} = - \sum A \omega^2 \\
 \sum A \omega^2 b &+ \sum B \omega R \quad \quad \quad \sum \omega^2 c_{1g} = \sum B \omega^3
 \end{aligned}
 \tag{9-44}$$

where N equals the number of frequencies and the summation is taken over all the frequencies at which data are obtained.

If the phase and amplitude of the normal acceleration response to sinusoidal elevator motion is measured, the coefficients of the transfer function

$$\frac{\eta}{\delta_e} = \frac{c_{2n} p^2 + c_{1n} p + c_{0n}}{p^2 + b p + R}
 \tag{9-45}$$

can be determined in a similar manner.

The aerodynamic coefficients can then be evaluated by a simultaneous solution of the transfer function coefficients. (This assumes the mass and inertia are known.)

b. Sinusoidal (Frequency) Response as Applied to the Equations of Motion.

If the frequency responses α/δ_e and q/δ_e are available, they can be converted into the following:

$$\frac{\alpha}{\delta_e} = A + i B \quad \quad \frac{q}{\delta_e} = C + i D
 \tag{9-46}$$

Also, the lift equation of motion,

$$(U m p - Z_\alpha) \alpha - (U m + Z_q) q = Z_{\delta_e} \delta_e$$

can be rewritten as

$$(U m i \omega - Z_\alpha) \alpha / \delta_e - (U m + Z_q) \frac{q}{\delta_e} - Z_{\delta_e} = 0
 \tag{9-47}$$

Then substituting equations (9-46) in equation (9-47) the following is obtained:

$$(\mathcal{U}m i \omega - Z_{\alpha})(A + iB) - (\mathcal{U}m + Z_g)(C + iD) - Z_{\delta_e} = 0 \quad (9-48)$$

Equating the real and imaginary parts results in the two equations:

$$-Z_{\alpha}A - \mathcal{U}m \omega B - \mathcal{U}mC - Z_gC - Z_{\delta_e} = 0 \quad \text{Real Equation} \quad (9-49)$$

$$\mathcal{U}m \omega A - Z_{\alpha}B - \mathcal{U}mD - Z_gD = 0 \quad \text{Imaginary Equation}$$

If the mass, the inertia and the values of A, B, C and D are known at two frequencies, then it is possible to set up four simultaneous equations, and solve for the unknowns Z_{α} , Z_g and Z_{δ_e} , using any three of the four equations. The equations are:

$$\begin{aligned} -Z_{\alpha}A_1 - \mathcal{U}m \omega_1 B_1 - (\mathcal{U}m + Z_g)C_1 - Z_{\delta_e} &= 0 \\ -Z_{\alpha}A_2 - \mathcal{U}m \omega_2 B_2 - (\mathcal{U}m + Z_g)C_2 - Z_{\delta_e} &= 0 \\ \mathcal{U}m \omega_1 A_1 - Z_{\alpha}B_1 - (\mathcal{U}m + Z_g)D_1 &= 0 \\ \mathcal{U}m \omega_2 A_2 - Z_{\alpha}B_2 - (\mathcal{U}m + Z_g)D_2 &= 0 \end{aligned} \quad (9-50)$$

where A_1 , A_2 , B_1 , B_2 , C_1 , C_2 , D_1 and D_2 are the values at frequencies ω_1 and ω_2 . The solution of these equations gives the values of Z_{α} , Z_g and Z_{δ_e}

corresponding to a frequency response curve that agrees exactly with the measured curve at the two frequencies selected.

Better values for Z_{α} , Z_g and Z_{δ_e} can be obtained by using data measured at more than two frequencies. A method of least-squares is used in this case

to evaluate the aerodynamic coefficients. The procedure outlined above can also be used to determine the coefficients (M_α , M_q and M_δ) from the moment equation.

The foregoing material has indicated that the least-squares solution is preferable to using the "method of selected frequencies" (or selected times). However, the circumstances should be pointed out under which one could obtain ill-conditioned equations (and matrices). The samples selected should contain significant values of all the variables; otherwise the "noise" (errors) may obscure some values. In the frequency domain, values obtained in the regions of resonance should give better "signal to error" ratios. On the other hand, if all the data points are taken from too narrow a frequency band, the fitting of the coefficients to the frequency response curve will be inaccurate. Thus some compromise is indicated. Also, for example, in a two-degree-of-freedom longitudinal case, using data at low frequencies, introduces errors due to speed changes (which are not accounted for by the equations). The response at frequencies well above resonance is small and leads to errors due to poor resolution (low signal-to-error or signal-to-noise ratios).

If data in the time domain contains noise it is sometimes difficult to select good data points. The primary asset of going through the transformation to the frequency domain is that good data can be separated from the noise (particularly when the frequency spectrum of the noise is well separated from the spectrum of the desired data). However, if data in the time domain must be used, take a sufficient number of samples so as to well define the time history and also have unequal time intervals between the samples.

9.6.3.3 Simplified Analysis Procedures. Sometimes when a fairly clear-cut mode can be seen in the frequency response of an aircraft, it is desirable to be able to at least determine the effective viscous damping and spring constants of the mode. If the mode in question is well separated from the other modes, the frequency response in the regime of the natural frequency of the mode usually behaves as a second order system. As an example of how such an analysis would be conducted consider the following example of the rigid-body response of an aircraft which is well separated in frequency from the elastic modes: (The same technique could be applied to an elevator response mode whose natural frequency is much higher and well separated than the rigid-body motion which would affect the elevator response in the lower frequency regime.)

The equation of motion for the normal acceleration of the airplane at the center of gravity can be written as:

$$(\ddot{n}-1) + b(\dot{n}-1) + k(n-1) = (U_0 M_{\delta_e} Z_w \delta_e) I_m e^{i\omega t} \quad (9-51)$$

where

b = effective viscous damping for the airplane (short period motion) mode,
 k = effective spring constant for the airplane mode, and
 I_m = the "imaginary part of".

The frequency response may be written as:

$$\frac{(\overline{n-1})}{\delta_e} = \frac{U_0 M_{\delta_e} Z_w}{\sqrt{(k - \omega^2)^2 + \omega^2 b^2}} e^{iLA(n-1)\delta_e} \quad (9-52)$$

where

$$LA_{(n-1)}\delta_e = -\tan^{-1} \frac{\omega b}{R - \omega^2}$$

$$(n-1) = (\overline{n-1}) I_m e^{i\omega t}$$

The imaginary component of the above vector at any frequency is

$$I_m \frac{(\overline{n-1})}{\delta_{e_a}} = \frac{(n-1)}{\delta_{e_a}} \sin LA_{(n-1)} \delta_e =$$

$$\frac{UM_{\delta_e} Z_{\omega}}{\sqrt{(R - \omega^2)^2 + \omega^2 b^2}} \times \frac{\omega b}{\sqrt{(R - \omega^2)^2 + \omega^2 b^2}} \quad (9-53)$$

since

$$\sin LA_{(n-1)}\delta_e = \frac{\omega b}{\sqrt{(R - \omega^2)^2 + (\omega^2 b^2)}}$$

Differentiating $I_m \frac{(\overline{n-1})}{\delta_e}$ with respect to ω , and setting the result equal to zero, we obtain:

$$(R - \omega^2)^2 + 4\omega^2(R - \omega^2) = \omega^2 b^2 \quad (9-54)$$

If we let

$$b = 2\omega_n \xi$$

$$R = \omega_n^2$$

where $\xi = \frac{c}{c_c}$ = effective viscous damping ratio

and $\omega_n = 2\pi \times$ the frequency at which the $LA_{(n-1)}\delta_e = 90^\circ$

$$\text{then } (\omega_n^2 - \omega^2)^2 + 4\omega^2(\omega_n^2 - \omega^2) = 4\xi^2 \omega^2 \omega_n^2 \quad (9-55)$$

Rewriting gives

$$\omega_n^4 \left[1 - \left(\frac{\omega}{\omega_n}\right)^2\right]^2 + 4\omega^2 \omega_n^2 \left[1 - \left(\frac{\omega}{\omega_n}\right)^2\right] = 4\xi^2 \omega^2 \omega_n^2 \quad (9-56)$$

and if we let $\frac{\omega}{\omega_n} = \beta$

where $\omega = 2\pi \times$ frequency of the maximum departure in the imaginary direction,

then
$$\xi^2 = (1 - \beta^2) + \frac{1}{4\beta^2} (1 - \beta^2)^2 \quad (9-57)$$

or
$$\xi = \sqrt{(1 - \beta^2)^2 + \frac{1}{4\beta^2} (1 - \beta^2)^2} \quad (9-58)$$

Having determined ξ and ω_n , b and k may be evaluated.

9.6.4 Techniques for Performing Error Analyses. An error analysis provides a means for determining the errors in the final results of any method of data analysis used. The error analysis can take into account the errors of the initial flight test data as well as the errors that arise from the mathematical manipulations within the data analysis method. There are two very useful types of error analyses that will be covered in the following pages. One determines the maximum error while the other determines the probable error present in the results of a data analysis method.

The theory involved in these analyses is concerned principally with the errors that are derived from the solution of a set of simultaneous equations (i.e., the errors that arise in the results due to the initial errors in the coefficients of the equations to be solved simultaneously).

A system of simultaneous equations can be written symbolically as follows:

$$\sum_{j=1}^n a_{ij} x_j = a_{i(n+1)} \quad i, = 1, 2, \dots, n \quad (9-59)$$

where the a_{ij} have initial errors (due to the errors in the flight test data) and the x_i are the unknowns which include the final errors. The errors can be related similarly (for relatively small errors):

$$\sum_{j=1}^n d(a_{ij} x_j) = \sum_{j=1}^n (x_j da_{ij} + a_{ij} dx_j) = da_{i(n+1)} \quad (9-60)$$

$$\sum_{j=1}^n a_{ij} dx_j = da_{i(n+1)} - \sum_{j=1}^n x_j da_{ij} = N_i \quad (9-61)$$

Hence a simultaneous set of algebraic equations can be found by Equation (9-61), (where the N_i are constants) from which the final errors, d_{x_i} can be calculated.

Since the initial errors, da_{ij} , can be either positive or negative, the summation for the N_i must consist of the absolute values for the maximum error analyses. Equation (9-61) is modified as follows:

$$\sum_{j=1}^n a_{ij} dx_j = \sum_{j=1}^n |x_j da_{ij}| + |da_{i(n+1)}| = N_{i_{max}} \quad (9-62)$$

Harmonic averages of precision factors, h_{ij} , are involved in computing the N_i constants for the probable error analyses (i.e., each N_i prob. is the probable error for the combination of $n+1$ initial probable errors; da_{ij} ; $j = 1, 2, \dots, n+1$). The precision factors, h_{ij} , are related to the initial probable errors, da_{ij} , by the equation:

$$h_{ij} = \frac{\rho}{da_{ij}} \quad \text{where } \rho = .4769 \quad (9-63)$$

The harmonic average is:

$$\frac{1}{h_i^2} = \frac{(x_1)^2}{(h_{i1})^2} + \dots + \frac{(x_n)^2}{(h_{in})^2} + \frac{1}{(h_{i(n+1)})^2} = \sum_{j=1}^{n+1} \frac{(x_j)^2}{(h_{ij})^2}, \quad (x_{n+1} = 1) \quad (9-64)$$

where the N_i prob. are related to the h_i as in Equation (9-63):

$$\sum_{j=1}^n a_{ij} dx_j = N_{i_{prob}} = \frac{\rho}{h_i} \quad (9-65)$$

Therefore Equation (9-61) is replaced, for the probable error analyses, by Equation (9-65) which incorporates Equations (9-63) and (9-64). See References 45 and 46 for the theory involved in Equations (9-63) and (9-65).

REFERENCES

1. Klein, H., and Sedney, R., Some Basic Concepts for Analyzing Dynamic Flight Test Data, Journal of the Aeronautical Sciences, Vol. 20, No. 11, Nov. 1953, pp 740-748.
2. Milliken, W. F., Dynamic Stability and Control Research, Cornell Aeronautical Laboratory Report No. CAL-39 (Presented at the Third International Joint Conference of the RAeS-IAS, Brighton, England, September 3-14, 1951)
3. Cole, H. A., Jr., Brown, S. C., and Holleman, E. C., Experimental and Predicted Longitudinal Response Characteristics of a Large Flexible 35° Swept-Wing Airplane at an Altitude of 35,000 Feet, NACA RM A54H09, November 1954.
4. Cole, H. A., Jr., Brown, S. C., and Holleman, E. C., The Effects of Flexibility on the Longitudinal and Lateral-Directional Response of a Large Airplane, NACA RM A55D14, May 1955.
5. Donegan, J. J. and Huss, C. R., NACA RM L54L16, May 1955. (CONFIDENTIAL)
6. Krug, E. H., B-36B Autopilot Program Final Summary Report, Consolidated Vultee Aircraft Corporation Report No. FZA-36-210, November 1950.
7. Clousing, L. A., Turner, W. N. and Rolls, L. S., Measurements in Flight of the Pressure Distribution on the Right Wing of a P-39N-1 Airplane at Several Values of Mach Number, NACA Report 859, 1946.
8. Wener, N. L., Oscillation Method of Stability Flight Testing, USAF Air Material Command, Flight Test Division Memorandum Report No. MCRFT-2253, March 1950.
9. Soule, H. A., and Miller, M. P., The Experimental Determination of the Moments of Inertia of Airplanes, NACA Report No. 467, 1933.
10. Turner, H. L., Measurement of the Moments of Inertia of an Airplane by a Simplified Method, NACA TN 2201, Oct 1950.
11. Cole, H. A., Jr. and Bennison, F. L., Measurement of The Longitudinal Moment of Inertia of a Flexible Airplane, NACA TN 3870, January 1956.
12. Widmayer, E., Jr., and Reese, J. R., Moment of Inertia and Damping of Fluid in Tanks Undergoing Pitching Oscillations, NACA RM L53E01a, June, 1953.
13. Boucher, R. W., Rich, D. A., Crane, H. L. and Matheny, C. E., A Method for Measuring the Product of Inertia and the Inclination of the Principal Longitudinal Axis of Inertia of an Airplane, NACA TN 3084 April, 1954.

14. Reese, J. R., and Sewall, J. L., Effective Moment of Inertia of Fluid in Offset, Inclined and Swept-Wing Tanks Undergoing Pitching Oscillation, NACA TN 3353, January 1955.
15. Bisplinghoff, H. L., Ashley, H., and Halfman, R. L., Aeroelasticity, Addison-Wesley, 1955.
16. Flutter Inspection of Boeing XB-47 Airplane, USAF Air Materiel Command, Engineering Division Memorandum Report No. MCREXAS-4262-36-29, 1948.
17. Mayo, A. P. and Ward, J. F., Experimental Influence Coefficients for the Deflection of the Wing of a Full-Scale, Swept-Wing Bomber, NACA Research Memorandum L53L23, 1954.
18. Perkins, C. D., Methods for Obtaining Aerodynamic Data Through Steady-State Flight Testing, Part I Longitudinal; Part II, Lateral, Princeton University, Dept. of Aeronautical Engineering (ASTIA Nos. ATI 76294 and ATI 114359).
19. Perkins, C. D., and Walkowicz, T. F., Stability and Control Flight Testing, AAF Technical Report 5242, July 1945.
20. Campbell, G. F., Whitcomb, D. W., and Breuhaus, W. O., Dynamic Longitudinal Stability and Control Flight Tests of B-25J Airplane. Forced Oscillation and Step Function Response Methods Utilizing an A-12 Automatic Pilot, Cornell Aero. Lab., Report No. TB-405-F-3, April, 1947.
21. Breux, G. P. and Zeiler, E. L., Dynamic Response Program on the B-36 Airplane: Part III - Presentation and Theoretical Considerations of the Transient Analysis Method Employed for Obtaining Frequency Response Functions from Flight Data, Convair Report No. FXA-36-195, Feb. 1952.
22. Goldman, S., Frequency Analysis, Modulation, and Noise, McGraw-Hill Book Co., Inc., New York, 1948.
23. Guillemin, E. A., The Mathematics of Circuit Analysis, John Wiley and Sons, Inc., 1949.
24. Muzzey, C. L., and Kidd, E. A., Measurement and Interpretation of Flight Test Data for Dynamic Stability and Control, Cornell Aeronautical Laboratory Report No. CAL-60, April 1954.
25. Perkins, C. D., et al., Flight Test Manual, Volume II: Stability and Control, Advisory Group for Aeronautical Research and Development (AGARD) of NATO.
26. Lappi, U. O., A Transient Method for Determining Frequency Responses in Lateral Stability, Cornell Aero Lab., Inc., Report No. TE 543-F-1, May, 1948 (Revised, April, 1949).

27. Eggleston, J. M. and Mathews, C. W., Application of Several Methods for Determining Transfer Functions and Frequency Response of Aircraft from Flight Test, NACA Report No. 1204, 1954 (also NACA TN 2997, Sept. 1953).
28. Bratten, F. W. and Brown, R. W., Analog Computer Techniques for Determining Transfer Function Coefficients, Corona Labs., NBS Report No. 1232, January 1953.
29. Wener, N. L. and Drum, H. C., The Accuracy of Frequency Spectra as Determined by Several Fourier Transformation Methods, USAF, Wright Air Development Center Technical Report 54-518, August, 1955.
30. Andrew, G. M., End Correction for Frequency Response by Laplace Transformation, AFFTC Tech. Report No. 52-15, February 1952.
31. Schumacher, L. E., Methods of Analyzing Transient Flight Data to Obtain Aircraft Frequency Response, WADC Memo Report NCRFT-2268, Jan. 1950.
32. Tranter, C. J., Integral Transforms in Mathematical Physics, John Wiley and Sons, Inc., 1951.
33. Filon, L. N. G., On a Quadrature Formula for Trigonometric Integrals, Proceedings of the Royal Society of Edinburgh, Scotland, Vol 49, 1928-1929, pp 38-47.
34. Rice, S. O., Mathematical Analysis of Random Noise, Bell System Technical Journal, Parts I and II, Volume 23, July, 1944, pp 282-332, and Parts III and IV, Volume 24, January, 1945, pp 46-156.
35. Lanczos, C., Smoothing of Noisy Data by Trigonometric Truncation, National Bureau of Standards Report Number 1582, National Bureau of Standards Project Number 1101-11-50100, 9 April 1952.
36. Wiener, N., The Extrapolation, Interpolation, and Smoothing of Stationary Time Series, Wiley Publishing Company, New York, 1949, also appears with DIC Contract 6031 of NRDC, Section D-2, 1 February 1942.
37. Bubb, F. W., Theory of Best Automatic Control Systems for Predicting and Smoothing, (Thumper Project), General Electric Company TR 55377, 19 April 1948.
38. Zadeh, L. A. and Ragazzini, J. R., An Extension of Wiener's Theory of Prediction, Journal of Applied Physics, Volume 21, July 1950, pp 645-55.
39. Walters, E. R. and Rea, J. B., Determination of Frequency Characteristics from Response to Arbitrary Input, Journal of the Aeronautical Sciences, Volume 17, Number 7, July 1950.
40. Rea, J. B., Analysis of Systems for Automatic Control of Aircraft, Aeronautical Engineering Review, Volume 10, No. 11, November 1951.

41. Courant, R., Differential and Integral Calculus, Volume 1, Interscience Publishers, Inc.
42. Greenberg, H., A Survey of Methods for Determining Stability Parameters of an Airplane from Dynamic Flight Measurements, NACA TN 2340, April 1951.
43. Donegan, J. J. and Pearson, H. A., Matrix Method of Determining the Longitudinal Stability Coefficients and Frequency Response of an Aircraft from Transient Flight Data, NACA TN 2370, June 1951.
44. Booth, A. D., An Application of the Method of Steepest Descents to the Solution of Systems of Non-Linear Simultaneous Equations, The Quarterly Journal of Mechanics and Applied Math, December 1949.
45. Scarborough, J. B., Numerical Mathematical Analysis, Edward Brothers, Inc., Ann Arbor, Michigan.
46. Margenau, H. and Murphy, G. M., The Mathematics of Physics and Chemistry, D. Van Nostrand, New York.

BIBLIOGRAPHY

1. Donegan, J. J., Robinson, S. W., Jr., and Gates, O. B., Jr., Determination of Lateral-Stability Derivatives and Transfer-Function Coefficients from Frequency-Response Data for Lateral Motions, NACA TN 3083, May 54.
2. Triplett, W. C., and Smith, G. A., Longitudinal Frequency-Response Characteristics of a 35° Swept-Wing Airplane as Determined from Flight Measurements, Including a Method for the Evaluation of Transfer Functions, NACA Research Memorandum A51G27, 1951.
3. Merten, K. F., and Stephenson, B. H., Some Dynamic Effects of Fuel Motion in Simplified Model Tip Tanks on Suddenly Excited Bending Oscillations, NACA TN 2789, 1952.
4. Ross, D. T., Improved Computational Techniques for Fourier Transformation, MIT Servomechanisms Laboratory Report No. 7138-R-5, June 1954.
5. Breuhaus, W. O. and Segal, L., Notes on Aircraft Dynamic Stability Testing and Analysis Techniques, Cornell Aeronautical Laboratory, Inc., Report No. CAL-51, April, 1953.
6. LaVerne, M. E., and Boksenbom, A. S., Methods for Determining Frequency Response of Engines and Control Systems from Transient Data, NACA TN 1935, August 1949.
7. Smith, G. A., and Triplett, W. C., Experimental Flight Methods for Evaluating Frequency-Response Characteristics of Aircraft, Trans ASME, Vol. 76, No. 8, Nov. 1954, pp 1383-93.
8. A Bibliography of Techniques for the Smoothing or Adjustment of Data, Aberdeen Proving Grounds, Technical Note 561, December 1951.
9. A Device for Computing Correlation Functions, U. S. Naval Research Laboratory, NRL-3679.
10. Arley, N. and Buch, Introduction to the Theory of Probability and Statistics, John Wiley and Sons, New York, 1950.
11. Bode, Blackman, and Shannon, Data Smoothing and Prediction in Fire-Control Systems, Research and Development Board, Washington, D. C., August 1948.
12. Booton, R. C., Jr., An Optimization Theory for Time-Varying Linear Systems with Nonstationary Statistical Inputs, Meteor Report Number 72, Massachusetts Institute of Technology, July 1951, also IRE August 1952.
13. Brooks, R. E., and Smith, H. W., A Computer for Correlation Functions, Review of Scientific Instruments, Volume 23, pp 121-6, March 1952.

14. Davenport, W. B., Jr. (Research Laboratory of Electronics, Massachusetts Institute of Technology), R. A. Johnson, and D. Middleton (Cruft Laboratories Harvard), Statistical Errors in Measurements on Random Time Functions, JAPS, Volume 23, Number 4, April 1952, pp 377-388.
15. Davis, R. C., Techniques for the Statistical Analysis of Continuous-Wave Doppler Data, Navord, Report 1312, 25 April 1951.
16. Fano, R. M., Signal-to-Noise Ratio Correlation Detectors, Technical Report 186, February 19, 1951, Massachusetts Institute of Technology.
17. Goldman, S., Frequency Analysis, Modulation, and Noise, McGraw-Hill Book Company, Inc., New York, 1948.
18. Goldman, S., Some Fundamental Considerations Concerning Noise Reduction and Range in Radar and Communication, IRE Proceedings, Volume 36, Number 5, pp 584-94, May 1948.
19. Grenander, Ulf, Stochastic Processes and Statistical Interference, Arkiv for Matematik, K. Svenska Vetinshap Akondimum, Band I, Hafte 3, Paper Number 18, pp 195-277, 1950.
20. Huggins, Wm. H., Network Approximation in the Time Domain, Air Force Report Number E-5048, Cambridge Research Laboratory.
21. Kolmogoroff, A., Foundations of the Theory of Probability, Chelsea Publishing Company, New York, 1950.
22. Lanczos, C., Analytical and Practical Curve Fitting of Equidistant Data, National Bureau of Standards Report Number 1591.
23. Lee, Y. W., Application of Statistical Methods to Communications Problems, Technical Report Number 181, Research Laboratory of Electronics, Massachusetts Institute of Technology.
24. Phillips, R. S., and Weiss, P. R., Theoretical Calculation of Best Smoothing of Position Data for Gunnery Prediction, Report 532, Radiation Laboratory, Massachusetts Institute of Technology, February 1944.
25. Representation Theory and Prediction of Stochastic Processes, University of Michigan EMF-11, 23 March 1950.
26. Rice, S. O., Statistical Properties of a Sine Wave Plus Random Noise, Bell Laboratories Technical Journal, Volume 27, 1948.
27. Shannon, C. E., A Mathematical Theory of Communication, Bell System Technical Journal Monograph B-1598.
28. Shannon, C. E., and Bode, H. W., Linear Least Square Smoothing and Prediction Theory, Proceedings of the IRE, Volume 38, pp 417-25, April 1950.

29. North American Aviation Aerophysics Laboratory Report Number AL-930, Presented jointly with UCLA on February 10, 11, and 12, 1949.
30. Uhlenbeck, G. E., and Lawson, Threshold Signals, Volume 24, Massachusetts Institute of Technology Radiation Laboratory Series, McGraw-Hill Book Company, Inc. 1948.
31. Wang, M. and Uhlenbeck, G. E., On the Theory of Brownian Motion, Review of Modern Physics, 1945.
32. Whittaker, J. M., Interpolatory Function Theory, Cambridge Tracts in Mathematics and Mathematical Physics. Number 33, Cambridge University Press, Chapter IV, 1935.
33. Wiener, N., The Fourier Integral, pp 150, Cambridge, 1939.
34. Schumacher, L. E., A Method for Evaluating Aircraft Stability Parameters from Flight Test Data, A. F. Technical Report No. WADC TR 52-71, June 1952.

NOMENCLATURE

General

| | |
|---------------------|---|
| α | angle of attack, radians |
| A,B | in- and out-of-phase components of oscillation |
| p | differential operator $\frac{d}{dt}$ |
| δ_e | elevator deflection, radians |
| E | residual error in an equation |
| g | acceleration due to gravity |
| θ | angle of pitch, radians |
| I_y | pitching moment of inertia, slug-feet squared |
| L | lift force pounds |
| L_α | $\frac{\partial L}{\partial \alpha}$ |
| L_δ | $\frac{\partial L}{\partial \delta}$ |
| m | mass of airplane, slugs |
| M | pitching moment, foot-pounds |
| M_α | $\frac{\partial M}{\partial \alpha}$ |
| $M_{D\dot{\alpha}}$ | $\frac{\partial M}{\partial D\dot{\alpha}}$ |
| M_δ | $\frac{\partial M}{\partial \delta}$ |
| M_q | $\frac{\partial M}{\partial q}$ |
| μ | relative density parameter $\frac{2m}{\rho S_w c} = \frac{2 \times \text{mass}}{\text{density} \times \text{wing area} \times \text{wing chord}}$ |
| n | normal acceleration, g units |
| q | angular pitching velocity, radians per second |
| R, ϕ | amplitude and phase of complex number |
| t | time seconds |

U velocity of airplane, feet per second
W weight of airplane, pounds
 ω angular frequency, radians per second

Transfer-Function Coefficients

b damping parameter $\frac{-M_q - M_{D\dot{\alpha}}}{I_y} + \frac{L_{\dot{\alpha}}}{mU_o}$

$C_{l_{\alpha}} \frac{-L_{\delta}}{mU_o}$

$C_{l_q} \frac{M_{\delta}}{I_y} - \frac{L_{\delta}}{mU_o} \frac{M_{D\dot{\alpha}}}{I_y}$

$C_{o_{\alpha}} \frac{M_{\delta}}{I_y} + \frac{L_{\delta}}{mU_o} \frac{M_q}{I_y}$

$C_{o_q} \frac{M_{\delta}}{I_y} \frac{L_{\alpha}}{mU_o} - \frac{M_{\alpha}}{I_y} \frac{L_{\delta}}{mU_o}$

$C_{o_n} C_{o_q} \frac{U_o}{g}$

$C_{l_n} (C_{l_q} - C_{o_{\alpha}}) \frac{U_o}{g}$

$C_{2_n} -C_{l_{\alpha}} \frac{U_o}{g}$

k stiffness parameter $-\frac{M_{\alpha}}{I_y} - \frac{L_{\alpha}}{mU_o} \frac{M_q}{I_y}$